

CARBONATE SEDIMENTATION IN AN EVOLVING MIDDLE
ORDOVICIAN FORELAND BASIN, WESTERN NEWFOUNDLAND

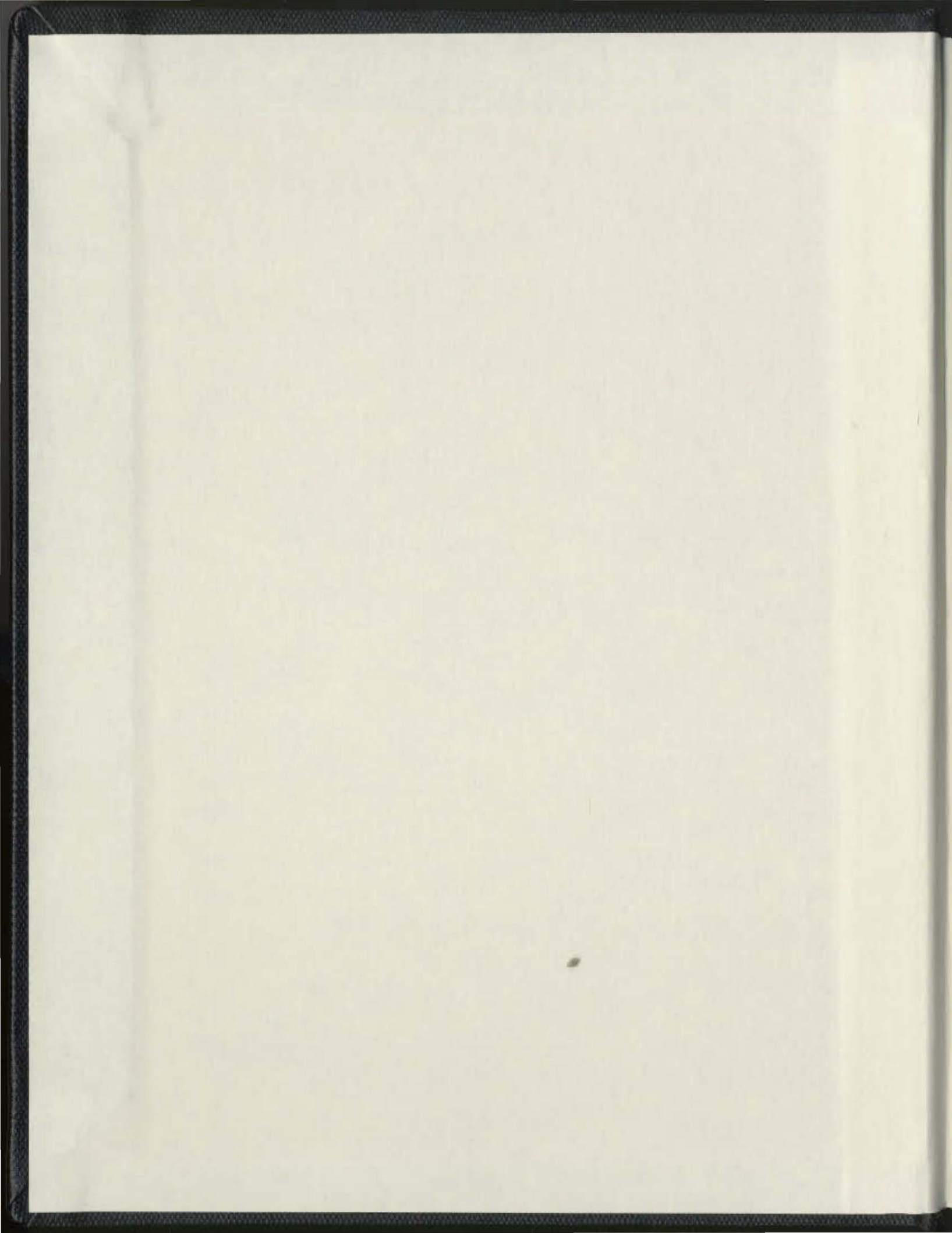
VOL. I

CENTRE FOR NEWFOUNDLAND STUDIES

TOTAL OF 10 PAGES ONLY
MAY BE XEROXED

(Without Author's Permission)

SHEILA RAE STENZEL





National Library
of Canada

Acquisitions and
Bibliographic Services Branch

395 Wellington Street
Ottawa, Ontario
K1A 0N4

Bibliothèque nationale
du Canada

Direction des acquisitions et
des services bibliographiques

395, rue Wellington
Ottawa (Ontario)
K1A 0N4

Your file *Votre référence*

Our file *Notre référence*

NOTICE

The quality of this microform is heavily dependent upon the quality of the original thesis submitted for microfilming. Every effort has been made to ensure the highest quality of reproduction possible.

If pages are missing, contact the university which granted the degree.

Some pages may have indistinct print especially if the original pages were typed with a poor typewriter ribbon or if the university sent us an inferior photocopy.

Reproduction in full or in part of this microform is governed by the Canadian Copyright Act, R.S.C. 1970, c. C-30, and subsequent amendments.

AVIS

La qualité de cette microforme dépend grandement de la qualité de la thèse soumise au microfilmage. Nous avons tout fait pour assurer une qualité supérieure de reproduction.

S'il manque des pages, veuillez communiquer avec l'université qui a conféré le grade.

La qualité d'impression de certaines pages peut laisser à désirer, surtout si les pages originales ont été dactylographiées à l'aide d'un ruban usé ou si l'université nous a fait parvenir une photocopie de qualité inférieure.

La reproduction, même partielle, de cette microforme est soumise à la Loi canadienne sur le droit d'auteur, SRC 1970, c. C-30, et ses amendements subséquents.

Canada

CARBONATE SEDIMENTATION IN AN EVOLVING
MIDDLE ORDOVICIAN FORELAND BASIN, WESTERN NEWFOUNDLAND

By

©Sheila Rae Stenzel, B. A., M. S.

A thesis submitted to the School of Graduate
Studies in partial fulfilment of the
requirements for the degree of
Doctor of Philosophy

Department of Earth Sciences
Memorial University of Newfoundland

August 1991

St. John's

Newfoundland



National Library
of Canada

Acquisitions and
Bibliographic Services Branch

395 Wellington Street
Ottawa, Ontario
K1A 0N4

Bibliothèque nationale
du Canada

Direction des acquisitions et
des services bibliographiques

395, rue Wellington
Ottawa (Ontario)
K1A 0N4

Your file *Votre référence*

Our file *Notre référence*

The author has granted an irrevocable non-exclusive licence allowing the National Library of Canada to reproduce, loan, distribute or sell copies of his/her thesis by any means and in any form or format, making this thesis available to interested persons.

L'auteur a accordé une licence irrévocable et non exclusive permettant à la Bibliothèque nationale du Canada de reproduire, prêter, distribuer ou vendre des copies de sa thèse de quelque manière et sous quelque forme que ce soit pour mettre des exemplaires de cette thèse à la disposition des personnes intéressées.

The author retains ownership of the copyright in his/her thesis. Neither the thesis nor substantial extracts from it may be printed or otherwise reproduced without his/her permission.

L'auteur conserve la propriété du droit d'auteur qui protège sa thèse. Ni la thèse ni des extraits substantiels de celle-ci ne doivent être imprimés ou autrement reproduits sans son autorisation.

ISBN 0-315-82662-2

Canada

ABSTRACT

Table Head and Goose Tickle group strata in western Newfoundland are a deepening-upward, carbonate to clastic sequence deposited on the convergent, paleosouth-facing, North American continental margin during Middle Ordovician time. Preceding passive margin platform growth was abruptly terminated by widespread, early Middle Ordovician block-faulting and differential uplift (St. George Unconformity) caused by migration of a peripheral bulge across the platform interior. Subsequent sea level rise led to widespread peritidal, then shallow subtidal, carbonate deposition (Table Point Formation) on a tectonically unstable platform that formed the western flank of the evolving Taconic foreland basin. Syntectonic faulting and differential subsidence profoundly influenced sedimentation, leading to marked variations in thickness and abrupt lateral and vertical changes in platform carbonate lithofacies. Episodic seismicity and changes in slope triggered gravitational slides and flows. This platform was in turn tectonically drowned by extensional faulting and differential collapse as it became part of the outer trench slope of the subduction zone. Thin-bedded, hemipelagic and turbiditic limestone and shale (Table Cove Formation) accumulated on discontinuous, gently-dipping carbonate slopes and basin margins of variable duration and facing direction. Massive, polymictic, carbonate debris flow conglomerate, calciturbidite and shale (Cape Cormorant Formation) were deposited in an isolated basin adjacent to a high relief fault scarp that exhumed several hundred metres of buried, older, passive margin platform carbonate. Laminated black shale (Black Cove Formation) accumulated in remote, sediment-starved basins, and on the tops of isolated, rapidly foundered, relict platforms. As the (collapsed) platform entered the trench it was buried by siliciclastic flysch (American Tickle Formation and Mainland Sandstone) derived from an advancing accretionary prism. Terrigenous

mud, silt and sand, transported mostly by turbidity currents travelling southwest parallel to the trench axis, accumulated in topographic depressions controlled by antecedent structural domains.

Contemporaneous reverse faulting generated new escarpments in the trench, sourcing limestone debris flow conglomerates and calciturbidites deposited in intra-trench depressions (Daniel's Harbour Member).

ACKNOWLEDGEMENTS

I sincerely thank my supervisor, Noel P. James, for his continuous interest, advice and encouragement during this study. I am also grateful to Ian Knight and Peter Cawood for pointing me to critical outcrops, and for their interest and helpful discussions in the field. I also benefited from the perspectives of and discussions with Rob Grenier, Rick Hiscott, Louise Quinn, and Bob Stevens. I also thank Roger Cuffey, Bernard Mamet, Felicity O'Brien, Neil O'Brien, Suzanne Pohler, S. Henry Williams, and Steve Westrop for consultation and identification of fossils.

Research was funded by a Natural Sciences and Engineering Research Council of Canada grant to Noel P. James. Helicopter flying time awarded by Seeland Incorporated is gratefully acknowledged. Teck Corporation gave me free access to drill core at the Daniel's Harbour Zinc Mine. Parks Canada permitted me to work in Gros Morne National Park.

Several people were helpful during various stages of this project. Alison Pye provided excellent assistance in the field. Flemming Mengel, David Van Everdingen, Jeroen Van Gool, and Judith James cheerfully found solutions to every computer problem I encountered. Darcy Taylor helped with drafting. Jeanette Rolefson-Ahl helped with photography and drafting. Heather Macdonald read parts of the manuscript and provided invaluable technical assistance during its final production. Many others among the office, administrative and technical staffs in the Department of Earth Sciences at Memorial University and in the Department of Geological Sciences at Queens University provided essential technical and logistical assistance.

This endeavour was propelled by never-ending emotional support and encouragement from family and friends. I especially thank my parents, Robert and Joyce Stenzel, and my dear friends, Heather Macdonald, Darcy Taylor, Tom Lane, and Julie Porter.

TABLE OF CONTENTS

	Page
ABSTRACT	ii
ACKNOWLEDGMENTS	iv
TABLE OF CONTENTS	v
LIST OF FIGURES	xi
LIST OF TABLES	xvii
CHAPTER 1 INTRODUCTION	1
1.1 Introductory Remarks	1
1.2 Geologic Setting	3
1.3 Summary of Previous Work	8
1.3.1 Stratigraphy	8
1.3.2 Paleontology and Biostratigraphy	10
1.3.3 Sedimentology	11
1.4 Scope and Aims of this Study	13
1.5 Organization of Results	14
PART I: SEDIMENTOLOGY	
CHAPTER 2 INTRODUCTION TO SEDIMENTOLOGY	15
CHAPTER 3 SEDIMENTOLOGY OF THE AGUATHUNA FORMATION	16
3.1 General Character and Stratigraphic Relationships	16
3.2 Lithofacies	16
3.2.1 Dololaminite	16
3.2.2 Stromatolite	22
3.2.3 Burrowed Dolostone	23
3.2.4 Limestone	23
3.2.5 Dolomitic Shale	24
3.2.6 Intraformational Breccia	25
3.3 Stratigraphy	25
3.3.1 Lower Aguathuna	28
3.3.2 Middle Aguathuna	28
3.3.3 St. George Unconformity	29
3.3.4 Upper Aguathuna	32
3.4 Summary and Environmental Reconstruction	32
3.5 Signals of Convergent Margin Tectonism	36
CHAPTER 4 SEDIMENTOLOGY OF THE TABLE POINT FORMATION	38
4.1 General Characteristic and Stratigraphic Relationships	38
4.2 Basal Peritidal Unit (BPU)	38
4.2.1 Peritidal Lithofacies	49
4.2.2 Restricted Subtidal Lithofacies	52
4.2.3 Peritidal Sequences	54
4.3 Middle Subtidal Unit (MSU)	54
4.3.1 Burrowed, Peloidal Packstone	54
4.3.2 Bioturbated, Fossiliferous Wackestone	58
4.3.3 Sponge Bioherms	59
4.3.4 Early Lithification; Diagenetic Bedding	61
4.4 Upper Subtidal Unit (USU)	62
4.4.1 Sponge-Oncolite Biostrome	63
4.4.2 Echinoderm-algal Limestone	66
4.4.3 <u>Stromatactis</u> Mound	67
4.4.4 USU Mineralized Hardground	69
4.5 Summary and Reconstruction of Depositional Environments	71
4.6 Discussion	73
4.7 Signatures of Convergent Margin Sedimentation	75

CHAPTER 5	SEDIMENTOLOGY OF THE TABLE COVE FORMATION	77
5.1	General Characteristics and Stratigraphic Relationships	77
5.2	Burrowed Limestone Lithofacies	77
5.2.1	Lithologies	92
	(i) Medium grey, muddy limestone	92
	(ii) Dark grey, trilobite-rich limestone	93
	(iii) Echinoderm-rich, skeletal sands lenses	94
	(iv) Limestone conglomerate	95
	(v) Bentonite	95
5.2.2	Synsedimentary Deformation	96
5.2.3	Interpretation	96
5.2.4	Regional Variations	97
5.3	Parted Limestone Lithofacies	101
5.3.1	Lithologies	104
	(i) Light grey, parted limestone	104
	(ii) Dark grey, trilobite-rich limestone	106
5.3.2	Trace Fossils	106
	(i) Description	106
	(ii) Significance of the assemblage	109
5.3.3	Synsedimentary Deformation	110
5.3.4	Interpretation	110
5.3.5	Comments	112
5.4	Ribbon Limestone Lithofacies	113
5.4.1	Lithologies of Sub-lithofacies A	114
	(i) Ribbon limestone	114
	(ii) Dark grey, trilobite-rich limestone	120
	(iii) Limestone conglomerate	121
5.4.2	Synsedimentary Deformation	122
5.4.3	Lithologies of Sub-lithofacies B	123
	(i) Ribbon limestone	123
	(ii) Bentonite	127
5.4.4	Synsedimentary Deformation	127
5.4.5	Interpretation	128
5.5	Paleoslope Direction	129
5.6	Summary and Reconstruction of Depositional Environments	130
5.7	Table Cove Formation vs. Continental Slope and Rise Carbonates	136
CHAPTER 6	SEDIMENTOLOGY OF THE CAPE CORMORANT FORMATION	138
6.1	General Characteristics and Stratigraphic Relationships	138
6.2	Lithologies	147
6.2.1	Shale	147
6.2.2	Ribbon Limestone	159
6.2.3	Lithoclast Conglomerate and Megaconglomerate	162
6.2.4	Lithoclast Calcirudite	169
6.2.5	Lithoclast Calcarenites and Calcisiltites	176
6.2.6	Bentonite	178
6.3	Gravitational Slides	178
6.4	Trace Fossils	179
6.5	Provenance of Lithoclastic Debris	184
6.5.1	Composition of Clasts	184
	(i) Limestone	184
	(ii) Dolostone	184
	(iii) Chert	190
	(iv) Other minor exotic lithologies	190
	(v) Clasts of Cape Cormorant aspect	190
6.5.2	Ages of Clasts	191
	(i) Fossiliferous clasts	191
	(ii) Barren clasts	194
6.5.3	Interpretation of the Lithoclast Debris Source	195
6.5.4	Temporal Changes in Sediment Gravity Flow Composition	196
	(i) Evidence of stratigraphic unroofing	196

(ii)	Influx of siliciclastic sand	198
6.6	Interpretive Reconstruction of the Depositional Setting	199
6.7	Cape Cormorant Formation Lithofacies	203
6.7.1	Megaconglomerate - Ribbon Limestone Lithofacies	203
(i)	Description	203
(ii)	Interpretation	206
6.7.2	Calcarenite - Conglomerate Lithofacies	207
(i)	Description	207
(ii)	Interpretation	207
6.7.3	Green Shale - Calcarenite Lithofacies	208
(i)	Description	208
(ii)	Interpretation	209
6.8	Paleocurrent and Paleoslope Data	210
6.8.1	Megaconglomerate - Ribbon Limestone Lithofacies	210
6.8.2	Calcarenite - Conglomerate Lithofacies	212
6.8.3	Green Shale - Calcarenite Lithofacies	213
6.9	Basin Configuration and Development	213
6.9.1	Location, Orientation and Morphology of the Faulted Margin	214
6.9.2	Basin Geometry and Dimensions	214
6.9.3	Basin Evolution	215
(i)	Phase 1	215
(ii)	Phase 2 ..	215
(iii)	Phase 3	218
(iv)	Phase 4	219
(v)	Phase 5	220
CHAPTER 7 SEDIMENTOLOGY OF THE BLACK COVE FORMATION		222
7.1	General Characteristics and Stratigraphic Relationships	222
7.2	Composition	222
7.3	Depositional Layering	229
7.3.1	Description	229
7.3.2	Interpretation	229
(i)	Hemipelagic muds	231
(ii)	Turbiditic muds	232
7.4	Other Sedimentary Structures	234
7.5	Reconstruction of the Depositional Environment	234
7.6	Relationship Between Anoxia and Starved Sedimentation	237
CHAPTER 8 SEDIMENTOLOGY OF THE AMERICAN TICKLE FORMATION AND THE MAINLAND SANDSTONE (GOOSE TICKLE GROUP)		240
8.1	General Characteristics and Stratigraphic Relationships	240
8.2	Lithofacies	243
8.2.1	Lithofacies 1 (Shale-dominated)	243
8.2.2	Lithofacies 2 (Siltstone- and Shale-dominated)	250
8.2.3	Lithofacies 3 (Siltstone-dominated)	250
8.2.4	Lithofacies 4 (Sandstone-dominated)	253
8.2.5	Correspondence to Submarine Fan Facies	253
8.2.6	Vertical Sequences	256
8.2.7	Lateral Distribution	256
8.3	Regional Paleocurrents	257
8.4	Sandstone Composition and Provenance	257
8.5	Fossils and Biogenic Structures	260
8.6	Reconstruction of the Depositional Environment	260
8.7	Discussion	261
CHAPTER 9 SEDIMENTOLOGY OF THE DANIEL'S HARBOUR MEMBER (GOOSE TICKLE GROUP)		263
9.1	General Characteristics and Stratigraphic Relationships	263
9.2	Limestone Conglomerate	263
9.2.1	Description	263
9.2.2	Interpretation	278

9.3	Lithoclast Calcarenite and Calcirudite	280
9.3.1	Description	280
9.3.2	Interpretation	285
9.4	Provenance of Lithoclasts	286
9.4.1	Composition and Age of Clasts	286
(i)	Grey-brown fossiliferous and/or peloidal limestone ..	286
(ii)	Interbedded limestone and shale	292
(iii)	Mottled <u>Stromatactis</u> limestone	292
(iv)	White fenestral limestone	293
(v)	Dolostone	294
(vi)	Chert	294
(vii)	Siliciclastic sediment	295
(viii)	Resedimented carbonates	296
9.4.2	Primary Origin of Lithoclast Debris	297
9.4.3	Multi-generation Origin of Daniel's Harbour Member Beds	300
9.5	Geographic and Stratigraphic Distribution of the Daniel's Harbour Mbr.	300
9.6	Dimensions of Individual Beds	301
9.7	Depositional Model	302

PART II: SEDIMENTATION AND TECTONICS

CHAPTER 10	REGIONAL FORELAND BASIN EVOLUTION: INTRODUCTION	307
CHAPTER 11	PHASE 1: FAULTING AND UPLIFT: THE ST. GEORGE UNCONFORMITY	313
11.1	Deformation Beneath the Unconformity	314
11.2	Structurally Controlled Karst	317
11.3	Stratigraphic Relief on the St. George Unconformity	318
11.4	Discontinuous Distribution of the Upper Aquathuna	322
11.5	Synthesis	322
11.6	Tectonic Significance	323
CHAPTER 12	PHASE 2: DEPOSITION ON A TECTONICALLY UNSTABLE PLATFORM	328
12.1	Synsedimentary Deformation Structures and Deposits	328
12.1.1	Intraformational Unconformities	330
12.1.2	Gravitational Slides	332
12.1.3	Pebbly Limestone Conglomerate	342
12.1.4	Fractured Limestone and Flaggy Limestone Conglomerate	344
12.2	Depositional Anomalies	348
12.2.1	Variation in Formation Thickness	349
12.2.2	Variations in Lithofacies Assemblages	352
(i)	Regional variations in thickness and lithofacies of the BPU	352
(ii)	Abrupt lateral and vertical changes in BPU lithofacies	357
(iii)	Anomalous peritidal sequences	361
12.3	Synthesis	362
12.4	Tectonic Significance	367
CHAPTER 13	PHASE 3: PLATFORM COLLAPSE	371
13.1	Deposition of the Table Cove Formation	374
13.2	Deposition of the Black Cove Formation	383
13.3	Deposition of the Cape Cormorant Formation	390
13.4	Reconstruction and Discussion	392
CHAPTER 14	PHASE 4: DEPOSITION OF SILICICLASTIC SEDIMENTS	395
14.1	Starved, Anoxic Basin Sedimentation	395
14.1.1	Origin and Significance of Anoxic Bottom Waters	398
14.2	Siliciclastic Turbidite Sedimentation	401
14.3	Mechanism of Basin Filling	404

CHAPTER 15	PHASE 5: INTRABASINAL FAULTING	411
15.1	Location of Escarpments	411
15.1.1	Port au Port Area	415
15.1.2	Gros Morne Area	418
15.1.3	Table Point Area	421
15.1.4	Hare Bay - Pistolet Bay Area	425
15.2	Cause and Style of Intrabasinal Faulting	429
CHAPTER 16	PHASE 6: EMPLACEMENT OF TACONIC ALLOCHTHONS	432
16.1	Regional Extent	432
16.2	Nature of the Autochthon - Allochthon Contact	434
16.3	Platform Carbonate Blocks in the Allochthons	435
16.4	Model for Allochthon Emplacement in the Foreland Basin	438
CHAPTER 17	MODEL FOR FORELAND BASIN DEVELOPMENT IN WESTERN NEWFOUNDLAND	441
17.1	Architecture and Mechanics of Convergent Margins	441
17.2	Models for Lithosphere Flexure	444
17.3	Pre-convergence Configuration of the Continental Margin	446
17.4	Ocean Closing and Initial Subduction of the Continent	451
17.5	Evolution of the Foreland Basin on the Platform	454
17.5.1	Phase 1: Faulting and Uplift	454
17.5.2	Phase 2: Sedimentation on an Unstable Platform	457
17.5.3	Phase 3: Platform Collapse	458
17.5.4	Phase 4: Deposition of Siliciclastic Sediments	462
17.5.5	Phase 5: Intrabasinal Faulting	462
17.5.6	Phase 6: Emplacement of the Accretionary Prism	465
17.6	Discussion	466
17.7	Modern Analogue	468
CHAPTER 18	CONCLUSIONS	477
REFERENCES	480
APPENDIX A	KEY TO SYMBOLS	516
APPENDIX B	BRYOZOAN MOUNDS: TABLE POINT FORMATION	518
B.1	Description	518
B.2	Interpretation	520
B.3	Discussion	521
APPENDIX C	SYNSEDIMENTARY DEFORMATION: TABLE COVE FORMATION	523
C.1	Introduction	523
C.2	Types of Synsedimentary Deformation	524
C.3	General Attributes of Slides in the Table Cove	524
C.4	Lithofacies Control on Deformation	530
C.5	Discussion	540
APPENDIX D	ORIGIN OF BEDDING IN PARTED AND RIBBON LIMESTONE: TABLE COVE FORMATION	541
D.1	Primary Compositional Layering	541
D.2	Early Lithification	544
D.3	Diagenetic Stratification	546
D.4	Pressure Dissolution	549
APPENDIX E	TRACE FOSSILS IN THE CAPE CORMORANT FORMATION	551
E.1	? <u>Planolites</u>	551
E.2	<u>Syncoprulus</u> (= <u>Alcyonidiopsis</u>)	552
E.3	<u>Gordia marina</u> ?	552
E.4	<u>Chondrites</u> spp.	553
E.5	<u>Diplichnites</u>	553
E.6	? <u>Diplocraterion</u>	554

E.7 <u>Ichnogenus incertae</u> type A	555
E.8 <u>Ichnogenus incertae</u> type B	556
APPENDIX F LITHOLOGIC DESCRIPTIONS AND CONODONT FAUNAS OF CARBONATE LITHOCLASTS FROM THE CAPE CORMORANT FORMATION	557
APPENDIX G LITHOLOGIC DESCRIPTIONS AND CONODONT FAUNAS OF CARBONATE LITHOCLASTS AND WHOLE ROCK SAMPLES FROM THE DANIEL'S HARBOUR MEMBER	568
APPENDIX H LOCATIONS OF MEASURED SECTIONS	575
MEASURED SECTIONS	(back pocket)

LIST OF FIGURES

Figure	Page
1.1 Lithostratigraphic framework for the Table Head and Goose Tickle groups	2
1.2 Simplified geologic map of the western Newfoundland Humber Zone showing section locations	5
1.3 Stratigraphic section of the Early Paleozoic autochthonous sedimentary sequence and allochthonous rocks in the Humber Arm Allochthon in western Newfoundland	7
3.1 Aguathuna Formation; field photos	21
3.2 Stratigraphy of the Aguathuna Formation	27
3.3 St. George Unconformity	31
3.4 Reconstruction of depositional environments recorded by Aguathuna Formation lithofacies	33
3.5 Depositional megacycles of the Lower Ordovician St. George Group	37
4.1 Generalized, diagrammatic distribution of Table Point Formation lithofacies	39
4.2 Basal Peritidal Unit lithofacies; photos	51
4.3 Shallowing-upward and deepening-upward sequences in the SPU .	55
4.4 Middle Subtidal Unit lithofacies; photos	57
4.5 Upper Subtidal Unit lithofacies; photos	65
4.6 Schematic section of the <u>Stromatactis</u> mud mound at Piccadilly	68
4.7 Schematic reconstruction of depositional environments recorded by Table Point Formation	72
4.8 Sea level curves for the late Early to Middle Ordovician in North America	74
5.1 Table Cove Formation sequences at Table Cove (a) and Black Cove (b)	79
5.2 Schematic summary of Table Cove Formation lithofacies	80
5.3 Burrowed limestone lithofacies (Table Cove Formation); field photos and photomicrographs	91
5.4 Regional variations in the burrowed limestone lithofacies; field photos and photomicrographs	100
5.5 Parted limestone lithofacies (Table Cove Formation); field photos and photomicrographs	103
5.6 Trace fossils in the parted limestone lithofacies	108

5.7	Ribbon limestone lithofacies (Type A) (Table Cove Formation); field photos and photomicrographs	116
5.8	Shelly fossils in Table Cove Formation ribbon limestones ..	119
5.9	Ribbon limestone lithofacies (Type B) (Table Cove Formation); field photos and photomicrographs	125
5.10	Table Cove Fm. at Table Cove: paleoslope data (back pocket)	
5.11	Interpretive reconstruction of depositional environments for the Table Cove Formation	131
6.1	Measured sections of the Cape Cormorant Formation	140
6.2	Geologic map of the west side of the Port au Port Peninsula	144
6.3	Stratigraphic relationships	146
6.4	Shale and ribbon limestone; outcrop photos and photomicrographs	154
6.5	Body fossils in Cape Cormorant Formation shale	157
6.6	Schematic summary of ribbon limestone components	160
6.7	Lithoclastic megaconglomerate and conglomerate; field photos and photomicrographs	164
6.8	Measured sections showing lateral changes in debris flow conglomerate thickness and texture	165
6.9	Types of lithoclast conglomerates; sketches	167
6.10	Polymictic, lithoclastic calcirudites, calcarenites and calcisiltites; slab and outcrop photos	171
6.11	Polymictic lithoclastic calcirudites, calcarenites and calcisiltites; photomicrographs	173
6.12	Trace fossils in the Cape Cormorant Formation	182
6.13	Composition of debris flow conglomerates at Caribou Brook ..	185
6.14	Lithoclasts; polished slabs and photomicrographs	187 & 189
6.15	Cambro-Ordovician platformal succession on Port au Port Peninsula	192
6.16	Ages of carbonate lithoclasts processed for conodonts	193
6.17	Schematic reconstruction of the depositional environment for the Cape Cormorant Formation	201
6.18	Paleocurrent and paleoslope data from the Cape Cormorant Fm. and the Mainland Sandstone at Caribou Brook	211
6.19	Paleogeographic reconstruction and evolution of the Cape Cormorant basin	217
7.1	Representative schematic sections of the Black Cove Formation	223

7.2	Black Cove Formation; field photos and photomicrographs ...	225
7.3	Stratigraphic distribution of hemipelagic and turbiditic muds in the Black Cove Formation	230
7.4	Idealized sequence of structures in a fine-grained turbidite	233
7.5	Reconstruction of the basinal environment envisaged for the Black Cove Formation	235
8.1	Schematic, composite sections of the American Tickle Formation and the Mainland Sandstone	241
8.2	Schematic depictions of flysch lithofacies	244
8.3	Siliciclastic flysch lithofacies; field photos and photomicrographs	252
8.4	Submarine fan model and depositional sequence	255
9.1	Measured sections of the American Tickle Formation showing the distribution of Daniel's Harbour Member beds	264
9.2	Schematic sections of clast-supported and matrix-supported conglomerates characteristic of Daniel's Harbour Member beds	265
9.3	Daniel's Harbour Member conglomerates; outcrop and slab photos and photomicrographs	267 & 269
9.4	Map of Daniel's Harbour Member conglomerates at Daniel's Harbour	271
9.5	Clast size distribution in clast-supported conglomerates ..	275
9.6	Clast fabric in Daniel's Harbour Member conglomerates	276
9.7	Daniel's Harbour Member calcarenites; outcrop photos and photomicrographs	282
9.8	Model for the origin of Daniel' Harbour Member resedimented carbonates	304
10.1	Phases of foreland basin evolution in the upper St. George, Table Head and Goose Tickle groups	308
10.2	Measured sections through the Table Head Group and overlying Goose Tickle Group from Port au Port Peninsula to Pistolet Bay	311
11.1	Sub-unconformity deformation of platform carbonates and structurally controlled karst	316
11.2	Stratigraphic relief on the St. George Unconformity; cross-section of measured sections	320
11.3	Schematic vertical cross-section across the platform (a) prior to, (b) during, and (c) after formation of the St. George Unconformity	324

11.4	Stratigraphic sections showing correlations of lithologic units and synsedimentary deformation events between the Aguathuna Formation and coeval deep water sediments of the Cow Head Group	327
12.1	Intraformational erosion surface in the BPU	331
12.2	Gravitational slides in the Table Point Formation at Table Point	334
12.3	Schematic sections in the Middle Subtidal Unit (MSU) at Gargamelle Cove and Table Point showing correlations between gravitational slides	336
12.4	Synsedimentary deformation features in the Table Point Formation; outcrop and slab photos	338
12.5	Location and orientation of synsedimentary fractures in the Table Point Formation	340
12.6	Schematic cross-section through the top of the Table Point in the Pistolet Bay area showing relationships between USU limestones, cross-cutting fractures, conglomerate veneer and their relationships to mineral phases of the hardground at the top of formation	345
12.7	Cross-section of measured sections of the Table Point Formation	351
12.8	Cross-section of measured sections through the BPU	354
12.9	Cross-section of measured sections through the BPU in cores at the DHZM	358
12.10	Maps showing drill core locations for Figure 12.9 and paleogeographic reconstructions for BPU sediments at the DHZM	360
12.11	Schematic vertical cross-section across the platform during deposition of the Table Point Formation	365
12.12	Relative sea level and subsidence curves for the Table Point Formation	369
13.1	Type examples of collapsed platform sequences	372
13.2	Aerial distribution of post-platform, deep-water formations	373
13.3	Collapsed platform sequences in the Table Point area	377
13.4	Map of the Table Point area showing the locations of measured sections in Figure 13.3	378
13.5	Schematic reconstruction of platform collapse in the Table Point area	381
13.6	Cross-section of post-platform sequences in the Pistolet Bay area	387
13.7	Models for platform collapse and generation of the drowning unconformity in the Pistolet Bay area	389

13.8	Schematic vertical cross-section across the western Newfoundland platform during the collapse stage (Phase 3) of foreland basin development	393
14.1	Cross-section of measured sections through the Goose Tickle Group	397
14.2	Models for the Oxygen Minimum Zone in the foreland basin ..	399
14.3	Map distribution of deep-water, siliciclastic turbidite lithofacies and paleocurrents	402
14.4	Model for turbidite dispersal in the foreland basin	408
14.5	Map distribution of American Tickle Formation lithofacies and paleocurrents in the Hare Bay - Pistolet Bay area	410
15.1	Regional distribution and transport directions for Daniel's Harbour Member beds	412
15.2	Daniel's Harbour Member beds in the Port au Port area	417
15.3	Daniel's Harbour Member beds in the Gros Morne area	420
15.4	Daniel's Harbour Member beds in the Table Point area	423
15.5	Daniel's Harbour Member beds in the Hare Bay - Pistolet Bay area	427
16.1	Map of western Newfoundland showing the distribution of Taconic allochthons and blocks or slivers of autochthonous carbonates in the Humber Arm Allochthon	433
16.2	Contact relationships between the Humber Arm Allochthon and the autochthon in the Fort au Port area	437
16.3	Tectono-sedimentary model for emplacement of Taconic allochthons in the foreland basin	440
17.1	Schematic vertical cross-section through a continent - ocean subduction zone	442
17.2	Summary diagram of the early Paleozoic stratigraphy in western Newfoundland and its relationship to radiometrically dated igneous/tectonic events in western and central Newfoundland	448
17.3	Interpretive reconstruction of the western Newfoundland margin at the end of its passive margin stage of development	450
17.4	Interpretive cross-section across the margin during initial closing of Iapetus Ocean	453
17.5	Tectonic model for foreland basin development on the platform in western Newfoundland (a, b)	456
	(c, d)	460
	(e, f)	464
17.6	Location map of the Australia-Banda Arc collision zone	469
17.7	Bathymetric profile from the Australian shelf to Timor	469

17.8	Tectonic models for the Australia - Banda Arc collision zone	471
B.1	Schematic measured section through bryozoan mounds and enclosing strata in the BPU at Shag Cliff in Bonne Bay	519
C.1	Deformation structures in gravity slides; Table Cove Formation at Table Cove	528 & 529
C.2	Slides in upper slope and middle slope limestones	535
C.3	Helicopter view of slides in the ribbon limestone lithofacies at Table Cove	537
C.4	Helicopter view of thin slide masses in the upper 30 m of the ribbon limestone lithofacies at Table Cove	539
D.1	Origin of bedding in parted and ribbon limestone	542
D.2	Stratigraphic distribution of synsedimentary deformation features and neomorphic crystal fabrics of parted and ribbon limestones in the Table Cove Formation	545
D.3	Diagenetic zones, geochemical properties and processes below the sediment-water interface	548

LIST OF TABLES

Table	Page
1.1 Evolution of Stratigraphic Nomenclature	9
3.1 Aguathuna Formation Lithofacies	18
4.1 Table Point Formation Lithofacies	41
4.2 Storm Lenses in the Burrowed, Fossiliferous Wackestone Lithofacies (MSU)	60
5.1 Table Cove Formation Lithofacies	82
6.1 Cape Cormorant Formation Lithologies	148
6.2 Body fossils in the Cape Cormorant Formation	155
6.3 Cape Cormorant Formation Lithofacies	204
7.1 Characteristics of the Black Cove Formation	227
8.1 American Tickle Formation and Mainland Sandstone Lithofacies	246
8.2 Detrital Components of American Tickle Formation and Mainland Sandstone Sandstones	259
9.1 Characteristics of Daniel's Harbour Member Conglomerates ...	273
9.2 Composition of Daniel's Harbour Member Conglomerates; point count data	277
9.3 Siliciclastic Components of Daniel's Harbour Member Calciturbidites	284
9.4 Clast Components of Daniel's Harbour Member Conglomerates ..	288
12.1 Deformation Features in the Table Point	329
17.1 Predictions of Flexural Models	445
C.1 Synsedimentary Deformation Structures; Table Cove Fm.	525
C.2 Gravitational Slides; Table Cove Formation	532
F.1 Lithoclasts Processed For Conodonts (Cape Cormorant Formation Lithoclasts)	559
F.2 Conodont Faunal Lists (Cape Cormorant Formation)	565
G.1 Lithologies and Conodont Faunas of Daniel's Harbour Member Clasts and Whole Rock Samples	569

CHAPTER 1
INTRODUCTION

1.1 Introductory Remarks

This is a stratigraphic and sedimentologic study of the Middle Ordovician Table Head Group and overlying Goose Tickle Group in the western Newfoundland segment of the Appalachian Orogen (Figure 1.1). The Table Head is a heterogeneous package of carbonates deposited above a regional, subaerial unconformity (St. George Unconformity). It comprises a muddy, fossiliferous, platformal limestone (Table Point Formation) overlain by one of three markedly different deep-water facies, 1) thin bedded muddy limestone and shale (Table Cove Formation), 2) interbedded polymictic, carbonate lithoclast conglomerate, calcarenite and shale (Cape Cormorant Formation), or (3) a thin black shale (Black Cove Formation). The bulk of the Goose Tickle is deep-water siliciclastic turbidites (American Tickle Formation and Mainland Sandstone) punctuated by limestone conglomerate and calcarenite (Daniel's Harbour Member). This deepening-upward, carbonate-to-clastic sequence accumulated along the margin of the North American continent during closure of the Proto-Atlantic (Iapetus) Ocean and attempted subduction of the continent beneath a volcanic island arc. It records the cataclysmic destruction of a long-lived, passive margin carbonate platform and formation of a foreland basin during initial stages of the Taconian Orogeny.

Similar convergent margin sedimentation has been described to the south along strike in the Taconian foreland of the U. S. A. Appalachians (Read, 1980; Shanmugam and Lash, 1982; Shanmugam and Walker, 1983; Bradley and Kusky, 1986; Houseknecht, 1986), and to the north in the Caledonian Orogen of east Greenland (Hurst and Surlyk, 1983, 1984), and in other ancient orogens of different ages (eg. Alpine-Mediterranean Orogen, Bernoulli and Jenkyns, 1974; Wompay Orogen, Hoffman and Bowring,

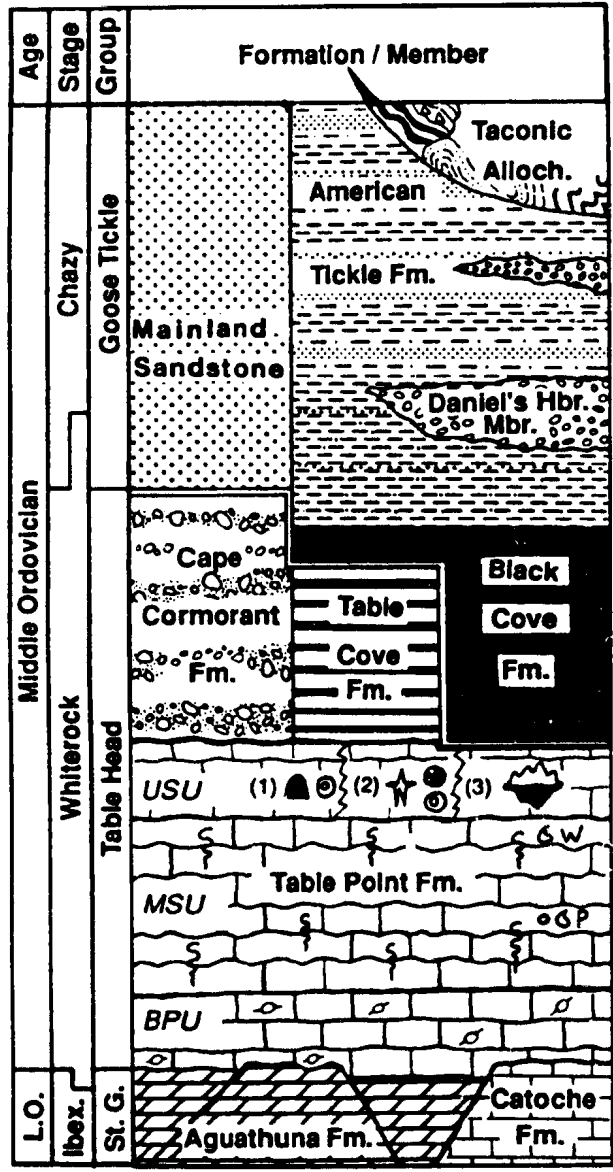


Figure 1.1 Lithostratigraphic framework for the Table Head and Goose Tickle groups (from Stenzel et al., 1990).

1984; Oman Mountains, Robertson, 1987a, b; New Guinea Orogen, Pigram et al., 1989). Most such studies have been regional in scope. The purpose of this study is to document, in detail, the nature of carbonate sedimentation during tectonism and, on the basis of these findings, interpret the incremental demise of the continental margin and birth of the foreland basin in Newfoundland.

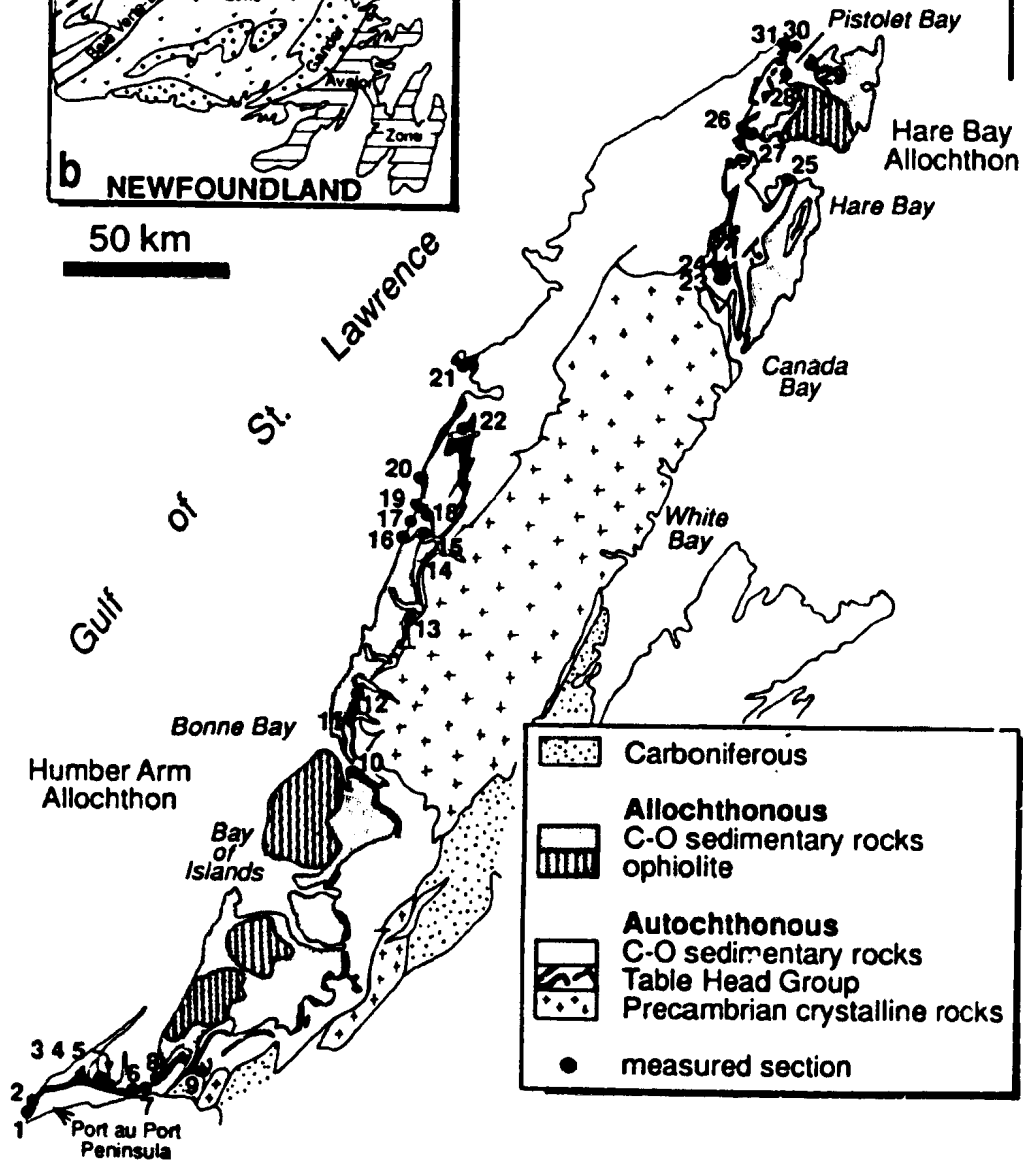
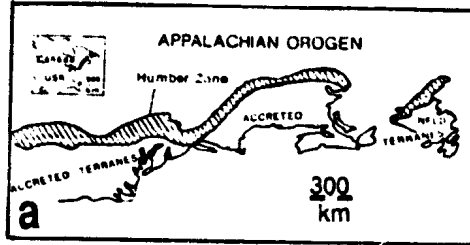
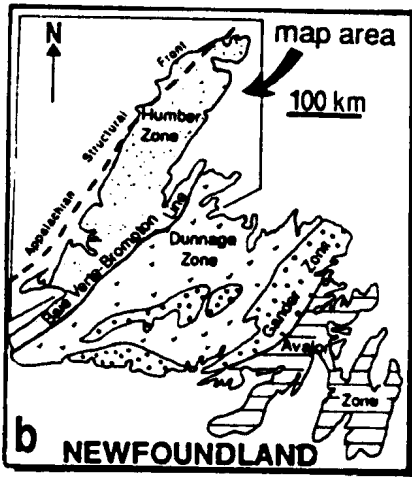
1.2 Geologic Setting

Newfoundland is a part of the Appalachian-Caledonian Orogen that extends along the eastern margin of North America, and from the British Isles through east Greenland, through Scandinavia and beyond to Spitzbergen (Williams and Stevens, 1974; Williams, 1978a, b; Figure 1.2, inset a). In North America the orogen is made up of five lithologically distinctive tectonostratigraphic zones, four of which comprise the geology of Newfoundland (Figure 1.2, inset b). The Table Head - Goose Tickle sequence occurs in the westernmost Humber Zone, which is the Early Paleozoic continental margin (Williams and Stevens, 1974; Williams, 1978a, b). The Humber Zone is bounded on the west by the Acadian Structural Front (Williams, 1979) which separates deformed rocks of the orogen from undeformed rocks of the craton, and on the east by the Baie Verte-Brompton Line, a fault zone marked by ophiolite and ophiolitic mélange (Williams and St-Julien, 1982).

The Dunnage, Gander and Avalon Zones which lie progressively further east are suspect terranes of uncertain paleogeographic origin, each accreted to North America during the Paleozoic (Williams and Hatcher, 1983). The Dunnage Zone, comprised of island arc volcanics and sediments, represents the vestiges of the Proto-Atlantic Ocean accreted to the Humber Zone during Middle Ordovician Taconian orogenesis.

The major geologic elements of the Humber Zone are Precambrian basement, an autochthonous sequence of early Paleozoic sedimentary rocks, and Taconic allochthons (Figure 1.2). Precambrian basement rocks

Figure 1.2 Simplified geologic map of the western Newfoundland Humber Zone showing section locations. Locations: 1, Big Cove; 2, Caribou Brook; 3, West Bay Center; 4, Piccadilly Park Roadcut; 5, Piccadilly roadcut; 6, Aguathuna Quarry; 7, Northwest Gravels; 8, Black Cove; 9, Cold Brook Quarry; 10, Shag Cliff; 11, Bakers Brook; 12, Stag Brook; 13, West Brook; 14, Southwest Feeder; 15, Portland Creek Pond; 16, Eastern Head-Cliffy Point; 17 Daniel's Harbour; 18, Daniel's Harbour Zinc Mine; 19, Spudgel's Cove; 20, Table Point; 21, Gargamelle Cove; 22, River of Ponds Lake; 23, Beaver Brook; 24, Roddickton Quarry; 25, Springs Inlet; 26, Hwy. 430 roadcuts; 27, Northern Arm; 28, Pistolet Bay (west coast); 29, Burnt Island peninsula; 30, Bakeapple Island; 31, Callieux Bay (Vaches Point). Inset maps: a) Appalachian Orogen in North America; b) Tectonostratigraphic zones in Newfoundland (modified from Williams (1978a, b, 1979), Williams and Hatcher (1983), and Williams et al. (1988).



are mostly granitic gneisses and minor anorthosites (Bostock, 1983; Williams, 1985). They are structural inliers of the Grenville Structural Province of the Canadian Shield.

The autochthonous sedimentary sequence unconformably overlies crystalline basement and is represented by ~1-2 km of latest Precambrian to Middle Ordovician clastics and carbonates (Figure 1.3). Most of these sediments were deposited along a paleosouth-facing shelf during the rifting and passive, drifting stages of the continental margin. The Table Head - Goose Tickle sequence deposited on the convergent margin caps the autochthonous succession. Younger Ordovician Long Point Group carbonates are the basal unit of a neoautochthonous, Ordovician to Siluro-Devonian age overlap sequence deposited on the Taconian foreland (Williams and Hatcher, 1983).

The Humber Arm and Hare Bay Allochthons, emplaced during Middle Ordovician Taconian orogenesis, structurally overlie the autochthonous sequence. They consist of imbricated thrust slices of Early Paleozoic sedimentary rocks of the continental slope and rise, i.e. deep-water equivalents of the autochthonous strata, plus slices of volcanic islands, oceanic crust, and mantle (Stevens, 1970; Williams and Stevens, 1974; Williams, 1975; Figure 1.3).

Structure of the Humber Zone is the product of three orogenic phases. Middle Ordovician Taconian orogenesis is manifest by structural emplacement of the Humber Arm and Hare Bay allochthons (Williams and Stevens, 1974). Siluro-Devonian Acadian orogenesis is in the form of large scale folding and thrusting and uplift of Precambrian basement (Cawood and Williams, 1988; Grenier, 1990). Early Carboniferous Alleghanian deformation is manifest by strike-slip faulting and minor thrusting (Williams *et al.*, 1982).

Carboniferous sediments that discontinuously cover Precambrian basement and early Paleozoic rocks (Figure 1.2) are relics of successor basins that formed on the Taconian and Acadian forelands (Knight, 1983).

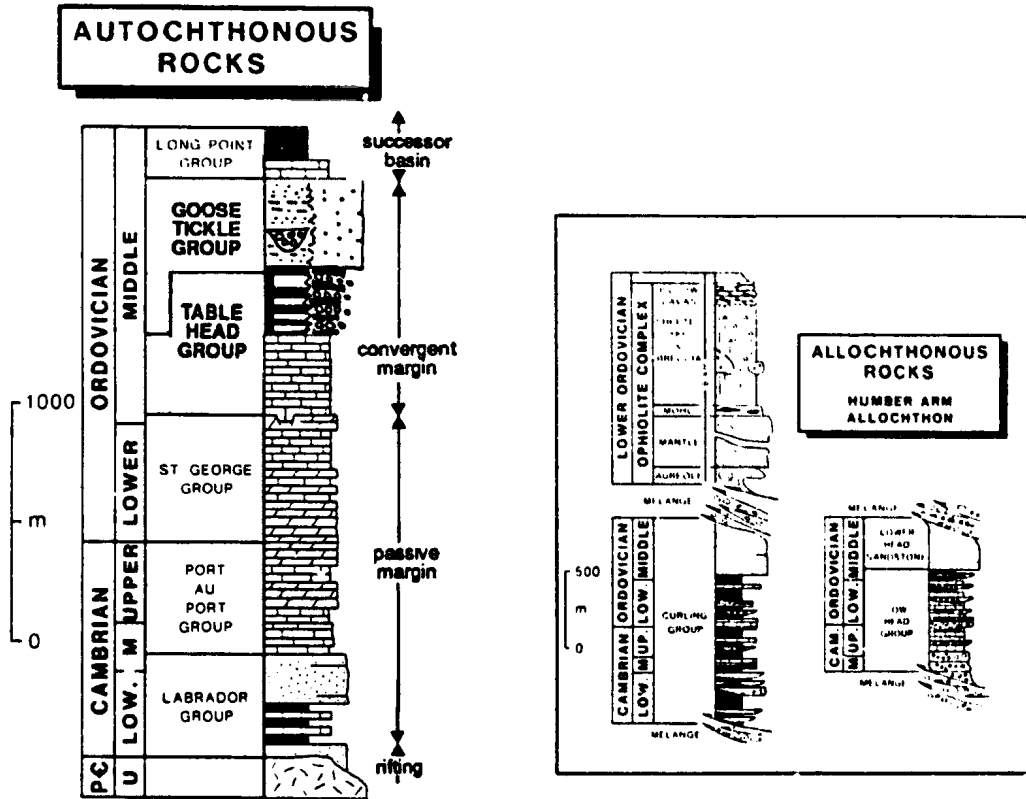


Figure 1.3 Stratigraphic section of the Early Paleozoic autochthonous sedimentary sequence and allochthonous rocks in the Humber Arm Allochthon in western Newfoundland (modified from James and Stevens (1986)).

1.3 Summary of Previous Work

1.3.1 Stratigraphy

Previous studies of what are now the Table Head and Goose Tickle groups have largely concerned stratigraphy. The evolution of lithostratigraphic hierarchy and nomenclature are summarized in Table 1.1.

James Richardson (in Logan, 1863) was first to establish an informal alphabetized stratigraphy for the Early Paleozoic strata exposed on the west coast of Newfoundland. Schuchert and Dunbar (1934) recognized Richardson's Divisions L, M and N as a natural grouping of strata disconformably overlying the St. George series, which they named the Table Point series and defined informal lower (limestone), middle (limestone and shale), and upper (shale) lithologic subdivisions. They correlated sandstones above the Table Point series with sandstones at Long Point on the Port au Port Peninsula and sandstones underlying limestone conglomerate at Lower Head and named them the Long Point series. All limestone conglomerates exposed in the west coast were included in the Cow Head Breccia, which they interpreted to overlie the Long Point series.

Whittington and Kindle (1963) redescribed the sequence at Table Point and renamed it the Table Head Formation. They retained Schuchert and Dunbar's informal divisions and provided detailed accounts of the faunal aspects of each. Overlying sandstones were correlated with other sandstones overlying the Cow Head Group and informally called the "unnamed green sandstones".

Schillereff and Williams (1979) mapped limestone conglomerate and shale sequences above the Table Point Formation and below sandstones and interbedded sandstone and shale in the Port au Port Peninsula area, which they informally named the Caribou Brook formation, and the Mainland Sandstone and Black Cove formation, respectively.

Klappa *et al.* (1980) raised the Table Head Formation to group status and expanded its definition to include the Caribou Brook formation. The lower, middle and upper Table Head were renamed the Table Point, Table

Table 1.1 Evolution of Stratigraphic Nomenclature

Richardson in Logan (1863)	
Point Riche Ls. at Table Head and Point Riche	Division Q
	P (limestone conglomerate)
	O
	$\frac{3}{2}$ N
	1
	$\frac{2}{1}$ M
	L
	K
	D-I

Schuchert and Dunbar (1934)		
MIDDLE ORDOVICIAN	Humber Arm Series	
	Cow Head Breccia	
	Long Point Series	
	Table Head Series	upper
		middle
	lower	
^L ORDOV.	St. George Series <small>Green Pt. Series</small>	

Whittington and Kindle (1963)		
MIDDLE ORDOVICIAN	Unnamed Green Sandstones	
		Upper
		Middle
	Lower	
^L ORDOV.	St. George Group	

Schillereff and Williams (1979)		
MIDDLE ORDOVICIAN	Black Cove Fm.	Mainland Sandstone
	Caribou Brook fm.	
	Table Head Formation	
^L ORDOV.	St. George Group	

Klappa et al. (1980)		
MIDDLE ORDOVICIAN	Unnamed Green Sandstone	Mainland Sandstone
	Table Head Group	Cape Cormorant Fm.
		Black Cove Fm.
		Table Cove Formation
		Table Point Formation
^L ORDOV.	St. George Group	

Cove and Black Cove Formations respectively, and the overlying breccias named the Cape Cormorant Formation.

Stenzel *et al.* (1990; Figure 1.1) redefined the Table Head Group to include only the Table Point and Table Cove formations and the conglomeratic Cape Cormorant Formation sequence that directly overlies the Table Point on Port au Port Peninsula. The Black Cove Formation was included at the base of the overlying clastic sequence, provisionally named the Goose Tickle Group (L. A. Quinn, pers. comm., 1988). Other carbonate conglomerates previously included in the Cape Cormorant, but proven to be interbedded locally with the overlying flysch, were named the Daniel's Harbour Member.

1.3.2 Paleontology and Biostratigraphy

Detailed accounts of the Table Head faunas have been presented by numerous workers. Important contributions have been made on the brachiopods (Cooper, 1956; Pickerill *et al.*, 1984b), trilobites (Raymond, 1925; Whittington and Kindle, 1963; Whittington, 1965), cephalopods (Flower, 1978), graptolites (Reudemann, 1947; Morris and Kay, 1966; Erdtmann, 1971; Finney and Skevington, 1979), conodonts (Fähræus, 1970; Stouge, 1984), sponges (Klappa and James, 1980; Paquette *et al.*, 1983), and the microfossil *Konyrium* (Bergström, 1979).

Stouge's (1984) study of conodonts in the Table Head Group documented a change in provincialism between the faunas of the Table Point and Table Cove formations. Genera and species in the Table Point are allied to a North American Midcontinent fauna, while those in the Table Cove are common to a North Atlantic fauna.

Studies of the graptolites by Morris and Kay (1966), Erdtmann (1971) and Finney and Skevington (1979) documented a change in provincialism between faunas of the Table Cove and Black Cove formations and the American Tickle Formation. Graptolites in the two lower units have strong Pacific affinities with species common to Australia, while those in the flysch are allied to a North Atlantic fauna.

Collectively, studies of the trilobites (Whittington and Kindle, 1963; Whittington, 1965), brachiopods (Ross and James, 1987), conodonts (Fåhraeus, 1970; Stouge, 1984), and graptolites (Morris and Kay, 1966; Erdtmann, 1971; Finney and Skevington, 1979) conclude that the Table Head is upper Whiterockian (early to middle Llanvirnian) in age, and the overlying Goose Tickle is uppermost Whiterockian (middle Llanvirnian to Llandeilian) in age. Lucid discussions on correlations between these faunas and biostratigraphic faunal zones established for North America, Europe and Australia are presented in Ross and James (1987) and Williams *et al.* (1987).

1.3.3 Sedimentology

General attributes and distribution of Table Head and Goose Tickle strata have been documented in the context of geological mapping by numerous workers, but the strata have largely escaped detailed sedimentological analyses. Delong and Middleton (1978) briefly described the Cape Cormorant Formation at Cape Cormorant in an abstract and interpreted the carbonate conglomerates and calcarenites as debris flows and turbidites. Klappa *et al.* (1980) described major lithofacies of each formation in their Table Head Group at its type locality. They interpreted the Table Point as a platform limestone deposited in peritidal and shallow subtidal environments, the Table Cove as upper to lower slope limestones, the Black Cove as a basinal deposit, and the Cape Cormorant as debris flows and turbidites originating along fault scarps in the basin. Stouge (1981) included preliminary sedimentologic study of the Table Head Formation (*sensu* Whittington and Kindle, 1963) in the Table Point - Port-au-Choix area, which he interpreted as a shallow shelf, slope and basin sequence deposited during rapid subsidence and transgression on a gently-dipping platform.

Stevens (1970) was first to consider the Table Head and overlying conglomerates within the Middle Ordovician tectonic framework. He interpreted the conglomerates as being shed from fault scarps related to

collapse of the miogeosyncline, and interpreted the entire sequence as a series of westward-migrating bank edge (Table Point), basin slope or margin (Table Cove) and basin (Black Cove) facies deposited as the miogeosyncline rapidly subsided. James et al. (1979) modified Stevens' (1970) hypothesis, and interpreted the Table Head strata as strandline to deep basin sediments deposited on the platform as it began to subside as a result of horst and graben tectonics. Klappa et al. (1980) documented highly variable thickness and complex stratigraphic relationships among formations they included in the Table Head and proposed that the sequence recorded the transformation of a stable margin into a pericratonic foreland basin with a major west-dipping slope. Their tectonic model postulated horst and graben fragmentation of the platform prior to deposition of the Table Point, deposition of the Table Cove and Black Cove formations during initial collapse of the platform, and subsequent west-directed thrusting in the basin which uplifted the platform and gave rise to Cape Cormorant Formation conglomerates. A similar sequence of tectonically-controlled sedimentation events for the Table Head sequence was outlined by James et al. (1989). Knight (1986c) documented the sedimentology and stratigraphic relationships of the Table Head and Goose Tickle groups in the Pistolet Bay - Hare Bay area. He described and illustrated sections where the top of the Table Point Formation is fractured and directly overlain by the Black Cove Formation, and described both matrix-poor and matrix-rich limestone conglomerates and calcarenites interbedded with the flysch and included in the Cape Cormorant Formation (sensu Klappa et al., 1980). For the anomalous Table Point-Black Cove sequences Knight proposed very rapid subsidence and drowning of the Table Point platform. Conglomerates were attributed to a protracted history of faulting of the platform as it collapsed and uplift after burial by basinal shale.

1.4 Scope and Aims of This Study

This study is a detailed, regional analysis of carbonate rocks formed during tectonism of the Middle Ordovician continental margin (Figure 1.1). It is focused on the Table Head Group but includes study of the Black Cove Formation and Daniel's Harbour Member, both of which are intimately linked to the Table Head but are now included in the Goose Tickle Group. The bulk of the Goose Tickle Group is under study by L. A. Quinn.

Stratigraphic sections were studied in numerous coastal outcrops between Port au Port Peninsula and the tip of the Great Northern Peninsula, in several inland brooks, and in numerous drill cores from the Daniel's Harbour Zinc Mine (Figure 1.2; Appendix H). Carbonates immediately underlying the Table Point Formation, most commonly the Aguathuna Formation (St. George Group), and the St. George Unconformity were also examined, as were siliciclastic sandstones of the Goose Tickle Group overlying the Cape Cormorant Formation and enclosing the Daniel's Harbour Member. Detailed measured sections are included in the back pocket. The data base covers an area approximately 400 km along and 50 km across the ancient margin.

The specific objectives of this study are to:

- 1) Describe the regional distribution and sedimentology of the Table Head Group and the Black Cove Formation and the Daniel's Harbour Member of the Goose Tickle Group. Emphasis is placed on the deep-water Table Cove and Cape Cormorant formations and the Daniel's Harbour Member which heretofore have not been studied in detail.

- 2) Document and evaluate sedimentologic and stratigraphic expressions of synsedimentary tectonism in each lithostratigraphic unit and relate them to temporal changes in bathymetry and configuration of the platform during foreland basin development.

- 3) Relate the temporal tectono-sedimentary stages to morphotectonic regimes along collisional plate margins and construct a tectonic model

for foreland basin development.

1.5 Organization of Results

Results are presented in two parts. Part I - Sedimentology - presents solely sedimentologic descriptions and interpretations of each lithostratigraphic unit comprising the foreland basin succession, as well as the underlying Aquathuna Formation, and including sandstone units in the Goose Tickle Group. Part II - Sedimentation and Tectonics - presents, in a temporal framework, descriptions and interpretations of the sedimentologic and stratigraphic evidence for synsedimentary tectonism and proposes a model for foreland basin evolution.

PART I
SEDIMENTOLOGY

CHAPTER 2
INTRODUCTION TO SEDIMENTOLOGY

The eight major lithostratigraphic units of the upper St. George, Table Head, and Goose Tickle Groups include a wide range of initially carbonate then clastic rock types which record both aerial variation and temporal changes in depositional setting. The purpose of the following chapters (3-9) is to document the sedimentologic attributes, characterize the styles of sedimentation, and interpret the depositional environments of each of unit. Detailed analyses are presented for the Table Point, Table Cove, Cape Cormorant and Black Cove Formations and for the Daniel's Harbour Member of the American Tickle Formation. The Aguathuna Formation and the American Tickle Formation and Mainland Sandstone which bracket that sequence and are essential components of the foreland basin are treated in less detail. The Aguathuna has been the focus of other regional and detailed studies by several previous workers (Levesque, 1977; Pratt, 1979; Pratt and James, 1986; Knight and James, 1987; Lane, 1990). Detailed study of sandstone units in the Goose Tickle Group is currently underway by L. A. Quinn.

CHAPTER 3
SEDIMENTOLOGY OF THE AGUATHUNA FORMATION

3.1 General Character and Stratigraphic Relationships

The Aguathuna Formation at the top of the St. George Group is composed mostly (70-95%) of unfossiliferous, microcrystalline dolostone, subordinate fossil-poor, grey limestone, and minor dolomitic shale. These strata vary markedly in thickness across the study area, ranging from as little as 2 m to 130 m, and are locally missing from the Ordovician succession. Stratigraphic relationships with underlying and overlying formations are complex. In most places they conformably overlie muddy and fossiliferous or peloidal limestone, or dolostone of the Catoche Formation, but locally that contact is defined by the erosional St. George Unconformity. They are everywhere overlain by fossil-poor, peritidal carbonates, mostly limestone, of the Table Point Formation (Table Head Group) (Chapter 4). That contact is locally conformable, but more commonly is also defined by the St. George Unconformity.

3.2 Lithofacies

The Aguathuna is made up of six lithofacies that record deposition in extremely restricted, peritidal environments (Table 3.1). The reader is referred to theses of Levesque (1977), Pratt (1979) and Lane (1990) and to Pratt and James (1986) for more detailed descriptions and discussions of these sediments.

3.2.1 Dololaminite (Lithofacies 1 in Table 3.1)

Dololaminite is the most conspicuous and common component of the Aguathuna (Figure 3.1.a, b). Commonly associated with desiccation cracks (Figure 3.1.c) and tepee structures (Kendall and Warren, 1987), these sediments are interpreted to have been deposited on low energy, muddy, high intertidal to supratidal flats. Crinkly, cryptalgal dololaminite bears the signature of organic binding, indicating that

Table 3.1 Aguathuna Formation Lithofacies: outcrop appearance, depositional and diagenetic characteristics, and interpretation. Abbreviations: Colours - lt.=light, med.=medium, dk.=dark, gy.=grey, gn.=green, yl.=yellow, bn.=brown. Textures: M=mudstone, W=wackestone, P=packstone, G=grainstone, F=floatstone. cgl.=conglomerate, microcryst.=microcrystalline, med. cryst.=medium crystalline. Structures - cross lam.=cross-lamination, par.=parallel, discon.=discontinuous, lam.=lamination.

* - indicates the predominant lithology, sedimentary structure, development of burrowing, or fossils.

** - cauliflower-shaped nodular evaporites pseudomorphed by silica and coarse dolomite, the former commonly retaining a crystalline fabric of fine lathes of an original evaporite mineral.

Table 3.1 Aguathuna Formation Lithofacies

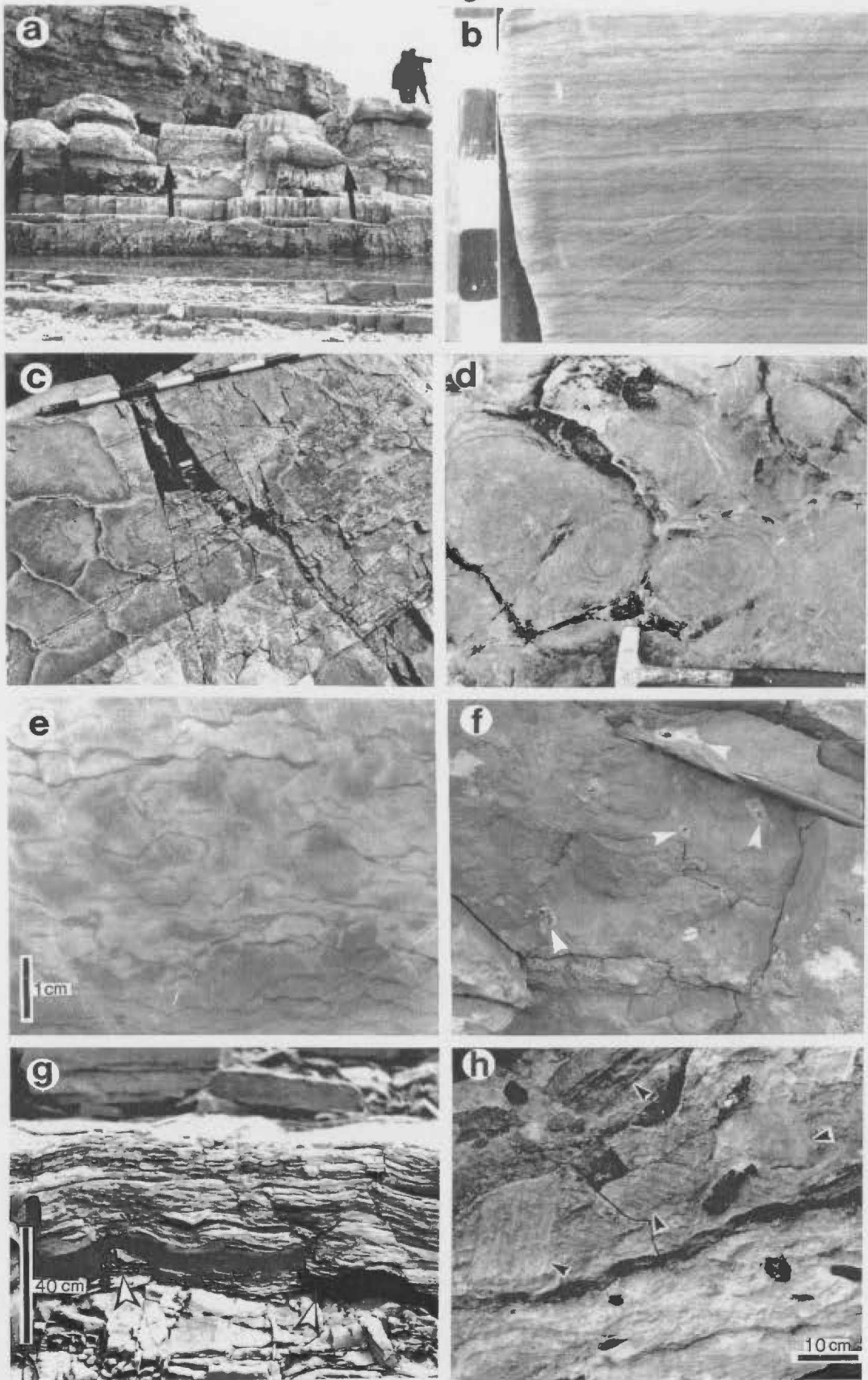
LITHOFACIES	COLOUR, BEDDING STYLE & THICKNESS	COMPOSITION	PRIMARY SEDIMENTARY STRUCTURES
(1) Dololaminite	lt. gn.-gy., dk. bn.-gy., yl.- & blocky-weathering, 10-100 cm beds	microcrystalline dolomite*, & dolomitic M & fine, peloidal G* with thin beds (1-10 cm) of dolostone intraclast cgl. & ripple-scale, cross-lam. peloidal G, small scours	crinkly, cryptalgal lamination* (a fraction of a mm to 1 mm thick); planar, hor. to low-angle lam.* (1-10 mm); desiccation cracks, tepee structures
(2) Stromatolite	gy.-bn., yl.-weathering, 30-100 cm beds that are laterally continuous a few metres to a few 10s of metres	same as for dololaminites	crinkly, cryptalgal lamination define LLH build-ups (<10-20 cm dia.); dolomitic shale drapes (1-10 cm thick) locally (see (5) below)
(3) Burrowed Dolostone	tan, bn., gy., blocky-weathering, 20-100 cm beds in units to 10 m thick	microcrystalline or medium crystalline dolomite	discontinuous lamination; bored &/or eroded hard-grounds on upper bedding planes locally
(4) Fossil-poor Peloidal Limestone	med. gy. or lt. gy. bn., rubbly &/or recessive-weathering, 10-40 cm beds in 10-400 cm intervals with stylonodular or stylotured bedding	peloidal, fossil-poor W & P	none*
		----- peloidal, fossil-poor P & G -----	structureless or parallel lamination & ripple-scale cross-lamination fenestral fabric locally
(5) Dolomitic Shale	lt. gn.-gy. to dk. bn., recessive-weathering, (i) cm-thick drapes, (ii) 1-75 cm beds (locally of great lateral extent, & (iii) several metres thick 'pods'	dolomitic shale with up to 25% silt*, & shaley dolomite*, minor 0.5-5 cm thick, quartz & chert sand, granule, pebble beds, shale intraclast cgl. & oncolite F	planar & wavy parallel lamination (<1-5 mm)*, desiccation cracks
(6) Intraformational Breccia	yl.-gy. & dk. bn., yl.- & blocky-weathering beds 20-50 cm thick	poorly-sorted & clast-supported, pebble to boulder size, angular dololaminite clasts & pebble to cobble size quartz/chert clasts in an argillaceous dolomite/dolomitic shale matrix	none

Table 3.1 continued

BIOGENIC STRUCTURES/ SKELETAL COMPONENTS	DIAGENETIC FEATURES	DEPOSITIONAL ENVIRONMENT
(1) minor burrowing locally no fossils	penecontemporaneous dolo- mitization, early nodular evaporites** & early multicoloured, banded chert nodules	extremely hypersaline, algal-microbial mat- covered high intertidal & supratidal mud flats exposed for prolonged periods of time
(2) none	penecontemporaneous dolo- mitization & early multi- coloured, banded chert nodules	hypersaline, algal-microbial mat-covered, shallow subtidal to low intertidal mud flats in protected, coastal embayments
(3) bioturbated* <u>Thalassinoides</u> , <u>Planolites</u> , & <u>Chondrites</u> locally no fossils	penecontemporaneous dolo- mitization; early nodular evaporites+ & black cryp- tocrystalline chert nod- ules	low energy, hypersaline shallow subtidal to low inter- tidal mud flats inhabited by a soft-bodied infauna & grazers
(4) bioturbated* sparse ostracodes*, tri- lobites*, gastropods, & small cephalopods	pressure dissolution-gen- erated stylo-bedding	restricted, shallow subtidal, mixed sand/mud flat supporting a soft-bodied infauna & low diversity shelly fauna
----- none no fossils	same	high energy, shallow subtidal mobile sand shoal or low intertidal sand flat
----- none no fossils	same	restricted, moderately high energy, shallow subtidal to low-intertidal, algal-microbial mat-covered sand flat
(5) none no fossils	none	extensively exposed & un- commonly inundated sabkhas & stranded tidal flat ponds that were 'sinks' for fine-grained, wind-blown clastics
(6) none no fossils	none	subsurface intrastratal dissolution of evaporite beds in sabkha sediments

Figure 3.1 Aguathuna Formation; field photos. a) Upper Aguathuna (blocky-bedded dolostones) - Table Point Formation (limestone) contact at Table Point. Contact is accentuated by pressure dissolution in the limestone. b) Polished slab of cryptalgal dololaminite; Table Point section. Scale is in centimetres. c) Polygonal desiccation cracks in dololaminite; Table Point section. Metre stick for scale. d) Bedding plane view of small hemispherical stromatolites; Table Point section. e) Slab of burrowed dolostone; Table Point section f) Burrowed dolostone with cauliflower-shaped evaporite nodules (arrows) replaced by coarse dolomite and/or silica; Aguathuna Quarry. g) Wavy-laminated, dolomitic shale overlying erosional topography on the St. George Unconformity (arrows) developed between middle and upper Aguathuna dolostones at Table Point. h) Intraformational (collapse) breccia with angular fragments of dololaminite (arrows) and dark chert surrounded by fine-grained dolomite matrix; north shore of Portland Creek Pond.

Figure 3.1



sediment accretion was controlled by algal-microbial mats that mantled the sediment surface (Logan *et al.*, 1964; Kendall and de'E Skipwith, 1968; Shinn *et al.*, 1969; Davies, 1970). Planar dololaminite, in contrast, is thought to have been deposited on mat-free flats, possibly in areas of high sedimentation (Lane, 1990).

Prolonged exposure and hypersaline waters excluded virtually all organisms from this zone of the tide flats. Restricted marine circulation combined with evaporation resulted in the generation of brines from which evaporites were precipitated, and which facilitated early dolomitization of the sediments (eg. Illing *et al.*, 1965; Shinn *et al.*, 1965; Butler, 1969; McKenzie *et al.*, 1980). Cauliflower-shaped nodules and thin beds of evaporites (Figure 3.1.f), most likely anhydrite (see Pratt and James, 1986, Fig. 6A), which grew displacively in the sediments before they were lithified and were dissolved and/or pseudomorphed by coarse dolomite or silica during early diagenesis (Kinsman, 1969; Butler, 1969; Chowns and Elkins, 1974; Tucker, 1976; Kendall, 1984).

3.2.2 Stromatolite (Lithofacies 2 in Table 3.1)

This lithofacies is represented by relatively thin and discontinuous beds of small, laterally-linked, hemispherical stromatolites (LLH-type of Logan *et al.*, 1964) (Figures 3.1.d and 3.2). Commonly interstratified with dololaminites, stromatolites are prominent components of Aguathuna sections only locally (eg. Shag Cliff in Bonne Bay and Port au Port). They are interpreted to have formed on algal-microbial mat-covered flats under conditions of low wave energy and current velocities either in protected, low intertidal areas (Logan *et al.*, 1964) or in shallow subtidal settings (Gebelein, 1969) within a peritidal complex. Since those in the Aguathuna do not bear evidence of prolonged subaerial exposure, their growth must have been permitted by elevated seawater salinity which excluded grazing and burrowing organisms, thereby allowing mats to proliferate (Garrett, 1970). Thin shale drapes (Lithofacies 5, Chapter section 3.2.5) commonly mantle stromatolite beds and may

indirectly indicate that these structures preferentially formed in protected, coastal embayments. Deposition of such fine, terrigenous sediments suggests the carbonate sediment supply was cut off, which in coastal embayments would likely have occurred as a consequence of tidal flat progradation that changed embayments into tidal flat ponds that became sinks for wind-blown sediment.

3.2.3 Burrowed Dolostone (Lithofacies 3 in Table 3.1)

Burrowed to bioturbated, finely crystalline dolostone either gradationally overlies dololaminite, forms discrete beds that punctuate dololaminite sequences, or comprises massive-looking, 1-10 m thick intervals in the Aguathuna locally (Figure 3.1.e). In the absence of conclusive evidence of prolonged exposure these sediments are interpreted to have been deposited in quiet, restricted, shallow subtidal to low intertidal environments. Harsh conditions imposed by abnormal seawater salinity and/or intermittent exposure prevented inhabitation by shelly organisms, but allowed a burrowing infauna to thrive. Variations from completely bioturbated beds to partly burrowed, laminated muds probably reflects a landward topographic and environmental gradient across the mud flat defined by increasingly inhospitable conditions (Shinn *et al.*, 1969). The finely-crystalline nature of the dolomite and common preservation of biogenic structures and fabrics suggest these sediments were also dolomitized early (Friedman, 1980; Hardie, 1987). This is further supported by the presence of nodular evaporite pseudomorphs in the sediments which indicate exposure to hypersaline brines during very shallow burial (Hardie and Shinn, 1986; Figure 3.1.f).

3.2.4 Limestone (Lithofacies 4 in Table 3.1)

Limestone beds are minor components, comprising between <10-30% of Aguathuna sequences. They are invariably fossil-poor and, in most cases, lack evidence of subaerial exposure, and so are interpreted to have been deposited in shallow subtidal to possibly low intertidal environments under comparatively normal, yet restricted marine waters.

Burrowed, muddy sediments were deposited in tranquil or protected, low energy, subtidal settings where a soft-bodied infauna thrived but abnormal sea water salinity prevented all but a low diversity shelly fauna to survive. Burrowed, peloidal sands were deposited under similar conditions but in comparatively shallow water where currents and waves were more effective at winnowing away fine sediment. Current-stratified, peloidal grainstone was deposited either in subtidal shoals or on intertidal sand flats that were regularly reworked by tidal currents and, or waves where substrate mobility, perhaps combined with abnormal seawater salinity, excluded both shelly organisms and burrowers. Peloidal sands with fenestral fabrics were deposited on more protected and restricted, intertidal sand flats where sediment accumulation was controlled by algal-microbial mats (Hardie and Shinn, 1986).

3.2.5 Dolomitic Shale (Lithofacies 5 in Table 3.1)

Thin beds of silty, dolomitic shale comprise <5-10% of most Aguathuna sections. They are commonly either (i) interbedded with dololaminites, (ii) drape stromatolites, or (iii) underlie intraformational breccias (see Chapter section 3.2.6; Figure 3.1.g). Anomalously thick shaley units (several metres) constitute the uppermost Aguathuna locally on Port au Port Peninsula (Big Cove section A, back pocket) and in the Daniel's Harbour Zinc Mine (DHZM) area (Lane, 1990).

These sediments are interpreted as accumulations of wind-transported, dominantly terrigenous sediment deposited in environments only rarely inundated by marine water. Thin, laterally extensive shales intimately associated with dololaminites are interpreted to have been deposited on sabkhas situated landward of mat-covered carbonate tidal flats, as are other thin, structureless shales immediately below intraformational breccias (Lithofacies 6, Chapter section 3.2.6) (Lane, 1990). Shales overlying stromatolites are thought to have accumulated in tidal flat ponds that evolved from protected, coastal embayments during tidal flat progradation. Anomalously thick shale units are

interpreted to have been deposited in sinkholes (Knight *et al.*, in press) or other topographically isolated depressions developed on the St. George Unconformity.

3.2.6 Intraformational Breccia (Lithofacies 6 in Table 3.1)

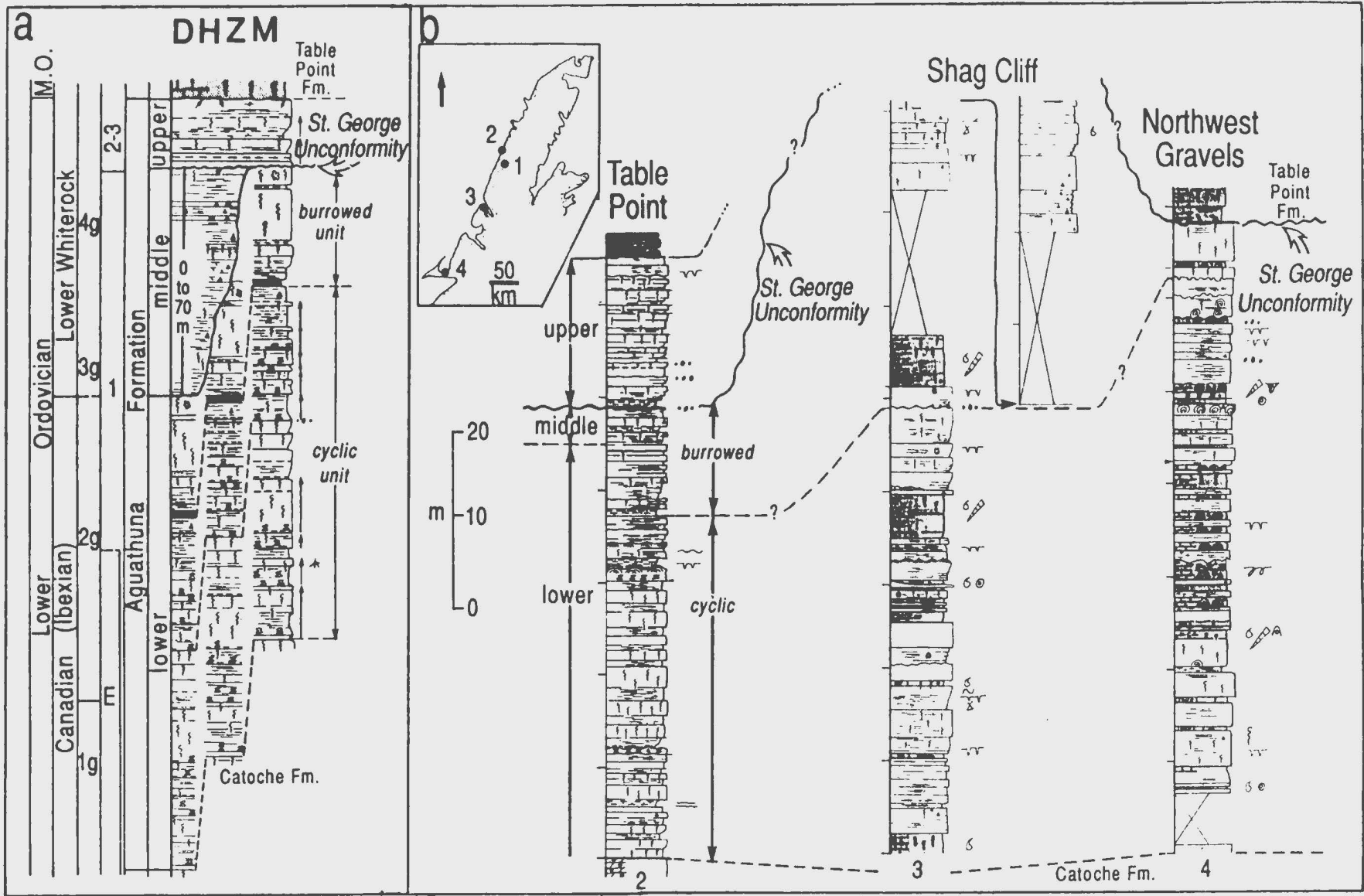
Intraformational breccia (intrastratal breccia of Lane, 1990) is a prominent component of Aguathuna sequences in which sabkha shales are also abundant, specifically in the Table Point - DHZM area (Figures 3.1.h and 3.2). The genesis of these beds is quite complex (Lane, 1990), but their (i) common occurrence above silica clast- and shale-mantled subaerial disconformities, (ii) lack of evidence of subaqueous transport or reworking, and (iii) common sagging and/or brecciation of overlying dolostones indicate that they formed in the shallow subsurface by collapse of lithified sediments due to dissolution of an underlying evaporite bed (Rubin and Friedman, 1977; Friedman, 1980). Thin sabkha shales immediately below these beds are inferred to have originally hosted the evaporite.

3.3 Stratigraphy

The Aguathuna Formation is comprised of three members originally delineated and informally defined by Lane (1990) in thick formation sequences at and around the DHZM (Figure 3.2.a). The lower member consists of a basal, cyclically-bedded unit overlain by a thick burrowed unit. The middle member, which is bounded at the top by the St. George Unconformity, is composed mostly of cherty dololaminites and lesser interbedded burrowed dolostone. The upper member consists of multiple, small-scale, dololaminite to burrowed dolostone cycles. Regional correlations made on the basis of lithology and/or style of sedimentation, and confirmed by identification of the St. George Unconformity based on physical evidence of exposure and biostratigraphic evidence of a depositional hiatus, has proven the Aguathuna elsewhere to be invariably incomplete, composed of only one or two of the members present

Figure 3.2 Stratigraphy of the Aguathuna Formation. a) Schematic composite section from the Daniel's Harbour Zinc Mine (DHZM) area from this study and Lane (1990, Figures 2.2 and 4.1). Columns, from left to right include: age; stage; graptolite zones (1g - Didymograptus protobifidus, 2g - D. bifidus, 3g - Isograptus victoriae (St. George Unconformity hiatus), 4g - Paraglossograptus etheridgei (tentaculatus); conodont zones; informal member. Scale is the same as for b). Offsets in the lower member (dashed correlation lines) show variation in thickness of the middle member in a subsidence doline at the DHZM. Arrows to the right denote deepening-upward sequences. b) Lateral variations in lithofacies of the lower member of the Aguathuna. Table Point section from this study and Knight and James (1987); Shag Cliff section from this study; Northwest Gravels section modified after Pratt (1979) and Knight and James (1987).

Locations of all sections in a and b shown in inset map. Limestone beds are light grey, dolomitic shale beds are dark grey, and dolostone is white. Key to other symbols is in Appendix A.



in the vicinity of the mine. Complications of Aguathuna stratigraphy are addressed in Chapter section 11.3.

3.3.1 Lower Aguathuna

The lower Aguathuna is most widespread and is consistently composed of a basal, cyclically-bedded unit and upper burrowed unit. Variations in the lithofacies make-up of the basal unit between the DHZM area and the Port au Port Peninsula suggest that the nature of the peritidal system varied along strike (Figure 3.2.b). In general, the number of sabkha shales and intraformational (collapse) breccias in the sequences decreases toward the south, whereas the number of stromatolite beds and proportion of more normal marine limestone increases. Moreover, in the north, beds and cyclic lithofacies sequences show great lateral continuity, some being traceable more than 300 km² (Lane, 1990), whereas those in the south are highly discontinuous (Pratt, 1979; Pratt and James, 1986). Collectively these features suggest that the peritidal system in the north was characterized by extremely restricted conditions, with tidal flats and sabkhas that covered large areas of a very gentle topography, possibly disposed in broad belts parallel to a shoreline, while in the south it was characterized by better marine circulation, areally restricted and/or highly transient tidal flats, and numerous protected embayments, all of which suggest it may have consisted of a complex of small islands, banks and shallow channels (Pratt and James, 1986). Increased dissection and complexity of the peritidal system may reflect increasing wave energy between the DHZM area and Port au Port, that was either determined by distance from the shelf margin or controlled by the distribution of barriers along it.

3.3.2 Middle Aguathuna

The middle Aguathuna is recognized only in the vicinity of the DHZM (Knight *et al.*, in press; Figure 3.2.a). It varies markedly in thickness (2-70 m), is interpreted to disconformably overlie the lower member, and is bounded at the top by another erosional surface that

correlates with the St. George Unconformity (Lane, 1990). Unusually thick sequences were deposited in subsidence dolines that formed locally and concurrently with subsurface dissolution and collapse, and the generation of rock matrix breccias in the underlying Catoche Formation (Lane, 1990).

3.3.3 St. George Unconformity

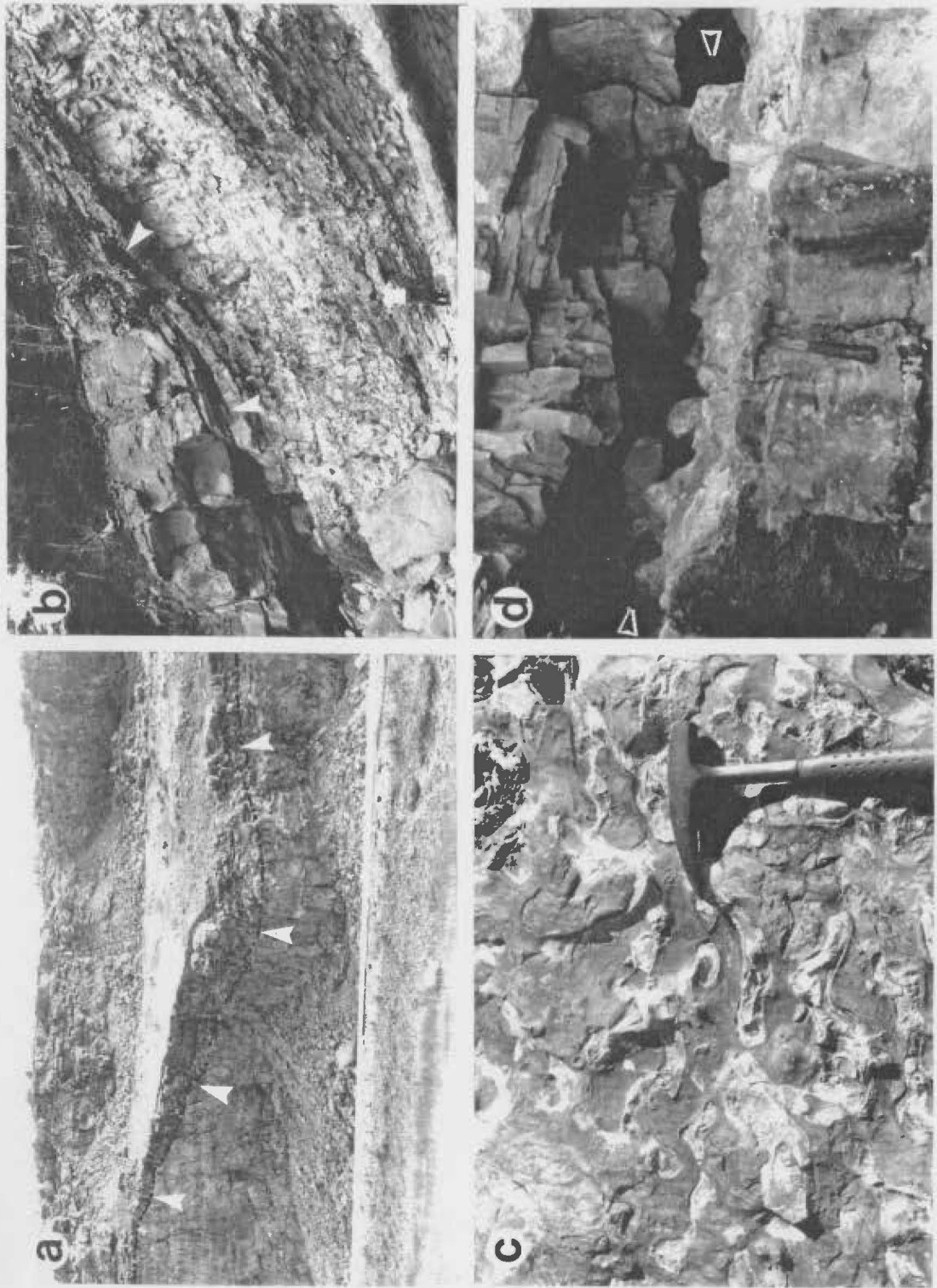
The St. George Unconformity is an erosional, commonly karstified surface that is recognized regionally (Knight *et al.*, in press). In sequences at and around the DHZM it separates lower from middle Aguathuna dolostones (Figure 3.2.a), but in all other areas it defines the contact between (i) the lower and upper Aguathuna, (ii) lower Aguathuna dolostones and basal Table Point Formation limestones, (iii) the Catoche Formation and upper Aguathuna dolostones, or (iv) Catoche limestones or dolostones and Table Point limestone.

Erosional relief on the unconformity in most outcrops is on the order of a few centimetres or tens of centimetres (Figure 3.1.g and 3.3.b). Exceptional is the exposure in Aguathuna Quarry where the surface is defined by a broad (>200 m) channel with more than 10 m relief (Figure 3.3.a). Even more extensive erosion, however, is demonstrated by the amount of stratigraphic relief on the unconformity regionally, which is in excess of 50 m. The surface is locally discontinuously mantled by a thin lag of insoluble quartz and chert sand or pebbles, and/or silica sands are incorporated in overlying carbonates.

Evidence of karst is widespread and includes both surface and subsurface features that are developed on and in both Aguathuna dolostones and Catoche Formation carbonates below the unconformity (Lane, 1990; Knight *et al.*, in press). The former include rillenkarrren, small, irregular-shaped, solution depressions (Figure 3.3.c), rubble breccias (paleosoils), small sinkholes, and solution-enlarged joints, fractures, and vugs that are filled with sediments derived from above the

Figure 3.3 St. George Unconformity. a) High-relief erosional contact between Aguathuna Formation dolostones and basal Table Point Formation limestones at Aguathuna Quarry. The unconformity defines a broad channel discontinuously mantled by silica pebbles and locally etched by dissolution pits (Figure 3.3.c) and rillenkarren. Lower quarry wall in the centre of the photo is about 5 m high. b) Low relief, erosional contact (arrows) between light-coloured, blocky-bedded, Aguathuna dolostone and dark, massive-weathering Table Point Fm. limestone; Black Cove section. The unconformity is mantled by a sandy, limestone lithoclast, silica pebble conglomerate. C. James (~1.5 m high) for scale. c) Surface karst on the unconformity; Aguathuna Quarry. Bedding plane view of dissolution pits on chert-bearing dolostone. Hammer for scale. d) 'Egg carton' cave (subsurface karst) between lower Aguathuna dolostone beds ~8 m below the unconformity; NW Gravels. Hammer for scale.

Figure 3.3



unconformity surface. Subsurface karst features include stratiform 'egg carton' caves (Figure 3.3.d) and rock matrix breccias that formed by dissolution of limestone beds, and vertical, tabular or pipe-shaped, rock matrix breccias.

The St. George Unconformity is recognized in nearly every sequence in western Newfoundland, thereby demonstrating widespread subaerial exposure of the shelf (Knight *et al.*, in press). Gaps in both conodont and shelly faunas at the unconformity suggest that the depositional hiatus represents only 1-3 million years (Fåhraeus, 1977; Stait and Barnes, 1988; Stait, 1988; Boyce *et al.*, 1988). Thus far the only place the unconformity is not recognized is in the anomalously thick Aguathuna sequence at Shag Cliff in Bonne Bay (Schuchert and Dunbar, 1934; Levesque, 1977; this study; Figure 3.2.b). Discontinuous exposure of the uppermost Aguathuna and basal Table Point Formation there, plus lack of biostratigraphic information from the section preclude demonstrating either continuous sedimentation or a depositional hiatus.

3.3.4 Upper Aguathuna

The upper member of the Aguathuna discontinuously overlies the St. George Unconformity (Knight *et al.*, in press; Figure 3.2.a). It generally ranges from 5-15 m thick, but is up to 60 m thick where it fills in sinkholes developed on the unconformity in the vicinity of the DHZM (Lane, 1990).

3.4 Summary and Environmental Reconstruction

Fine-grained dolostones, fossil-poor limestones, and thin, silty shales which comprise the Aguathuna Formation record deposition in very restricted, low energy, peritidal environments (Figure 3.4). Dololaminites accumulated on extensively exposed, high intertidal and supratidal flats. Burrowed dolostones were deposited on restricted, low intertidal to shallow subtidal flats. Stromatolites grew in protected, hypersaline, coastal embayments. Limestones were deposited in comparatively

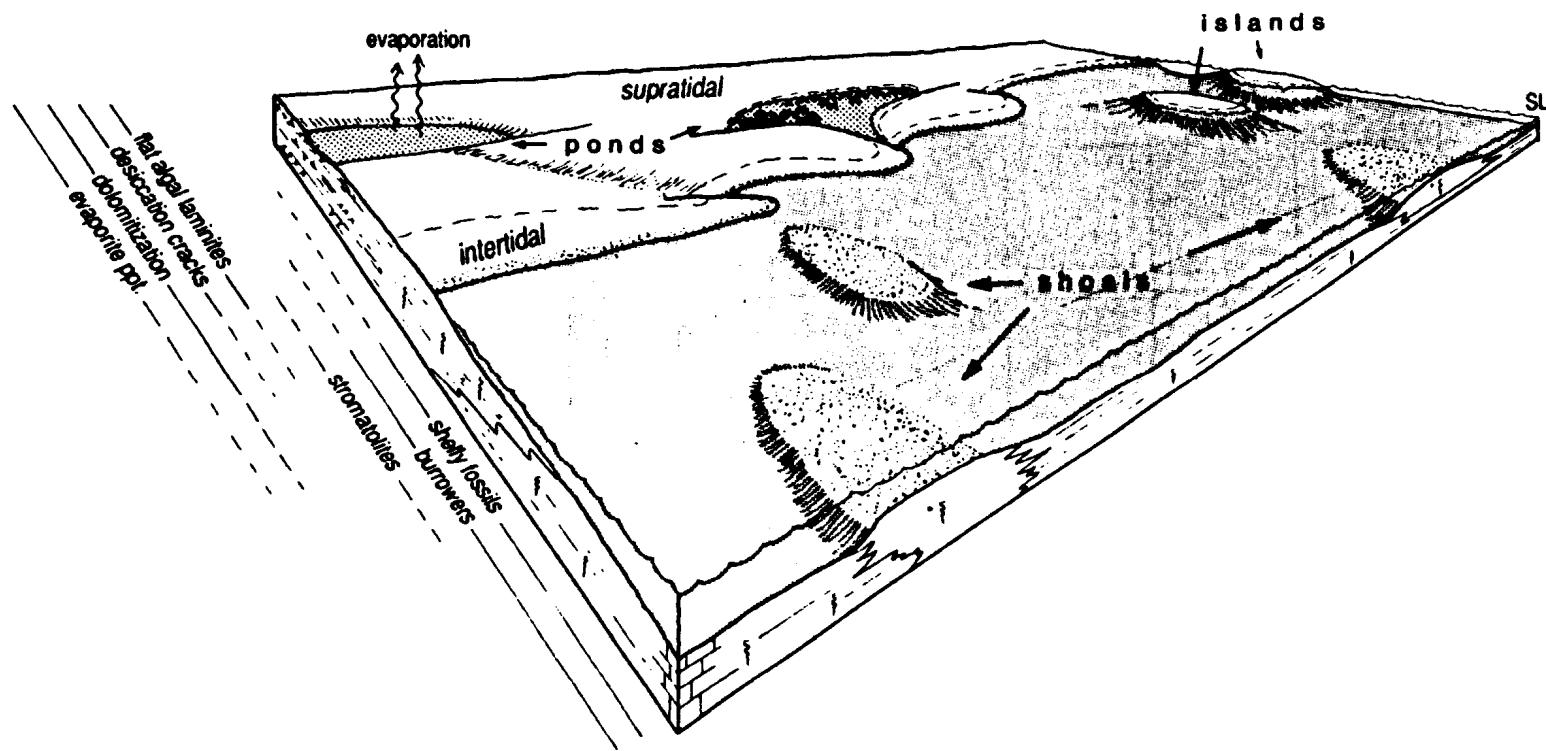


Figure 3.4 Reconstruction of depositional environments recorded by Aguathuna Formation lithofacies. Lateral changes in peritidal complex are inferred from lithofacies distributions in the lower member of the Aguathuna. Key to symbols is in Appendix A.

normal marine, nearshore environments. Shales composed mostly of wind-blown, terrigenous sediment, accumulated on sabkhas and in stranded, tidal flat ponds isolated from a marine carbonate supply. Elevated salinity of ambient marine and groundwater, more so than any other physical parameter, appears to have determined the distinctive characteristics of the carbonate sediments deposited in each environment, controlling not only the distribution and diversity of shelly and soft-bodied organisms and, consequently, the distribution of algal-microbial mats, but also early dolomitization of original lime sediment in the most restricted environments and precipitation of evaporites in tidal flat and sabkha sediments.

Nodular and bedded evaporites associated with syndepositional dolostone are peculiar to the Aguathuna, and suggest that these sediments accumulated under extremely arid climatic conditions (Schopf, 1980; Hardie and Shinn, 1986). Evidence of evaporites is lacking in underlying and overlying peritidal deposits including analogous, dolostone-dominated sequences in the Boat Harbour Formation and limestone-dominated sequences of the upper Catoche Formation and basal Table Point Formation, all of which are interpreted to have been deposited under semi-arid or humid climatic conditions (Pratt and James, 1986; Knight and James, 1987; Ross and James, 1987; Knight *et al.*, in press; this study), a conclusion that agrees with the paleogeographic position of the ancient shelf at 20-30° south of the Equator during this time (Scotese *et al.*, 1979).

Since the continental margin did not shift dramatically in latitude during this period of time, and therefore it is unlikely that Aguathuna sediments record a complete change in climate, evaporite precipitation must either reflect a marked change in local climate, or is an expression of extremely restricted marine circulation. A change in local climate could conceivably be an orographic effect of encroaching volcanic highlands (eg. Press and Siever, 1982, Figure 6-6), but sudden

reversion back to humid climatic conditions indicated by basal Table Point peritidal sediments, which demands either very rapid erosion or great lateral displacement of the arcs, makes this unlikely. Alternatively, restricted circulation imposed by temporary barriers along the shelf margin that limited exchange with open ocean waters and severely dampened wave-induced movement of water across the shelf, could have generated extremely saline waters conducive to evaporite precipitation.

Lithologically distinctive, lower, middle, and upper members of the Aguathuna Formation record a three-phase depositional history. Lower Aguathuna strata were deposited regionally across the shelf. Variations in lithofacies comprising the basal, cyclic unit (Figure 3.2.b) suggest that the configuration of the peritidal system varied along strike (Figure 3.4), probably in response to different local hydrodynamic conditions determined either by distance from the shelf margin or by the distribution of barriers along it. The regional distribution of the upper, burrowed unit, however, indicates a relative rise in sea level and establishment of more uniform conditions across the shelf.

Middle Aguathuna dolostones are preserved only in the DHZM area. Their distribution may be in part a function of subsequent erosion and formation of the St. George Unconformity. However, the intimate association of these deposits with contemporaneous, subsurface karst and dissolution collapse suggests deposition reflects local flooding by marine waters in a topographic low while surrounding areas were sub-aerially exposed.

The St. George Unconformity records a period of shelf-wide exposure, nondeposition, and erosion. The surface truncates middle Aguathuna dolostones in the DHZM area, and lower Aguathuna strata elsewhere, locally eliminating them entirely from the Ordovician succession. Widespread development of karst at and below the unconformity records the effects of prolonged exposure to meteoric water.

Upper Aguathuna carbonates were deposited only locally above the

unconformity. Their restricted distribution suggests they record inundation by marine waters and reestablishment of very restricted, peritidal environments locally on the shelf while adjacent areas remained subaerially exposed and were sites of nondeposition.

3.5 Signals of Convergent Margin Tectonism

The Aguathuna Formation comprises the top half of a large-scale, shallowing-upward sequence deposited on the platform from late Early Ordovician through early Middle Ordovician time (Knight and James, 1987; James et al., 1989; Figure 3.5). The upper Boat Harbour - Catoche - Aguathuna succession is interpreted as a third-order sequence (sensu Mitchum et al., 1977 and Vail et al., 1977) that records deposition in response to a relatively rapid sea level rise, followed by a slow down in the rate of sea level rise or lowering of sea level. Similar to other Early Paleozoic, third-order sequences, notably the Cambrian Grand Cycles (Aitken, 1966), sea level fluctuations indicated by changes in the type of sediment deposited are considered to be eustatic.

There are several features of the Aguathuna, however, that are uncharacteristic of passive margin carbonate sequences and indicate that regional and local tectonics overprinted eustasy and influenced peritidal sedimentation. They include: 1) temporary establishment of extremely restricted circulation across the shelf; 2) gentle folding of lower Aguathuna dolostones prior to deposition of the middle member and the latter's limited distribution in the DHZM area; 3) tilting and gentle folding of Aguathuna strata locally prior to subaerial exposure and formation of the St. George Unconformity; 4) evidence of structural control on the distribution and development of karst; 5) great variation, both regionally and locally, on the level of erosion on the St. George Unconformity; 6) highly discontinuous deposition of upper Aguathuna dolostones above the unconformity. Each of these is addressed in Part II: Sedimentation and Tectonics, Chapter 11.

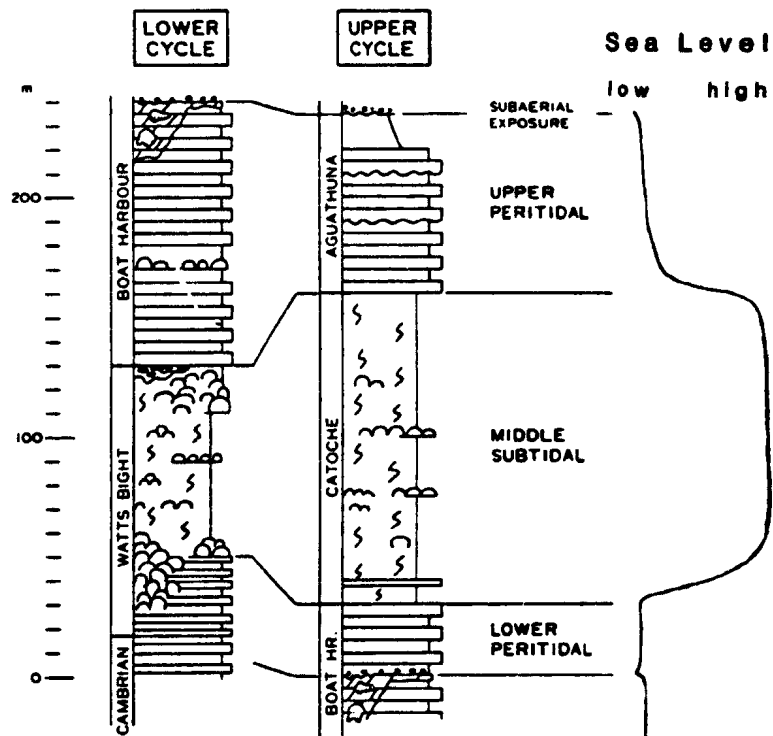


Figure 3.5 Depositional megacycles of the Lower Ordovician St. George Group (Watts Bight, Boat Harbour, Catoche and Aguathuna formations); modified after Knight and James (1987).

CHAPTER 4

SEDIMENTOLOGY OF THE TABLE POINT FORMATION

4.1 General Characteristics and Stratigraphic Relationships

The Table Point Formation is a variably thick package (60-250 m) of grey, fossiliferous limestone and minor dolostone. In most places these strata disconformably or conformably overlie the Aguathuna Formation, but locally they disconformably overlie older Catoche Formation carbonates. Disconformable contacts are defined by the St. George Unconformity (S. G. U.) (Chapter section 3.3.3). Table Point limestones are most commonly gradationally overlain by thin-bedded, shaley limestones of the Table Cove Formation (Chapter 5). Locally on the Port au Port Peninsula they are disconformably overlain by resedimented carbonate conglomerates, calcarenites, and shale of the Cape Cormorant Formation (Chapter 6). Elsewhere the Table Point is abruptly overlain by black, laminated shale of the Black Cove Formation (Chapter 7).

The Table Point Formation is made up of twelve marine and marginal marine lithofacies (Figure 4.1). The lithofacies are distributed among three units that everywhere comprise the formation. The Basal Peritidal Unit (BPU) is an extremely heterogeneous package of restricted, shallow subtidal, intertidal and supratidal limestones and dolostones. The Middle Subtidal Unit (MSU) is a comparatively uniform package of shallow subtidal sediments that overlie the BPU. The Upper Subtidal Unit (USU) is a second heterogeneous package of limestones deposited in comparatively shallow subtidal settings. Sedimentologic and diagenetic attributes of each lithofacies are detailed in Table 4.1.

4.2 Basal Peritidal Unit (BPU)

This unit is an assemblage of seven lithofacies deposited in supratidal, intertidal and restricted subtidal environments (Lithofacies 1 through 8 in Table 4.1; Figure 4.1). It is equivalent to the Spring Inlet Member of the Table Point (Ross and James, 1987). Diagnostic

Table Point Formation Lithofacies

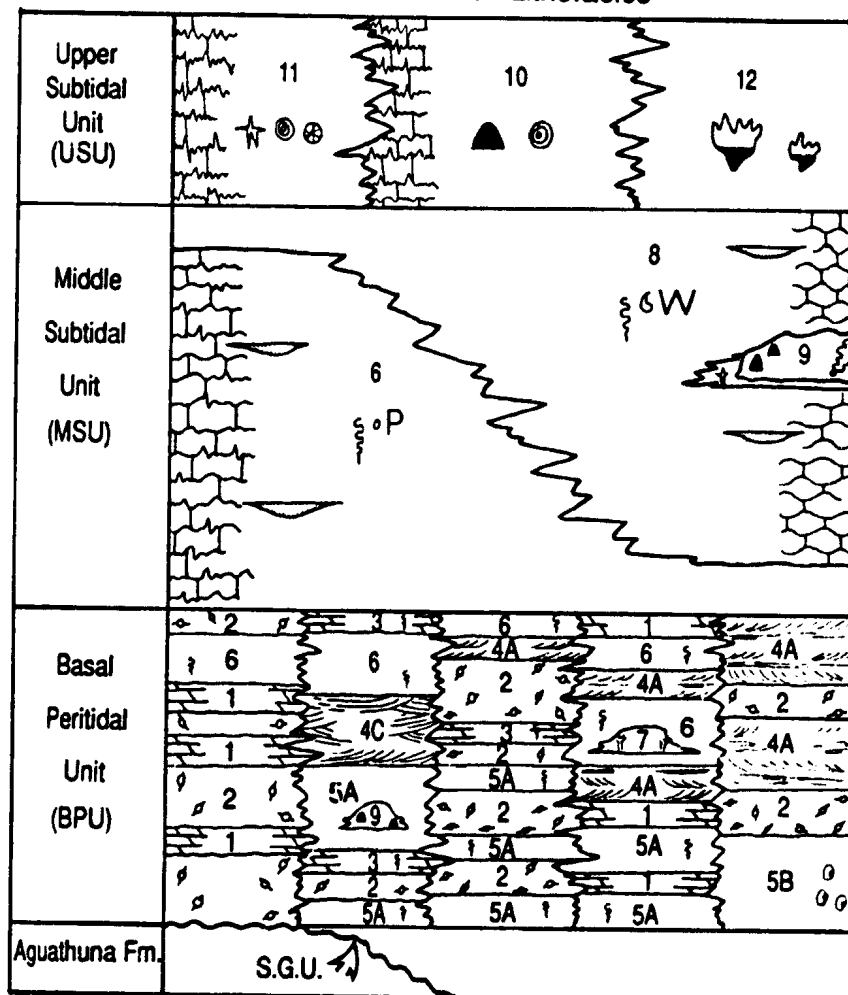


Figure 4.1 Generalized, diagrammatic distribution of Table Point Formation lithofacies. Numbers 1 through 12 correspond to Table 4.1. Key to symbols is in Appendix A.

Table 4.1 Table Point Formation Lithofacies. Environmental interpretations are based on comparison with both modern, shallow marine, carbonate deposits and other ancient, platformal carbonate sequences (Laporte, 1967; Bathurst, 1975; Ginsburg, 1975; Wilson, 1975; Enos, 1983; Shinn, 1983; Wilson and Jordan, 1983). Water depth estimates based largely on assemblages of photosynthesizing microbes and calcareous algae (Ginsburg *et al.*, 1971; Guilbault *et al.*, 1976; Wray, 1977).

Colours: lt.=light, dk.=dark, gy.=grey, yl.=yellow, bn.=brown, gn.=green, bk.=black.

Composition: M=mudstone, W=wackestone, P=packstone, G=grainstone, R=rudstone, F=floatstone; pel.=peloidal, fossil.=fossiliferous, intra.=intraclastic, cgl.=conglomerate, microcryst.=microcrystalline.

Structures: lam.=lamination, hor.=horizontal, par.=parallel, discon.=discontinuous, dimen.=dimensional, strat.=stratification, dia.=diametre, amp.=amplitude, wave.=wavelength, mic. envelopes= micrite envelopes.

Fossils: ostra.=ostracode, gastro.=gastropod, art. (inart.) brach.=articulate (inarticulate) brachiopod, trilo.=trilobite, echin.=echinoderm, crin.=crinoid, cyst.=cystoid, ortho. ceph.=orthoconic cephalopod, bryo.=bryozoan, lg.=large.

Algae: on=oncolite, fr=fragment, no=nodule, en=encrusting/coating, ra=raft.

DH2M=Daniel's Harbour Zinc Mine.

The symbol (*) denotes the predominant lithology, sedimentary structure, development of burrowing, or fossils which for the case of fossil-poor sediments does not mean abundant.

' - Lithofacies 6 in the MSU is more fossiliferous than it is in the BPU; faunal list in column 5 represents MSU occurrences.

Table 4.1 Table Point Formation Lithofacies

LITHOFACIES	COLOUR, BEDDING STYLE & THICKNESS	COMPOSITION	PHYSICAL SEDIMENTARY STRUCTURES	BIOGENIC STRUCTURES
(1) CRYPTALGAL LAMINITE (BPU)	lt. gn. gy., yl.- & blocky-weathering 5-100 cm beds	M*, dolomitic M* & fine pel. P/G, microcryst. dolomite	crinkly, cryptalgal lamination (a fraction of a mm to 1 mm thick)	minor burrowing locally
(2) FENESTRAL LIMESTONE (BPU)	tan, lt. bn., or lt. gy. massive or flaggy-weathering 1-300 cm beds in units up to 15 m thick	fenestral pel. intra. P/W*, clotted, pel. M*, thrombolitic pel. M/W & thin beds of: laminated or burrowed M, oncolitic F, LLN & LLH/SH stromatolites (1-10 cm), gastropod coquina, coquina, rippled pel. G; minor fine quartz sand &/or silt	laminoid & irregular fenestree*; small stromatocoid cavities*; desiccation cracks, hardgrounds locally; intraformational (collapse) breccia (10-40 cm) in DHZM cores	no distinct burrows*; neospar burrows or spar-filled burrows in some beds; <u>Palaeophycus</u> locally
(3) BURROWED DOLOSTONE (BPU)	lt. gn. gy., dk. gy., yl.- & blocky-weathering, 10-90 cm beds in units up to 3 m thick	dolomitic M*, microcryst. dolomite*, fossil. W, thin (<2 cm), discontinuous ostra. coquinas ostra. coquinas	none* disrupted, fine parallel lamination in some beds	vague mottling (bioturbated); <u>Chondrites</u> & <u>Palaeophycus</u> locally
(4) CROSS-BEDDED, PELOIDAL GRAINSTONE (3 types) (BPU)	lt. gy. bn., yl.- weathering, massive or blocky, or flaggy beds 5-50 cm thick in units up to 11 m thick	(4A) fine to medium-grained peloidal, intraclastic, fossil-poor G*; minor fine quartz sand & silt (eg. Caribou Brook)	5-20 cm, high-angle trough cross-stratification*; parallel lamination, dolomitic M flasers	locally burrowed; <u>Palaeophycus</u> on the tops of some beds
		----- (4B) fine to medium-grained intraclastic, peloidal G/P (Gargamelle section only) -----	5-50 cm tangential cross-stratification* (unidirectional foresets in a thinning- & fining upward package)	burrows in finer-grained, thinner cross-sets
		(4C) very fine-grained, dolomitic peloidal G* with interbeds of pel. fossil P/W & thin mollusc coquinas in the upper part of the unit (Table Point section only)	5-20 cm, low-angle, trough cross-stratification* (in thinning-upward sets); hor. to low-angle, parallel lamination*; mm-thick dolomitic M flasers; 2-dimen., flat-topped? ripples; bimodally oriented gastro. & ortho. cephalopods; irregular relief erosion surface at one horizon (karst? or hardground)	scattered <u>Chondrites</u> in cross-stratified G; large <u>Chondrites</u> (6-8 mm dia.) & large (1-2 cm wide) branching, horizontal burrows (? <u>Palaeophycus</u>) in associated muddier sediments

Table 4.1 continued

SKELETAL COMPONENTS	DIAGENETIC FEATURES	DEPOSITIONAL ENVIRONMENT
(1) rare ostracodes	penecontemporaneous dolomitization	extensively-exposed, hypersaline, high intertidal to supratidal, microbial mat-covered flat; marine invertebrates excluded
(2) ostra.*, trilo.*, gastro*, sponge spicules*	mic. envelopes/bored grains; early vadose & phreatic cements (pendant columnar & blocky calcite); internal sediment; vadose silt; partial early dolomitization	restricted, microbial mat-covered, very shallow subtidal to high intertidal flats; periodic subaerial exposure &/or abnormal seawater salinity limit marine biota
(3) ostracodes & trilobites* (commonly moldic)	penecontemporaneous dolomitization	quiet-water, extremely restricted, semi-enclosed shallow subtidal, intra-platform basin to ?intertidal mud flat
(4A) sparse leperditiid & other ostracodes*, gastro.*, small ortho. cephalopods*, trilo., art. brach., echin., <u>Nuis</u> & <u>Halysis</u>	oolitic coatings on grains in some beds; partially dolomitized (early?); molluscs silicified locally; micro-stylolitic bedding	current- &/or wave-agitated, mobile sand flat; as discontinuous patches on a muddy seafloor & as belts or areas marginal to mat-covered tidal flats
(4B) leperditiid & other ostracodes*, trilo.*, echin., <u>Halysis</u> fragments	partially dolomitized ?early; minor authigenic quartz	shallow subtidal sand bar or tidal channel bar; sands deposited from high-energy currents in migrating dunes & ripples under progressively decreasing water depth &/or flow strength
(4C) ostracode valves & <u>Merchisoni</u> in G; gastro., trilo., art. brach. ortho. cephalopods & small (1-7 mm) globular sponges in associated muddier sediments	early? dolomitization; silicified molluscs above omission surface	shallow subtidal sand body (?)formed in the breaker zone of normal waves; sands deposited from both unidirectional currents and oscillatory flow by migrating megaripples

Table 4.1 continued

LITNOFACIES	COLOUR, BEDDING STYLE & THICKNESS	COMPOSITION	PHYSICAL SEDIMENTARY STRUCTURES	BIOGENIC STRUCTURES
(5) BURROWED, FOSSIL-POOR, MUDDY LIMESTONE (BPU) (two types)	(5A) dk. gy., blocky to rubbly-weathering (locally recessive, wavy-parted bedding), 10-300 cm beds in units up to 35 m thick (5B) dk. gy. & bk., recessive-weathering, parted, nodular bedding in a unit ~8 m thick (Big Cove & Caribou Brook sections only)	fossil-poor M*, peloidal W*, pel. fossil. W & P; small sponge bioherms (50-100 cm dia., 10-15 cm high) locally (see (9) below)	none*; fine parallel lamination in some thin M beds; 1-2 m thick coarsening-upward units	bioturbated*; neospar (& less commonly peloidal G burrows); <u>Chondrites</u> prevalent in some units; <u>Palaeophycus</u> prevalent in wavy-parted beds
(6) BIOTURBATED, FOSSIL-POOR, PELOIDAL PACKSTONE (BPU & NSU) ¹	lt. to med. gy., massive-weathering beds 50-300 cm thick in units 2-50 m thick	fossil-poor, peloidal, intraclastic P*, pel. W; thick units with thin, coarse-grained lenses & beds of peloidal, intraclastic G/R & mollusc coquinas	none*; rare parallel lamination; coarse lenses with erosional bases, shelter porosity, infiltration fabrics, normal grading, parallel lamination, aligned fossils (see Table 4.2)	bioturbated*; neospar, dolomitic & peloidal P/G burrows; <u>Palaeophycus</u> on some bedding planes; <u>Chondrites</u> locally
(7) BRYOZOAN BIONEEM (BPU) (Appendix B) (Shag Cliff only)	mottled dk. gy., bk., white, & yl. bn., rubbly-weathering, cryptic lumps (0.5-1.5 m dia., 1-1.5 m high) in a 1.5 m thick bed	mound proper: bryozoan bindstone flanking beds: fossil. P; inter-mound sediments: dolomitic M; cap bed: fossiliferous, intra-clastic oncolitic G/R	none*	bioturbated*
(8) BIOTURBATED, FOSSILIFEROUS, MACKSTONE (NSU)	med. gy. to dk. gy., rubbly-weathering, thick to massive beds (1-7 m) in units up to 145 m thick	ranges from fossil-bearing M to very fossiliferous, pel. W/P - discontinuous lenses (1-30 cm thick, 3-100 cm long) of fossiliferous, pel. intra. P/R, fine-grained, peloidal, fossil. G/P & spiculitic M or finely-fossil. W (see Table 4.2)	none* lenses with erosional bases & flat or rippled tops; shelter porosity & infiltration fabrics; preferentially oriented concave-down shells, parallel lamination, ripple-scale, cross-lamination	bioturbated* lenses burrowed or with burrowed tops

Table 4.1 continued

SKELETAL COMPONENTS	DIAGENETIC FEATURES	DEPOSITIONAL ENVIRONMENT
(5A) ostra.*, trilo.*, gastro.*, sponge spicules*; sparse echin. bryo., art. brach., ortho. cephalopods <u>Girvanella</u> * (fr, m, on, n) <u>Hedstroemia</u> , very minor <u>Nuia</u> & <u>Malysis</u>	mic. envelopes/bored grains; partially dolomitized (?early) & early-formed phosphatic chert nodules in some units; weakly- to well-developed pressure dissolution generated, stylo-nodular bedding	protected and restricted, shallow-water, intra-platform basin; abnormal sea water salinity and/or low oxygen levels caused by limited exchange with open marine water and poor circulation restricted the marine biota
(5B) leperditiid & other ostracodes*, gastropods	pressure-dissolution enhanced, early diagenetically-unmixed(?) bedding	restricted depression as (5A) above, but possibly a brackish water, stranded tidal flat pond episodically flooded by marine waters but a continuous sink for fine, windblown sediment and catch-basin for freshwater runoff
(6) ostra.*, trilo.*, <u>Maclurites</u> *, <u>Merchisoni</u> * & other gastro.*, ortho. & coiled ceph.*, <u>Lapidipanis</u> *, <u>Pulchritamina</u> (in some beds); minor echin., bryo., art. brach., lithistid sponges, <u>Girvanella</u> * (fr, n, on), <u>Hedstroemia</u> (n), <u>Wetheradella</u> ?, <u>Malysis</u> , <u>Nuia</u>	mic. envelopes/bored grains; chert nodule horizons common; weakly-developed, pressure-dissolution generated stylo-nodular or stylo-brecciated bedding	gently agitated, restricted, stable sand flat above normal wave base; sediments winnowed by currents &/or waves, but stabilized by organic films or early cement; depth and energy intermediate between mobile sands (4) and burrowed muds (5 or 8); <10 m water depth
(7) encrusting & stick-shaped bryozoans* (25-30%), gastro. small coiled ceph., art. brach. (mound); echin.*, ostra.*, gastro.*, trilo.*, ortho. ceph.*, bryo.*, <u>Girvanella</u> oncolites (to 2 cm) (cap bed)	mic. envelopes/bored grains; partially dolomitized	small organic buildups that formed in the subtidal on a stable, grainy substrate (eg. (6) above) in ~7-10 m water (see Appendix C)
(8) abundant & diverse biota: leperditiid & other ostra.*, illaenid & bathyrid trilobites, orthid art. brach.*, echin., <u>Maclurites</u> *, <u>Merchisoni</u> & other gastro.*, lg. (to 80 cm long) ortho. cephalopods, bryo.*; lithistid sponges, <u>Lapidipanis</u> ; <u>Girvanella</u> * (fr, no, m, en), <u>Hedstroemia</u> , <u>Nuia</u> , <u>Malysis</u>	mic. envelopes/bored grains; chert nodule horizons (common); well-developed pressure dissolution generated stylo-nodular bedding	quiet water, open? marine subtidal platform setting below normal wave base & above storm wave base, well within the photic zone & probably in no more than a few to several tens of metres water; light & oxygen levels, salinity & temperature conditions suitable for a diverse assemblage of organisms

Table 4.1 continued

LITHOFACIES	COLOUR, BEDDING STYLE & THICKNESS	COMPOSITION	PHYSICAL SEDIMENTARY STRUCTURES	BIOGENIC STRUCTURES
(9) SPONGE BIONEERM (NSU)	dk. gy., rubbly weathering, circular to elliptical mounds (50-200 cm dia., 30-70 cm high) in 1-2 m thick horizons	mound proper: sponge-bearing fossil. W/F underlying & flanking beds: echinoderm-rich, peloidal intra. G/R	none* in the mound flanking beds structureless or megarippled (ampl.=10 cm; wave.=45 cm)	bioturbated*, neospar burrows
(10) SPONGE-ONCOLITE BIOSTRONE (USU)	med. gy. to lt. gy, massive or rubbly-weathering, 0.5-5 m beds in 5-40 m thick	sponge-bearing limestones range from W,P, F & R containing variable amounts of fossil fragments, peloids, intraclasts & <u>Girvanella</u> oncolites (0.3-1.5 cm dia.) (grain-supported textures increase up-section)	none	bioturbated* neospar burrows common, dolomitic & peloidal G burrows locally
(11) ECHINODERM-ALGAL-LINESTONE (USU)	lt. gy. or tan, massive or blocky-weathering, 30-100 cm beds in units 1-5 m thick	echinoderm-algal P & echin.-algal intra. P, echin. G or echin.-trilo. G/R (latter locally with black shale matrix); minor fine quartz sand & silt in P/G/R	none in P/W; vague parallel lamination, shelter pores & infiltration fabrics in some G beds; syndimentary, tectonic, shale-filled fractures locally	bioturbated* or neospar burrows in muddy sediments; none in G/R; black, argillaceous carbonate-filled burrows or borings at the top locally

Table 4.1 continued

SKELETAL COMPONENTS	DIAGENETIC FEATURES	DEPOSITIONAL ENVIRONMENT
(9) globular, cylindrical, vase-shaped, stick-like & encrusting lithistid sponges* & spicules, leperditiid & other ostra.*, <u>Maclurites*</u> , <u>Merchisoni*</u> & other gastro.*, art. brach.*, echin.*, trilo.*; <u>Girvanella*</u> , <u>Solenopora</u> , <u>Hedstroemia</u> , <u>Malysis</u> & <u>Nuia</u>	mic. envelopes/bored grains	open marine, shallow subtidal organic buildups that formed on grainy sediment patches on a muddy seafloor above normal wave base &/or in the presence of gentle currents; water less than 25 m & possibly only a few metres (eg. 3-5 m) deep
(10) globular, irregular & vase-shaped lithistid sponges* (spicules & holdfasts), lg. (to 75 cm) ortho. & (to 25 cm) coiled ceph.*, echin. (crin. & cyst.)*, ostra.*, cheirurid, illaenid & ?asaphid trilobites*, art. brach.*, small gastro.*, bun & twig-like bryo.* <u>Lepidipenis</u> , <u>Pulchrellamina</u> , <u>Girvanella*</u> (no, fr, on), <u>Nuia*</u> , <u>Malysis*</u> , unnamed green alga*, <u>Sphaerocodium</u> , <u>Wetheradella</u> , coccoid algae	mic. envelopes/bored grains; pre-pressure dissolution v-shaped ?tension cracks, authigenic quartz & albite; weak stylo-nodular to micro-stylolitic bedding; pyrite-replaced fossils & intraclasts at the top	open marine, shallow subtidal setting, regularly agitated by gentle waves &/or currents in water less than 25 m to possibly only a few metres deep; optimum conditions of light, water movement & salinity conducive for proliferation of sponges, echinoderms, & algae & a diverse assemblage of other invertebrates
(11) echin. (crin. & cyst.)*, ostra., trilo., small (<15 cm) ortho. & coiled (<6 cm) ceph., art. brach., lithistid sponges (uncommon), spicules, <u>Lepidipenis</u> , inart. brach., bryozoans, <u>Girvanella*</u> (ra, on, no, en), <u>Nuia*</u> , unnamed desycladacean alga*, <u>Malysis</u> , coccoid algae	dense micrite envelopes, syntaxial overgrowths & displacive neomorphic spar on echinoderm fragments; neomorphic pseudospar intraclasts; micritic firmgrounds & a mineralized hardground at the top locally; partial replacement of sediment by calcium phosphate, microquartz, micro-crystalline dolomite & pyrite	open marine, shallow subtidal, crinoid-cystoid & algae-covered, meadows probably in less than 10 m of water; depending on depth bottom currents & waves were weak (muddy sands) to vigorous (clean sands); sedimentation interrupted by depositional hiatuses, the final one (locally) resulting in a mineralized hardground

Table 4.1 continued

LITHOFACIES	COLOUR, BEDDING STYLE & THICKNESS	COMPOSITION	PHYSICAL SEDIMENTARY STRUCTURES	BIOGENIC STRUCTURES
(12) <u>STROMATACTIS</u> <u>MOUND</u> (USU)	dk. gy. with lt. gy. mottles or lt. bn. with tan mottles, massive- weathering limestone up to 35 m thick	mound base: complex assemblage of massive or thin-bedded, pel., intra. G/R, fenestral limestone (pel. W/P) & ostracode M (Piccadilly)	synsedimentary <u>high-angle frac-</u> <u>tures</u> (few mm to several cm wide, up to several 10s of cm vertical extent) filled with ostra. M or microsparitic internal sediment & fibrous marine cement; M-filled <u>sheet-cracks</u> (1-3 cm wide, sev- eral 10s of cm long)	minor burrowing
		mound: fossiliferous to fossil- poor, peloidal. intra. W/F*; minor echinoderm-rich G/R & onco- lite <u>Lapidipanis</u> F (Piccadilly); fossil-poor W (Burnt Island)	pervasive fine fenestral fabric; dolomitic M-filled <u>sheet cracks</u> (as at base); synsedimentary, high-angle, marine cement-filled <u>fractures</u> (few mm wide) & echino- rich, peloidal G-filled <u>fissure</u> (0-50 cm wide) at the top (Picca- dilly); high-angle, echinoderm G- filled <u>fractures</u> (<10 cm wide, in- determinate vertical extent) (Burnt Island)	bioturbated*, microsparitic burrows

Table 4.1 continued

SKELETAL COMPONENTS	DIAGENETIC FEATURES	DEPOSITIONAL ENVIRONMENT
(12) echinoderms* ostr., trilo., bryo., <u>Girvanella</u> , <u>Halysis</u> , <u>Medstroemia</u> , <u>Nuis</u>	micritized hardgrounds on G; pendant (vadose) & isopachous (phreatic) fibrous marine cement in fenestrae & syndimentary fractures	shallow subtidal to intertidal, algae-microbe & sponge? constructed buildup developed above a tidal flat/sand shoal complex; overall quiet water or protected setting experiencing gentle currents & periodically accreting to sea level; episodes of syndimentary fracturing caused by displacements on nearby faults
----- leperditiid & other ostr.*, echin.*, globular & stick- like lithistid sponges* & spicules*, <u>Lapidipenis</u> , gastro., art. brach., trilo., ortho. ceph. <u>Girvanella</u> * (no, on) <u>Halysis</u> , <u>Nuis</u> , unnamed dasycladacean alga	micrite envelopes & bored skeletal grains; classical cm-size <u>Stromatactis</u> , larger interconnected <u>Stromatactis</u> , & sheet-like <u>Stromatactis</u> (<5 cm wide & >1 m long) complexly filled with internal sediment (M or peloidal G) & roof-thickened (vadose) or isopachous (phreatic) fibrous marine cement	

lithofacies are fenestral limestone, cryptalgal laminite, burrowed, microcrystalline dolostone, and cross-bedded, peloidal grainstone. They occur together with muddy and peloidal sediments bearing a restricted assemblage of shelly fossils.

4.2.1 Peritidal Lithofacies (Lithofacies 1-4, Table 4.1)

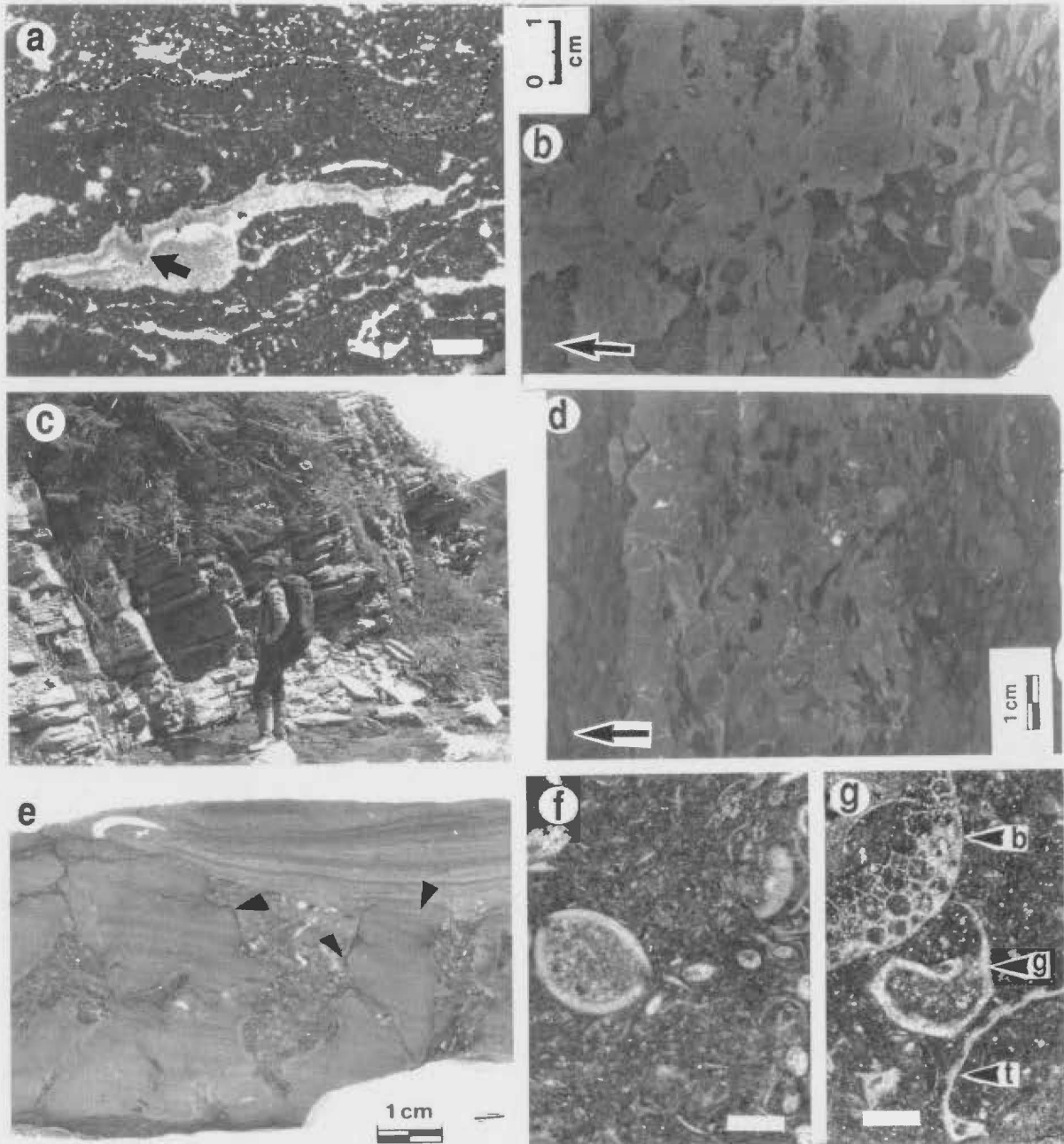
Fenestral limestone (Figure 4.2.a) and cryptalgal laminite (see Figure 3.2.b) are distinctive and characteristic tidal flat deposits (Ginsburg, 1975; Hardie and Shinn, 1986). Fenestrae and crinkly lamination indicate that sediment accumulation was influenced by algal-microbial mats. Desiccation cracks and vadose silt and cement in fenestrae prove that the sediments accumulated on periodically exposed surfaces. Scarcity of dolomitized sediments and apparent absence of evaporites suggest deposition under semi-arid to humid climatic conditions.

Burrowed dolostones (Figure 4.2.b), some of which contain relict fine, (?) cryptalgal lamination, are interpreted to have been deposited in very shallow, highly restricted, possibly stranded depressions. Limited lateral distribution of this lithofacies indicates the depositional environment was aeriually restricted. Its common occurrence immediately above restricted, subtidal limestones (Lithofacies 5 in Table 4.1) and overlain by fenestral limestone, further suggests that this environment evolved by filling in of a semi-enclosed, intra-platform depression subsequently covered by prograding tidal flat deposits. Early dolomitization is interpreted to have been caused by exposure to hypersaline waters generated in the depression due to limited exchange with normal marine water.

Cross-bedded, peloidal grainstone was deposited in three settings by different processes. 1) Parallel-laminated and small-scale, high-angle, cross-bedded sands (Lithofacies 4A in Table 4.1; Figure 4.2.c) are interpreted to have been deposited on high energy, shallow subtidal to low intertidal, mobile sand flats. Common association with fenestral

Figure 4.2 Basal Peritidal Unit lithofacies; outcrop and thin section photos. a) Photomicrograph of fenestral limestone; Aquathuna Quarry. Laminoid fabric suggests algal-microbial mat binding. Arrow points to pendant fibrous marine cement. Dotted line marks a surface between two fenestral fabric types. Bar scale is 1 mm. b) Polished slab of Chondrites burrowed, limy dolostone; Table Point. Up is to the left. c) Blocky-bedded, cross-bedded peloidal grainstone (Lithofacies 4A); Caribou Brook. d) Polished slab of partly dolomitized, burrowed wackestone (Lithofacies 5A); Table Point. Up is to the left. e) Polished slab through an irregular omission surface in dolomitic peloidal grainstone (Lithofacies 4C); Table Point. Echinoderm grainstone fills topography on the surface. f) Photomicrograph of ostracode-rich wackestone (Lithofacies 5B); Big Cove section A. Bar scale is 0.5 mm. g) Photomicrograph of dolomitic fossiliferous wackestone (Lithofacies 5A); Table Point (as d, above). b, bryozoan; g, gastropod; t, trilobite. Bar scale is 0.5 mm.

Figure 4.2



limestone suggests that these flats formed seaward fringes on mat-covered tidal flats or formed in adjacent, less protected settings.

2) Unidirectionally cross-stratified peloidal sands characterized by thinning-upward set size, fining-upward grain size, and an upward increase in burrowing (Lithofacies 4B in Table 4.1) were deposited by migrating sandwaves and ripples under progressively weaker, unidirectional currents and/or decreasing water depth. They are interpreted to have been deposited in either in a migrating tidal channel bar (eg. Shinn, 1983) or a shallow subtidal sand bar (eg. Ball, 1967) where bedform migration and sediment deposition occurred primarily during one phase of the tidal cycle.

3) Exceptionally well-sorted and very fine-grained peloidal sands with distinctively low-angle, trough cross-stratification reminiscent of swaley cross-stratification (Leckie and Walker, 1982; Walker *et al.*, 1983) (Lithofacies 4C in Table 4.1) are more difficult to interpret. Sediment size (0.03-0.1 mm) and paucity of high-angle cross-beds almost demand that these sands were deposited from high velocity, oscillatory flows (see Harms *et al.*, 1975, Fig. 2). However, the presence of some high-angle cross-bedding and vertical burrows in the sands that are not obviously linked to an overlying truncation surface suggest the sediments could have been deposited by continually migrating dunes under unidirectional currents. To accommodate the possibility that both processes were operating, it is postulated that these sands accumulated in a breaker zone where wave action was dominant and currents were generated (eg. Bourgeois and Smith, 1984). An irregular omission surface near the top of the lithofacies (Figure 4.2.e) suggests that the sand bar was at one point subaerially exposed. Early dolomitization could have occurred in a mixing zone around a freshwater lens developed beneath the emergent bar at that time (Choquette and Steinen, 1980).

4.2.2 Restricted Subtidal Lithofacies

Fossil-poor muddy limestone, burrowed, peloidal packstone and

bryozoan mounds (Lithofacies 5, 6, and 7, Table 4.1) in contrast to other BPU lithofacies are comparatively fossiliferous and/or burrowed, and lack evidence of exposure. They are interpreted to have been subtidally deposited, though it is possible that Lithofacies 5 and 6 accumulated in the lowest portions of intertidal flats as well. Paucity of shelly fossils and the low diversity assemblage in these sediments indicate that the depositional environments were generally inhospitable to most marine organisms. Calcareous algae in all of the lithofacies indicate very shallow water, while predominance of Girvanella suggests water depth probably was not more than 5-10 m (Ginsburg et al., 1971; Wilson, 1975; Moore, 1977).

Fossil-poor muddy limestones include lithologies that vary in style of bedding, skeletal components or burrows, and diagenetic features. Distinctive parted-nodular, ostracode wackestone (Figure 4.2.f) could also have been deposited in a stranded, brackish water depression where carbonate sediment was diluted by windblown clays. Chondrites-burrowed, dolomitic limestone with phosphatic chert nodule horizons (Figure 4.2.d,g) indicate deposition in a poorly-oxygenated, abnormal marine (either hypersaline or brackish), subtidal setting where abundant organic matter deposited with and preserved in the sediment catalyzed several early diagenetic processes (Badiozamani, 1973; Knauth, 1979; Southgate, 1986; Soudry and Lewy, 1988).

Small bryozoan mounds not previously recognized in the Table Point Formation are described and compared with similar, but slightly younger buildups, in Appendix B. Greater diversity of the shelly fauna associated with the mounds, plus their appearance in a BPU sequence in which cross-bedded peloidal sands and burrowed, peloidal packstones are prominent components, suggest they formed under more normal marine conditions in an area of greater current activity and less restricted circulation.

4.2.3 Peritidal Sequences

BPU lithofacies commonly occur in repeated vertical sequences interpreted to record shallowing-upward (Figure 4.3). Lithofacies which define them are not everywhere the same, but most complete sequences are 1) muddy and/or peloidal, burrowed, subtidal limestone (Lithofacies 5a and 6), 2) fenestral limestone or rippled, peloidal sands (Lithofacies 2 and 4a) deposited on restricted and exposed tidal flats, and 3) a cryptalgally-laminated dolostone or dolomitic limestone cap (Lithofacies 1 in Table 4.1) deposited on high intertidal and supratidal flats. Subtidal and supratidal components are not present in every sequence.

Fenestral limestones in these sequences commonly display a fining-upward fenestral fabric (Figure 4.3.b,c). A coarsening-upward fabric is developed in some shallowing-upward sequences as well. However, where a coarsening-upward fenestral fabric is accompanied by increasingly muddy texture and the uppermost sediments are burrow-mottled, and evidence of subaerial exposure or a supratidal cap lacking, the coarsest fenestrae are interpreted to represent burrows in semi-lithified subtidal sediments, and the entire sequence is interpreted to record deepening-upward (Figure 4.3.d).

4.3 Middle Subtidal Unit (MSU)

This unit is composed mostly of burrowed, peloidal packstone and fossiliferous, stylo-nodular wackestone, but small sponge bioherms also occur locally within the muddier lithofacies (Figure 4.1). None of these sediments bears evidence of subaerial exposure, nor are they interstratified with sediments deposited in the intertidal. They are interpreted as wholly subtidal.

4.3.1 Burrowed, Peloidal Packstone (Lithofacies 6, Table 4.1)

This lithofacies makes up anywhere from only the lower tier to all of the MSU (Figures 4.1 and 4.4.a-c). Although it also occurs in the underlying Basal Peritidal Unit, here it comprises much thicker units,

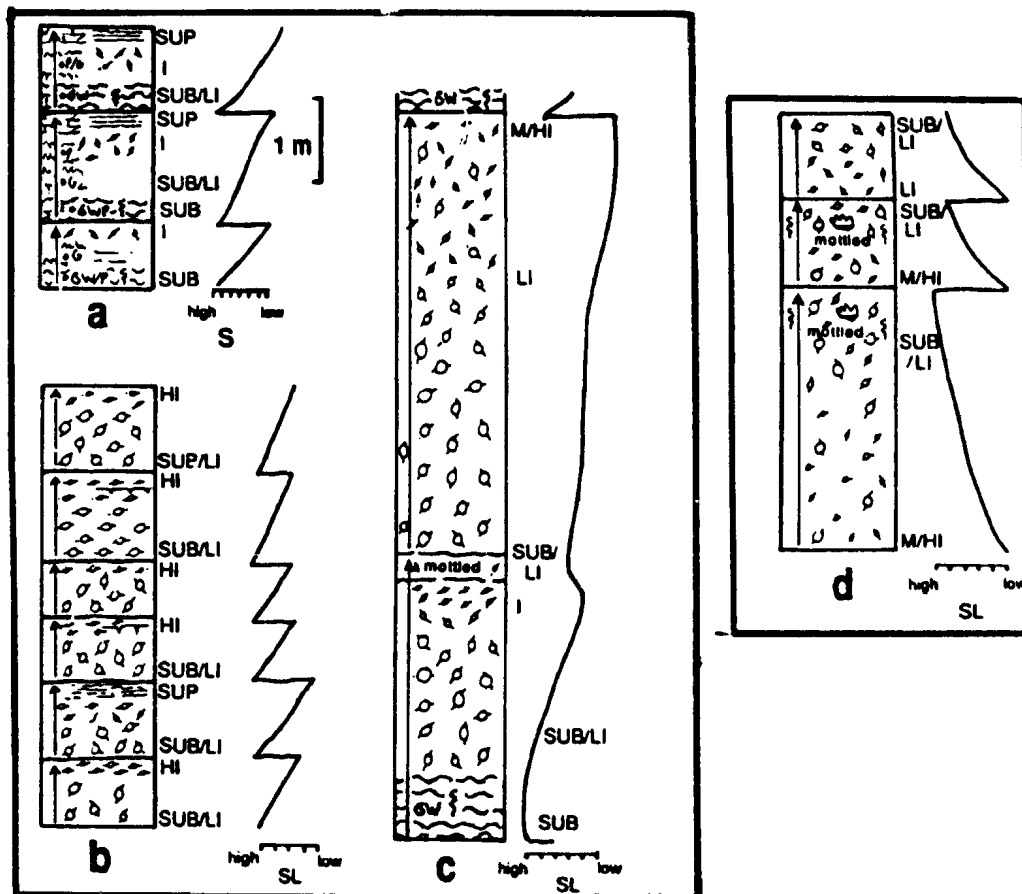
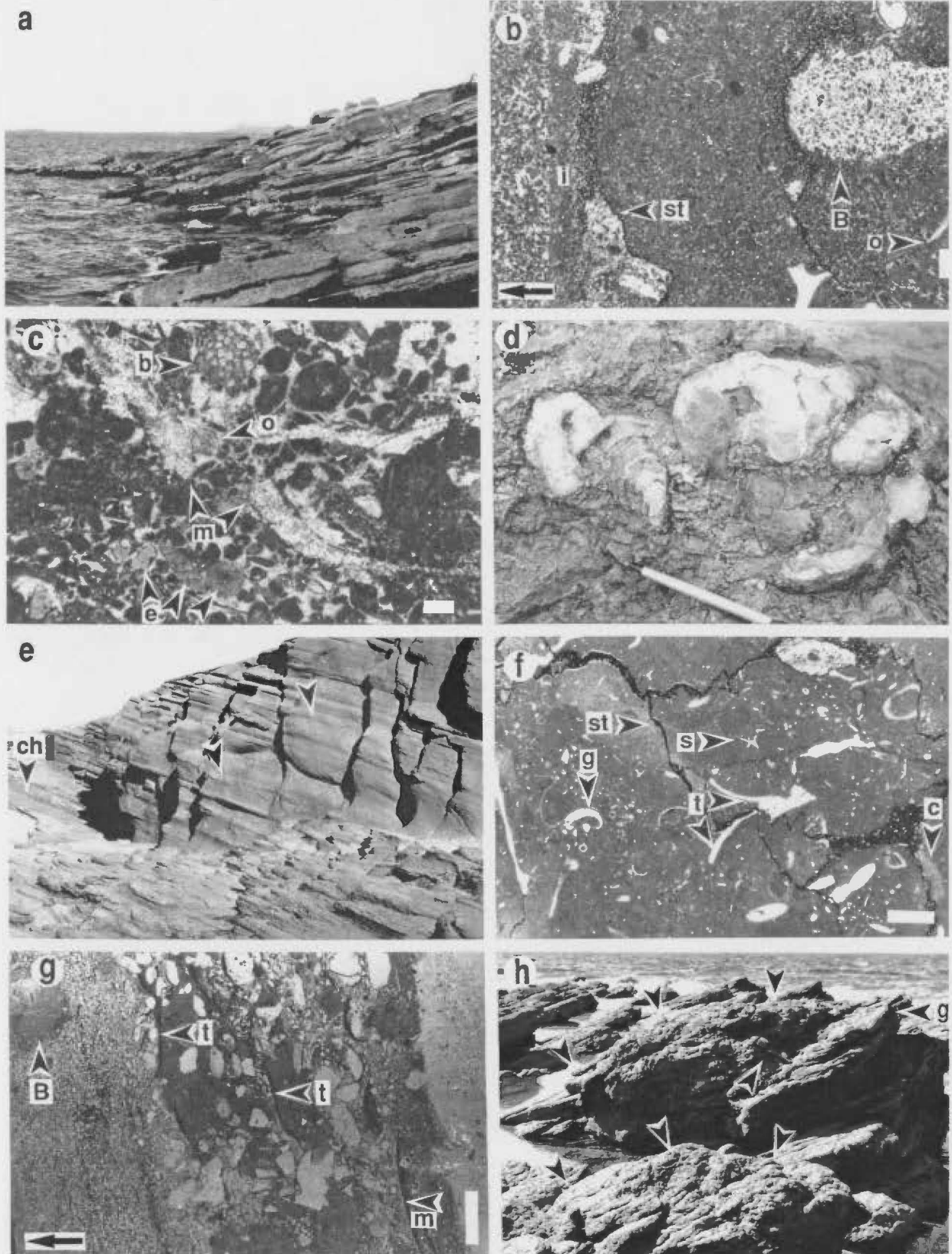


Figure 4.3 Shallowing-upward and deepening-upward sequences in the BPU. Curves to the right show changes in relative sea level (SL). a) Thin sequences with subtidal bases and supratidal caps; Southwest Feeder. b) Stacked fenestral limestone beds with a fining-upward fenestral fabric and supratidal caps; Burnt Island. c) Thick shallowing-upward sequences with fining-upward fenestral fabric in fenestral limestone components; DHZM core DH-2513. d) Stacked beds of fenestral limestone with coarsening-upward fabrics interpreted to record deepening-upward; DHZM core DH-2512. SUP=supratidal, I=intertidal, HI=high intertidal, M/HI=mid to high intertidal, L=low intertidal, SUB=subtidal, SL=sea level. Key to other symbols is in Appendix A.

Figure 4.4 Middle Subtidal Unit lithofacies; outcrop and thin section photos. Bar scales on all photomicrographs are 0.5 mm long. o, ostracode; i, intraclast; st, stylolite; b, bryozoan; e, echinoderm; m, mollusc; g, gastropod; s, sponge spicule; c, cystoid; t, trilobite; B, burrow. a) Blocky-bedded, burrowed peloidal packstone (Lithofacies 6); Black Cove. Beds in foreground are 30-40 cm thick. b) Photomicrograph of burrowed packstone (Lithofacies 6); Aguathuna Quarry. Up is to the left. Fine-grained, peloidal packstone is overlain by coarse peloidal grainstone, possibly a storm layer, that also fills a burrow. c) Coarse-grained, peloidal, intraclastic, fossiliferous grain-/packstone (Lithofacies 6); Aguathuna Quarry. Micrite envelopes define spar-replaced mollusc fragments. d) Lapidipanis in burrowed, fossiliferous wackestone (Lithofacies 8); Table Point. e) Typical outcrop of burrowed, fossiliferous wackestone (Lithofacies 8); Table Point. Cliff is approximately 22 m high. Chert-covered bedding plane (ch) is 102 m above the base of the formation. White arrows point to tops of gravitational slides 12 m and 19 m above the chert. f) Photomicrograph of burrowed, fossiliferous wackestone (Lithofacies 8); drill core DH-1382. g) Thin-section negative of a normally-graded, intraclastic storm deposit in burrowed, fossiliferous wackestone (Lithofacies 8); drill core U. S. Borax #2 (BO-2). Micritic intraclasts and peloids are light grey; skeletal fragments (mostly trilobites and ostracodes) are dark grey; very dark grey, inter- and intraclast material is neomorphic calcite. Upper peloidal grainstone is burrowed. h) Sponge bioherms (arrows) (Lithofacies 9); Table Point. Bioherms overlie and are flanked by echinoderm grain-/rudstone (g). Hammer (centre of the photo) for scale.

Figure 4.4



is punctuated by intraclast lenses and coquinas, and commonly contains large numbers of the sclerosponge Lapidipanis (Paquette et al., 1983; eg. Figure 4.4.d) or the possible coelenterate Pulchrilamina (Toomey and Ham, 1967; Toomey and Nitecki, 1979). These grainy sediments are interpreted to have been deposited on stable sand flats, similar to those in the interior of the Bahama platform (Bathurst, 1975), that were affected by gentle currents and/or waves which prevented large amounts of mud from accumulating but allowed a burrowing infauna to thrive. Sediment stability may have been provided by organic films or mats, or by micritic cement (Shinn, 1969; Bathurst, 1975). Such cement may contribute to the muddy texture of these sediments.

Although waters above the sand flat may have been gently and continuously agitated, only evidence of exceptionally high energy currents and waves is preserved. Coarse-grained, intraclastic and bioclastic beds and lenses that punctuate burrowed sediments possess features of storm deposits (column 3, Lithofacies 6 in Table 4.1; cf. Kreisa, 1981; Kreisa and Bambach, 1982; Aigner, 1982). Also, coarse grainstone-filled burrows (Figure 4.4.b) resemble 'tubular tempestites' described in modern platform carbonates and generated when coarse sediment transported by storm-generated currents falls into open burrows (Wanless et al., 1988). The sea floor is inferred to have been above normal wave base, but within a depth range where only records of episodic high energy depositional events escaped homogenization by burrowers. The cyanophyte Girvanella, and the green and red algae present are not indicative of a specific water depth, but their presence agrees with inferred shallow conditions and, like the Bahama platform, the sea bottom may have been mostly less than 10 m deep (eg. Bathurst, 1975; Moore, 1977).

4.3.2 Bioturbated, Fossiliferous Wackestone (Lithofacies 8, Table 4.1)

This lithofacies is either the dominant component or constitutes the

upper tier of the MSU in most sections (Figures 4.1 and 4.4.e,f). The enormous amount of mud, the generally unbroken and unabraded nature of the shelly fossils, and pervasive bioturbation indicate that these sediments were deposited in very quiet water. Large abundances and diverse shelly taxa indicate normal marine, oxygenated waters and imply good circulation.

Evidence of waves and currents in the muddy sediments is confined to thin lenses or beds interpreted as storm deposits (Figure 4.4.g; Table 4.2). The coarsest of these are thought to be storm wave-generated lags that have undergone little lateral transport. Finer-grained sediments that overlie the lags or occur alone in lenses were deposited both from wave-generated suspensions and from waning, turbidity or density flows. There is no detectable, systematic change in the type of storm deposit up section indicating that water depth did not change directionally - either deepen or shallow - with time.

The depth at which these sediments were deposited cannot be precisely determined. The combination of normal, very quiet water sediment accumulations and storm beds implies deposition somewhere between below normal wave base and above, or just below, storm wave base. The calcareous algae indicate the sea floor lay within the photic zone which, combined with the prolific, shelly invertebrate assemblage, suggests depths of less than 100 m (Benedict and Walker, 1978; Wilson and Jordan, 1983). The presence, but scarcity of green algae (*Halysia* and *Nuia*) may, based on occurrences of modern forms, indicate depths greater than 25 m deep (Wray, 1977). Associated sponge bioherms (section 4.3.3 below), which appear to have formed in very shallow water, strongly suggest that unless there were dramatic changes in water depth, the muddy sediments were probably deposited in no more than a few to several tens of metres of water.

4.3.3 Sponge Bioherms (Lithofacies 9, Table 4.1)

Small, muddy sponge build-ups formed locally on the subtidal shelf

Table 4.2

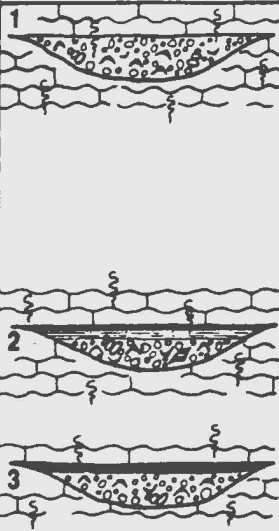
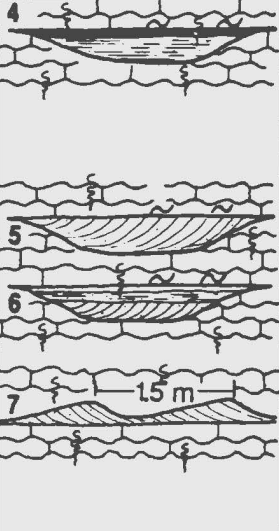
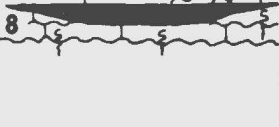
	COMPOSITION AND SEDIMENTARY STRUCTURES	DEPOSITIONAL MECHANISM
	<p>(1)* coarse, poorly-sorted, fossiliferous intraclastic peloidal packstone/rudstone</p> <ul style="list-style-type: none"> - erosional bases; autochthonous commonly unbroken fossils; mudstone and wackestone intraclasts; plate-shaped fossil fragments parallel to bedding; valves oriented concave-down; shelter porosity and infiltration fabrics common <p>(2) as (1) with normally-graded, parallel-laminated, fine-grained peloidal, fossiliferous grainstone to mudstone cap</p> <p>(3) as (1) but abruptly overlain by a thin mudstone layer</p>	<ul style="list-style-type: none"> - in situ reworking by storm waves with a unidirectional component of flow during storm peak - deposition of coarse material as a winnowed lag or after short lateral transport - deposition of fine sediment during waning stages; absence of rippled sands suggests this may have occurred solely from suspension, though laminated sand may also have been deposited in upper flow regime plane bed under either unidirectional or oscillatory flow
	<p>(4)** well-sorted, fine-grained, peloidal fossiliferous grainstone</p> <ul style="list-style-type: none"> - erosional bases; parallel-laminated with or without a thin mudstone cap <p>(5) as (4) but cross-laminated</p> <p>(6) as (4) but ripple cross-laminated to parallel-laminated sand (couplet) to mudstone cap (triplet)</p> <p>(7) as (4) but with a flat base and ripple form top</p>	<ul style="list-style-type: none"> - high flow stage erosion of muddy sediments by either waves or currents; incomplete Bouma sequences suggest deposition from low velocity gravity currents - parallel-laminated sands deposited in upper flow regime plane bed from either unidirectional or high velocity oscillatory flows - cross-laminated sands deposited from unidirectional flows - mudstone deposited from suspension - ripple cross-laminated sand, parallel-laminated sand/laminated mud couplets and triplets deposited from waning low-velocity gravity currents
	<p>(8) mudstone or finely-fossiliferous spiculitic wackestone</p> <ul style="list-style-type: none"> - low relief, erosional? bases; parallel lamination 	<ul style="list-style-type: none"> - deposited from suspension from low-velocity gravity currents (possibly upper plane bed unidirectional or high velocity oscillatory currents)

Table 4.2 Storm lenses in the bioturbated, fossiliferous wackestone lithofacies (MSU). Lenses range from 1-30 cm thick; most are less than 5 cm. Disruption by burrowing is common; *Palaeophycus* is common on upper surfaces of 4-6 and 8. Similar deposits occur in the burrowed, peloidal packstone lithofacies. Interpretations of depositional mechanisms based on Bowen *et al.*, (1974), Harms *et al.*, (1975), Kreisa (1981), and Kreisa and Bambach (1982).

* = common in MSU wackestone below and above sponge bioherms;

** = most common in MSU wackestone directly above burrowed, peloidal packstone

(Figure 4.4.h). Klappa and James (1980; 1989) have documented the sedimentological, paleontological and ecological attributes of these mounds and have discussed their significance in the evolution of early Paleozoic buildups.

Elongation of these bioherms in response to prevailing currents or waves and the asymmetric distribution and rippled character of pelmatozoan grainstones around some of the mounds (Figure 4.4.h) indicate that the bioherms formed at depths shallower than those which ambient muddy wackestones (Lithofacies 8) were deposited. Although Klappa and James (1980) concluded that the mounds accreted to sea level and were subaerially exposed, evidence of this was not observed by the writer. The presence of dominantly cyanobacteria and calcareous green algae suggests depths of less than 25 m (Wray, 1977); a similar assemblage in other small, Ordovician-age organic buildups has been interpreted to signify depths of less than 10 m, and possibly as little as 3 m (Moore, 1977).

4.3.4 Early Lithification; Diagenetic Bedding

Thin (1-2 cm), lumpy, stylo-nodular bedding is a characteristic feature of the bioturbated, fossiliferous wackestone lithofacies of the MSU. It is also developed in subtidal limestones in the BPU, and to various degrees in the sponge-oncolite biostrome and echinoderm-algal limestone of the Upper Subtidal Unit (Chapter section 4.4), as well as in the burrowed limestone lithofacies of the Table Cove Formation (Chapter section 5.2). There is compelling evidence that this bedding is an early diagenetic stratification (Bathurst, 1987) overprinted by pressure dissolution during burial.

Evidence of early lithification of these sediments includes the following. 1) Near surface-derived mudstone intraclasts and fossil fragments with attached sediment in storm lenses demonstrate cohesion or incipient lithification of sediments at the surface. 2) Discrete burrows show no evidence of compaction; some are filled with peloidal

sediment demonstrating that they were open to the sediment-water interface. 3) Thin gravitational slides generated at the sediment-water interface include conglomerate domains generated by brittle failure of lithified sediments. (These structures are described, illustrated and discussed in Chapter section 12.1).

These muddy sediments are homogeneously burrowed. With the exception of storm lenses, observed thin bedding does not correspond to discrete, primary depositional layers. Surface-generated gravitational slides in these sediments, however, include folded domains defined by thin, stylo-nodular bedding. If thin bedding were solely generated by pressure dissolution during burial, stylolites and pressure dissolution seams would invariably be oriented parallel to the depositional/burial surface, cross-cutting, rather than outlining folded sediments. Therefore, bioturbated sediments must have been overprinted by an early diagenetic stratification before sliding.

Lithification at or just below the sediment-water interface was probably accomplished by a combination of cementation and neomorphism (Bathurst, 1975). Predominance of pebble-size limestone clasts in conglomerate domains of gravitational slides, similar in dimension to nodules comprising present thin bedding, indicates that lithification proceeded in thin horizons by heterogeneous cementation of limestone lumps or nodules which with time coalesced to form more or less continuous beds. The process is analogous to submarine nodule cementation and hardground formation documented in Recent subtidal sediments (Taylor and Illing, 1969; Fischer and Garrison, 1967; Müller and Fabricius, 1974; Mullins *et al.*, 1980). Similar mechanisms have been invoked for the generation of nodular limestones and hardgrounds in other ancient fine-grained carbonates (Kennedy and Garrison, 1975; Jones *et al.* 1979).

4.4 Upper Subtidal Unit (USU)

Three different lithofacies comprise the top of the Table Point

(Figure 4.1). All contain evidence of deposition in environments shallower than those inferred for underlying MSU limestones.

4.4.1 Sponge-Oncolite Biostrome (Lithofacies 10, Table 4.1)

A sponge-oncolite biostrome gradationally overlies burrowed, fossiliferous wackestone (Lithofacies 8) at several localities. In contrast to underlying deposits, the sediments are lighter in colour, are more fossiliferous (and increasingly so up section), host large numbers of lithistid sponges (up to $>35 \text{ m}^2$), and contain a diverse and abundant assemblage of calcareous algae and Girvanella oncolites (Figure 4.5.a, c-e).

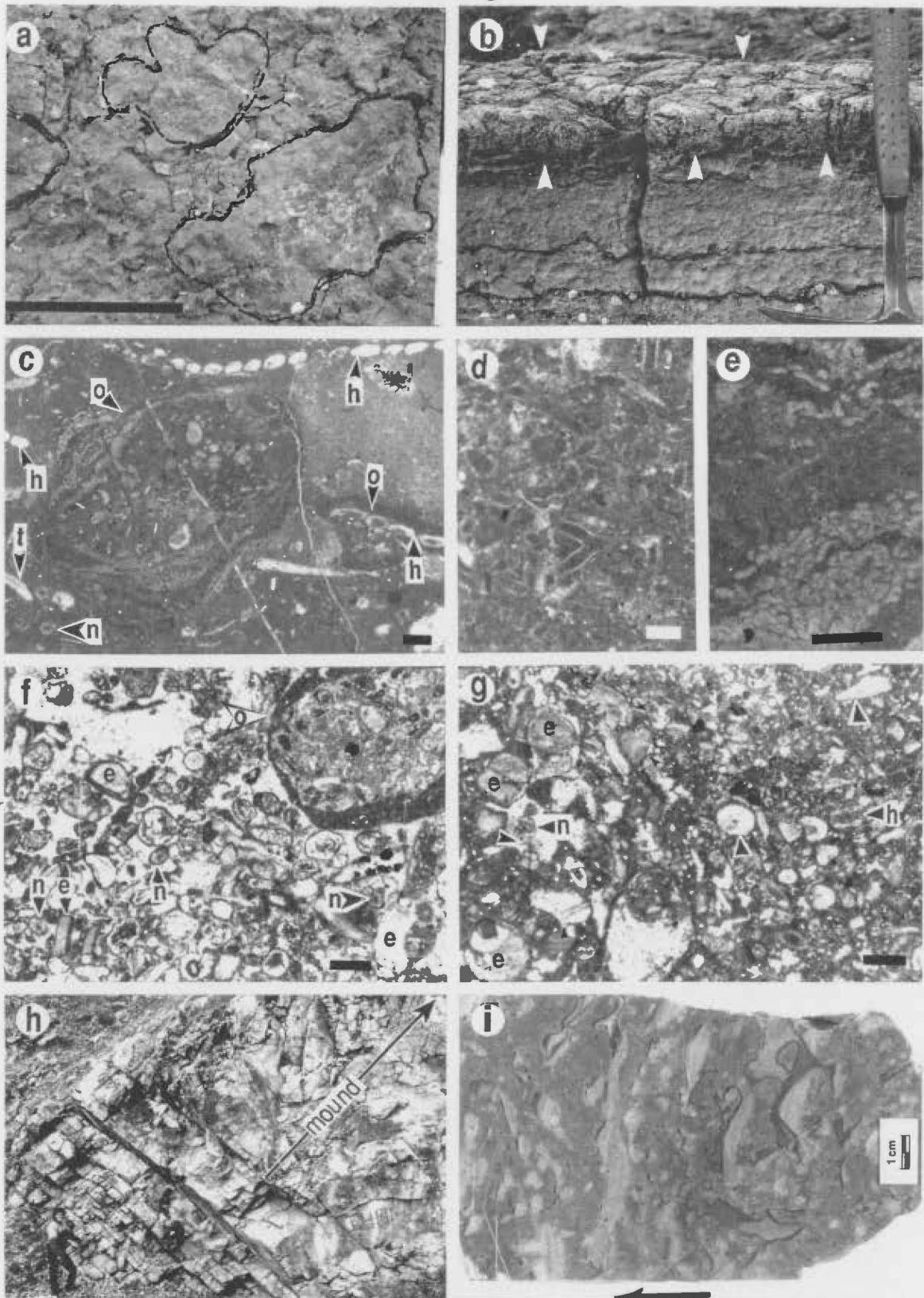
The high diversity of organisms present indicates that these sediments were deposited in an open marine, shallow subtidal setting with optimum conditions of water depth, water movement and salinity that permitted proliferation of sponges and calcareous algae and inhabitation by a variety of epifaunal organisms and a soft-bodied infauna. Numerous upright invertebrates and calcareous algae that would have been effective bafflers, and organisms that would have been effective encrusters or sediment binders, such as Girvanella, Sphaerocodium (Figure 4.5.e), Wetheredella, laminated bryozoans, and Pulchrilamina, indicate that sedimentation was profoundly influenced by the community itself.

Oncolites dispersed throughout the muddy sediment and locally concentrated in coarse layers indicate at least intermittent agitation of the seafloor. More or less continuous, albeit gentle, current and wave activity is suggested by the abundance of sessile, filter-feeding invertebrates (eg. sponges, bryozoans, Pulchrilamina, echinoderms) that require moving water to supply nutrients. Nearly pervasive bioturbate fabrics agree with such moderate energy conditions, implying relatively slow and continuous processes of deposition and erosion conducive to infaunal inhabitation and reworking of the sediment (Howard, 1975, 1978).

Biostromal limestones lack evidence of exposure and so are inferred

Figure 4.5 Upper Subtidal Unit lithofacies; outcrop and thin section photos. o, oncolite; h, Halysia; n, Nuia; t, trilobite; e, echinoderm. Bar scales on all photomicrographs are 0.5 mm. a) Globular, colonial, and vase-shaped (Archaeoscyphia?) lithistid sponges (outlined) in the sponge-oncolite biostrome (Lithofacies 10); Table Point. Bar scale is 10 cm long. b) Siliceous-dolomitic crust on echinoderm-algal limestone (Lithofacies 11) at the top of the Table Point; west coast Pistolet Bay. c) Photomicrograph of Girvanella oncolite floatstone with algae-rich, fossiliferous wackestone matrix from the sponge-oncolite biostrome; Table Point. d) Photomicrograph of branching, tubular green algae (unnamed) from the sponge-oncolite biostrome; drill core DH-1382. e) Photomicrograph of Sphaerocodium in the sponge-oncolite biostrome; Table Point. f) Photomicrograph of echinoderm-algal pack-/grainstone; west coast Pistolet Bay. Nuia is most abundant; large Girvanella-coated oncolite is in the upper right. Pseudospar intraclasts with micrite coats and micritic cores are either recrystallized micritic grains or Nuia. g) Photomicrograph of echinoderm-algal pack-/wackestone; Bakeapple Island. h) Outcrop of underlying fenestral limestones and base of the Stromatactis mud mound at Piccadilly. Up is to the right. A. Pye for scale. i) Polished slab of limestone from the Piccadilly mound with complex internal sediment- and cement-filled Stromatactis. Up is to the left.

Figure 4.5



to be wholly subtidal. Increasingly grain-supported textures up through the biostrome suggest sedimentation occurred in progressively shallower water under increasingly agitated conditions. The abundant and diverse assemblage of calcareous algae (Figure 4.5.c-e) indicates a shallow environment. Halysia has been reported only in restricted intertidal and very shallow subtidal sediments where it is associated with Girvanella and algal mats (Guilbault et al., 1976). Nuia, known to occur in many early Paleozoic, shallow subtidal limestones (Toomey and Klement, 1966; Toomey, 1967; Stricker and Carozzi, 1973; Guilbault et al., 1976; Wray, 1977; Toomey and Nitecki, 1979; Gnoli and Serpagli, 1980; Mamet and Roux, 1982; Ross et al., 1988), is thought to be a green alga that grew in shallow, agitated settings. Encrusting Wetheredella and Sphaerocodium near the top of the biostrome are prominent sediment binders and framework components in early Paleozoic reefs and reef flats (Ginsburg et al., 1971; Wray, 1977; Bourque et al., 1981, 1986), which suggests that here they are also indicative of high-energy conditions. Encrusting bryozoans and Pulchrilamina at the same level are sediment binders and frame builders in other, possibly wave-resistant, early Paleozoic buildups (Pitcher, 1964; Toomey and Ham, 1967; Toomey and Nitecki, 1969), which further supports the conclusion that these sediments were deposited in progressively shallower water.

The sponge-oncolite biostrome is similar to a sponge-algal facies described by Alberstadt and Repetski (1989) in Lower Ordovician carbonates in the southern United States. The lateral distribution of those deposits, between restricted shelf carbonates and deep-water clastics, in contrast, indicates they formed in an outer shelf or deep-ramp setting.

4.4.2 Echinoderm-algal Limestone (Lithofacies 11, Table 4.1)

This lithofacies includes both grain-supported and lesser mud-supported limestone rich in echinoderm debris and a variety of calcareous algae (Figure 4.5.f,g). Profuse echinoderms suggest clear,

shallow, normal marine waters (Broadhead and Waters, 1980). Shallow depth is also indicated by the algae - Nuia, dasyclads, and Girvanella, which collectively suggest depths of less than 10 m (Stricker and Carozzi, 1973; Wilson, 1975; Wray, 1977; Ross et al., 1988). Muddy packstone and echinoderm-algal wackestone are interpreted as in situ accumulations of skeletal debris and baffled sediment on a crinoid, cystoid and Nuia covered seafloor where currents and/or waves were less effective than burrowers at reworking the sediment. Clean echinoderm sands are interpreted as current or wave winnowed accumulations in adjacent, shallower water flats.

4.4.3 Stromatactis Mound (Lithofacies 12, Table 4.1)

Massive, mottled, muddy Stromatactis mounds, previously unrecognized in the Table Point, occur at the top of the formation at Piccadilly (Port au Port Peninsula) and on Burnt Island (Pistolet Bay) (Figures 4.5.h,i and 4.6). More widespread development on the platform, however, is indicated by occurrences of mound limestone clasts in Daniel's Harbour Mbr. conglomerates (Chapter 9).

The well-exposed mound at Piccadilly is ~35 m thick and at least 150 m wide (Figure 4.6). Its absence from nearby outcrops demonstrates that it is less than 10 km wide in east-west cross-section. Detailed sedimentology and diagenesis of this buildup is documented by Stenzel and James (in press). The mound on Burnt Island is similar in composition, texture, fabric, and diagenetic features, but limited exposure (only the top 80-100 cm in an area a few tens of metres square) precludes the same degree of analysis.

These buildups are envisaged as isolated, shallow subtidal to intertidal islands of mud, similar in disposition if not origin to mud mounds currently forming in Florida Bay (Bathurst, 1975; Enos and Perkins, 1979; Boscence et al., 1985). Fenestral limestone and peloidal grainstone underlying and at the base of the Piccadilly mound indicate nucleation on a topographic high. Synsedimentary fracturing of basal

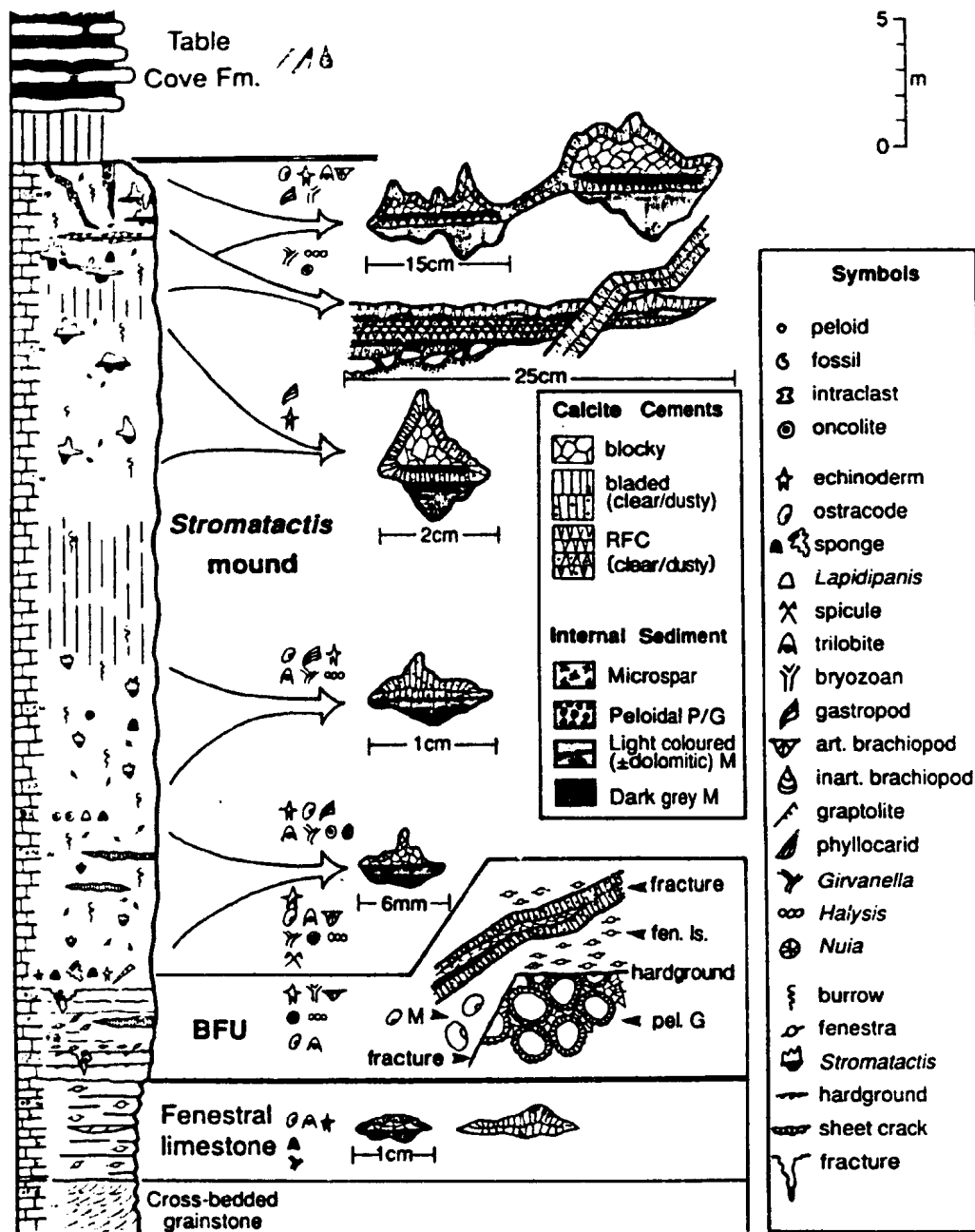


Figure 4.6 Schematic section through the *Stromatactis* mud mound at Piccadilly (from Stenzel and James, in press). BFU = basal fractured unit; vertical lines represent poorly-exposed or covered intervals. Sketches to the right show stratigraphic changes in cavity size and morphology, and in internal sediments and cements that fill them. Location is shown in Figure 1.3.

mound sediments is interpreted to have been caused by displacements on a nearby fault, suggesting that local topography was structurally controlled. Compositional, textural and biotic attributes indicate mound growth continued under shallow, somewhat restricted, low energy conditions. Sediment accumulation was influenced by stalked echinoderms, sponges, and algae on the mound surface that baffled currents and trapped fine sediment, and by algal-microbial mats, masses or films that trapped and bound the sediment and probably played an active role in early lithification (Monty *et al.*, 1982; Bridges and Chapman, 1988).

Pervasive early lithification of mound sediments is indicated by the general absence of evidence of compaction and is demonstrated by early marine cements, hardgrounds, internal sediment- and cement-filled Stromatactis, sheet cracks and synsedimentary fractures. The distribution of marine cements within some Stromatactis cavities indicate precipitation in the vadose zone and prove that the mound was at times exposed.

The origin of Stromatactis in the mounds cannot be attributed to a single mechanism. Small, classical Stromatactis cavities could have originated as shelter pores, as decayed algal material or sponges, or as partially filled burrows (eg. Pratt, 1982; Shinn, 1968; Bourque and Gignac, 1983), but their final size, shape and distribution appears to have been controlled by sediment texture and the amount and volume of water flushing through the sediment (eg. Wallace, 1987), both ultimately determined by tidal current and/or wave activity on the mound surface. Up-through-the-mound increase in the size and complexity of these structures indicates increasingly agitated, probably shallower conditions. Sheet-like Stromatactis associated with high-angle, synsedimentary fractures at the top of the mound, in contrast, are interpreted to have originated as fractures generated by slumping or nearby faulting.

4.4.4 USU Mineralized Hardground

Echinoderm-algal limestone and Stromatactis mound limestone at the

top of the Table Point exposed around Pistolet Bay are locally mantled by a thin (<4 cm), resistant, orange-weathering, phosphatic, siliceous, dolomitic and pyritic crust (Figure 4.5.b). Uppermost limestones of both lithofacies are invariably syndimentarily fractured and/or veneered by conglomeratic limestone, and are abruptly overlain by Black Cove Formation shale (Chapter 7). Orthoconic and coiled cephalopods are conspicuously concentrated with other skeletal debris in echinoderm-algal limestones immediately beneath the crust. Uppermost Stromatactis mound limestones are cross-cut by sub-vertical burrows or borings filled with black shale or shaley pseudospar.

Relationships among the mineral phases seen in thin-section indicate phosphatization occurred before silicification and dolomitization. Silicification either preceded or occurred at the same time as dolomitization. All three phases predate shale deposition. The timing of pyrite formation is not constrained and may have occurred before, during, and/or after the other minerals formed.

Phosphatization of the limestones is compelling evidence that crust is a submarine hardground that formed during a period of little or no sediment accumulation (Bathurst, 1975; Kennedy and Garrison, 1975; Read and Grover, 1977). Accumulations of pelagic cephalopods in the sediments just beneath the crust are also indicative of a condensation horizon (Wendt, 1973; Wendt and Aigner, 1985). Phosphate formation requires a high concentration of organic matter and is favoured in poorly-oxygenated environments (Bromley, 1967; Baturin, 1982). Therefore, phosphatization is interpreted to have occurred after carbonate sedimentation in shallow water ceased and during subsidence of the platform to a depth at which it intercepted dysaerobic water.

The intimate association of microquartz and dolomite suggests the two minerals formed at nearly the same time. Both mineral phases are interpreted as expressions of continued nondeposition and hardground formation. Silicification may have resulted from longterm exposure to

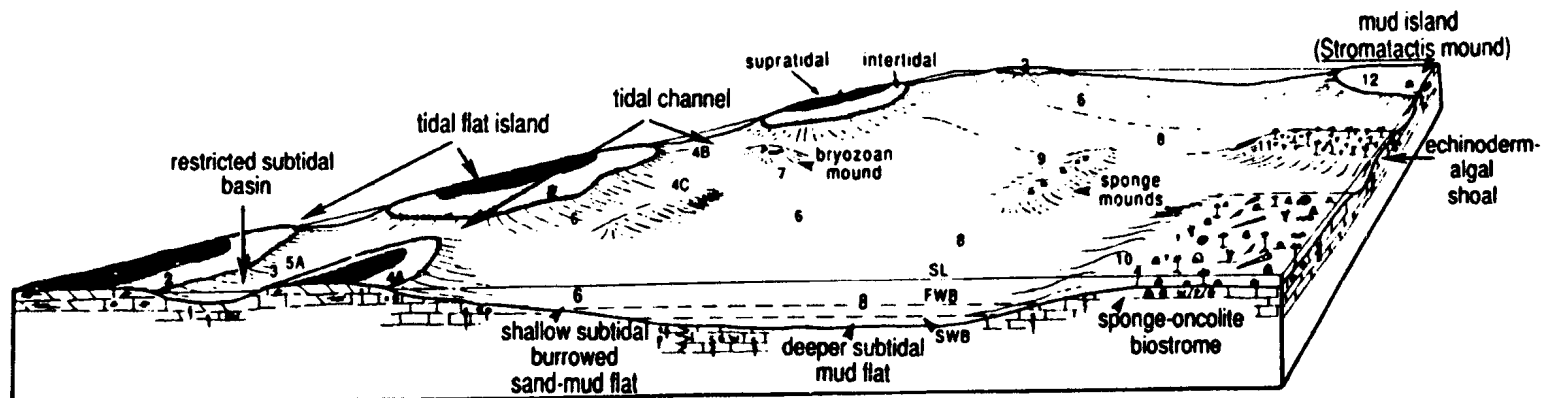
silica saturated basinal waters or from redistribution of biogenic silica (ie. radiolarians, spicules) that accumulated during subsidence. Dolomite may have precipitated directly from seawater or reducing pore waters (Marlowe, 1971; Baker and Burns, 1985; Coniglio and James, 1988), or formed during silicification (Jacka, 1974).

Relationships between the hardground and deformation structures at the top of the Table Point are discussed in Chapter section 12.1.4.

4.5 Summary and Reconstruction of Depositional Environments

The Table Point Formation records deposition in several shallow marine and marginal marine environments (Figure 4.7). Fossil-poor limestones and dolostones deposited above the St. George Unconformity and comprising the Basal Peritidal Unit were deposited in a complex of shallow subtidal, intertidal and supratidal environments. Restrictions imposed by limited circulation, abnormal seawater salinity, and/or exposure precluded inhabitation of most environments by a diverse taxa. Predominance of fenestral tidal flat limestone, paucity of early dolomite, and absence of evaporites indicate sedimentation under humid climatic conditions (Read and Grover, 1977; Hardie and Shinn, 1986). Overall less restrictive environmental conditions than are inferred for underlying Aguathuna Formation carbonates further suggest improved marine circulation across the platform during this time.

Overlying limestones comprising the Middle Subtidal Unit were deposited in wholly subtidal, normal marine environments (Figure 4.7). Burrowed, muddy, peloidal sands accumulated in relatively shallow water, probably above normal wave base. Bioturbated, fossiliferous muds were deposited in deeper environments below normal wave base, where consistently low energy conditions permitted accumulation of large volumes of mud. Small sponge bioherms formed on the muddy sea bottom during periods of shoaling. Stratigraphic relationships between the two main subtidal lithofacies indicate deepening-upward, but the absence of



- | | | |
|---------------------------|----------------------------|------------------------------|
| 1 cryptalgal dololaminite | 5 restricted wackestone W | 9 sponge bioherm |
| 2 fenestral ls. | 6 burrowed peloidal P | 10 sponge-oncolite biostrome |
| 3 burrowed dolostone | 7 bryozoan bioherm | 11 echinoderm algal ls. |
| 4 cross-bedded peloidal G | 8 burrowed fossiliferous W | 12 <u>Stromatactis</u> mound |

Figure 4.7 Schematic reconstruction of depositional environments recorded by the Table Point Formation. Peritidal, subtidal, and shoal water environments for Basal Peritidal (BPU), Middle Subtidal (MSU), and Upper Subtidal (USU) lithofacies, respectively, are shown as laterally equivalent in order to illustrate variable water depth and are not meant to depict a cross-section across the platform at any given time. Numbers correspond to those for lithofacies in Table 4.1. Key to symbols is in Appendix A.

systematic changes in the style of storm beds in the deeper-water, fossiliferous wackestone lithofacies indicates that those sediments were not deposited under ever increasing water depth.

Youngest platform limestones comprising the Upper Subtidal Unit were deposited in shallower settings than underlying subtidal deposits (Figure 4.7). A sponge-oncolite biostrome formed locally in the shallow subtidal at depths of persistent but gentle currents and waves, where optimum conditions of water depth, water movement and salinity allowed proliferation of sponges, a diverse assemblage of calcareous algae, a variety of epifaunal invertebrates, and a soft-bodied infauna. In other areas crinoids, cystoids and a variety of short, stalked, calcareous algae flourished in shallow subtidal meadows on the seafloor. Muddy, echinoderm-algal sediments accumulated in situ; clean, echinoderm-algal sands were transported and reworked by currents and/or waves on adjacent, shallower water flats. In isolated areas large volumes of muddy sediment accumulated in low relief mounds that episodically accreted to or were uplifted to sea level. Peculiar hydrodynamic conditions must have dictated nucleation of these buildups. Continued growth was controlled by biotic components of the mound, especially algal-microbial mats, masses or films that acted to trap and bind the sediment and played an active role in early, pervasive lithification.

4.6 Discussion

Table Point Formation sequences record inundation of the exposed platform and deposition in restricted, peritidal environments, followed by deepening and deposition in the wholly shallow, subtidal settings and, finally, late stage shoaling of the platform (Figure 4.8.a). These changes in relative sea level show some correspondence to both the sea level curve interpreted from late Early and early Middle Ordovician strata around Canadian North America (Barnes, 1984) and that interpreted from same age strata in the southwestern U. S. A. (Ross *et al.*, 1989)

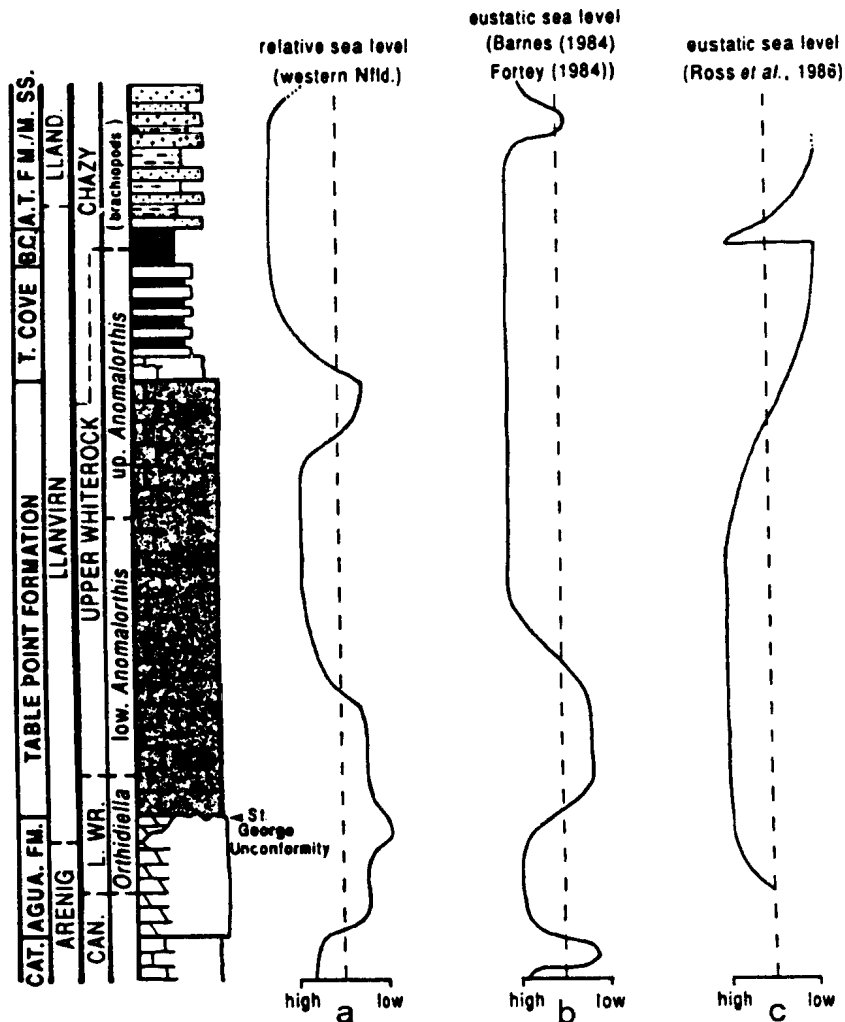


Figure 4.8 Sea level curves for the late Early to Middle Ordovician in North America. a) Interpretive sea level changes based on sedimentology of the Lower and Middle Ordovician sequence in Newfoundland. b) Sea level curve based on sedimentology of coeval strata elsewhere in Canada, and on displacements of shelf, island and oceanic graptolite faunas in Ordovician strata in North America, Europe, and Australia. c) Eustatic curve interpreted for coeval sedimentary rocks in Nevada deposited on the passive margin of North America. Cat., Catoche Fm.; T. Cove, Table Cove Fm.; B.C., Black Cove Fm.; A. T., American Tickle Fm.; M. SS., Mainland Sandstone; Llan., Llandello; Can., Canadian (= Ibexian), L. WR., lower Whiterock (North American stages). Brachiopod zonation is from Ross and James (1987); the position of the lower - upper *Anomalorthis* zone is approximate.

(Figure 4.8.b,c). The former, however, was constructed without consideration for probable tectonic influences on sea level changes, hence sedimentation, so its value as a eustatic signal is suspect. Ordovician sediments in Nevada, however, are interpreted to have been deposited on a passive continental margin of North America, and so sea level changes are inferred to be primarily eustatic.

There is no counterpart in Newfoundland to initial (earliest Whiterock), rapid sea level rise and platform flooding recorded in Nevada. That period of time coincides with 1) the St. George Unconformity, and/or (2) deposition of middle and upper Aguathuna Formation dolostones, and/or (3) deposition of basal peritidal Table Point limestones. Both Aguathuna and Table Point peritidal carbonates indicate that the platform was not nearly drowned, but was a site of very shallow marine sedimentation where sediments periodically accreted to sea level. Effects of eustatic sea level rise, however, may be recorded by MSU limestones which indicate widespread establishment of shallow subtidal environments. Also, late stage shoaling of the Table Point platform appears to correlate with sea level fall and progradation on the passive margin in Nevada. USU limestones could similarly reflect a decrease in the rate of sea level rise that allowed vertical accretion of the platform and deposition in progressively shallower water.

4.7 Signatures of Convergent Margin Sedimentation

Table Point Formation limestones are compositionally and texturally similar to other ancient and modern platform carbonates. Perception of possible eustatic controls on sedimentation further suggests deposition on a passive margin experiencing uniform, thermal subsidence. There are, however, several anomalous features which indicate that the Table Point was deposited on an unstable platform where sedimentation was profoundly influenced by regional and local tectonics: 1) local subaerial erosion and dissolution surfaces in the BPU; 2) gravitational

slides in BPU, MSU, and USU lithofacies; 3) gravitational slides, sediment gravity flow deposits, and synsedimentary, tectonic fractures at the top of the platform; 4) great lateral variation in the thickness of the formation and of the lithofacies assemblages which comprise it; 5) nondirectional variation in the lithofacies make-up of BPU sequences, abrupt changes in the style of peritidal sedimentation, and anomalous, shallowing-upward, depositional sequences. These are described, illustrated and discussed in Part II: Sedimentation and Tectonics, Chapter 12.

CHAPTER 5
SEDIMENTOLOGY OF THE TABLE COVE FORMATION

5.1 General Characteristics and Stratigraphic Relationships

The Table Cove Formation consists of thin-bedded, muddy, grey limestone and partings or thin interbeds of calcareous shale which are commonly slump-folded, imbricated or conglomeratic. In many places these strata gradationally overlies shallow subtidal limestones of the Table Point Formation (Chapter 4), but the formation is highly variable in thickness, ranging from as little as 9 m to 126 m (Figure 5.1), and locally is not present in the stratigraphic sequence. Where it is present it is most commonly gradationally overlain by Black Cove Formation shale (Chapter 7) (Figure 5.1); locally it is directly overlain by coarser-grained lithofacies of the American Tickle Formation (Chapter 8).

Table Cove sequences are represented by three lithofacies: the burrowed limestone lithofacies and parted limestone lithofacies, both of which occur at the base of the formation, and the ribbon limestone lithofacies which occurs at the top (Figure 5.2). In all sequences limestones change from burrowed and fossiliferous, to laminated or massive and fossil-poor, and shale becomes increasingly abundant up section. Outcrop, compositional, and diagenetic characteristics of each lithofacies are detailed in Table 5.1. The reader is referred to Figure 1.2 for locations of sections cited in the following text.

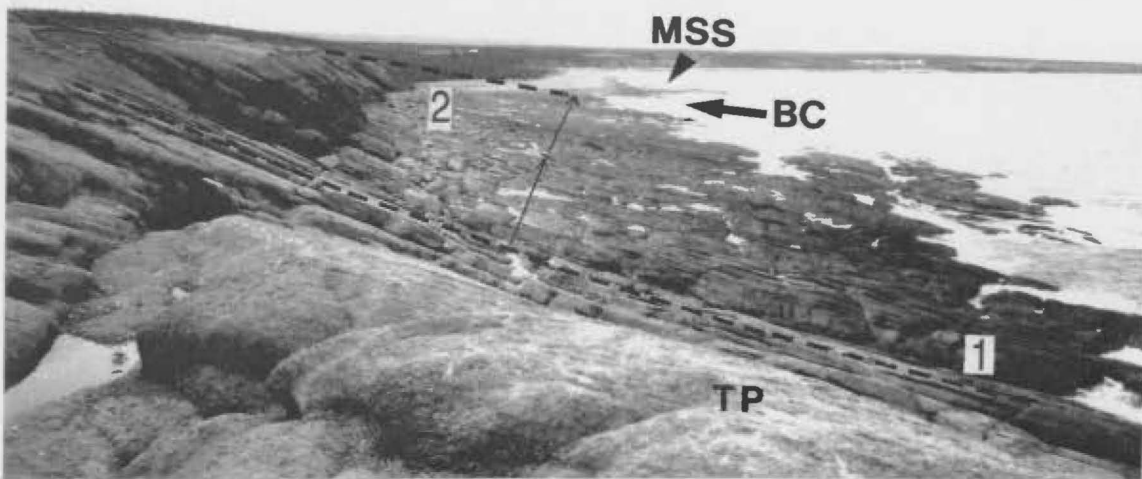
5.2 Burrowed Limestone Lithofacies (Lithofacies 1 in Table 5.1)

This lithofacies is composed mostly of thin-bedded, medium to dark grey, muddy, burrowed, fossiliferous limestone with millimetre-thick, argillaceous partings (Figures 5.2 and 5.3.a-c). These strata occur at the base of the Table Cove, gradationally overlying USU platformal limestones of the Table Point Formation (Chapter section 4.4) at most localities (eg. Figures 5.1 and 5.3.a). They are differentiated from

Figure 5.1 Table Cove Formation. a) Overview of the 93 m thick formation sequence (between dashed lines) from the top of the Table Point Formation at Table Point. b) Outcrop of the 9 m thick Table Cove Formation at Black Cove. A. Pye (arrow) for scale. TP, Table Point Formation; 1, burrowed limestone lithofacies; 2, ribbon limestone lithofacies; BC, Black Cove Formation; AT, American Tickle Formation; MSS, Mainland Sandstone; DH, Daniel's Harbour Member calcarenite.

Figure 5.1

a



b



Table Cove Formation Lithofacies

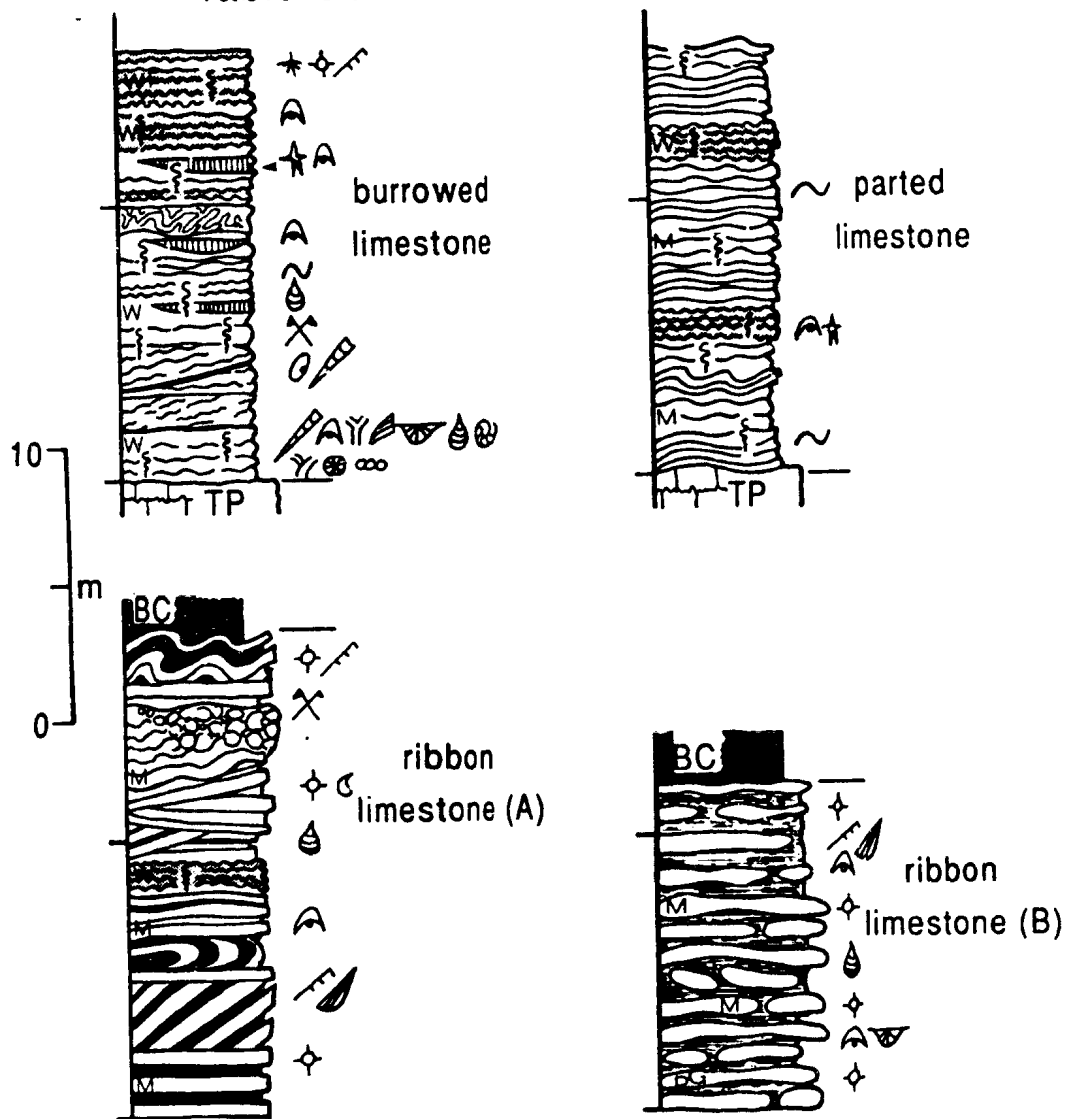


Figure 5.2 Schematic summary of Table Cove Formation lithofacies. Shaded bedding represents dark grey, trilobite-rich limestone. Key to other symbols is in Appendix A.

Table 5.1 Table Cove Formation Lithofacies: outcrop appearance, depositional and diagenetic characteristics, and interpretation. Interpretations of depositional environment based on comparison with both modern and other ancient, deep-water slope and basin margin carbonate sequences as documented by Cook and Enos (1977) and papers therein, Keith and Freidman (1977), Cook (1979), Cook and Mullins (1983) and references therein, McIlreath and James (1984), Mullins *et al.* (1984), Coniglio (1985), James and Stevens (1986), Brooks and Holmes (1990), Watts and Blome (1990).

Composition: M=mudstone, W=wackestone, P=packstone, G=grainstone, R=rudstone, F=floatstone; pel.=peloidal, fossil.=fossiliferous, intra.=intraclastic, congl.= conglomerate, clast-sup.=clast-supported, mtx.-sup.=matrix-supported, mtx.-poor(-rich)=matrix-poor(-rich), f.-cryst.=finely-crystalline, c.-cryst.=coarsely-crystalline, dolo.=dolomite; silic. silt=siliciclastic silt, glauc.= glauconite, musc.=muscovite, bio.=biotite, feld.=feldspar, volc. lithic=volcanic lithic; det.=detrital, auth.=authigenic, argil.=argillaceous, ls.=limestone

Structures: lam.=lamination, hor.=horizontal, par.=parallel, subhor.=subhorizontal, subvert.=subvertical, struc.=structure, dia.=diameter, cross-lam.=cross-lamination, trunc.=truncation; nor. graded=normally graded.

Fossils: ostra.=ostracode, gastro.=gastropod, art.(inart.) brach.=articulate (inarticulate) brachiopod, trilo.=trilobite, echin.=echinoderm, ortho.(coiled) ceph.=orthoconic (coiled) cephalopod, bryo.=bryozoan, spic.=spicules; lith. sponge= lithistid sponge (glob.=globular, disc.=discoidal, cylind.= cylindrical), radio.=radiolarian, grapt.=graptolite, phyllo.= phyllocarid, lg.=large, v. small=very small, skel.=skeletal, invert.=invertebrates

Algae: onco.=oncolite, calc. algae=calcareous algae, dasyclad.=dasycladacean alga

Diagenesis: pres. diss.=pressure dissolution, stylo-nod.=stylo-nodular, pseudo-congl.=pseudo-conglomeratic, bdg.= bedding, agg. neomorph.=aggrading neomorphic

DRZM=Daniel's Harbour Zinc Mine, WBCQ=West Bay Centre Quarry

The symbol (*) denotes the predominant lithology, sedimentary structure, development of burrowing, or fossils which for the case of fossil-poor sediments does not mean abundant.

Base⁺ refers to base of the lithofacies sequence; Top⁺⁺ refers to the top of the lithofacies sequence.

Table 5.1 Table Cove Formation Lithofacies
1) BURROWED LIMESTONE LITHOFACIES

Lithologies	Colour, Bedding and Thickness	Physical Sedimentary Structures	Biogenic Structures	Skeletal Components	Diagenetic Features	Depositional Environment
<p>1) Medium grey, muddy limestone</p> <p>- fossil-poor M, - fossiliferous W, - muddy, fossiliferous P</p>	<p>medium to dark grey, thin (1-5 cm), stylo-nodular bedding</p>	<p>none</p>	<p>bioturbated*; small (2-4 mm dia.), subhor. to subvert., microsparitic or sparry calcite-filled burrows; <u>Planolites</u> (3-10 mm dia.) and small <u>Chondrites</u> (0.5-1 mm dia. tunnels) locally</p>	<p>fragments of echino.*, bryo.*; art. brach.*, ostra.*, small gastro.*, sponge spic.*, <u>Halysis</u>*, <u>Girvanella</u>*, <u>Nuia</u>*, unnamed dasyclad.; rare sponges; large lingulids; diverse assemblage of trilobites; scattered ortho. and coiled ceph.; radio. and grapt. near the top⁺⁺</p>	<p>matrix-rich, pressure dissolution generated, stylo-nodular bedding auth. pyrite, quartz & albite</p>	<p><u>In situ</u> accumulation of carbonate mud and skeletal debris on a relatively shallow, well-oxygenated, upper slope</p>
<p>2) Dark grey, trilobite-rich limestone</p> <p>- fossiliferous, peloidal W/F - muddy, fossiliferous P/R</p>	<p>dark grey to black, very thin (0.5-1.5 cm), knobbly bedding; isolated thin beds near base⁺ & units a few 10s of cm to 2 m thick near top⁺⁺</p>	<p>none</p>	<p>bioturbated*</p>	<p>similar to Lithology 1 plus abundant large fragments (1-3 cm) of illaenid trilobites and coarse echino. debris</p>	<p>pres. diss. - generated, matrix-rich, stylo-nod. to pseudo-congl. bdg.; pervasively replaced by c. cryst. pseudospar; abundant pyrite; strong petroliferous odor from fresh broken surfaces</p>	<p>platform-derived, organic-rich sediments transported and deposited by gravity currents or flows? onto the upper slope</p>

1) BURROWED LIMESTONE LITHOFACIES continued (Table 5.1 continued)

Lithologies	Colour, Bedding Style and Thickness	Physical Sedimentary Structures	Biogenic Structures	Skeletal Components	Diagenetic Features	Depositional Environment
<p>3) Echino-germ-rich, skeletal sand</p> <p>- fossiliferous, peloidal, intraclastic P/F and G/R</p>	<p>medium grey, 1-25 cm thick lenses; isolated or stacked to form diffuse sand bodies</p>	<p>erosional bases & flat tops; some with rippled (5-15 cm λ) tops; hor. lamination, shelter porosity & infiltration fabrics in some beds</p>	<p>partly burrowed* to bioturbated</p>	<p>echino. debris* & lg. fragments of illaenid and other trilobites*; lingulid valves, fragments of art. brach. and bryo., small gastro., ostra. & <u>Girvanella onco.</u></p>	<p>patchy to pervasive replacement of micritic components by coarsely-cryst. pseudospar; skel. fragments concentrated in press. diss. seams between ls. layers</p>	<p>platform-derived sediment episodically transported and deposited by storm-generated bottom currents onto the upper slope; locally reworked by persistent bottom currents</p>
<p>4) Limestone Conglomerate (DH-1516 only)</p> <p>- clast-sup., mtx.-poor (<10%), pebble-grade (2-5 cm) congl.; clasts are very fossiliferous, peloidal u*</p>	<p>medium grey; massive; 4 m thick</p>	<p>none</p>	<p>none; clasts preserve bioturbate textures</p>	<p>none in conglomerate; clasts with abundant fragments of shelly fossils like those in Lithology 1 and in Table Point Fm. platform limestones (see Table 4.1)</p>	<p>stylolites and/or thin, argillaceous pres. diss. seams between clasts</p>	<p>partly lithified, upper slope- or platform-derived carbonate sediment transported and deposited by debris flow; triggered by seismicity or nearby faulting</p>
<p>5) Bentonite (DH2M cores & WBCO and Black Cove sections)</p>	<p>light grey or white; recessive-weathering; 2.5-8 cm thick</p>	<p>none</p>	<p>none</p>	<p>none</p>	<p>----</p>	<p>volcanic ash layer deposited by suspension settling through the water column</p>

2) PARTED LIMESTONE LITHOFACIES Table 5.1 continued

Lithologies	Colour, Bedding Style and Thickness	Physical Sedimentary Structures	Biogenic Structures	Skeletal Components	Diagenetic Features	Depositional Environment
<p>1) Parted limestone</p> <p>limestones: fossil-bearing M* & lesser fossiliferous, peloidal W</p>	<p>limestones: light grey; 1-10 cm thick, planar wavy and wavy nodular limestone beds</p>	<p>none in ls.</p>	<p>ls. bioturbated*; burrows defined by quartz silt stringers or small tubes (2-4 mm dia.) of pseudospar (agg. neomorph. fabrics developed toward burrow centres that contain a small amount of argil. sediment), blocky calcite cement, micrite, or pyrite;</p> <p><u>Taenidium</u>, <u>Palaeophycus</u>, <u>Chondrites</u>, <u>Ichnogona</u> <u>incertae</u></p>	<p>M with fragments of thin-walled trilo.*, small (<0.5 mm) ostra.*, small articulate brach.*, radio.*; echino., sponge spic., lacy bryo., gastro., & calc. algae typical of Table Pt. Fm. platform limestones; scattered trilo., ortho. ceph. & lg. lingu-lids (3-10 mm)</p>	<p>limestones partly altered to pseudospar; abundant disseminated pyrite and pyrite-replaced skeletal fragments in W beds; limestone bed margins with aggrading neomorphic fabric or with stylolite at limestone-parting contact</p>	<p>mostly hemipelagic carbonate sediment and lesser autochthonous carbonate deposited in a relatively deep (below normal wave base), low energy, well-oxygenated to dysaerobic, lower upper slope or middle slope environment</p>
<p>dolomitic shale partings: clay, f.-cryst. dolomite (5-15 μm), with scattered coarse (25-60 μm) euh. dolomite, silic. silt & small skel. fragments</p>	<p>dolomitic shale: dark brown; recessive-weathering; 2-10 mm thick partings</p>	<p>dolomitic shale with compaction-generated bedding-parallel foliation defined by elongate skeletal fragments</p>	<p>none in shale</p>	<p>W similar, also with trilo., echino., stick bryo., small high-spined gastro. debris concentrated with lg. and small ortho. and coiled ceph., articulate brach., glob., disc., & cylind. lith. sponges in 30-40 cm dia. 'build-up.'</p>		

2) PARTED LIMESTONE LITHOFACIES continued (Table 5.1 continued)

Lithologies	Colour, Bedding Style and Thickness	Physical Sedimentary Structures	Biogenic Structures	Skeletal Components	Diagenetic Features	Depositional Environment
<p>2) Dark grey, trilobite-rich limestone</p> <p>- similar to same named lithology in Lithofacies 1</p>	<p>similar to same named lithology in Lithofacies 1</p>	<p>none; orthocone cephalopods aligned on some bedding planes</p>	<p>bioturbated*</p>	<p>similar to same named lithology in Lithofacies 1; also with common to abundant fragments of stick bryo., articulate brach., osia., <u>Muia</u>, radio., <u>Maclurites</u>, <u>Merchisoni</u>, other small, high-spined gastro.; lith. sponges (to 15 cm dia.) & spiculitic sponge holdfasts, ortho. ceph. (30-120 cm long) & coiled ceph. (2-20 cm dia.)</p>	<p>similar to same named lithology in Lithofacies 1</p>	<p>organic-rich, platform-derived carbonate sediments transported and deposited on the lower upper slope or mid-slope by gravity currents or flows</p>

3) RIBBON LIMESTONE LITHOFACIES (TYPE A) (Table 5.1 continued)

Lithologies	Colour, Bedding Style and Thickness	Physical Sedimentary Structures	Biogenic Structures	Skeletal Components	Diagenetic Features	Proositional Environment
<p>1) Ribbon limestone</p> <p>limestone: - fossil-poor &/or peloidal W* - fossil-bearing M* - rare fossiliferous, peloidal P/R near base**</p> <p>calcareous shale interbeds: variable amounts of clays, auth. dolo. (5-60 μm), auth. & det. quartz & albite, small skel. fragments; minor musc., biot., chlor., glauc., CaPO₄, feld., and volc. lithic fragments near top**; decrease in dolo. content (80-30%) and increase in silic. silt content (5-20%) up-section</p>	<p>limestone: dark grey brown; 1-15 cm thick; tabular beds with planar contacts; pinch out laterally over several 10s of metres</p> <p>shale: dark brown to black; yellow and recessive-weathering; few mm to 30 cm thick</p>	<p>M/W: structureless near base*; par. lam. & thin bdg. (few mm - 2 cm thick) defined by abundance of peloids, quartz silt, radio., pyritic skel. grains or by different neomorph. calcite crystal sizes near top**; P/R layers: erosional bases, nor. grading, aligned skel. fragments, shelter pores and infiltration fabrics</p> <p>shale: massive or with weak foliation defined by elongate skel. fragments near base*; compaction foliation or fine, argil. and silty lam. near top**</p>	<p>limestones: rare horizontal and vertical neosparitic burrows, burrows defined by stringers of quartz silt, & small <u>Chondrites</u> present locally near base*</p> <p>none in shale interbeds</p>	<p>M & W with small (<1 mm) fragments of shelly, shallow-water invert. & calc. algae (cf. Lithofacies 1, lithology 1) plus ?indigenous lingulids, thin-walled trilo., small art. brach., radio. & grapt.</p> <p>P/R similar</p> <p>shale with fragments of & intact grapt., phyllo., olenid, nielid, endymionid & telephinid trilo., small (few mm) inert. brach; rare small (6-10 mm) art. brach.</p>	<p>carbonate mud invariably re-crystallized to microspar (3-5 μm) with agg. neomorph. fabrics toward bed margin (50-80 μm); minor (<10%) silt-size auth. & det. quartz & albite, & auth., nonfer. dolomite</p>	<p>mostly platform-derived, hemipelagic and lesser turbiditic sediment deposited in a deep (below normal wave base), quiet water, poorly-oxygenated, lower slope to basin margin environment</p>

3) RIBBON LIMESTONE LITHOFACIES (TYPE A) continued (Table 5.1 continued)

Lithologies	Colour, Bedding Style and Thickness	Physical Sedimentary Structures	Biogenic Structures	Skeletal Components	Diagenetic Features	Depositional Environment
<p>2) Dark grey, trilobite-rich limestone</p> <p>- fossiliferous W and F</p>	similar to same named strata in Lithofacies 1 and 2; 10-80 cm thick	none	bioturbated*	similar to same named strata in Lithofacies 1 and 2	similar to same named strata in Lithofacies 1 and 2	same as for dark grey, trilobite-rich limestones in Lithofacies 1 and 2, but deposited in a lower slope - basin margin environment
<p>3) Limestone conglomerate</p> <p>Vaches Point: mtx.-poor, clast-sup., pebble-grade (1-5 cm) with scattered cobbles, boulders & megaboulders?; clasts mostly bur. fossil. W & fossil. pel. P/G; minor (<2%) echino. G/P, M plates and calc. shale patches (ie. ribbon ls.)</p> <p>DH-1382: poorly-sorted, clast-sup. & mtx.-sup., pebble-grade congl.; clasts mostly fossil., pel., conco. W/P</p>	<p>light to medium grey; massive-weathering; (three congl.) 5-22 m thick</p> <p>medium to dark grey; (nine beds) 5 cm to 4 m thick</p>	<p>none</p> <p>none</p>	<p>none; clasts preserve bioturbate textures</p> <p>none in conglomerates; clasts preserve bioturbate textures</p>	<p>none in conglomerates; clasts with fragments of shelly fossils as in MSU and USU lithofacies limestones of the Table Point fm. (cf. Table 4.1)</p> <p>none in congl.; clasts with fragments of shelly fossils & grains as in Table Pt. fm. sponge-onco. biostrome (Table 4.1) and Lithofacies 1</p>	<p>stylolitic contacts between clasts; minor interclast coarsely-cryst. blocky calcite cement</p> <p>stylolitic contacts between clasts in matrix-poor conglomerate beds</p>	<p>partly lithified, platform- & upper slope-derived carbonates transported and deposited by debris flows onto the lower slope / basin margin; probably originating from fault-generated escarpments that exhumed shallowly buried sediments</p>

3) RIBBON LIMESTONE LITHOFACIES (TYPE B) (Table 5.1 continued)

Lithologies	Colour, Style and Thickness of Bedding	Physical Sedimentary Structures	Biogenic Structures	Skeletal Components	Diagenetic Features	Depositional Environment
<p>1) Ribbon limestone limestones: fine-grained, peloidal, spiculitic P/G and radiolarian M/W either 1) forming discrete beds, 2) thinly-interbedded, or 3) arranged in nor. graded couplets (few mm to few cm thick)</p> <p>dolosiltite interbeds: variable amounts of clay, auth. nonferroan dolo. and quartz; alternating siliceous laminae¹ & argillaceous laminae² correspond to peloidal P/G and radio. M/W layers in limestones</p>	<p>limestones: dark grey-brown; continuous layers (1-15 cm thick) defined by discontinuous hummocky strips or plates (20-50 cm across) that appear as cigar-shaped nodules (10 cm to several m long) in cross-section</p> <p>dolosiltite: dark brown, light green-weathering; 1-15 cm, rarely to 30 cm thick</p>	<p>P/G massive or massive to par.-laminated; some nor. graded; rare fluid escape struct.; M/W layers massive or with lam. defined by radio. or grapt. or very thin beds defined by different neomorphic calcite cryst. size or abundance of fossils</p> <p>dolosiltite: fine par. & low-angle lam.; local ripple-scale cross-lam., low-angle truncations, small-scale soft-sed. folds & faults, & convolute lam.; siliceous laminae¹ with current aligned spicules</p>	<p>minor burrowing & very small (<5 mm dia.) burrows near base defined by concentrations of pyrite</p> <p>none in dolosiltite</p>	<p>P/G: calcite-replaced or siliceous sponge spic., calcite-replaced radio., & v. small (<0.5 mm) fragments of trilo., echino., ostra., <u>Halysis</u>, <u>Nuia</u>, & <u>Girvanella</u>; grapt. & phyllo. M/W with radio., grapt., phyllo., <u>Konyrium</u>³ intact trilo., small art. brach., inart. brach.</p> <p>dolosiltite: abundant grapt., phyllo. & inart. brach. (current aligned on some surfaces)</p>	<p>carbonate mud recrystallized to fine (20-60 μm) pseudospar with aggrading neomorphic fabrics toward bed margins (50-200 μm); minor silt-size auth. quartz & nonfer. dolo.</p>	<p>platform-derived and lesser wholly pelagic material transported and deposited from turbidity currents and suspensions onto a deep (below normal wave base), quiet water, poorly-oxygenated, lower slope to basin margin environment adjacent to a by-pass margin</p>

3) RIBBON LIMESTONE LITHOFACIES (TYPE B) continued (Table 5.1 continued)

Lithologies	Colour, Style and Thickness of Bedding	Physical Sedimentary Structures	Biogenic Structures	Skeletal Components	Diagenetic Features	Depositional Environment
2) Bentonite (WBCO & Black Cove sections only)	light greenish grey, recessive-weathering; 1-12 cm thick	none	none	none	----	altered volcanic ash deposited by suspension settling through the water column

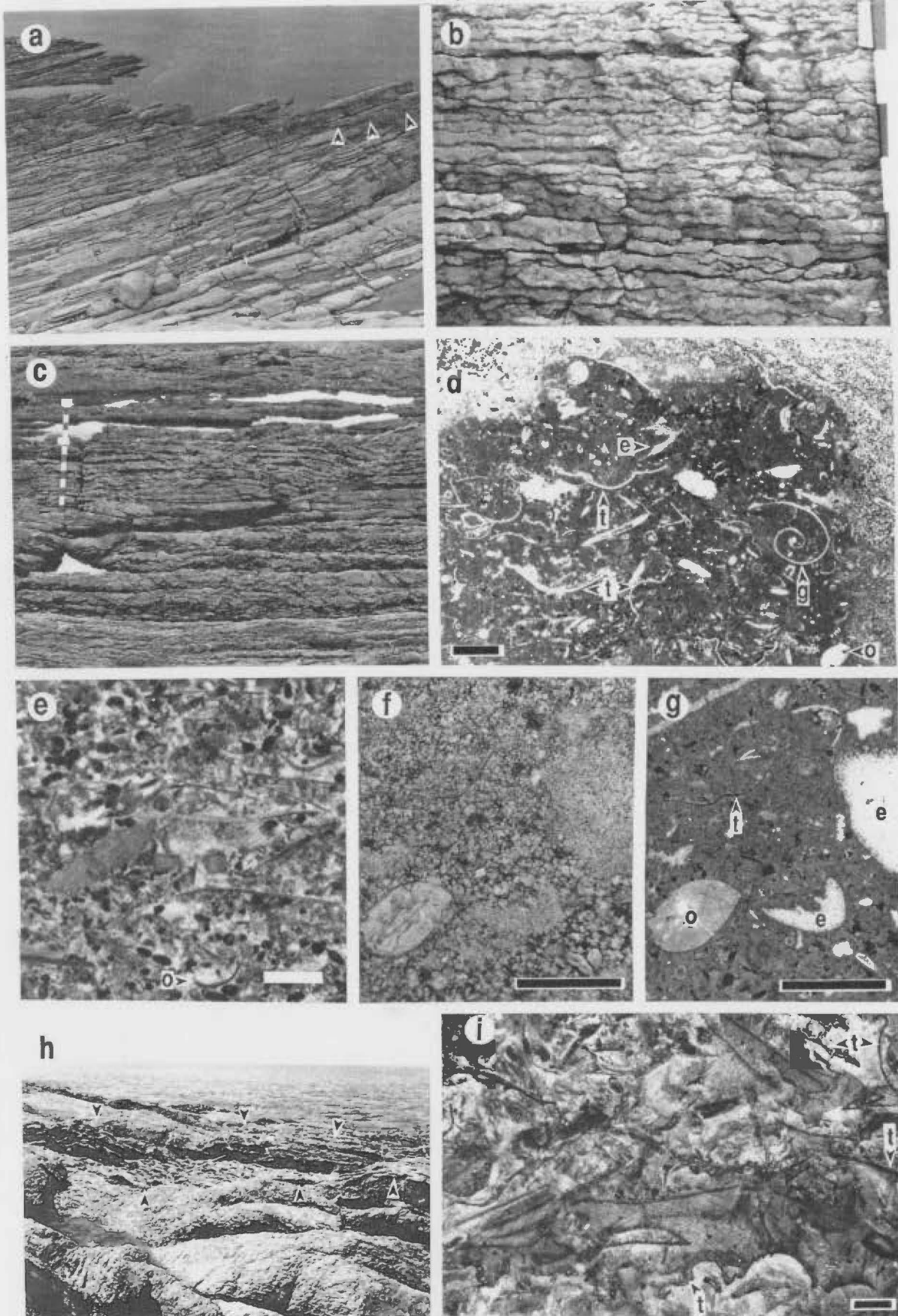
¹ - siliceous laminae are light grey, clay-poor, rich in siliceous sponge spicules, quartz silt, and dolomitized peloids and contain minor micritic peloids, small calcitic skeletal fragments, glauconite and CaPO₄.

² - argillaceous laminae are brown, clay-rich, contain widely-dispersed, silt-size dolomite and quartz, and lack calcitic or siliceous skeletal fragments.

³ - siliceous microfossil described by Bergström (1979)

Figure 5.3 Burrowed limestone lithofacies (Table Cove Fm.); field photos and photomicrographs. e - echinoderm; t - trilobite; o - ostracode; g - gastropod; i - inarticulate brachiopod; p - pelcid; py - pyrite. Bar scales on all photomicrographs except f and g are 1 mm. a) Aerial view of the basal Table Cove Formation sequence at Table Cove. Light grey beds bounded by major bedding plane breaks in foreground are about 10 m thick. Small arrows (right side) delineate a low-angle, basal truncation surface of a relatively large slide mass. b) Medium grey, muddy limestones (lithology 1 in Table 5.1) with thin, stylo-nodular bedding from near the base of the lithofacies at Table Cove. c) Transition from stylo-nodular bedding to planar, ribbon limestone type bedding near the top of the lithofacies at Table Cove. Warped bedding in the foreground is a result of gravitational sliding. Divisions on measuring stick are 10 cm. d) Photomicrograph of typical medium grey, muddy limestone from Table Cove. e) Photomicrograph of peloidal, fossiliferous grainstone lense from Table Cove. Flat, elongate fragments are mostly echinoderm plates. f) Photomicrograph of neomorphosed, dark grey, trilobite-rich limestone at Table Cove. Bar scale is 0.5 mm. g) Photomicrograph of f) under cathodoluminescence. Bar scale is 0.5 mm. h) Coarse, echinoderm-rich grain-/rudstone lenses forming a diffuse sand body (arrows); Table Cove - Bellburns section at the head of Table Cove about 1 km southeast of the Table Cove section. Metre stick (centre of photo) for scale. i) Photomicrograph of echinoderm-rich rudstone shown in h).

Figure 5.3



the latter by 1) their darker colour and well-defined, thin (1-5 cm), matrix-rich, stylo-nodular or pseudo-conglomeratic bedding, 2) the presence of large inarticulate brachiopods (Ectonoglossa sp., Pickerill et al., 1984b), an abundant and diverse assemblage of deep-water trilobites (Whittington, 1965; Whittington and Kindle, 1963; Fortey, 1975) and a deeper-water conodont assemblage (Stouge, 1981, 1984), and 3) common, though subtle, evidence of gravitational sliding. Generally the limestones become less fossiliferous and the argillaceous partings become thicker up section, thereby grading in texture, composition, and style of bedding into overlying ribbon limestones (Chapter section 5.2.3, below; Figure 5.3.c). At one exceptional location (see Chapter section 5.2.1 (iv)) this lithofacies comprises the entire Table Cove Formation and is directly overlain by the Black Cove Formation.

5.2.1 Lithologies

(i) **Medium grey, muddy limestone** This category includes bioturbated, fossil-poor mudstone, fossiliferous wackestone, and muddy, fossiliferous packstone with thin, stylo-nodular bedding (Table 5.1; Figure 5.3.b-d). These lithologies make up most of the lithofacies, but decrease in abundance up section. Sediments are compositionally similar, specifically with respect to biotic components, though muddier in texture than underlying Table Point Formation limestones (cf. USU lithofacies in Table 4.1). Shelly fossils decrease in abundance up section, while radiolarians and graptolites become conspicuous, though minor components in the uppermost beds. Bioturbation is pervasive but generally cannot be ascribed to a particular ichnofossil. Sinuous, Planolites-like burrows, circular intersections of vertical (or sub-horizontal) burrows, and small Chondrites occur on the upper surfaces of only a few beds.

These strata are interpreted to be largely in situ accumulations of carbonate mud and skeletal debris deposited in somewhat deeper water than underlying Table Point Formation platform limestones. Diverse

benthic invertebrates and calcareous algae indicate fairly shallow, normal marine water. Predominance of infaunal deposit feeding organisms and bioturbate sediment textures imply stability of surface sediments and suggest that current and wave activity was weak. Increasingly muddy textures of the limestones, diminishing numbers of calcareous shelly fossils, and the appearance of pelagic radiolarians and graptolites up section indicate progressive deepening and increasing importance of hemipelagic sedimentation.

(ii) **Dark grey, trilobite-rich limestone** Dark grey, fossiliferous, peloidal wacke-/floatstone and muddy, fossiliferous pack-/rudstone comprise thin beds that punctuate medium grey limestone near the base of the lithofacies sequence, and comprise knobby-weathering units a few tens of centimetres to 2 metres thick further up section (Table 5.1; Figures 5.2 and 5.3.e-g). Thin beds generally pinch out laterally over a few metres; it is not readily apparent whether the lensoid morphology is strictly depositional or is accentuated by pressure dissolution. Thicker units are further distinguished from enclosing, lighter coloured limestones by even thinner, very matrix-rich, stylo-nodular to pseudo-conglomeratic bedding.

These beds contain an assortment of skeletal grains similar to that found in enclosing, lighter coloured limestones ((i), above) and are also invariably bioturbated (Figure 5.3.e-g). In contrast, the sediments are exceptionally rich in large fragments of illaenid trilobites and, commonly, coarse echinoderm debris. In addition, they are noticeably more pyritic and are pervasively replaced by coarsely-crystalline pseudospar (Figure 5.3.f).

Fragments of illaenid trilobites, indigenous arthropods of the Table Point platform (Whittington and Kindle, 1963; Whittington, 1965), suggest that these sediments originated on the platform and were transported into the deeper water setting (Fortey, 1975). The darker colour and petroliferous odour of these sediments plus abundant pyrite are also

indicative of relatively high concentrations of organic matter and suggest rapid deposition of sediment derived from a shallower, more biologically productive area. Although bioturbation has obliterated primary depositional structures, the mixture of organic-rich muds and coarse skeletal debris suggests the sediments were deposited from waning bottom currents or sediment gravity flows with both bedload and suspended sediment components. Currents directed off the platform may have been generated by storm waves that entrained sediments in shallower water, or could have been triggered by seismicity. Increasing abundance of these allochthonous sediments up section and concurrent decline in *in situ* carbonate accumulation suggest that water depth increased to a point where dissolved oxygen level, light level, and/or temperature were not conducive to biogenic carbonate production and the majority of sediment was transported in from adjacent shallow water areas.

(iii) **Echinoderm-rich, skeletal sand lenses** Very fossiliferous pack-/floatstone and grain-/rudstone lenses are minor components of the lithofacies (Table 5.1; Figures 5.2 and 5.3.h, i). In some sequences they are randomly distributed and widely disseminated, but locally they are closely stacked and define diffuse skeletal sand bodies (Figure 5.3.h; compare Table Point and Table Cove-Bellburns sections in back pocket).

These sediments are also interpreted to have come from the platform and were transported by currents into deeper water. Oncolites link the sediments to a contemporaneous sponge-oncolite biostrome. However, predominance of coarse, clean echinodermal sands and paucity of mud suggests the sediments were derived specifically from areas where crinoids and cystoids proliferated, possibly shoals adjacent to the biostrome. Scattered skeletal sand lenses in the muddier, deeper-water deposits indicate episodic transport and deposition from high energy bottom currents probably generated by powerful waves during storms. Diffuse sand bodies made up of stacked skeletal sand lenses are thought

to have developed locally in areas most proximal to the echinoderm shoal. Relative to surrounding areas these sand bodies may also have been local highs on the seafloor that were more susceptible to normal waves, and possibly tidal currents, that promoted their development.

(iv) **Limestone conglomerate** Unique fossiliferous limestone conglomerate is recognized in a single drill core from the Daniel's Harbour Zinc Mine (DH-1516, back pocket; Table 5.1). It comprises the top 4 m of the lithofacies, which anomalously constitutes the entire formation sequence, and is directly overlain by Black Cove Formation shale (Chapter 7). The conglomerate is clast-supported and matrix-poor, and is composed of granule- to pebble-size clasts of light grey, very fossiliferous limestone.

Clast size and bed thickness suggest the conglomerate was transported and deposited by a debris flow or, possibly, a high concentration turbidity current (Middleton and Hampton, 1976). Composition of the clasts indicate a shallower-water origin. Clast size and shape suggest the pebbly sediment was generated by disaggregation of at least partially lithified, nodular limestone during transport. The sediment gravity flow could have evolved during transport and break-up of coherent strata in a gravitational slide involving surficial sediments in adjacent shallower water areas. It may also have been generated by mass-wasting of shallowly-buried sediments exhumed by faulting. Abrupt deepening after conglomerate deposition, indicated by overlying black, basinal shale, suggests that fault displacement was likely involved.

(v) **Bentonite** Centimetre-thick, sticky clay beds punctuate this lithofacies in both the Daniel's Harbour Zinc Mine and Port au Port Peninsula areas (Table 5.1). XRD analysis indicates that they are composed of expandable, mixed layer illite-smectite clays. They are interpreted as altered volcanic ash layers that accumulated on the sea floor by suspension settling through the water column. The mixed-layer composition of the clays indicates further conversion of smectite, the

original weathering product of siliceous volcanic ash, to illite during burial (Eslinger and Sellars, 1981).

5.2.2 Synsedimentary Deformation

Deformation structures and fabrics generated by gravitational sliding are common, albethey typically obscure in this lithofacies. Most slides are only a few tens of centimetres thick and are characterized by predominantly brittle deformation features, namely rotated, imbricated bedding, broken beds and conglomeratic fabric, and low-angle (5-15°) faults (Figure 5.3.a; Appendix C). Broad, open folds ($\lambda \geq 1$ m; $A = 10-20$ cm) manifest by undulatory bedding planes (Figure 5.3.c), and indicative of ductile deformation, are also present; smaller wavelength folds are vaguely defined by broken limestone nodules.

5.2.3 Interpretation

These strata are interpreted to have been deposited on a gently-dipping, moderately shallow but progressively deepening, upper slope created by tilting and subsidence of the predeceasing, shallow-water platform. Sediments deposited included in situ accumulations of mud and skeletal debris, plus material derived from the adjacent platform and deposited via bottom currents and sediment gravity flows.

Numbers and diversity of invertebrates living on and in the sediments indicate normal marine, well-oxygenated bottom waters. Darker colour of the sediments compared to underlying platform limestones, however, suggests a greater quantity of unoxidized organic matter, possibly an indication that bottom waters were not as well oxygenated. Chondrites burrows in the youngest, and inferred to be deepest, upper slope limestones, may signify dysaerobic, interstitial, bottom waters (Bromley and Eckdale, 1984).

Low energy, below normal wave base conditions are inferred from the muddy, bioturbated texture of most sediments. Progressive deepening of the upper slope environment is indicated by 1) a gradual decrease in the numbers of benthic organisms and appearance of pelagic radiolarians and

graptolites, and 2) the change from primarily in situ carbonate accumulations to mostly platform-derived, transported sediments up section. Calcareous green algae in the initial upper slope deposits may indicate water depths of less than 25 m (Wray, 1977), but may have been a few or several tens of metres greater for younger sediments deposited in more distal regions.

Common remobilization of these sediments in gravitational slides signals a rather abrupt change from a more or less level platform to an inclined depositional slope. Predominance of brittle deformation structures and fabrics indicate the sediments were fairly well-lithified at the sediment-water interface. Limited thicknesses of sediments involved in sliding probably reflects the lithification state, but also suggests that mass movement was triggered by either rapid increases in the angle of the depositional slope or by sudden changes in pore water pressure caused by earthquake shocks or passing storm waves rather than by local sediment overloading or by sudden depositional loading. Seismicity may have been related to plate convergence and volcanism outboard of the continental margin or it could have accompanied small displacements on nearby faults that controlled local subsidence. Exotic, pebbly, debris flow conglomerate derived from the platform or very high up on the slope may be a dramatic consequence of catastrophic faulting and extremely rapid subsidence locally.

5.2.4 Regional Variations

The general character and lithologic components of the burrowed limestone lithofacies described above come from outcrops at Table Cove and from drill cores at the adjacent Daniel's Harbour Zinc Mine where the lithofacies is well-developed. In other areas limestones which comprise the lithofacies are compositionally and texturally similar, but there are important lateral variations.

The most striking difference is the thickness of lithofacies sequences, which ranges from as little as 1.5 m to as much as 22 m (cf.

Figure 5.1.a and b); lithofacies thickness is invariably proportional to the thickness of the entire Table Cove Formation. Since the thickness of upper slope deposits essentially records the duration of in situ carbonate sediment production, thinner upper slope sequences are inferred to have been deposited during more rapid subsidence.

Comparatively thin lithofacies sequences differ from thick sequences described above in four respects.

1) Sediments commonly cannot be differentiated into autochthonous and platform-derived components. This is probably partly due to thorough mixing of sediments by burrowing organisms. It is also probably a function of rapid demise of the upper slope and the adjacent platform due to rapid subsidence.

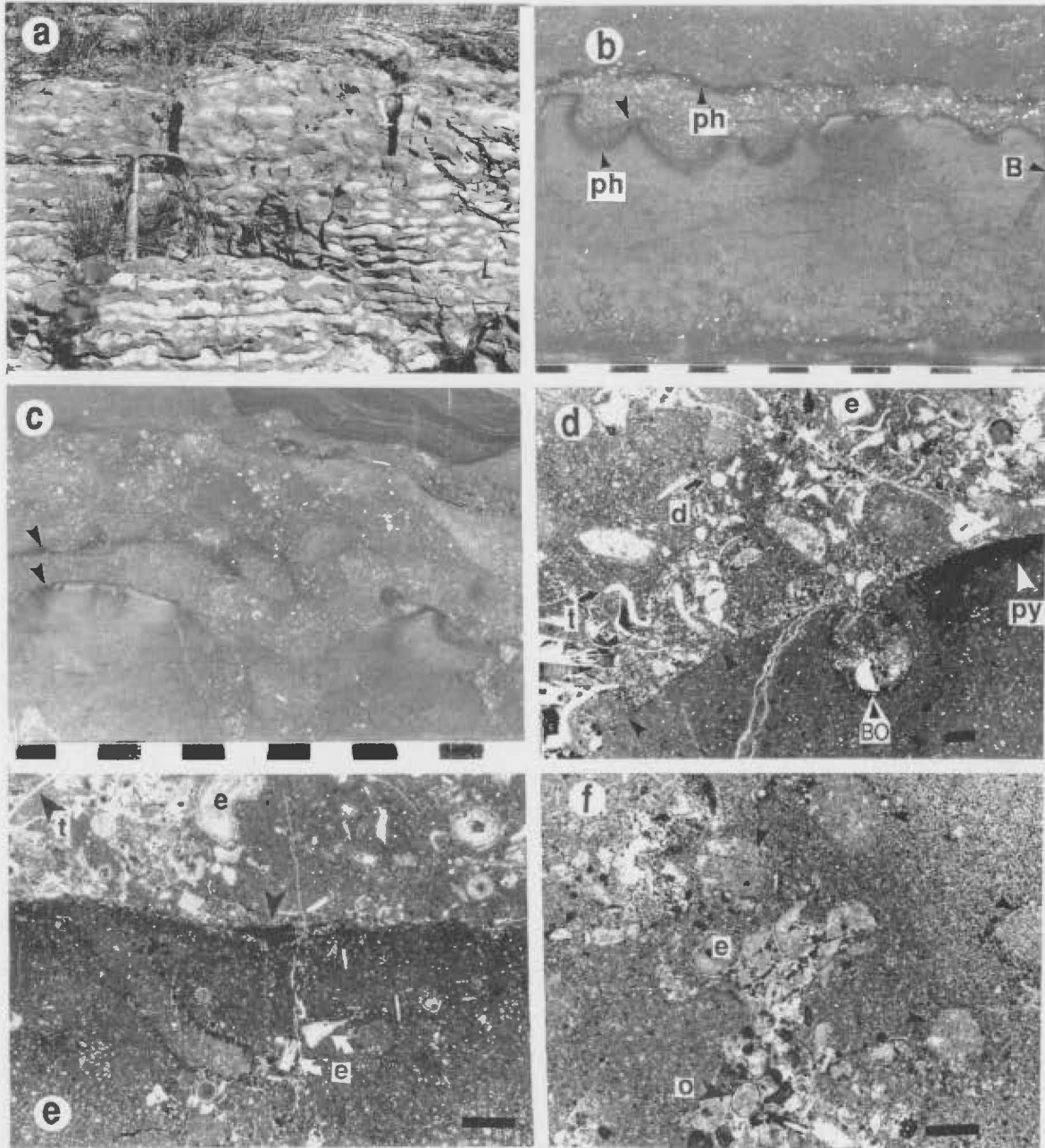
2) There is little evidence of downslope transport in gravitational slides or slumps. This suggests subsidence in those areas was accompanied by minimal tilting.

3) Locally thin upper slope deposits are characterized by very argillaceous, nodular bedding (Figure 5.4.a) interpreted as a pressure dissolution fabric generated in sediments that were incompletely lithified before burial. Incomplete lithification indicates that either the contribution of clays from the water column was greater at the onset of slope formation and sedimentation, or the upper slope was deeper, bottom waters were less well-oxygenated, and/or a larger proportion of sediment deposited was organic-rich material derived from shallower water areas.

4) Thin upper slope sequences locally have multiple hardgrounds or firmgrounds (Figure 5.4.b,c). Hardgrounds defined by pyritic rinds and/or concentrations of CaPO_4 can be traced for a few tens of metres along the length of the outcrops. Most are developed on muddy, burrowed sediments and vary from smooth to undulatory to highly irregular surfaces that display 2-5 cm relief in series of scallop-shaped depressions separated by narrow pinnacles (Figure 5.4.b,c). In the absence of

Figure 5.4 Regional variations in the burrowed limestone lithofacies; field photos and photomicrographs. e - echinoderm; t - trilobite; d - dasycladacean alga; py - pyrite; ph - phosphatized sediment/grain. All bar scales on photomicrographs are 1 mm. a) Very argillaceous limestone with nodular bedding at the base of the Table Cove Formation at Beaver Brook. b) Polished slab of eroded and mineralized hardgrounds (arrows) from West Bay Centre Quarry. Echinoderm-rich sediment above the prominent, scalloped hardground is mixed into underlying, Chondrites-burrowed muddy sediment via larger burrows (B) that penetrate the hardground, extend 4-6 cm below it, and concentrate the material above another? hardground. Divisions on scale are one centimetre. c) Similar to b), also from West Bay Centre Quarry. Laminated argillaceous sediment overlies the uppermost, pyritized hardground. Divisions on scale are one centimetre. d) Photomicrograph of a phosphatized (dense shading) and pyritized hardground that is bored (BO) and overlain by echinoderm-rich sediment. e) Photomicrograph of the same hardground surface as in d) with a truncated Chondrites burrow (outlined). f) Photomicrograph of twice burrowed, muddy sediment below a mineralized hardground at West Bay Center Quarry. First generation burrows are circular, microspar patches (arrows); second generation burrows, which do not cross-cut earlier burrows, are filled with peloidal, echinoderm grainstone.

Figure 5.4



evidence of subaerial exposure and meteoric diagenesis, and lack of large boring bivalves in these sediments, irregular topography is interpreted to reflect heterogeneous mechanical erosion of the hardground dictated by patchy distribution of well-lithified sediment. Muddy sediments beneath the hardgrounds record multiple stages of burrowing (Chondrites) and complex diagenetic histories involving neomorphism, cementation, glauconitization, phosphatization and pyritization, all intimately related to hardground formation (Figure 5.4.d-f).

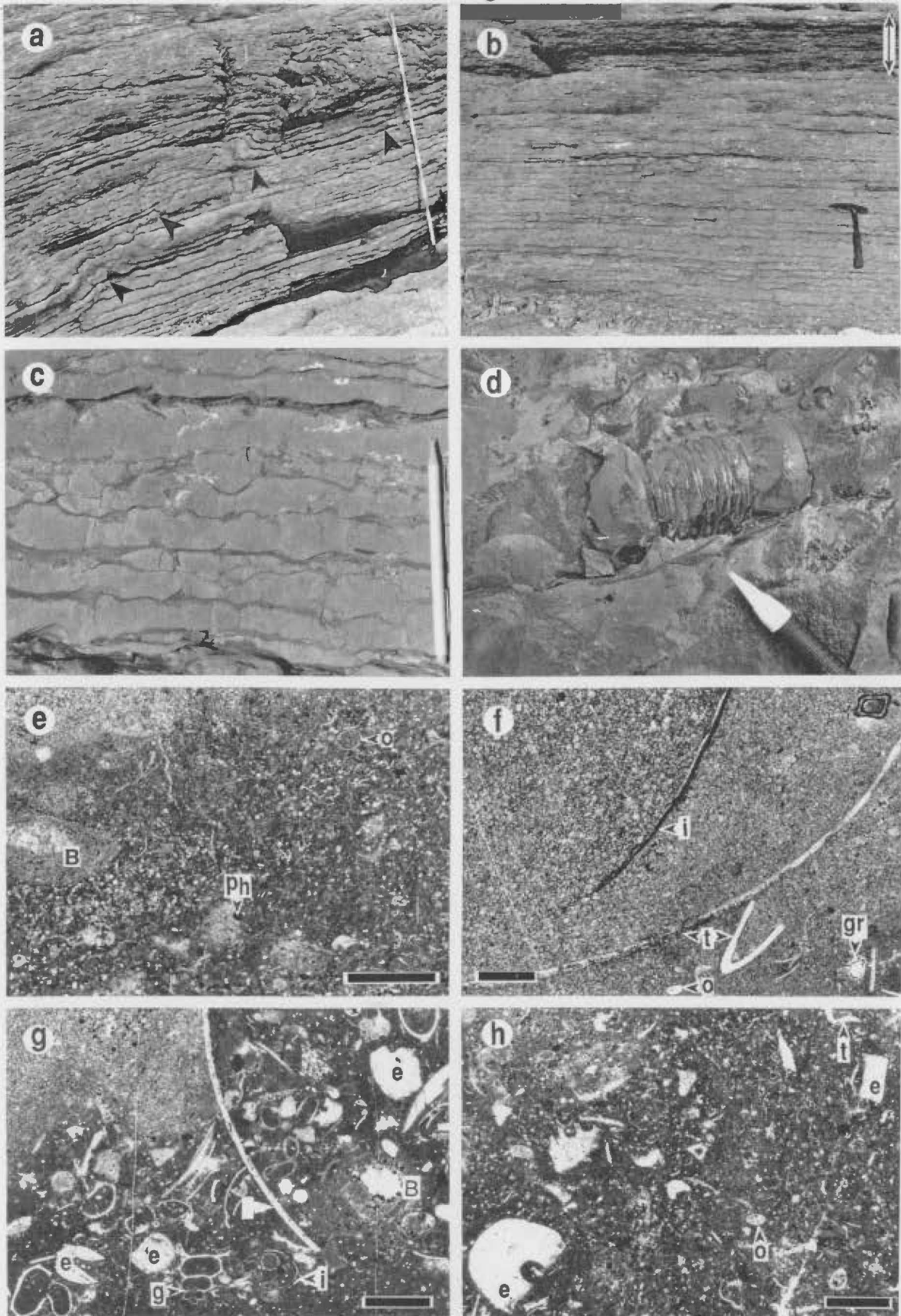
Mineralized hardgrounds and firmgrounds indicate lithification of sediments during periods of very slow sedimentation or nondeposition (Fischer and Garrison, 1967; Shinn, 1969; Kennedy and Garrison, 1975; Fürsich, 1979). Reduced carbonate production may have been the result of ever increasing water depth and/or abrupt changes in depth caused by pulses of rapid subsidence (Purser, 1969; Read, 1980, 1982; Pedley and Bennett, 1985). The presence of phosphate and paucity of glauconite in the hardgrounds suggests that lithification and mineralization occurred in relatively shallow water, perhaps between 30 and 50 m deep (Bromley, 1967).

5.3 Parted Limestone Lithofacies (Lithofacies 2 in Table 5.1)

This lithofacies is composed of thin-bedded, light grey, planar to wavy, fossil-poor, parted limestone and lesser dark grey, stylo-nodular to pseudo-conglomeratic, fossiliferous limestone, both pervaded by deformation structures generated by gravitational sliding (Figures 5.2 and 5.5.a). It abruptly overlies massive, sponge-oncolite biostromal limestone at the top of the Table Point Formation (Chapter section 4.4) only in the Bellburns-Spudgel's Cove section. Basal beds locally rest discordantly on the platformal limestones, but limited exposure of the contact precludes judging whether it is truly an angular unconformity or an apparition caused by syndepositional sliding and folding of the basal sediments. This lithofacies is laterally equivalent and compositionally

Figure 5.5 Parted limestone lithofacies (Table Cove Fm.); field photos and photomicrographs. All from the Bellburns-Spudgel's Cove section. e - echinoderm; t - trilobite; o - ostracode; g - gastropod; i - inarticulate brachiopod; gr - graptolite; B - burrow; ph - phosphate grain. Bar scales on all photomicrographs are 1 mm. a) Parted limestone near the base of the section. Folding occurs in the hanging wall of a synsedimentary fault (arrows) at the base of a gravitational slide. Divisions on the measuring stick are 10 cm. b) Light grey, planar-wavy parted limestone overlain by dark grey, trilobite-rich limestone (arrow). c) Close-up of parted limestone with planar-wavy to wavy-nodular bedding; thin, dark grey layers are dolomitic shale. Pencil for scale. d) Large nileid? trilobite on the upper surface of a mudstone bed. e) Photomicrograph of finely-fossiliferous, silty (white specks), burrowed mud-/wackestone (parted limestone). Most skeletal fragments are valves of very small ostracodes. Black specks are disseminated pyrite and pyrite-replaced skeletal grains. f) Photomicrograph of recrystallized wackestone (parted limestone) with large fragments of trilobites and an inarticulate brachiopod, all partly replaced by pyrite. g) Photomicrograph of very fossiliferous, burrowed wackestone (parted limestone) patchily replaced by pseudospar. Black specks are pyrite. h) Photomicrograph of dark grey, trilobite-rich limestone. Siliciclastic silt and echinoderm debris are more abundant in field of view than trilobite material. Black specks are pyrite.

Figure 5.5



similar to the burrowed limestone lithofacies (Chapter section 5.2, above), differentiated from it by more continuous and much less fossiliferous limestone beds and thicker argillaceous partings, and by a distinctive trace fossil assemblage. These strata are abruptly overlain by ribbon limestone (Chapter section 5.4, below,) which are even less fossiliferous and are interbedded with thicker beds of calcareous shale (Figure 5.2).

5.3.1 Lithologies

(i) **Light grey, parted limestone** This lithology is the dominant component of the lithofacies (Figure 5.2). It is composed of thin, planar-wavy to wavy-nodular beds of mudstone and fossil-poor wackestone separated by very thin, argillaceous partings (Table 5.1; Figure 5.5.a-c). Field and petrographic aspects of these strata indicate that this bedding is largely defined by an early diagenetic stratification influenced by primary compositional layering and subsequently modified by pressure dissolution during burial (Appendix D).

Limestone beds are mostly fossil-bearing mudstones with skeletal components similar to, but finer-grained and less abundant than those present in the burrowed limestone lithofacies (Chapter section 5.2.1, above) and in platformal limestones (Figure 5.5.d,e). They are interstratified with lesser fossiliferous, peloidal wackestone beds that contain a similar biotic assemblage (Figure 5.5.f,g) that decrease in numbers up section. On some bedding planes skeletal debris is concentrated with orthoconic and coiled cephalopods, articulate brachiopods and lithistid sponges, forming small (30-40 cm diameter), ill-defined, low-relief buildups reminiscent of sponge bioherms in the Table Point Formation (Chapter section 4.3.3). Disseminated pyrite and pyrite-replaced skeletal fragments are more abundant in these beds than in the mudstones, also suggesting originally higher concentrations of organic matter (Figure 5.5.g).

All limestone beds lack primary, physical sedimentary structures and

are interpreted to be bioturbated (Figure 5.5.e-g). Burrow mottling is generally recognized by irregular patches of microspar and pseudospar; it is also defined in some beds by discontinuous stringers of quartz silt. Discrete burrows, mostly less than 5 mm in diameter, are alternatively filled with neomorphic calcite, blocky calcite cement, micrite, or pyrite. Upper bedding planes also commonly display several types of large horizontal traces (see Trace Fossils, Chapter section 5.3.2, below).

Partings are essentially argillaceous mosaics of finely-crystalline dolomite with scattered siliciclastic silt, and small, mostly unidentifiable, skeletal fragments. They are interpreted as carbonate-depleted sediment layers equivalent to enclosing limestones that escaped early lithification and were subjected to mechanical compaction and pressure dissolution during burial (Appendix D).

Parted limestones are interpreted to be a combination of hemipelagic sediment and lesser autochthonous carbonates deposited in a quiet water environment below fairweather wave base. Predominance of mud, the fine, fragmental nature of skeletal grains, and paucity of calcareous algae suggest that these sediments accumulated in deeper water than the burrowed limestone lithofacies (Chapter section 5.2). Mudstones with very small fragments of typical shallow-water invertebrates and calcareous algae, and radiolarians are interpreted as hemipelagic sediments (Wilson, 1969) composed mostly of fine sediment derived from either the adjacent platform or higher up on the slope, plus as pelagic material deposited from suspension from the water column. Dilute suspensions of fine sediment may have been continually transported out into deeper water via normal tidal currents and waves (Neumann and Land, 1975). More voluminous suspensions were probably generated by storms and transported seaward by storm ebb flows (Ball *et al.*, 1967; Perkins and Enos, 1968; Boardman and Neumann, 1984). Diffuse clusters of sponges, cephalopods and other shelly invertebrates, however, also suggest that

some sediment was generated in situ by benthic organisms localized on the seafloor in small buildups. Declining abundance of these sediments up section indicates deteriorating environmental conditions, probably a consequence of deepening.

(ii) **Dark grey, trilobite-rich limestone** Knobbly-weathering, dark grey, fossiliferous limestone comprises 1.5-3 m thick beds interstratified with the parted limestone (Table 5.1; Figures 5.2 and 5.5.b). It is compositionally, texturally and diagenetically similar to same named strata in the burrowed limestone lithofacies (Chapter section 5.2.1 (ii); Figure 5.5.h), but they commonly contain an even more conspicuous and diverse assemblage of typical shallow-water, shelly invertebrates and calcareous algae (Table 5.1). Orthocones on bedding planes of some of these units show a preferred orientation (see Spudgel's Cove section, back pocket).

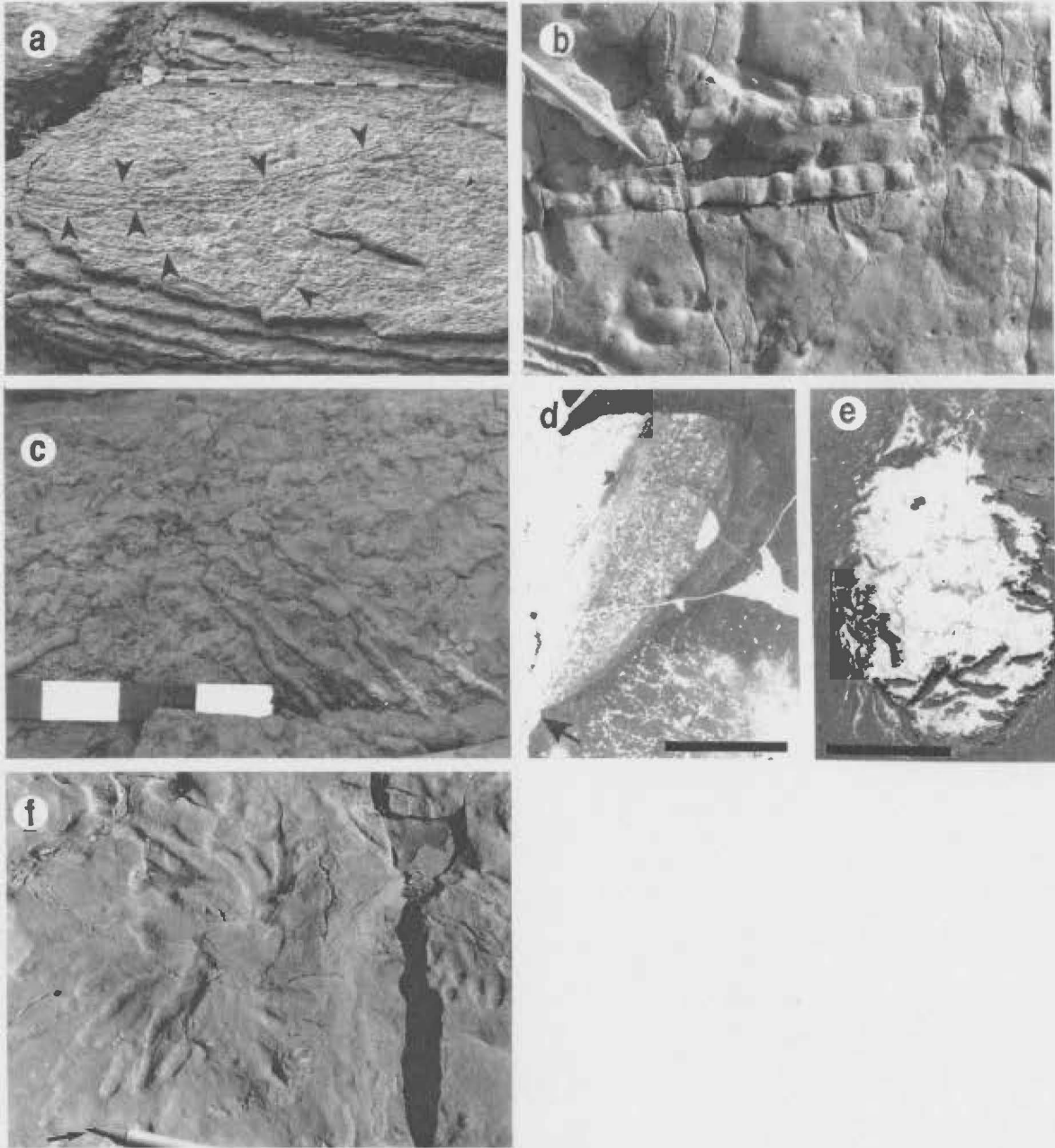
Like similar beds in the burrowed limestone lithofacies these strata are interpreted to have derived from the platform, specifically a sponge-oncolite buildup, and were transported downslope and rapidly deposited by gravity-driven bottom currents generated by storms or, possibly, triggered by episodic seismicity. Complete reworking of the sediments by burrowers indicates that relatively small amounts of sediment were deposited by each current event. Thick accumulations, therefore, must record long periods of episodic current deposition either when the source was comparatively shallow and more susceptible to disruption by high energy storms or, when seismic activity was frequent.

5.3.2 Trace Fossils

(i) **Description** Several types of trace fossils are found on the upper surfaces of parted limestone beds and, to a lesser extent, on dark grey limestones. Most common are large (7 mm to 2 or 3 cm diameter), straight to broadly sinuous, horizontal to gently inclined burrows, some of which are up to several metres long (Figure 5.6.a). Both burrows expressed in positive relief and those defined by shallow grooves are

Figure 5.6 Trace fossils in the parted limestone lithofacies. All specimens are from the Bellburns - Spudgel's Cove section. a) Large, gently-curved burrows (arrows) on the upper bedding plane of muddy, parted limestone. Divisions on the measuring stick are 10 cm. b) Taenidium on the upper bedding plane of a mudstone bed; pencil for scale. Peristaltic wall morphology and internal meniscus structure are apparent only when the upper wall of the tunnel and internal sediment have been removed by weathering. Other large, full relief burrows composed of micrite and lacking these features may be manifestations of Taenidium. c) Palaeophycus on an upper bedding plane; divisions on the measuring stick are 10 cm. d) Photomicrograph of Palaeophycus burrow floored by internal sediment, lined with bladed calcite cement, and filled with equant spar; up is to the left. Other Palaeophycus burrows are lined with bladed calcite and filled with lime mud or are filled solely with blocky calcite cement. That the burrows remained open implies that either that walls of the structure were reinforced with mucous or enclosing muds were firm (see e), below). Sparry, fenestral-looking sediment patch on the left is a sponge. Bar scale is 0.5 cm. e) Photomicrograph of Palaeophycus burrow occluded by blocky calcite cement. Minute, spar-filled fractures around the burrow and the presence of fragments of the burrow wall (partly replaced by pyrite) in the burrow record partial collapse of the burrow in semi-lithified sediment. Bar scale is 0.5 cm. f) Large Chondrites on upper bedding plane near the top of the section; pencil for scale.

Figure 5.6



partly responsible for the lumpy topography on upper and lower surfaces of parted limestone beds (Figure 5.5.c).

The trace fossil assemblage includes the following. Taenidium (sensu D'Alessandro and Bromley, 1987), is a large (1.5-3 cm diameter), low relief, straight to gently-curved burrow with peristaltic wall morphology and meniscate internal structure (Figure 5.6.b), interpreted as a tunnel generated by an infaunal, deposit-feeder that back-filled its burrow as it moved through the sediment. Palaeophycus spp. (Pemberton and Frey, 1982), are large (0.5-2 cm diameter), smooth-walled, sub-horizontal tunnels with sharply defined walls and several different types of burrow fill (Figure 5.6.c-e), interpreted to have been generated by a deposit-feeding organism, or possibly constructed as a domicile for protection and/or filter-feeding. Chondrites is a complex burrow system consisting of a central, vertical shaft from which extends a whorl of branching, smooth-walled, gently-inclined tunnels (Figure 5.6.f), interpreted as a feeding structure of a sessile, deposit-feeding organism. Ichnogenus incertae is another large, straight to gently-curving burrow expressed as a shallow groove with low (4-5 mm) lateral ridges on the tops of limestone beds which may be either be a surface trail of an epifaunal grazer or scavenger, a tunnel generated by an infaunal, deposit-feeder that migrated along the interface between sediments of somewhat different composition, or a pressure dissolution enhanced cast of Taenidium from an overlying limestone bed.

(ii) **Significance of the assemblage** This assemblage of traces indicates a soft, stable substrate containing an adequate supply of fine, organic matter to support inbenthic organisms, thereby confirming other sedimentologic evidence that these sediments accumulated in a quiet water environment. Though it is not diagnostic of a specific environment or water depth, similar assemblages dominated by infaunal deposit-feeders are common to both modern and ancient, fine-grained, deep-water sediments (Eckdale and Berger, 1978; Kern, 1978; Pickerill,

1980; Eckdale *et al.*, 1984). Inhabitation of the sediment by large soft-bodied organisms indicates that bottom waters and near surface, interstitial waters were well-oxygenated (Byers, 1977). The appearance of Chondrites may signal decreasing O₂ levels (Bromley and Eckdale, 1984), probably a reflection of increasing water depth.

Actual distribution of burrows in these strata is uncertain; neither lower bedding planes of limestones nor bedding planes in argillaceous interbeds are exposed in outcrop. Apparent absence of burrows in argillaceous partings is thought to be at least partly due to obliteration by compaction. However, weakly-developed nodular fabrics in limestone beds indicate little vertical mixing of sediment by burrowers. This suggests that burrowing activity may have been influenced by either primary compositional layering and/or the interstitial water chemistry of different sediment layers (Appendix D).

5.3.3 Synsedimentary Deformation

Deformation structures and fabrics generated by gravitational sliding are pervasive in this lithofacies. Discrete slides range from only a few tens of centimetres up to ~12 m thick. The thinnest are analogous to those in the burrowed limestone lithofacies (Chapter section 5.2.2) and are characterized by similar brittle deformation features. Metre-scale slides display nearly the entire spectrum of brittle (faults, rotated and imbricated bedding, pebbly limestone conglomerate) and ductile (folds, sheared bedding) structures in approximately equal proportion (Figure 5.5.a), while deformation in one large slide mass at the top of the lithofacies is manifest almost solely by imbricate thrusts and pebbly limestone conglomerate (Appendix C).

5.3.4 Interpretation

This lithofacies records sedimentation on a moderately deep, gently-dipping carbonate slope generated by abrupt subsidence of the Table Point platform. Predominance of mud indicates overall low-energy conditions, while paucity of important carbonate-producing organisms,

notably calcareous algae, suggests that little sediment was generated in situ. Most mud and skeletal debris originated on an adjacent platform or higher up on the slope and was deposited either by suspension settling through the water column (parted limestone) or from episodic gravity flows (dark grey, trilobite-rich limestone). Skeletal components of the latter indicate the presence of a contemporaneous, upslope, shallow-water, lithistid sponge buildup. Compositional and textural contrasts with the burrowed limestone lithofacies indicate deposition in somewhat deeper water, either in a lower upper slope or mid-slope environment.

The mid-slope was normally inhabited by a limited assemblage of shelly invertebrates. Restrictions on their numbers and diversity may have been imposed by reduced light intensity, low oxygen level, low water temperature, or a combination of these, each of which decreases with increasing depth. Intermittently improved environmental conditions, possibly oxygenation of bottom waters, allowed proliferation of a more diverse assemblage of invertebrates, including sponges, gastropods and echinoderms.

Soft-bodied, deposit-feeding organisms thrived in the muddy sediments. Their ability to obliterate all primary depositional structures suggests that sedimentation was relatively slow and continuous (Howard, 1975, 1978). Their presence implies that normally bottom waters and near surface interstitial waters were well oxygenated; dysaerobic to anoxic interstitial waters appear to have been generated in dark grey limestones deposited rapidly with higher concentrations of organic matter.

Predominance of very fine-grained, carbonate sediment and absence of current- and wave-generated structures indicate quiet water deposition, certainly below fairweather wave base and possibly below storm wave base. Minimum water depth inferred from the general absence of indigenous green algae is about 25 m (Wray, 1977). Deposition below

fairweather wave base implies a similar minimum depth (Walker, 1985). Intermittent proliferation of diverse shelly invertebrates suggests that water depth probably did not exceed 100 m (Benedict and Walker, 1978; Wilson and Jordan, 1983). Gradual disappearance of fossiliferous sediments generated by indigenous organisms up through the lithofacies sequence indicates that water depth increased with time.

The abrupt appearance of these mid-slope carbonates atop very shallow limestones indicates very rapid subsidence of the platform. Soft-sediment folds and other early deformation structures in even the basal slope deposits prove that subsidence was accompanied by tilting. Pervasive deformation due to sliding implies that virtually all sediments deposited on the mid-slope were subsequently transported some distance further downslope in gravitational slides. In this setting episodic seismicity may have been a more important triggering mechanism than was changing pore water pressure associated with passing storms. Greater instability of these sediments compared to those deposited on the upper slope is probably due to the presence of unlithified, argillaceous interbeds which readily succumbed to shear stresses and served as glide surfaces even on very gentle slopes.

5.3.5 Comments

This lithofacies comprises an anomalously thick sequence at the base of the Table Cove Formation only in the Bellburns - Spudgel's Cove area. It is laterally equivalent to, though much thicker than the burrowed limestone lithofacies strata at the base of the Table Cove at nearby Table Cove and the Daniel's Harbour Zinc Mine. Deposition of these deeper-water sediments implies more rapid subsidence of the underlying platform than in surrounding areas. The anomalous thickness of the sequence may in part be due to synsedimentary structural thickening in gravitational slides, and/or record a unique balance between adjacent, slowly subsiding, shallower, carbonate source areas and the slope which was able to accommodate the mass of sediment deposited on it by

subsiding more rapidly.

5.4 Ribbon Limestone Lithofacies (Lithofacies 3 in Table 5.1)

This lithofacies consists mostly of rhythmically-interstratified, thin-bedded, fossil-poor, muddy or peloidal limestone and graptolitic shale, commonly referred to as ribbon limestone (Figures 5.1 and 5.2). In contrast to previously described Table Cove Formation lithofacies, limestone beds are on average thicker, less conspicuously burrowed or not burrowed at all, and contain fewer and smaller fragments of shallow water organisms and increasing numbers of pelagic radiolarians and graptolites. Interbedded shales are also thicker and contain a similar pelagic faunal assemblage. Field and petrographic aspects of these strata indicate that this bedding is defined by an early diagenetic stratification influenced by primary compositional layering and subsequently modified by pressure dissolution during burial (Appendix D).

These strata gradationally overlie the burrowed limestone and parted limestone lithofacies (Chapter sections 5.2 and 5.3), constituting the upper Table Cove almost everywhere the formation occurs; an exception is noted in Chapter section 5.2.1 (iv), above. They are almost everywhere gradationally overlain by the Black Cove Formation (Chapter 7) (Figure 5.2). Exceptional is the section at Piccadilly on the Port au Port Peninsula (back pocket) where ribbon limestone is directly overlain by coarser siliciclastic sediments of the American Tickle Formation (Chapter 8).

This lithofacies includes two sub-lithofacies (Type A and Type B) differentiated by style of bedding, composition, and primary sedimentary structures (Figure 5.2; Table 5.1). They also differ in their associated carbonate lithologies, degree and styles of synsedimentary deformation, and diagenetic features. Type A comprises both very thin and very thick sedimentary sequences on the Great Northern Peninsula. Type B comprises thin sequences only on and near Port au Port Peninsula.

5.4.1 Lithologies of Sub-lithofacies A

(i) **Ribbon limestone** These strata are characterized by remarkably tabular beds of limestone and recessive-weathering shale generally interbedded on a scale of 1-10 cm (Table 5.1; Figure 5.7.a,b). Limestone beds appear continuous, but may change gradually in thickness and pinch out along strike over several metres or tens of metres. The limestone:shale ratio within discrete, 50 cm to 15 m thick stratigraphic intervals varies from 20:1 to 1:5; it does not everywhere systematically decrease up section, but calcareous shale is always the dominant component near the top of lithofacies sequences.

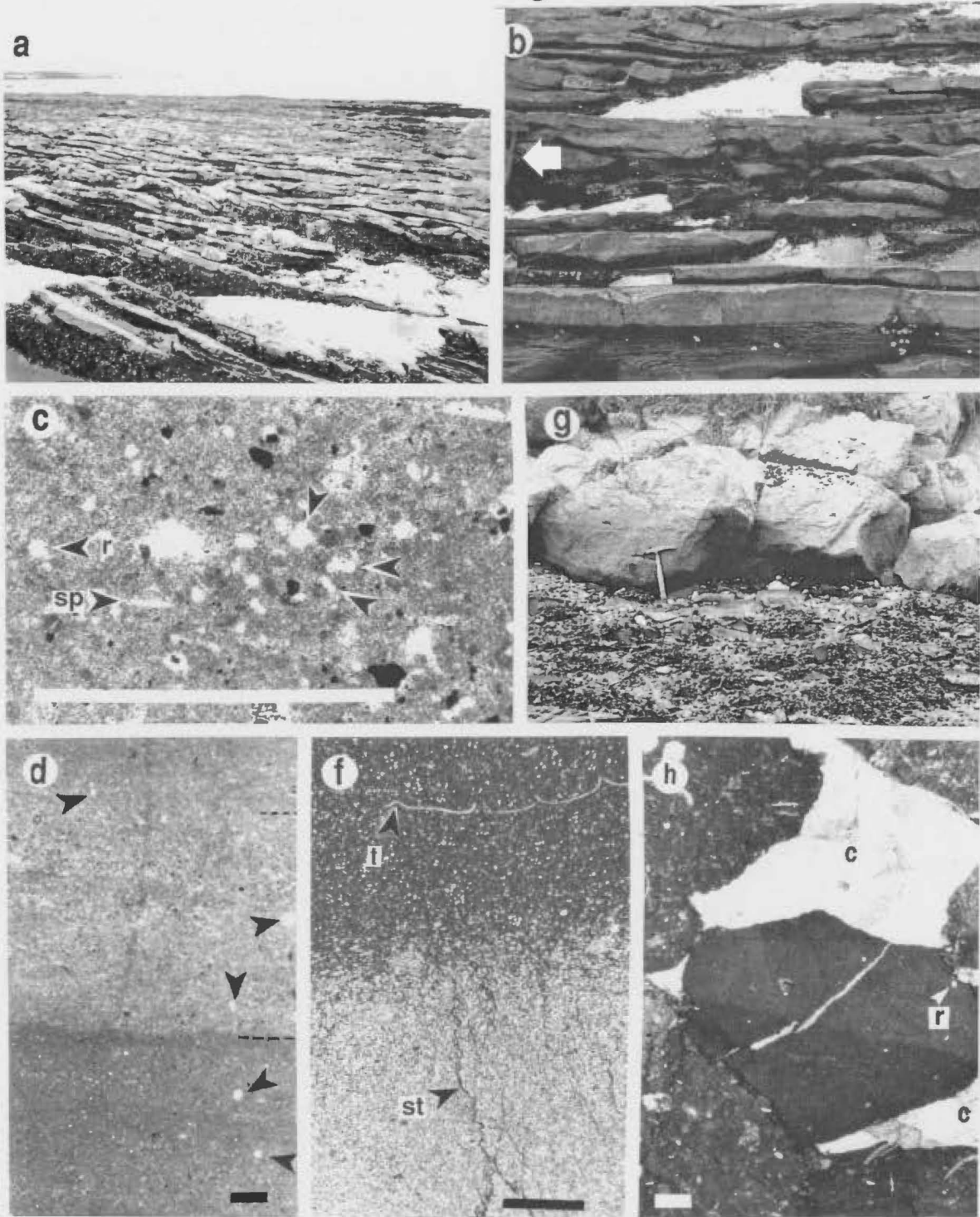
Limestone beds are mostly fossiliferous and/or peloidal wackestone and fossil-bearing mudstone (Figure 5.7.c-e); thin beds of fossiliferous pack-/rudstone are present near the base of lithofacies sequences locally. Muddy limestones contain very small fragments of shelly invertebrates and calcareous algae typically found in platformal and upper slope limestones, as well as radiolarians and graptolites, and disarticulated, but not pulverized fragments of thin-walled trilobites, lingulids, and rare small articulate brachiopods (Figure 5.8). Those near the base lack primary sedimentary structures suggesting they may be bioturbated, but discrete burrows are sparse. Only coarse, skeletal layers show structures indicative of deposition from turbidity currents (Table 5.1). Higher up section muddy limestone beds are typically laminated or are composed of several sediment layers a few millimetres to 2 cm thick (Figure 5.7.d) proving that individual limestone beds do not record single depositional events. Ambient lime mud is invariably neomorphosed to equidimensional microspar which increases in crystal size to equidimensional or loaf-shaped pseudospar toward the margins of the beds (Figure 5.7.e).

Interbedded shale is composed of variable amounts of clay, authigenic dolomite, silt-size, authigenic and detrital quartz and albite, and minor calcareous skeletal fragments (Figure 5.7.e). Overall, shale

Figure 5.7 Ribbon limestone lithofacies (Type A) (Table Cove Fm.); field photos and photomicrographs. e - echinoderm, t - trilobite, r - radiolarian, o - ostracode, m - mollusc, b - articulate brachiopod, sp - spicule. Bar scales on all photomicrographs are 1 mm.

a) Ribbon limestone at Table Cove. Divisions on measuring stick are 10 cm. b) Close-up of ribbon limestone at Table Cove. Hammer (left) rests on deformed limestones beneath a detachment surface of a gravitational slide; truncated upper limb of fold on right suggests displacement of the slide to the left. c) Photomicrograph of microsparitic mudstone from the middle part of the ribbon limestone sequence in drill core U.S. Borax #2 from the DHZM. Most white grains are small skeletal fragments; angular grains (arrows) are authigenic quartz. Dense, micritic grains are relict peloids; black grains are authigenic pyrite. d) Photomicrograph of mudstone with very thin bedding defined by a change in neomorphic calcite crystal size (2-7 μm crystals in the lower layer, 10-30 μm crystals in the upper layer) which grades up into radiolarian mudstone; Table Cove. Arrows point to radiolarians. e) Photomicrograph showing aggrading neomorphic crystal fabric toward the margin of a limestone bed and gradational contact with overlying shale; U.S. Borax #2 drill core from the DHZM. f) Limestone conglomerate overlying ribbon limestone (algae covered foreground) at Callieux Bay (Vaches Point). Hammer for scale. g) Photomicrograph of conglomerate in f. Massive, dark grey clast in centre is radiolarian mudstone derived from underlying ribbon limestone; other clasts are partly neomorphosed, burrowed, peloidal, fossiliferous packstone and wackestone. Coarse calcite cement (c) fills interclast pores; clast-clast contacts are stylolitic.

Figure 5.7



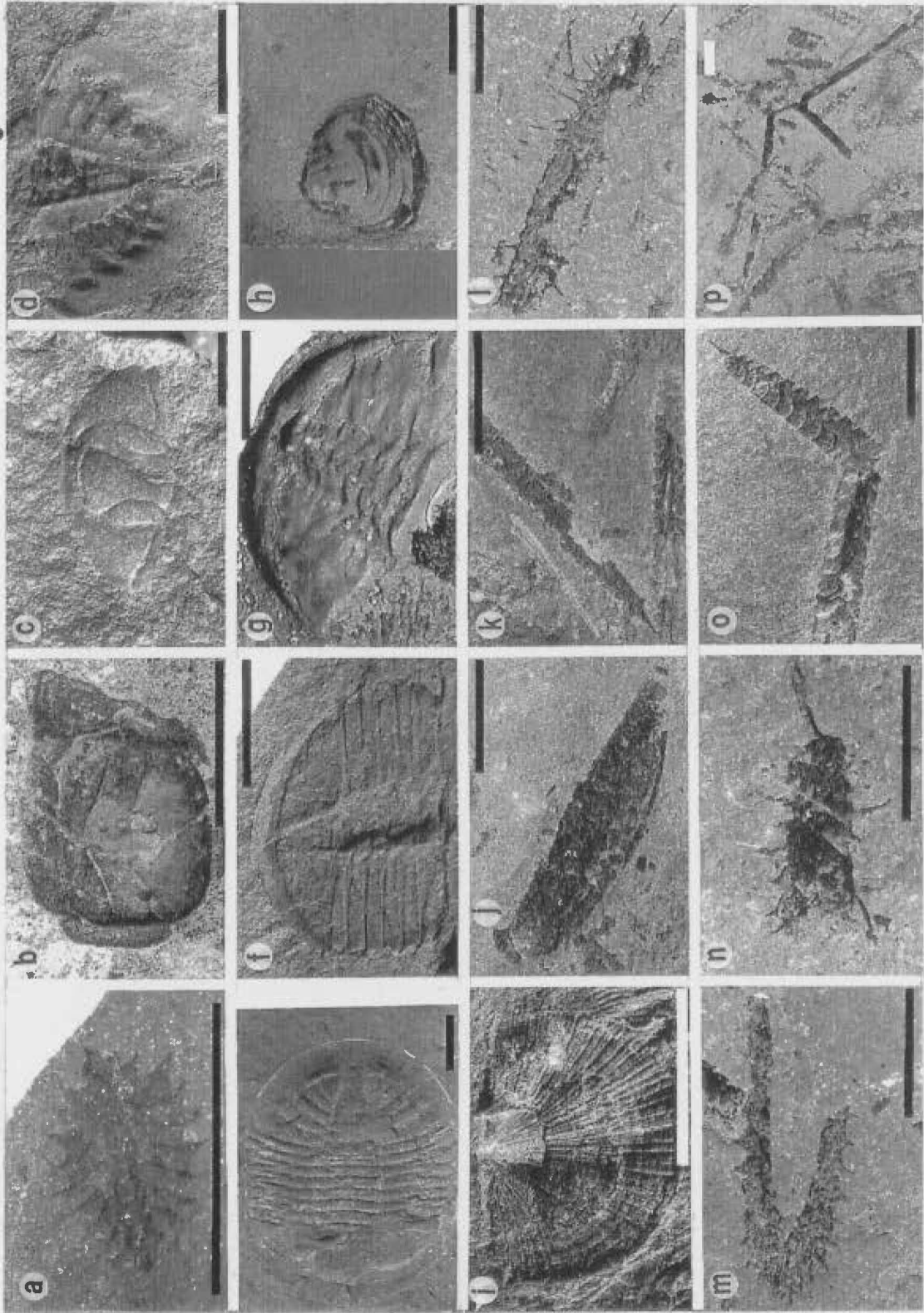
layers decrease in dolomite content and increase in clay and siliciclastic silt content, and change from structureless to finely-laminated up section. Common, but widely-dispersed skeletal components in the shale include graptolites, phyllocarids, cephalons and pygidia of numerous types of trilobites (Table 5.1), very small inarticulate brachiopods, and rare small, articulate brachiopods (Figure 5.8; Whittington and Kindle, 1963; Whittington, 1965; Erdtmann, 1971). They are essentially the same as the pelagic and benthic components the limestones but, in contrast to those, are commonly flattened or broken by compaction.

These strata are interpreted to be predominantly accumulations of hemipelagic sediment deposited in deep water below fairweather wave base, and given the absence of wave-generated structures in these generally unburrowed sediments, probably below storm wave base as well. Paucity of calcareous skeletal debris of indigenous invertebrates and algae indicate little, if any, in situ carbonate production, implying even greater water depths than those at which either of the two underlying Table Cove lithofacies were deposited. Comminuted debris of typical shallow water organisms and pelagic creatures dispersed in large volumes of carbonate mud indicate that most carbonate sediment was supplied from shallower water environments, while a fraction was supplied directly from the water column (eg. Scholle *et al.*, 1983; Mullins *et al.*, 1984). Siliciclastic clays and silt originating from either continental or oceanic terranes were continuously supplied to the water column as eolian dust, or by dilute suspensions generated by turbidity currents transporting and depositing coarser clastics elsewhere in the basin.

Fine depositional textures and overall absence of current structures suggest that most sediment accumulated by suspension settling. Rare graded beds of coarse skeletal debris, intraclasts and peloids record deposition from episodic turbidity currents. Very fine-grained carbonate sediment may have been continually extrained by daily tidal currents and waves and transported out into deeper water (Neumann and

Figure 5.8 Shelly fossils in Table Cove Fm. ribbon limestones. (A) - ribbon limestone type A; (B) - ribbon limestone type B. Bar scales are 0.5 cm. a) Phyllograptus cf. anna; Black Cove (B). b) Triarthrus cf. fischeri (cephalon); Roddickton Quarry (A). c) Endymionia cf. schucherti (cephalon); Spudgel's Cove (A). d) Pygidium of unidentified asaphid trilobite; Black Cove (B). e) Unidentified trilobite (cf. nielid); Black Cove (B). f) Thorax and pygidium of a raphiophorid trilobite (cf. Ampyx sp.); West Bay Centre Quarry (B). g) Pygidium of another raphiophorid trilobite (cf. Lonchodomus sp.; Beaver Brook (A). h) Inarticulate brachiopod (lingulid, cf. Obolus sp.) Black Cove (B). i) Small articulate brachiopod (orthid); Black Cove (B). j) Phyllocarid Caryocaris sp.; West Bay Centre Quarry (B). Phyllocarids are primitive relatives of the modern shrimp (eg. Calianassa) (Copeland and Boltmon, 1985). k) Diplograptid fragments, cf. Diplograptus; West Bay Center Quarry (B). l) Cryptograptid (Glossograptus? sp.; West Bay Center Quarry (B). m) Tetragraptus?; West Bay Center Quarry (B). n) Cryptograptid (Glossograptus? sp. (cf. n, above); West Bay Centre Quarry (B). o) Diplograptid; Black Cove (B). p) Dichograptid (?Tetragraptus or ?Schizograptus) and other unidentified graptolite fragments; West Bay Centre Quarry coast (B).

Figure 5.8



Land, 1975). Dense clouds of suspended sediment and turbidity currents originating in shallower areas were probably generated during storms (Ball *et al.*, 1967; Boardman and Neumann, 1984; Perkins and Enos, 1968).

The sedimentary structures (or lack of them) and the benthic, skeletal components in shale layers suggest those beds record the same depositional processes and environmental conditions as the limestones. Carbonate depletion in these layers is interpreted to be partly primary in origin and partly the product of early diagenetic carbonate redistribution and pressure dissolution during burial (Appendix D). Since individual limestone beds record more than a single depositional event, alternating limestone and shale layers are interpreted to record long period fluctuations in the composition of the sediment supplied to the slope (eg. relative abundances of carbonate, clay and/or organic matter) (Appendix D). Striking rhythmicity of the limestone and shale layers suggests sediment supply was governed by long period climatic changes.

(ii) Dark grey, trilobite-rich limestone Dark grey, burrowed wacke-/floatstone rich in coarse fragments of trilobites constitute 10-80 cm thick, knobbly-weathering units near the base of ribbon limestone sequences (Table 5.1; Figure 5.2). These strata are similar in appearance, composition, texture, and diagenesis to same-named limestones in the other, lower Table Cove lithofacies (Chapter sections 5.2.1 (ii) and 5.3.1 (ii)). Here, however, they notably directly overlie discrete gravitational slide masses in ribbon limestone.

Like their counterparts in the other two lithofacies, these sediments are interpreted to have come from an adjacent platform and to have been transported and rapidly deposited from waning bottom currents or sediment gravity flows. Similarly, thorough bioturbation suggests that the sediment was incrementally deposited and that thick accumulations record long periods of episodic deposition. Moreover, burrowing of these sediments and paucity of burrowing in enclosing ribbon limestones implies that depositing currents were oxygen-enriched and

transported infaunal organisms along with the sediment into this deep environment (eg. Föllmi and Grim, 1990). Coincidence of these deposits above slide masses suggests that whatever triggered mass movement also controlled the generation of sediment gravity flows. Mass movement may signal an increase in depositional slope caused by faulting or a period of increased seismic activity. Gravity driven currents may also indicate faulting and uplift of the source area into shallower water where sediments were more susceptible to disruption by high energy storms.

(iii) **Limestone conglomerate** Massive limestone conglomerate is interstratified with muddy (Type A) ribbon limestone at two localities. Three conglomerates comprise most of the upper 60 m of the Table Cove Formation at Vaches Point (Figure 5.7.f; back pocket). They are matrix-poor, lack primary depositional structures, and are composed mostly of clast-supported, equidimensional limestone pebbles with scattered cobble and boulder-size clasts; weakly brecciated areas in the conglomerate suggest mega-boulders are also present. Most clasts are either burrowed, fossiliferous wackestone or burrowed, peloidal packstone (Figure 5.7.g), identical in composition to limestones which comprise same-named lithofacies in the Table Point Formation (Chapter sections 4.3.1 and 4.3.2 ; Table 4.1). Other conspicuous, but very minor clast types include echinoderm pack-/grainstone, which is characteristic of both the uppermost Table Point Formation and lower Table Cove Formation limestones (Chapter sections 4.4.2 and 5.2.1 (iii)), plus plate-shaped clasts of radiolarian mudstone (Figure 5.7.g) and formless patches of dark, calcareous shale, both of which are constituents of enclosing ribbon limestone.

Several limestone conglomerates also occur in the upper 8.2 m of the Table Cove in drill core DH-1382 (back pocket). The basal bed (~ 4 m thick) changes from matrix-supported and pebbly to clast-supported and barely disarticulated limestone up section. Above it are several poorly-sorted, matrix-supported, pebbly conglomerates (5-130 cm thick).

Most clasts are very fossiliferous and/or peloidal and/or oncolitic wacke-/packstone, identical to limestones which comprise the sponge-oncolite biostrome at the top of the Table Point Formation (Chapter section 4.4.1) and the burrowed limestone lithofacies of the Table Cove Formation (Chapter section 5.2.1) in the immediate area.

Matrix-supported fabrics in the thinner and finer-grained conglomerates in DH-1382 and great bed thickness, poor size sorting, the presence of megaboulders, and the absence of stratification in the conglomerates at Vaches Point and the base of DH-1382 suggest these sediments were transported and deposited by debris flows (Middleton and Hampton, 1976). Predominant pebbly debris is thought to have originated by disintegration of semi-lithified, nodular limestones during transport, the process of which appears to be frozen in the conglomerates where weakly brecciated megaboulders grade almost imperceptibly into pebbly, polymictic conglomerate.

Debris flows may have evolved from slides that originated on an adjacent, contemporaneous platform or on the upper slope. Alternatively they may have originated by mass wasting along an escarpment generated by submarine faulting that exhumed buried platform and/or upper slope carbonates. The composition of the clasts comprising the conglomerates in DH-1382 suggests that they could have been derived solely from contemporaneous environments, but those making up the Vaches Point conglomerates, which are representative of a greater stratigraphic thickness of platform sediments, indicate faulting and uplift were involved.

5.4.2 Synsedimentary Deformation

Synsedimentary deformation structures and fabrics generated by gravitational sliding are more pervasive and complex in thick sequences of ribbon limestone Type A than in other lithofacies previously described or in Type B ribbon limestone. Discrete slides range from only a few tens of centimetres to ~4 m thick. Deformation is manifest by a complete spectrum of brittle and ductile structures and fabrics including

faults, rotated and imbricated beds, pebbly and chaotic limestone conglomerate, folds (Figure 5.7.a), sheared bedding and quasi-conglomeratic limestone (Appendix C). Brittle and ductile features are of equal importance in the stratigraphically lowest beds, while ductile deformation predominates in slides at the top of the lithofacies (Appendix C).

5.4.3 Lithologies of Sub-lithofacies B

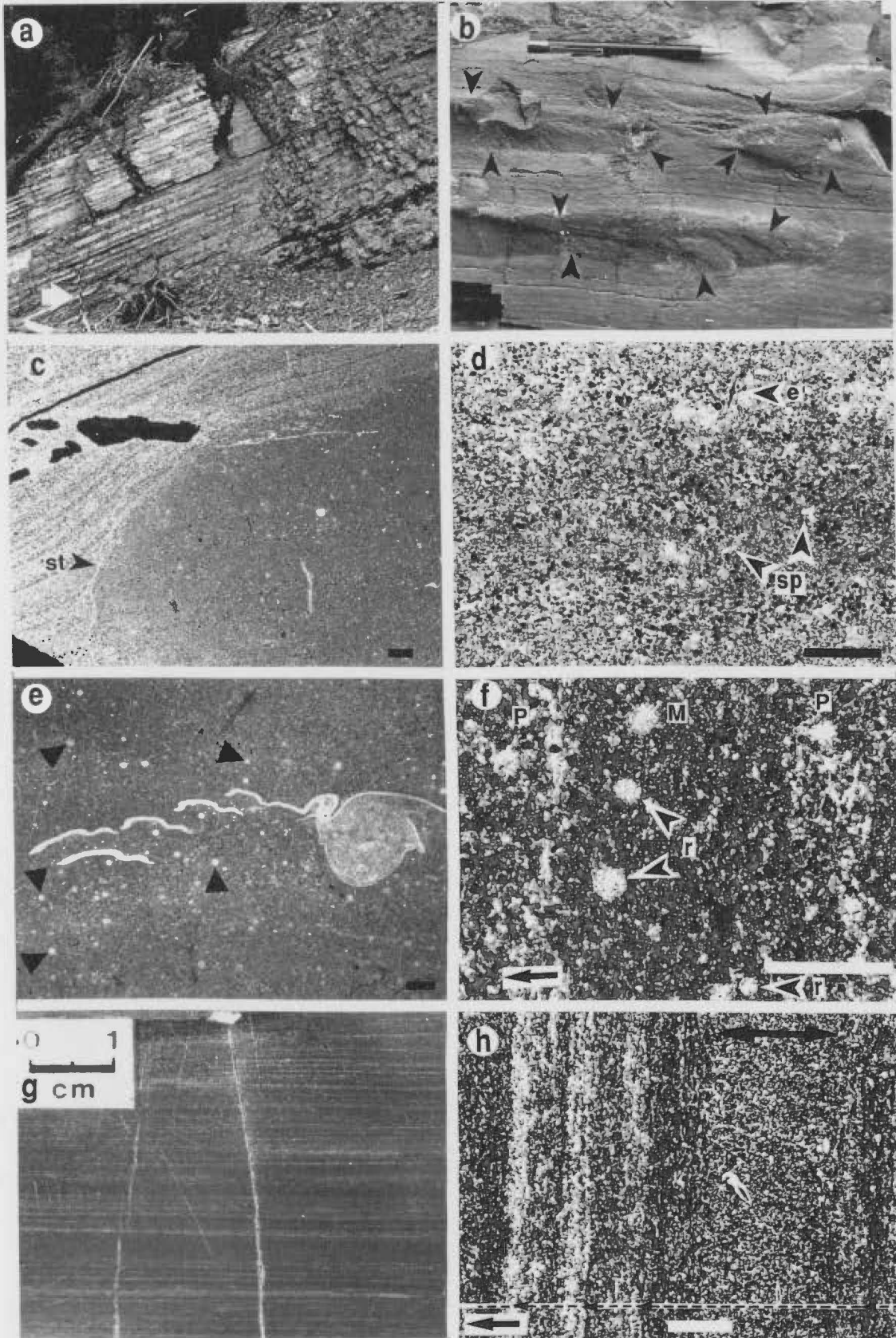
(i) **Ribbon limestone** These ribbon limestones form blocky-weathering outcrops composed of nearly equally resistant, thin beds of limestone and argillaceous dolosiltite generally interbedded on a scale of 2-15 cm (Table 5.1; Figures 5.2 and 5.9.a). In contrast to ribbon limestones previously described, bedding in these strata is defined by discontinuous, cigar-shaped limestone nodules with smooth or irregular bounding surfaces (Figure 5.9.b,c), which in plan view are proven to be either hummocky, rectangular strips or irregular, polygonal limestone plates. Limestone:dolosiltite ratios are highly variable among different outcrops, but limestone beds decrease in thickness and number, and argillaceous dolosiltite becomes the dominant lithology up section.

Limestone beds are composed of peloidal, spiculitic pack-/grainstone and radiolarian mud-/wackestone. Either lithology may comprise a single limestone bed (Figure 5.9.d,e), but more commonly they occur as superposed or alternating layers a few millimetres to a few centimetres thick in a limestone bed (Figure 5.9.f); alternating packstone-mudstone layers define normally-graded couplets. Peloidal pack-/grainstone, which is most abundant at the base of lithofacies, typically contains very small fragments of shallow water, shelly invertebrates and calcareous algae (Table 5.1). Most layers lack distinct structure, but some relatively thick beds are partial Bouma sequences (Table 5.1). Radiolarian mud-/wackestone, which predominates at the top of the lithofacies, also contains scattered graptolites and phyllocarids, as well as benthic trilobites, and small inarticulate and articulate brachiopods (Figures 5.8 and 5.9.e), similar to those which occur in Type A ribbon limestone.

Figure 5.9 Ribbon limestone lithofacies (Type B) (Table Cove Formation); field photographs and photomicrographs. All bar scales are 1 mm.

a) Blocky-weathering ribbon limestone at the top of the Table Cove Formation at Black Cove; see also Figure 5.3.b. Metre stick (arrow) for scale. b) Ribbon limestone in West Bay Centre Quarry. Arrows delineate discontinuous limestone nodules that grade into laminated dolosiltite. c) Thin section negative of limestone nodule and enclosing dolosiltite; West Bay Centre Quarry. Grainy, turbiditic laminae in limestone are defined by sponge spicules (black specks). Those in the centre of the nodule are traceable directly into adjacent dolosiltite. Featureless hemipelagic mudstone laminae in the nodule trace into argillaceous (white) laminae in the dolosiltite. Bending of dolosiltite laminae around the top of the limestone nodule is due to differential compaction, which has reduced the thickness of the carbonate-depleted dolosiltite ~50%. st = stylolite; black areas in the dolosiltite are holes in the thin section. d) Photomicrograph of vaguely laminated, coarse microsparitic peloidal packstone and mudstone; West Bay Centre Quarry. Peloidal (dense micrite) layers contain very small skeletal fragments of platformal invertebrates (o=ostracode, e=echinoderm, sp=spicule). e) Radiolarian (small white spheres) mudstone with a large trilobite; coastal outcrop east of Boswarlos. f) Photomicrograph of alternating peloidal, spiculitic packstone (P) and radiolarian (r) mudstone (M) laminae; West Bay Centre Quarry. Dense micritic grains are peloids; white grains in peloidal layers are siliceous spicules and quartz silt. g) Polished slab of laminated dolosiltite; West Bay Centre Quarry. Light laminae are siliceous; dark laminae are argillaceous. h) Photomicrograph of laminated dolosiltite; West Bay Centre Quarry. Light laminae are clay-poor, contain high concentrations of siliceous sponge spicules, quartz silt, and dolomitized peloids, and minor micritic peloids and very small, calcitic skeletal fragments. Massive lamina in centre (double arrow) is composed primarily of siliceous spicules; predominance of circular cross-sections indicates they are aligned. Dark laminae are clay-rich, dolomite- and quartz silt-poor, and devoid of radiolarians. Alternating siliceous and argillaceous laminae define normally-graded couplets (arrows).

Figure 5.9



Beds generally appear structureless, but faint lamination is commonly defined by radiolarians and graptolites, and thin superposed mud-/wackestone layers are commonly defined by different neospar crystal sizes and/or abundance of radiolarians. As in Type A limestones, carbonate mud is invariably replaced by neomorphic calcite and aggrading crystal fabrics on bed margins are distinct.

Argillaceous interbeds, in contrast to calcareous shale in ribbon limestone Type A, are very dolomitic and siliceous and very fossiliferous (Figure 5.9.g,h). They are invariably finely-laminated; ripple-scale cross-lamination, low-angle truncations, small-scale, soft-sediment faults, folds, and convolute lamination occur in a few horizons. They pass laterally into adjacent limestone nodules and are proven to be calcite- and radiolarian-depleted, and compacted (~50%) equivalents of sediments comprising limestone layers (Figure 5.9.b-c; Table 5.1). Graptolites, phyllocarids and small inarticulate brachiopods are very abundant (Figure 5.8; Morris and Kay, 1966; Erdtmann, 1971; Finney and Skevington, 1979). On most bedding planes they are broken and/or randomly oriented, but on some surfaces all three components are current aligned.

Similar to muddy (Type A) ribbon limestones described above (Chapter section 5.4.1(i)), these strata are predominantly composed of fine, resedimented carbonate derived from shallow water areas, and lesser wholly pelagic skeletal material, deposited in a deep, quiet water environment. Structureless, radiolarian-bearing muds are interpreted to represent the pulsating background of hemipelagic sediments deposited from suspension. Spiculitic, peloidal sands are interpreted to record episodic transport and deposition from turbidity currents. The latter indicate that adjacent platform(s) were sites of fine peloidal and skeletal sand accumulation and so were probably shallower than platforms that were sources for muddy (Type A) ribbon limestone sequences.

Thin layering within limestone beds demonstrates that they do not

record single depositional events. Moreover, preservation of similar, albeit compacted, layers in enclosing dolosiltite prove that those sediments are carbonate-depleted hemipelagic sediments and turbidites. If limestone-dolosiltite rhythms that define bedding record long period, cyclic changes in the average composition of the sediment as defined by relative abundances of carbonate, fine siliciclastics, and organic matter, then these strata demonstrate that compositional differences were subtle at best. Discontinuous limestone beds that pass laterally into compacted dolosiltite demonstrate that bedding is at least partly controlled by carbonate redistribution before deep burial (Appendix D).

(ii) **Bentonite** Several cm-thick beds of sticky clay are interbedded with ribbon limestones in West Bay Centre Quarry (Port au Port Peninsula), the lowest of which is correlated with the single clay bed at the base of the ribbon limestone lithofacies in the Black Cove section, 27 km to the east. XRD analysis indicates that they are composed of expandable, mixed layer illite-smectite clays. Like similar beds in the burrowed limestone lithofacies (Chapter section 5.2.1 (v)), they are interpreted to be altered volcanic ash layers that accumulated on the sea floor by suspension settling through the water column.

5.4.4 **Synsedimentary Deformation**

Deformation structures generated by gravitational sliding are less common and more subtle than those in thick, muddy ribbon limestone sequences. Difficulties in recognizing deformed horizons is partly due to limited exposure and to uniform, blocky-weathering nature of these strata which obscures rhythmic bedding. Centimetre-scale folds in dolosiltite interbeds are the only distinct expression of ductile deformation. Brittle failure is manifest by cryptic, low-angle truncation surfaces, thin (<1 m) discontinuous domains of disoriented limestone nodules (plates) dipping at odd angles to bedding, and, locally, cm-wide fractures that extend into limestone nodules and are filled with dolosiltite.

5.4.5 Interpretation

The ribbon limestone lithofacies is interpreted to have been deposited at the base of a carbonate slope and adjacent basin margin. Most sediments came from adjacent shallower environments and were episodically deposited from hemipelagic suspensions and turbidity currents (ribbon limestone and dark grey, trilobite-rich limestone). They were commonly displaced further downslope in gravitational slides. Seismicity or faulting also triggered slides or generated escarpments on the upper slope or adjacent platform locally from which originated debris flows that transported semi-lithified, shallower water carbonates (limestone conglomerate) onto the slope and into the basin.

A deeper-water setting than is inferred for the other Table Cove Formation lithofacies is indicated by the apparent absence of *in situ* generated carbonate sediment, the low diversity of benthic, shelly invertebrates, and low numbers and small size of soft-bodied infaunal organisms. Collectively these features point to restrictions imposed by limited light, colder temperatures, and/or limited availability of O₂ in bottom waters. The presence of a benthic fauna indicates that bottom waters were never anoxic, but their small size and low diversity, and the small size of burrowers, suggest that bottom waters were dysaerobic (0.1-1.0 ml/l, Rhoads and Morse, 1971; Byers, 1977). Disappearance of burrows up section suggests that interstitial waters became increasingly dysaerobic or anoxic, thereby precluding inhabitation by infaunal organisms. This further implies that oxygen levels in bottom waters gradually diminished, probably as a consequence of gradually increasing water depth.

Actual water depth can only be broadly bracketed. Absence of indigenous green algae implies depths of greater than 25 m (Wray, 1977), inferred below storm wave base conditions signal depths of at least several tens of metres, and the general absence of an abundant and diverse, indigenous, calcareous benthos probably indicates depths

greater than 100-150 m (Benedict and Walker, 1978; Wilson and Jordan, 1983). Absence of evidence of carbonate dissolution (eg. red clay deposits or siliceous oozes), implies deposition above the Calcite Compensation Depth and, possibly, the Aragonite Compensation Depth. Depths to the CCD and ACD in modern oceans are highly variable (Li *et al.*, 1969; Berger, 1970, 1971, 1974; Broecker, 1974), and are unknown for Paleozoic oceans. Based on data from modern tropical oceans, specifically in areas of high organic productivity adjacent to a continent, such as is envisaged for deposition of the Table Cove, estimated maximum depths to the CCD and ACD, above which ribbon limestone was deposited, are 2500 m and 500 m, respectively.

Rhythmic bedding in these deposits is partly due to periodic changes in the composition of sediment supplied to lower slope - basin margin which has been accentuated by early diagenetic redistribution of carbonate and later pressure dissolution (Appendix D). Nevertheless, a decrease in the limestone:shale (limestone:dolosiltite) ratio up section indicates that progressively less carbonate sediment was deposited. That change, which is accompanied by a decrease in thickness and number of carbonate beds and by either fining of the sediment and/or a change from mixed turbidites and hemipelagites to hemipelagic deposits up section, indicates either increasing distance from shallow water sediment sources and/or that source areas subsided to depths at which biogenic carbonate production gradually ceased and only infrequent, exceptionally powerful storms were capable of disrupting surficial sediments and transporting them out over the slope.

5.5 Paleoslope Direction

Most Table Cove Formation sequences include horizons of synsedimentary deformation structures indicative of gravitational sliding. Very few, however, are either pervasively deformed or well-enough exposed to permit measurements of fold axes, faults, and/or rotated and imbricated

bedding from which transport direction, hence slope orientation, can be determined (Woodcock, 1976, 1979). Numerous data collected from anomalously thick slope sequences well-exposed at Table Cove and along the Bellburns-Spudgel's Cove coast (Figure 1.2) indicate an unconventional slope history, namely a reversal from northwest- to southeast-dipping during the course of sedimentation (Figure 5.10 and the Bellburns-Spudgels Cove section in the back pocket). Sparse data from the Port au Port Peninsula indicate displacement on a north-dipping paleoslope.

Among Table Cove sequences there is no consistent directional change in thickness or lithofacies distribution indicative of a regional paleoslope. This, in conjunction with data from Table Cove outcrops, is interpreted as evidence that there was no single, regional slope flanking a single platform and that these sediments accumulated on numerous slopes of variable facing directions.

5.6 Summary and Reconstruction of Depositional Environments

The Table Cove Formation consists of thin-bedded, dark grey limestone and calcareous/dolomitic shale deposited in carbonate slope to basinal environments. It is differentiated from underlying platform limestones of the Table Point Formation not only by style of bedding, but by a deeper-water benthic fauna and conspicuous pelagic fauna, and by common to pervasive synsedimentary deformation structures generated by gravitational sliding. Schematic reconstructions of environments in which these strata were deposited are shown in Figure 5.11.

Muddy, bioturbated, fossiliferous carbonates (burrowed limestone lithofacies) were deposited on the shallow upper slope where favourable light levels, nutrient supply, water temperature and oxygenation of bottom waters allowed a diverse, benthic flora and shelly fauna, and soft-bodied infauna to thrive on and in the sediments (Figure 5.11.a, b). Most carbonate sediment was generated in place by the indigenous *Lenthos*, but some was transported onto the slope by bottom currents

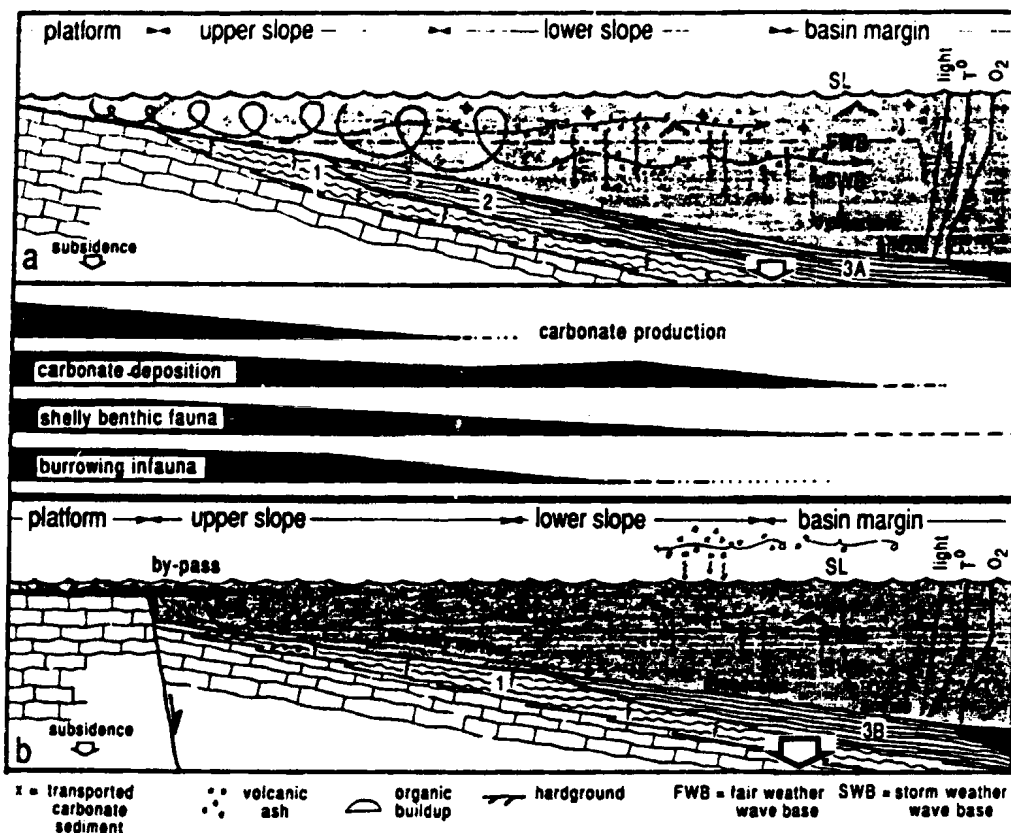


Figure 5.11 Interpretive reconstruction of depositional environments for the Table Cove Fm. 1, burrowed limestone lithofacies deposited on the upper slope; 2, parted limestone lithofacies deposited on the middle slope; 3, ribbon limestone lithofacies deposited on the lower slope and basin margin. a) Ramp-style carbonate slope envisaged for deepening-upward sequences in which upper slope sediments gradationally overlie platform limestones and grade up into muddy ribbon limestone. b) By-pass margin slope envisaged for Table Cove sequences in which upper slope sediments gradationally overlie platform carbonates and are overlain by mixed, sandy and muddy ribbon limestone.

originating in adjacent platformal environments. Locally, platform-derived echinoderm debris accumulated in diffuse sand bodies on the upper slope, their development partly determined by the location of crinoid-cystoid shoals on the adjacent platform, and by persistent bottom currents that concentrated the debris (Figure 5.11.a). Elsewhere discontinuous sedimentation on the upper slope, caused either by pulses of subsidence that inhibited carbonate production or by bottom currents that prevented sediment from accumulating, resulted in the formation of firmgrounds and mineralized hardgrounds (Figure 5.11.b).

Burrowed muds with comparatively little and finer-grained skeletal material (parted limestone lithofacies) accumulated on the lower upper slope and mid-slope, at depths well below normal wave base, but possibly above storm wave base (Figure 5.11.a). Most sediments came from higher up on the slope or the platform and were deposited from muddy suspensions or low concentration turbidity currents. A soft-bodied infauna, including several large deposit feeders, thrived in the sediment, but at most times restrictions imposed by poor light, low temperature, and/or low dissolved oxygen content of bottom waters prevented most shelly invertebrates and calcareous algae from inhabiting the environment.

Sparsely-burrowed or laminated radiolarian mudstone, peloidal-spiculitic sands, and terrigenous clays (ribbon limestone lithofacies) accumulated on the lower slope and basin margin at depths below storm wave base (Figure 5.11.a,b). Carbonate sediment came almost solely from the platform and upper slope and was deposited from storm-generated suspensions and turbidity currents. Rhythmic alternations of limestone and argillaceous layers resulted from long period fluctuations in carbonate sediment supply in concert with an increasing supply of terrigenous clays originating from within the basin. Very restrictive conditions imposed by limited light, cold temperatures and/or limited oxygen availability precluded inhabitation, even temporarily, by a diverse, carbonate-producing, benthic community. Poorly-oxygenated

bottom waters permitted small species of trilobites and brachiopods to live on the seafloor. Very dysaerobic or anoxic interstitial waters generated by rapid consumption of the available oxygen by bacterial oxidation of organic matter in near surface sediments excluded inhabitation by a soft-bodied infauna in all but the shallowest regions of the lower slope.

There is no evidence that sediments deposited on the middle and lower slope and basin margin were dispersed via major channels or canyons that dissected the slope. Thus, shallow-water-derived hemipelagites and turbidites deposited in these environments are envisaged to have formed linear aprons parallel to the strike of the adjacent platform source and the slope (eg. Mullins and Cook, 1986).

Locally 'normal' sedimentation in all subenvironments on the slope to basin gradient was temporarily superseded by deposition of platform-derived sediments rich in organic matter and trilobite and echinoderm debris (dark grey, trilobite-rich limestone) that were transported onto the slope by gravity currents or flows (Figure 5.11.a). During these times platform sediments may have been more susceptible to disruption and downslope transport either because 1) the platform shoaled and was frequently impinged upon by powerful waves, 2) seismic activity was frequent, or 3) the angle of the depositional slope was temporarily increased by synsedimentary faulting.

As carbonate deposition on the slope occurred, volcanism outboard of the continent generated clouds of ash that were transported by wind toward the continent, settled out through the air and water column, and were deposited on the sea floor (Figure 5.11.a,b). Near the end of slope sedimentation, powerful seismic events, possibly related to outboard volcanism, locally triggered major slides and/or generated submarine escarpments from which originated debris flows that transported the semi-lithified, shallow water carbonates onto the slope and basin margin (Figure 5.11.a).

Deposition of the deep-water, slope carbonates atop shallow water, platform limestones signals an increase in water depth accompanied by tilting of the platform. Table Cove Formation lithofacies sequences, in turn, invariably record gradual cessation of *in situ* carbonate production followed by deposition of shallow water-derived, hemipelagic and turbiditic sediment under steadily deteriorating environmental conditions. Each constitutes a single, deepening-upward succession that involved drowning of the adjacent platform, lateral migration of deep water environments and sediments over shallower ones and, eventually, basin formation. Since deposition of the Table Cove coincides approximately with an eustatic sea level fall (Ross *et al.*, 1989; Figure 4.6.c), deepening over the Newfoundland platform is interpreted to have been caused by rapid subsidence.

Slope configurations and subsidence histories varied across the region with three different styles recognized.

1) Table Cove sequences composed of fossiliferous, upper slope limestones (burrowed limestone lithofacies) that gradationally overlie platform limestones and grade up into muddy ribbon limestone (Type A) are interpreted to have deposited on a gently-dipping, uniformly subsiding ramp (Ahr, 1973; Figure 5.11.a). Gradational changes in sediment composition and texture up section suggest that depositional environments graded on a cline between the relict platform and the basin, along which there were no abrupt topographic breaks or changes in declivity of the slope. Deposition of predominantly muddy, hemipelagic sediment on the lower slope and basin margin indicates contemporaneous source areas were sites of fine carbonate sediment accumulation and probably lay at depths below fairweather wave base. Concurrent deepening of the shallow water sediment source and the slope suggests subsidence of the two areas, though not necessarily identical in rate, were intimately related, and further suggests that ramp-style slopes were not structurally disjointed from adjacent relict platforms.

2) Table Cove sequences consisting of upper slope carbonates overlain by peloidal-spiculitic ribbon limestone (Type B) are interpreted to have been deposited on a very gently dipping slope adjacent to a by-pass margin (McIlreath and James, 1984; Figure 5.11.b). Gradational contacts with, and compositional and textural similarities between, upper slope and platform sediments indicate the former record continued carbonate production and accumulation under steadily increasing water depth. However, the composition of lower slope ribbon limestone indicates derivation, in part, from an adjacent, relict platform that remained in fairly shallow water where normal wave or current activity favoured accumulation of fine carbonate sand rather than mud. Paucity of peloidal and spiculitic sediments in upper slope limestones suggests that currents which delivered carbonate sand to the lower slope and basin by-passed the upper slope. Those nondepositional currents traveling across the upper slope may have promoted the generation of firmgrounds and mineralized hardgrounds locally. Scarcity of deformation structures caused by sliding in these slope deposits indicates an extremely low-angle depositional slope, but sediment by-passing of the upper slope suggests that the platform to slope transition was relatively steep. The platform - slope break is thought to have been defined by a fault or fault zone which was not likely expressed as an escarpment, but permitted the platform and slope to subside independently of each other, thereby creating the vertical drop necessary to generate high velocity currents that by-passed the upper slope.

3) Table Cove sequences composed of muddy, parted limestone overlain by muddy, ribbon limestone are also interpreted to have been deposited during continued subsidence of a gently-inclined, ramp-style slope. However, the abrupt, and possibly discordant, contact between basal, parted limestone and underlying platform limestone indicates that initial subsidence was so rapid that carbonate production ceased rapidly and was largely replaced by hemipelagite and turbidite deposition. This

expression of differential subsidence also suggests that the slope was structurally separated from the relict platform that supplied sediment to deep water environments.

The thickness of slope to basinal carbonates deposited was fundamentally, and predominantly controlled by subsidence. The rate of subsidence of the slope determined how long in situ carbonate production continued. The rate of subsidence of the adjacent relict platform, whether it represented the shallowest region of a ramp or was separated from the slope by a fault, determined the availability of carbonate sediment transported into adjacent deep-water settings. Therefore, to a first approximation, thick Table Cove sequences (eg. Table Cove, Figure 5.1.a) are inferred to have been deposited in areas of relatively slow subsidence; thin sequences (eg. Black Cove, Figure 5.1.b), are inferred to have been deposited in areas where subsidence was rapid. Gravitational sliding, which is most evident in thick Table Cove sequences, may have increased the thickness of those sequences by either repeating stratigraphy in discrete slide masses or by introducing 'allochthonous' slide masses into the environment. Those processes, however, probably only exaggerated or accentuated what would have been the primary depositional thickness. Conversely, thinning caused by gravitational sliding may present a very misleading picture of the depositional history of the area. Since there commonly is little evidence of sliding in thin Table Cove sequences, they are thought to closely reflect the interplay of local subsidence and sedimentation.

5.7 Table Cove Formation vs. Continental Slope and Rise Carbonates

Slope to basinal carbonates of the Table Cove Formation differ in several respects from other deep water carbonates sequences deposited in continental margin settings and margins of large carbonate platforms (cf. Cook and Taylor, 1977; Keith and Freidman, 1977; Reinhardt, 1977; Yurewicz, 1977; Mullins and Neumann, 1979; Cook, 1979; Cook and Mullins,

1983 and references therein; McIlreath and James, 1984; Mullins et al., 1984; Coniglio, 1985; Demicco, 1985; James and Stevens, 1986; Brooks and Holmes, 1990; Eberli and Ginsburg, 1990). 1) Table Cove sequences are thinner. 2) Table Cove sequences vary markedly, and nondirectionally both along strike and across strike and are locally not present in the stratigraphic section. 3) The depositional slope faced different directions and, locally, changed facing direction during the course of sedimentation. 4) Slope sequences contain no platy conglomerates. 5) Slope sequences only continually deepen, and do not shoal. These aspects of the Table Cove Formation are thought to reflect the fact that the deep-water slopes formed on a tectonically deformed platform, well inboard of the margin of the continent, in an evolving foreland basin. They are addressed in Part II - Sedimentation and Tectonics, Chapter 13.

CHAPTER 6

SEDIMENTOLOGY OF THE CAPE CORMORANT FORMATION

6.1 General Characteristics and Stratigraphic Relationships

The Cape Cormorant Formation consists of polymictic, carbonate lithoclast conglomerate and calcarenite, and lesser peloidal, fossiliferous ribbon limestone, interstratified with slightly calcareous to noncalcareous, graptolitic shale. These strata disconformably overlies muddy, bioturbated, fossiliferous Table Point Formation limestone (Chapter 4) only on the extreme western side of Port au Port Peninsula (Figures 6.1, 6.2 and 6.3.a,b) and are conformably overlain by the Mainland Sandstone (Chapter 8; Figures 6.1.a, 6.2, and 6.3.d).

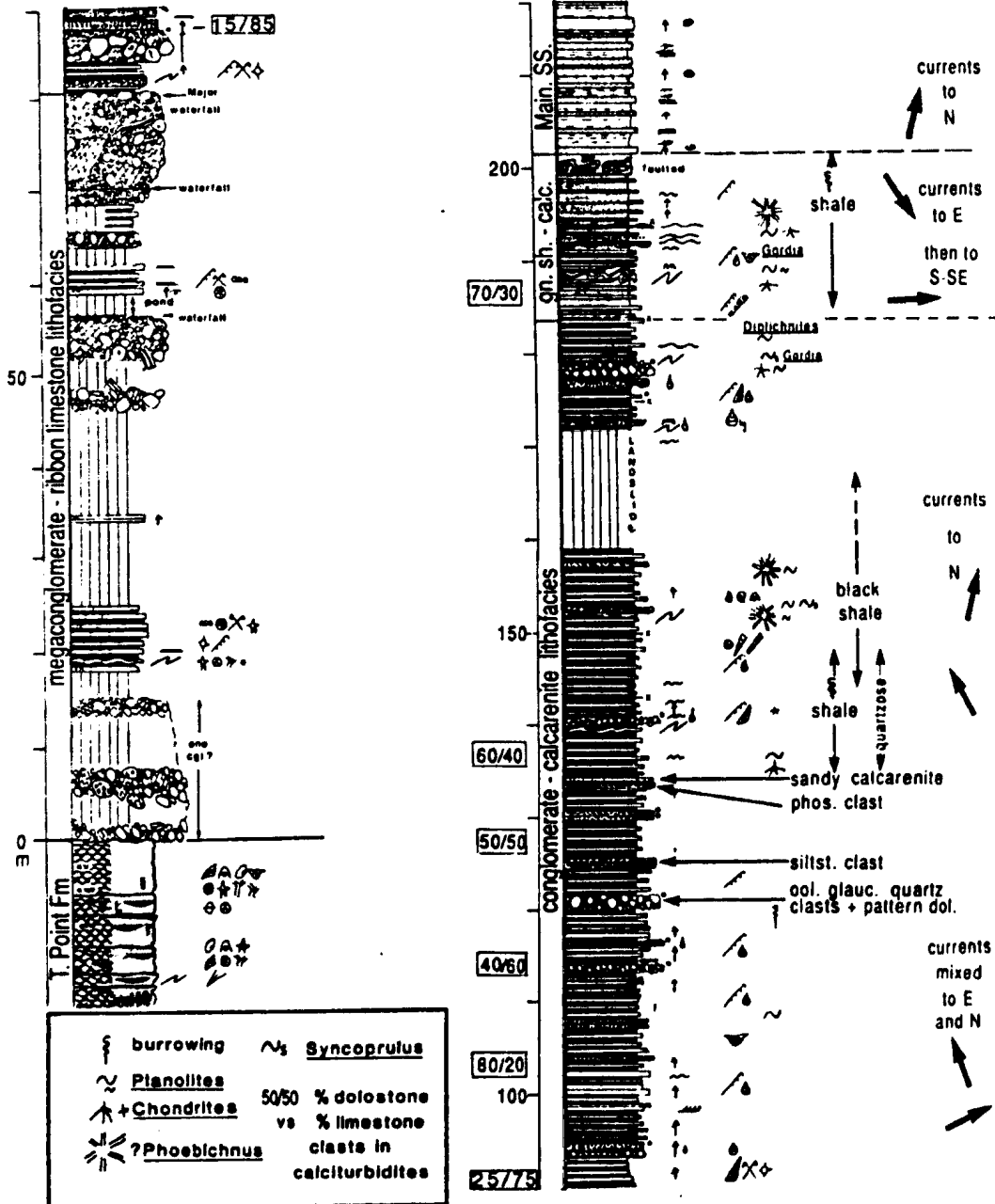
The following sedimentologic analysis of the Cape Cormorant is based primarily on detailed study of the most complete, structurally intact, and accessible section exposed in Caribou Brook and in coastal outcrops several hundred metres north and south of the brook (Figures 6.1.a and 6.2). The lower 70 m of the approximately 200 m thick section is poorly-exposed in Caribou Brook proper and so has been documented in lesser detail than the overlying strata.

Cape Cormorant strata exposed along the coast north of, within, and south of Big Cove proper were also examined but were not documented in detail simply because of limited outcrop accessibility. Big Cove Section A (Figures 6.1.b and 6.3.a,b), superbly exposed along the coast north of Big Cove, was measured by traverse along the top of the sea cliff (Figure 6.2). Observations were made from the top of the cliff and from a boat offshore. Big Cove Section B (Figure 6.1.c) is a composite of two partial sections in Big Cove proper (Figure 6.2). The Table Point - Cape Cormorant contact is exposed near the north end of the cove (Figure 6.3.c), but the sequence does not extend high enough up section to expose the upper contact with the Mainland Sandstone. Although neither of these Cape Cormorant sequences are complete they are

Figure 6.1 Measured sections of the Cape Cormorant Formation. a) Caribou Brook. b) Big Cove section (A) north of Big Cove; megaconglomerate-ribbon limestone lithofacies only. c) Big Cove (B) in Big Cove proper; megaconglomerate-ribbon limestone lithofacies only. Paleoslope indicators to the right of the column are: soft sediment thrust fault = half arrow, fold axis = line (sense of fold asymmetry = solid arrow), direction of thinning of megaconglomerate = outline arrow. Each represents one measurement unless otherwise indicated. Locations are shown in Figure 6.2. Key to symbols is in Appendix A.

Neither the structural integrity of Big Cove section (B) nor correlation of discrete beds (primarily megaconglomerates) in Big Cove proper have been established with certainty. The conglomerate at the base of the upper section (B2) may be laterally equivalent to the olistolith conglomerate (4a) at the top of the lower section (B1). However, calculations made from aerial photographs, assuming constant strike and dip between (4a) and (5a), indicate that as much as 25 m of section may be missing. The highest megaconglomerate (5d) underlies the entire promontory at the south end of Big Cove. Cliff exposures south of the cove indicate that it is at least 40 m thick. However, if the bed is not repeated by faulting at the promontory, it may be >200 m thick.

Cape Cormorant Formation (Caribou Brook)



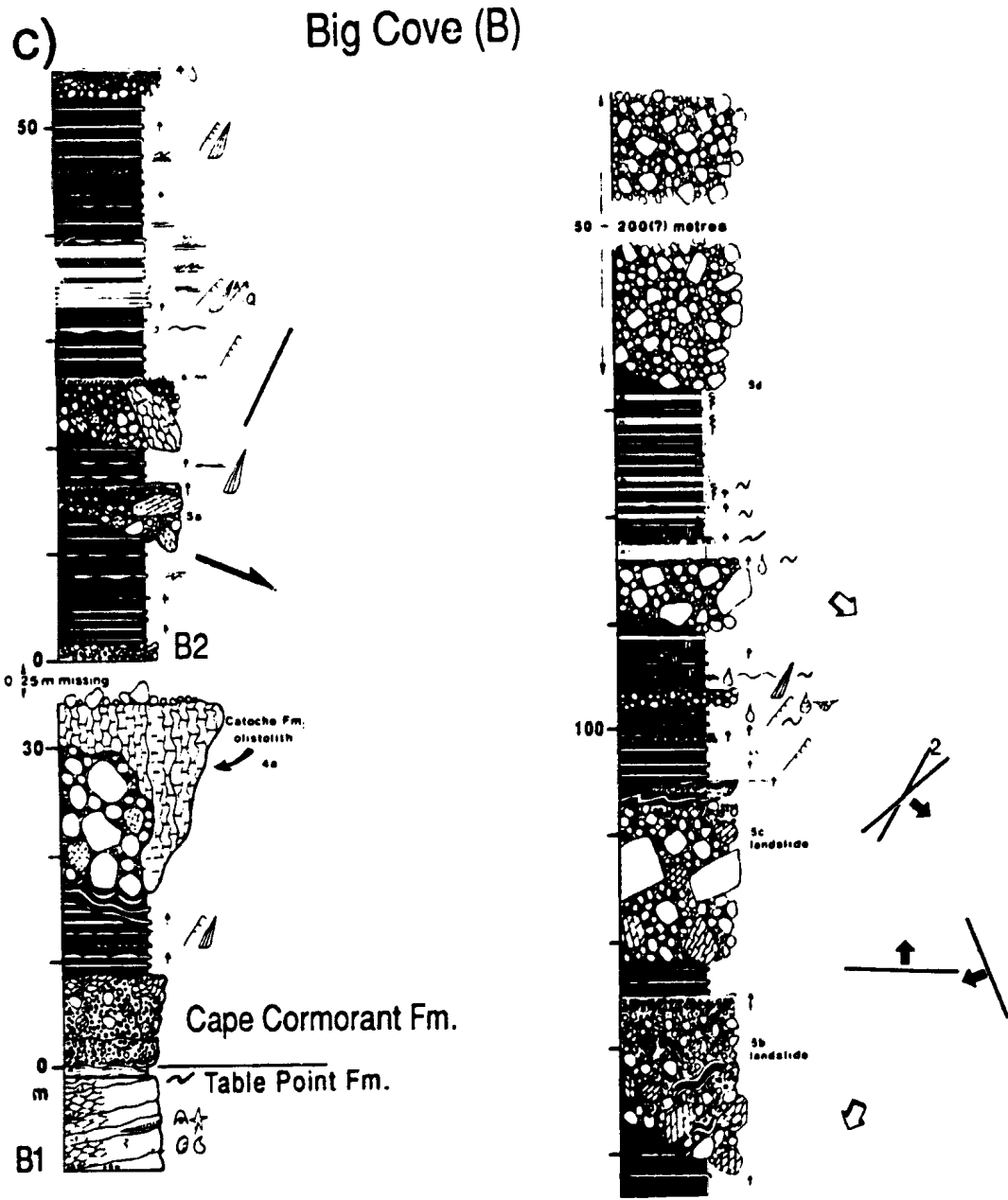


Figure 6.2 Geologic map of the west side of the Port au Port Peninsula (this study). Caribou Brook section (Figure 6.1.a) was measured in Caribou Brook proper and along the coast north of the brook. Big Cove section (A) (Figure 6.1.b) was measured by traverse (double lines) above the sea cliffs north of Big Cove. Both incomplete sequences comprising Big Cove section (B) (Figure 6.1.c) were measured in Big Cove proper. 1 = Mega-conglomerate in section A with Catoche Formation olistolith (Figure 6.7.a). 2 = Megaconglomerate in section A with Petit Jardin Formation olistolith (Figure 6.7.b). 3 = Megaconglomerate at the top of section A with Upper or Middle(?) Cambrian parted limestone olistolith (Figure 6.7.c). 4 = Table Point Formation-Cape Cormorant Formation contact, base of section B. 4a = Megaconglomerate with a Catoche Formation olistolith (Figure 6.3.d) 20 m above the Table Point-Cape Cormorant contact in section B. 5 = Megaconglomerates in the upper part of the Cape Cormorant of Big Cove section B2; 5a = matrix-rich conglomerate at 20; 5b = megaconglomerate at 60 m (corresponds to a prominent landslide on the coast); 5c = megaconglomerate at 80 m (corresponds to another landslide on the coast); 5d = megaconglomerate at 140 m.

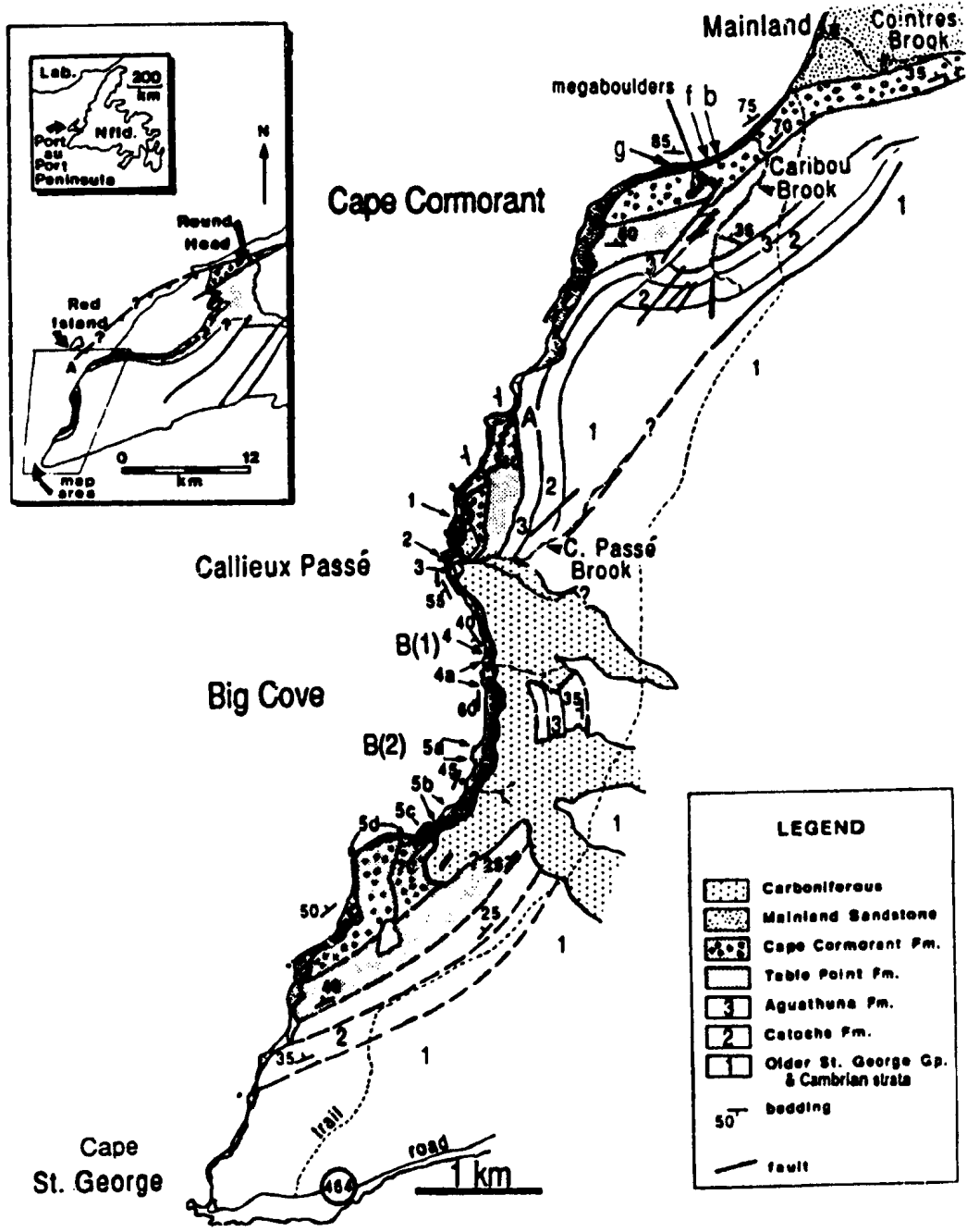
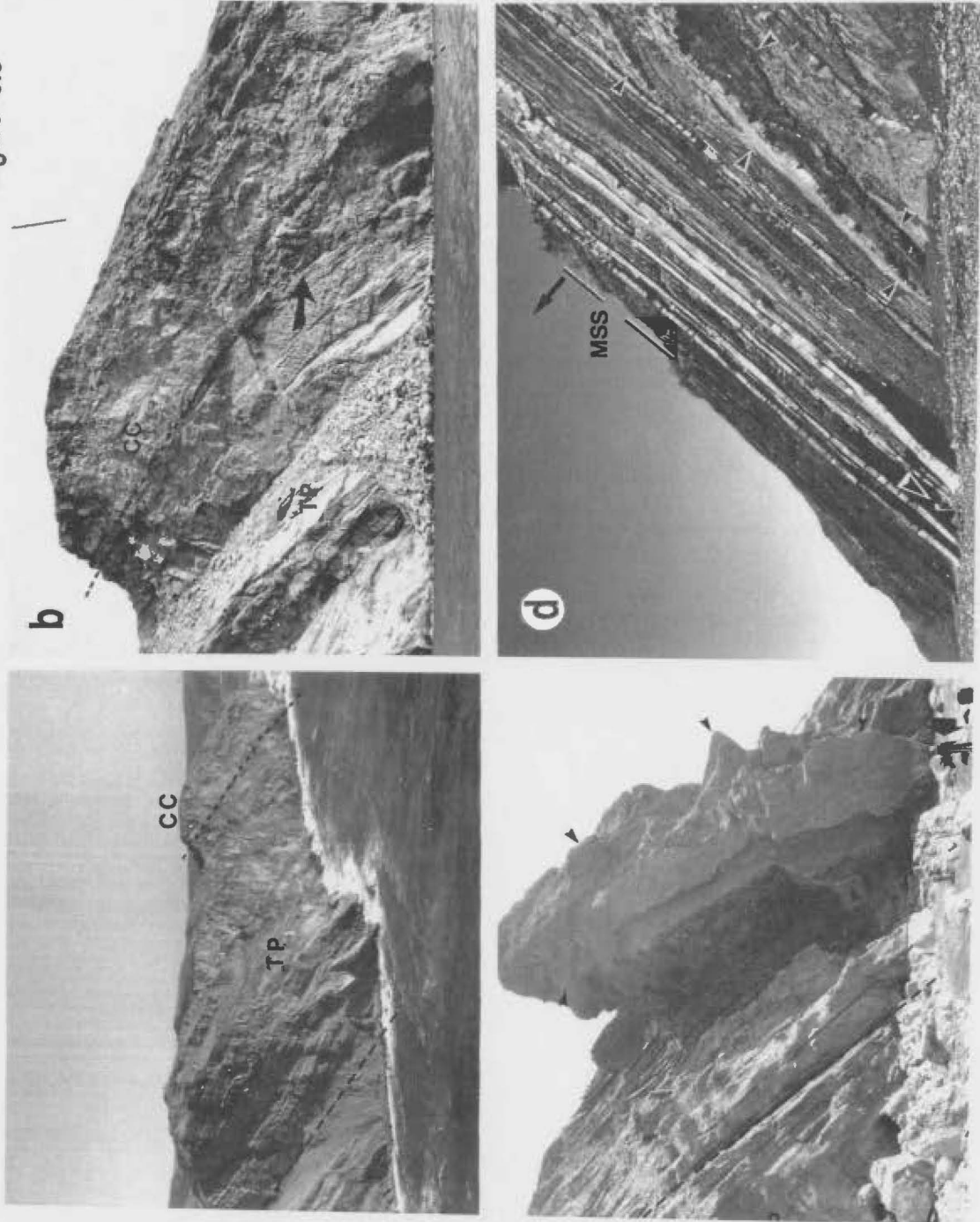


Figure 6.3 Stratigraphic relationships. a) Helicopter view of the Table Point-Cape Cormorant section (Big Cove (A)) north of Big Cove. The cliff of Table Point Fm. limestone in the foreground is about 150 m high. b) Table Point-Cape Cormorant contact; Big Cove (A). Traced in the hills behind the sea cliff, the contact displays ~8 m erosional relief and is discontinuously mantled by lithoclast calcirudite. The Cape Cormorant part of the cliff is a single, 39 m thick megaconglomerate. Beds in the top 10 m of the Table Point are folded and rotated (arrow). The cliff is approximately 150 m high. c) Table Point-Cape Cormorant contact; Big Cove (B). The contact is marked by a minor angular unconformity; the 8.5 m thick basal conglomerate is made up mostly of pebbly debris. Arrows point to an olistolith (40 m by 5-40 m by 7-15 m) of Catoche Formation limestone in a 15-20 m thick megaconglomerate about 20 m above the contact. The flat surface of the clast is primary bedding; the longest dimensions are nearly perpendicular to primary bedding and nearly parallel to conglomerate bedding. A. Pye (arrow) for scale. d) Cape Cormorant - Mainland Sandstone contact in the Caribou Brook section. The cliffs are ~20 m high; A. Pye (large arrow) for scale. Prominent light coloured beds are calcirudites in the green shale-calcarenite lithofacies of the Cape Cormorant Fm. Small arrows point to the bottom and top of a gravitational slide ~14 m below the top of the formation. A, Aquathuna Fm.; TP, Table Point Fm.; CC, Cape Cormorant Fm.; MSS, Mainland Sandstone.

Figure 6.3



both several tens of metres thicker than the Caribou Brook section.

The Cape Cormorant was also briefly studied in outcrop at the south end of Round Head (Figure 6.2). Polymictic boulder conglomerate forms the west-facing, vertical escarpment of Round Head, but it is pervasively dolomitized and the attitude of bedding is unknown. The escarpment could either represent a single, flat-lying, 60 m (\pm) thick bed or a bedding plane exposure of a nearly vertical conglomerate of unknown thickness.

6.2 Lithologies

The Cape Cormorant is made up of five major and one minor lithologies: shale, ribbon limestone, megaconglomerate/conglomerate, calcirudite, calcarenite/calcsiltite, and bentonite. Their sedimentologic and diagenetic characteristics are detailed in Table 6.1.

6.2.1 Shale (Table 6.1(1))

Dark, organic-rich shale constitutes the voluminous background sediment in the formation, comprising between 40-80% of discrete intervals. It is mostly composed of clay minerals with minor very fine, siliciclastic silt, but millimetre-thick laminae of carbonate sand, silt and mud are volumetrically important components. At Caribou Brook the shale changes from dark grey-brown, predominantly laminated and calcareous to black, laminated and noncalcareous to olive green and dark grey, mottled and noncalcareous up section (Figures 6.1.a and 6.4.a-e). There are a few thin horizons with disrupted laminae indicative of burrowing near the base of the section, but the mottled fabric of the green-grey shale at the top of the section indicates more pervasive burrowing.

The shale contains relatively low numbers of a limited variety of invertebrate fossils (Table 6.2 and Figure 6.5). The assemblage, of which graptolites, phyllocarids, and small inarticulate brachiopods are most abundant, is similar to those which occur in the Table Cove, Black

Table 6.1 Cape Cormorant Formation Lithologies

Lithology	General Character	Additional Components	Sedimentary Structures	Body Fossils	Interpretation
1) Shale					
(0-168 m CB) (Figure 6.4.a)	dark brown-grey, slightly calcareous to noncalcareous upsection; gritty, slightly fissile; clays in thin section mostly aligned parallel to bedding	minor silt-size, nonferroan, authigenic dolomite (commonly with dusty, detrital cores), detrital quartz, siliceous sponge spicules & radiolarians; scattered spherical to elliptical, blocky calcite (\pm ferroan) grains (0.1-0.3 mm across) of uncertain origin; minor pyrite (minute framboids either disseminated or concentrated in discontinuous streaks (0.3-0.5 mm by a few cm long); replaces radiolarians)	fine parallel lamination defined by numerous yellow-weathering carbonate laminae; very minor burrowing	common graptolites, phyllocarids, & inarticulate brachiopods; scattered small articulate brachiopods, small coiled & orthoconic cephalopods; rare segmented arthropod antennae? & carbonaceous algal? debris (Figure 6.5)	mostly pelagic sediments deposited by suspension settling in a deep, quiet water, dysoxic to anoxic basin or basin margin; carbonate-rich shale layers may be i) platform-derived carbonate-depleted hemipelagites or ii) suspension settling deposits of carbonate-bearing turbidity currents
(168--183 m CB) (Figure 6.4.b & c)	black, noncalcareous; lacks fissility; clays in thin section aligned parallel to bedding	very minor & very fine silt-size authigenic dolomite rhombs & detrital quartz; scattered blocky calcite grains (as above); rare siliceous spicules & radiolarians; very minor pyrite; <u>pervaded</u> by microcrystalline, ferroan dolomite	fine parallel lamination; minor burrowing in the top 4.5 m		
(183-202 m CB) (Figure 6.4.d & e)	olive green & dark grey, noncalcareous; lacks fissility; clays in thin section mostly aligned parallel to bedding	very minor, disseminated, silt-size authigenic dolomite & detrital quartz; comparatively pyritic (minute framboids disseminated & in discontinuous streaks (as above) & replaces spicules, radiolarians & elliptical grains of similar dimension to blocky calcite grains in underlying shale	mostly mottled or with discontinuous, relict parallel lamination suggestive of burrowing; lesser parallel lamination		

Table 6.1 continued

Lithology	Thickness	Contacts	Sedimentary Structures	Biotic Components	Interpretation
2) Ribbon Limestone i) peloidal, spiculitic W/P & radiolarian M	5-30 cm, up to 60 cm	sharp, commonly erosional bases; sharp, commonly concretionary tops	massive or parallel lamination; minor convolute lamination; W/P and M form 1-few cm thick, normally-graded couplets	radiolarians & sponge spicules plus very small fragments of shallow water fossils (eg. echinoderms, ostracodes, trilobites, inarticulate brachiopods, <u>Girvanella</u> , <u>Nuia</u> , & <u>Halysis</u>)	fine-grained, platform-derived carbonates episodically transported and deposited by turbidity currents & hemipelagic muds deposited from suspension; like limestone components of Table Cove Formation ribbon limestones (Chapter 5)
ii) calcareous, dolomitic shale	1-20 cm, up to 2 m	sharp contacts with limestones (diagenetically enhanced); flat sharp or gradational contacts with noncalcareous shale	parallel lamination	graptolites, phyllocarids, sponge spicules, radiolarians	pelagic sediments deposited by suspension settling and carbonate-depleted fine-grained carbonate turbidites and hemipelagites (as above); like calcareous shale/dolosiltite components of Table Cove Formation ribbon limestone (Chapter 5) - carbonate depletion <u>possibly</u> accentuated by redistribution during shallow burial
iii) massive M	20-100 cm	flat sharp or gradational at base; flat and sharp at top	massive or vague but pervasive mottled fabric; upper bedding planes commonly with small (0.3-0.5 mm dia.), subhorizontal burrows	none	platform-derived muds deposited by settling of voluminous, but dilute suspensions; <u>possibly</u> a product of carbonate redistribution during shallow burial

Table 6.1 continued

Lithology	Bed Thickness & Morphology	Composition & Texture	Internal/Sedimentary Structures	Interpretation
<p>3) Lithoclast Conglomerate & Megaconglomerate (beds >5 m thick composed of boulder-size & larger clasts)</p>	<p>-20 cm to ~65 m</p> <p>beds pinch and swell due to a combination of erosional relief on base & depositional topography on the top; topography accentuated by protruding cobbles or boulders; sloping surface topography indirectly inferred from evidence of gravitational sliding (eg. soft-sediment folds & wrinkles) in immediately overlying strata</p>	<p>poorly-sorted; clast size ranges from granules & pebbles to Volkswagen size blocks & olistoliths to at least 65 m across (average clast size generally parallels bed thickness)</p> <p>mostly clast-supported; matrix varies from <5-30%</p> <p>mostly equidimensional dolostone & limestone clasts of shallow marine aspect; minor chert & clasts of Cape Cormorant aspect; dolostones generally more angular than limestones; metres long slabs, blocks & olistoliths are angular, their shapes controlled by primary bedding (broadest surface of many is perpendicular or at a high angle to primary bedding in the clast)</p> <p>very dark brown, black or dark greenish-grey argillaceous matrix (identical to enclosing shale) contains floating granule- to silt-size carbonate lithoclasts plus radiolarians & small calcitic skeletal fragments; partly replace by cryptocrystalline quartz & microcrystalline dolomite in some beds</p>	<p>poorly-sorted, no preferred orientation of clasts, no stratification</p> <p>clast size & matrix content decrease & the degree of organization generally increase with decreasing bed thickness</p> <p>disorganized & inversely-graded beds most common in both relatively thin & very thick beds; inverse grading mostly identified by presence of outsized clasts at the tops of beds, locally by a gradual increase in clast size through entire bed; grading most obvious in megaconglomerates with several metres long clasts concentrated at the top</p> <p>normally-graded (two types): normal, coarse tail grading accompanied by a decrease in matrix up through the bed occurs in relatively thin (<1 m) pebbly conglomerates; normal, coarse-tail grading accompanied by an increase in matrix up through the bed more common in thick to massive (0.7-7 m), boulder-grade beds</p> <p>grooves (uncommon): 20-30 cm wide, 10-20 cm deep, <1-2 m long fluid escape structures (uncommon): low relief, relatively fine-grained sediment ridges on upper bedding planes (see (4), below)</p>	<p>transported and deposited by subaqueous debris flows (sediment is transported above the bed by strength and buoyancy of the fluid & dispersive pressures caused by clast collisions and deposited rapidly from suspension by frictional freezing at the base of the flow)</p> <p>thickness of the deposit decreases toward flow margins; clast size & amount of matrix decrease with decreasing bed thickness (increasing transport distance); disorganized, normally-graded, & inversely-graded beds may define a proximal to distal trend</p>

Table 6.1 continued

Lithology	Thickness & Morphology	Composition & Texture	Internal Structure	Sedimentary Structures	Interpretation
4) Lithoclast Calcirudite	<p>few cm to 1.2 m; most <50 cm</p> <p>flat or erosional bases; flat to wavy (rippled) or hummocky tops (caused by projection of outsized clasts)</p>	<p>- mostly granule to small pebble size clasts (2 mm to 3 cm); outside clasts 5-10 cm common, some 30-40 cm across</p> <p>- clast-supported & matrix-poor; interclast porosity occluded by silica (fine equigranular or fibrous quartz or chalcedony) &/or very coarsely-crystalline calcite or ferroan calcite cement</p> <p>- polymictic: lithoclasts are a mixture of dolostone, limestone & minor chert (identical to debris flow conglomerates); invariably sub-round to angular & equidimensional</p>	<p>Disorganized: erosional bases & flat or hummocky tops; most beds <15 cm thick</p> <p>Inversely-graded: (either an increase in grain size up through entire bed or outside clasts concentrated near top); relatively flat bases & (especially in the coarser beds) hummocky tops; most beds <10-50 cm thick</p> <p>Inversely- to normally-graded: low relief erosional bases & flat or wavy tops; most beds 15-25 cm thick (layering defined by grading similar to crude stratification)</p> <p>Crudely-stratified: vaguely-bound layers defined by changes in average grain size); markedly erosional bases & hummocky tops; beds 15-50 cm thick; common in top 25 m of the Caribou Brook section</p> <p>Normally-graded: (decrease in average clast size): sharp or gradational base*, sharp flat or wavy top; 10 cm->1 m thick (*commonly gradationally overlie debris flow conglomerates)</p> <p>Normally-graded, stratified: coarse, graded base overlain by low-angle cross-stratified calcirudite or calcarenite with Bouma sequence structures; beds 20-40 cm thick</p>	<p>megaripples: sinuous to crescent-shaped; $\lambda = 1.5-5$ m, $A = 10-20$ cm; ripple crests of fine pebble to medium sand size sediment (comparable to the fine fraction in underlying sediment) \pm with out-sized cobbles; troughs expose underlying calcirudite or are mantled by very fine-grained \pm rippled & burrowed calcarenite/ calcisiltite; most common atop crudely-stratified calcirudites</p> <p>fluid escape structures (upper bedding planes): large, irregular, wedge-shaped bulges or toothpaste-like ridges (to >20 cm across, 10-15 cm high, >3 m long); some branch & rejoin, defining irregular polygonal areas; composed of mixtures of coarse sand & granules (rare pebbles), finer than sediment comprising entire bed); cross-cut bedforms on upper bedding planes, but do not cross-cut overlying shale</p>	<p>transported and deposited from concentrated clast dispersions at the base of large, high velocity, turbidity currents; coarse sediment transported in suspension above the base of the flow by dispersive pressure generated by high numbers of collisions between clasts and deposited rapidly or in pulses by frictional freezing due to shear at the base or top? of the dispersion</p>

Table 6.1 continued

Lithology	Thickness & Morphology	Composition & Texture	Internal Structure	Sedimentary Structures	Interpretation
5) Lithoclast Calcarenite & Calcsiltite	<1 mm to -50 cm (commonly amalgamated) thinnest beds & laminae are tabular, thicker beds pinch and swell due mostly to channeling at base & ripples at the top	- grain size ranges from very coarse sand to very fine silt - poorly- to moderately well-sorted (varies between beds & within a single bed) - predominantly clast-supported & matrix-poor; minor interclast porosity occluded by silica & calcite cement (see 4, above); some thin sand-grade beds & laminae are matrix-supported - polymictic: compositionally identical to calcirudites (4); siliciclastic sand is a conspicuous component of some beds -135 m & in the upper several metres of the Caribou Brook section	partial or complete Bouma sequences; thickest, coarsest beds have the most complete sequences of structures; fine sand calcarenites & calcsiltites are generally i) vaguely normally-graded, parallel-laminated or massive (T^A, O^A, E^A)	* normal grading, parallel lamination, ripple cross-lamination; 2- and 3-dimensional ripples occur on upper bedding planes <u>loaded bases</u> common; <u>convolute lamination</u> common in ripple cross-laminated horizons (T^C); concave-up inarticulate brachiopod valves in the finest laminated or massive portions (T^E); <u>fluid escape structures</u> on upper bedding planes: i) <u>echelon ridges</u> (1-2 cm wide, 1-2 cm high, a few cm to 20 cm long) composed of sand & granule size sediment (invariably coarser than sediment comprising the top of the bed), ii) sharp-crested, runzel-like structures ($\lambda = 2-4$ mm, $A=0.5-1$ mm), locally grade laterally into non-linear warts	mostly transported and deposited by turbidity currents into a deep, quiet water basin or basin margin; some thin, matrix-supported, sand-grade beds probably emplaced by thin debris flows

Lithology	Bed Thickness	Colour & Composition	Sedimentary Structures	Interpretation
6) Bentonite	1-10 cm	light greenish-white, recessive-weathering sticky clay; XRD analyses indicate mixed-layer illite-smectite clays	none	volcanic ash deposited by suspension settling through the water column

Figure 6.4 Shale and ribbon limestone; outcrop photos and photomicrographs. CB=Caribou Brook. BC (A or B)=Big Cove section A or B. Bar scales on all photomicrographs are 0.5 mm. a) Photomicrograph of calcareous, spiculitic (round grains marked by arrows) shale; 83 m in the CB section. Grainy layer at the bottom is the top of a very fine-grained, lithoclast calcarenite. Spicules are siliceous; most other white grains in the shale are dolomite. b) Polished slab of black, noncalcareous shale with laminae and very thin beds of calcarenite and calcisiltite; 143 m in CB section. Uppermost calcisiltites and shale are cross-cut by very small burrows (dark, shale-filled in the calcisiltites, arrows). Bar scale is 1 cm. c) Photomicrograph of black, noncalcareous shale (as b, above) punctuated by dolomitic calcarenite laminae; 146 m in CB section. Large white grains are mostly dolomite rhombs (arrows) with dusty (detrital) cores. Most disseminated, white silt-size grains in the shale are nonferroan dolomite. g=graptolite, i=inarticulate brachiopod. d) Polished slab of mottled, greenish-grey shale with discontinuous calcarenite laminae disrupted by burrowing; 187 m in the CB section. e) Photomicrograph of mottled greenish-grey shale (as d, above); ~194 m in CB section. Discontinuous stringers of concentrated organic material (arrow) are commonly oblique to bedding and are thought to be burrows. Black grains are pyrite; some are replaced skeletal grains. White silt-size grains are mostly dolomite. f) Polished slab of graded and laminated, peloidal, fossiliferous packstone (ribbon limestone) from near the base of the Cape Cormorant Fm. exposed south of Big Cove. Liesegang over-prints parallel lamination. Small divisions on scale are 1 mm. g) Photomicrograph of peloidal-fossiliferous packstone (ribbon limestone); ~23 m in CB section. Some white, elongate grains are siliceous spicules (arrows); most are unidentifiable calcitic skeletal grains. h) Interbedded calcareous shale (*), noncalcareous shale (black), pebbly conglomerates and calcarenites in the 120-124 m interval of Big Cove (B). Up is to the right; metre stick (arrow) for scale. The top two calcareous shale beds overlie pebbly conglomerates; beds 1 and 3 have burrowed tops; bed 4 appears burrowed throughout. Some horizons in the noncalcareous shale are also burrowed.

Figure 6.4

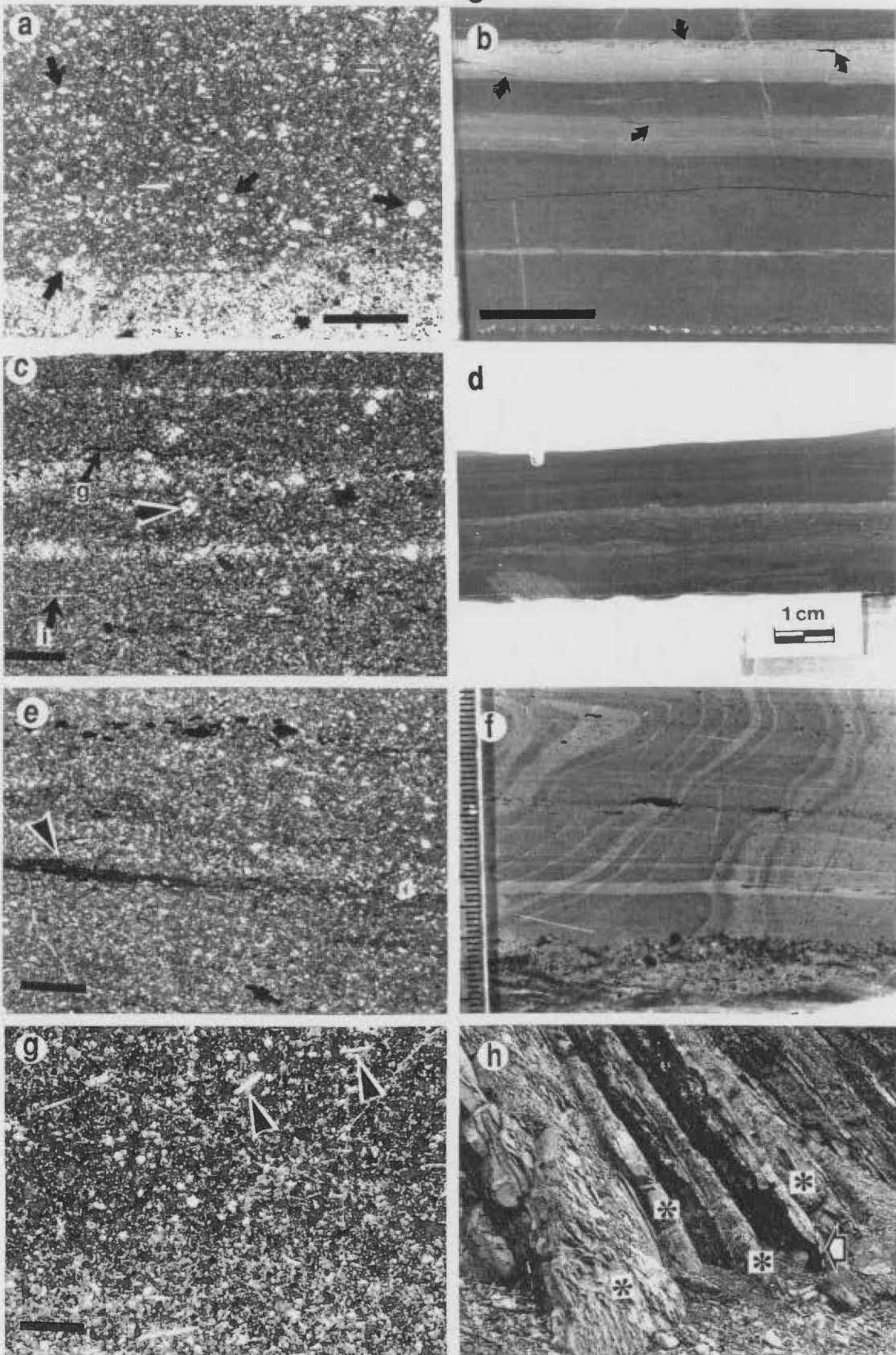


Table 6.2 Body Fossils in the Cape Cormorant Formation

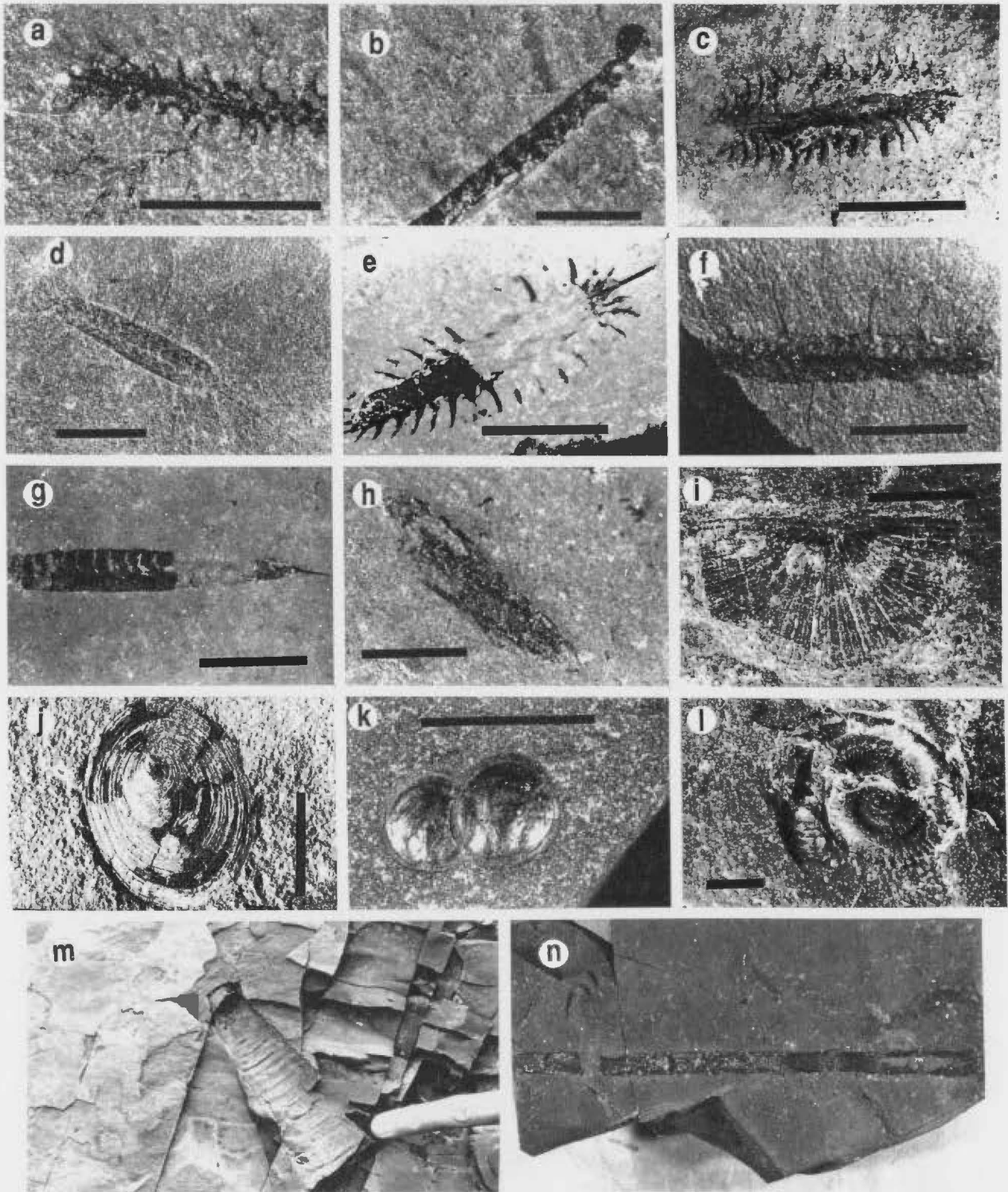
Body Fossil	Abundance	Distribution	Forms/Genera Present
Graptolites	abundant	widely dispersed and randomly oriented; current aligned on some bedding planes	<u>Climacograptus riddellensis</u> Harris ^{1,4} <u>Cryptograptus inutilis?</u> (Hall 1858) <u>Diplograptus decoratus</u> Harris and Thomas ^{1,2,3,5} <u>Glossograptus hincksii</u> (Hopkinson) ^{3,5} <u>Paraglossograptus tentaculatus</u> (Hall 1858) <u>Pseudoclimacograptus</u> sp. <u>Pseudophyllograptus</u> sp. diplograptids, dentatus group diplograptid sp., sigmoidraptid spp., dendroid spp., unidentified spp.
Phyllocarids	common	same as for graptolites	similar to those in the Table Cove and Black Cove formations, <u>Caryocaris</u> (Morris and Kay, 1966)
Inarticulate Brachiopods	common	widely scattered; smaller forms commonly articulated; larger forms found mostly in the upper 30 m	at least four species present; very small (1-5 mm dia.) with nearly round valves (most common); small (5-10 mm) with stout, conical valves; large (10-20 mm) with oval valves; very large (30-60 mm) with elongate, subrectangular valves
Articulate Brachiopods	rare	widely scattered; unbroken, commonly articulated	(1) less than 1.5 cm maximum dimension; similar to forms in the Table Cove Fm. (cf. Figure 5.8)
Cephalopods	very rare	widely scattered	(1) coiled, annulated forms 1 cm or less in diameter (2) smooth wall orthocones; partial specimens 1.5-4 cm wide, 8-12 cm long
Arthropod Antennae?	very rare	widely scattered	elongate (≥ 10 cm), slightly tapering (1-1.3 cm), hollow, calcitic, segmented tube with transverse walls forming 1-1.5 cm long chambers

Table 6.2 Body fossils in the Cape Cormorant Formation. Graptolites collected during this study identified by S. H. Williams, Memorial University of Newfoundland). See also Figure 6.5.

1 Reported by Whittington and Kindle (1963) in the Upper Table Head (Black Cove Formation) at Table Point. 2 Reported by Whittington and Kindle (1963) in the (Black Cove Formation) at Black Cove, Port au Port Peninsula. 3 Reported by Morris and Kay (1966) from the Black Cove Formation at Black Cove on Port au Port. 4 Reported by Erdtmann (1971) from the Table Cove Formation at Table Cove. 5 Reported by Erdtmann (1971) from the Table Cove Formation at Black Cove. 6 Reported by Finney and Skevington (1979) from the Table Cove Formation at West Bay Centre Quarry, Port au Port Peninsula.

Figure 6.5 Body fossils in Cape Cormorant Formation shale. Graptolites identified by S. H. Williams (Memorial University). Bar scales for all specimens (except m) are 5 mm. a) Cryptograptus inutilis. b) Diplograptus decoratus. c) Pseudophyllograptus sp. d) Glossograptus hinckei. e) Paraglossograptus sp. f) Cryptograptid (cf. Glossograptus). g) Diplograptid? fragment. h) Poorly preserved phyllo-carid. i) Small orthid brachiopod. j) Large inarticulate brachiopod; incomplete shell, internal mould. Genus is indeterminate. k) Very small inarticulate brachiopod (cf. Paterula); valves are commonly found together. l) Small coiled cephalopod. m) External mould of an orthoconic cephalopod. n) Problematic segmented fossil probably an antenna of either a trilobite or eurypterid (L. Fähræus, pers. comm., 1988); bar scale is 5 cm.

Figure 6.5



Cove, and American Tickle formations (see Chapter sections 5.4.1 and 5.4.3, 7.2 and 8.5).

The shale is interpreted to have been deposited mostly via suspension settling in a deep, quiet-water environment well below storm wave base, suggesting a basinal or basin margin setting for the lithologically diverse formation. Terrigenous clays are inferred to have come from weathered, continental areas and oceanic terranes. Fine, particulate organic matter came from highly-productive, surface waters. Graptolites, phyllocarids, radiolarians, and cephalopods inhabited near surface waters and settled through the water column onto the seafloor.

Fine, parallel lamination and randomly oriented graptolites at most horizons indicate that the sediment was deposited primarily from suspension. However, aligned graptolites on some bedding planes indicate current activity and suggest the sediments were also deposited from, or reworked by, bottom currents. Laminae of fine-grained carbonate which punctuate the shale are interpreted as traction or suspension deposits of weak, low concentration, turbidity currents (see Chapter section 6.2.4, below). Large numbers of these laminae indicate that low velocity bottom currents were common.

Preservation of delicate parallel-lamination throughout most of the formation and the presence of a sparse, shelly benthic fauna suggest that bottom waters and near-surface pore waters were usually very poorly-oxygenated. Scattered inarticulate and articulate brachiopods in the shale are inferred to be indigenous to the basin floor (see Chapter section 7.5). Their presence implies that bottom waters were not anoxic, but such low faunal diversity suggests the waters were dysaerobic and incapable of supporting a wide variety of shelly organisms. Paucity of burrows indicates that pore waters in near surface sediments were usually anoxic (Byers, 1977; Savrda *et al.*, 1981). In the presence of abundant particulate organic matter, anoxic pore waters may have evolved rapidly from dysaerobic bottom waters below the sediment-water

interface (Fenchel and Riedl, 1970). Burrowed shale at the top of the formation suggests oxygenation of bottom waters improved with time.

Changes in shale composition up through the Cape Cormorant section and the vertical distribution of burrowing record long-term, basin-wide changes in sediment provenance and circulation. They are discussed in Chapter sections 6.7.3 and 6.8.

6.2.2 Ribbon Limestone (Table 6.1(2))

Ribbon limestone is a relatively minor component of the Cape Cormorant and occurs only at the base of the formation (Figure 6.1). This category includes thin to thick beds of 1) dark grey-brown, muddy, peloidal and/or fine, fossil-bearing limestone, 2) barren or radiolarian mudstone, and 3) carbonate-rich shale (Figures 6.4.f-h and 6.6). In some horizons these lithologies are intimately interstratified to form typical ribbon limestone, similar to that which comprises the upper Table Cove Formation in outcrops on the east side of the Port au Port Peninsula (Chapter section 5.4.3). Otherwise the limestones and calcareous shale form discrete beds interstratified with noncalcareous shale and lithoclastic carbonate sediments (eg. Figure 6.4.h).

These lithologies are comparable to same-named strata in the Table Cove and are similarly interpreted to have come from a shallow water platform and to have been deposited by a combination of suspension settling and dilute turbidity currents. Rationale for this interpretation and discussion of depositional mechanisms were presented in Chapter section 5.4.

The limestone-calcareous shale rhythms, like those in the Table Cove, are thought to record deposition during alternating periods of high and low carbonate productivity and availability which may have been controlled by climate (eg. Einsele, 1982; Kaufmann, 1982). The significance of unusually thick beds of calcareous shale and massive mudstone is more problematic. That they sporadically punctuate noncalcareous shale suggests that the overall contribution of platform-derived

Ribbon limestone components (Cape Cormorant Formation)

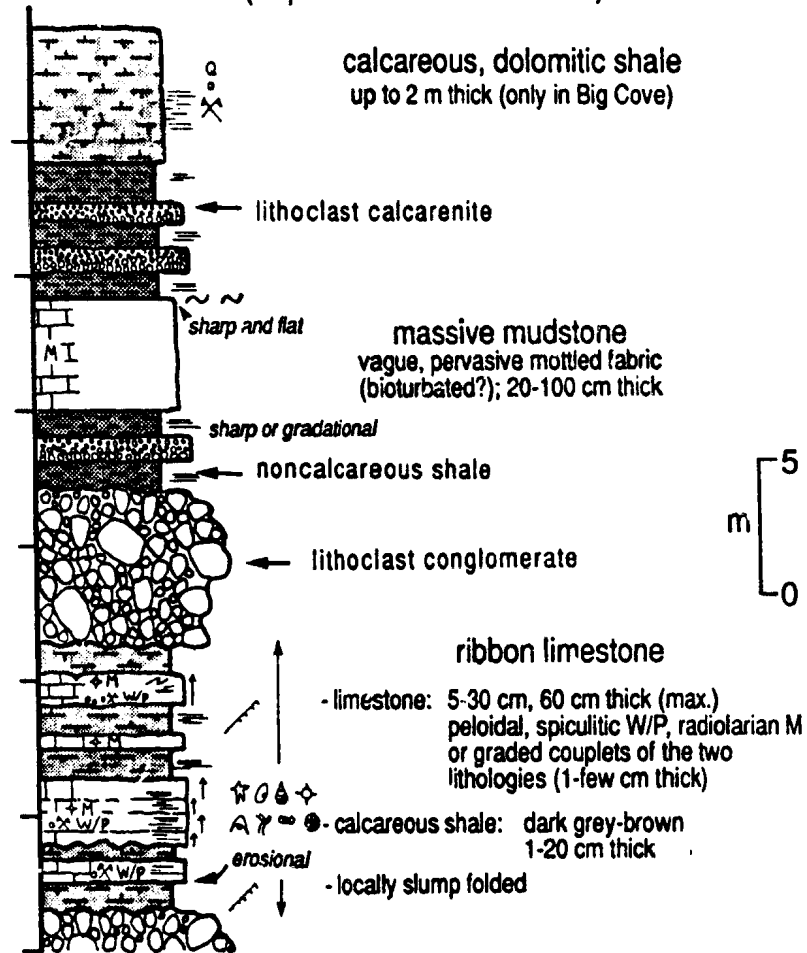


Figure 6.6 Schematic summary of ribbon limestone components. Intervals of rhythmically-interbedded limestone and calcareous shale occur in the Caribou Brook section (Figure 6.1.a). Discrete beds of mudstone and calcareous shale are more common in Big Cove proper (Figures 6.1.c and 6.4.g). Key to symbols is in Appendix A.

sediment was diminished and was not solely or predominantly controlled by cyclic climate changes. If the beds are depositional in origin, then their great thickness implies either a prolonged period of sedimentation or deposition from a voluminous suspension or flow. Thick calcareous shale beds may have accumulated over a long period of time during which adjacent platforms contributed a small, but steady supply of carbonate sediment. Massive mudstones, in contrast, may have been deposited when carbonate productivity was comparatively high, but the platform(s) were at a depth where only mud accumulated and was effectively entrained by waves and transported basinward. Burrowing in the mudstones, which are interstratified with generally laminated shale, suggests that either the sediment was transported and deposited by oxygenated currents or deposition coincided with improved oxygenation of bottom waters. An alternative explanation for the anomalously thick calcareous shale and mudstone beds is that they are, at least in part, diagenetic in origin, formed by migration of CaCO_3 from enclosing shale and reprecipitation during early burial.

Importantly, ribbon limestone in the Cape Cormorant proves the presence of contemporaneous carbonate platform(s) at the onset of deposition and reconfirms the general interpretation of the depositional setting deduced from enclosing shale. A deep, basinal environment is supported by: 1) predominance of fine-grained sediment and absence of wave-formed structures, which indicates the sediments accumulated below storm-wave base; 2) presence of only transported, hemipelagites and turbidites, which indicates water depths below that of *in situ* biogenic carbonate production; 3) the apparent absence, or at least scarcity, of even a restricted shelly benthos and absence (in most beds) of a soft-bodied infauna, which indicates low oxygen availability of bottom waters; and 4) paucity of slump-folded horizons, thereby indicating deposition on a very low slope.

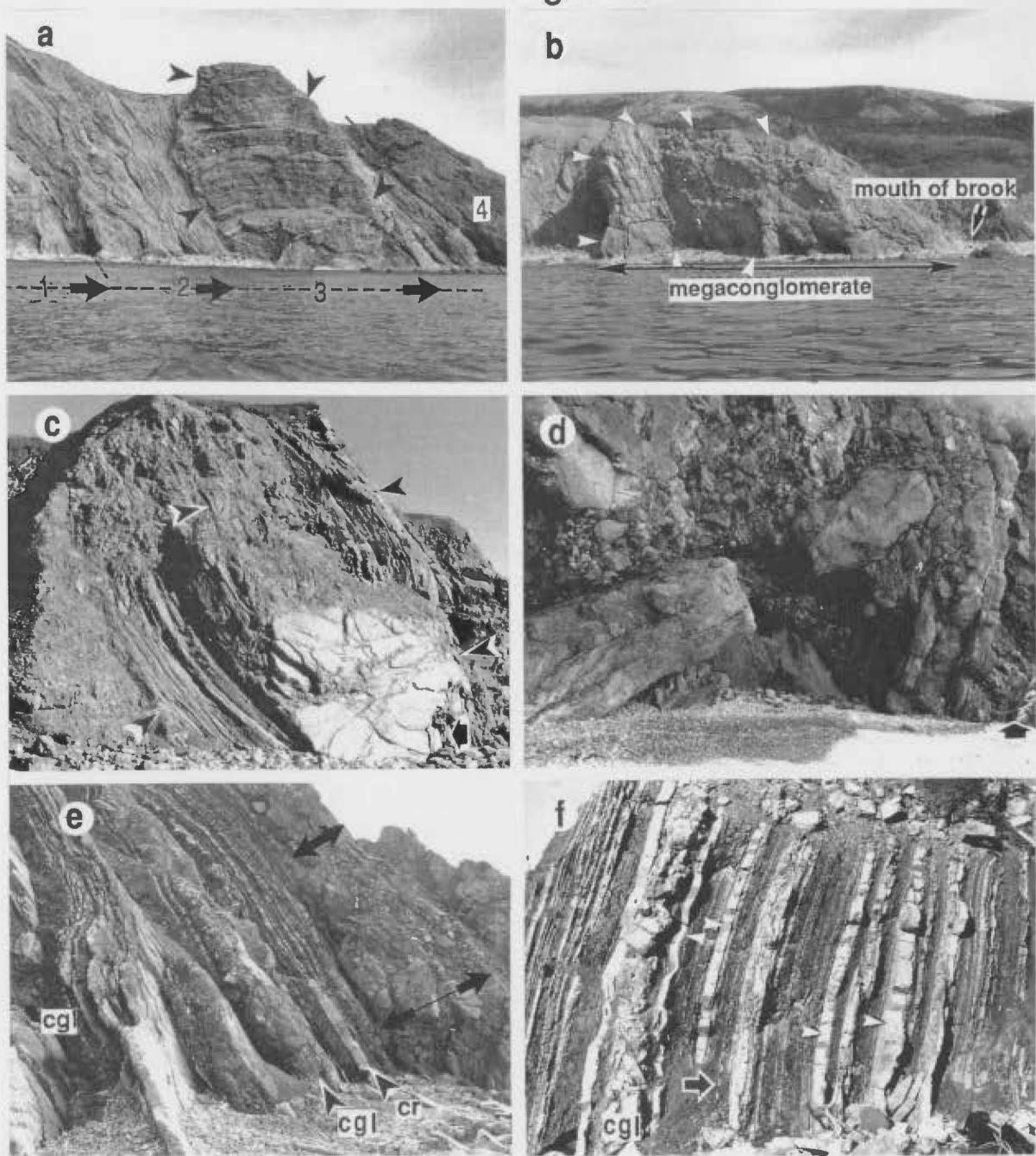
6.2.3 Lithoclast Conglomerate and Megaconglomerate (Table 6.1(3))

Carbonate lithoclast conglomerate and megaconglomerate are the most outstanding components of the Cape Cormorant (Figures 6.1, 6.3.a-c, 6.4.h and 6.7), constituting approximately 25-75% of formation sequences. Beds range from as little as 20 cm up to ~65 m in thickness (Figure 6.7). They typically pinch and swell in thickness over distances of several or several tens of metres due to a combination of erosional relief at the bases and depositional topography on the tops of the beds (Figures 6.7.a,e,f and 6.8). Erosional relief accounts for most thickness variation and is most evident at the base of the thicker, coarser conglomerates. Bed surface topography is accentuated by protruding cobbles and boulders.

Both conglomerates and megaconglomerates are poorly-sorted and clast-supported, and are composed of a polymictic suite of mostly shallow marine limestone and dolostone lithoclasts. (Clast diversity, age and origin are discussed in Chapter section 6.5.) Clasts range in size from granules to olistoliths up to at least 65 m across (Figures 6.3.c and 6.7). Argillaceous matrix is compositionally similar to enclosing shale. Generally all clasts of all sizes are subround to subangular and nearly equidimensional. Conspicuous angularity of cobble and boulder size dolostone clasts compared to more rounded limestone clasts is thought to reflect the inherent hardness of the two lithologies; dolostones are generally homogeneously well-lithified and fracture brittly, whereas many limestones have irregular zones of weakness defined by burrows, patchy dolomite, or argillaceous, pressure dissolution seams, which facilitate breakdown during transport. Megaboulders and olistoliths of all lithologies, whether equidimensional, rectangular or slab-shaped, are also generally angular, their shapes largely controlled by primary bedding (Figures 6.3.c and 6.7.a-d). The longest dimension of many of these is perpendicular, or at a high angle to, primary bedding in the clast.

Figure 6.7 Lithoclastic megaconglomerate and conglomerate; field photos and photomicrographs. a) Olistolith-bearing megaconglomerate (3) ~65 m above the base of Big Cove (A); bedding dips moderately to the right. 1-basal conglomerate of the Cape Cormorant Fm., 2-interbedded shale, calcarenite and conglomerate, 4, boulder conglomerate. Olistolith (arrows) is ~65 m high and 45 m wide; its primary bedding is nearly perpendicular to that of enclosing megaconglomerate (~25 m thick). Conodonts in the clasts prove it came from the Catoche Fm. Underlying Cape Cormorant strata are folded and truncated. b) Megaconglomerate ~135 m above the base of Big Cove (A) with a Petit Jardin Fm. olistolith (interbedded oolitic grainstone, digitate stromatolites, pattern dolomite) (arrows); up is to the right. The cliff is ~35 m high. Massive, rubbly conglomerate (dashed outline) mantles the olistolith which extends several tens of metres further southeast away from the coast and is cross-cut by Callieux Passé brook. c) Megaconglomerate at the top of section A with a thin-bedded, parted limestone clast from either the Middle or Upper Cambrian which, although broken apart in the conglomerate, extends for about 65 m along the coast further south. Bedding in the megaconglomerate dips in approximately the same direction and inclination as bedding in the parted limestone slab in the upper right. C. James (large arrow) for scale. d) Bedding plane exposure (near vertical bed) of several metres long blocks and slabs in a megaconglomerate south of Caribou Brook that is equivalent to the conglomerate 120 m above the base of the Caribou Brook section; see also Figure 6.8.f. Several of the slabs show thrombolite build-ups. N. P. James (arrow) for scale. e) Matrix-rich megaconglomerate (far right) with ~2 m erosional relief; maximum thickness is ~7 m. Located 110 m above the base of Big Cove section (B2). Up is to the right. cgl=conglomerate; cr=calcirudite. f) Small boulder conglomerate (cgl) and interstratified calcirudites (arrowheads) and calcarenites; 134-142 m interval in Caribou Brook section. Angular boulders are predominantly dolostone. Up is to the left; metre stick (arrow) for scale. a, b, c and e represent the megaconglomerate - ribbon limestone lithofacies. d and f are in the calcarenite - conglomerate lithofacies.

Figure 6.7



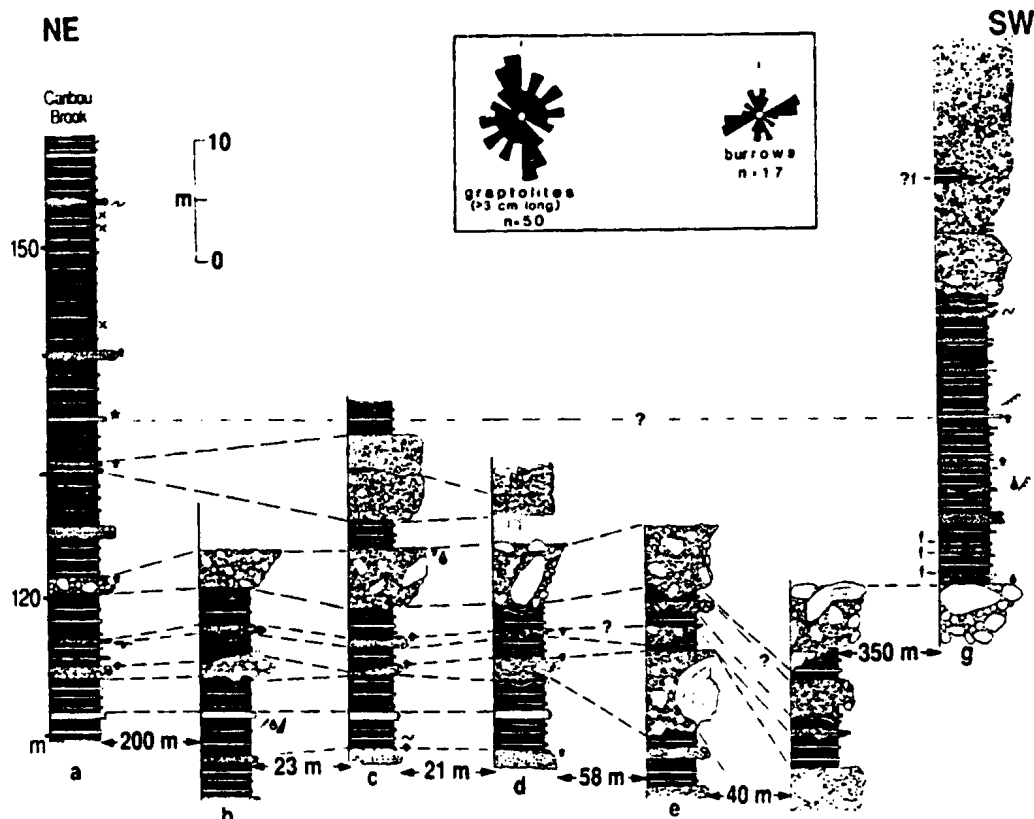


Figure 6.8 Measured sections showing lateral changes in debris flow conglomerate thickness and texture. Metre values left of a) Caribou Brook correspond to those in Figure 6.1.a. Locations of the tops of sections b), f), and g) are shown in Figure 6.2. The highest conglomerate in f) is shown in Figure 6.7.d. Correlation of section g) is based on a sandy calcarenite which also occurs in the Caribou Brook section (star). Small arrows indicate normally-graded calcirudite/calcarenite caps on the conglomerates. Key to other symbols is in Appendix A. Histograms show the orientations of graptolites and *Diplocraterion* burrows at ~4 m above the base of section c).

All conglomerates and megaconglomerates lack stratification. Moreover, since the vast majority of clasts are equidimensional, there is no obvious preferred orientation of clasts within beds. Exceptional are very large slab-shaped clasts which are commonly oriented with their broadest dimension sub-parallel to megaconglomerate bedding (Figures 6.3.c and 6.7.c,d). Beds fall into one of four categories based on internal structure: 1) disorganized, homogeneously poorly-sorted, 2) inversely-graded, 3) normally-graded with matrix decreasing up through the bed, and 4) normally-graded with matrix increasing up through the bed (Table 6.1(3); Figure 6.9). Overall, clast size and matrix content decrease and the degree of organization of clasts increases with decreasing bed thickness.

The only sedimentary structures associated with these beds are large grooves at the base of some cobble- to boulder-grade beds, and irregular, low relief, sediment ridges (<5 cm) on the tops of calcarenite-mantled conglomerates. The former are similar to smaller-scale tool marks common at the base of turbidites and are interpreted to have been generated by clasts scraping soft muds during transport (Reineck and Singh, 1980). Upper bedding plane sediment ridges are similar to others which occur on the tops of coarse calcarenites and calcirudites and are interpreted to be expressions of fluid escape (see Chapter section 6.2.4).

These thick- to massively-bedded, coarse-grained, and unsorted sediments are interpreted to have been transported and deposited by subaqueous debris flows (Johnson, 1965, 1970; Hampton, 1975, 1979; Middleton and Hampton, 1976; Pickering et al., 1986). Disorganized and inversely-graded conglomerates in the Cape Cormorant are typical of debris flow deposits described in other ancient, submarine sequences (Cook et al., 1972; Cook and Mullins, 1983; Enos and Moore, 1983; Hiscott and James, 1985; Srivastava et al., 1972). Absence of grading indicates deposition from a flow of uniform competency throughout its

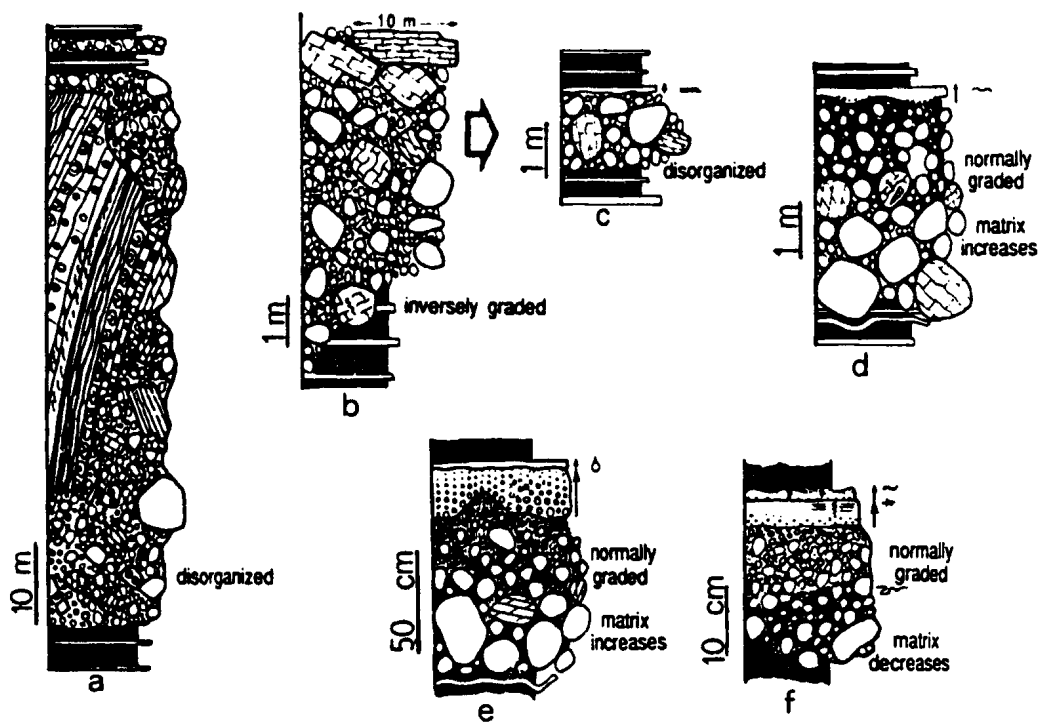


Figure 6.9 Types of lithoclast conglomerates; sketches. CB=Caribou Brook section; BC (A or B)=Big Cove section (A) or (B). a) Disorganized megaconglomerate; 135 m in BC (A). b) Inversely-graded megaconglomerate; equivalent to 120 m in CB (top bed in Figure 6.8.f). Grading is defined by concentration of large, bedded slabs at the top of the bed. c) Disorganized conglomerate with fine sand calcarenite cap; 120 m in CB. d) Normally-graded conglomerate with a graded calcirudite cap; 85 m in CB. Grading partly defined by an increase in matrix up through the bed. (Decrease in clast size exaggerated; clasts predominantly in clast-support.) e) Normally-graded conglomerate with graded calcirudite cap; 140 m in CB. As for d), grading is accompanied by an increase in inter-clast matrix. f) Normally-graded conglomerate with graded, sandy calcarenite cap (with second amalgamated, graded calcarenite; 175 m in CB. Grading is accompanied by a decrease in matrix up through the bed. Key to symbols is in Appendix A.

thickness, whereas inverse-grading indicates increased competency of the flow above an intensely sheared zone at its base (Middleton and Hampton, 1976, Fig.7; Naylor, 1980). Enormous blocks and slabs in the very thick flows are thought to be buoyed up and rafted along near the top of the flow by overpressured fluids at the base (Pickering *et al.*, 1986).

Normal-grading, though not a common characteristic of debris flow deposits, has been documented in other ancient sequences (eg. Eberli, 1987). Normally-graded beds in the Cape Cormorant in which matrix increases up through the bed may reflect decreased competency of the upper layer of the flow due to shearing at the top during transport (Middleton and Hampton, 1976, Fig.7; Naylor, 1980). Those in which matrix content decreases up through the bed, and which are overlain by graded calcarenite, may instead record deposition from a degenerating debris flow overridden by a high concentration turbidity current that entrained fine sediment at the top of the flow.

Disorganized, normally-graded, and inversely-graded conglomerate, in that order, are thought to define a proximal to distal trend for debris flow deposits (Naylor, 1980; Eberli, 1987).

Erosional bases and matrix-lean, clast-supported texture distinguish Cape Cormorant conglomerates from ideal debris flow deposits. Basal erosion suggests the flows, especially the most coarse-grained and voluminous ones, were channelized and that flow was not purely laminar (eg. Hampton, 1970). It indicates that clasts rolled, bounced, and scraped underlying sediments at the base of the flow and suggests that dispersive pressures due to clast collisions were of greater importance than buoyancy or matrix strength in sediment transport (Lowe, 1982). Low abundance of matrix may reflect relatively small amounts of fine sediment incorporated at the source of the flow and thereby confirm the greater importance of dispersive pressure during transport. It could otherwise be an artifact of compaction, ie. water and volume loss during burial. However, the positive correlation between bed thickness, clast

size and matrix-content suggests that fine sediment was commonly lost during transport, most likely entrained and transported in turbulent currents accompanying the debris flow (Hampton, 1972).

6.2.4 Lithoclast Calcirudite (Table 6.1(4))

Polymictic calcirudites in the Cape Cormorant either constitute sharply bounded beds that punctuate ambient shale or they gradationally overlie debris flow conglomerates (Figures 6.7.e,f, 6.9.d,e and 6.10.a). They are, in turn, commonly overlain by graded lithoclast calcarenite (Chapter section 6.2.5). The tops of the beds are commonly burrowed (see Trace Fossils, Chapter section 6.4).

Beds range from a few centimetres to 1.2 m in thickness; most are less than 50 cm thick. The thickest ones invariably overlie very thick debris flow deposits (eg. 15 m and 26 m in Big Cove (B2), Figure 6.1.c). Some beds are tabular, but more commonly they have erosional bases and/or wavy to hummocky tops generated by bedforms or by outsized clasts projecting above the top of the bed (Figure 6.10.a).

Calcirudites are generally composed of granule to small pebble-size clasts (Figure 6.10.a-d), but commonly contain outsized clasts 5-10 cm, or even 30-40 cm across. They are clast-supported and matrix-poor; interclast porosity is typically occluded by silica and/or blocky calcite cement (Figures 6.10.a-d and 6.11.a-f). Lithoclasts are identical to those comprising the debris flow conglomerates (Figures 6.10.a-d and 6.11.a-f; Chapter section 6.5).

Six types of calcirudite beds are differentiated on the basis on internal organization and presence/absence of stratification, four of which correspond to clast-supported conglomerate facies of Walker (1975). They are: 1) disorganized, 2) inversely-graded (Figure 6.10.b), 3) inversely- to normally-graded (Figure 6.10.c), 4) crudely-stratified (Figure 6.10.d), 5) normally-graded, and 6) normally- graded, stratified. Detailed descriptions of each are in Table 6.1(4).

The only sedimentary structures commonly associated with the

Figure 6.10 Polymictic, lithoclastic calcirudites, calcarenites and calcisiltites; slab and outcrop photos. CB=Caribou Brook. a) Calcirudites (arrows) near the top of the CB section (green shale-calcarenite lithofacies; ~203-206 m). Thinner light coloured beds are predominantly calcarenites and calcisiltites. Up section is to the left; MSS=Mainland Sandstone. Pinch and swell morphology is mostly due to basal erosion, but is accentuated by bedforms at the top. b) Slab of an inversely-graded calcirudite; ~134 m in the CB section. Scale is in centimetres. c) Slab of inversely- to normally-graded calcirudite; 130 m in the CB section. d) Crudely-stratified calcirudite; 196 m in the CB section. Bar scale is 10 cm. e) Sinuously-crested megaripples (small arrows) atop calcirudites at ~192 m in the CB section; metre stick (arrow) for scale. Bedding dips steeply toward the reader; up-section is to the left. Flow direction is toward the upper right (east-southeast). f) Normally-graded calcarenite with partial Bouma sequence; 110-140 m interval in the CB section. Marker pen for scale. g) Slab of shale with very thin calcarenite and calcisiltite beds. 1-matrix-supported and normally-graded mini debris flow(?). 2-vague lower boundary and uneven upper boundary, irregular internal lamination a result of synsedimentary deformation or possibly burrowing. 3-calcisiltite/mudstone with tiny burrows (dark spots filled with shale). 4-normally-graded, loaded base. h) Large, toothpaste-like fluid escape structure protruding from the upper bedding plane of a 10-15 cm thick calcirudite; equivalent to ~123 m in the Caribou Brook section (section g) in Figure 6.8). Bedding dips steeply toward the reader; divisions on measuring stick are 10 cm. i) Upper bedding plane view of wrinkle-like, fluid escape structures (arrows) atop a ~25 cm thick, graded calcirudite-calcisiltite cap on debris flow conglomerate; ~140 m in the Caribou Brook section. Bar scale is 10 cm.

Figure 6.10

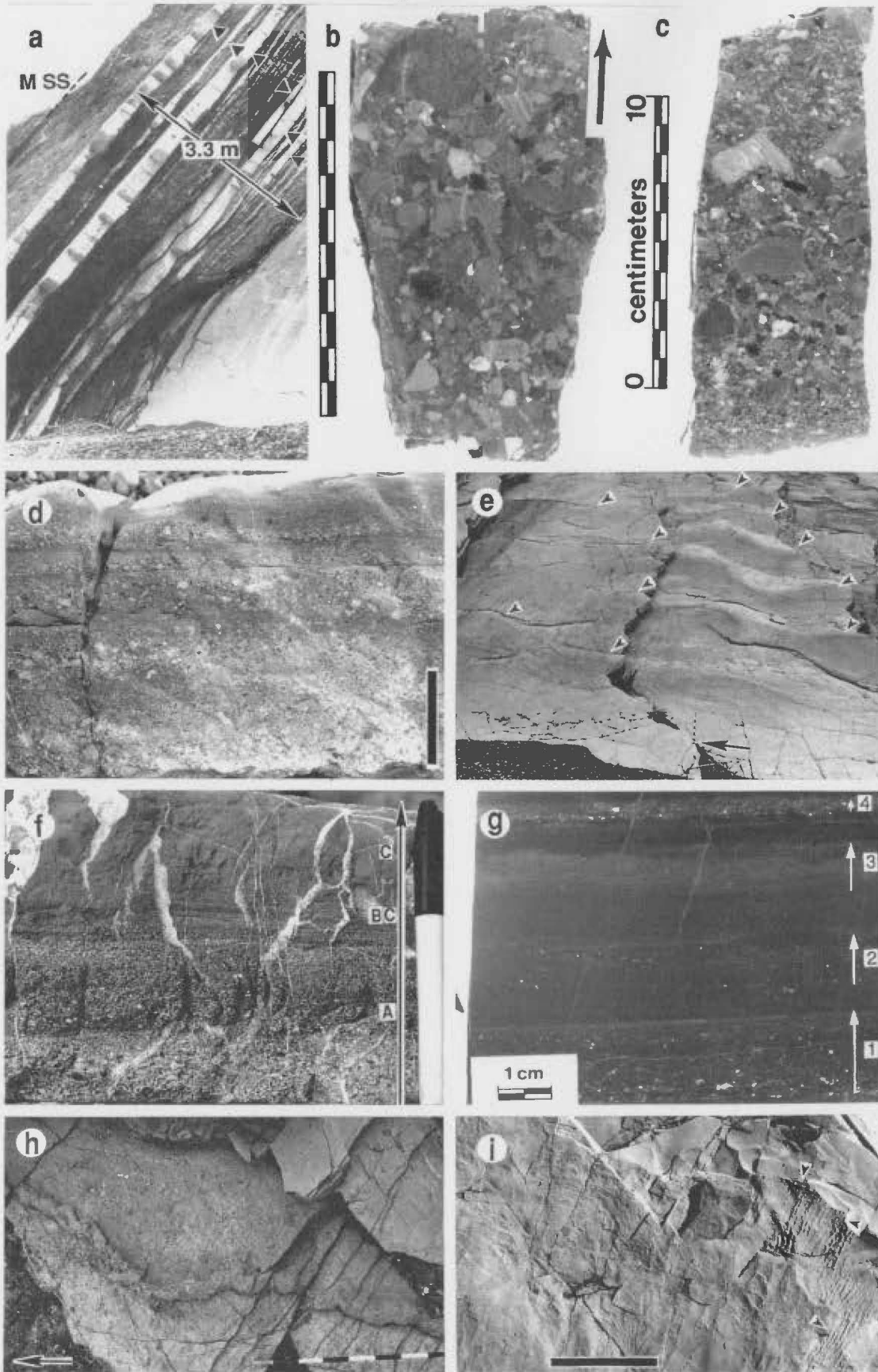
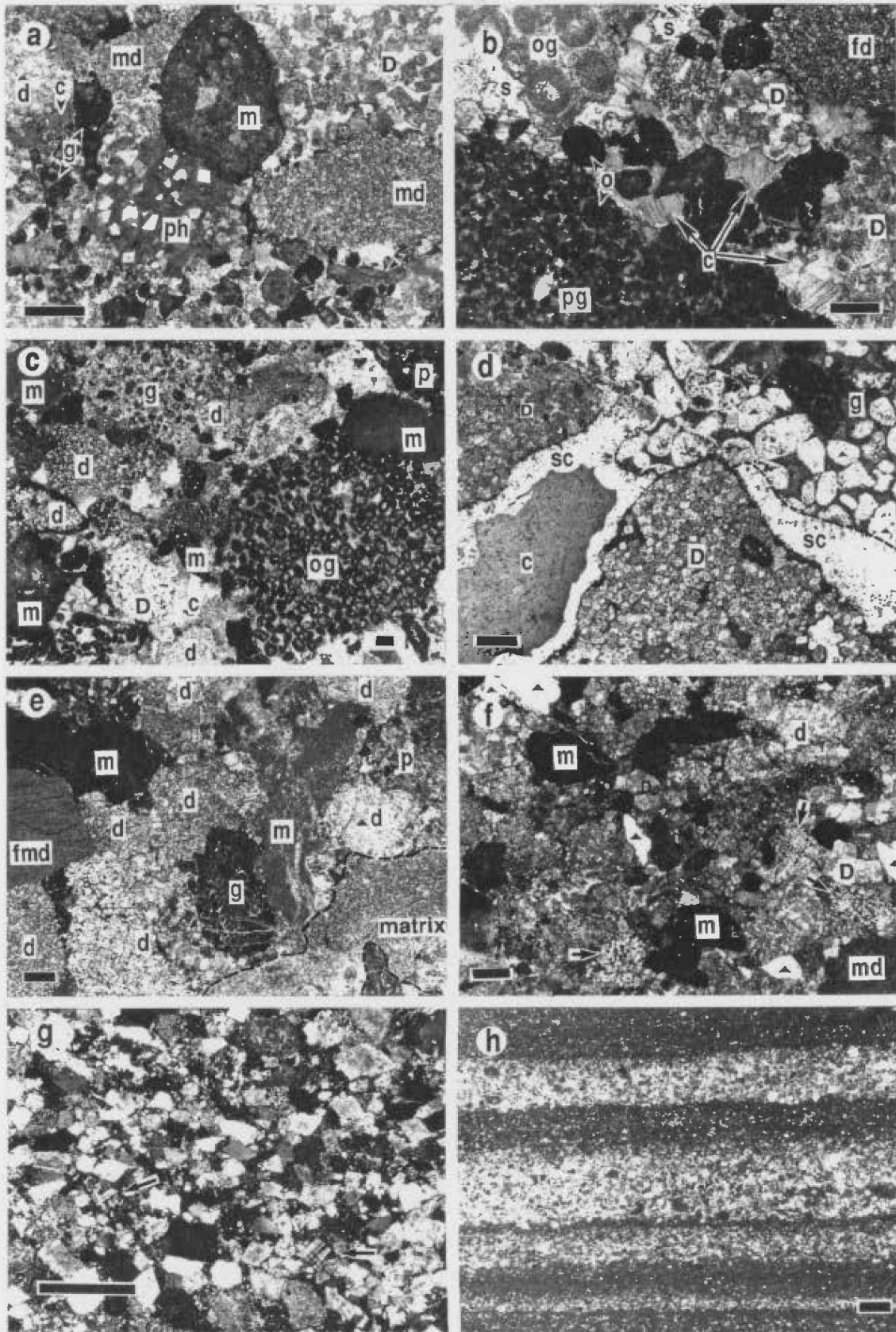


Figure 6.11 Polymictic, lithoclastic calcirudites, calcarenites and calcisiltites; photomicrographs. All thin sections are stained with Dual stain; limestones appear dark and dolostones appear light. Bar scales are all 0.5 mm. m=mud-/wackestone, microsparitic limestone; p=packstone; g=grainstone; p=peloidal; o=oid/oolitic; md=microcrystalline dolostone; d=fine- or medium-crystalline dolostone; D=very coarsely-crystalline dolostone; (Δ)d=dolostone with chert matrix; (▲)=chert; f=ferroan; c=cement; s=silica. CB=Caribou Brook. a) Calcirudite with a calcium phosphate pebble (ph) with floating dolomite rhombs; ~183 m in the CB section. Cement includes an early, very thin rim of silica and later, very coarse, blocky calcite. Arrows point to skeletal grain clasts. b) Calcirudite with neomorphosed (microsparitic) ooid grainstone clast (upper left); ~157 m in the CB section. Cement is very coarse, blocky, slightly ferroan calcite. Silica may be partly cement and partly a replacement of carbonate. c) Calcirudite; 177 m in the CB section. Oolitic coatings on grains in the large grainstone pebble are micritized. Cement is very coarse, blocky calcite. d) Calcirudite with first generation chalcedony and second generation blocky, ferroan calcite cements; ~158 m in the CB section. Most intraclasts in the grainstone pebble (top right) are replaced by chert. e) Dolostone-dominated calcirudite; cap on conglomerate at ~140 m in the CB section. Argillaceous matrix is compacted shale rip-ups. f) Calcirudite with abundant quartzose siltstone clasts (arrows) and chert; ~197 m in the CB section. g) Sandy calcarenite with abundant simple and polycrystalline quartz (subangular to subround, white and black grains) and minor feldspar grains (twinned, arrows) from ~134 m in the CB section; crossed polars. Very large rhombs are nonferroan dolomite. h) Very fine-grained, massive or graded, polymictic calcarenites; ~173 m in the CB section. Dark grains are mostly limestone (mudstone/microspar) and lesser skeletal fragments. White grains are mostly dolomite; some are chert. Overlying shale laminae are calcareous.

Figure 6.11



calcirudites are megaripples and fluid escape structures (Table 6.1 (4)). Megaripples (Figure 6.10.e) occur at the top of every type of calcirudite, but are most common on crudely-stratified beds. They are composed of fine pebble- to medium sand-size sediment, comparable in size to the fine fraction of the underlying bed. Most are starved bedforms that lack distinct internal structure; intervening troughs expose underlying pebbly sediment.

Fluid escape structures are irregular, low relief, protrusions of sediment on the tops of the beds. They assume a variety of shapes, most commonly large, irregular, wedge-shaped bulges or toothpaste-like ridges (Figure 6.10.h), and are generally composed of mixtures of coarse sand and granules, rarely small pebbles, on average finer-grained than sediment comprising the entire calcirudite. Only one such structure was exposed in cross-section and appeared to be linked to a vertical dyke that cross-cut bedding. Most demonstrably cross-cut bedforms on the tops of the beds, but none were proven to cross-cut overlying shale. Although these relationships do not unequivocally determine where the structures formed with respect to the sediment-water interface, significant topographic relief on many of them suggests they formed beneath a sedimentary cover during shallow burial.

Fluid escape structures are not commonly generated in permeable, coarse-grained sediments (Lowe, 1975), but they have been documented in other pebble-grade deposits (eg. Hein, 1982; Postma, 1983; Johnson, S. Y., 1986). Although the structures in the Cape Cormorant are not the same as those occurrences, they do closely resemble (in plan view) sandstone dykes described in finer-grained, fluvial deposits (Aspler and Donaldson, 1986), and are similarly interpreted to have formed by forceful fluid injection during burial. Limited expulsion of sediments and fluid above the tops of the calcirudites and the absence of dykes cross-cutting enclosing shale suggest fluid injections were not extremely forceful, possibly due to lower water volume and pressures in the

relatively thin and coarser-grained beds.

Matrix-poor calcirudites in the Cape Cormorant are analogous to clast-supported, siliciclastic gravels commonly found in association with turbiditic sands in deep-water, submarine fan sequences (Davies and Walker, 1974; Walker 1975; Hein, 1982; Pickering *et al.*, 1986). They are similarly interpreted to have been transported and deposited from concentrated clast dispersions at the base of large, high velocity, turbidity currents (Walker, 1975). Hein (1982) calculated that a gravel dispersion 27 cm thick, comparable in thickness to many calcirudites in the Cape Cormorant, would form beneath a turbidity current 100 m thick.

Different types of grading in the calcirudites record different hydrodynamic conditions during deposition (Walker, 1975; Hein, 1982; Pickering *et al.*, 1986). Disorganized, inversely- and inversely- to normally graded beds indicate very rapid deposition from suspension. Crudely-stratified beds indicate rapid, pulsating deposition from suspension. Normally-graded beds record comparatively slow deposition from a waning flow. Normally-graded, stratified beds record similar conditions, followed by traction deposition. Walker's (1975) model for similar siliciclastic gravels proposes that increasing segregation and organization of sediments records increasing degree of sediment transport and predicts that disorganized, inversely- and inversely- to normally graded beds are proximal deposits while normally-graded and normally-graded, stratified beds are distal deposits.

Besides normally-graded, stratified beds, megaripples on select calcirudites are the only other evidence of tractive currents. Since the megaripples, in most cases, overlie coarse sediments deposited from suspension (ie. they are not the 'cap' of a classical turbidite), and are generally starved bedforms, they are interpreted to have formed by high velocity, nondepositional currents that reworked the relatively fine-grained sediments on the upper, hummocky surfaces of the calcirudite beds. A crude estimate of flow velocity based on the size

of grains comprising the ripples (0.5-5 mm) obtained from Hjulstrom's diagram (see Blatt *et al.*, 1980, Fig. 4-8) is 20-200 cm/sec. The flows are inferred to have operated shortly after emplacement of the coarse sediments, and were most likely the same currents from which the coarse sediments were initially deposited.

Compositional similarities between calcirudites and debris flow conglomerates indicate they derived from the same source. Gradational contacts with underlying conglomerates further suggest that high concentration turbidity currents were commonly generated concurrently above moving debris flows (Hampton, 1972; Krause and Oldershaw, 1979; Crevello and Schlager, 1980). Turbidity currents generated in this manner could continue to flow for much greater distances than the debris flow, depositing fine sediment even further from the source area (eg. Cossey and Ehrlich, 1979). Therefore, most calcirudites not directly linked to a debris flow conglomerate may have been similarly related to debris flows that deposited coarser-grained, matrix-rich sediments in more proximal regions in the basin.

6.2.5 Lithoclast Calcarenites and Calcisiltites (Table 6.1(5))

Lithoclast calcarenites and calcisiltites in the Cape Cormorant most commonly form sharply bounded beds that punctuate ambient shale (Figures 6.3.d, 6.7.e,f and 6.10.a). Calcarenites also commonly gradationally overlie, and calcisiltites more abruptly overlie, both debris flow conglomerates and calcirudites. The tops of the beds are commonly burrowed (see **Trace Fossils**, Chapter section 6.4).

Beds range from only a millimetre up to 50 cm in thickness; they are commonly amalgamated. The thinnest ones are generally tabular but thicker beds commonly pinch and swell along strike due mostly to channeling at the base. The vast majority are clast-supported and matrix-poor (Figure 6.11.h); some very thin beds and laminae made up of sand-size grains appear matrix-supported. Predominant detrital components are carbonate lithoclasts identical to those in the debris

flow conglomerates and calcirudites (Chapter section 6.5); siliciclastic sand is a conspicuous component of some calcarenites (Figure 6.11.g), especially near the top of the Caribou Brook section.

Calcarenites almost invariably display partial or complete Bouma sequences (Bouma, 1962; Figure 6.10.f,g). The exceptions are very thin, matrix-supported beds and laminae, only some of which are normally-graded (eg. Figure 6.10.g). Bouma sequences of structures are most complete in the thickest, coarsest calcarenites. Thin, fine-sand calcarenites and calcisiltite, in contrast, are generally either vaguely graded, parallel-laminated, or massive (Figure 6.11.h), corresponding only to the base (T_A) and highest portions (T_{Df}) of the Bouma sequence.

Calcarenite bases are also commonly loaded, convolute lamination commonly overprints ripple cross-laminated horizons, and their upper surfaces commonly exhibit fluid escape structures (Table 6.1(5)). Most of the latter are short, en echelon, comparatively coarse-grained sediment ridges that protrude above the top of the bed. They appear to be more regular and smaller-scale analogues of fluid escape structures atop calcirudites (Chapter section 6.2.4; Figure 6.10.h) and are similarly interpreted as manifestations of sediment dykes produced by liquifaction during shallow burial. Also present in the upper, very fine sand and silt layers are runzel-like structures (Figure 6.11.i) which are too small and irregular to be ripples formed by tractive processes and are interpreted to be expressions of either very small pillars formed by fluid escape or convolute lamination.

These sediments are interpreted to have been transported and deposited primarily by turbidity currents. Calcarenites with Bouma sequence structures that indicate deposition from a waning flow are classical turbidites (Bouma, 1962; Middleton and Hampton, 1976; Walker, 1984). Complete sequences record first rapid deposition from suspension (T_A), then slower deposition from suspension combined with tractive currents (T_{B-C-Di}), and finally slow suspension settling of the very fine sediment

components of the flow (T_{D2}). Beds that begin with division T_B , T_C , and T_D are interpreted to record sedimentation from progressively lower velocity flows (Walker, 1967). Laminated calcisiltites similarly record deposition from very thin, low velocity and low concentration suspensions.

Matrix-supported beds and laminae could be artifacts of compaction (ie. turbidites with abundant small shale intraclasts). Alternatively, they may have been deposited by thin, sandy debris flows.

Compositional similarities between these calciturbidites and the calcirudites and debris flow conglomerates, plus the fact that they commonly gradationally cap the debris flows, suggest they came from the same source and that turbidity currents were commonly generated above debris flows during transport.

6.2.6 Bentonite (Table 6.1(6))

Five thin beds of recessive-weathering, sticky clay occur in the Caribou Brook section (Figure 6.1.a). XRD analysis indicates that they are composed primarily of mixed layer, smectite-illite clay. Like other sticky clays that occur in the Table Point and Table Cove formations they are interpreted to be diagenetically altered layers of volcanic ash.

6.3 Gravitational Slides

Soft-sediment deformation structures caused by sliding are not abundant, but are scattered throughout formation sequences. They include slump folds, mullions and small wrinkles (amplitudes <1 cm), plus blocks of rotated and imbricated bedding and small throw (cm-scale) faults (Figures 6.1 and 6.3.b,d).

Most deformation occurs in discrete horizons a few tens of centimetres thick immediately below or directly above a debris flow conglomerate or, less commonly, a thick calcirudite. Deformation of strata beneath a conglomerate is interpreted to have been caused by a

combination of shearing and loading during emplacement of the coarse debris. Deformation of overlying strata is interpreted to be the result of sliding down depositional topography on top of the bed, possibly triggered by repacking or remobilization of grains in the very shallow subsurface.

Slides in interbedded shale and calcarenite sequences that are not closely associated with a conglomerate (eg. Figure 6.3.d) also involve only a few to several tens of centimetres of section. Beds involved are identical to enclosing undeformed strata indicating they are locally derived. A thin zone of rubbly bedding defines a shear zone above the basal detachment, but preservation of bedding within the slide indicates little internal remoulding and suggests little lateral displacement. Post-slide shale and calciturbidites are ponded in depressions and even out irregular depositional topography on some of the thicker slide masses.

Paucity of evidence of gravitational sliding suggests that sedimentation occurred on a very low angle slope. This agrees with the basin margin or basin setting indicated by the voluminous accumulation of laminated shale in Cape Cormorant sequences (Chapter section 6.2.1). Sliding in unconsolidated sediment can occur on slopes of only a few degrees (Lewis, 1970). In this particular setting it may have been triggered by seismicity or possibly by a small, but sudden change in slope due to faulting.

6.4 Trace Fossils

A variety of biogenic structures are found on the tops of most calcarenites and calcarenite-mantled calcirudites. Vertical sections through beds indicate that only the upper few millimetres are burrowed. Most are exposed on steeply-dipping bedding planes along the coast, the accessible portions of which are wave-battered and the upper portions of which are inaccessible. Consequently, though many different trace

fossil forms are recognized, morphologic detail that allows more certain identification is limited. Poorly-preserved casts of burrows also occur on the base of a few calcarenites near the top of the Caribou Brook section; the skewed distribution may reflect the paucity of exposed lower bedding planes lower in the section.

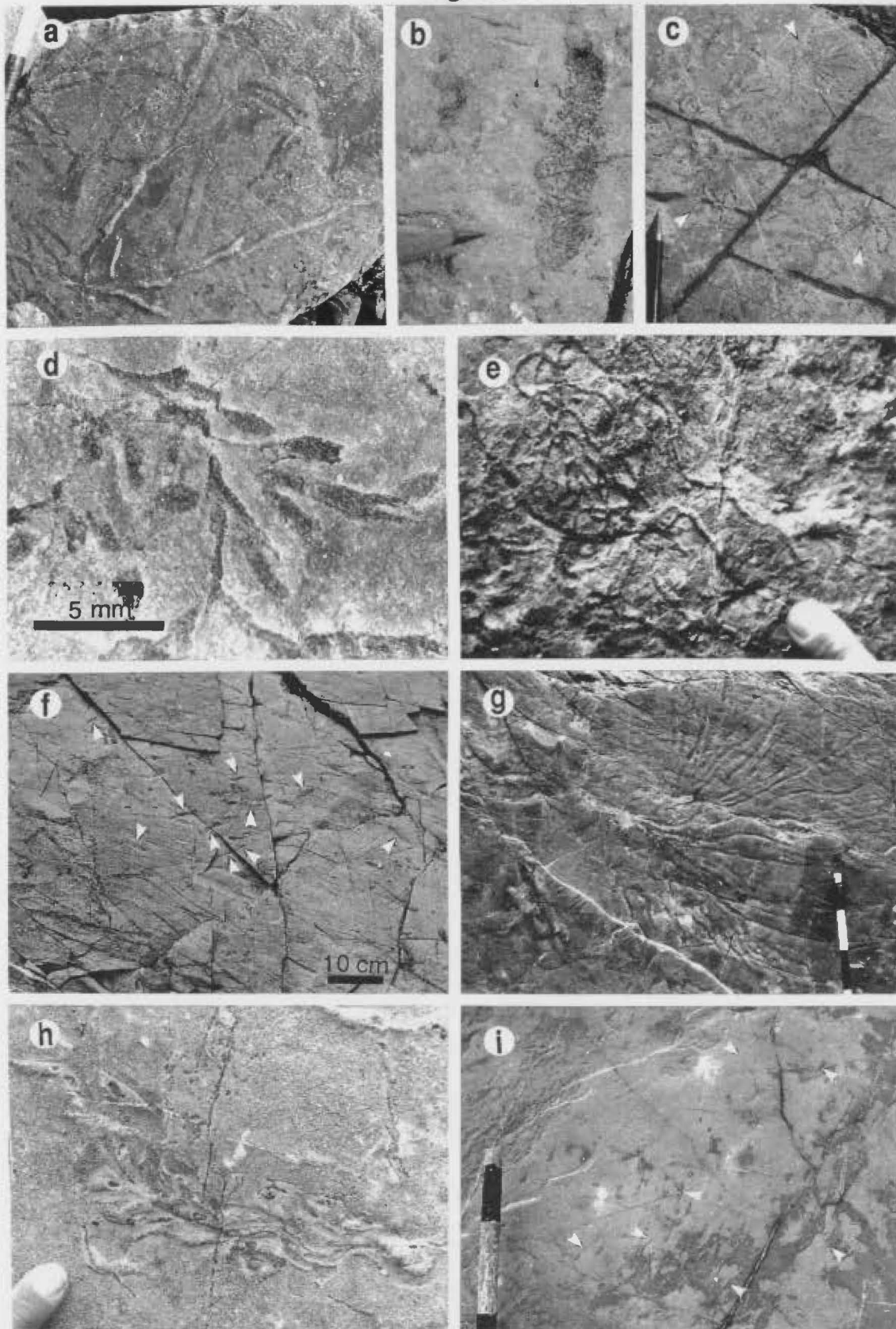
Traces present include: Planolites and possibly Palaeophycus, Syncoprulus, Gordia marina?, Chondrites spp., Diplichnites, Diplocraterion?, and two unidentified genera, one a large, star-like burrow reminiscent of Phoebichnus, the other a cluster of tubes similar to Chondrites. Descriptions and interpretation of these traces are in Appendix E, their stratigraphic distributions in the Caribou Brook section are shown in Figure 6.1.a, and several are illustrated in Figure 6.12.

None of the trace fossils present is diagnostic of a particular depositional environment or water depth. Predominance of surface or near surface feeding trails of sediment-ingesting organisms generally point to a quiet water setting where very fine-grained sediment and organic matter accumulated on the sea floor. The exception, Diplocraterion, indicates persistent bottom current activity, which is also indicated by numerous carbonate laminae in the shale (eg. Figures 6.4 and 6.11.h).

Overall, the assemblage is most closely allied to the Nereites ichnofacies typically found in deep-water, turbiditic slope and basin sequences (Seilacher, 1967; Chamberlain, 1971a, 1971b; Crimes, 1973, 1977; Kern, 1978; Pickerill, 1980). The relatively low diversity of the assemblage, though not uncommon for Early Paleozoic deep-water strata (Pickerill, 1981; Narbonne, 1984; Pickerill *et al.*, 1987), may be an artifact of poor preservation of the burrows on exposed bedding planes, or may indicate even more restricted conditions. Chondrites, in particular, signals dysaerobic (0.1-1.0 ml/l O₂, Rhoads and Morse, 1971) conditions on the sea floor (Bromley and Eckdale, 1984), but the large

Figure 6.12 Trace fossils in the Cape Cormorant Fm. All burrows except i) are on upper bedding planes of lithoclastic calciturbidites in the Caribou Brook section or laterally equivalent strata between Caribou Brook and Cape Cormorant. a) Planolites?; float from the 160-170 m landslide interval. Divisions on the measuring stick are 10 cm. b) Faecal pellet filled Syncopruhus; ~153 m. c) Chondrites sp. (arrows); ~186 m. d) Very small Chondrites sp.; 110-130 m interval in CB. e) Gordia marina?; ~194 m. f) Diplocraterion? (arrows); outcrop south of Caribou Brook equivalent to ~110 m in the Caribou Brook section (Figure 6.8.c). g) Large radiating burrow system similar to Phoebichnus trichoides; 157 m. Divisions on the measuring stick are 10 cm. g) Inchnogenus incertae, a small tunnel system of overlapping and ?branching burrows somewhat similar to Chondrites; ~175 m. h) Planolites? (arrows) on the upper bedding plane of a mottled mudstone bed; ~101 m in Big Cove section (B2).

Figure 6.12



burrows and evidence of indigenous benthic trilobites (Diplichnites) suggest that at least at times bottom waters were well oxygenated (Byers, 1977).

In contrast to the distribution of trace fossils in other ancient flysch sequences, the vast majority of burrows in the Cape Cormorant Formation occur on the tops of the calcarenites and are post-depositional (compare with Seilacher, 1962; Chamberlain, 1971a, 1971b; Kern, 1978). Although there are some poorly-preserved Planolites-like traces on the soles of some beds, possible casts of predepositional burrows whose scarcity may be due to limited exposure of lower bed surfaces, the apparent distribution of the burrows is compatible with the paucity of burrowed fabrics in enclosing shale and suggests that the seafloor was not normally inhabited by an abundant soft-bodied infauna. Anomalous selection of organic-poor calcarenites by deposit-feeders that normally select organic-rich muds for their feeding forays suggests that inhabitation was controlled by environmental parameters other than food supply or substrate. In light of evidence that bottom waters were normally dysaerobic or anoxic (ie. preservation of lamination in shale) burrows atop the calcarenites are interpreted to indicate more well-oxygenated conditions. Given the episodic nature, but high frequency of the calciturbidites, it is unlikely that the burrowed beds coincide with either basin-wide fluctuations in the degree of oxygenation of bottom waters or even reflect fluctuations in the level of an O₂-minimum zone. Instead, it is postulated that the calciturbidites were transported and deposited by aerated currents that also may have transported a soft-bodied, invertebrate fauna (eg. Sholkovitz and Souter, 1975; Potter et al., 1982; Föllmi and Grim, 1990). The allochthonous creatures, and possibly other tolerant, indigenous forms, temporarily thrived in the rapidly deposited sediment layers bathed in more well-oxygenated waters until strongly dysaerobic or anoxic conditions were reestablished. This mechanism implies that the currents originated in shallower, more

aerated water and that the Cape Cormorant basin was stratified.

6.5 Provenance of Lithoclastic Debris

6.5.1 Composition of Clasts

Debris flow conglomerates and calciturbidites are composed mostly of a polymictic suite of shallow marine limestone and dolostone clasts with minor chert and clasts of Cape Cormorant aspect (Figure 6.13). General descriptions of the major clast components and some other less common lithologies are provided below. More detailed descriptions of representative lithoclasts are in Table F.1 in Appendix F.

(i) **Limestone** Limestone lithoclasts range in colour from tan, to light or dark greyish-brown, to dark greenish-grey. They span a vast array of compositions and depositional textures typical of platformal environments (Figure 6.14.a-c,m,n). Common skeletal components in clasts confirm a shallow marine (Table F.1). Very large blocks and olistoliths reveal outcrop scale bedding styles and large structures which are not apparent in smaller clasts including: (i) 1-3 m high thrombolites (Figure 6.7.d), (ii) interstratified small, digitate stromatolite mounds, rippled, ooid grainstone, small thrombolite mounds, glauconitic calcarenite, parted mudstone, and cryptalgal and pattern dolomite (Figure 6.7.b), and (iii) thin-bedded, wavy-parted, burrowed mudstone, glauconitic flat pebble conglomerate, and laminated, micaceous shale (Figure 6.7.c).

(ii) **Dolostone** Dolostone lithoclasts range in colour from off white to brown to green to grey, and commonly weather yellow (Figure 6.7.g). Microcrystalline to very finely-crystalline types include cryptalgal dololaminite, mudcracked or brecciated dolostone, and pattern dolomite (Figure 6.14.i,j). More common are medium- to coarsely-crystalline dolostone clasts which include: 1) replaced oolitic, grain-supportstone (Figure 6.14.c,d,h), 2) replaced very fine, peloidal and/or intraclastic grain-/packstone, and 3) dolostones devoid of any

Debris Flow Composition

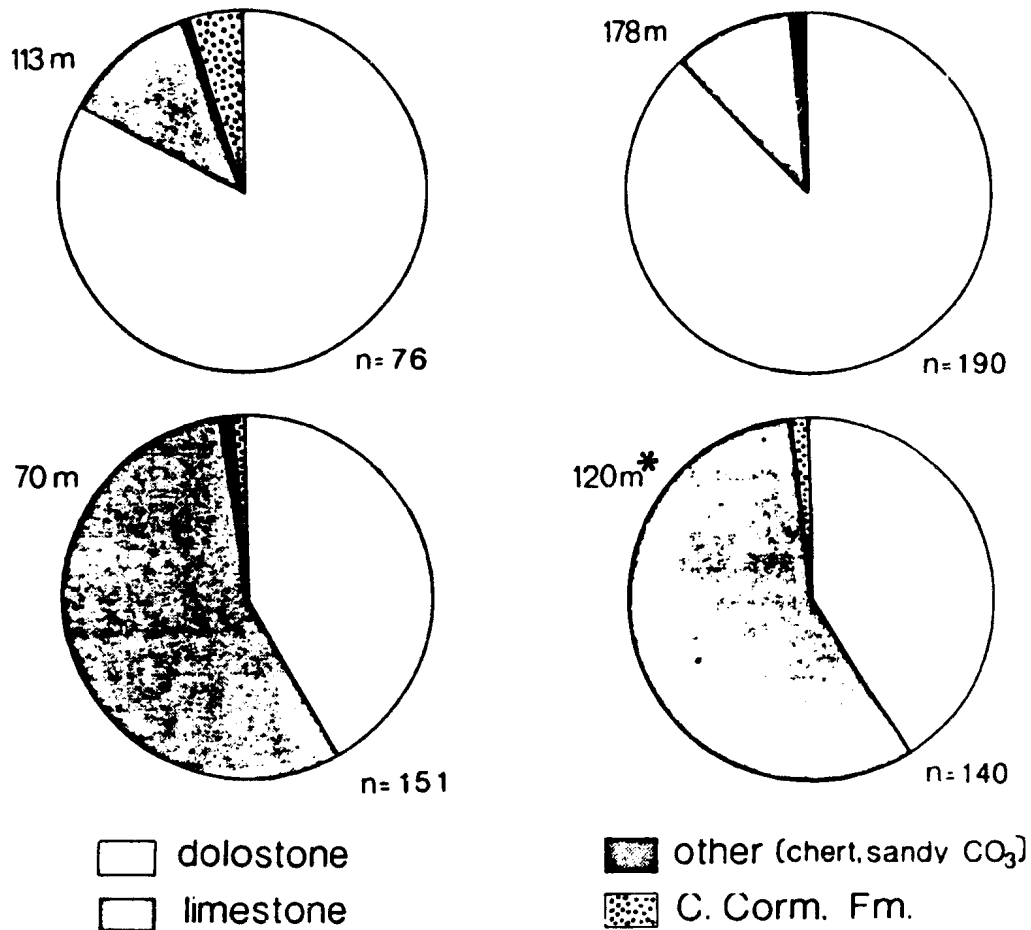


Figure 6.13 Composition of debris flow conglomerates at Caribou Brook. Positions of beds in the section are to the left of the pie diagrams; n = number of clasts counted. Data were collected by point counting on a grid on the outcrop, the spacing of which was based on average clast size. Number of data points was determined by the size of the accessible outcrop. Data for the 70 m conglomerate was collected in Caribou Brook; 30 cm grid spacing is smaller than the average clast size of the bed, which contains megaboulders up to 4 m long, but was chosen because outcrop was limited. Megaboulders were counted only once. Data for the (113 m) conglomerate was collected south of Caribou Brook (Figure 6.8.e); 30 cm grid spacing. Data for the (120 m) conglomerate was collected south of Caribou Brook (Figure 6.8.b); 30 cm grid spacing. Data for the (178 m) conglomerate was collected in the Caribou Brook section; 60 cm grid spacing.

Figure 6.14 Lithoclasts; polished slabs and photomicrographs. Bar scales on all photomicrographs except f) and p) are 0.5 mm. M=mudstone; W=wackestone; P=packstone; G=grainstone; R=rudstone; F=floatstone. Sample number and (inferred) or determined age and derivation are in parentheses. More complete descriptions are in Appendix F. a) Slab of partly pyritized (dark grey), clotted, peloidal, intraclastic, fossiliferous W with peloidal, intraclastic G pockets; several metres long slab in outcrop shows thrombolite macrostructure (#77; early Arenig, Boat Harbour Fm.). b) Slab of partly dolomitized (tan), intraclastic R/F with peloidal, fossiliferous W/P/G matrix. (CB. 82; Arenig, Catoche Fm.). c) Slab of intraclastic R. (#270; Cambrian). d) Photomicrograph of intraclastic F with peloidal, oolitic G matrix. All grains and cement are replaced by dolomite. m=mudstone intraclast; g=oolitic, peloidal G intraclast. (#67; Cambrian). e) Slab of wavy laminated to mottled, very finely crystalline, nonferroan dolostone with round, quartz sand grains (dark spots); divisions on scale are 1 mm. (CB33I; Cambrian). f) Photomicrograph of CB33I in e), above; crossed polars. Large grains are quartz; most are simple quartz, some are polycrystalline. Very small white grains dispersed in the dolomite are quartz silt. g) Photomicrograph of finely crystalline, nonferroan dolostone with floating glauconite grains (dark), angular quartz silt (arrows), and inarticulate brachiopod fragment (i). (CB33A; Cambrian). Vein is blocky calcite. h) Photomicrograph of dolomitized oolitic G; white interclast cement is chert. (CB33R; Cambrian).

Figure 6.14

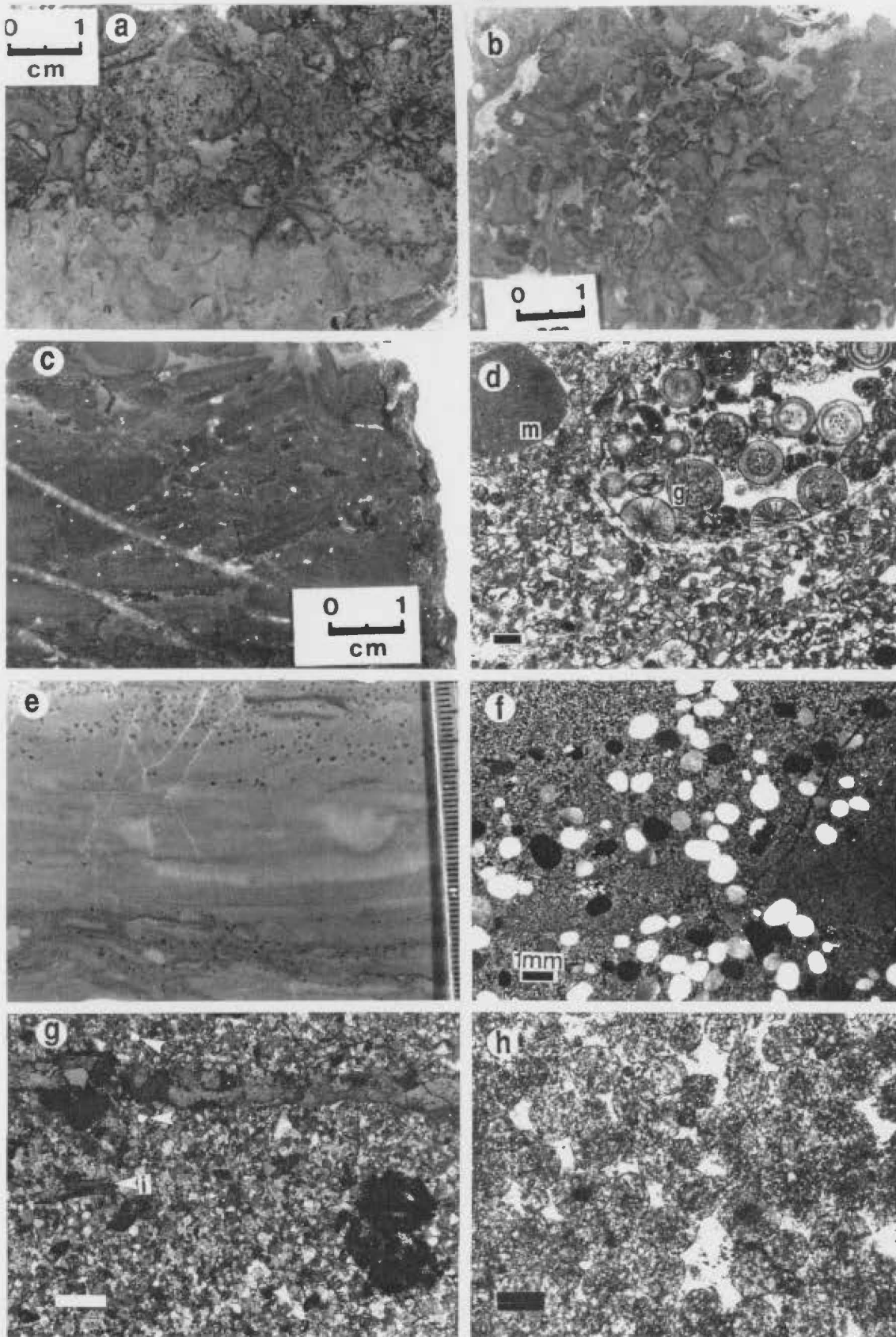
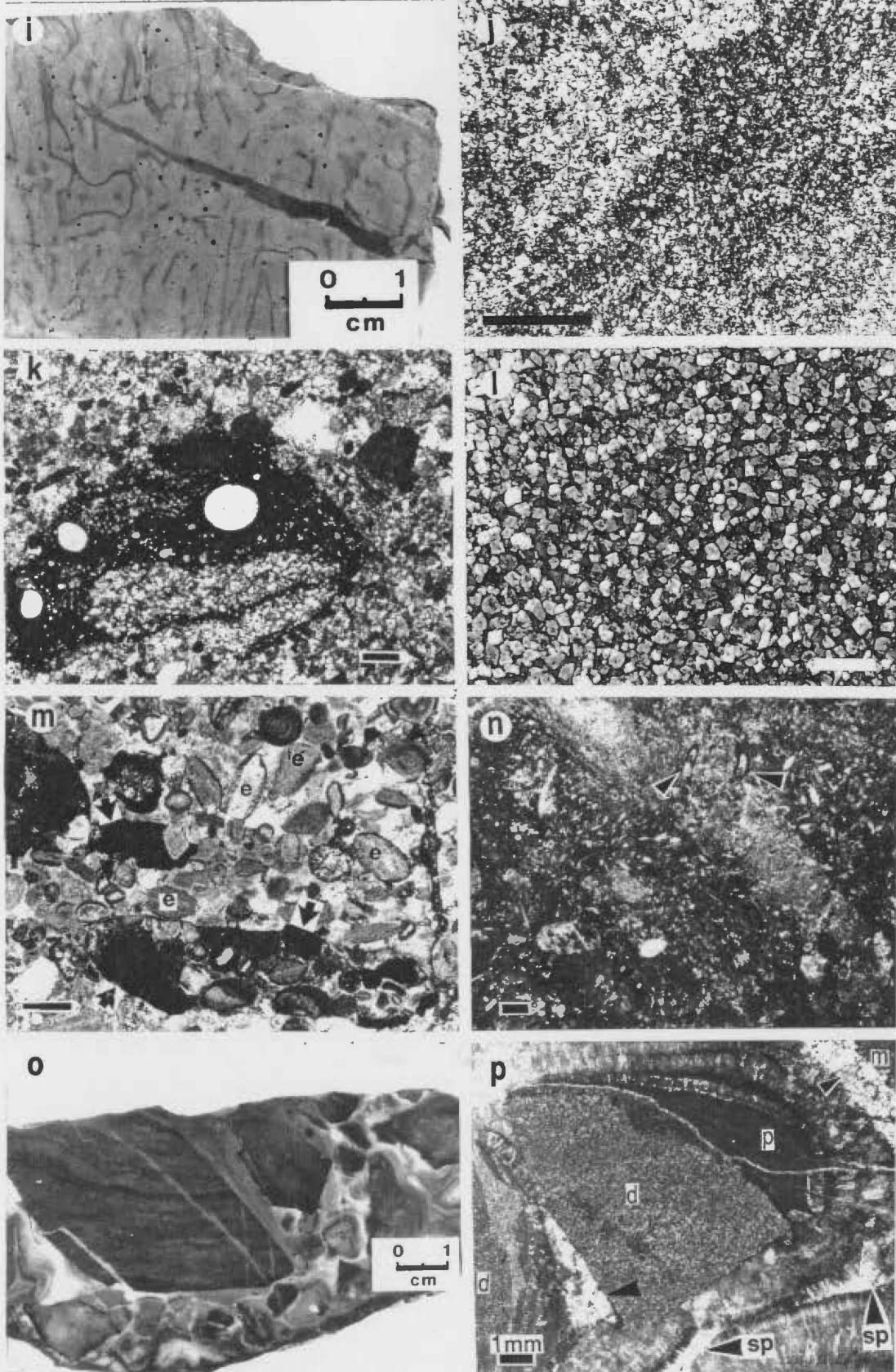


Figure 6.14 continued i) Slab of pattern dolomite; cross-cutting fracture is filled with shale matrix from the enclosing conglomerate. (0724-7; Upper Cambrian, Berry Head Fm.). j) Photomicrograph of barren very finely-crystalline dolostone. (#158; age and derivation indeterminate). k) Photomicrograph of partly dolomitized, lithoclast calcarenite with phosphatic shale clast with quartz sand grains. (CB.110; 151 m in the Caribou Bk. section; (Cambrian)). l) Photomicrograph of medium crystalline, nonferroan dolostone (#149; age and derivation indeterminate). m) Photomicrograph of intraclastic, glauconitic F with echinoderm (e) G matrix. Very dark grey grains and patches are glauconite (arrows); echinoderm fragments have oolitic coats. (#289; (Cambrian)). n) Photomicrograph of muddy, burrowed, peloidal, fossiliferous P (CB33P; indeterminate, probably Lower Ordovician). Most skeletal fragments (white) are calcitic spicules.; *Girvanella* coats (arrows) common. o) Slab of polymictic, lithoclast breccia (0714-4). Clasts are cemented with fibrous calcite. p) Photomicrograph of lithoclast breccia in o, above. d=medium crystalline dolostone; m=mudstone; p=perched internal sediment. Fibrous cement is partly recrystallized to coarse, anhedral calcite with undulose extinction. sp=late stage blocky calcite.

Samples in a, d, e, f, g, h, j, l and n are from the highest boulder conglomerate at ~178 m in the Caribou Brook section. Sample in b and o and p is from the boulder conglomerate at ~120 m in the Caribou Brook section. Samples c, i, and m are from a megaconglomerate equivalent to the conglomerate at 120 m in the Caribou Brook section; uppermost conglomerate in Figure 6.8.f.

Figure 6.14



relict grains or structures (Figure 6.14.1). Ooid-bearing lithologies vary considerably in composition and texture, but commonly contain well-rounded, medium- to coarse-grained quartz sand, fine, angular, quartz sand or silt, and glauconite (Figure 6.14.e,f,g) (Table F.1). All dolostone clasts are composed of nonferroan crystals with variable amounts of ferroan dolomite overgrowths and/or cement. Intercrystalline porosity in the coarser crystalline fabrics is commonly occluded by silica cement and blocky calcite (Figure 6.14.h; Table F.1).

(iii) **Chert** Chert clasts are minor, but conspicuous components of almost all gravity flow deposits (Figures 6.11.f and 6.13). Most are pebble-size, but small cobble-size clasts occur in some debris flow conglomerates. They range in colour from brown to dark grey to black. Most lack any discernible texture or fabric, but some overprint oolitic or peloidal grainstone and spiculitic mudstone, and some bear ghosts of anhydrite crystals (ie. evaporite pseudomorphs).

(iv) **Other minor exotic lithologies** Sedimentary lithic fragments which are not obvious in the debris flow conglomerates, but which are conspicuous components of the calciturbidites, especially above 120 m in the Caribou Brook section, include 1) dark brown, phosphatic and silicified shale, some with exceptionally round, coarse-grained, quartz sand, 2) mica-bearing, quartz siltstone, and 3) dolomitic siltstone (Figures 6.11.a,f and 6.14.k).

(v) **Clasts of Cape Cormorant aspect** Two types of clasts that are compositionally allied to the Cape Cormorant Formation occur in the debris flow conglomerates. Most are folded or broken, decimetre to metre-size rafts of interbedded lithoclast calcarenite and shale which are thought to have been incorporated by plucking or scraping at the base of the flow during transport. Also present, but extremely uncommon, are clasts of polymictic, carbonate breccia that is composed of angular, pebble-size carbonate lithoclasts, displays infiltration fabrics, and is cemented by fibrous, marine cement (Figure 6.14.o,p).

Texturally the breccia is unlike any lithology found in the stratified formation sequence, more closely resembling talus than debris transported and deposited in a gravity flow. Transport as a clast in a debris flow implies it derived near the source of the debris.

6.5.2 Ages of Clasts

All limestone and dolostone lithoclasts, as well as the chert and other minor sedimentary lithics found in the debris flows and calciturbidites have in situ counterparts in the early Paleozoic carbonate platform succession exposed on the south shore of the Port au Port Peninsula (Figure 6.15). Some of the more distinctive lithoclasts can be correlated directly with a specific lithostratigraphic unit. Most carbonate lithologies, however, occur in several formations in the succession, so correlation is problematic. Moreover, although a large percentage of clasts are fossiliferous, the skeletal debris is mostly too small and broken to be identified and dated.

To determine the ages of the clasts sixty-seven limestone and dolostone clasts were processed for conodonts (Table F.1). Of those samples, 58% were barren and 42% contained identifiable conodont elements (Figure 6.16.a; Tables F.1 and F.2 in Appendix F).

(i) **Fossiliferous clasts** Conodonts were recovered only from limestone clasts. Assemblages indicate that the clasts range in age from latest Tremadocian to early Llanvirnian (Table F.2; Figure 6.16.b) and therefore were derived from limestones as old as the Watts Bight Formation of the St. George Group and as young as the Table Point Formation (Figure 6.15). Conodont faunas indicating derivation from the Table Cove Formation were not found. The largest percentage of clasts sampled are interpreted to have come from the Catoche Fm. (Figure 6.16.b), an early to middle Arenigian unit which constitutes the thickest sequence of pre-Table Point limestones on the Port au Port Peninsula; all other formations consist of a very large percentage of dolostone (Figure 6.15).

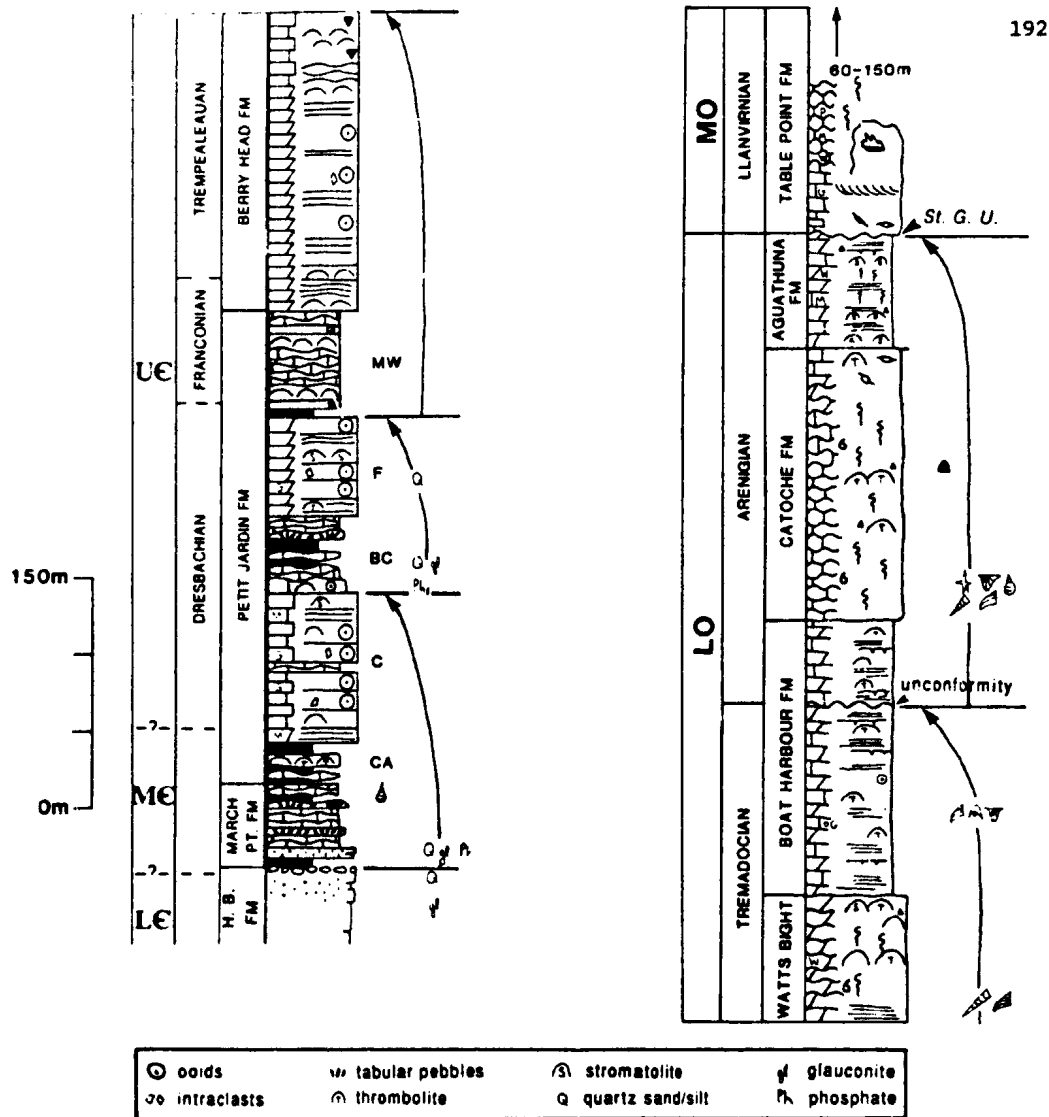


Figure 6.15 Cambro-Ordovician platformal succession on Port au Port Peninsula. Cambrian clastics and carbonates from Chow and James, 1986. Early Ordovician and early Middle Ordovician carbonate succession (modified after Knight and James, 1987; this study). CA=Cape Ann Mbr.; C=Campbells Cove Mbr.; BC=Big Cove Mbr.; F=Felix Mbr.; MW=Man O'War Mbr. St. G. U.= St. George Unconformity. Arrows delineate grand cycles.

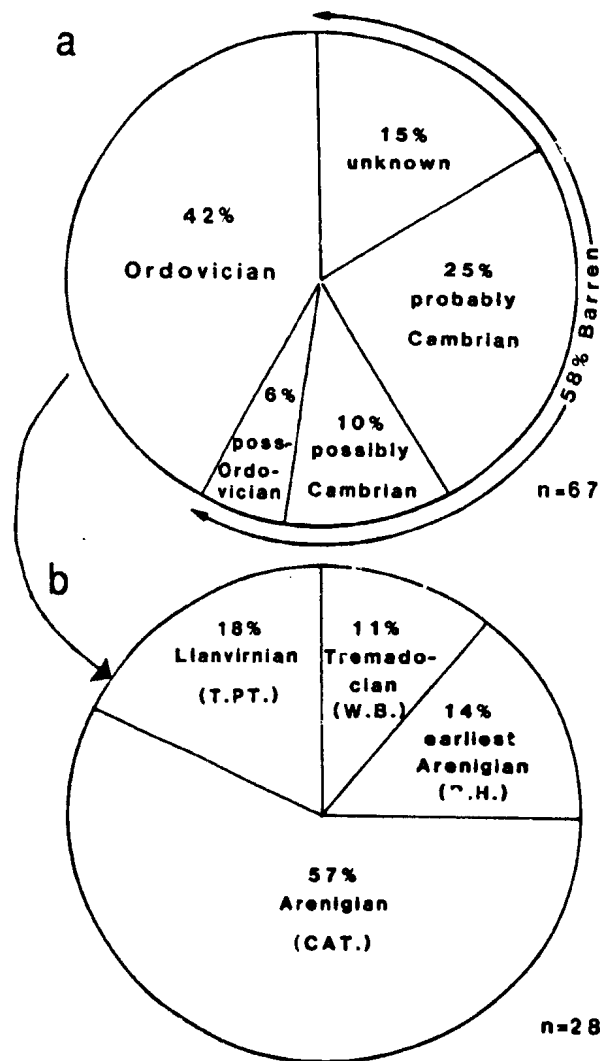


Figure 6.16 Ages of carbonate lithoclasts processed for conodonts; pie diagrams. a) Percentages of barren clasts versus fossiliferous clasts that contained Ordovician conodont elements. Designation of barren clasts as Cambrian or Ordovician is based on their compositional and textural similarities to same age formations on the Port au Port Peninsula. b) Percentages of fossiliferous clasts (exclusively limestone) determined by their conodont faunas to be Tremadocian, Arenigian, and Llanvirnian in age. Most are early and middle Arenigian in age, indicating derivation from the Catoche Formation (CAT.) of the St. George Group. The remaining 43% were approximately equally divided among the Tremadocian Watts Bight Formation (W.B.), the earliest Arenigian Boat Harbour Formation (B.H.), and the Llanvirnian (Whiterockian) Table Point Formation (T.P.T.). None of the conodont assemblages recovered from the clasts was diagnostic of either the late Arenigian Aquathuna Formation or the Llanvirnian Table Cove Formation.

(ii) **Barren clasts** All dolostone clasts processed, as well as several of the limestone clasts, were barren (Table F.1; Figure 6.16.a). Paucity of conodonts in early-formed dolostones, such as cryptalgal laminite and pattern dolomite, is probably a reflection of the extremely restricted environments in which the sediments were deposited. The absence of conodonts from more coarsely-crystalline, epigenetic dolostones may reflect their original absence from the sediments, since many are high energy grainstones, or their destruction during dolomitization.

Several barren dolostone and limestone lithologies, plus several clast types that were not processed for conodonts, are inferred on the basis of composition to be Upper to Middle Cambrian in age (Table F.1; Figure 6.16.a). These include: (i) ooid-bearing, quartzose, and/or glauconitic carbonates, (ii) pattern dolomite, (iii) dark grey, wavy-parted, glauconitic mudstone or dolostone and micaceous shale, (iv) dark brown, phosphatic and silicified shale clasts (\pm quartz sand), and (v) mica-bearing, quartz siltstone and dolomitic siltstone (Figure 6.14). All are characteristic of the Cambrian succession on the Port au Port Peninsula and are virtually absent from the overlying Ordovician strata (Figure 6.15). Both ooid limestone/dolostone and pattern dolomite are predominant lithofacies of the carbonate-dominated units of each of the three grand cycles comprising the Port au Port Group (Chow, 1986; Chow and James, 1986). Notable quantities of round, medium- and coarse-grained, quartz sand are also present in these units, particularly the Felix Cove Member of the Petit Jardin Formation (Chow, 1986). Wavy-parted limestone is the definitive lithofacies component of the shaley half-cycles of the grand cycles. Parted limestones bearing glauconite, micaceous silt and flat pebble conglomerates specifically occur in the oldest, Cape Ann Member of the Petit Jardin. That member, as well as the underlying March Point Formation, also contains quartzose, glauconitic calcarenites and silty shale. Phosphatized sediments and siliciclastic siltstone are components of the March Point.

6.5.3 Interpretation of the Lithoclast Debris Source

The composition and age of the carbonate lithoclasts indicate derivation from the early Paleozoic platform succession. Sudden exposure of those buried strata to erosion and redeposition as clasts in sediment gravity flows, plus the angular shape and enormous size of many clasts, suggest they were exhumed by faulting. The age range of lithostratigraphic units represented in the resedimented beds, as estimated from the thickness of the in-place stratigraphic succession on the Port au Port, indicates that at least 500 m of section were uplifted, exposed and eroded. In the absence of evidence that the resedimented carbonates had experienced subaerial exposure (eg. nonselective dissolution of carbonate sediments, karst sculpturing), the fault scarp is inferred to have been entirely submarine.

Mass wasting of exhumed, lithified carbonates along the escarpment would likely have involved minor to catastrophic rock falls, which consequently formed enormous piles of very coarse, angular talus at the base of the scarp. Large slabs in the debris flow conglomerates with broad dimensions at high angles to bedding (eg. Figures 6.3.c and 6.7.c,d) indicate that mass-wasting was controlled by high angle fractures parallel to the escarpment, or at least at a high angle to bedding. Lithified, polymictic breccia clasts in the debris flow conglomerates likely represent cemented talus that was exhumed and retransported after a long period of exposure to marine waters.

In this unstable setting several interrelated mechanisms could have triggered flows that transported coarse debris away from the escarpment into the basin. Episodic faulting could have increased the slope of the talus piles above the angle of repose, thereby triggering rock slides which during transport incorporated fine-sediment and evolved into sediment gravity flows as the material moved down slope. Earthquakes that accompanied fault displacements may also have sent shock waves that either increased pore water pressure of enclosing clays and

other finer-grained carbonates near the base of the talus piles, thereby reducing the strength and inducing mass movement of the sediment (Dott, 1963). Lastly, mass wasting, especially rock falls involving enormous blocks, may also have triggered rock slides or, by sudden loading, increased pore fluid pressure leading to instability of the sediment pile and gravity flows.

6.5.4 Temporal Changes in Sediment Gravity Flow Composition

All debris flow conglomerates and calciturbidites are polymictic, composed of a variety of limestone and dolostone lithoclasts derived from different stratigraphic levels (Figure 6.13). Since the vast majority of clasts in any given bed are of indefinite origin it is impossible to determine stratigraphic changes in the ages of clasts comprising the beds in the field. The large number of indistinct, barren dolostone clasts make this task extremely difficult even by combined analyses of extensive point count, petrographic, and microfossil data.

(i) Evidence of stratigraphic unroofing There are three compositional aspects of the debris flows and calciturbidites which suggest progressive, stratigraphic unroofing of the exhumed, early Paleozoic platform.

First, among megaconglomerates in the Caribou Brook and Big Cove sections there is a distinct increase in the age of the largest clasts up section. 1) In Big Cove (A) (Figure 6.1.b) the basal conglomerate contains large blocks of mottled mound lithofacies limestone, cryptalgal dololaminite, light brown, peloidal grainstone, very similar to lithologies that comprise the Table Point, Aguathuna, and Catoche formations, respectively (Figure 6.15). Basal conglomerates in Caribou Brook and in Big Cove (B) (Figures 6.1.a, c) are compositionally similar but finer-grained, and in all locations distinctive Cambrian lithologies are absent. 2) The megaconglomerate ~15 m above the base of the formation in Big Cove (B) (Figures 6.1.c and 6.3.c) contains an enormous,

fossiliferous-peloidal limestone slab determined by conodonts to have come from the Catoche Formation (sample 0718-5 in Tables F.1 and F.2).

3) At 65 m above the base of Big Cove (A) (Figures 6.1.b, 6.3.a, and 6.7.a), a second megaconglomerate contains an olistolith determined by conodonts to have been derived from the early Early Ordovician Catoche or Boat Harbour formation (sample CB-COC in Tables F.1 and F.2).

4) The next megaconglomerate, about 135 m above the base (Figures 5.1.b and 6.7.b), contains an enormous clast composed of interstratified small, digitate stromatolite mounds, rippled, ooid grainstone, small thrombolite mounds, glauconitic calcarenite, parted mudstone, and cryptalgal and pattern dolomite, inferred to have been derived from the Upper Cambrian Petit Jardin Formation.

5) Finally, at 225 m above the base (Figures 6.1.b and 6.7.c), a fourth thick conglomerate contains a very large, disintegrating, wavy-parted, silty and glauconitic limestone raft, inferred to have been come from the Middle Cambrian Cape Anne Member of the Petit Jardin or, possibly the underlying March Point Formation.

Second, distinctive Cambrian lithologies are not obvious components of lithoclastic beds until ~120 m in the Caribou Brook section (Figure 6.1.g). Calcarenites and calcirudites below this level contain sparse ooid-bearing limestone clasts, but the fact that none are sandy or silty or glauconitic and that no oolitic dolostone clasts are present suggest they may have come from only Ordovician units. The abrupt and conspicuous appearance of the spectrum of Cambrian lithologies in the 120 m conglomerate suggests those strata were not initially exhumed along the fault scarp.

Third, petrographic examination of calcarenites and calcirudites in the Caribou Brook section indicates a qualitative increase in the dolostone clast:limestone clast ratio between 80 m and ~140 m in the section (Figure 6.1.a). A similar change in composition is recorded in debris flow conglomerates (Figure 6.13). If most dolostone came from

lithostratigraphic units older than the Catoche Formation (Figure 6.15), then the increase in abundance of dolostone clasts in this lower part of the section suggests those deeply buried strata were gradually uncovered. The fact that this compositional change precedes and accompanies the appearance of distinctive Cambrian clasts in the section supports this interpretation.

Collectively these observations suggest gradual unroofing of the buried platform sequence along the fault scarp.

(ii) **Influx of siliciclastic sand** Lithoclast calcarenites with noticeably large amounts of siliciclastic grains occur in two stratigraphic intervals of the Cape Cormorant at Caribou Brook, between 134 and 149 m and from ~183 m to the top of the section (Figure 6.1.a). The base of the lower interval is marked by a 30 cm thick, greenish-grey coloured, very small pebble-based (<1 cm) calcirudite that grades up into sandy calcarenite with Bouma sequence structures. The colour of the bed, which distinguishes it from other calciturbidites and allies it to the Mainland Sandstone, reflects a relatively high percentage of argillaceous matrix. Siliciclastic grains are not prominent components of the pebbly base, but angular to subround, quartz and untwinned or albite-twinned feldspar comprise 25-35% and 5-15%, respectively, of the overlying calcarenite portion of the bed (Figure 6.11.g). Several very thin, siliciclastic-rich calcarenites and calcisiltites occur in the 15 m section above this bed.

The top 20 m of the formation bears several calcarenites in which the fine-grained, ripple-cross-laminated and/or parallel-laminated portions of the beds consist predominantly of quartz and feldspar. Some very thin, laminated siltstones are also present in this interval.

Siliciclastic sediments in the calcarenites near the top of the formation are similar enough in composition and size to those that make up the overlying, turbiditic Mainland Sandstone to infer a sedimentologic linkage. Their presence suggests they were entrained by litho-

clast-bearing turbidity currents as they travelled over areas in the basin where fine-grained, siliciclastic turbidites were being concurrently deposited.

The origin of siliciclastic sands in calcarenites much lower in the Cape Cormorant section is not as certain. Their compositional and textural immaturity links them to the Mainland Sandstone. However, other outstanding detrital components of the basal Mainland, such as iron-rich chlorite and a variety of shale intraclasts and lithoclasts, are not present. Moreover, quartz and feldspar grains in the calciturbidite at 134 m are much coarser-grained (0.25-2 mm) than they are in the sandstone at the base of the Mainland (0.04-0.2 mm). The differences suggest that despite similar weathering characteristics, this sandy interval is not linked to the Mainland turbidites.

An alternative origin is breakdown and resedimentation of Cambrian sandstones uplifted and exposed along the fault scarp from which all the carbonate debris was derived. It is supported by the fact that the basal sandy calcarenite occurs only 13 m above the first debris flow conglomerate with oolitic and pattern dolomite clasts, only 10 m above the first appearance of siltstone clasts in a calcirudite, and directly above the first calcirudite bearing distinctive phosphatic shale clasts (Figure 6.1.a) all of which are inferred to have come from Upper and Middle Cambrian formations. Either the March Point or underlying Hawkes Bay Formation (Figure 6.15), or possibly lateral equivalents, could be the source of the sand. Derivation from a lower stratigraphic level in the Paleozoic succession is unlikely given the scarcity of siliciclastic grains in the calcarenites and apparent absence of coarse, resedimented sandstone clasts in the calcirudites and debris flow conglomerates.

6.6 Interpretive Reconstruction of the Depositional Setting

The thick sequence of dark shales, resedimented lithoclastic conglomerates, calcirudites and calcarenites, and ribbon limestone is

interpreted to record sedimentation in a deep-water, basin margin to basinal environment. The basin was bounded along at least one margin by an escarpment generated by faulting that exhumed early Paleozoic platform carbonates. For some time early in its history the basin was also bordered by one or more shallow-water platforms. A schematic reconstruction of this setting is shown in Figure 6.17.

Enormous quantities of terrigenous mud accumulated on the basin floor, delivered by a continuous rain of fine sediment suspended in the water column. Highly productive surface waters also supplied abundant organic debris to the basin floor including graptolites, phyllocarids, cephalopods, and radiolarians, as well as fine organic matter contributed by phytoplankton living in the photic zone. Volcanism outboard of the continent gave rise to clouds of ash which were episodically blown into the area and settled onto the sea floor.

Platform(s) bordering the basin were sites of in situ carbonate production. Peloidal sands, mud, and fine skeletal debris accumulating in the shallow-water environments were periodically swept away by powerful waves and currents and transported into deep water. The transported sediment was delivered to the basin floor both by slow suspension settling through the water column and by rapid deposition from turbidity currents, forming distinctive ribbon limestones in the basinal sequence.

Fault scarps defining at least one margin of the basin exposed old, buried, platform carbonates. Intense fracturing and faulting of the lithified strata facilitated mass wasting, resulting in the formation of enormous talus piles of coarse, angular debris. That debris was episodically destabilized by catastrophic rock falls and earthquakes shocks, and was disrupted by faulting, all of which could have triggered rock slides or avalanches from which sediment gravity flows were generated. Debris flows evolved from masses of tumbling, rolling, and sliding rocks as they incorporated water and fine sediment, forming slurries that transported pebbles, cobbles, boulders, and blocks or slabs up to

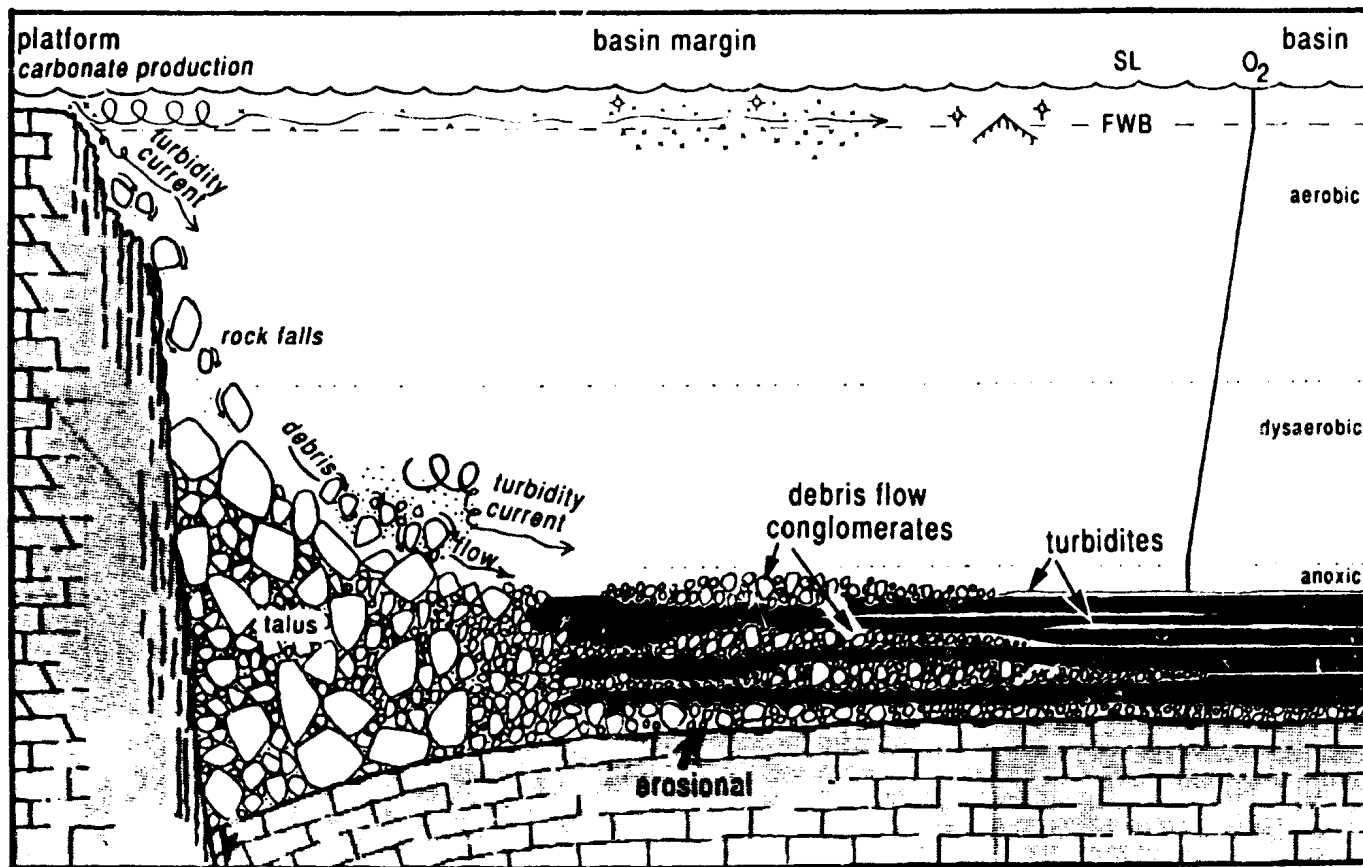


Figure 6.17 Schematic reconstruction of the depositional environment for the Cape Cormorant Formation. SL, sea level; FWB, fairweather wave base. Key to other symbols is in Appendix A.

several tens of metres long into the basin. Flow size and size of transported debris would have depended on the area, volume and size of debris initially involved in the avalanche, and flow competency would have been determined by the consistency of the clay-water fluid. The largest debris flows would have been generated when and where faulting was most frequent and the escarpment(s) had greatest vertical relief.

Turbidity currents may have similarly originated by avalanching of talus piles when large volumes of fine debris, either in the piles or generated by crushing in an avalanche, were thrown into suspension, and flowed down into the basin depositing thin sheets of sandy and silty sediment. They were also generated above moving debris flows. Sometimes the entrained sediment was rapidly deposited atop the coarse, debris flow deposit. More commonly the currents travelled beyond the snout of the debris flow, transporting and depositing sediment farther out in the basin.

Debris flows and turbidity currents likely would have emanated from all points along the length of the escarpment(s). Small, submarine fans may have developed locally and temporarily (eg. Watts, 1988), but sediment dispersal in the basin as a whole is unlikely to have occurred via a single, large, channelled, fan complex such as emanate from the mouths of submarine canyons on modern continental slopes (eg. Normark, 1970). Instead, flows originating at the escarpment(s) would have formed discontinuous sheets or lobes, with highly variable width:length ratios, in which the coarsest sediment was deposited in an escarpment-parallel zone nearest the source, while the finest material was deposited in the far reaches of the basin.

Bottom waters in the basin were normally very poorly-oxygenated. A limited brachiopod fauna tolerant of low O_2 levels inhabited the basin floor, presumably living on the sediment surface. Near-surface muds were commonly anoxic and did not allow inhabitation by a burrowing infauna, but small numbers of burrowers inhabited the sediments during

times of improved aeration of bottom waters. Turbidity currents transporting lithoclastic sediment into the basin carried with them more well-oxygenated waters derived from shallower depths. Once transported into the basin, the oxygenated waters veneered the sediment interface, temporarily creating a hospitable environment for a limited soft-bodied, mostly deposit-feeding infauna that fed in the finest sediment layers of the turbidites.

Poorly-oxygenated bottom waters may have been a consequence of poor circulation, probably caused by submarine topography that limited exchange with aerated surface waters and/or normal marine bottom waters. Oxygen stratification of the water column would have been exacerbated by high organic productivity of surface waters; abundant decaying organic matter settling through the water column rapidly consumes available dissolved oxygen. Fluctuations between dysaerobic and strongly dysaerobic or anoxic conditions could have been caused by changes in surface water productivity or episodic lowering of barriers to circulation.

6.7 Cape Cormorant Formation Lithofacies

The five predominant lithologies that make up the Cape Cormorant comprise three lithofacies: 1) megaconglomerate-ribbon limestone, 2) calcarenite-conglomerate, and 3) green shale-calcarenite (Table 6.3). Lithofacies 1) forms the lower 80 m of the Caribou Brook section and all of Big Cove sections (A) and (B); lithofacies 1), 2) and 3) form a single vertical succession at Caribou Brook (Figure 6.1).

6.7.1 Megaconglomerate-Ribbon Limestone Lithofacies

(i) **Description** This lithofacies is distinguished by exceptionally coarse and voluminous debris flow conglomerates and the presence of ribbon limestone, both interstratified with a large amount of dark shale and relatively minor lithoclastic calciturbidites (Table 6.3). These strata, and specifically the outstanding megaconglomerates, are spectacularly exposed along the coast in and around Big Cove (Figures

Table 6.3 Cape Cormorant Formation Lithofacies

Lithofacies	Geographic & Stratigraphic Distribution	Shale	Ribbon Limestone	Debris Flow Conglomerates	Turbiditic Calcarenites
Megaconglomerate-Ribbon Limestone	<ul style="list-style-type: none"> - all of Big Cove sections (A) & (B) - lower 80 m of the Caribou Brook section - megaconglomerate comprises Round Head (Figure 6.2); neither thickness nor stratigraphic position are known 	<ul style="list-style-type: none"> - very abundant (CB) to extremely abundant (BC) (>60-80%) - dark grey-brown (CB) or black (BC) - slightly calcareous to noncalcareous - minor burrow-mottling (100-130 m) in BC (B2) - common pelagic invertebrates, benthic brachiopods common 	<ul style="list-style-type: none"> - relatively minor, but conspicuous ribbon limestone intervals at CB - discrete beds of muddy limestone & calcareous shale interstratified with lithoclastic turbidites and non-calcareous shale at BC - anomalous burrowed mudstone above 126 m in BC (B2) 	<ul style="list-style-type: none"> - major component (comprises ~75% of BC(A)) - extremely thick/massive & matrix-rich - 40 cm - >65 m thick, most >10 m - coarse- to extremely coarse-grained; predominantly boulders, megaboulders, & olistoliths (commonly several 10s of metres maximum dimension) - disorganized & normally-graded beds most common - thick turbiditic calcirudite 'caps' common above graded beds 	<ul style="list-style-type: none"> - relatively minor component - 1 mm - 20 cm thick, mostly calcarenites & calcisiltites sparsely punctuating dark shale - uncommonly amalgamated - graded calcirudites mostly above debris flow conglomerates - burrowing inconspicuous except in the upper 30 m of BC (B2)
Calcarenite - Conglomerate	<ul style="list-style-type: none"> Caribou Brook 80-183 m interval also in Cointres Brook (north of Mainland) & in Three Rock Cove Brook (south of Round Head) (Figure 6.2) 	<ul style="list-style-type: none"> - very abundant (>50-60%) increasing to >70% between 140 and 160 m - dark brown-grey, slightly calcareous between 80-140 m, black noncalcareous between 140-159 m, dark grey brown, noncalcareous between 172-184 m - minor burrow-mottling at 120 m & 134-149 m - common pelagic & benthic invertebrates 	<ul style="list-style-type: none"> - extremely minor component - sparse muddy limestone beds between 80-125 m (may be confused with fine-grained lithoclastic turbidites) - discrete calcareous shale beds absent 	<ul style="list-style-type: none"> - relatively minor component - thick to relatively thin & matrix-lean <25 cm to 7-8 m thick, most <1.5 m - relatively fine- to coarse-grained; predominantly pebbles, cobbles & small boulders, few metre diameters blocks & slabs to 10 m long present in the thickest flows only 	<ul style="list-style-type: none"> - major component - <1 mm - 1.2 m thick, mostly thin calcarenites & calcisiltites - 'distal', normally-graded and graded, stratified calcirudites prominent in the lower 50 m (where debris flows are also most numerous); 'proximal', disorganized, crudely-stratified & inversely-graded calcirudites prominent above 153 m

Table 6.3 continued

Lithofacies	Geographic & Stratigraphic Distribution	Shale	Ribbon Limestone	Debris Flow Conglomerates	Turbiditic Calcarenites
Calcarenite - Conglomerate (continued)	-----	-----	-----	<ul style="list-style-type: none"> - disorganized, normally- & inversely-graded beds present - turbiditic calcarenite caps very common; most are <5-10 cm thick 	<ul style="list-style-type: none"> - megaripples present atop beds in the upper 35 m - tops typically burrowed (conspicuous above 135 m) - quartzose/feldspathic calcarenite at 134 m; sandy calcarenites & thin siltstones between 134-146 m
Green Shale - Calcarenite	Caribou Brook only uppermost 20 m	<ul style="list-style-type: none"> - very abundant (50-80% in intervals between major calcirudites) - dark greenish-grey, noncalcareous - burrow mottling very common - common pelagic & benthic invertebrates 	none	none	<ul style="list-style-type: none"> - major component - <1 mm to 30 cm thick - bimodal population of thin, fine calcarenites & calcisiltites & thin to medium calcirudites - 'proximal', disorganized & crudely stratified calcirudites most common; inversely- & inversely- to normally-graded, normally-graded & graded stratified beds also present - megaripples atop several calcirudites - tops invariably burrowed - (siliciclastic) sandy & silty calcarenites present

6.3.a-c and 6.7.a-c, e). Though poorly-exposed and comparatively thin in Caribou Brook proper, the megaconglomerates have prominent topographic and (aerial) photographic expression in the hills 400-650 m southwest of the brook; one bed (~50-70 m thick) contains clasts up to 10 m by 50 m in cross-section (note 'megaboulders' in Figure 6.2). No one megaconglomerate has been traced between adjacent sections, due in part to limited exposure and/or accessibility of some outcrops and structural complexities between sections. However, marked variations in thickness and texture of the basal conglomerate in the three measured sections (compare Figure 6.1.a-c) suggest that the debris flows are in fact discontinuous sheets of highly variable dimensions, lateral extent and volume.

(ii) **Interpretation** These strata are interpreted as proximal deposits of a newly formed, fault scarp-bounded basin which was supplied with carbonates derived both from one or more tectonically active, escarpments and one or more adjacent, relict platforms. Deposition of these strata directly atop shallow water, platformal limestones (Table Point Formation) implies that basin formation was an immediate consequence of down-faulting. Predominance of megaconglomerates and paucity of lithoclastic turbidites identify this lithofacies as proximal with respect to the faulted basin margin (Crevello and Schlager, 1980; Cook and Mullins, 1983). Deposition of coarse debris adjacent to the fault may have been accentuated by a structural depression, specifically a roll-over structure on the hanging wall of the down-faulted, basin block (Gibbs, 1984), which trapped, or at least hindered basinward transport of debris (eg. Eberli, 1987). More fluid and higher velocity turbidity currents, in contrast, by-passed proximal areas and transported and deposited relatively fine sediment further out in the basin.

The intercalated ribbon limestones attest to one or more contemporaneous platforms, mere relics of the preceding, regional carbonate shelf platform. One likely site of carbonate production was atop the escarp-

ment-bounded horst which experienced relative uplift and remained a topographic high while the Cape Cormorant basin formed. However, since ribbon limestone constitutes the sole deep-water, carbonate deposited atop platformal limestones east of the immediate basin (Table Cove Formation, Chapter 6), it is possible that these sediments came from other submarine highs flanking the basin.

6.7.2 Calcarenite-Conglomerate Lithofacies

(i) **Description** This lithofacies is distinguished by numerous calciturbidites, comparatively fewer and thinner debris flow conglomerates, and very minor ribbon limestones interstratified with slightly calcareous to noncalcareous shale (Table 6.3). An approximate time line defined by the first appearance of Cambrian lithoclasts in debris flow deposits and turbidites indicates that these strata are coeval with the upper 100-140 m of megaconglomerate-ribbon limestone lithofacies in the Big Cove area (Figure 6.1.a,c).

Debris flow deposits are the most striking components of the lithofacies, but compared to those in the megaconglomerate-ribbon limestone lithofacies they are on average thinner, finer-grained, and matrix-lean, constitute a lesser percentage of the whole stratigraphic thickness, and decrease in number and thickness up section. The thickest flows in the lower 45 m contain very large blocks and rafts (Figure 6.7.d), but none comparable in size to those in underlying and adjacent megaconglomerates.

Calcirudites, calcarenites, and calcisiltites, all present in large numbers, generally become thinner-bedded and finer-grained and display less complete Bouma sequences up section. Calcirudites with 'distal' internal structure are conspicuous in the lower 50 m where debris flow conglomerates are also most numerous. Calcirudites with 'proximal' internal structure reappear in the upper 15-25 m of the lithofacies.

(ii) **Interpretation** Predominance of calciturbidites identifies the lithofacies as distal with respect to the faulted margin. Transport and

deposition by less voluminous and finer-grained debris flows in the Caribou Brook area while deposition of megaconglomerates and ribbon limestones continued around Big Cove is thought to reflect diminished supply of coarse, lithoclastic debris and reduced size of the flows at their origin, and, possibly, trapping of debris flows in a structural depression in front of the fault scarp. Whether the turbidity currents originated at the escarpment or were generated above debris flows, they generally indicate by-passing of the proximal area where debris flow deposition continued. The calcirudites, calcarenites and calcisiltites record a wide range of flow strengths, but their general fining- and thinning-upward trend mirrors that of the debris flow conglomerates, further indicating that the escarpment was becoming an increasingly benign source of sediment. Reappearance of calcirudites near the top of the lithofacies sequence, however, suggests reactivation of the fault.

Scarcity of ribbon limestones, and their eventual disappearance up section, implies that relict platforms, including the escarpment-bounded block, subsided to depths at which biogenic carbonate sediment was no longer produced and/or waves and currents were no longer capable of entraining sediments and transporting them basinward.

6.7.3 Green Shale - Calcarenite Lithofacies

(i) **Description** This lithofacies consists of a bimodal population of fine calcarenites and very coarse calcirudites interstratified with dark green and grey, noncalcareous shale (Table 6.3). It is further differentiated from the other two lithofacies by the absence of debris flow conglomerates and ribbon limestone.

Greenish-grey, burrow-mottled shale is the diagnostic feature of the lithofacies (Figure 6.4.d,e). Its colour, thought to reflect a high percentage of chlorite, links the sediment to overlying Mainland Sandstone graywackes (Chapter 8), as does the presence of siliciclastic sand and silt in some of the calciturbidites (Chapter section 6.5.4(ii)).

Predominant thin, fine-grained calcarenites and calcisiltites are mostly parallel-laminated (T_4), but more complete Bouma sequences are not uncommon. Outstanding calcirudites in the otherwise fine-grained sequence (Figures 6.3.d and 6.10.a,d) display a range of internal structures, but are primarily of 'proximal' aspect. Megaripples that veneer many of these (Figure 6.10.e) record post-depositional reworking by nondepositional tails of the gravel-bearing flows.

(ii) Interpretation Predominance of fine-grained calciturbidites and absence of debris flow conglomerates identify this lithofacies as distal. In contrast to underlying strata, however, these strata record simultaneous deposition of escarpment-derived carbonate sediment and terrigenous muds of an encroaching, siliciclastic depositional system. Overall, the marginal escarpment contributed relatively minor amounts of sediment. However, renewed influx of lithoclastic calcirudites to the basin, which marks a reversal in the fining-upward trend recorded in the underlying lithofacies, suggests reactivation of at least a segment of the fault that triggered mass wasting and/or more voluminous sediment gravity flows. The greenish-grey shale is interpreted to have been deposited from dilute suspensions at the tails of siliciclastic-bearing turbidity currents, and thus heralds encroachment of sandy turbidites in the basin. Siliciclastic silt and sand incorporated in calciturbidites further indicate that currents originating at the escarpment travelled over areas where siliciclastic turbidites were being deposited, thereby also signalling proximity of the siliciclastic depositional system.

The appearance of a more persistent burrowing infauna in the basin-al muds suggests that oxygenation of bottom waters had improved. The change may have been 1) the consequence of continuous sedimentation or tectonic uplift which raised the seafloor above the oxygen minimum zone in the water column, or 2) the result of improved circulation due to reduced submarine topography or, possibly, 3) frequent influx of well-aerated, siliciclastic-bearing turbidity currents into the basin.

6.8 Paleocurrent and Paleoslope Data

Field measurements and observations indicative of paleocurrent and/or paleoslope direction include: ripple and megaripple strike, ripple foreset and ripple trough orientation, graptolite orientation, orientation of grooves, thinning direction of debris flow conglomerates, orientation and asymmetry of slump fold axes, orientation of soft-sediment wrinkles, orientation and thrust direction of soft-sediment faults, and orientation of imbricated bedding. Data collection was restricted by limited exposure in some locations and/or parts of the section, and by the nature of the outcrop. Near vertical bedding limited accessibility at both Caribou Brook and Big Cove; weathering commonly obscured details of internal structure of calciturbidites and reduced relief on upper bedding planes thereby obscuring asymmetry of bedforms. The majority of data are compiled in Figure 6.18; additional data are in Figures 6.1.c and 6.8.

6.8.1 Megaconglomerate-Ribbon Limestone Lithofacies

Most paleoslope/-current data from this lithofacies come from Big Cove (B) (Figure 6.1.c); exposure is poor in Caribou Brook and Big Cove (A) is inaccessible. They are too sparse to generate a clear picture of basin configuration. Orientations of fold axes and wrinkles suggest a northerly-striking slope. Inferred directions of displacement are inconsistent, but in conjunction with the single soft-sediment thrust suggest the slope dipped eastward. Thinning directions of debris flows conglomerates in the section, which given the short distances over which thickness changes were noted are probably more reliable indicators of basal channel margins or lateral margins of the flows, indicate ambiguous northeast/southwest and south-east/northwest flow, which is compatible with the slope suggested by the other data. Similarly, the outcrop/topographic expression of a megaconglomerate in the inland area around Caribou Brook (see 'megaboulders' in Figure 6.2) outlines a 1500 m long lens which thins markedly to both the northeast and southwest.

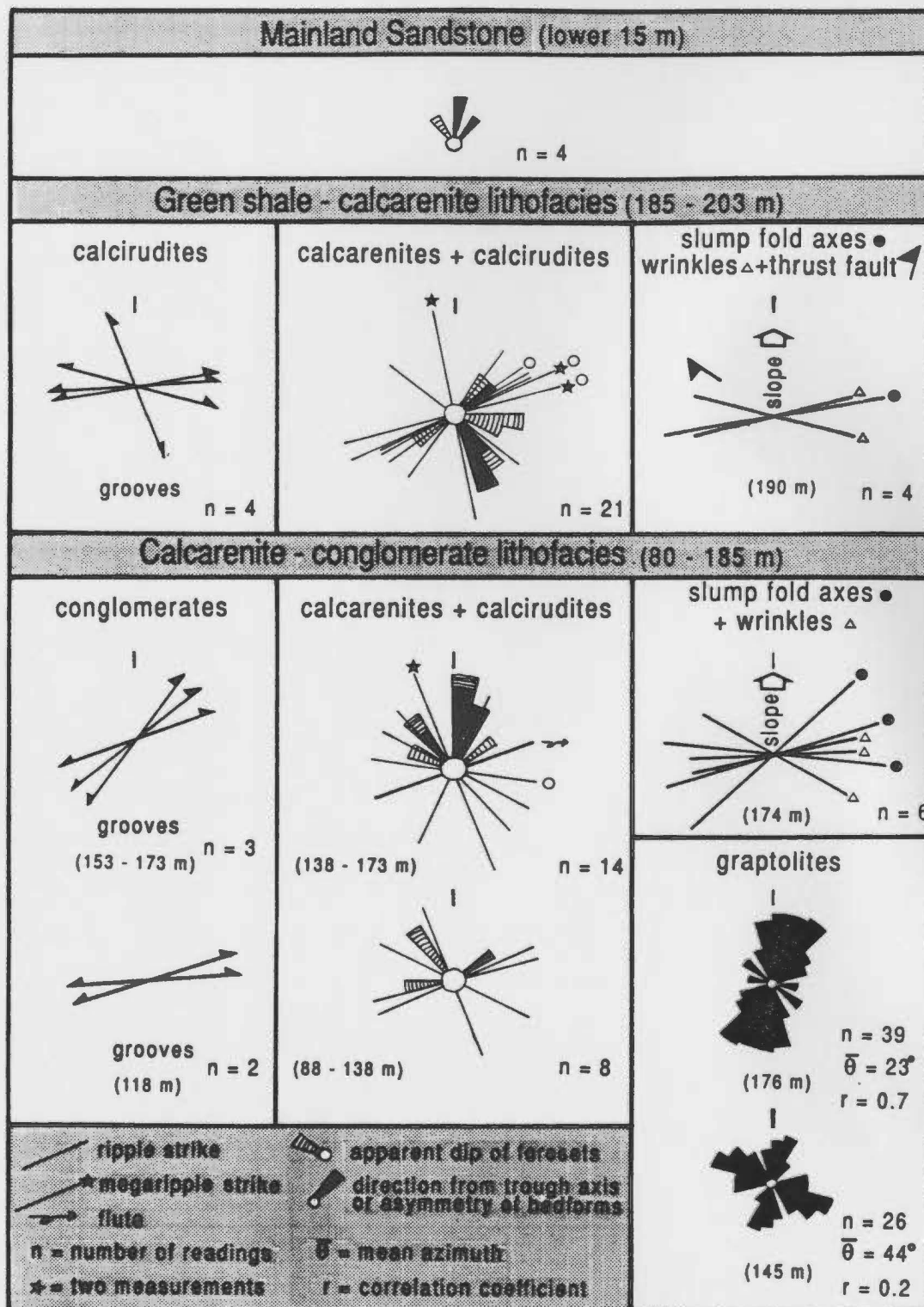


Figure 6.18 Paleocurrent and paleoslope data from the Cape Cormorant Fm. and the Mainland Sandstone at Caribou Brook. Data have been rotated once with respect to bedding. A second rotation about the gently plunging axis of the large-scale syncline of which the outcrop is a part (Figure 6.2) would change the values shown by only $\sim 10-15^\circ$ (counter clockwise).

The thinning directions are inferred to define lateral flow margins, implying (ambiguous) southwest/northeast transport, consistent with the orientation of the slope inferred for Big Cove.

None of the data come from ribbon limestone components; rare ripple cross-lamination was typically convoluted. Relatively few but thick beds of platform-derived sediments in Big Cove (B) (Figure 6.1.c), and thinner, but more numerous beds at Caribou Brook (Figure 6.1.a) may represent a southwest to northeast, proximal to distal trend away from an up slope, relict platform. However, since ribbon limestone constitutes the sole deep-water, carbonate lithofacies (Table Cove Formation, Chapter 5) east of the Cape Cormorant basin, it is possible that these sediments came from several relict platforms so the significance of the directional change in bed thickness and number is suspect.

6.8.2 Calcarenite-Conglomerate Lithofacies

Paleoslope and paleocurrent data from these strata at Caribou Brook indicate two transport directions: north and (ambiguous) east-northeast/west-southwest (Figure 6.18). Fold axes, mulliens and soft-sediment wrinkles define an east-west trending, north-dipping paleoslope. That configuration is supported by most paleocurrent data from calcarenites which, though widely-dispersed, overall indicate transport to the north, as does a single, northwest-striking, megaripple train inferred to record flow to the northeast. Oriented graptolites show two, ambiguous orientations (north-northeast/south-southwest and southeast/northwest) at one horizon, but strongly define ambiguous, north-northeast/south-southwest flow at another (see also Figure 6.8). The latter agrees with current data from the calcarenites and is interpreted to reflect north-flowing currents.

In contrast, grooves at the bases of debris flow conglomerates indicate ambiguous east/west or northeast/southwest flow. In light of the slope direction inferred for the underlying and coeval megaconglomerate-ribbon limestone lithofacies, they are interpreted to indicate

transport toward the east.

6.8.3 Green Shale-Calcarenite Lithofacies

Paleocurrent data from these strata at Caribou Brook are markedly different from those in the underlying lithofacies (Figure 6.18). Strikes of small ripples range from southeast- to east-northeast and trough axes and dip directions of foreset laminae indicate transport to the east or southeast. Strikes of megaripples atop calcirudites are divided among two populations, one oriented nearly north-south (a single data) deposited from east-flowing currents and a second, nearly east-west trending set deposited from currents flowing to the south-southeast. A groove at the base of one of these, though ambiguous, is inferred to indicate transport to the southeast. Structures indicating flow to the east occur at the base of the lithofacies, while those indicating flow to the southeast occur at the top (see Figure 6.1.a).

Measurements of fold axes, wrinkles, and imbricated bedding come from a single gravitational slide at 188 m (Figure 6.1.a) and indicate a nearly east-west striking, north-northwest dipping paleoslope - the same as that inferred for the underlying lithofacies. The slide approximately marks the stratigraphic interface between sequences with calciturbidites transported to the east and those with calciturbidites transported to the southeast. In light of similar bimodal transport directions in the underlying lithofacies, east-flowing currents and a north-dipping slope are still considered compatible, while deposition from southeast flowing currents implies a nearly 180 degree reversal of the slope of the basin.

6.9 Basin Configuration and Development

Integration of information on stratigraphic relationships, the lateral and vertical distribution of lithofacies (and changes in sediment composition), and paleocurrent and paleoslope data permit

reconstruction of the Cape Cormorant basin and interpretation of its history.

6.9.1 Location, Orientation and Morphology of the Faulted Margin

The lateral distribution of Cape Cormorant Formation lithofacies (Table 6.3) give some indication of the location of the fault scarp source of carbonate lithoclastic and, therefore, the location and trend of one basin margin. Extraordinarily thick and coarse-grained sequences of the megaconglomerate-ribbon limestone lithofacies around Big Cove compared to that around Caribou Brook (Figure 6.1) suggest the escarpment was located south-southwest of Port au Port Peninsula. However, massive megaconglomerate at Round Head (Figure 6.2), hence the inferred presence of the megaconglomerate-ribbon limestone lithofacies north of Caribou Brook, more strongly suggests the basin margin fault trended north or north-northeast and was located west of the peninsula (Figure 6.19.a). That interpretation is supported by the fact that nowhere on the Port au Port Peninsula east of Cape Cormorant outcrops are Early Paleozoic carbonates missing from the autochthonous sequence. It is also supported by interpreted eastward transport directions of both debris flow conglomerates and some calcirudites.

Whether the fault scarp trended north or northeast it would have created between ~1.5 km and 3 km across-strike distance between the Big Cove and Caribou Brook areas, enough to account for marked thinning of proximal, sediment gravity flow deposits documented between the two areas (cf. Eberli, 1987). The structure, which extended a distance of at least 30 km, may have been linear, or it may have had an more irregular morphology due to offsets along cross-faults (Figure 6.19.a). The apparent absence of megaconglomerates from Cape Cormorant sequences between Caribou Brook and Round Head supports the latter configuration, suggesting that area lay basinward of a reentrant along the escarpment.

6.9.2 Basin Geometry and Dimensions

The outcrop distribution of the Cape Cormorant (Figures 6.2 and

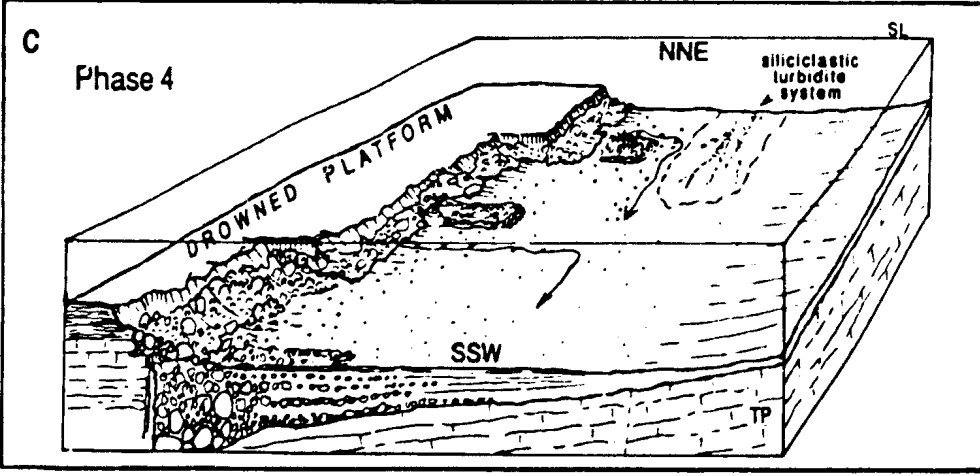
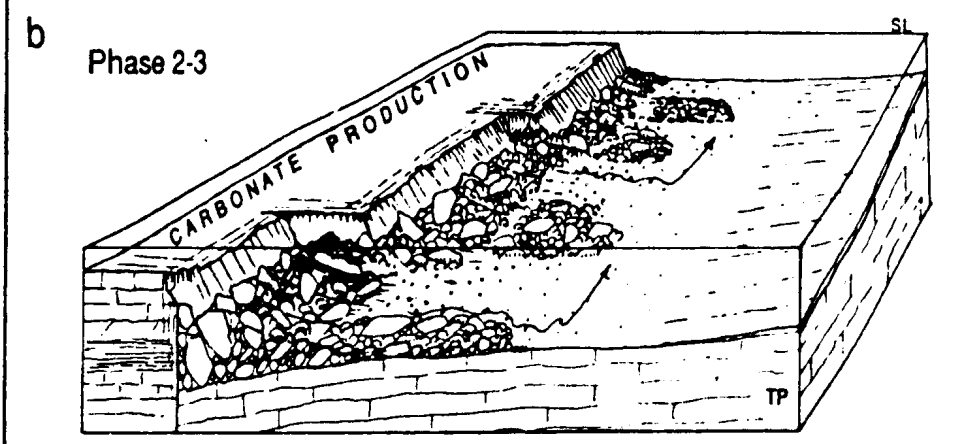
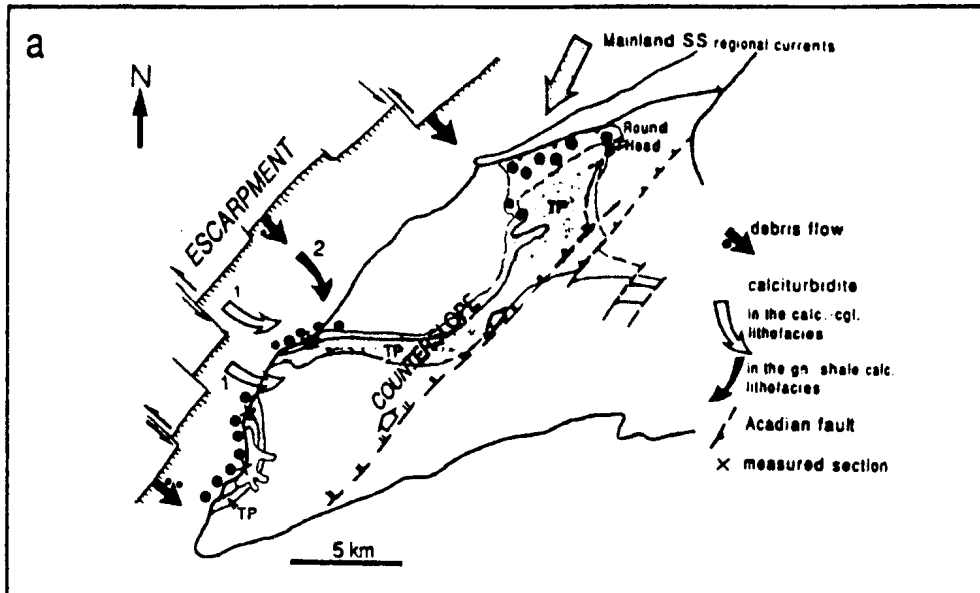
6.19.a) indicates the basin was at least 30 km long and at least 4-5 km wide. The faulted margin can only be placed at some uncertain distance west of present day outcrops, ie. out in the Gulf of St. Lawrence. Great thickness and enormous clast size in megaconglomerates around Big Cove suggest the fault may have been within a few kilometres of where the debris was deposited (eg. Eberli, 1987). However, debris flows with enormous clasts in other ancient sequences are proven to have travelled more than 10 km, and up to 50 or 75 km away from the source (Cook and Mullins, 1983), so proximity of the Cape Cormorant scarp cannot be certain. Moreover, in light of the interpretation of Stockmal and Waldron (1990) that the entire early Paleozoic, autochthonous succession on the peninsula has been transported at least 30 km from the southeast, the actual location of the scarp may have been located many kilometres to the east of present day outcrops. The location of the eastern basin margin, the nature of which is discussed below, is more precisely constrained by outcrop data; Cape Cormorant strata are not part of the autochthonous succession exposed inland more than ~5 km from the west coast.

6.9.3 Basin Evolution

(i) Phase 1 The initial phase of basin development involved catastrophic faulting and rapid subsidence and drowning of the shallow water platform, and formation of a deep basin bounded to the west by a high relief, submarine fault scarp. Synsedimentary deformation of the youngest platformal strata (Figure 6.1.a-c) suggest subsidence was accompanied by gravitational sliding. The west-dipping, rotated and imbricated limestone beds in Big Cove (A) indicate a northerly-striking, east-dipping slope for the nascent basin.

(ii) Phase 2 The second phase coincides with deposition of the megaconglomerate-ribbon limestone lithofacies in the Big Cove and Caribou Brook areas, as well as in the vicinity of Round Head. At least a few hundred metres of the Early Paleozoic carbonate sequence was

Figure 6.19 Paleogeographic reconstruction and evolution of the Cape Cormorant basin. a) Map showing the inferred location of the fault scarp and opposing counterslope, and transport directions of debris flows and turbidity currents during different stages of basin development. b) Schematic reconstruction of the basin with a north dipping axis during deposition of the megaconglomerate - ribbon limestone and calcarenite - conglomerate lithofacies c) Schematic reconstruction of the basin with a south dipping axis during deposition of the green shale - calcarenite lithofacies.



exhumed along the western fault scarp which was highly unstable and contributed an enormous volume of exceptionally coarse debris transported by debris flows several kilometres out into the basin (Figure 6.19.b). Straightforward stratigraphic unroofing of the exhumed platform sequence recorded in the sediment gravity flows implies that either an escarpment-bounded horst was narrow and completely destroyed by mass wasting as relative uplift continued, or mass wasting was confined to a narrow fracture zone parallel to the fault, inboard of which well lithified carbonates were resistant to gravitational collapse. The latter implies that the escarpment persisted with several hundred metres vertical relief from the top to the basin floor. It is the favoured reconstruction because of overwhelming evidence that bottom waters were stagnant, a condition that likely would have evolved and persisted in the presence of submarine topography that restricted circulation.

One or more relict, shallow water platforms flanked the basin during this time and carbonate mud and fine skeletal and peloidal sands accumulating on them were episodically transported into the deep water basin via turbidity currents and suspensions. One platform was probably atop the fault-bounded horst west of the basin (Figure 6.19.b), but it is possible that some of the sediment was supplied from relict platforms off to the east as well.

(iii) Phase 3 The third phase coincides with deposition of the calcarenite-conglomerate lithofacies at Caribou Brook while deposition of megaconglomerates and ribbon limestones continued around Big Cove. Uplift along the western fault reached its maximum by this time, exposing buried carbonates down to at least the lower Upper Cambrian and possibly the upper Middle Cambrian; total vertical displacement must have been at least 500 m. Regression of proximal, escarpment-derived sediment gravity flows back toward the margin and deposition of this distal assemblage at Caribou Brook, however, implies the escarpment had

reached a relatively stable configuration and mass wasting along it had diminished. Deprivation of the Caribou Brook area of coarse, resedimented debris could also in part reflect trapping of very coarse and voluminous debris flows in a structural depression adjacent to the escarpment. Greater stability of the fault suggests that movement on it slowed down and/or occurred less frequently. If differential movement was sufficiently reduced, the basin, rather than steadily deepening, may have begun to fill with sediments supplied to it from the escarpment, from the water column, and from adjacent relict platforms. Paucity and eventual disappearance of ribbon limestones from these deposits imply that those platforms were drowned as a result of continued subsidence.

Paleocurrent and paleoslope data from the calcarenite-conglomerate lithofacies (Caribou Brook) indicate that the Cape Cormorant basin was elongate, trending parallel to the western faulted margin, and its axis sloped toward the north (Figure 6.19.b). Voluminous debris flows travelled directly into the basin, perpendicular or at a very high angle to the trend of the escarpment. Turbidity currents, at least those transporting relatively fine sediment (current structures in calcirudites are largely absent), were deflected along the basin axis and flowed north, down-slope. Current deflection implies a west-dipping counterslope on the eastern margin of the basin. Reflection of east-flowing currents off the counterslope also explains the dispersion of transport directions recorded by the calciturbidites. Since no Cape Cormorant Formation deposits are found more than about 4.5 km east of the west coast of the peninsula, the counterslopes must have been immediately to the east. Whether it was simply defined by westerly tilt of the Cape Cormorant basin block (eg. Gibbs, 1984), or was generated by an independent submarine high off to the east is not known, but it served to positionally isolate this basin from the one created in the east Port au Port area.

(iv) **Phase 4** This phase coincides with deposition of the distal,

green shale-calcarenite lithofacies at Caribou Brook, strata which record two significant changes in sedimentation: 1) renewed influx of coarse lithoclastic debris from the western escarpment which temporarily reversed the thinning- and fining-upward trend defined by the two underlying lithofacies, and 2) introduction of chloritic, green shale and siliciclastic silt in the basin which signalled encroachment of a turbiditic, siliciclastic depositional system (Figure 6.19.c).

Paleocurrent and paleoslope data from these strata indicate that renewed influx of coarse lithoclastic sediments and the introduction of allochthonous siliciclastics into the basin were accompanied by significant changes in its configuration (Figure 6.19.c). Structures in calcarenites and calcirudites indicate a rather sudden change from north-flowing currents (in the underlying assemblage) to east-flowing, then to southeast-flowing currents. One hundred-eighty degree reversal in flow along the basin axis requires tilting to the south. North-northwest displacement in the slide mass only a few metres below calcirudites deposited from southeast-flowing currents indicates that the change was abrupt. Simultaneous influx in coarse lithoclastic debris suggests that tilting involved reactivation of a northern segment of the fault scarp. Structural adjustments that altered the slope of the basin also permitted the flow of siliciclastic-bearing, turbidity currents into the region.

(v) Phase 5 The final phase of basin development coincides with the onset of almost exclusively siliciclastic turbidite sedimentation - the Mainland Sandstone. Several thin to thick-bedded calcarenites and calcirudites interbedded with the sandstones both in the Caribou Brook section (Figure 6.1.a) and in Cointres Brook (Figure 6.2) suggest the fault scarp probably still had significant relief and was flanked by talus piles, but the infrequency of gravity flows that travelled into the basin indicate minimal mass wasting, probably a reflection of both the stable configuration of the scarp and infrequency of seismicity

which triggered it.

Current structures in sandstone beds in at least the lower 15 m of the Mainland at Caribou Brook indicate unidirectional flow toward the north (Figure 6.18). That direction is nearly opposite to both the flow direction of calcarenites in the underlying Cape Cormorant and to the transport direction for turbidites higher up in the formation (L. A. Quinn, 1990, pers. comm.; Williams, 1985; Figure 6.19.a). The north flowing currents indicate that either 1) siliciclastic sediment initially entered this sub-basin from the south, or 2) currents travelling south into the basin ricocheted off a counterslope, or some remaining submarine barrier, and were reflected back up slope (eg. Hiscott and Pickering, 1984). In light of the regional paleocurrent data for the Mainland Sandstone (Chapter section 8.3) the second hypothesis is favoured.

CHAPTER 7

SEDIMENTOLOGY OF THE BLACK COVE FORMATION (GOOSE TICKLE GROUP)

7.1 General Characteristics and Stratigraphic Relationships

The Black Cove Formation is a black, finely-laminated, graptolitic, noncalcareous shale with minor silt laminae (Figure 7.1). It is everywhere a distinctive unit at the base of the Goose Tickle Group except at two localities on the Port au Port Peninsula: 1) Piccadilly, where Table Cove Formation ribbon limestones are directly overlain by American Tickle Formation siliciclastics and 2) on the far west side of the peninsula, where the Cape Cormorant Formation is directly overlain by the Mainland Sandstone (Figure 1.2, locations). Regionally the Black Cove ranges from 1.5 m to 22 m thick. In many places it conformably and gradationally overlies upper Table Cove ribbon limestone (Chapter section 5.4; Figures 5.1 and 7.1.a), at one locally it directly overlies lower Table Cove strata (see Chapter section 5.2.1(iv)), and elsewhere it abruptly overlies massive, fossiliferous limestone of the Table Point Formation (Chapter 4; Figures 7.1.b and 7.2.a). The shale is everywhere gradationally overlain by interstratified shale, siltstone and sandstone of the American Tickle Formation (Chapter 8; Figures 5.1 and 7.1).

7.2 Composition

The shale is composed of illitic and chloritic terrigenous clays plus variable amounts of dolomite, siliciclastic silt, authigenic pyrite, and noncalcareous skeletal debris and unidentifiable organic matter (Table 7.1; Figure 7.2.c-f). Invariably high concentrations of unoxidized organic matter in the sediment are implied by its black colour (Potter *et al.*, 1980). Greatest compositional variation is in abundances of dolomite and siliciclastic silt; the former invariably decreases up section, while the latter increases up section. The dolomite is authigenic and is interpreted to have replaced and overgrown

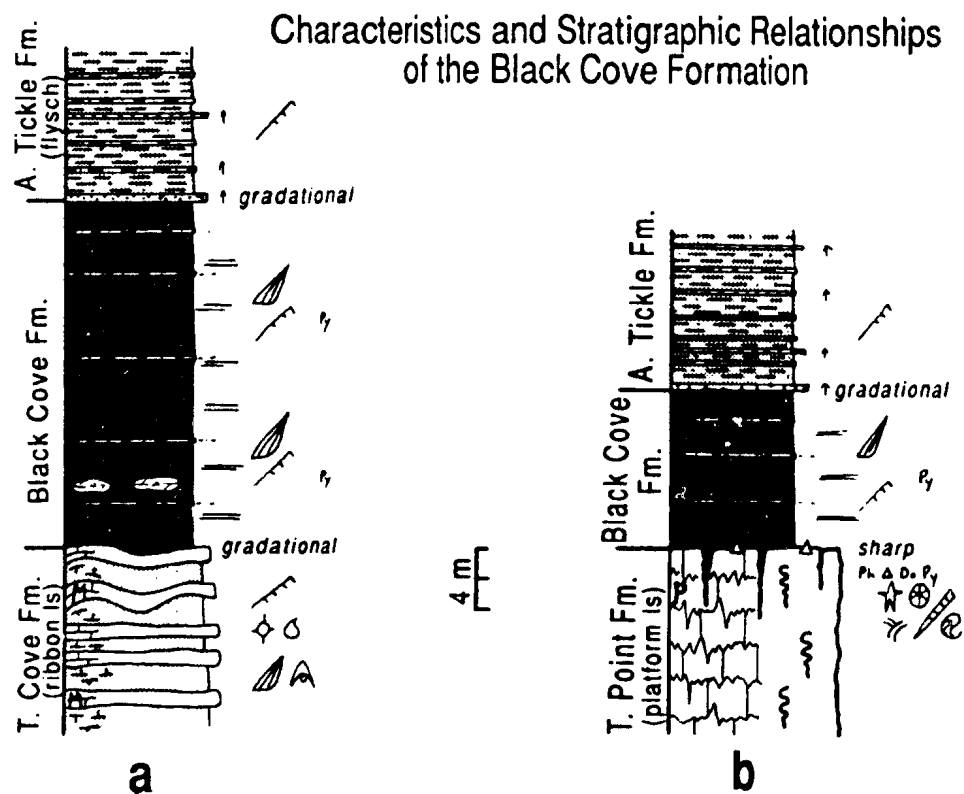


Figure 7.1 Representative, schematic sections of the Black Cove Formation. Stratigraphic relationships shown - a) overlying ribbon limestones (Spudgel's Cove) and b) overlying platformal limestones (west Pistolet Bay), are most common. Key to symbols is in Appendix A.

Figure 7.2 Black Cove Formation; field photos and photomicrographs. Bar scales on all photomicrographs are 0.5 mm. Prominent white lines crossing photomicrographs are epoxy-filled fractures in the thin section. a) Table Point - Black Cove contact on Bakeapple Island; beds dip moderately to the left. C. James (arrow) for scale. b) Laminated shale on Bakeapple Island. c) Finely-laminated shale in Beaver Brook. Light-weathering laminae have higher concentrations of dolomite. Pencil for scale. d) Photomicrograph of pelagic shale (type A) with flattened graptolites; Spudgel's Cove. e) Photomicrograph of silty pelagic shale (dark; type A) with interlaminated, silt-poor, chloritic shale turbidites (type C; arrows); top of the Black Cove on Bakeapple Island. Clay domains are sparse in the pelagic laminae, but discontinuous, single grain thick silt laminae (second arrow from bottom) define layering as do changes in organic matter content (darkness). f) Photomicrograph of alternating, streaky, pelagic laminae (h; type A) and massive, sparsely dolomitic (white grains) turbidites (not labeled; type B); Black Cove. Streaky foliation in the former is defined by discontinuous clay domains (light coloured). Arrow points to small, dolomite silt lense. (i) = inarticulate brachiopod. g) Photomicrograph showing graded, siliciclastic turbidite (light) - pelagic shale (dark, graptolitic) couplets (arrows); Spudgel's Cove. Lower couplet defined by siltstone turbidite (type E) that grades up into silty shale (type D) and pelagic shale (type A). Second couplet defined by silty shale turbidite (type D) gradationally overlain by pelagic shale (type A). Dark streaks are flattened graptolites.

Figure 7.2

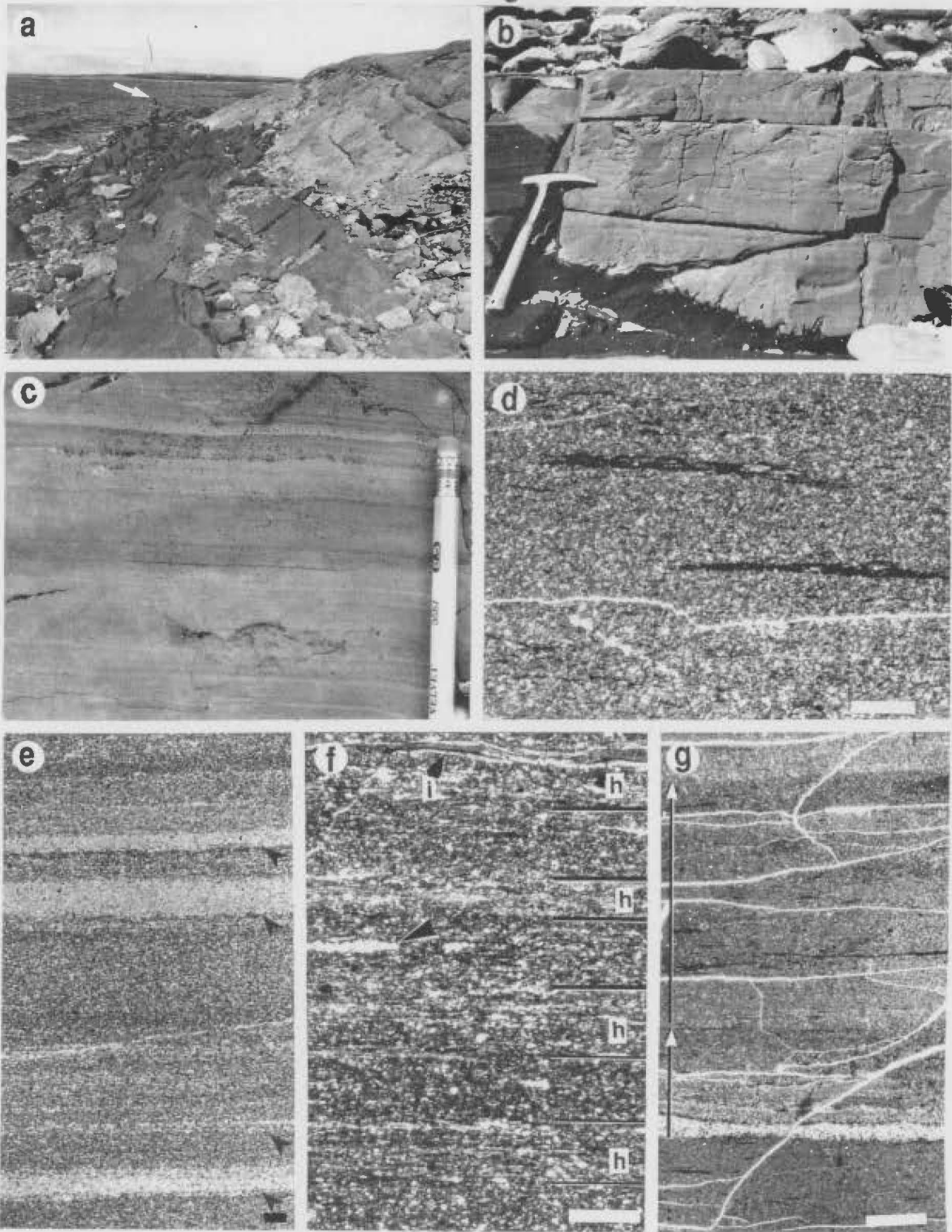


Table 7.1 Characteristics of the Black Cove Formation.

Part 1: Inorganic and Organic Components of the Shale.

T.Pt.Fm. = Table Point Fm.; T.C.Fm. = Table Cove Fm.

OG=overgrowths; inc.=increases; qtz.=quartz; feld.=feldspar; plagio.= plagioclase; micro.=microcline; musc.=muscovite; biot.=biotite; chlor.=chlorite; glau.=glaucinite; phosph.=phosphatic; skel. frag.=skeletal fragments; dia.=diametre; lg.=large; org.=organic; ppt.=precipitation; ppl.=plane polarized light

! - Most chlorite grains are compositionally similar to enclosing shale (ie.pale, iron-poor chlorite and illitic clay); they are commonly deformed by compaction and are thought to be minute shale rip-ups. Other grains are composed of dark green, strongly pleochroic, iron-rich chlorite with a fibrous (serpentine-like) crystal habit; some are polymineralic, occurring together with very small, clear, nonpleochroic and low birefringent, equidimensional to lath-shaped, silicate minerals of uncertain identity (?quartz, feldspar, clay mineral, zeolite). These grains are not bent or compacted and are believed to be mafic igneous or, possibly, sedimentary lithic fragments.

Part 2: Description and Interpretation of Depositional Layers.

Table details colour of the sediment in thin section under plane polarized light, thickness range of individual laminae, relative abundances of organic matter, dolomite and siliciclastic silt, and the nature of the lower and upper contacts of the laminae with enclosing sediments. T (turbidite) subdivisions correspond to those of Stow and Shanmugam (1980) in Figure 7.4.

**Table 7.1 Characteristics of the Black Cove Formation
Part 1: Inorganic and Organic Components of the Shale**

Terrigenous Clays	Dolomite	Siliciclastic Silt/Very Fine Sand	Pyrite	Organic Matter/ Fossils
illitic: clear or pale brown, pleochroic, low birefringent chloritic: clear or pale green, very low birefringent admixed with dark organic matter; mineral grains aligned with c-axis parallel to bedding	5-60% of the shale (generally more dolomitic where it directly overlies the T.Pt. Fm. than where it overlies the T.C. Fm.); invariably decreases in abundance up-section); 50-60 μ m, anhedral to euhedral, mostly nonferroan (commonly with ferroan OG); some with detrital cores; compaction deformation of organic stringers around crystals indicate some dolomite formed before significant burial	5-30% of the shale (inc. in abundance & changes from disseminated to concentrated in laminae upsection); mostly qtz. (~75-95%), plus feld. (plagio. >> micro. & untwinned), plus minor musc. (>) biot., chlor. or chlor.-bearing lithic frag., glauc. & phosph. skel. frag.; qtz., feld. & micas most abundant near base, chlor. grains increasingly abundant higher up-section	conspicuous throughout the shale; minute (<0.05 mm dia.) spheres (disseminated), oblate aggregates (0.04-0.25 mm dia.) of minute spheres & lg. cubes (to 2-3 mm across) (commonly concentrated in laminae); compaction deformation of org. stringers around aggregates indicates ppt. before deep burial; cubic crystals that cross-cut laminae or have qtz. beards in pressure shadows formed later	fragments and intact specimens of graptolites, phyllocarids (<i>Caryocaris</i>), small (5-7 mm) inarticulate brachiopods (<i>?Obolus</i> &/or <i>?Leptobolus</i>); pervasive particulate organic matter (orange-brown cast to sediment in ppl.), plus minute blebs and discontinuous organic stringers (probably compacted graptolites & phyllocarids & algal? debris)

Part 2: Description and Interpretation of Depositional Layers

Type	Colour	Thickness	Organic Matter	Dolomite	Silic. Silt	Lower Contact	Upper Contact	Internal Structure	Interpretation
A	dark orange brown	1-20 mm	very high	moderate to high	low	sharp or gradational	sharp	<ul style="list-style-type: none"> - organic-rich/organic-lean couplets, 0.5-1.0 mm thick - foliation defined by organic matter & lenticular clay domains (0.1-0.3 mm by 0.5-3 mm) - clays aligned parallel to bedding - discontinuous dolomite laminae (1-2 grains thick) 	<p style="text-align: center;">PELAGITE</p> <ul style="list-style-type: none"> - deposited by suspension settling - reworked by gentle bottom currents

Table 7.1 - Part 2 continued

Type	Colour	Thickness	Organic Matter	Dolomite	Silic. Silt	Lower Contact	Upper Contact	Internal Structure	Interpretation
B	dark orange brown	0.5-6 mm	low	moderate to high	low	sharp	gradational	<ul style="list-style-type: none"> - structureless or with discontinuous dolomite laminae at the base & within laminae - clays moderately well aligned parallel to bedding 	<p>CARBONATE-RICH TURBIDITE (T⁴ or T⁶)</p> <ul style="list-style-type: none"> - deposited from suspension from high density, low velocity flows
C	light green grey	0.1-25 mm	very low	absent to very low	absent to moderate	sharp or gradational (above E)	sharp or gradational	<ul style="list-style-type: none"> - structureless - clays poorly- to well-aligned parallel to bedding - scattered graptolites define foliation in thicker laminae 	<p>SILICICLASTIC TURBIDITE (T⁷)</p> <ul style="list-style-type: none"> - deposited from suspension from low density, low velocity flows
D	light green grey	0.1-1 mm	low	low	moderate to high	sharp	gradational	<ul style="list-style-type: none"> - structureless or with discontinuous silt laminae (1-2 grains thick) at the base and within laminae - vague coarse-tail grading 	<p>SILICICLASTIC TURBIDITE (T⁴ or T⁶)</p> <ul style="list-style-type: none"> - deposited from suspension from high density, low velocity flows
E	light green grey	1-3 mm	low	low	very high	sharp	sharp or gradational	<ul style="list-style-type: none"> - structureless or with parallel- to low-angle lamination - erosional or micro-loaded bases 	<p>SILICICLASTIC TURBIDITE (T⁸)</p> <ul style="list-style-type: none"> - deposited by traction at the base of turbidity flows

very small calcitic grains. Siliciclastic silt and very fine sand grains are compositionally similar to those comprising siltstone and sandstone beds in the overlying American Tickle (Chapter 8). Common skeletal components include graptolites, phyllocarids and small inarticulate brachiopods (Figure 7.2.d,f,g; see Whittington and Kiedle (1963) and Morris and Kay (1966) for faunal lists). They are generally sparsely distributed in the shale, but are also concentrated in specific laminae.

7.3 Depositional Layering

7.3.1 Description

The shale is invariably finely, parallel-laminated (Figure 7.2.b-g). In outcrop, laminations are defined by subtle colour changes that reflect differences in carbonate content, particularly dolomite, at the base of the sequence, and in siliciclastic silt content in the upper part. No other physical or biogenic structures are apparent. Five types of laminae are differentiated (Table 7.1). Their general distribution in Black Cove sequences is shown schematically in Figure 7.3; several are illustrated in Figure 7.2.

7.3.2 Interpretation

Differences in abundance of organic matter, dolomite, and siliciclastic silt indicate Black Cove shales were derived from three sources. Subtle differences in sedimentary structures and microfabric suggest more than one depositional mechanism was involved. Interpretations are based on comparison with fine-grained sediments on modern marine slopes and in basins, and with other ancient counterparts, interpreted to have been deposited by slow suspension settling and from dilute turbidity flows and weak bottom currents (O'Brien, 1970; Rupke, 1975; Piper, 1978; Stow, 1979; O'Brien *et al.*, 1980; Stow and Shanmugam, 1980; many authors in Stow and Piper, 1984).

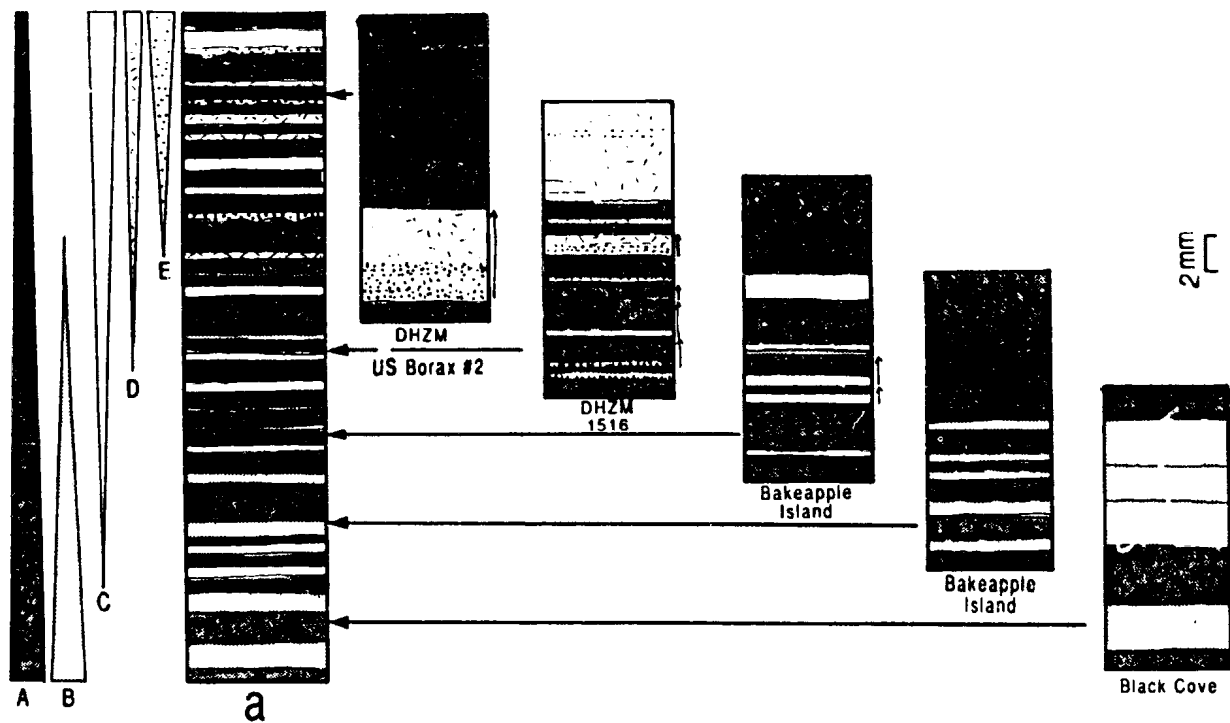


Figure 7.3 Stratigraphic distribution of hemipelagic and turbiditic muds in the Black Cove Formation. a) Schematic representative Black Cove sequence showing changes in composition up section. Letters A-E correspond to laminae types described in Table 7.1 and in the text. Width of bars to the left of the column denote relative abundance of the laminae. Columns 1-5 on the right come from thin-sections of Black Cove samples (in parentheses) that demonstrate variations in composition at different heights above the base of the formation.

(i) Hemipelagic muds Type A laminae, which are punctuated by all other laminae types (Figures 7.2.d-f and 7.3; Table 7.1), are interpreted as hemipelagites. Diffuse lower contacts and sharp upper contacts indicate continuous deposition periodically interrupted by other sedimentation events. Large numbers of pelagic graptolites and phyllocarids point to derivation of the sediment directly from the water column. Very thin, organic-lean:organic-rich couplets resemble varves and are thought to record periodic changes in primary planktonic productivity in surface waters (eg. Thornton, 1984). Small amounts of dolomite correspond to altered carbonate mud and silt grains derived from coeval, distant platforms or adjacent slopes and transported seaward in surface suspensions or nepheloid layers at intermediate depths (eg. Pierce, 1976). Siliciclastic silt is probably partly eolian dust and partly grains put into suspension by gravitational sliding and/or turbidity currents transporting coarser siliciclastic sediment in other areas of the basin. Preferential alignment of clays suggests that they accumulated by slow suspension settling (O'Brien *et al.*, 1980). Discontinuous dolomite and silt laminae suggest the sediments were episodically winnowed by gentle bottom currents.

The origin and significance of lenticular clay domains (Figure 7.2.e), which together with organic matter stringers define the streaky foliation in these laminae, are uncertain. Alternative explanations include: 1) expressions of a compacted bioturbate fabric (N. O'Brien, 1989, pers. comm.); 2) compacted faecal pellets; 3) compacted floccules; 4) miniature clay flasers deposited from low velocity bottom currents (N. O'Brien, 1989, pers. comm.). The pure clay composition of the domains argues against a biogenic origin, either as burrows or faecal pellets. Interpretation of the domains as clay flocs is reasonable given the importance of flocculation in transport and deposition of fine-grained sediment (Potter *et al.*, 1980, references cited therein). The large size of the domains, however, argues against this origin, for

although floccules as large as 1 mm in diameter have been described from Tertiary sediments (Pryor and Van Wie, 1971), those generated experimentally and documented in nature are generally much smaller (Kranck, 1975; Gorsline *et al.*, 1984). The least controvertible interpretation is that the domains represent flasers. As such they demonstrate very small scale depositional relief on the muddy sea bottom and are indicative of the high frequency of very gentle, depositional bottom currents operating while pelagic sedimentation continued.

(ii) **Turbiditic muds** Other clay, dolomitic or silty clay, and silt laminae (Types B-E) (Figures 7.2.d-f and 7.3; Table 7.1) are interpreted as turbidity current deposits. Low abundances of organic matter and pelagic skeletons indicate the sediments were not derived directly from the water column. Sharp basal contacts, some with minor erosional relief, indicate rapid onset of deposition. Moderately to weakly developed clay micro-fabric implies rapid sedimentation rather than slow settling (O'Brien *et al.*, 1980). Laminae Types B-E compare well with subdivisions of the ideal silt and mud turbidite sequence proposed by Stow and Shanmugam (1980) (Figure 7.4) interpreted to be deposited primarily from suspension from a muddy turbidity flow.

Type B laminae are carbonate-enriched turbidites; the dolomite content reflects original mud and silt-size CaCO₃ components transported with the clay. Laminae Types C, D, and E are fine, siliciclastic turbidites that generally form discrete layers in the shale; the vertical sequence E-D is recognized locally. Their compositional similarities to turbiditic sandstones in the overlying American Tickle (Chapter 8) indicate that these deposits are fine-grained equivalents.

Reciprocal distribution of the carbonate turbidites and siliciclastic turbidites up through Black Formation sequences (Figure 7.3) indicates a temporal change in sediment provenance. Concomitant decrease in the pelagic sediment component up section indicates that this was accompanied by a change to turbidity current-dominated

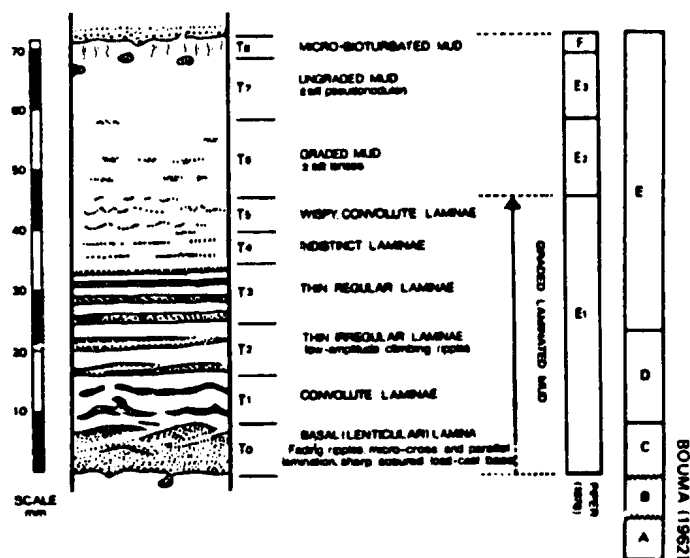


Figure 7.4 Idealized sequence of structures in a fine-grained turbidite (from Stow and Shanmugam, 1980); complete sequences are uncommon. Relationship to other turbidite sequence schemes is shown in the columns to the right.

sedimentation.

7.4 Other Sedimentary Structures

Black, cobble-size, disc-shaped concretions composed of dolomitic, microcrystalline quartz occur locally in discrete horizons (Figure 7.1). Concretionary limestone layers are also present in the shale, but are very uncommon. They range from 10-20 cm thick and are composed of coarse to very coarse, equidimensional to wormy pseudospar; cone-in-cone structure (Franks, 1969; Coniglio, 1985) is well-developed on the margins of some.

7.5 Reconstruction of the Depositional Environment

Black Cove shale is interpreted to have been deposited in a deep, quiet-water, sediment-starved, anoxic basin (Figure 7.5). Fine sediment size attests to low energy conditions; absence of wave-formed structures or evidence of continuous bottom currents implies deposition well below storm wave base. Absence of evidence of gravitational sliding points to a basinal rather than lower slope or basin margin setting. Predominance of pelagic graptolites and phyllocarids and absence of soft-bodied and shelly benthic organisms, except possibly inarticulate brachiopods, indicates bottom waters were normally toxic. Gradational stratigraphic relationships between the shale and underlying ribbon limestones (Table Cove Formation) and the presence of some carbonate concretions and beds in the shale indicate that the basins lay beyond the toes of carbonate slopes. Deposition of shale directly atop platformal limestone (Table Point Formation), however, indicates that starved, basinal conditions were also generated by very rapid deepening over the platform.

Pelagic sediments composed of terrigenous clays, fine carbonate, siliciclastic silt, and remains of pelagic organisms and organic matter originating in biologically productive surface waters, comprised the continuous background sedimentation (Figure 7.5). Varve-like,

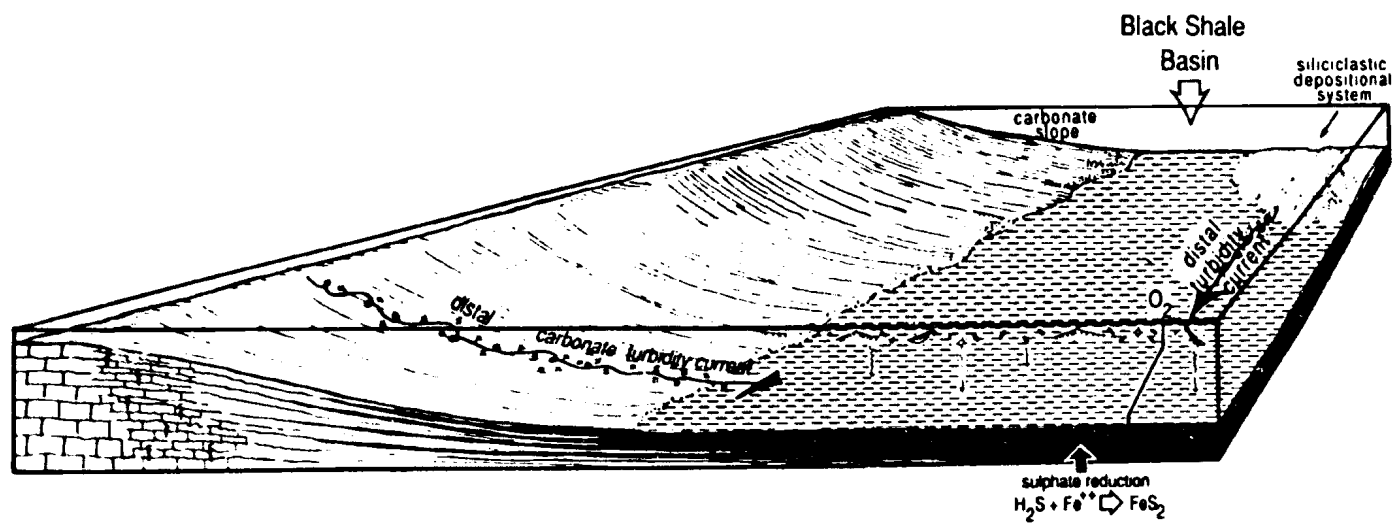


Figure 7.5 Reconstruction of the basinal environment envisaged for the Black Cove Formation.

organic-rich:organic-lean couplets suggest periodic, possibly seasonal, fluctuations in primary productivity. An apparent decrease in abundance of organic matter up section indicates that either biologic productivity gradually declined, basinal waters became increasingly well-oxygenated such that more organic material was oxidized as it settled through the water column, or, most likely, organic matter became diluted by ever increasing amounts of terrigenous sediment transported into the basin.

Very thin, fine-grained turbidites composed of clays and variable amounts of fine carbonate and siliciclastic silt and comparatively little organic debris, were episodically delivered by thin and weak, low density currents. With the exception of those depositing laminated, siliciclastic silt and very fine sand, flows were solely depositional, the prevailing mechanism being suspension settling. Mineral markers in these deposits, namely dolomite and siliciclastic silt, indicate they came from two different sources. During initial basin sedimentation hemipelagite accumulation was interrupted by deposition of turbiditic muds enriched in fine-grained carbonate. Those sediments came from coeval, albeit very distant, carbonate depositional environments, and were deposited by currents most likely generated by storms that entrained sediment on relict platforms or by mass movements on an adjacent carbonate slopes (Figure 7.5). Later, pelagic sedimentation was interrupted by deposition of fine, and increasingly coarse-grained, siliciclastic turbidites. Silt- and very fine sand-size mineral and lithic components of those layers link them to overlying, coarser-grained siliciclastics (American Tickle Formation; Chapter 8) which came from a complex terrane made up of plutonic, volcanic and sedimentary rocks. The fine-grained turbidites record deposition from the most distal flows of high velocity, high concentration turbidity currents that transported and deposited coarse-grained siliciclastics elsewhere in the basin, and herald the arrival of prograding, turbidity current-dominated depositional systems (Figure 7.5).

Absence of infaunal organism and preservation of very fine lamina-on indicates that bottom waters were strongly dysaerobic or anoxic (Byers, 1977; Savrda et al., 1984). Preservation of abundant organic matter in the sediment and early precipitation of pyrite are also indicative of such conditions. The former implies that neither basinal nor interstitial waters contained enough dissolved O₂ to permit complete oxidation of organics either during transport or after deposition. Pyrite precipitation, which requires H₂S, a by-product of bacterial sulphate reduction, also indicates strongly reducing conditions in the shallow subsurface (Fenchel and Riedl, 1970).

The only organisms which may have lived on the basin floor were tiny, inarticulate brachiopods. Although their presence in the black, graptolitic shale is not anomalous, their life mode is uncertain and they may have been epiplanktic (Reudemann, 1934; Watkins and Berry, 1977; Williams and Lockley, 1983), epibenthic (Sheehan, 1977), or benthic organisms (Cherns, 1979). Their small size, delicate shell, and mode of preservation are compatible with both a benthic existence on a soft substrate and with an epiplanktic mode of life. However, since all modern day inarticulate brachiopods are benthic (Boardman et al., 1987), some known to be tolerant of very low O₂ levels (Cloud, 1948), those in the Black Cove are thought to have been benthic as well and indicate that bottom waters were at least periodically dysaerobic rather than perpetually anoxic.

7.6 Relationship Between Anoxia and Starved Sedimentation

Coincidence of anoxic bottom water and starved sedimentation recorded by the Black Cove Formation suggests the two phenomena are interrelated. Paucity of carbonate, in particular, suggests deposition below the ACD (Aragonite Compensation Depth) and/or the CCD (Calcite Compensation Depth). Such an interpretation is ruled out for the following reasons. 1) Strongly dysaerobic to anoxic bottom waters are inferred for lower slope and basin margin environments in which

Table Cove Formation ribbon limestones were deposited (Chapter section 5.4); black shale is the major component of ribbon limestones at Piccadilly (Port au Port Peninsula) where the Black Cove Formation is not recognized as a discrete unit. 2) Black shale is a major component of deep-water flysch sequences of the Goose Tickle Group (Chapter 8), also indicating poor oxygenation of bottom waters. 3) Anoxic conditions are recorded in the deep-water Cape Cormorant Formation (Chapter 6); black shale is the distinctive background sediment of a ~20 m thick unit in the calcarenite - conglomerate lithofacies at Caribou Brook and constitutes a large proportion of the voluminous background sediment of the megaconglomerate - ribbon limestone lithofacies in Big Cove. 4) There is no evidence of partial seafloor dissolution of carbonate grains in any of the carbonate-bearing formations. 5) There are no conspicuous accumulations of siliceous fossils, specifically radiolarians, which might be expected in such deep-water environments.

These relationships suggest that black basinal shale was deposited above the CCD and probably above the ACD. Reasonable depths of these compensation depths in the Ordovician basin, previously estimated for the depth of the lower slope (Table Cove Formation, Chapter section 5.4.5), are 2500 m and 500 m, respectively.

The relationships also point to the existence of an Oxygen Minimum Zone (OMZ; <0.5 ml/l) at some critical depth in the water column which transected several depositional environments. Its presence is supported by a progressive decrease in abundance and diversity of benthic fauna between platform limestones (Table Point Formation, Chapter 4), upper to lower slope limestones (Table Cove Formation, Chapter 5), and basinal shale, which indicates a progressive decrease in the degree of oxygenation of bottom waters with increasing depth. Oxygen demand would have been determined by the amount of organic matter suspended in the water column, whereas oxygen supply would have been controlled by diffusion from well-aerated surface waters and/or by diffusion from or mixing with

an even deeper, well-oxygenated water layer (Richards, 1957). Therefore, the generation of strongly dysaerobic or anoxic bottom waters implies a large supply of organic matter and/or very limited vertical and lateral circulation.

The origin of the OMZ in the Middle Ordovician foreland basin and possible implications for basin configuration and bathymetry are addressed in Part II - Sedimentation and Tectonics, Chapter 14.

CHAPTER 8
SEDIMENTOLOGY OF THE AMERICAN TICKLE FORMATION
AND MAINLAND SANDSTONE
(GOOSE TICKLE GROUP)

8.1 General Characteristics and Stratigraphic Relationships

The American Tickle Formation and the Mainland Sandstone are thick sequences of dark greenish-grey, turbiditic sandstones and siltstones and shale (Figure 8.1). The two formations are differentiated primarily by texture and scale of bedding, but they also differ in several other important respects.

The American Tickle Formation is mostly very thin- to medium-bedded shale, silty shale and siltstone with minor thin to medium beds of very fine- to medium-grained, and rarely coarse-grained sandstone (Figure 8.1.a). These strata are widespread in the study area, nearly everywhere gradationally overlying black shale of the Black Cove Formation (Chapter 7; Figure 5.1.b). Sequences are punctuated at several different stratigraphic levels at many localities by thick to massive beds of grey limestone conglomerate and/or thin to very thick beds of quartz-bearing, limestone lithoclast calcarenite (Figure 8.1.a) which constitute the Daniel's Harbour Member of the formation (Chapter 9). In the Hare Bay and Pistolet Bay areas (Figure 1.2) there are also other carbonate lithoclast-bearing conglomerates and calcarenites near the top of the siliciclastic sequences, distinguished from Daniel's Harbour beds by abundant green and black shale clasts, and thought to have come from the Northwest Arm Formation of the Hare Bay Allochthon (Tuke, 1968; Stevens, 1970; Knight, 1986c; Quinn, 1988a). The total thickness of the American Tickle Formation is difficult to assess, largely because sequences are commonly severely deformed or poorly-exposed. Thicknesses of relatively intact sequences range from at least 80 m to 100 m in the Pistolet Bay and Hare Bay regions, respectively

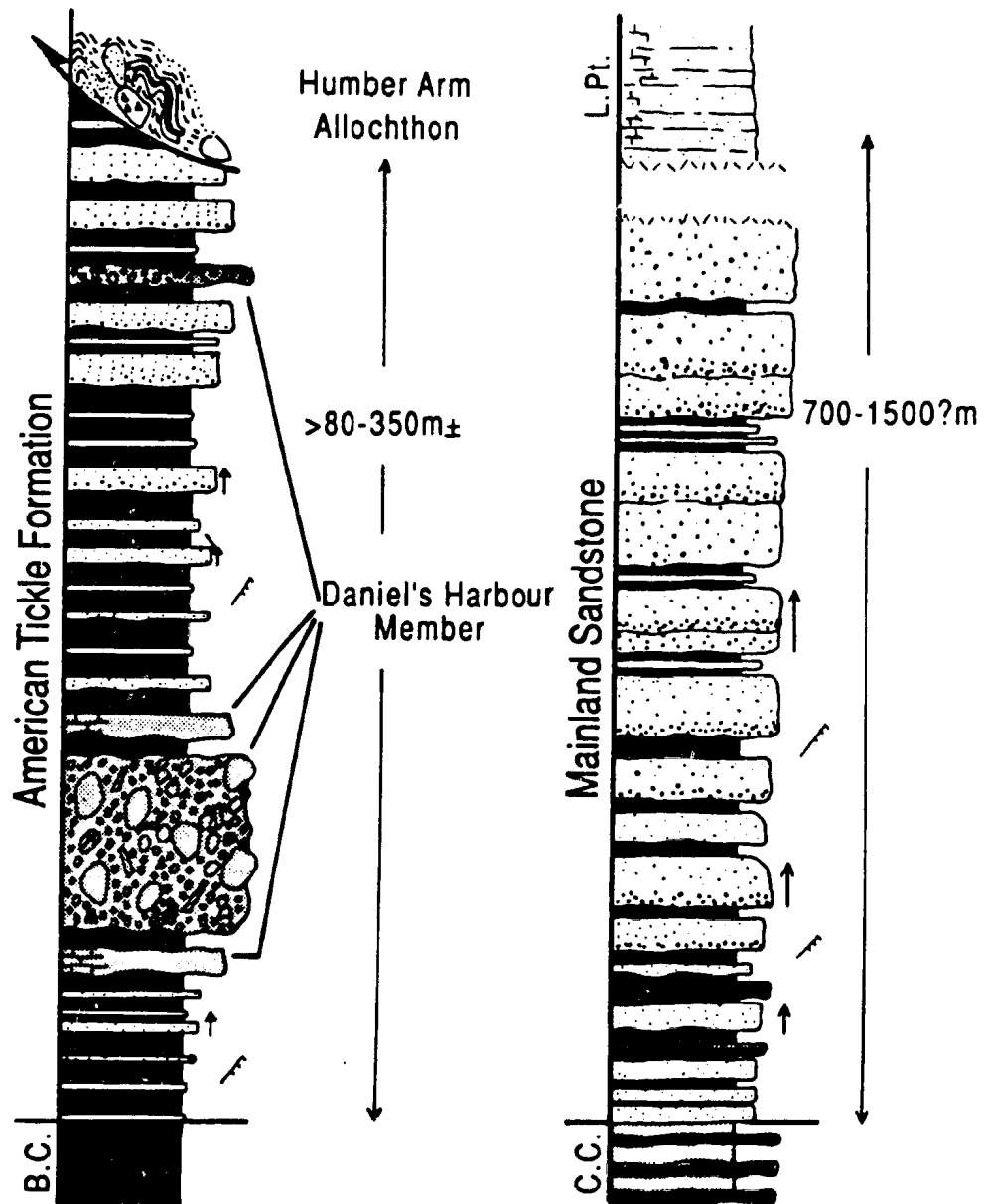


Figure 8.1 Schematic, composite sections of the American Tickle Formation and the Mainland Sandstone. B. C., Black Cove Fm.; C. C., Cape Cormorant Fm.; L. Pt., Long Point Gp. Key to other symbols is in Appendix A.

(Quinn, 1988a), to at least 250 m to 350 m (approximated) in West Brook and west of Shag Cliff in Bonne Bay (this study) (Figure 1.2). True thicknesses may indeed be highly variable due to relief on the structural contact with overlying *mélange* at the base of the allochthons.

In contrast, the Mainland Sandstone is composed mostly of medium to very thick beds of fine- to very coarse-grained sandstone and comparatively minor thin-bedded, very fine-grained sandstone, siltstone and shale (Figure 8.1.b). The formation is defined (Schillereff and Williams, 1979) and conventionally identified only on the west coast of the Port au Port Peninsula, but similar thick-bedded sandstones also comprise parts of siliciclastic sequences between Spudgel's Cove and Table Point on the Great Northern Peninsula (Figure 1.2). On Port au Port the Mainland overlies interstratified polymictic, carbonate lithoclast conglomerate and calcarenite, and shale of the Cape Cormorant Formation (Chapter 6; Figure 6.3.d). A few thin (<10 cm) and rare, thick-bedded (75-90 cm), polymictic calcarenites of Cape Cormorant Formation aspect occur near the base of the Mainland there. Daniel's Harbour Member conglomerates and calcarenites are not present. The Mainland Sandstone has a directly measurable thickness of 700 m (Quinn, 1988a), but may be as much as 1500 m thick (Stevens, 1970).

The American Tickle Formation and the Mainland Sandstone constitute the youngest strata in the Middle Ordovician foreland basin succession. American Tickle clastics are, in many places, structurally overlain by *mélange* at the base of the Humber Arm and Hare Bay Allochthons. The Mainland Sandstone on west Port au Port Peninsula, beyond the western extent of the Humber Arm Allochthon, grades up into limey sandstones and limestones that are lithologically similar and age equivalent (Stevens, 1970; Cawood *et al.*, 1988a, b) to strata at the base of the neoautochthonous Long Point Group (Rodgers, 1965; Bergström *et al.*, 1974).

A separate, detailed sedimentologic analysis of these strata, with

particular emphasis on sediment provenance, is currently under way by L. A. Quinn. The purpose of this chapter is establish the character of these strata and the general style(s) of sedimentation during this phase of foreland basin evolution.

8.2 Lithofacies

The two formations are comprised of four main lithofacies distinguished by their predominant lithologies. Diagnostic characteristics, distribution, and interpretation of each are summarized in Table 8.1; representative schematic sections are in Figure 8.2. The reader is referred to Figure 1.2 for locations of sections cited in the text.

8.2.1 Lithofacies 1 (Shale-Dominated) (Table 8.1)

Turbiditic sequences composed mostly of black, graptolitic shale with minor, thin siltstone and fine-grained sandstone turbidites (Figures 8.2.a and 8.3.a,b) are best developed at the base of the flysch, gradationally overlying Black Cove Formation shale. Siltstone and sandstone beds invariably increase in number and thickness up section. Shale-dominated strata are also minor components of other coarser-grained and thicker-bedded lithofacies (Table 8.1).

These sequences are mostly pelagic muds deposited slowly from suspension and/or by very dilute turbidity flows, and lesser silts and sands deposited by low concentration, silt-dominated and high concentration, higher velocity turbidity currents, respectively. Predominance of pelagic sediments and the overall thin-bedded nature of the turbidites, as well as the gradational relationship of these strata with underlying shale indicate that these are the most distal deposits of a turbidity current-dominated depositional system in a basinal setting. Based on relative abundances of silt and sand turbidites, sub-lithofacies 1a, 1b and 1c record deposition in increasingly proximal regions of the system.

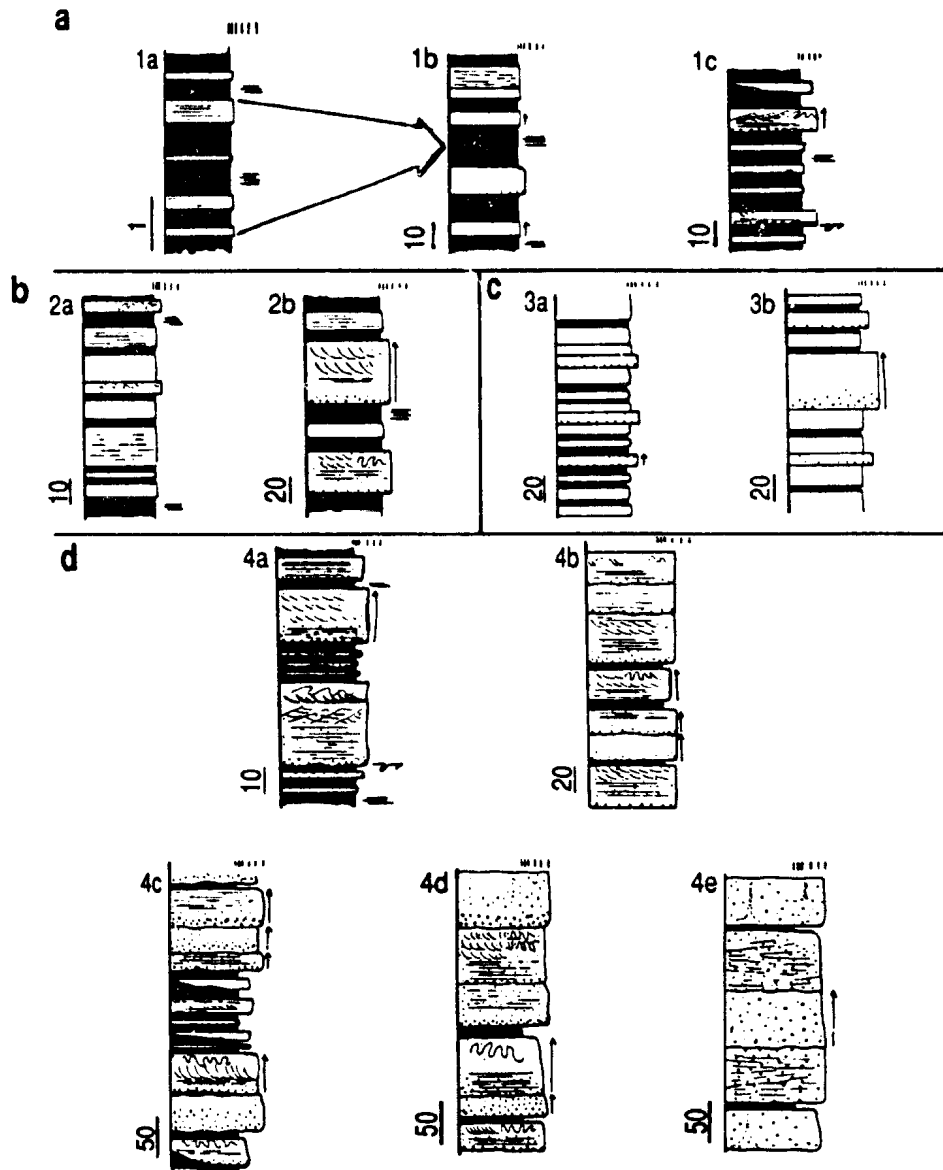


Figure 8.2 Schematic depictions of flysch lithofacies. a = shale-dominated. b = siltstone- and shale-dominated. c = siltstone-dominated. d = sandstone-dominated. Numbers correspond to those in Table 8.1. Scales are in centimetres. Key to symbols is in Appendix A.

Table 8.1 American Tickle Formation and Mainland Sandstone Lithofacies: lithologic components, sedimentary structures, location and stratigraphic position, and interpretation. Lithofacies are cross-referenced (in parentheses, eg. D2.2) with deep-water facies of Pickering *et al.*, (1986). In Components & Style of Bedding grain size refers to coarsest fraction at the base of the bed. Asterices are used to correlate between lithology in this column and Bed Thickness and Sedimentary Structures. Interpretation of depositional mechanisms and environment are based on Pickering *et al.* (1986) and on comparison with other similar, ancient siliciclastic turbidite sequences (eg. Rickard and Fisher, 1973; Morris, 1974; Poole, 1974; Walker and Keller, 1977; Shanmugam, 1980; Belt and Bussi eres, 1981; Shanmugam and Lash, 1982; Ricci Lucchi, 1985; Lash, 1988).

Idealized Bouma sequence: A - normal grading, B - parallel lamination, C - ripple cross-lamination, D - parallel lamination, E - laminated or burrowed, pelagic mud.

grad.=gradational, lam.=lamination, med.=medium, bdg.=bedding, GMNP=Gros Morne National Park

¹ - crude lamination interpreted to be generated by frictional freezing on traction carpets at the base of turbidity flows (Hiscott and Middleton, 1979, 1980).

Table 8.1 American Tickle Formation and Mainland Sandstone Lithofacies

Lithofacies 1 (Shale-Dominated)

Lithofacies	Components & Style of Bdg.	Bed Thickness	Sedimentary Structures	Occurrence In Study Area	Interpretation
1a	interlaminated or thinly-interbedded black shale* (E2.2) (50-70%) & argy green siltstone or shaley siltstone** (D1.1/D1.2) (30-70%)	*0.1-10 cm **0.1-2 cm	* parallel lamination ** sharp base & sharp or grad. top; structureless or fine parallel lamination; some convolute lam.	1a, 1b, & 1c occur at the base of the flysch between Table Point & Portland Creek Pond & locally in the Pistolet Bay area (west side & Burnt Island)	distal turbidites: mostly pelagic muds deposited by suspension settling &/or by dilute turbidity flows and lesser silts & sands deposited by low concentration & high velocity turbidity currents, respectively
1b	similar shale-silt couplets as 1a plus minor thin to medium beds of green siltstone to very fine-grained sandstone*** (D1.1)	***3-15 cm	*** sharp, planar upper & lower contacts; lack obvious internal structure	1a & 1c comprise all of the American Tickle Fm. between Parsons Pond & Baker's Brook in GSNP & at Black Cove	
1c	similar to 1b plus minor thin to medium beds of fine- to medium-grained (rarely coarse) sandstone* (C2.2/C2.3)	*1-20 cm, some to 50 cm thick	* planar or erosional bases; flutes; some pinch out laterally over a few tens of metres; normal grading; Bouma: B or C * thicker, fine-grained beds with Bouma: A, AB, ABC, AC, BC, B, & C; med. scale cross-bdg., climb. ripple cross-lam. &/or loaded ripples/convolute lam. common		

Table 8.1 continued

Lithofacies 2 (Siltstone- and Shale-Dominated)

Lithofacies	Components & Style of Bdg.	Bed Thickness	Sedimentary Structures	Occurrence In Study Area	Interpretation
2a	thin to medium beds of green-grey silty shale* (D1.2) with minor black shale** (E2.2) & thin beds of tan-weathering, fine-grained sandstone*** (C2.3); rare medium to thick beds**** (C2.2)	*5-15 cm	* sharp & planar contacts; structureless or vaguely laminated	2a at the base of the American Tickle Fm. on Bakeapple Island (Pistolet Bay) & all? of the American Tickle in Mare Bay	distal turbidites (more proximal than 1): mostly turbiditic muddy silts deposited rapidly from high concentration, silt- or mud-dominated flows & lesser pelagic sediment & classical sandy turbidites deposited from high concentration currents
		**0.5-5 cm	** parallel laminated		
		***1-5 cm	*** sharp & planar contacts; Bouma: B or D, C; convolute lam. & loaded ripples common	2b all of the American Tickle Fm. around Bonne Bay	
		****20-50 cm	**** thicker beds with vague normal grading and med. scale cross-bdg.		
2b	similar to 2 but thicker bedded; greenish-grey siltstone*, black shale**, orange-weathering, fine- to medium-grained sandstone***	*10-60 cm	* as above		
		**1-15 cm	** as above		
		***15-60 cm	*** normal grading; Bouma: B or D, C, AC, BC; medium-scale cross-bdg. in some of the thicker beds (commonly convoluted)		

Table 8.1 continued

Lithofacies 3 (Siltstone-Dominated)

Lithofacies	Components & Style of Bdg.	Bed Thickness	Sedimentary Structures	Occurrence In Study Area	Interpretation
3a	thin to medium beds of green-grey siltstone* (D1.1) interbedded with minor shaley strata (1a) and minor medium beds of fine- to medium-grained sandstone** (C2.2?)	*10-20 cm	* planar upper & lower contacts; lack distinct internal structure	3a & 3b occur in vertical succession above 1b in Southwest Feeder, together forming a single ~70 m thick thickening- and coarsening-upward sequence	intermediate to proximal turbidites: mostly turbiditic silts deposited rapidly from suspension from low concentration, silt-dominated flows & lesser sand deposited from comparatively large, high concentration currents
		**15-20 cm	** planar upper & lower contacts; normal grading; lack distinct internal structure		
3b	similar to 3a plus thick beds of medium- to very coarse-grained sandstone* (C2.2)	*60-80 cm	* normal grading; lack distinct internal structure		

Lithofacies 4 (Sandstone-Dominated)

4a	thin to thick beds of fine- to medium-grained sandstone* (C2.2/C2.3) and lesser (<50%) interbedded shale or thinly-interstratified shale, siltstone & very fine-grained sandstone**	*5-60 cm	* planar lower & upper contacts; flutes common; erosional channelling & lateral pinching out of beds uncommon; uncommonly amalgamated; Bouma: B, BC, C; climb. ripple cross-lam. & convolute lamination common	4a: base of the Mainland Sandstone at Mainland; occurs in a structurally isolated outcrop on the coast at WBC; base of the American Tickle Fm. at Springs Inlet	proximal turbidites: all sub-lithofacies composed mostly of turbiditic sands deposited from high velocity, high concentration currents; 4a - 4d are classical turbidites; absence of typical turbidite structures in 4e sandstones (except crude lamination) may indicate rapid deposition from a dense, cohesionless suspension or be the result of fluidization
		**5-150 cm			

Table 8.1, Lithofacies 4 (Sandstone-Dominated) continued

Lithofacies	Components & Style of Bdg.	Bed Thickness	Sedimentary Structures	Occurrence In Study Area	Interpretation
4b	mostly (80%) medium to thick beds of medium-grained sandstone & lesser fine- and coarse-grained sandstone* (C2.2) & minor thin black shale** interbeds	*30-100 cm **<10 cm	* planar lower & upper contacts; thickest beds commonly amalgamated; * medium-grained beds with Bouma: A, B, ABCD, BC, C, CD * thinner & finer-grained beds with Bouma: AC, CD; loaded ripples & convolute lamination common * thick, coarse beds with Bouma: AB or BC	4b gradationally overlies 4a at Springs Inlet, comprising a ~40 m thick, thickening- & coarsening-upward sequence	(previous page)
4c	medium to thick beds of fine- to very coarse-grained sandstone (C2.2/C2.1) & minor argillaceous interbeds** (ie. 1b & 1c)	*20-120 cm **5-200 cm	* thickest & coarsest beds with erosional or loaded bases; commonly amalgamated; normal grading; Bouma A, AB, AC; some rippled horizons convoluted * finer-grained & thinner beds with planar or erosional bases; some pinch out laterally over several tens of metres; normal grading; Bouma: A, ABC, AC, ABCD; division C commonly with medium-scale cross-bdg., climb. ripple cross-lam. &/or convolute lam.	4c & 4d in Table Point and Spudgel's Cove sections only; Table Cove: 4c overlies 1a, 1b & 1c at the base, comprising the top half of a 40 m thick coarsening-upward sequence; 4d overlies a second, 1c interval forming the top 17 m of a second, 37 m thick, thickening- & coarsening-upward sequence; Spudgel's Cove: 4c overlies 1a & 1c at the base, forming the upper 100 m of the sequence	
4d	thick to very thick, coarse-grained sandstone or granule-based beds* (C2.1) with minor argillaceous interbeds**	*70-200 cm **<15 cm	* commonly amalgamated; normal grading; Bouma: A, AB, AC; division C commonly convoluted		
4e	thick to very thick, medium- to coarse-grained sandstone* (B1.1 or B2.1) & minor argillaceous interbeds**	*50-200 cm	* planar or erosional bases; some pinch out laterally; thicker beds commonly amalgamated; crude, low-angle stratification in some beds; fluid escape structures in others	4e: top of the Mainland Sandstone at Mainland (Winn, 1988), overlying 4a & thereby defining a single >700 m thick thickening- & coarsening-upward sequence	

8.2.2 Lithofacies 2 (Siltstone- and Shale-Dominated) (Table 8.1)

Siliciclastic sequences composed primarily of thin to medium beds of silty shale and black shale with minor, thin or medium beds of fine-grained sandstone (Figures 8.2.b and 8.3.c) comprise the base of the American Tickle Formation locally in Pistolet Bay and characterize most of the formation in Hare Bay (Quinn, 1988a) and in Bonne Bay.

These strata are interpreted to be mostly turbiditic, silty muds deposited rapidly from high concentration, silt- or mud-dominated flows and lesser pelagic shale and classical, sandy turbidites deposited from high concentration currents. Predomination of fine-grained turbidites and the gradational relationship with underlying black basinal shale locally indicate these sediments also comprise a relatively distal, basinal assemblage. Comparatively low abundances of pelagic muds suggests the depositional setting lies in a more proximal position within the basin than that inferred for lithofacies 1 sequences. Greater bed thickness and coarser grain size in sub-lithofacies 2b turbidites suggest it is a more proximal assemblage than is sub-lithofacies 2a.

8.2.3 Lithofacies 3 (Siltstone-dominated) (Table 8.1)

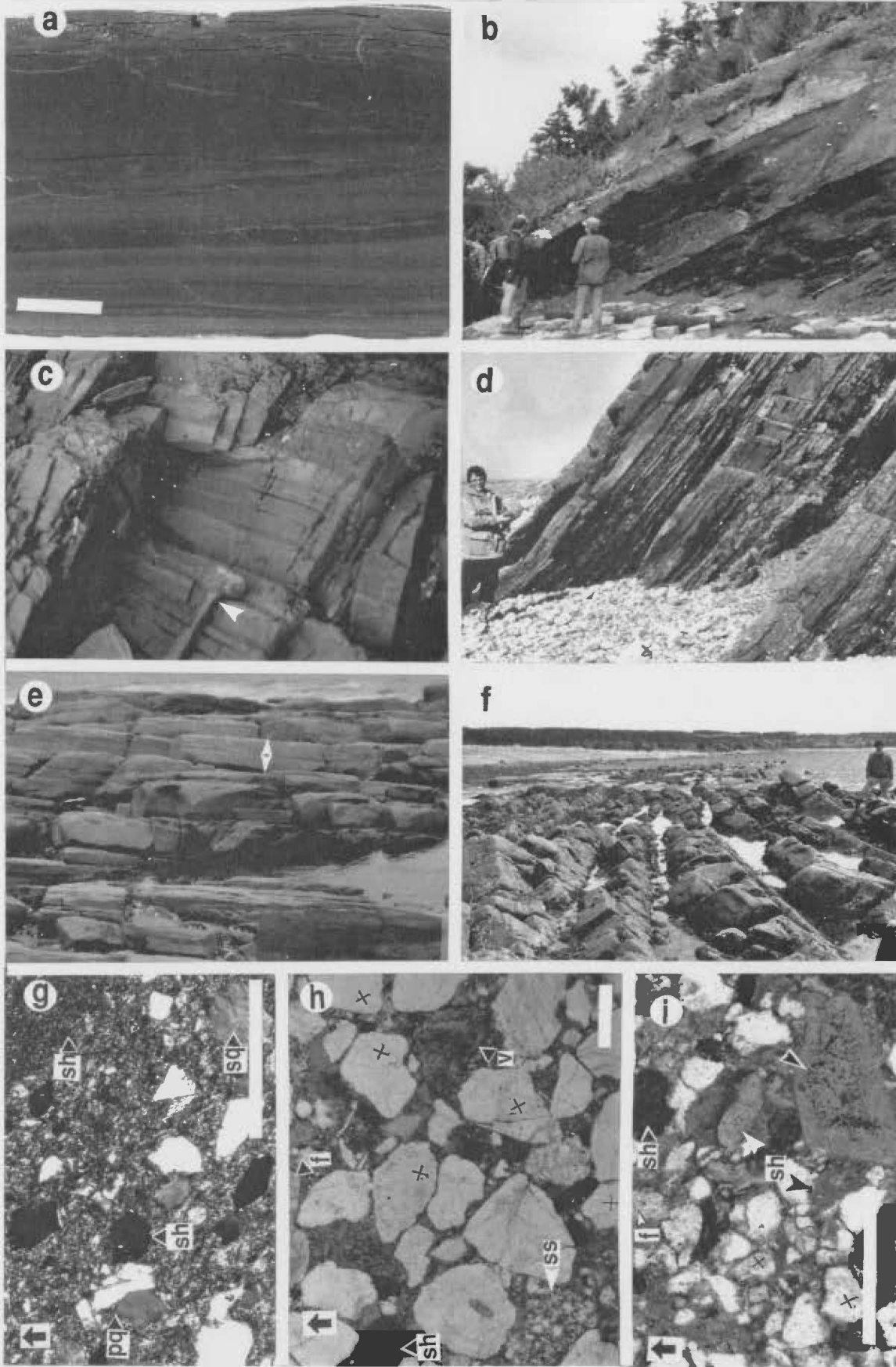
Strata composed mostly of thin to medium beds of structureless siltstone with minor shale and medium to thick beds of fine- to medium-grained (rarely coarse) sandstone (Figure 8.2.c) makes up most of the American Tickle in Southwest Feeder.

Sub-lithofacies 3a and 3b are interpreted to be mostly turbiditic silts deposited rapidly by suspension from low concentration, silt-dominated flows and lesser sand deposited by comparatively large, high concentration currents. Lack of typical turbidite structures other than grading in the sandstones may be a function of poor exposure (brook bed) rather than true absence. Paucity of pelagic shale identifies the depositional setting as higher energy, more persistently turbidity current-dominated than is inferred for lithofacies 2.

Figure 8.3 Siliciclastic flysch lithofacies; field photos and photomicrographs. Bar scales on all photomicrographs are 0.5 mm.

a) Polished slab of thinly-interbedded shale and siltstone turbidites, Lithofacies 1a (American Tickle Fm., 'banded argillite' facies of Quinn (1988a); Portland Creek Pond. b) Thick shale, minor siltstone and medium-scale, medium-grained turbidites, Lithofacies 1c (American Tickle Fm.); Black Cove. c) Thin, planar-bedded siltstone (light), shaley siltstone (medium) and shale (dark), Lithofacies 2a (American Tickle Fm., 'silty argillite facies' of Quinn (1988a); Northern Arm, Hare Bay. Hammer (arrow) for scale. d) Classical, thin and medium bedded, fine- to medium-grained turbidites, Lithofacies 4a (base of the Mainland Sandstone); Caribou Brook. e) Amalgamated, medium to thick beds of medium-grained turbidites, Lithofacies 4b (American Tickle Fm.); Spring Inlet, Hare Bay. Bed marked by arrows is about 60 cm thick. f) Amalgamated, very thick-bedded, very coarse-grained turbidites, Lithofacies 4d (top of the Mainland Sandstone (Quinn, 1988a); Table Cove. Up is to the right. g) Thin section photomicrograph of fine-grained, quartz-rich greywacke (crossed polars); American Tickle Fm., Pistolet Bay (west side). Most large grains are simple quartz; (sh) - shale lithic; (pq) - coarse polycrystalline quartz; (sq) - strained quartz; (f) - feldspar. h) Photomicrograph of coarse, quartz-rich; American Tickle Fm., Portland Creek Pond. Matrix has been replaced by coarse calcite (grey, interclast material); (ss) - siltstone fragment; (sh) - phosphatic shale fragment; (v) - volcanic lithic (aphanitic, plagioclase lathes); (x) - coarse, polycrystalline quartz. Other clear grains are simple quartz. i) Photomicrograph of medium-grained, quartz-rich greywacke; Mainland Sandstone, Spudgel's Cove. Majority of dusty grains (x) are feldspar (f). (sh) - shale lithic fragments. Arrow points to iron-rich, fibrous chlorite and pyrite grain, believed to be an altered mafic volcanic fragment.

Figure 8.3



8.2.4 Lithofacies 4 (Sandstone-dominated) (Table 8.1)

Siliciclastic sequences dominated by thin to very thick beds of sandstone (Figure 8.2.d) occur locally at the base of the flysch (eg. 4a, Table 8.1; Figure 8.3.d), but more commonly gradationally overlie finer-grained turbidite lithofacies and/or comprise the stratigraphically highest flysch. Sub-lithofacies 4a (Figure 8.3.d), 4b (Figure 8.3.e), 4c, 4d (Figure 8.3.f), and 4e (Quinn, 1988a, Figure 4), in that order, are differentiated by increasing sandstone bed thickness and grain size, increasing commonness of amalgamated beds, and decreasing abundance of interbedded fine-grained sediments.

These lithofacies are composed predominantly of turbiditic sands deposited rapidly from high velocity, high concentration currents. Predomination of sandstone beds suggests they all record deposition in positions within depositional systems more proximal than those indicated for the other lithofacies. Sub-lithofacies 4a, 4b, 4c and 4d are classical turbidite sequences with sandstones bearing sedimentary structures that record deposition from a waning flow (Bouma, 1962). High percentages of amalgamated beds in 4b, 4c, and 4d point to a higher frequency of powerful depositional currents than in sub-lithofacies 4a and so are inferred to be of more proximal aspect. Increasing grain size and bed thickness in these lithofacies records an increasing energy gradient which may also define a distal to proximal trend. Massive, amalgamated sandstones of sub-lithofacies 4e which lack typical Bouma sequence structures are also interpreted to have been deposited from thick, high velocity, high concentration currents. Absence of sedimentary structures in some beds may indicate rapid sedimentation of a dense, cohesionless suspension or reflect post-depositional liquefaction.

8.2.5 Correspondence to Submarine Fan Facies

All American Tickle Formation and Mainland Sandstone lithofacies clearly record deposition in a turbidity current-dominated, depositional system. Each can be assigned in a general way to an environment

within a submarine fan complex (Figure 8.4). Parallel-bedded, unchannelized turbidites, which characterize the vast majority of these lithofacies (1, 2, 3, 4a), are considered diagnostic of sedimentation in smooth fan environments, either the outer parts of a suprafan lobe, the lower fan, or basin plain. Since turbidite thickness and grain size in those settings decrease out toward the basin (eg. Normark, 1978), lithofacies 4a, 3, 2, and 1, in that order, may be visualized as proximal to distal deposits from the outer fan to the basin floor. Actual gradational, spatial relationships between their respective depositional environments, however, cannot be established regionally and can only be inferred from lithofacies sequences within a single, vertical succession. Maximum grain size, for example, could be determined by the nature of the source rather than distance of transport (or flow velocity). As such, shale-poor, siltstone-dominated sub-lithofacies 3a and 3b, which occur in a sequence devoid of sandstone-dominated lithofacies, may actually record deposition in a more proximal position of a fan system than does sandstone-dominated lithofacies 4a above basinal shales in another sequence.

Thick- to very thick-bedded, amalgamated and/or channelized, coarse-grained sandstones, such as comprise sub-lithofacies 4d and 4e, are diagnostic of mid-fan channel deposits (Figure 8.4; Hiscott, 1980). Preservation of typical Bouma sequence structures in 4d sandstones and paucity of such structures in 4e sandstones may reflect more rapid emplacement and fluidization of the latter in a more proximal channel position (Walker, 1984).

Other medium- to thick-bedded sandstones which comprise sub-lithofacies 4b and 4c share characteristics with both unchannelized and channelized fan deposits (ie. planar contacts and channelling, amalgamated sandstones and classic turbidites), and so in the context of the submarine fan model are best assigned to either a distal mid-fan or proximal outer fan setting (Figure 8.4).

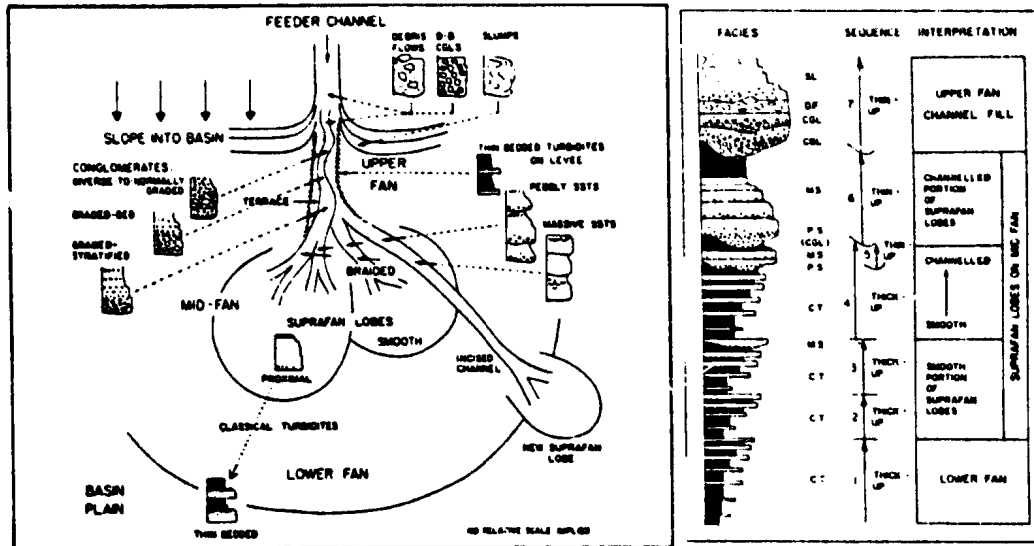


Figure 8.4 Submarine fan model (a) and generalized depositional sequence generated during fan progradation (b) (from Walker, 1978). In (b): CT=classical turbidites, MS=massive sandstones, PS=pebbly sandstone, CGL=conglomerate, DF=debris flow, SL=slump.

9.2.6 Vertical Sequences

American Tickle and Mainland Sandstone lithofacies are commonly arranged in coarsening- and thickening-upward packages (Table 8.1). They are recognized at the formation scale, ie. in sequences a few to several hundred metres thick which are thought to be the most complete. Similar trends are also recognized in the basal few to several tens of metres of siliciclastic sequences in most other localities, but whether they continued up through the entire section was not determined. In the Pistolet Bay region Cumming (1983) and Quinn (1988a) report coarsening-upward then fining-upward in the lower 100 m (by their descriptions) of the American Tickle Formation.

Smaller thickening- and coarsening-upward packages are recognized in the siliciclastic sequence at Table Cove (lithofacies 4c and 4d, Table 8.1) and are reported in the lower Mainland Sandstone (lithofacies 4a) at Mainland (Quinn, 1988a).

In the submarine fan model for turbidite sequences (Figure 8.4) coarsening- and thickening-upward packages are attributed to progradation of depositional lobes of a fan (Mutti and Ghibaudo, 1972 cited in Walker, 1984; Walker and Mutti, 1973). Those which are a few metres thick are thought to record progradation of the lobe fringe, while sequences a few tens of metres thick are thought to be generated by progradation of an entire lobe. These processes may be responsible for the small-scale, coarsening- and thickening-upward sequences in these Ordovician turbidite sequences. Coarsening- and thickening-upward sequences recorded over a few to several hundred metres of section, however, can not be attributed to these processes, and instead is inferred to record progradation of entire depositional system(s). Reversal of this trend in the Pistolet Bay area suggests progradation was followed by abandonment of the system.

8.2.7 Lateral Distribution

Across the study area there is a fairly consistent polarity to the

distribution of lithofacies comprising the siliciclastic sequences (Quinn, 1988a, b; this study). In general, sequences composed predominantly of shale, siltstone and fine-grained sandstone are best developed in the most eastern and northern parts of the study area. For example, lithofacies 1 comprises the entire flysch sequence in Black Cove and West Brook and lithofacies 2 comprises the entire siliciclastic sequence in Northern Arm. In contrast, flysch sequences dominated by sandstone are nearly restricted in outcrop to the most western localities, specifically on west Port au Port Peninsula (Mainland Sandstone, lithofacies 4a and 4e) and at Spudgel's Cove and Table Cove (lithofacies 4c and 4d). The only conspicuous exception to this trend is the sandstone-dominated American Tickle sequence at Big Spring Inlet (Hare Bay). Comparatively and consistently finer-grained siliciclastic sequences further east and south in Canada Bay, however, are reported by Cumming (1983).

8.3 Regional Paleocurrents

Current structures in the turbidite sequences regionally indicate flow generally to the south. Measurements from Port au Port Peninsula and in the Spudgel's Cove - Table Cove area on the Great Northern Peninsula indicate flow direction to the southwest (Quinn, 1988a). Those in the Hare Bay and Pistolet Bay areas of the Great Northern Peninsula indicate transport to the west and south (Williams and Smyth, 1983; Knight, 1986c). Few data collected in these areas during this study agree with these findings.

8.4 Sandstone Composition and Provenance

Sandstones in the two formations are compositionally and texturally immature, quartz-rich feldspathic and lithic greywackes (classification of Dott, 1964). They are poorly-sorted and are composed mostly of angular to subrounded grains enclosed in an argillaceous, illitic-

chloritic matrix (15-40%). Detrital components are itemized in Table 8.2 and representative thin sections are in Figure 8.3.g, h, and i. Very fine-grained sandstones and siltstones, in comparison, are mostly quartz and feldspar, the paucity of identifiable lithic fragments attributed to breakdown of such polymineralic grains by weathering and during transport.

Detrital components of the sandstones indicate a geologically complex source. Given the high abundance of sedimentary lithic fragments and conspicuous presence of volcanic lithics, and the presence of chromite in the heavy mineral assemblage, the writer agrees with Stevens' (1970) hypothesis that the sediment came from the Humber Arm and Hare Bay allochthons when they formed an advancing accretionary prism at the margin of the continent. That hypothesis is supported by (i) the ability to correlate many of the sedimentary and igneous lithic fragments with specific lithologic components of the allochthons (Stevens, 1970) and by (ii) trace element analyses of the sandstones which show high concentrations of chromium and nickel and underscore the contribution from ultramafic sources (Hiscott, 1984). However, relatively high abundances of quartz and feldspar in the sandstones raise the question of some other, or an additional sediment source (Quinn, 1988b). They could simply reflect the fact that easily disaggregated quartzose-feldspathic sandstones in the accretionary prism (eg. Summerside, Irishtown and Blow Me Down Brook formations in the Humber Arm Allochthon (Stevens, 1970; Williams and Godfrey, 1980; Williams *et al.*, 1982; Quinn and Williams, 1983; Williams and Cawood, 1986) and the Maiden Point Formation in the Hare Bay Allochthon (Williams and Smyth, 1983)) were major sediment contributors. Alternatively, they may indicate that an exposed granitic terrane, specifically Precambrian basement, supplied detritus to the basin (Quinn, 1988b). Resolution of this provenance question awaits completion of more detailed petrographic and geochemical analyses of the

Table 8.2 Detrital Components of American Tickle Formation and Mainland Sandstone Sandstones

Quartz	50-75%	1) monocrystalline 2) fine polycrystalline 3) coarse polycrystalline ¹ (some strained)
Feldspar	10-25%	1) albite 2) microcline 3) untwinned K-spar
Lithic Fragments	10-40%	1) sedimentary - quartzose siltstone; quartzose, fine- to medium-grained sandstone; shale/argillite (several types distinguished by colour); chert; microsparitic calcite (limestone); medium crystalline dolostone 2) igneous - altered intermediate and mafic volcanics: (i) - fine crystallite, fibre, and spherulitic fibre aggregates of iron-rich chlorite; (ii) - aphanitic aggregates of plagioclase lathes and/or chlorite and/or pyrite; (iii) - fibrous serpentine; siliceous plutonic fragments: (i) - phaneritic intergrowths of quartz, K-spar and biotite
Other Grains	few % maximum	minor muscovite, biotite, chlorite trace amounts of sphene, zircon, rutile, ilmenite, clinopyroxene, chromite

¹ - some polycrystalline grains may be siliceous plutonic lithic fragments.

Table 8.2 Detrital components of American Tickle Formation and Mainland Sandstone sandstones. General compositional and textural characteristics are based on field observations and petrographic examination of twenty-six thin-sections. Percentages of quartz, feldspar, and lithic fragments are visual estimates from ten thin sections of fine- to very coarse-grained sandstones and are in agreement with relative abundances given by Quinn (1988b). Numbers 1, 2, etc. denote order of abundance.

sandstones being conducted by L. A. Quinn.

8.5 Fossils and Biogenic Structures

Graptolites are the only common skeletal components. They occur mostly in shale, but broken fragments are also concentrated near the base of some turbidites.

There is very little evidence of burrowing. Pelagic black shale is invariably laminated and primary depositional structures are invariably preserved in the turbidites. Small (few mm diameter), poorly-preserved Planolites are present on the base of some sandstone beds.

8.6 Reconstruction of the Depositional Environment

Siliciclastic sediments comprising the American Tickle Formation and the Mainland Sandstone record rapid, but episodic deposition of compositionally and texturally immature sediment by turbidity currents in a deep-water basin. Primary depositional structures in the sandstone and siltstone beds are diagnostic of rapid deposition from a waning flow. A deep-water setting is inferred from the occurrence of these strata conformably above other deep-water strata, namely the Black Cove and Cape Cormorant formations, and is confirmed by absence of wave-generated structures and by the presence of a solely pelagic, graptolite fauna. Absence of benthic organisms, except for a sparse soft-bodied infauna, and preservation of primary sedimentary structures suggest the basinal waters were strongly dysaerobic or anoxic (Byers, 1977; Savrda *et al.*, 1984). Sandstone composition indicates derivation from geologically complex sources comprised of sedimentary, volcanic, plutonic, and possibly metamorphic elements.

Regional paleocurrents suggest the turbidites were deposited in an elongate, northeast-trending basin that dipped off to the south. The distribution of thick, coarse, channel-like sandstones suggests that the major depositional axis of the basin was situated on the western flank

of the outcrop belt. Coarsening and thickening of turbidites up through the siliciclastic sequences indicate that sedimentation was accompanied by progradation of the depositional system(s) into the basin.

8.7 Discussion

American Tickle Formation and Mainland Sandstone siliciclastics are similar to other ancient flysch sequences, particularly counterparts further south in the Appalachian orogen (eg. Rickard and Fisher, 1973; Morris, 1974; Hiscott, 1977; Walker and Keller, 1977; Shanmugam, 1980; Belt and Bussi eres, 1981; Shanmugam and Lash, 1982; Lash, 1988), as well as in other foreland basins (eg. Poole, 1974; Ghibaudo, 1980; Hoffman, 1987; Ricci Lucchi, 1985;). Moreover, the lithofacies which comprise them correspond closely to those which form the framework for the submarine fan model for deep-water turbidite sedimentation. Regional paleocurrents from the two formations, however, do not indicate a fan geometry for the entire basin, and detailed lithofacies and paleocurrent data necessary to establish their presence locally were not obtained in the course of this study.

A tilted, trough configuration for the basin is a reasonable reconstruction based on limited paleocurrent data. However, there is no obvious north to south, proximal-distal gradient indicated by grain size, bed thickness or depositional structures in the siliciclastic sequences to suggest sediment was supplied to the basin mostly or solely via its up-slope, northern end. Instead, some features of the siliciclastic sequences suggest that the sediment was introduced to the basin at several points: 1) distinctive outcrop expression of siliciclastic sequences different regions of the study area; 2) presence of proximal turbidite lithofacies at Big Spring Inlet (Hare Bay); 3) restriction of some lithofacies to limited areas, such as lithofacies 2a to the Pistolet Bay and Hare Bay areas and Lithofacies 2b to the Bonne Bay area. Furthermore, the regional west to east, proximal - distal

trend defined by the distribution of lithofacies is quite unlike what would be predicted given evidence that the source of the sediment was located off to the east.

All of these features have important implications for foreland basin configuration, sediment dispersal and depositional history. They are addressed in Part II - Sedimentation and Tectonics, Chapter 14.

CHAPTER 9**SEDIMENTOLOGY OF THE DANIEL'S HARBOUR MEMBER (GOOSE TICKLE GROUP)****9.1 General Characteristics and Stratigraphic Relationships**

The Daniel's Harbour Member of the Goose Tickle Group is thin to massive beds of limestone lithoclast conglomerate and thin to very thick beds of quartz-bearing, limestone lithoclast calcarenite which locally punctuate fine-grained, American Tickle Formation siliciclastics (Chapter 8) (Figure 9.1). Daniel's Harbour Member conglomerate also occurs locally as isolated lumps in mélangé at the base of the Humber Arm Allochthon. Neither lithology is recognized in the Mainland Sandstone.

Daniel's Harbour Member beds differ from Cape Cormorant Formation conglomerates and calcarenites (Chapter 6) in three respects. 1) They are not rhythmically-interstratified with shale, but sporadically punctuate turbiditic, siliciclastic sediments. 2) The conglomerates are, on average, very thick or massive and, rather than being conspicuously polymictic, are composed mostly of grey-brown limestone clasts. 3) The calcarenites are a mixture of carbonate lithoclast and siliciclastic grains, including sedimentary, igneous, and metamorphic lithic fragments.

9.2 Limestone Conglomerate**9.2.1 Description**

Two distinctive types of limestone conglomerate are present (Figure 9.2). **Clast-supported conglomerate** characteristically comprises light grey, massive-appearing beds which lack obvious primary sedimentary structures and internal organization (Figure 9.3.a,b). Of the two conglomerate lithologies it is most widespread, occurring in many American Tickle sequences between Port au Port Peninsula and Cape Norman at the tip of the Great Northern Peninsula (Figure 9.1, inset).

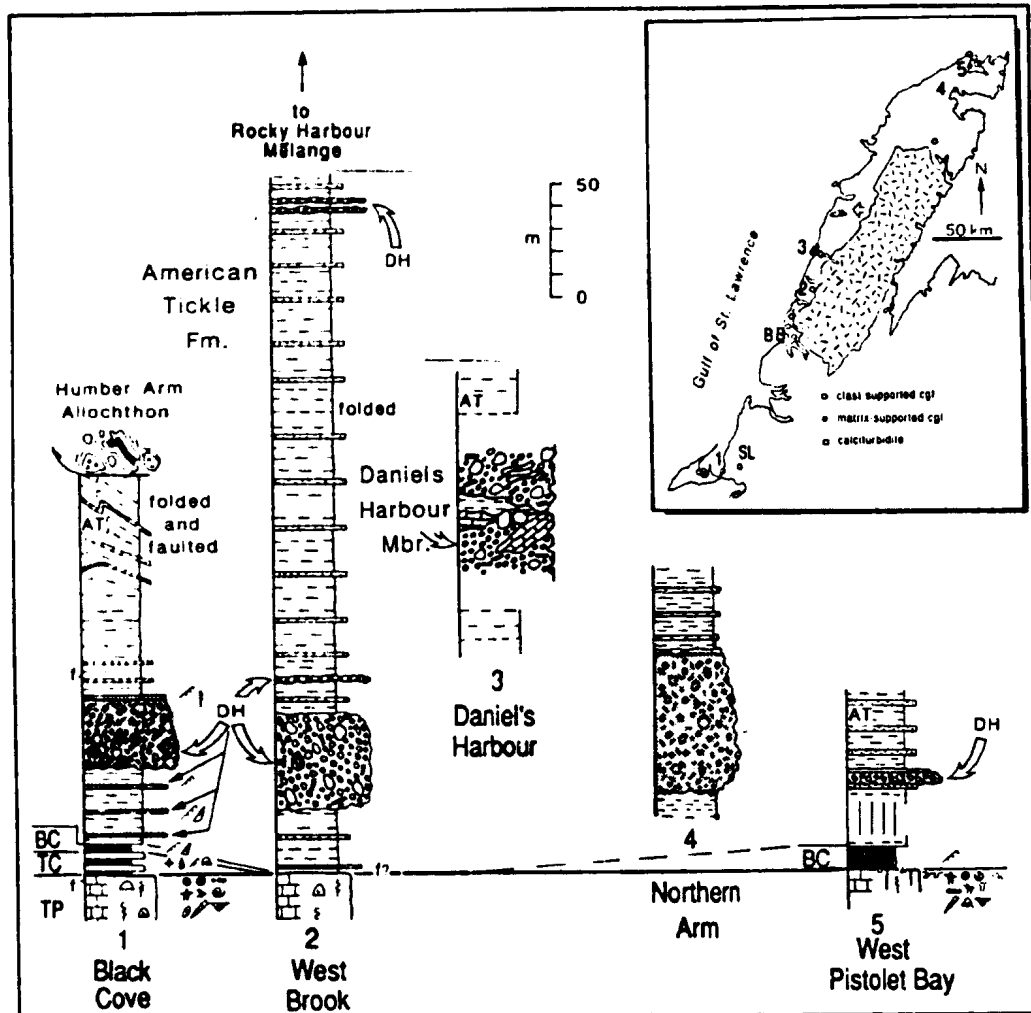
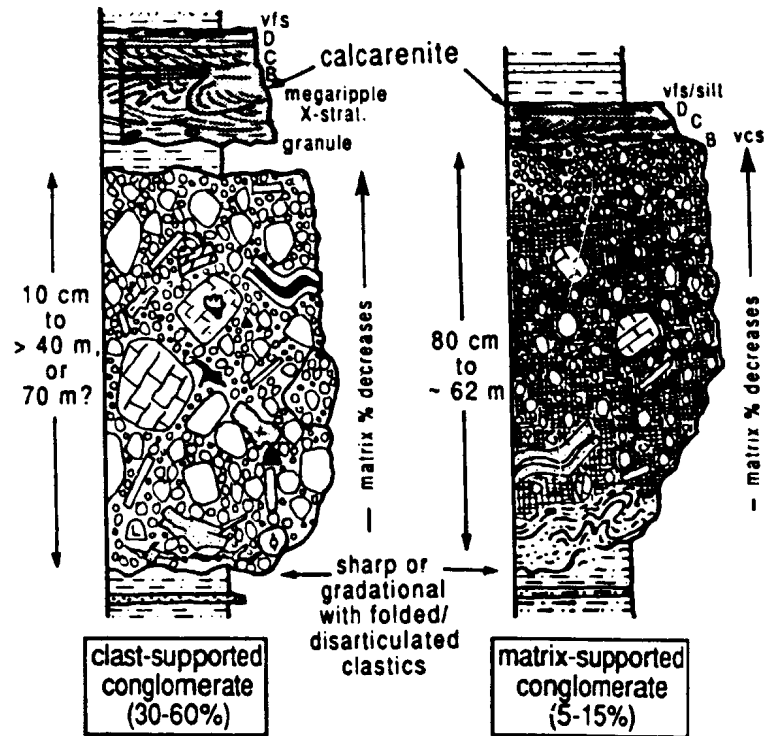


Figure 9.1 Measured sections of the American Tickle Fm. showing the stratigraphic distribution of Daniel's Harbour Member beds (shaded). TP, Table Point Fm.; TC, Table Cove Fm.; BC, Black Cove Fm.; AT, American Tickle Fm.; DH, Daniel's Harbour Member. Inset map shows the locations of all measured sections with conglomerates and/or calcarenites in the American Tickle. They are absent between Serpentine Lake (SL) and Bonne Bay (BB) (Williams and Godfrey, 1980; Williams *et al.*, 1982; Quinn and Williams, 1983; Williams and Cawood, 1986).

Daniel's Harbour Member Beds



- | | |
|---|--|
| <ul style="list-style-type: none"> - coarse-grained, poorly-sorted - maximum clast size ≈ 28 x 45 m - mostly disorganized, local normal + inverse grading - common M plates and conspicuous, exotic ribbon + parted limestone clasts, white fenestral limestone, <u>Stromatactis</u> limestone, sandstone, calcarenite and limestone conglomerate | <ul style="list-style-type: none"> - finer-grained, poorly-sorted - maximum clast size ≈ 2 x 6 m - normally-graded, bimodal limestone granules + black shale cobbles at the top - M plates + other exotic clasts very uncommon |
|---|--|

Figure 9.2 Schematic sections of clast-supported and matrix-supported conglomerates characteristic of Daniel's Harbour Member beds. Abbreviations are as follows: M, mudstone; vfs, very fine sand; vcs, very coarse sand; x-strat., cross-stratification. Arrows in calcarenites signify normal grading; B, C and D refer to Bouma sequence divisions.

Figure 9.3 Daniel's Harbour Member conglomerates; outcrop and slab photos and photomicrographs. a) Massive, clast-supported conglomerate at Black Cove (Figure 9.1.1). Up is to the left. Metre stick (arrow) for scale. Boulder debris in the foreground is weathered conglomerate. b) Pebbly clast-supported conglomerate with out-sized limestone boulders (arrows) at Daniel's Harbour (upper bed in Figures 9.1.3 and 9.4). Hammer for scale. c) Polished slab of clast-supported conglomerate from Eastern Head. Different colours of clasts demonstrate the polymictic nature of the conglomerate. Most grains in clasts are skeletal fragments. Interclast matrix is a mixture of carbonate and clays; clast contacts are marked by dark pressure dissolution seams or micro-stylolites (arrows). d) Ribbon limestone rafts in clast-supported conglomerate at Daniel's Harbour (upper bed in Figures 9.1.3 and 9.4). Hammer (arrow) for scale. e) Clast-supported conglomerate with fossiliferous wackestone megaclast (directly behind and left of measuring stick) and rounded coarse-grained sandstone boulder (sst); Eastern Head locality south of Clifty Point. Bedding is preserved in the limestone clast; its contact with enclosing conglomerate is gradational. Divisions on scale are 10 cm. f) Broken up and folded quartzose calcarenite clasts in clast-supported conglomerate at Black Cove. Metre stick for scale. g) Massive, pebbly, clast-supported conglomerate with outsized, quartzose sandstone boulder (arrow) and white fenestral limestone block (to the right); Eastern Head locality south of Clifty Point. Divisions on measuring stick are 10 cm. h) Polished slab of mottled Stromatactis mound limestone clast from the conglomerate at Piccadilly. Scale is in centimetres.

Figure 9.3

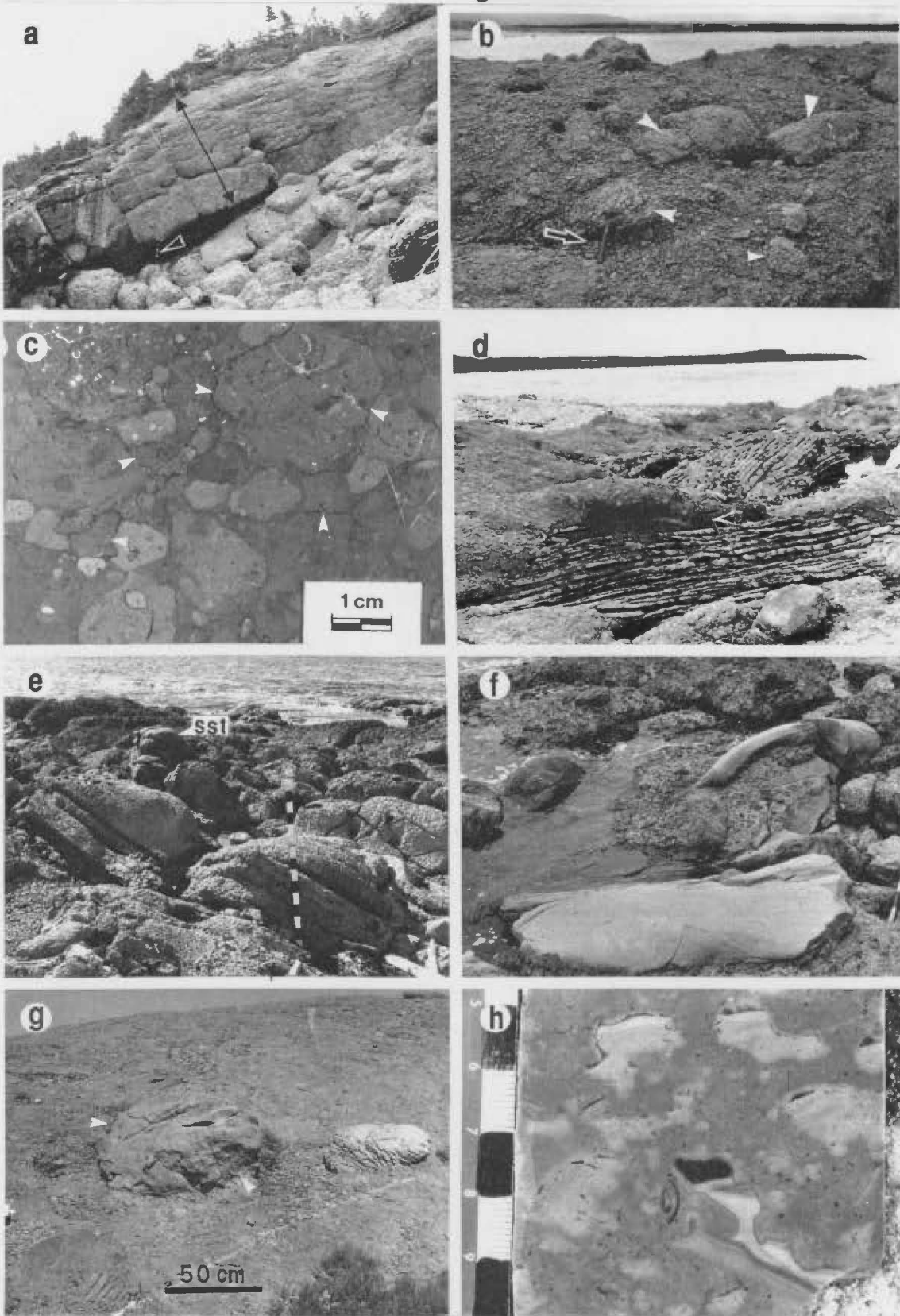
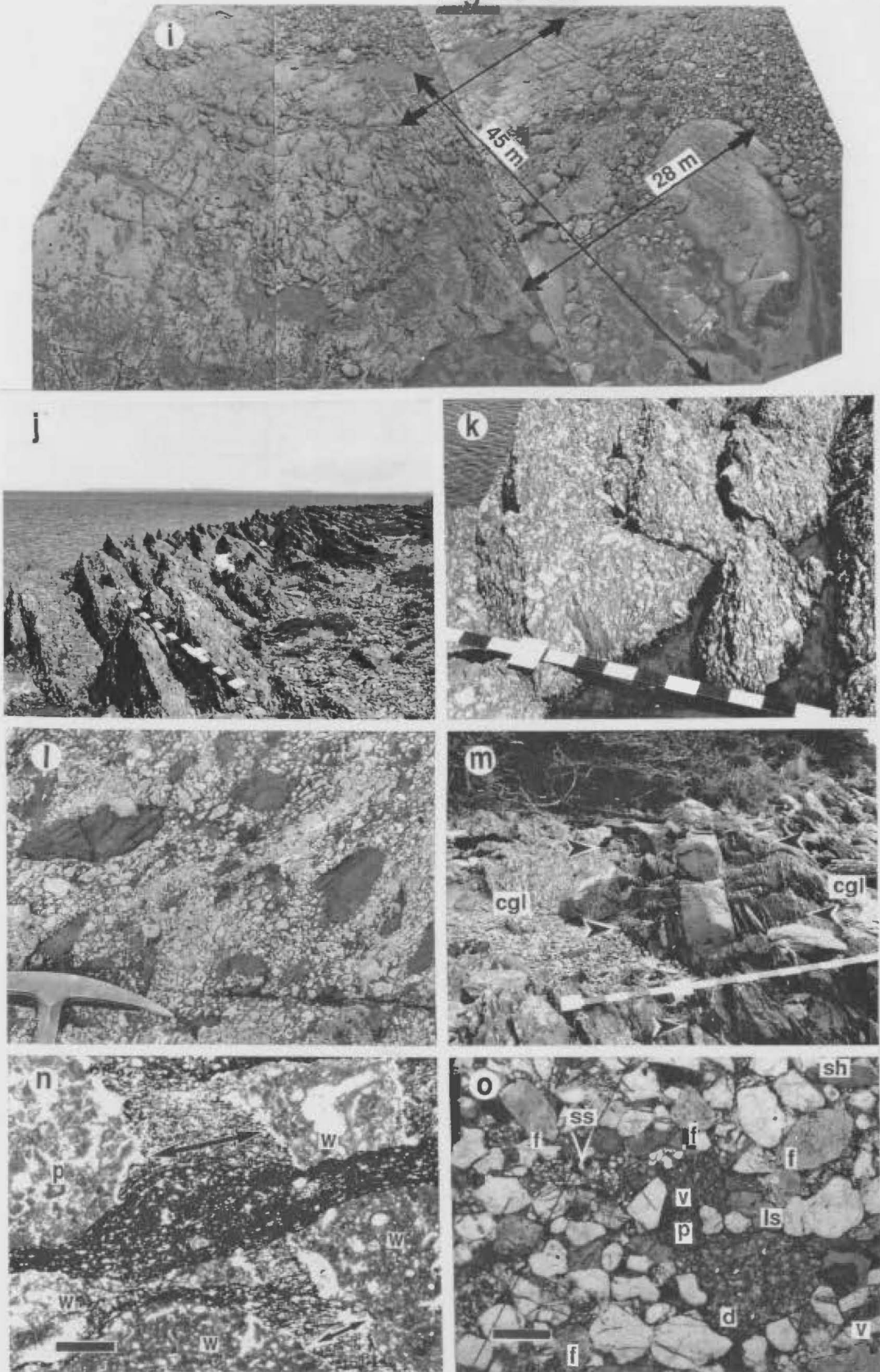


Figure 9.3 continued i) Helicopter view of the fossiliferous wackestone olistolith at the south end of Cliffy Point. Lithistid sponges in the clast indicate derivation from the sponge-oncolite biostrome of the Table Point Fm. Massive debris on the left is clast-supported, pebbly conglomerate. j) Rubbly, matrix-supported conglomerate on the west side of Pistolet Bay (Figure 9.1.5). Bedding is nearly horizontal; prominent stylo-foliation is nearly vertical. Divisions on scale are 10 cm. k) Close-up of pebbly, matrix-supported conglomerate shown in j). Divisions on scale are 10 cm. l) Fine pebble conglomerate with outsized shale clasts; top of the conglomerate at Northern Arm (Figure 9.1.4). m) Raft of interbedded shale and coarse-grained, turbiditic sandstone (arrows) in the matrix-supported conglomerate (cgl) at Northern Arm. Bedding in the conglomerate dips -75° to the left (west); prominent stylo-foliation dips -55° to the right (east). Divisions on scale are 10 cm. n) Photomicrograph of matrix-supported conglomerate from Northern Arm. Very closely-spaced pressure dissolution seams of argillaceous material and scattered siliciclastic silt and dolomite (white grains) characterize the matrix between clasts in the plane of stylo-foliation. More widely-spaced pressure dissolution seams and pseudospar make up the matrix between clasts in the plane perpendicular to the foliation (between arrows); very thin rinds of bladed calcite are a pressure shadow phenomena that occur along those contacts. w, fossiliferous, peloidal wackestone; p, peloidal, fossiliferous packstone. Bar scale is 0.5 mm. o) Photomicrograph of coarse-grained quartzose lithic sandstone clast from Eastern Head. f, feldspar; ss, fine sandstone; d, dolostone; sh, shale; ls, limestone; v, volcanic lithic (plagioclase lathe-chlorite-pyrite (centre); fibrous chlorite (bottom)); p, phosphatic shale?. Matrix is replaced by ferroan calcite.

Figure 9.3



It is best exposed at, and in the vicinity of, the type locality, Daniel's Harbour (Figure 9.4). Matrix-supported conglomerate, in contrast, forms speckled, light grey and black, knobby weathering beds (Figure 9.3.j,k). It occurs in American Tickle sequences only in the northern part of the study area (Figure 9.1, inset).

Physical attributes of the two conglomerate lithologies are shown schematically in Figure 9.2 and are detailed in Table 9.1. In common they 1) show the same range of thickness, forming thin to massive beds, 2) are primarily composed of pebbly limestone debris (Figure 9.5), 3) generally lack internal organization, oriented clast fabric (Figure 9.6), and sedimentary structures and 4) are overprinted by a prominent stylo-foliation commonly at a high angle to bedding (Figures 9.2, 9.3.j,k,n and 9.4).

The most outstanding difference between the two lithologies is abundance of matrix, hence the clast- versus matrix-supported texture of the beds. They are further distinguished from each other by the following: 1) Pebbly clast-supported beds commonly contain dispersed cobbles and small boulders, scattered, out-sized boulders, and, locally, enormous limestone blocks or slabs ranging from 5 to 10 m up to more than 45 m in maximum dimension (Figure 9.3.b,d-g,i). Matrix-supported beds, in contrast, are on average, even more uniformly fine-grained; limestone clasts exceeding 20-30 cm in diameter are uncommon. 2) Clast-supported conglomerates contain a noticeable, albeit small percentage of 'exotic' clast types including other distinctive types of limestone, dolostone, chert and siliciclastic clasts (Figure 9.3.d-g; Table 9.2). Matrix-supported beds are more compositionally homogeneous; all 'exotic' clast types (with the possible exception of siliciclastic ones) are even more uncommon than they are in clast-supported conglomerates and some (eg. parted and ribbon limestone, white fenestral limestone, dolostone, and chert) are not present (Table 9.2). 3) The most common outsize clast in massive, clast-supported beds is

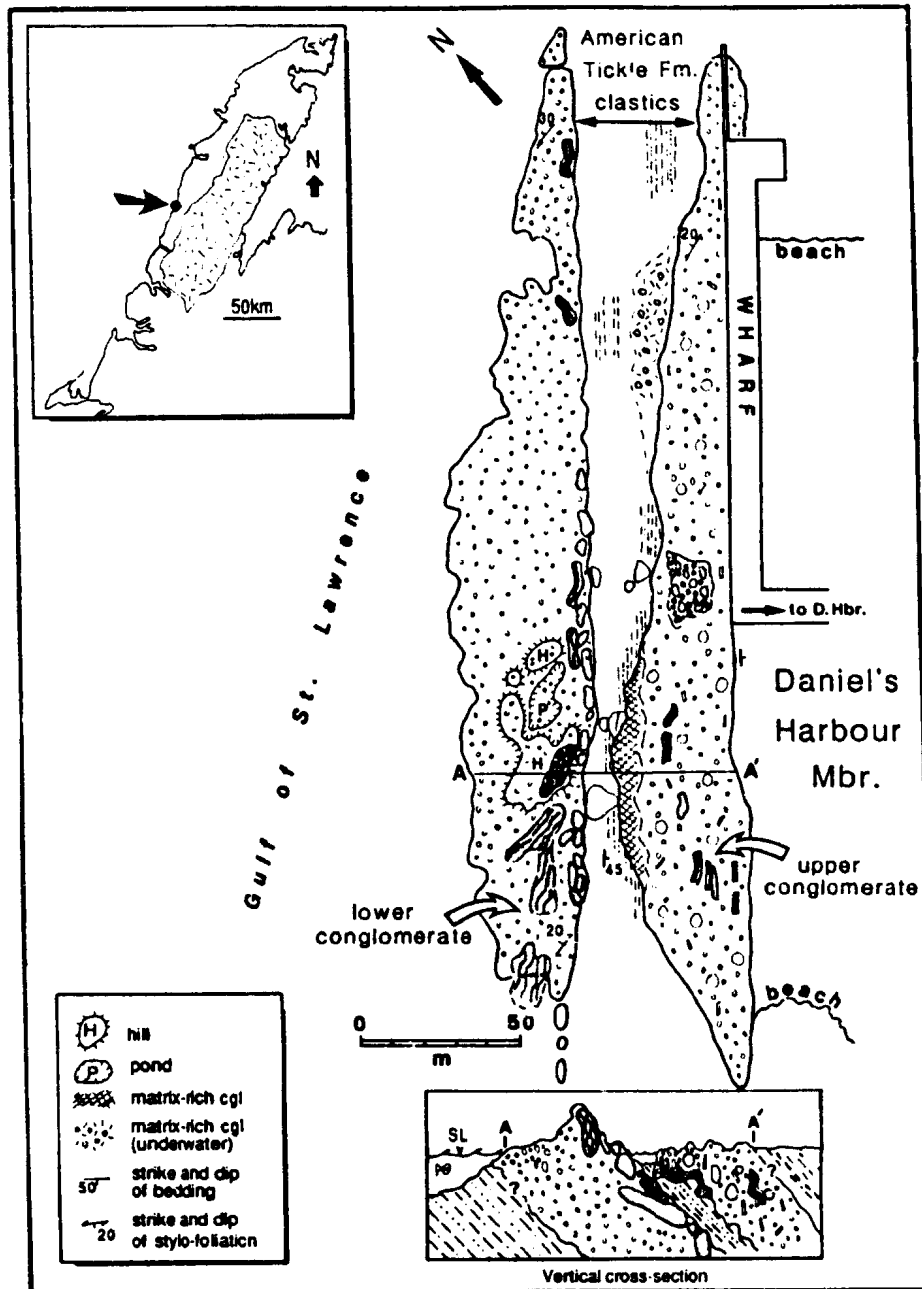


Figure 9.4 Map of Daniel's Harbour Member conglomerates at Daniel's Harbour. The lower bed has very large clasts (shaded) mostly concentrated near the top. Upper bed has a high relief lower contact and is matrix-rich in the lower several metres. Both beds contain large pebbly conglomerate clasts. American Tickle Fm. clastics underlie the subtidal gut between the two beds and are exposed only at very low tide.

Table 9.1 Characteristics of Daniel's Harbour Member Conglomerates; Abbreviations are as follows: D.Hbr., Daniel's Harbour; C.Pt., Clifty Point; E.Head, Eastern Head; cgl., conglomerate; ls, limestone; A.T., American Tickle Fm.; Q, quartz; F, feldspar; M, mudstone; bdg. bedding.

¹ At several localities precise measurements are difficult to obtain because contacts with enclosing siliciclastics are not exposed and the attitude of bedding is uncertain, or the possible effects of tectonic folding or faulting cannot be determined.

Table 9.1 Characteristics of Danie's Harbour Member Conglomerates

	Clast-Supported Conglomerate	Matrix-Supported Conglomerate
Thickness	0.1-70 m; most are >10 m thick	0.1-62 m; most are <10 m thick
Contacts	<ul style="list-style-type: none"> - <u>basal</u>: sharp with a few cm/cm erosional relief or loading (except bed 1 at D.Hbr. with 7-8 m, Figure 9.4); underlying clastics commonly folded & rip-ups (up to several m long) concentrated near the base; some very thick beds with a basal mélange-like zone that grades up into pebbly cgl. (Figure 9.1.4) - <u>upper</u>: sharp & relatively flat with a few cm hummocky relief (except the lower bed at D.Hbr. with protruding megaboulders, Figure 9.4) 	same as for clast-supported beds
Morphology	<ul style="list-style-type: none"> - thick & massive beds tabular at the scale of the outcrop - relatively thin beds (<3 m) pinch & swell due to erosion at the base & hummocky topography on the top of the bed 	similar to clast-supported beds
Texture (Figure 9.5)	<p>poorly-sorted, but mostly composed of pebble-size & smaller (<5 cm) clasts; commonly with dispersed cobbles & small boulders (10-40 cm), scattered oversized boulders (1-4 m), & locally enormous blocks or slabs from 5-10 m up to 45 m in maximum dimension (eg. D.Hbr., C.Pt., E.Head)</p> <ul style="list-style-type: none"> - thinner beds (<3 m) are consistently finer-grained, lacking clasts ≥1 m across 	poorly-sorted, predominantly rubble-size clasts; on average finer-grained than clast-supported conglomerates, clasts greater than 20-30 cm across are rare; largest clasts (up to 5-10 m long) are either black shale, siltstone or sandstone
Composition (Table 9.2)	<p>mostly fossil-bearing, peloidal ls clasts (over the entire clast size range); scattered fossils as clasts include lithistid & calcareous sponges & sponge holdfasts, & orthoconic & coiled cephalopods</p> <ul style="list-style-type: none"> - largest limestone clasts commonly disintegrating along the margins into pebble size debris <p>minor amounts of 'exotic' limestone & clastic clasts</p> <ul style="list-style-type: none"> - large clasts of ribbon & parted ls commonly folded &/or broken into plate-shaped clasts; siliciclastic clasts commonly folded & disintegrating along the margins contributing matrix to the cgl. 	<p>similar to clast-supported cgl.; large fossils rarely occur as discrete clasts</p> <ul style="list-style-type: none"> - rare large ls clasts also disintegrating along the margins into pebble size debris <p>'exotic' limestone & clastic clasts more uncommon than in clast-supported cgl.</p> <ul style="list-style-type: none"> - large siliciclastic clasts commonly folded & disintegrating along the margins contributing matrix to the cgl.
Matrix (Table 9.2)	5-15%; dark grey-brown, black, or greenish-grey mixture of carbonate mud, clays, disseminated silt & sand size calcite grains (some skeletal fragments) & authigenic nonferroan dolomite; minor Q & F silt & sand, very minor sand-size lithics (as occur in A.T. clastics (Chapter 8) & clastic clasts in the cgl.) (Figure 9.3.c)	35-60% (generally decreases in abundance up through the bed); black calcareous shale with silt- to granule-size grains of microsparitic ls & comminuted skeletal debris plus disseminated silt-size, authigenic nonferroan dolomite; minor (<5%) silt and vf sand-size Q, F & muscovite (except in the vicinity of disintegrating clastic clasts) (Figure 9.3.n)

Table 9.1 continued

	Clast-Supported Conglomerate	Matrix-Supported Conglomerate
Internal Structure	<p>predominantly disorganized</p> <ul style="list-style-type: none"> - discontinuous, roughly bedding-parallel parting defines thick to massive layers, but does not correspond to discernible changes in composition or texture - inverse grading at D.Hbr. (Figure 6.4) defined by concentration of outsized blocks & rafts at the top of the lower bed - crude normal grading (accompanied by a decrease in matrix) in some beds that are gradationally overlain by graded calcarenite/calcirudite 	<p>predominantly disorganized</p> <ul style="list-style-type: none"> - vague normal grading in two of the thicker beds; top few to several cm composed of a bimodal mixture of gran. - small pebble ls clasts & lg. shale clasts (10-30 cm long) (Figure 9.3.1) overlain by graded calcarenite
Clast Fabric (Figure 9.6)	<p>most clasts are equidimensional & show no preferred orientation</p> <ul style="list-style-type: none"> - M plates disposed at all angles to bdg., are preferentially oriented sub-parallel to bdg. or gently-inclined - large inequidimensional clasts & rafts also with highly variable orientation (original bdg. in those clasts locally parallels cgl. bdg. suggesting that clast bedding defines the broadest a-b plane of the clast (Figure 9.6.c)) 	<p>same as for clast-supported cgl.; paucity of plate-shaped M clasts precludes establishing whether they are preferentially oriented; siliciclastic clasts appear to be oriented with their broadest dimension sub-parallel to bdg.</p>
Sedimentary Structures	<p>mostly lacking</p> <ul style="list-style-type: none"> - tapering, sediment-filled fissures (<10 cm wide) extending 0.5-2 m down from the top of the bed present locally; filled with 1) finer-grained limestone conglomerate (where overlain by calcarenite, eg. Baker's Brook) or 2) black silty shale (where directly overlain by A.T. clastics, eg. Stag Brook) 	<p>none</p>
Stylo-foliation	<p>prominent; commonly oriented at moderate to very high angles to bdg.; clast contacts commonly defined by micro-stylolites or pressure dissolution seams</p> <ul style="list-style-type: none"> - does not overprint limestone clasts, but is expressed as cleavage in some siliciclastic clasts - proven locally to parallel axial planar cleavage in adjacent A.T. clastics which is interpreted to have formed in response to folding during Acadian (Siluro-Devonian) orogenesis (eg. Cawood and Williams, 1988) 	<p>very well-developed; expressed as very closely-spaced pressure dissolution seams within the matrix & at clast-matrix contacts</p> <ul style="list-style-type: none"> - locally overprints limestone clasts; invariably expressed as cleavage in clastic clasts - also parallels axial planar cleavage (eg. Williams and Smyth, 1983)

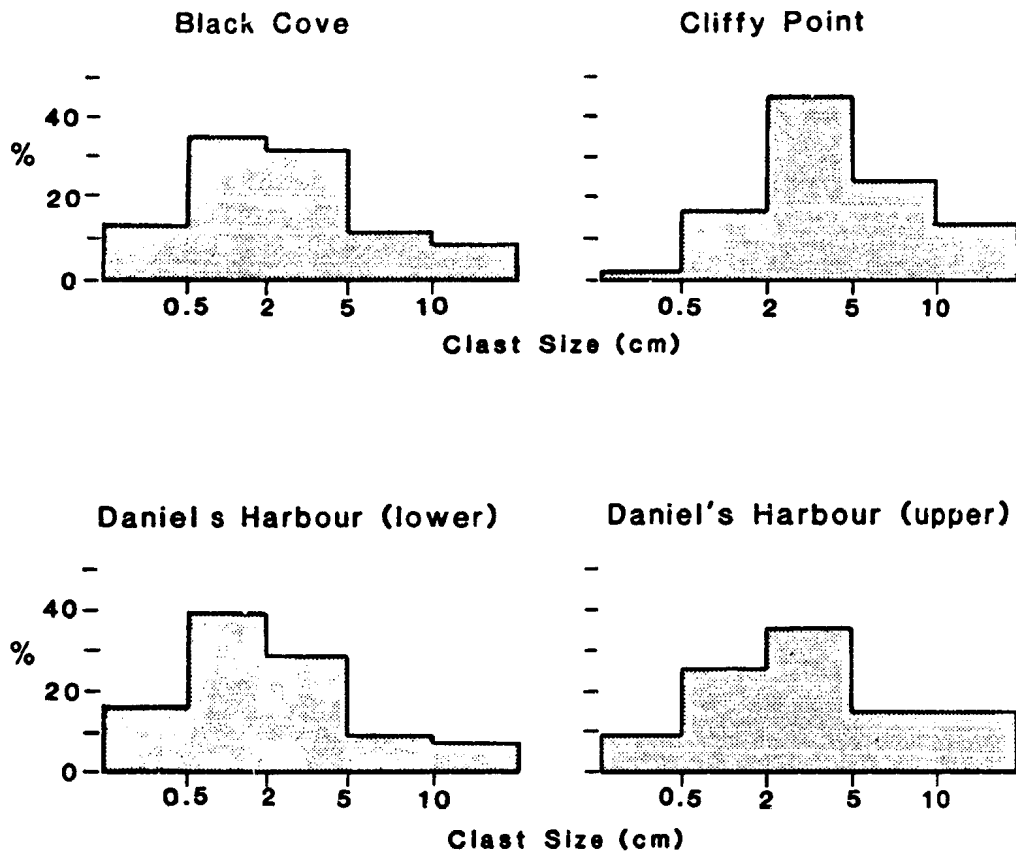


Figure 9.5 Clast size distribution in clast-supported conglomerates. Graphs are based on point counts using a spacing of 10 cm in transects spaced 2-6 m apart perpendicular to strike, generally up through the bed. At Black Cove the number of points (n) = 184; maximum clast size in transects (max) = 40 cm in diameter. At Clifty Point n = 327, max = 4 m by 4 m. At Daniel's Harbour (lower conglomerate) n = 232, max = 80 cm by 50 cm by 15 cm. At Daniel's Harbour (upper conglomerate) n = 251, max = 5 m by 2.4 m by 1.3 m.

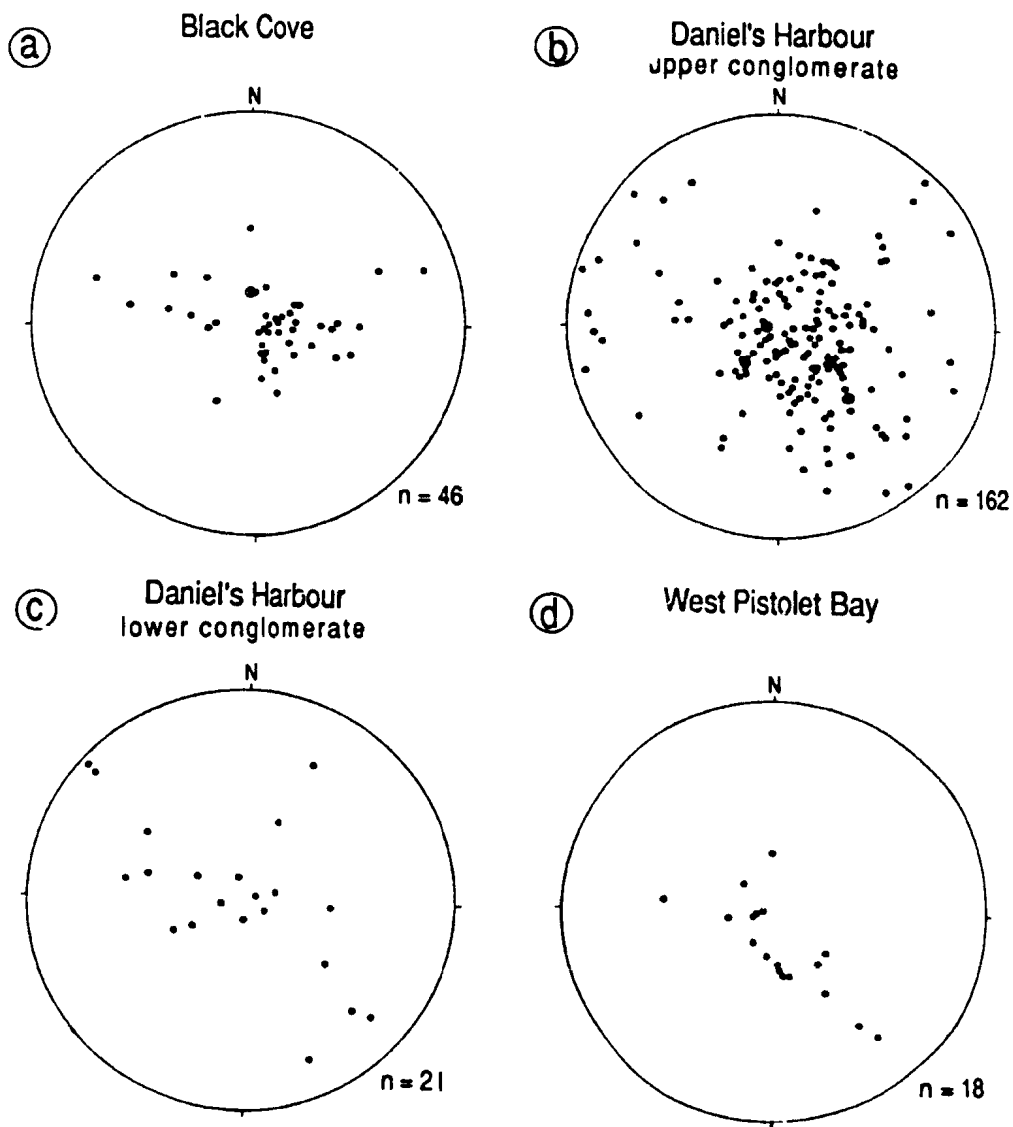


Figure 9.6 Clast fabric in Daniel's Harbour Member conglomerates. Equal area lower hemisphere projections of poles to plate-shaped mudstone clasts in clast-supported conglomerates at a) Black Cove and b) Daniel's Harbour and in matrix-supported conglomerate at d) Pistolet Bay. Clasts range in size from 10-50 cm long, 2-10 cm thick and have variable widths. They are sub-parallel or gently inclined with respect to bedding in clast-supported beds, but show no preferred orientation in the matrix-supported one. c) Projection of poles to primary bedding in megaclasts in the conglomerates at Daniel's Harbour.

Table 9.2 Composition of Daniel's Harbour Member Conglomerates

Clast Type	Black Cove	Daniel's Mbr. (lower bed)	Daniel's Mbr. (upper bed)	Cliffy Point	West Pistollet Bay
	%	%	%	%	%
brown-grey equidimensional limestone*	95	86	86	90	92
grey-brown plate-shaped limestone**	4	7.5	11	7	<5
white fenestral limestone	<1	2.5	0	1.5	0
mottled <u>Stromatolites</u> limestone	0 (present)	2	0	<1	0
dolostone	<1	0 (present)	0	0 (present)	0
chert	0 (present)	0	0	0 (present)	0
dark grey, black or green, fine to coarse clastics	<1	2	3	<1	4
lithoclast calcarenite	0 (present)	0 (present)	0 (present)	0 (present)	0 (present)
pebbly limestone conglomerate	0 (present)	0 (present)	0 (present)	(present)	
Matrix	7	9	7	?	50
N (number of points)	148	199	235	200	203

Table 9.2 Composition of Daniel's Harbour Member Conglomerates; point count data.

* - containing variable amounts of skeletal debris, peloids, intraclasts and oncolites over the range of depositional textures from mudstone to grainstone, floatstone and rudstone

** - predominantly mudstone or fossil-poor wackestone, commonly neomorphosed to microspar or pseudospar

fossiliferous limestone, commonly with preserved thin, stylo-sutured or stylo-nodular bedding and typically disintegrating along the margins into pebbly debris (Figure 9.3.b,d,h). The largest clasts in matrix-supported conglomerates are either black shale, siltstone or sandstone which are typically folded, are disintegrating along the margins and merge with ambient matrix of the conglomerate (Figure 9.3.1,m).

More detailed descriptions of clasts components and their inferred or determined provenance are presented in Chapter section 9.5.

9.2.2 Interpretation

Daniel's Harbour Member conglomerates are interpreted as subaqueous debris flow deposits. Poor size sorting, absence of stratification, and chaotic disposition of plate-shaped clasts relative to bedding imply that tractive currents were not involved in sediment transport or deposition (Middleton and Hampton, 1976). The general absence of channelling along the bases of most beds demonstrates that the debris was largely transported above the seafloor. For matrix-supported conglomerates deposited from flows with abundant argillaceous material the predominant mechanisms by which clasts were held in suspension during transport would have been the cohesive strength of the fluid matrix and buoyancy (Hampton, 1975, 1979; Lowe, 1982). For clast-supported conglomerates deposited from flows lacking abundant argillaceous sediment the predominant supporting mechanisms more likely would have been grain to grain contacts, dispersive pressures caused by collisions between clasts, and possibly turbulence (Pierson, 1981; Lowe, 1982). (The reader is referred to relevant discussions on the significance of grading (or lack of it) in Chapter section 6.2.3 presented for similar debris flow conglomerates and megaconglomerates in the Cape Cormorant Formation.)

Relatively abundant siliciclastic clasts and greater percentage of matrix at the base of the beds indicate that soft, underlying sediment was plucked and incorporated during transport, thereby contributing

watery, argillaceous and silty matrix to the moving debris. Zones of folded or disarticulated clastics beneath some beds suggest that transport and emplacement of very thick flows triggered sliding and folding of the underlying sediments. Given the basinal setting for the ambient siliciclastics (Chapter 8), deposition is inferred to have occurred by frictional freezing at the base of the flow rather than by an abrupt decrease in depositional gradient. Fissures that formed at the top of some beds demonstrate cohesive strength of the conglomeratic sediment after deposition. Tensile stresses which produced them may have originated by displacement of underlying clastics, suggesting that in some cases the underlying zones of folded and disarticulated sediment were generated after conglomerate emplacement.

Striking differences in the amount of matrix and general texture between the two types of conglomerates is inferred to reflect fundamental differences in the source of the flows. Predominance of limestone clasts and paucity of matrix in clast-supported conglomerates indicates a predominantly limestone source of the debris and that very little fine, siliciclastic sediment was incorporated either at the origin or during transport. The pebbly texture is proven to be, at least in part, the product of disintegration of large stylo-bedded limestone clasts during transport. However, the presence of pebbly limestone conglomerate clasts (Table 9.2) proves that the sources included other similar conglomerates, the reworking of which probably contributed to the large volume of pebble size debris. Abundant calcareous shale matrix in the matrix-supported beds, in contrast, is inferred to have been generated by total remoulding of unlithified, argillaceous sediment incorporated at the source of the flows. Furthermore, derivation from a pebble-grade source appears to have been of even greater importance for these beds. Large limestone clasts that could have disintegrated to pebble-size debris are uncommon, and the large volume of matrix, by reducing the numbers and impact of collisions

between clasts and frictional stress, would have minimized breakdown of clasts during transport. Implications of the presence of reworked conglomerate and calcarenite clasts for provenance and origin of both types of debris flow conglomerates are addressed in Chapter section 9.4.3.

Only some of the thin clast-supported conglomerate beds, which are finer-grained and less poorly-sorted, may have been transported and deposited by mechanisms other than debris flow. Texturally they are similar to clast-supported, disorganized gravels reported from other ancient submarine sequences (Davies and Walker, 1974; Walker, 1975; Hein, 1982), which are interpreted to have been transported and deposited from concentrated clast dispersions at the base of large, high velocity turbidity flows (Walker, 1975). Smaller clast size in these beds, however, may simply be a reflection of further disaggregation with increased transport distance and, therefore, an expression of distal debris flow deposition. Paucity of matrix may be accentuated by compaction and pressure dissolution during burial.

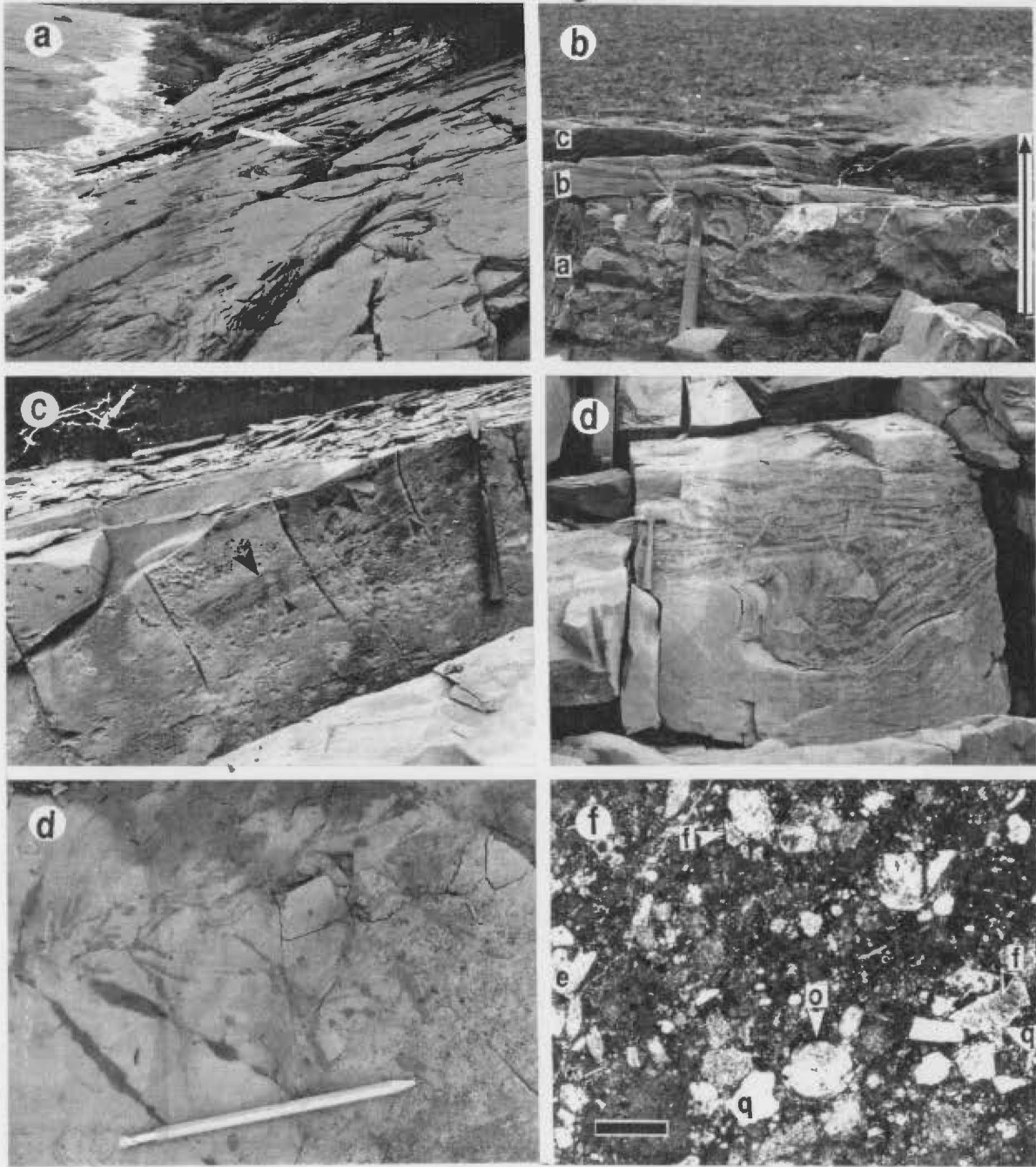
9.3 Lithoclast Calcarenite and Calcirudite

9.3.1 Description

Quartz-rich, limestone lithoclast calcarenite and calcirudite form thin to massive beds (5 cm- \geq 3 m) that either gradationally overlie a limestone conglomerate or are discrete beds in the American Tickle Formation (Figures 9.1, 9.2 and 9.7.a,b). Most thick beds appear tabular in outcrop; basal surfaces are either planar or exhibit a few to several centimetres erosional relief and upper surfaces are flat. Marked lateral changes in thickness are demonstrable only on the west side of Pistolet Bay (Figure 9.1.e) where the calcarenite overlying a matrix-supported conglomerate changes from 1.5 to 0.8 to 1.6 m over a distance of ~1 km. The coarsest size fraction of individual beds ranges from granules or very small pebbles (<1 cm), to medium sand. The

Figure 9.7 Daniel's Harbour Member calcarenites; outcrop photos and photomicrographs. Locations are in Figure 9.1. a) Outcrop of the highest calcarenite (upper bedding plane) at Black Cove. Up is to the left. Hammer (arrow) 10r scale. b) Graded calcarenite atop the matrix-supported conglomerate at Northern Arm. a, b and c indicate massive, parallel laminated and ripple cross-laminated horizons, respectively, of a Bouma sequence. c) Large-scale cross-stratification in the second calcarenite at Black Cove. d) Convolute lamination in the uppermost calcarenite at Black Cove. Hammer for scale. e) Chondrites at the top of the uppermost calcarenite at Black Cove. f) Photomicrograph of quartzose calcarenite from Black Cove. Contacts between predominant mudstone/microsparitic limestone clasts (grey) are stylolitic and indistinct. Black specks are authigenic pyrite. q, quartz; f, feldspar; o, ostracode; e, echinoderm. Bar scale is 0.5 m long.

Figure 9.7



thicker beds are generally coarser-grained than the thinner ones and commonly contain flat, pebble-size, dark shale intraclasts in the lower several centimetres; the coarsest beds typically gradationally overlie a conglomerate.

These strata are composed mostly of limestone lithoclasts and lesser broken skeletal debris (Figure 9.7.f). The former are predominantly microsparitic mudstone and peloidal and/or fossiliferous wacke-/pack-stone, compositionally and texturally identical to clasts that make up the bulk of Daniel's Harbour conglomerates. Skeletal grains, the most common being echinoderm, ostracode and trilobite fragments, and Nuia, are also identical to those which occur in the lithoclasts. 'Exotic' siliciclastic components of these beds, the most common being quartz and feldspar, are listed in Table 9.3; all are characteristic of Goose Tickle Group sandstones and sandstone clasts in the conglomerates. They vary in abundance from <1-2% in the very coarse sand - granule fraction to as much as 30-40% in the medium to coarse sand size fraction in some beds (Figure 9.7.f). They are invariably finer-grained than the carbonate grains with which they occur.

Most calcarenite and calcirudite beds are clast-supported and matrix-poor. Contacts between grains are typically stylolitic (Figure 9.7.f); finely-crystalline, blocky calcite cement never exceeds <5% and is usually absent. Some calcarenites that directly overlie matrix-rich conglomerate contain a high percentage (20-40%) of argillaceous matrix and are more appropriately classified as carbonate lithoclast greywacke.

All beds are normally-graded and exhibit sequences of structures that indicate deposition from a waning flow (Figure 9.2). Thinner, finer-grained calcarenites have Bouma sequence structures (eg. Tbcd, Tbc, or Tcd) (Figure 9.7.b). Basal parts of the thicker, coarser-grained beds, in contrast, are characterized by a zone of (i) structureless or graded granules or very small pebbles, (ii) planar to low-angle lamination, or (iii) planar to low-angle lamination and

Table 9.3 Siliciclastic Components of Daniel's Harbour Member Calciturbidites

Quartz

Simple
Coarse, polycrystalline
Fine, polycrystalline
Strained

Feldspar

Albite
Untwinned, sericitized orthoclase
Microcline

Sedimentary Lithics

quartz-feldspar-mica-chlorite very fine sandstone/siltstone
quartzose, fine-grained sandstone/siltstone with calcite cement
quartz-feldspar, dolomitic siltstone
finely-crystalline, nonferroan dolostone
medium-crystalline (0.05-0.1 mm), nonferroan dolostone
clear chert
orange-brown, phosphatic chert
clear, fibrous megaquartz
dark orange-brown to black (phosphatic) strongly foliated shale
pale green-brown, illitic, chloritic shale

Volcanic Lithics

iron-rich chlorite-plagioclase microlathe intergrowth
iron-rich, fine to medium, fibrous, crystalline chlorite

Plutonic Lithics

medium-crystalline, plagioclase-untwinned feldspar-quartz intergrowth
mermykite or perthite?

Other Grains

Biotite
Chromite

megaripple-scale (10-20 cm), trough cross-stratification, in turn overlain by finer-grained calcarenite with Bouma sequences (Figures 9.2.a and 9.7.c). Convolute lamination and/or loaded ripples are typically developed in rippled or megarippled horizons (Figure 9.7.d). Fluid escape dykes (<30 cm long, 0-10 cm wide) composed of comparatively coarse-grained sediment intersect bedding planes in the upper, fine-grained portions of a few thick beds. Sparse, current-aligned graptolites occur in the upper, parallel-laminated unit of some beds. Chondrites and Planolites burrows occur on the top of one calcarenite at Black Cove (Figure 9.7.e).

9.3.2 Interpretation

Daniel's Harbour Member calcarenites and calcirudites are interpreted to have been transported and deposited by turbidity currents (cf. Bouma, 1962; Middleton and Hampton, 1976; Walker, 1984). Basal zones of unstratified granules and laminated or cross-bedded pebbly sands in thick calcirudites are comparable to normally-graded, pebbly sands and graded, stratified pebbly sands in other submarine sequences (Pickering *et al.*, 1986, references cited therein) that are interpreted to record rapid deposition from suspension and sedimentation from traction bedload, respectively, from a high velocity, high concentration turbidity flow. Soft-sediment deformation structures generated by liquifaction or fluidization of the sediments shortly after deposition, attest to their original high water content and loose packing and further indicate that they were rapidly deposited.

Striking compositional similarities between these beds and the debris flow conglomerates indicate that the two types of deposits share a common sediment source and are closely related. That they commonly cap debris flow deposits further suggests that the currents from which they were deposited were generated above debris flows during transport (Hampton, 1972; Krause and Oldershaw, 1979; Crevello and Schlager, 1980). As turbidity currents would likely travel further than

associated debris flows and deposit finer-grained sediment even further from the source, calcarenite and calcirudite beds which occur independent of a conglomerate are inferred to signal debris flow activity in other areas of the basin (eg. Cossey and Ehrlich, 1979). Limestone lithoclasts comprising the calciturbidites are essentially comminuted equivalents of the limestone pebbles and larger clasts in the conglomerates, while siliciclastic grains are inferred to derive from disintegrating siliciclastic clasts transported in the debris flows. Common provenance is further supported by fossil evidence; conodont elements recovered from a calcarenite at Black Cove (BC-46 in Table G.1 in Appendix G) are also common to clasts in the conglomerates (see Chapter section 9.4, below).

9.4 Provenance of Lithoclasts

Clasts that make up Daniel's Harbour Member conglomerates fit into one of eight categories (Table 9.4). Based solely on their gross field characteristics the majority can be directly correlated with lithologies comprising the Table Point Formation and younger Middle Ordovician sedimentary units. In order to confirm the lithologic correlations and establish ages of clasts of uncertain derivation 21 clast and 5 whole rock conglomerate samples were processed for conodonts. Table 9.4 details the lithologies included in each clast category, lists their correlative formations and lithofacies in the autochthonous, sedimentary sequence, and provides additional comments on their distribution and occurrence pertinent to their origins. More detailed petrographic description of clast types and faunal lists of conodonts recovered from dissolved clast and whole rock conglomerate samples are in Table G.1.

9.4.1 Composition and Age of Clasts

(i) **Grey-brown fossiliferous and/or peloidal limestone** This category encompasses all light brown to dark grey brown limestones which constitute the overwhelming majority of clasts in the conglomerates

Table 9.4 Clast Components of Daniel's Harbour Member Conglomerates. Abbreviations are as follows:
M, mudstone; W, wackestone; F, packstone; G, grainstone; P, floatstone; R, rudstone; pel., peloidal; echino.,
echinoderm; intra., intraclastic; lam., lamination; convo., convolute; sed., sedimentary; volc., volcanic;
plut., plutonic; meta., metamorphic; fer., ferroan; vcs, very coarse sand-size; ms, medium sand size; cs,
coarse sand size; gran., granule.

Table 9.4 Clast Components of Daniel's Harbour Member Conglomerates

CLAST CATEGORY	CLAST SIZE & SHAPE	LITHOLOGIES	CORRELATIVE FORMATION &/OR LITHOFACIES (*)	DISTRIBUTION / OTHER COMMENTS
(1) GREY-BROWN FOSSILIFEROUS &/OR PELOIDAL LIMESTONE	subangular to subround pebbles, cobbles & boulders (<1 cm--4 m) plus inequidimensional megaclasts up to 28 m by 45 m in cross-section	mostly fossiliferous W (ranges from fossil-poor M to very fossiliferous & peloidal W/P & pel. intraclastic fossil-bearing P/G/R) 1) fossil. W with echino. & sponges 2) fossil. W with <u>Lapidipanis</u> 3) fossil. W with pel., intra., fossil. P or M lenses (uncommon) - <u>Girvanella</u> onco., intra., fossil. F/R - echinoderm P/G/R - trilobite-peloidal R - fine peloidal G & pel. fenestral P/G	Table Point Fm. and lower Table Cove Fm. (*) - sponge-oncolite biostrome lithofacies - burrowed, fossiliferous wackestone lithofacies - burrowed, fossiliferous wackestone lithofacies - sponge-oncolite biostrome lithofacies - echinoderm-algal limestone lithofacies - burrowed limestone lithofacies (T. Cove Fm.) - ?Basal Peritidal Unit	Major limestone components of all conglomerates; largest clasts are in beds in the Daniel's Hbr. area. Most large boulders are echinoderm-rich and bear sponges. Many large clasts exhibit original stylo-sutured or stylo-nodular bedding. Peloidal limestone lithologies are more abundant in conglomerates in the Port au Port and Pistolet Bay areas.
	(2) INTERBEDDED LIMESTONE & SHALE	plates (10-60 cm long, 2-5 cm thick, variable widths) deformed, bedded clasts a few tens of cm long & rafts up to 5-10 m long same as for parted limestone	(1) mudstone/microsparitic limestone* (2) <u>parted limestone</u> (1-3 cm, planar or wavy, structureless or burrowed limestone* & <1 cm shale) (3) <u>ribbon limestone</u> (2-10 cm, planar, structureless or laminated limestone* & 1-5 cm, dolomitic shale) *1, 2 & 3 are fossil-poor with sparse trilobites, ostracodes, radiolarians, graptolites & phyllocarids	Table Cove Formation (*) burrowed, parted limestone lithofacies ribbon limestone lithofacies

Table 9.4 continued

CLAST CATEGORY	CLAST SIZE & SHAPE	LITHOLOGIES	CORRELATIVE FORMATION &/OR LITHOFACIES (*)	DISTRIBUTION / OTHER COMMENTS
(2) INTERBEDDED LIMESTONE & SHALE cont.	deformed, bedded clasts a few tens of centimetres up to a few metres long	(4) dolomitic shale with limestone nodules 3-5 cm thick, 10-15 cm long); both components with parallel lam.; nodules with sparse trilobite fragments	?thin-bedded, burrowed limestone lithofacies (eg. Beaver Brook, Rod-ickton Quarry & Baker's Brook)	Conspicuous but minor components of several conglomerates in the Gros Morne Park area & River of Ponds.
	folded clasts up to a few metres long	(5) black mudstone without discrete shale interbeds; microsparitic, vaguely parallel-lam.; sparse trilobite fragments & small, unidentified skeletal grains	no <i>in situ</i> counterpart; probably equivalent to the Table Cove fm.	Present only in matrix-supported conglomerate at Northern Arm (nearly indistinguishable from black calcareous shale (below))
(3) MOTTLED STROMATACTIS LIMESTONE	angular blocks, mostly >20 cm across, up to 4-5 m across, maximum	light brown, burrowed, fossiliferous W or ostracode-rich W with tan, peloidal, fossiliferous P/G mottles & internal sediment- &/or cement-filled (radial fibrous & blocky calcite) <u>Stromatactis</u> cavities	Table Point Formation (*) <u>Stromatactis</u> mound lithofacies	Present in almost all conglomerates except matrix-supported beds in the Pistolet Bay area. Largest clasts occur at Piccadilly developed at the top of the Table Point. Large clasts in conglomerates in the Daniel's Harbour area have no <i>in situ</i> counterparts in the vicinity.
(4) WHITE FENESTRAL LIMESTONE	angular, pebble- to small boulder-size clasts (30-50 cm across); 1 m by 25 cm in cross-section, maximum	fine, peloidal, intraclastic P or G with sparse ostracodes, trilobites & <u>Girvanella</u> mats; fine laminoid to coarse irregular fenestral fabric; fibrous marine & blocky calcite cement	?Catoche Formation, possibly the Table Point Formation	Largest clasts are in beds in the Daniel's Harbour area. Clasts are notably absent from matrix-rich conglomerates in Hare Bay and Pistolet Bay areas.
(5) DOLOSTONE	angular, pebble- to small cobble-size clasts <10 cm across	structureless, rarely laminated, very finely-crystalline (0.01-0.02 mm) & mottled, finely-crystalline (0.02-0.06 mm) dolostone (both nonferroan with thin ferroan overgrowths)	Table Point Formation? (possibly the burrowed dolostone lithofacies of the Basal Peritidal Unit) or the Aguathuna fm.	Volumetrically minor, but conspicuous components of all conglomerates except matrix-supported bed in the Hare Bay - Pistolet Bay area

Table 9.4 continued

CLAST CATEGORY	CLAST SIZE & SHAPE	LITHOLOGIES	CORRELATIVE FORMATION &/OR LITHOFACIES (*)	DISTRIBUTION / OTHER COMMENTS
(6) CHERT	subround to subangular, pebble- to small cobble-size clasts, <10 cm across, maximum	pale green, off white, light brown & black; dark clasts commonly dolomitic & weather yellow; some light-coloured clasts are mosaics of equant micro-quartz & megaquartz & fibrous quartz	Table Point Formation (either the Basal Peritidal or Middle Subtidal Unit) or the Aguathuna Fm.	Volumetrically minor components of most conglomerates except matrix-supported beds in the Hare Bay - Pistolet Bay area. Black clasts conspicuous in beds in the Gros Morne Park area where locally underlying Table Point Fm. contains many black chert nodule horizons.
(7) SILICICLASTIC SEDIMENTS	deformed, flat clasts, mostly a few cm to 30-50 cm long, up to a few metres, maximum	(1) black <u>shale</u> ; slightly to very calcareous; slightly dolomitic; pyritic; sparse poorly-preserved graptolites	Table Cove Formation, (ribbon limestone lithofacies), Black Cove Formation, &/or Goose Tickle Group (shale-dominated lithofacies)	'Pure' shale clasts are minor components of most conglomerates. Calcareous shale clasts are major components of matrix-supported beds in the Hare Bay - Pistolet Bay area.
	deformed, flat clasts, mostly a few cm to 30-50 cm long, up to 3 by 14 m in cross-section	(2) <u>interstratified</u> black, noncalcareous <u>shale</u> , green <u>siltstone</u> & very fine- to fine-grained sandstone; quartzose or quartz-rich, feldspathic greywacke; normal grading, parallel & convo. lam.	Goose Tickle Group (shale- and siltstone-dominated lithofacies)	Conspicuous, but minor components of all conglomerates. Commonly concentrated near the base of the bed, but scattered throughout as well.
	round, equidimensional cobbles & boulders (0.2-2 m diameter) & medium- to thick-bedded (40-80 cm) rafts up 6-8 m long (commonly folded)	(3) greenish-grey, medium to very coarse-grained sandstone; calcareous, lithic arenite & lithic greywacke (35-75% quartz, 10-25% feldspar, 15-40% lithics (mostly sed., plus minor volc. & plut. & rare meta.); matrix (<5-20%) partially replaced by calcite, fer. calcite &/or dolomite; normal grading, large-scale cross-stratification, convo. lam., flutes	Goose Tickle Group (sandstone-dominated lithofacies)	The largest clasts and highest concentration of them occur at Eastern Head; they are present but sparse at Clifty Pt. Large, bedded rafts are major components at the base of the conglomerate at Northern Arm.

Table 9.4 continued

CLAST CATEGORY	CLAST SIZE & SHAPE	LITHOLOGIES	CORRELATIVE FORMATION &/OR LITNOFACIES (*)	DISTRIBUTION / OTHER COMMENTS
(8) RESEDIMENTED CARBONATE	equidimensional blocks or elongate slabs <1 m long to 10 m by 5 m by >1.5 m (maximum) (thinner clasts commonly folded)	(1) quartz-bearing, limestone lithoclast calcarenite/calcirudite; very fine sand to granule-size sediment; normal grading, parallel lam. or structureless; % Q,F,L varies from <1% in some vcs-gran. clasts to 30-35% in some ms-cs clasts (majority of siliciclastic grains are quartz)	Daniel's Harbour Member	Distinctive, but minor components of nearly all matrix-poor conglomerates. Most clasts are medium-grained or coarser. Largest clasts are in beds in the Daniel's Hbr. area and at Black Cove. Coarse-grained clasts in matrix-supported beds recognized as amorphous pockets of sand- & granule-size lithoclasts in pebbly conglomerate.
	vaguely defined 'boulders' and megaclasts, <1 m across to ~10 m by 15 m in cross-section	(2) pebbly, limestone lithoclast conglomerate; poorly-sorted, clast-supported pebbles, cobbles & small boulders (in come); most clasts similar to those in CLAST CATEGORY (1) plus M & white fenestral limestone; low abundance of siliciclastic grains in matrix	Daniel's Harbour Member	Largest clasts recognized in the conglomerate at Daniel's Harbour. Clasts in matrix-poor beds differentiated from disintegrating stylo-nodular limestone clasts by 'polymictic' composition, & from enclosing conglomerate by subtle textural differences (which influence weathering style) such as lesser matrix, scarce M plates &/or absence of large boulders.

(Tables 9.2 and 9.4; Figure 9.3.a, b). Lithologies included are similar in all respects to limestones that make up the Table Point Formation (Chapter 4) and the lower Table Cove Formation (Chapter section 5.2) (Table 9.4); most clasts are too small and not compositionally or texturally distinctive enough to correlate them precisely with a particular lithofacies.

Conodonts recovered from representative clasts confirm the lithologic correlations (Table G.1). Moreover, conodonts recovered from whole rock conglomerate samples include many long ranging species which suggest that the limestone debris came from all stratigraphic levels in the Table Point and Table Cove formations.

(ii) **Interbedded limestone and shale** This category includes clasts of typical parted and ribbon limestone, plus mudstone plates derived from them, as well as more atypical clasts of dolomitic shale with mudstone nodules and of black, even-bedded, argillaceous mudstone (Table 9.4; Figure 9.3.d).

Clasts of parted and ribbon limestone and associated plate-shaped mudstone clasts are identical to same-named, slope lithofacies in the Table Cove Formation (Table 9.4; Chapter sections 5.3 and 5.4). Conodonts recovered from representative clasts substantiate the lithologic correlation (Table G.1).

The other, locally occurring lithologies in this category are also inferred to have come from the Table Cove Formation (Table 9.4). Clasts of dolomitic shale with limestone nodules are comparable to shaley, nodular limestone which occurs at the base of the Table Cove at a few localities in the study area (Chapter section 5.2.4). Clasts of black mudstone have no *in situ* counterparts, but their composition, texture and state of deformation most closely ally them to the Table Cove. One representative clast processed for conodonts was barren (Table G.1), so the lithologic correlation is not proven.

(iii) **Mottled Stromatactis limestone** Clasts of light brown and

tan mottled limestone with internal sediment- and cement-filled Stromatactis are distinctive, but volumetrically minor components of the conglomerates (Tables 9.2 and 9.4; Figure 9.3.h). In contrast to most other limestone lithoclasts they are typically angular and are found breaking apart into smaller angular clasts in the conglomerates, suggesting that they were well-lithified and brittle at the time of transport.

These clasts are lithologically identical to Stromatactis mound lithofacies limestones that occur at the top of the Table Point Formation locally (Chapter section 4.4.3). This correlation is confirmed by conodont assemblages recovered from clasts at several localities (Table G.1).

(iv) **White fenestral limestone** These clasts are also conspicuous, but minor components of many conglomerates (Tables 9.2 and 9.4; Figure 9.3.g). Like (iii), above, they are generally angular and commonly are clustered within a bed, suggesting they were well-lithified and were broken up during transport.

These clasts are similar in composition, texture and fabric to fenestral limestones at the base of the Table Point Formation (Basal Peritidal Unit; Chapter section 4.2.1). Those beds, in contrast, are characteristically light grey or light brown in colour. White fenestral limestone, however, is a distinctive lithofacies at the top of the Lower Ordovician Catoche Formation (Costa Bay member) both on the Port au Port Peninsula and in the Pistolet Bay area (DeGrace, 1974; Knight and James, 1987).

Two of three clasts processed for conodonts were barren (Table G.1). The sparse assemblage recovered includes Cornuodus longibasis (Lindström), a long-ranging species reported from Beds 9-11 (Arenig) in the Cow Head Group (Stouge and Bagnoli, 1987) and from the Table Point and Table Cove formations (Stouge, 1984). It is possible that white fenestral limestone is a lithofacies in the Table Point Formation in

areas outside the outcrop belt, perhaps intimately associated with the Stromatactis mound lithofacies. (The two types of clasts commonly occur together or are both absent in some conglomerates.) Other evidence that supports derivation from the Catoche Formation comes from conodonts recovered from whole rock conglomerate samples (Table G.1) which includes three species (Protopanderodus rectus Stouge, Pteracntiodus cryptodens (Mound), Tripodus laevis Bradshaw) which have been previously reported from Arenig age strata but not from the LLanvirnian Table Point or Table Cove formations.

(v) **Dolostone** Yellow-weathering, very fine or finely-crystal-line dolostone are minor components of most conglomerates (Tables 9.2 and 9.4). Most are structureless or vaguely mottled; some are finely (\pm cryptalgally) laminated.

This lithology is common to many Early Paleozoic platformal formations (see Figure 6.15). With respect to the more immediately underlying stratigraphic sequence, two possible origins are the burrowed dolostones in the lower Table Point Formation (Basal Peritidal Unit, Chapter section 4.2.1) and the Aguathuna Formation (Chapter 3). A single sample processed for conodonts was barren (Table G.1). Conodonts in whole rock conglomerate samples which could have come from lower Table Point lithofacies (eg. ?Erraticodon balticus Dzik) and from the Aguathuna (eg. Tripodus laevis Bradshaw) (Table G.1) support both possibilities.

(vi) **Chert** This category includes all siliceous, pebble- to small cobble-size clast which are sparsely scattered in the conglomerates (Tables 9.2. and 9.4).

On the basis of shape, colour, crystalline fabrics, and dolomitic nature of some clasts, these clasts are inferred to be sedimentary in origin. Their exact derivation(s) are uncertain and are likely from more than one stratigraphic unit. Light coloured chert nodules are common components of several carbonate lithofacies in the Aguathuna

Formation (Chapter 3). Dark chert nodules occur in both the Aguathuna Formation and in peritidal and shallow subtidal lithofacies of the Table Point Formation (Chapter sections 4.2.3 and 4.3).

(vii) **Siliciclastic sediment** This category includes shale, siltstone and sandstone clasts, all of which are distinctive but minor components of the conglomerates (Tables 9.2. and 9.5; Figure 9.3.d,g,l,m,o). Common preservation of bedding and sedimentary structures in these clasts, combined with the fact that they are invariably disaggregating along their margins, demonstrate that the sediment was consolidated but not totally lithified at the time of transport.

Black shale clasts may have come from any of three formations: the ribbon limestone lithofacies of the Table Cove Formation (Chapter section 5.4), the Black Cove Formation (Chapter 7), and the shale-dominated lithofacies of the Goose Tickle Group (Chapter section 8.2.1). Graptolites in the clasts are too poorly-preserved to confirm these correlations. A single sample of calcareous shale dissolved for conodonts and graptolites yielded no identifiable specimens (Table G.1).

Clasts of thinly interbedded black shale, green siltstone, and very fine- to fine-grained sandstone, as well as discrete clasts of the latter two lithologies, are identical in colour, style of bedding, composition and texture to lithologies comprising the shale and siltstone-dominated lithofacies of the Goose Tickle Group (Chapter sections 8.2.1-3). Higher concentrations of these clasts near the base of conglomerate beds suggest that a significant proportion came from immediately underlying strata.

Clasts of medium- to very coarse-grained sandstone are compositionally and texturally similar to medium- or thick-bedded, sandstone-dominated lithofacies of the Goose Tickle Group (Chapter section 8.2.4). They are also similar to sandstones which make up the allochthonous Lower Head Formation which overlies the Cow Head Group, and is regarded

as an older (late Arenig-early Llanvirn) equivalent of the Goose Tickle Group (James and Stevens, 1986; Quinn, 1988a). One clast processed for conodonts yielded no specimens, so the age can not be determined (Table G.1). However, since no other clasts in the conglomerates are proven to have come from older, deep-water carbonates or clastics of the Humber Arm and Hare Bay allochthons, these sandstone clasts are interpreted to have come from the Goose Tickle Group. With one exception, conglomerates do not directly overlie medium- or thick-bedded sandstone, so the presence of these clasts cannot be readily attributed to plucking of immediately underlying sediments at the base of the debris flows. Moreover, most clasts occur well above the base of the beds and are much larger than would readily be entrained in that manner. They are inferred to have been incorporated in the flows at the source.

(viii) **Resedimented carbonates** This category includes clasts of quartz-rich limestone lithoclast calcarenite and calcirudite, and poorly-sorted, limestone pebble conglomerate (Table 9.4; Figures 9.3.f and 9.4). Both lithologies are relatively minor components of all conglomerates but are more common in clast-supported beds than in matrix-supported ones. Calcarenite and calcirudite are coherent, commonly folded clasts that are disaggregating along their margins. In matrix supported conglomerates they are tentatively identified as amorphous pockets of fine lithoclastic sediment in the otherwise pebbly conglomerate. Clasts of limestone conglomerate are almost indistinguishable from enclosing conglomerate, comprising discrete boulders less than 1 m across to ill-defined blocks or slabs up to 10 by 15 m in cross-section (Figure 9.4). Both calcarenite and conglomerate clasts are inferred to have been coherent but not lithified at the time of transport.

These clasts are compositionally and texturally identical to Daniel's Harbour Member beds. Conodonts recovered from one conglomerate clast from Daniel's Harbour include species which indicate the

clasts forming the conglomerate similarly come from the Table Point and Table Cove formations, including lower Table Point lithofacies, as well as older, St. George Group strata (Table G.1). At Eastern Head calcarenite clasts are noticeably abundant and intimately associated with large numbers of American Tickle Formation clasts in the basal, matrix-rich part of the conglomerate, suggesting that they may have come from a calcarenite interstratified with immediately underlying clastics. In all other cases these clasts are not associated with clastic clasts and are widely distributed from the base to the top of the conglomerate beds, suggesting that they were originally depositionally linked to conglomerate.

9.4.2 Primary Origin of Lithoclast Debris

Original sources of the sediment transported and deposited by debris flows and turbidity currents were predominantly the Table Point Formation, plus all slightly younger Middle Ordovician, deep-water carbonate and siliciclastic sediments overlying it (except the Cape Cormorant Formation), plus some older, platform carbonates of the upper St. George Group. The wide stratigraphic range represented by the lithoclast debris demands that these reseedimented carbonates were related to faulting and uplift while deposition of siliciclastic turbidites continued in the basin.

Two plausible, fault-related origins are considered. 1) Faults could have affected contemporaneous, albeit relict, platforms flanked by carbonate slopes that merged with the basin floor (eg. Figure 5.11.a). Debris flows generated by mass wasting along the shallow escarpments could have entrained slope and basin sediments either by plucking at the base of the flow or by triggering slides in underlying strata that were incorporated in the moving debris during transport.

Alternatively, debris flows and associated calcarenites may have been generated by mass wasting along fault scarps which uplifted and exhumed entire foreland basin successions in the basin - ie. shallow

water platformal carbonates and all deep-water carbonate and siliciclastic sediments which buried them. This explanation is favoured for the following reasons.

1) There is no conclusive evidence of contemporaneous platforms. All debris flow conglomerates and turbiditic calcarenites are interstratified with siliciclastic turbidites which everywhere succeed and are not interbedded with deep-water carbonates. If faulting affected a contemporaneous platform one might expect these debris flow conglomerates to be interstratified with toe of slope or basinal carbonates such as occur locally in Table Cove Formation ribbon limestones (Chapter section 5.4.2). Those debris flows, in contrast to Daniel's Harbour Member beds, contain very little slope-derived clasts which are mostly confined to the base of the flow, and lack both reworked Daniel's Harbour Member carbonate lithoclasts and siltstone and sandstone clasts, supporting transport down slope from a shallow source.

2) Clasts in the conglomerate that come from the sponge-oncolite biostrome, uniquely developed at the top of the Table Point platform sequence, as well as upper slope deposits of the burrowed limestone lithofacies of the Table Cove Formation, exhibit well-defined, stylo-sutured or stylo-nodular bedding (Table 9.4). Although lithification and thin bedding is proven to have formed early in the shallow sub-surface (Chapter section 4.3.4), some burial was required to have induced pressure dissolution. Burial depth can not be precisely defined. Bathurst (1980) suggests vertical stresses would become significant in dissolution processes under more than 300 m overburden, a depth which agrees with experimental compaction studies on unlithified, muddy carbonates (Shinn and Robbin, 1983). However, evidence of pressure dissolution has been documented in similar limestones subject to overburdens of no more than 90 m (Schlanger, 1964), and it is possible that pressure dissolution also began under only several tens of metres burial in these early lithified platform and upper slope

carbonates, especially in the presence of clay-rich partings.

3) Broken mudstone plates are the most common evidence of parted and ribbon limestone clasts in the conglomerates, indicating limestone beds were well lithified at the time of transport. In in situ Table Cove Formation sequences these strata are cross-cut by synsedimentary faults related to sliding which demonstrate brittle failure of the limestone beds but nowhere, however, are the beds broken up into plates. Even in gravitational slides in which primary bedding is least well-defined, disarticulated beds comprise lumpy nodules, rather than plates. This suggests that parted and ribbon limestones transported in these debris flows were more well-lithified than in situ counterparts, further suggesting they were subject to burial.

4) Clasts of semi-lithified, intrabasinal sediments, both Goose Tickle Group clastics and Daniel's Harbour Member carbonates, in some debris flow conglomerates are very large (Table 9.4) and are distributed well above the base of the bed. These features argue against incorporation by plucking at the base of the flows during transport, and suggest instead incorporation at the source of the flow in the basin.

The lithostratigraphic sequence from which the resedimented carbonates were derived is nearly everywhere the same. The only outstanding exceptions are debris flow conglomerates in the Pistolet Bay - Hare Bay area which appear to bear no clasts from either the Aguathuna Formation or the Catoche Formation. Great regional variation in the thickness of all lithostratigraphic units involved precludes determining exact amounts of uplift on escarpment sources. Taking into account what is known about thickness variations, and assuming that pressure dissolution does not necessitate very deep burial, vertical uplift could have ranged from a minimum of 80-100 m to a maximum of 400-500 m. The latter value approximates that interpreted to have occurred along the escarpment that gave rise to resedimented carbonates in the Cape Cormorant Formation (Chapter 6).

9.4.3 Multi-generation Origin of Daniel's Harbour Member Beds

Clasts of calcarenite, calcirudite, and conglomerate in the Daniel's Harbour Member conglomerates demonstrate that the immediate sources of transported debris included previously deposited debris flows and calciturbidites. Calciturbidites interstratified with American Tickle clastics below the first debris flow in some sequences (eg. Figure 9.1.1) signal earlier debris flow activity in adjacent areas of the basin. The fact that calciturbidite clasts do not occur with enclosing siliciclastics suggests they were originally interstratified with conglomerates, further suggesting that a large proportion of debris in the conglomerates have undergone more than one episode of transport and deposition.

A multi-generation origin also explains why the conglomerates are generally a heterogeneous mixture of clasts derived from a wide range of lithostratigraphic units. Had the debris flows originated by straight-forward unroofing of source areas along fault scarps, then debris flows should be comprised of only basinal and slope sediments, or solely platform carbonates.

9.5 Geographic and Stratigraphic Distribution of the Daniel's Harbour Member

Daniel's Harbour Member conglomerates and calciturbidites are widespread in the study area (Figure 9.1, inset map). Among the 23 measured sections in which American Tickle Formation clastics are exposed, there are only 9 in which these resedimented carbonates are not present. In all of those cases absence due to limited exposure cannot be ruled out. These beds are not interstratified with either the Cape Cormorant Formation or the Mainland Sandstone on the far west side of the Port au Port Peninsula. The only other area they appear to be missing from the siliciclastic sequences is in the area between just south of Bonne Bay further south to Serpentine Lake (Figure 9.1, inset). Although Goose

Tickle Group clastics occur in that area, Daniel's Harbour Member beds have not been described or mapped as components of the autochthonous sequence.

The conglomerates and calciturbidites punctuate American Tickle Formation clastics at all stratigraphic levels above the base of the formation. They appear to be more common near the base, but that this is a biased distribution introduced by limited exposure cannot be dismissed; in several places their precise stratigraphic positions, in fact, cannot be determined. The sequence in West Brook (Figure 9.1.2) demonstrates that they are present upwards of 250 m above the base of the American Tickle; the presence of Daniel's Harbour Member conglomerate lumps in the mélangé at the base of the Humber Arm Allochthon (eg. Shag Cliff) further suggests these carbonates occur relatively high in the clastic sequence.

Only a single conglomerate or calciturbidite, or conglomerate - calciturbidite couplet occurs in most measured sections. However, those in which more than one bed is present either 1) become coarser-grained and/or thicker-bedded up section, or 2) become finer-grained and/or thinner-bedded up section (eg. Figure 9.1.2), or 3) first coarsen and thicken then fine and thin up section. The third sequence, which is recognized at Black Cove (Figure 9.1.1), defines a prograding then regressing wedge of debris. 1) and 2), above, are thought to record only the lower and upper parts, respectively, of similar debris wedges.

9.6 Dimensions of Individual Beds

None of the Daniel's Harbour Member beds are thought to extend the length and width of the outcrop area. Even among closely-spaced sections in small regions it is extremely difficult to correlate with certainty any Daniel's Harbour Member beds. To some extent this is due to: 1) the inability to place many Daniel's Harbour Member beds in a precise stratigraphic context or relate them to marker beds, 2)

compositional and textural homogeneity among beds which renders one indistinguishable from another, and 3) potential lateral equivalency of debris flow conglomerates and calciturbidites. Consequently, although some beds may be correlative, especially those which occur within fairly small regions, both the debris flow conglomerates and calciturbidites are visualized as discontinuous sheets of variable thickness, length, and width in the siliciclastic basin sequence.

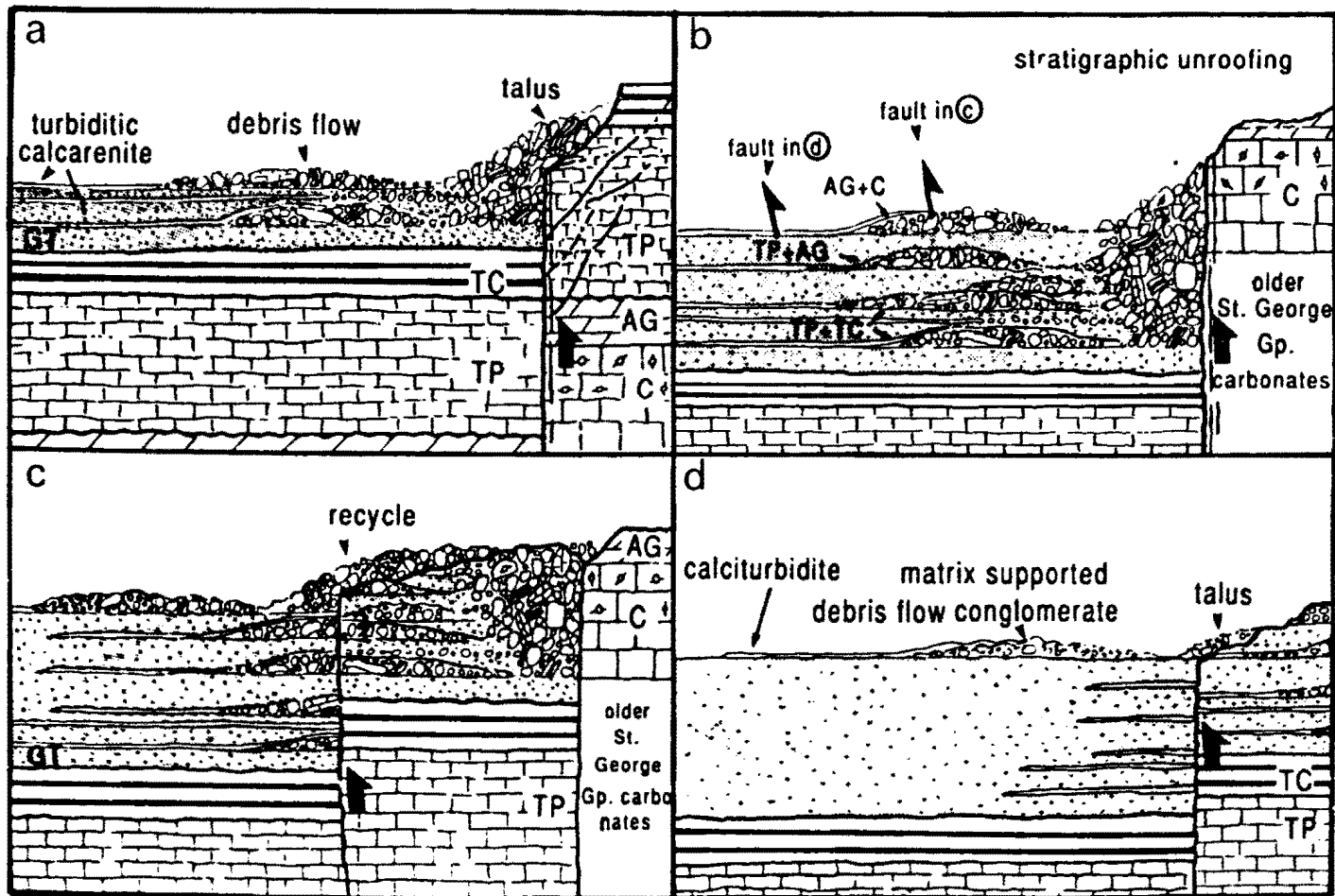
9.7 Depositional Model

Daniel's Harbour Member conglomerates and calciturbidites came from submarine escarpments that uplifted previously deposited deep-water clastics and carbonates and underlying platformal carbonate strata. They were ultimately generated by mass wasting along the escarpments and were deposited in a deep-water basin which was rapidly being filled by siliciclastic turbidites (Goose Tickle Group) derived from a geologically complex terranes located off to the east. Regionally the basin was an elongate, northeast-trending trough in which the siliciclastics were dispersed primarily toward the south.

A model which best accounts for 1) the multi-generational nature of the Daniel's Harbour Member debris flow conglomerates, 2) thickness and textural differences among the individual beds, 3) marked textural differences between clast-supported and matrix-supported conglomerates, and 4) textural trends recorded by the resedimented carbonates in many siliciclastic sequences is presented below and summarized schematically in Figure 9.8.

Initial faulting generated escarpments which uplifted surficial, basin sediments and exhumed buried carbonate slope and platform strata (Figure 9.8.a). Uplifted, unlithified siliciclastic sediments were probably transported quickly basinward in slides or slumps that, with further displacement, evolved into debris flows and turbidity currents which redeposited the sediment away from the escarpments. Mass-wasting

Figure 9.8 Model for the origin of Daniel's Harbour Member resedimented carbonates. a) Initial faulting in the basin and exhumation of platformal carbonates (Table Point Fm. (TP), Aguathuna Fm. (A), Catoche Fm. (C)) and overlying carbonate slope (Table Cove Fm. (TC)) and siliciclastic basin strata (Goose Tickle Gp. (GT)). b) Continued uplift and stratigraphic unroofing recorded by predominant clast composition in first generation debris flows. c) Uplift of basinal strata and proximal resedimented carbonates along another fault basinward of the original giving rise to clast-supported conglomerates with clasts of limestone conglomerate and calciturbidites. d) Uplift of basinal strata and distal resedimented carbonates along another fault yet further basinward of the original giving rise to matrix-supported debris flow conglomerates composed almost exclusively of pebble size limestone debris and large clasts of siliciclastic sediment remoulded into matrix during transport.



of exposed carbonates along the escarpments gave rise to talus piles generated by rock falls and slumps. Such debris, destabilized by further mass wasting or changes in slope or seismic shocks associated with faulting, was episodically transported basinward in rock slides which evolved into flows that transported coarse debris away from the escarpment. The thickest, coarsest and, possibly amalgamated, flows were deposited nearest the escarpment. Successive flows were probably compositionally distinct, recording stratigraphic unroofing of the source as long as uplift continued (Figure 9.8.b). Turbidity currents, either generated independently at the escarpment or developed above the debris flows transported finer-grained, lithoclastic debris, in some cases depositing it directly atop a conglomerate, but more commonly traveling beyond the snout of the flow and depositing the material further out in the basin.

First generation debris flows and turbidites deposited adjacent to the escarpment were subsequently incorporated in younger debris flows (Figure 9.8.c). Second generation flows and currents could also have been triggered by wholesale uplift along faults basinward of the original escarpment which, like the older structures, uplifted and exposed buried slope and platform strata. Alternatively, uplift along the younger structures may have been much less, triggering slides that evolved into debris flows in only the surficial, basinal sediments, including resedimented carbonates and interstratified siliciclastic turbidites. Remobilization of proximal, first generation debris flows and turbidites gave rise to limestone-dominated, clast-supported conglomerates composed of clasts representing a wide stratigraphic range due to mixing of several first generation flows, and a wide range of sizes inherited from the older flows, including barely disintegrated olistoliths. Basinward migration of fault scarps generated a prograding wedge of resedimented debris, while subsequent decline in faulting and mass wasting at the escarpment caused regression of the debris back

toward the escarpment.

Uplift and remobilization of more distal, thinner and finer-grained, first generation flows (Figure 9.8.d), in contrast, involved gravitational sliding of underlying and interbedded basinal, siliciclastic sediments. Remoulding of those sedimentary packages during transport gave rise to matrix-supported, second generation flows.

PART II
SEDIMENTATION AND TECTONICS

CHAPTER 10
REGIONAL FORELAND BASIN EVOLUTION: INTRODUCTION

The vertical sequence of sedimentary rocks that make up the Ordovician foreland basin everywhere record a deepening-upward depositional history expressed by the dramatic change from shallow marine, carbonate sediments to deep water, siliciclastic sediments prior to emplacement of the Humber Arm Allochthons. Phases of foreland basin development that are common to all sequences in the study area (Figure 10.1) include: 1) tectonic uplift and subaerial exposure of the passive margin, carbonate platform resulting in a period of nondeposition, erosion and/or karstification (Aguathuna Formation and the St. George Unconformity); 2) marine flooding of the deformed and eroded platform and renewed carbonate deposition, first in peritidal environments, then in shallow subtidal settings, and finally in more shallow subtidal to peritidal environments (Table Point Formation); 3) rapid deepening and drowning of the platform succeeded by deposition of deep-water carbonates (Table Cove and Cape Cormorant Formations) and/or shale (Black Cove Formation) in slope and basinal environments; 4) influx of compositionally and texturally immature siliciclastic sediments eroded from lithologically complex source terranes adjacent to the foreland basin and rapidly deposited by turbidity currents in a deep, basinal setting (American Tickle Formation and the Mainland Sandstone); 5) exhumation of foreland basin carbonates and clastics and, locally, underlying passive margin carbonates, along faults in the basin and redeposition as debris flows and calciturbidites (Daniel's Harbour Member). These phases record the physical response of a stable, carbonate platform to convergence and subduction of the North American

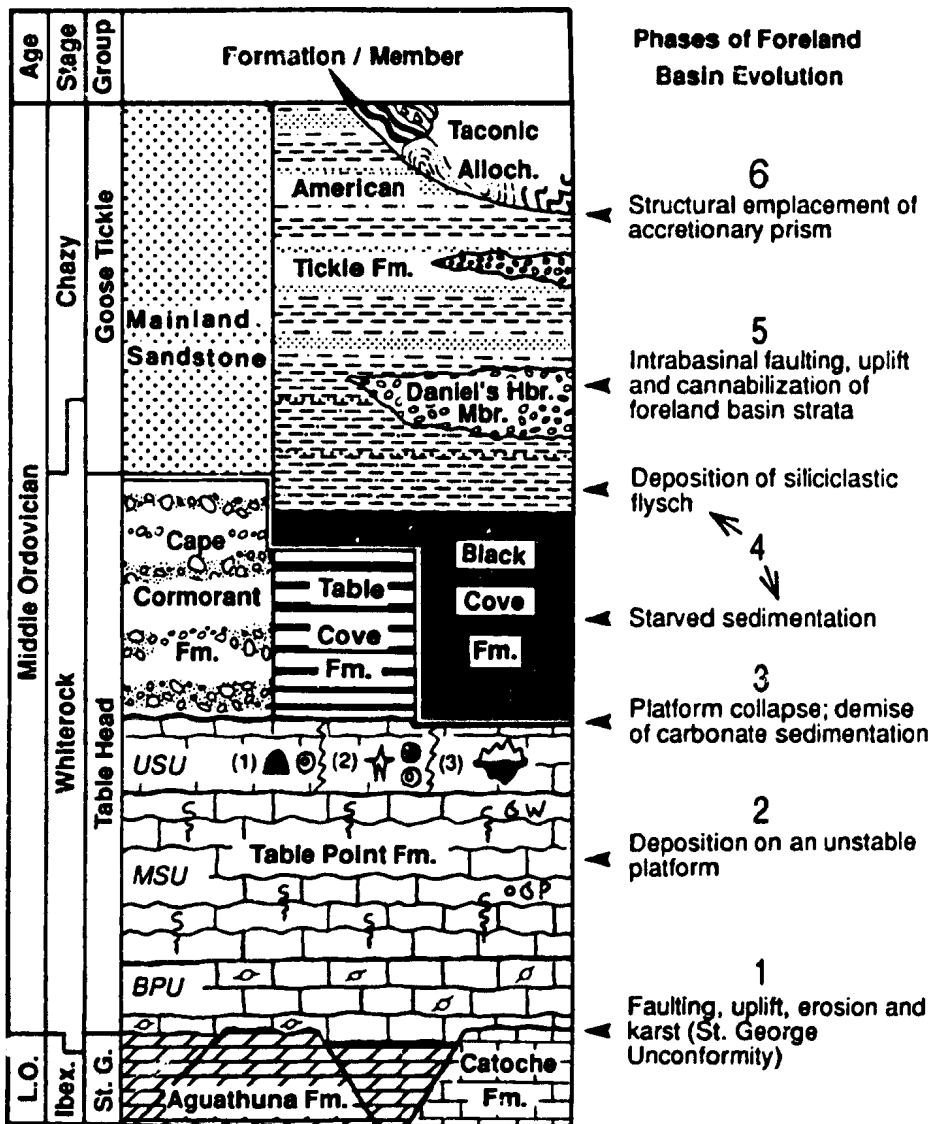


Figure 10.1 Phases of foreland basin evolution in the upper St. George, Table Head and Goose Tickle Groups. L.O., Lower Ordovician; Ibex., Ibexian; St. G., St. George Group; BPU, Basal Peritidal Unit; MSU, Middle Subtidal Unit; USU, Upper Subtidal Unit. Key to other symbols is in Appendix A.

continent.

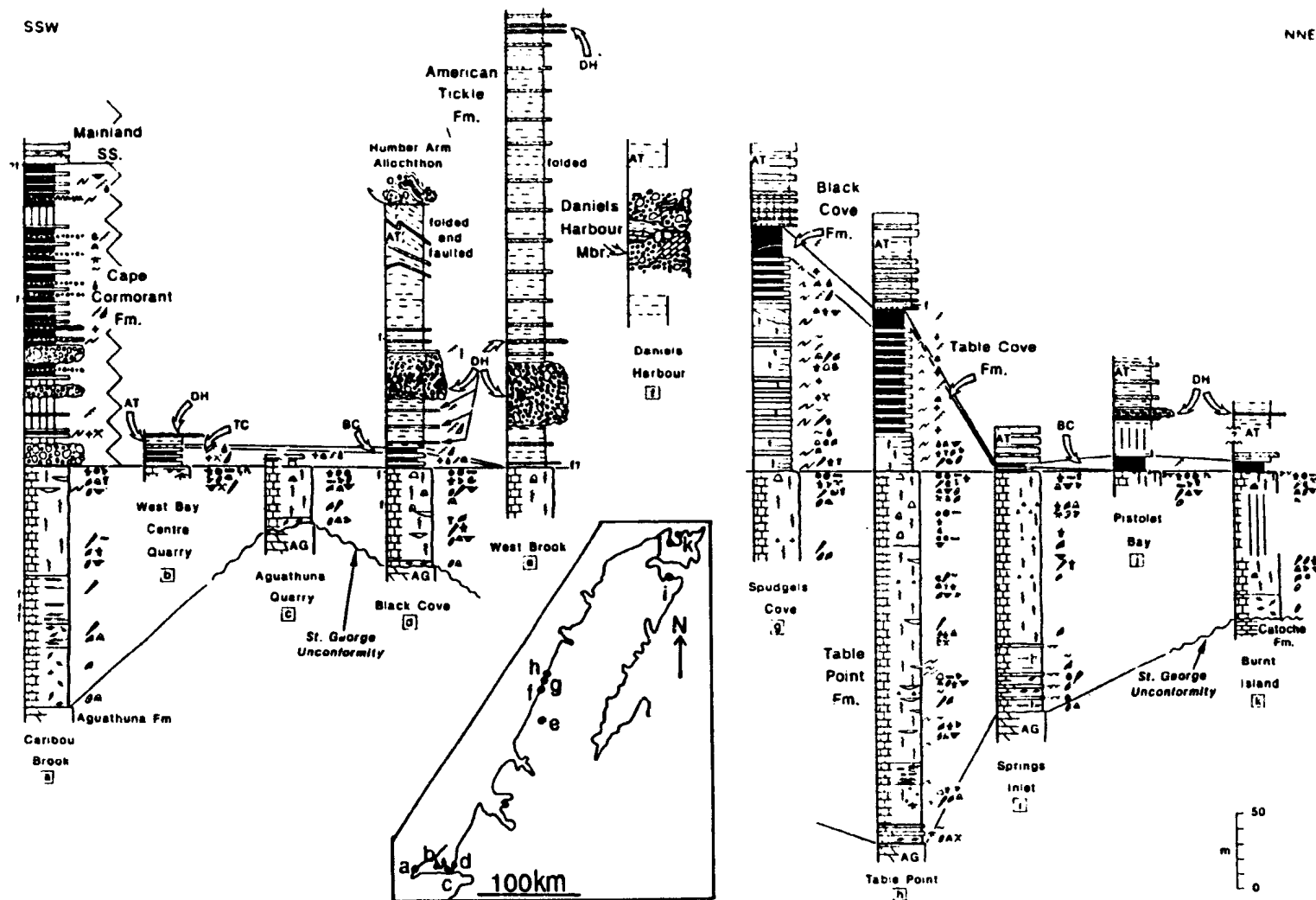
A cross-section of measured sections across the study area demonstrates that the foreland basin is most accurately visualized as a complex, three-dimensional mosaic of carbonate and terrigenoclastic units (Figure 10.2) which reflects a combination of: 1) lateral changes in stratigraphic relief on the St. George Unconformity; 2) large variations in the thickness of overlying platform limestones and in the vertical and lateral distribution of lithofacies which comprise them; 3) major differences in the type and thickness of deep-water sediments deposited directly atop the platform, namely two different types of slope to basinal carbonates and, locally, shale, plus variations in the vertical and lateral distribution of lithofacies which comprise them; 4) lateral and vertical variations in the distribution of siliciclastic lithofacies that fill the basin and in resedimented conglomerates and calciturbidites interstratified with them; and 5) lateral changes in contact relationships with the overlying allochthons. Heterogeneity among the sedimentary sequences reflects the overprint of local tectonics on regional foreland basin development.

It will be shown in the following chapters that a major factor controlling both regional basin evolution and local sedimentation is synsedimentary faulting. It is postulated that the structures which were active were reactivated, rift-related faults linked to crystalline basement. Although the exact configuration of the rifted basement cannot be demonstrated by field relationships, original horst and graben structure is interpreted to be indirectly expressed (to various degrees) by the trend, facing direction and polarity of Acadian faults which cross-cut early Paleozoic strata and uplift basement, and are interpreted to have been reactivated with reverse-sense displacement during Siluro-Devonian orogenesis (Grenier, 1990). In support of this interpretation is evidence that some mapped Acadian faults influenced

Figure 10.2 Measured sections through the Table Head Group and overlying Goose Tickle Group from Port au Port Peninsula to Pistolet Bay (from Stenzel et al., 1990). Key to symbols is in Appendix A.

SSW

NNE



early Ordovician (passive margin) carbonate sedimentation (Knight and Saltman, 1980). Evidence that this fault system influenced middle Ordovician foreland basin development lies in the fact that major changes in sediment thickness or lithofacies commonly occur across mapped Acadian structures. Reactivation of preexisting, rift-generated faults is also documented in other ancient forelands (eg. Froitzheim and Eberli, 1990).

Each of the five tectono-sedimentologic phases of foreland basin development and emplacement of the allochthons are described and discussed in Chapters 11-16. The influence of local tectonics on sedimentation are exemplified in each; all cross-sectional and aerial reconstructions employ mapped Acadian faults as basement-linked structures that were active during Ordovician time. A tectonic model for regional foreland basin evolution is presented in Chapter 17.

CHAPTER 11

PHASE 1: FAULTING AND UPLIFT:

THE ST. GEORGE UNCONFORMITY

The regional distribution of the Aguathuna Formation (Chapter 3) demonstrates that peritidal environments occupied the entire western Newfoundland zone of the continental shelf from late Early Ordovician (Ibexian) through early Middle Ordovician (Whiterockian) time. Similar peritidal carbonates of the same age (Romaine Formation) occur on the Mingan Islands in the St. Lawrence Lowlands indicating that the same conditions characterized the shelf another 50-100 km further inboard of the margin (Desrochers, 1985). Deposition of the Aguathuna above the dominantly subtidal Catoche Formation indicates shoaling of the platform and is interpreted to reflect either slowing of sea level rise that had begun at the beginning of the late Early Ordovician (basal Arenig), or a sea level fall (Figure 4.8).

Perception of eustasy as a fundamental control on platform sedimentation during this time, as is recorded in underlying Middle Cambrian through early Early Ordovician carbonate sequences (Chow and James, 1987; Knight and James, 1987), suggests deposition occurred on a shelf experiencing uniform, thermal subsidence. The St. George Unconformity, originally thought to simply define the top of the Aguathuna, is correlated with Knox Unconformity in the U. S. A. Appalachians, and with numerous other unconformities at approximately the Lower - Middle Ordovician boundary continent-wide, which are interpreted to record a major regression resulting from eustatic sea level fall (Mussman and Read, 1986). However, there are several aspects of the Aguathuna, all intimately related to the St. George Unconformity, that are anomalous to stable, passive margin carbonate accumulations and strongly suggest that tectonics influenced peritidal sedimentation. They include: 1) deformation of carbonates beneath the unconformity, 2) structurally

controlled karst, 3) great stratigraphic relief on the unconformity, and 4) discontinuous distribution of the upper Aguathuna dolostones above the unconformity. These features are detailed in a regional sedimentologic and stratigraphic study of the Aguathuna Formation and St. George Unconformity by Knight et al. (in press) which links them to synsedimentary tectonic uplift. They are briefly described and illustrated, and their tectonic significance discussed below.

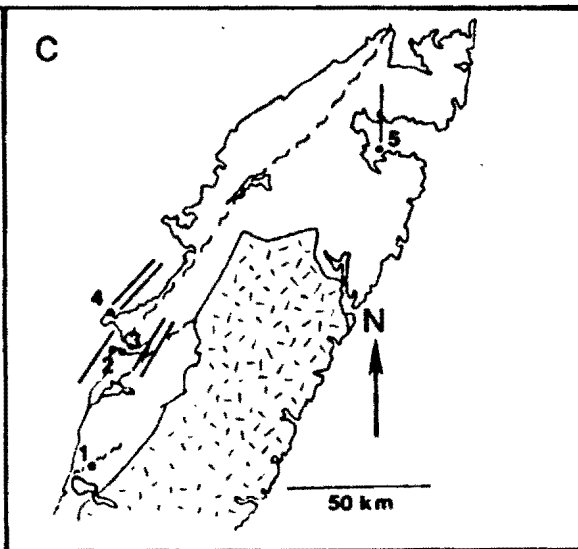
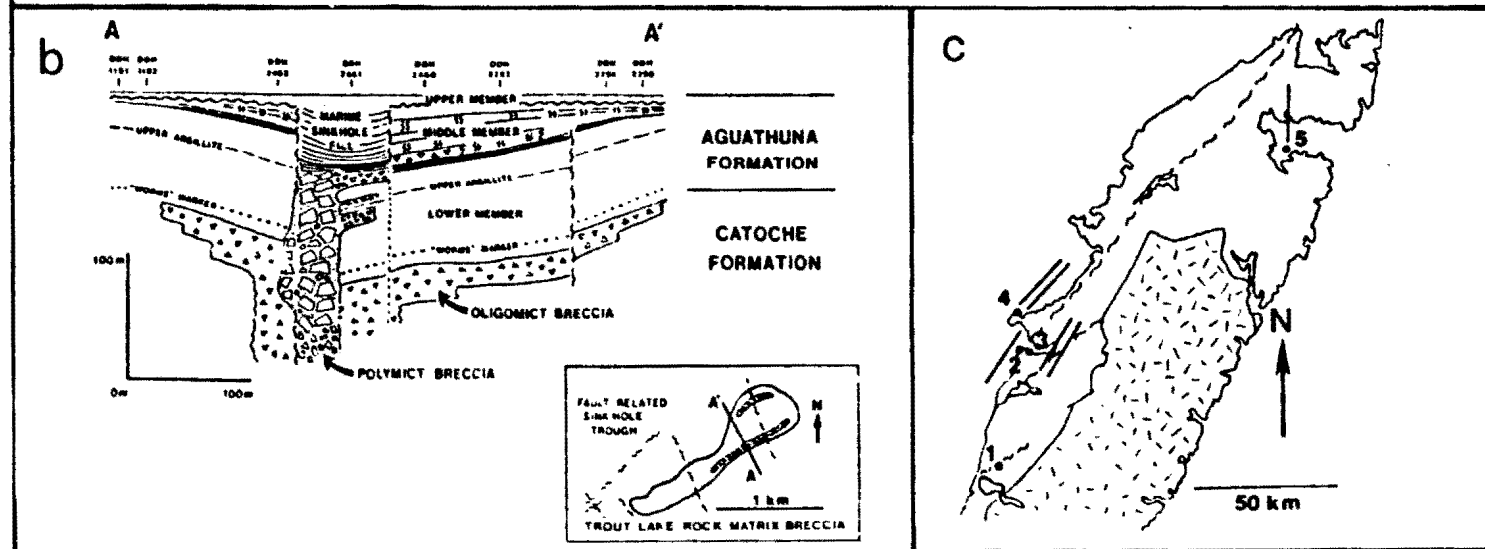
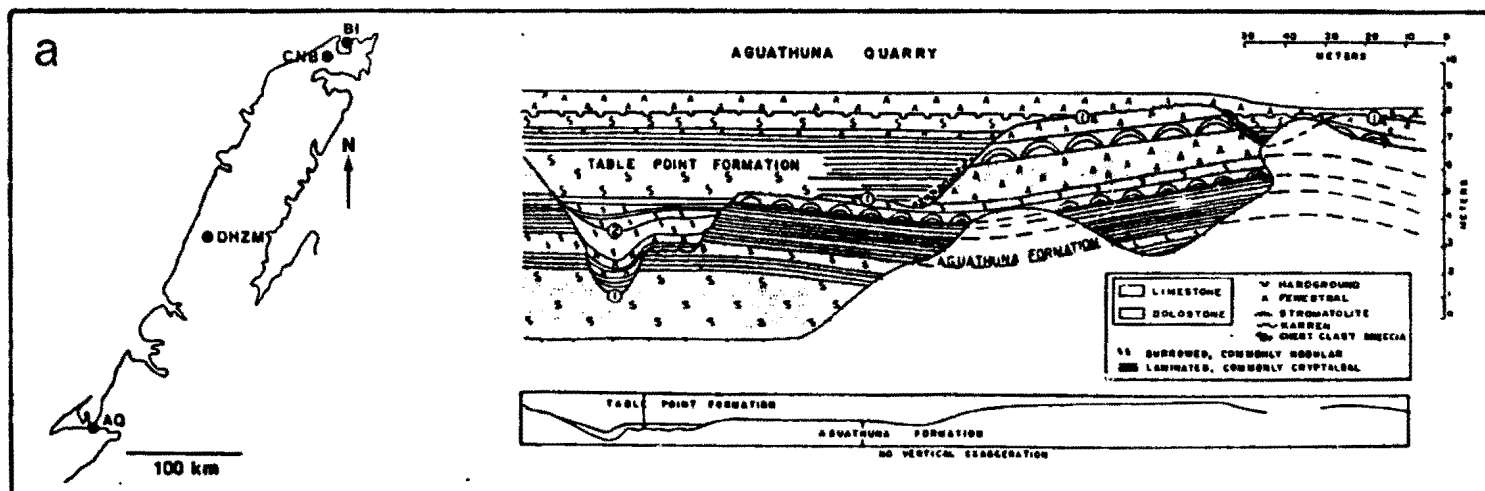
11.1 Deformation Beneath the Unconformity

Carbonates directly beneath the St. George Unconformity are tilted or folded at several localities (Figure 11.1.a). Deformation is seen in Aguathuna Quarry on Port au Port Peninsula where lower Aguathuna dolostones are disposed in broad, low amplitude folds, while overlying Table Point Formation limestones onlap the unconformity with angular discordance to Aguathuna bedding. Similar folding is recognized in the Catoche Formation directly below the unconformity on Burnt Island peninsula, as well as in outcrop on the Cape Norman barrens immediately adjacent to a lineament interpreted as a paleofault (Knight, 1986). Tilting of the platform is also recognized in subcrop in the Daniel's Harbour Zinc Mine area where cores at the mine and in areas immediately to the north show the St. George Unconformity to bevel a gently south-dipping, lower and middle Aguathuna sequence (Lane, 1990).

Folding and tilting of strata directly below the unconformity indicate deformation of the platform prior to, or contemporaneous with subaerial exposure and erosion. Since folding is not recognized everywhere it is unlikely to have been caused by regional, horizontal compression. Instead, local deformation is thought to be related to stresses generated by differential displacements along nearby faults (Chapter section 11.3, below).

Figure 11.1 Sub-unconformity deformation of platformal carbonates and structurally controlled karst.

a) Vertical cross-section through the Aguathuna and Table Point formations in Aguathuna Quarry, Port au Port Peninsula, showing gentle folding of Aguathuna dolostones beneath the St. George Unconformity (1) (from James et al., 1989). (2) marks an intraformational erosion surface in peritidal limestones at the base of the Table Point Formation. Inset map shows other locations where carbonates beneath the unconformity are folded or tilted. AQ, Aguathuna Quarry; DHZM, Daniel's Harbour Zinc Mine; CNB, Cape Norman barrens; BI, Burnt Island peninsula. b) Vertical cross-section through the Trout Lake Breccia at the Daniel's Harbour Zinc Mine (from Lane, 1990). Northeast-trending fracture and fault zones controlled the movement of undersaturated groundwaters and subsurface dissolution of limestone beds in the Catoche Formation giving rise to stratabound, oligomictic collapse breccias and later discordant, tabular bodies of polymictic collapse breccia. Inset shows a plan view of the Trout Lake Breccia and the location of other fractures in the area. c) Locations and orientations of karst features on the Great Northern Peninsula (data from Knight et al., in press). 1 = linear cave, 2 = solution-enlarged joints, 3 = joints with dolomite halos, 4 and 5 = fissure.



11.2 Structurally Controlled Karst

Karst features that formed during deposition of the Aguathuna and generation of the St. George Unconformity are widespread and proven in many places to be closely related to local fracture and/or fault zones. The most well-documented example is at the Daniel's Harbour Zinc Mine where two discrete episodes of karst are recognized (Lane, 1990; Figure 11.1.b). The first episode occurred during deposition of middle Aguathuna dolostones. Subsurface dissolution of limestone beds in the Catoche Formation caused collapse and gave rise to a large, rock-matrix breccia body, the Trout Lake Breccia, which subsequently became host for zinc and lesser lead sulphides. Location and development of the collapse structure and individual, stratabound breccias which comprise it are related to two, northeast-trending, fault and fracture zones. Continued dissolution collapse and differential displacements along bounding structures permitted anomalously thick accumulations of middle Aguathuna dolostones in a subsidence doline above the breccia. The second episode of karsting accompanied formation of the St. George Unconformity and deposition of overlying upper Aguathuna dolostones. Dissolution was restricted to near vertical zones along the margin of the Trout Lake Breccia and gave rise to tabular and discordant, polymictic breccias. Several tens of metres of vertical offset on lower and middle Aguathuna dolostones on either side of these bodies indicates concurrent faulting. Elongate, steep-sided sinkholes that formed on the unconformity above these breccias became sites of anomalously thick upper Aguathuna carbonate accumulations.

North of the mine karst features include comparatively small, discordant caves (30 cm wide), fissures, and solution enlarged joints, all filled with dolomitic, sandy or pebbly mud believed to come down from the unconformity, and joints with dolomite halos, all of which occur in Catoche Formation limestones (Knight *et al.*, in press; Figure 11.1.c). In the Hawke Bay - Port au Choix area these structures consistently

trend northeast, while that which occurs in Hare Bay trends nearly north-south.

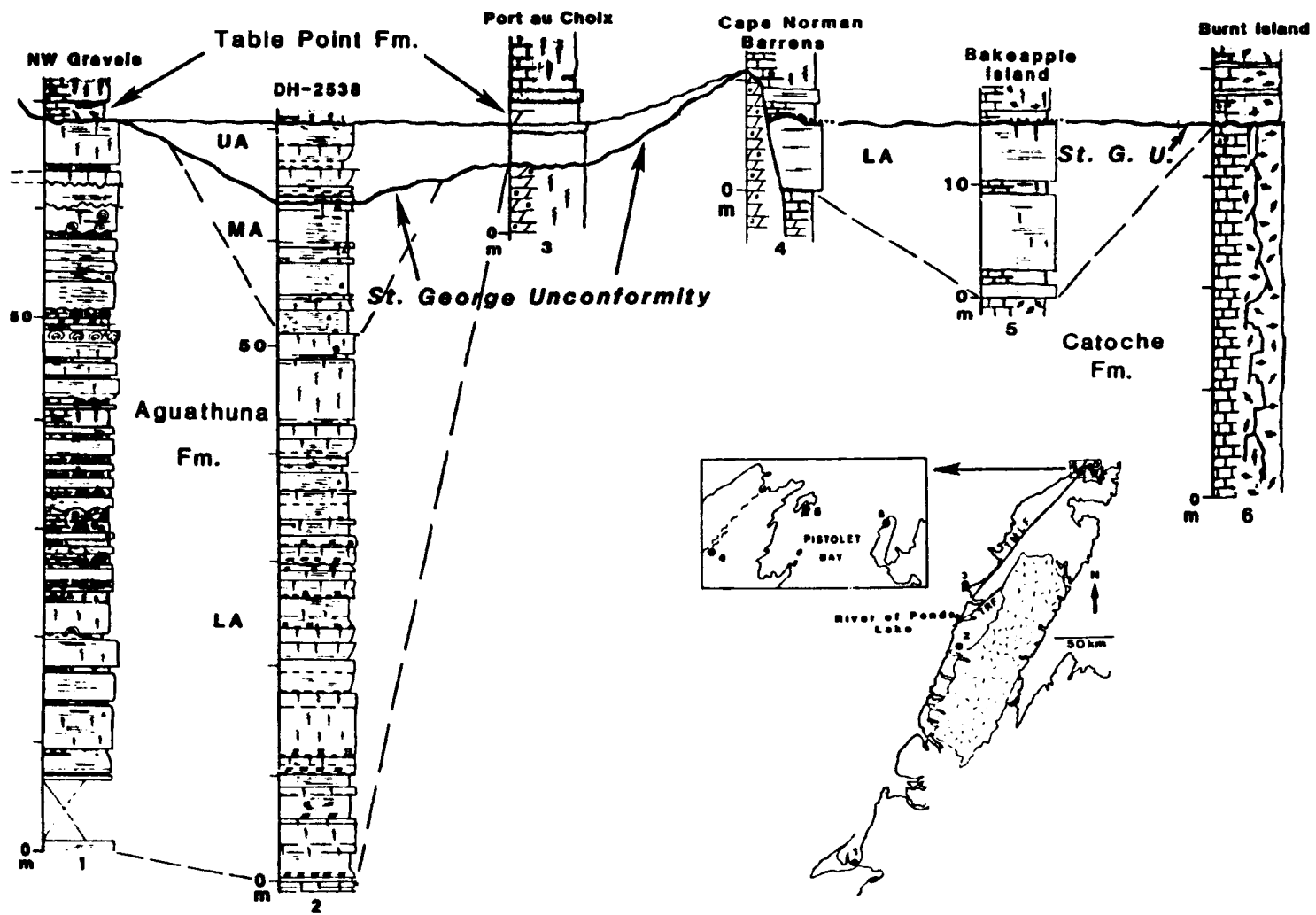
Fractures, faults and joints facilitated movement of undersaturated, meteoric or mixed groundwaters that caused dissolution of carbonates in the subsurface and, locally, dolomitization (Lane, 1990; Knight *et al.*, in press). They are interpreted as expressions of platform deformation that preceded or accompanied exposure and formation of the St. George Unconformity. Parallelism of these structures suggests they formed in response to regionally imposed stress.

11.3 Stratigraphic Relief on the St. George Unconformity

The most obvious, anomalous feature of the Aguathuna Formation is dramatic variations in thickness which, to a large extent, is an expression of great stratigraphic relief on the St. George Unconformity (Figure 11.2). This phenomenon is recognized on a regional scale, as well as on a local scale in all places where these strata are exposed. In neither case are directional, along-strike or across-strike variations perceived.

Between Daniel's Harbour and Port au Choix Peninsula, for example, the Aguathuna consists of three, markedly different stratigraphic sequences. At the Daniel's Harbour Zinc Mine (Figure 11.2.2) the Aguathuna is generally 65-70 m thick and is represented by all three informal members; the St. George Unconformity defines the top of the middle Aguathuna. A comparably thick sequence occurs as far north as the northeast shore of River of Ponds Lake (not illustrated, see inset map in Figure 11.2 for location), but the middle member is not recognized as a discrete unit and the unconformity separates lower Aguathuna from upper Aguathuna dolostones. The Aguathuna thins dramatically from there toward the northwest. On the northwest shore of River of Ponds Lake and on Pointe Riche Peninsula (Figure 11.2.3) the unconformity truncates upper Catoche Formation dolostones and is

Figure 11.2 Stratigraphic relief on the St. George Unconformity; cross-section of measured sections. 1 is modified after Pratt (1979) and Knight and James (1987). 2 is from this study. Comparable Aguathuna sequences occur in all cores from around the mine (except those that penetrate collapse structures) and in outcrop at Table Point. 3 and 4 are from Knight *et al.* (in press). On the Cape Norman barrens the Aguathuna thins to zero thickness along a northeast-trending lineament (paleofault) flanked on the west by a rubble breccia (paleosol) that overlies gently folded Catoche Formation dolostones and is overlapped by Table Point Formation limestones (Knight, 1986c). 5 and 6 are modified after Knight *et al.* (in press). White beds are dolostone; shaded beds are limestone; dashes are shale. LA, lower Aguathuna; MA, middle Aguathuna; UA, upper Aguathuna; St. G. U., St. George Unconformity. TRF, Torrent River Fault; TMLF, Ten Mile Lake Fault. Key to other symbols is in Appendix A.



directly overlain by the upper Aguathuna.

These contrasting sequences demonstrate more than 50 m stratigraphic relief on the St. George Unconformity. Preservation of very thick lower and middle Aguathuna sequences below the unconformity in the south and complete erosion of the lower Aguathuna in the northwest indicates those two areas underwent very different histories of exposure and erosion that are easily explained only by differential uplift. The locus of dramatic thinning between sections coincides with the northeast trending Torrent River Fault (Figure 11.2, inset) which is inferred to have been active and to have defined a major structural boundary between an uplifted crustal block in the north and a more continuously subsiding one to the south.

Similar relationships are seen in a series of three, even more closely-spaced sections exposed between the Cape Norman barrens and Burnt Island peninsula at the tip of the Great Northern Peninsula (Figure 11.2.4-6). They demonstrate ~20 m stratigraphic relief on the unconformity and define a block-faulted terrane consisting of a graben flanked by two topographic highs. The lineament that marks the western crustal block boundary approximately coincides with the northeast-trending Ten Mile Lake Fault zone (Figure 11.2, inset), which must have been active and controlled differential uplift of the platform during this time. Rapid lateral thinning to the east is similarly thought to reflect the presence of a second, major structural boundary between Bakeapple Island and Burnt Island peninsula in Pistolet Bay. Furthermore, complete erosion of the Aguathuna on the Cape Norman barrens and Burnt Island and preservation of a very thin lower Aguathuna section on Bakeapple Island, especially compared to sequences found around Daniel's Harbour, suggest that this entire area experienced greater and/or more prolonged uplift and exposure.

Along- and across-strike changes in stratigraphic relief on the St. George Unconformity demonstrate that subaerial exposure and erosion

accompanied heterogeneous uplift of the platform regionally. Coincidence of rapid lateral changes in the thickness of Aguathuna strata preserved with proven, albeit younger, fault zones indicates that differential erosion resulted from differential displacement along synsedimentary faults that dissected the platform. Identical relationships between a subaerial erosion surface and a block-faulted carbonate terrane are recognized on the island Jamaica adjacent to the Cayman Trough (Hendry, 1987).

11.4 Discontinuous Distribution of the Upper Aguathuna

Upper Aguathuna dolostones discontinuously mantle the St. George Unconformity (Figure 11.2); that surface is otherwise disconformably overlain by peritidal carbonates at the base of the Table Point Formation. It is possible that upper Aguathuna sediments were deposited widely across the shelf and that their absence locally is the result of later erosion. Possible evidence in support of that hypothesis are sub-unconformity karst features filled with dolomitic sediments that came from the unconformity surface (Chapter section 11.2) and could, therefore, be remnants of the upper Aguathuna (eg. Burnt Island). Alternatively, the limited distribution of the upper Aguathuna suggests that inundation of the platform and reestablishment of peritidal environments was dictated by topography on the tectonized shelf. Whether upper Aguathuna sediments are erosional remnants or reflect original, depositional distribution, they indicate that topography generated and/or perpetuated by differential uplift and subsidence of independent blocks continued to control sedimentation after wholesale uplift.

11.5 Synthesis

The sedimentologic and stratigraphic features outlined above indicate that deposition of the Aguathuna Formation was interrupted by a period of regional tectonism that transformed the intact, passive margin

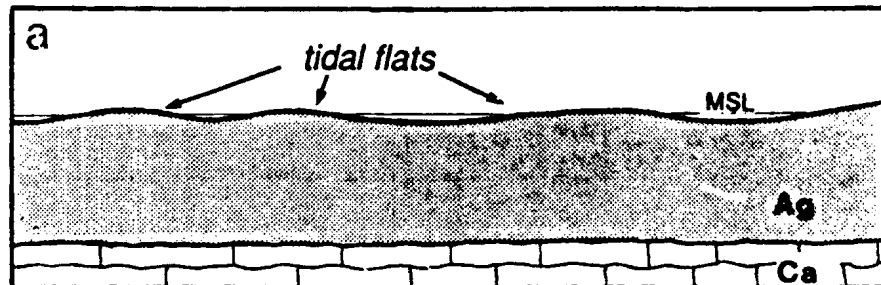
platform into a heterogeneous mosaic of fault-bounded blocks (Figure 11.3). Deformation was accompanied by regional uplift and subaerial exposure. Erosion and dissolution of the exposed platform created an irregular karst terrane recognized regionally as the St. George Unconformity. Coincidence of regional uplift of the platform with eustatic sea level fall may have exacerbated the effects of exposure. Differential displacements along faults that defined the platform blocks resulted in different depths of erosion, recognized by several tens of metres of stratigraphic relief on the unconformity. Continued differential subsidence perpetuated topography across the shelf that controlled the locus of marine flooding, reestablishment of very restricted peritidal environments, and deposition of upper Aguathuna dolostones above the unconformity.

Synsedimentary faulting generated a shelf-wide, low relief horst and graben terrane. The absence of sedimentary conglomerates or breccias suggests that faulting did not generate high relief escarpments. Platform blocks were predominantly defined by north-east-trending faults; similarly oriented structures influenced subsurface karst at the Daniel's Harbour Zinc Mine. Northeast-trending faults best account for lateral changes in the Aguathuna in other areas as well, but easterly-trending faults are inferred to have been active locally (eg. west Port au Port Peninsula).

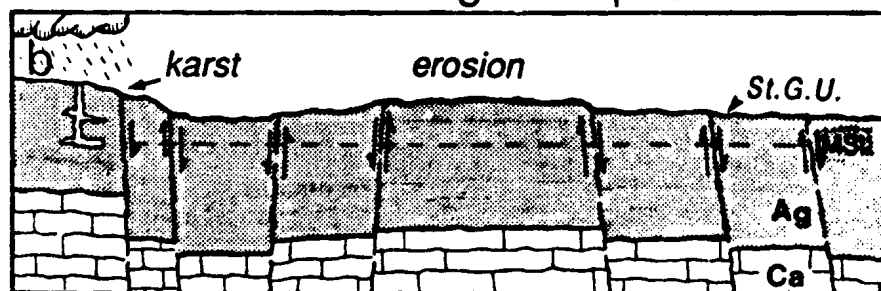
11.6 Tectonic Significance

Closure of the Iapetus Ocean and formation of a subduction zone outboard of the North American continental margin is inferred to have begun no later than early Ordovician time. Isotopic ages for obducted ophiolites in the Hare Bay Allochthon and in the Dunnage Terrane range from 477-494 Ma, which spans late Tremadocian to early Llanvirnian time (Dunning and Krough, 1985). Proximity of the continent to volcanic island arcs is indicated by the influx of chloritic clays derived from

Deposition of the lower Aguathuna



Block-faulting and Uplift



Local Subsidence; Deposition of upper Aguathuna

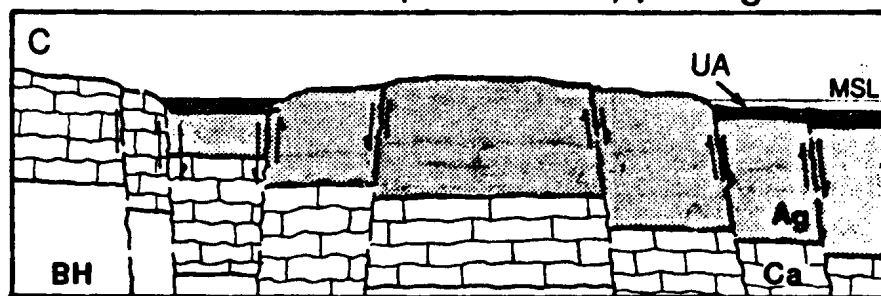


Figure 11.3 Schematic vertical cross-section across the platform (a) prior to, (b) during, and (c) after formation of the St. George Unconformity (St. G. U). Ag, Aguathuna Fm.; UA, upper Aguathuna; Ca, Catoche Fm.; BH, Boat Harbour Fm.; MSL, mean sea level.

mafic sources deposited on the continental slope and rise beginning in the early Arenig (Botsford, 1987).

Widespread block-faulting and uplift of the carbonate platform that interrupted deposition of the Aguathuna Formation and gave rise to the St. George Unconformity during the late Arenig postdates initial ocean closing by at least 10 million years. There is little indication that sedimentation on the platform was influenced by the change in the tectonic regime of the continental margin prior to this. Weak signals of tectonically influenced sedimentation may be recorded in the lower Aguathuna (Lane, 1990); 1) variations in the thickness of the basal, cyclic unit which suggest that subsidence of the platform was not uniform regionally and may have been controlled by differential displacements along synsedimentary faults and 2) widespread deposition of burrowed, subtidal sediments at the top of the lower member indicates regional deepening of the platform, possibly a consequence of a pulse of rapid subsidence prior to uplift.

Deformation and differential uplift of the platform was protracted and regional in extent. Initial fracturing and faulting is recognized only in the Daniel's Harbour Zinc Mine area, where deformation was accompanied by karsting (Figure 11.1.b). The actual extent of deformation across the shelf is difficult to assess because in most other areas the middle Aguathuna, which brackets the event, is not present or has yet to be recognized. (One possible exception is at Bonne Bay where the formation is very thick and, thus, may record fairly continuous sedimentation; faunal data necessary to determine which members of the Aguathuna are present has not been obtained.) Widespread development of the St. George Unconformity and, more importantly, differential erosion of the carbonates which underlie it and the discontinuous distribution of upper Aguathuna sediments which overlie it, demonstrate that a later, major episode of block-faulting affected the platform regionally.

These expressions of tectonically influenced sedimentation are

interpreted to mark the first response of the continental shelf to convergence between the continent and subduction zone and, thus, define the first phase of foreland basin evolution. Corroborative evidence that deformation of the platform was a consequence of continued convergence comes from coeval, continental slope and rise sediments of the Cow Head Group (Figure 11.4). In most sequences catastrophic faulting and tectonic collapse of the carbonate platform margin is interpreted to be recorded by deposition of two megaconglomerates, Beds 12 and 14, both composed of variety of carbonate lithoclasts ranging in age from late Cambrian to late early Ordovician, and indicating derivation from high relief fault scarp sources (James and Stevens, 1986). Locally tectonic collapse of the margin is interpreted to be recorded by abrupt cessation of carbonate sediment delivered to the slope from the platform margin and deposition of abundant shale (James et al., 1987; Botsford, 1987). That change, which coincides with emplacement of Bed 12, indicates drowning of margin directly upslope, most likely caused by synsedimentary faulting. Initial deformation of the platform recorded in the Daniel's Harbour area is not precisely dated by shelly fossils or conodonts, but its relative biostratigraphic age suggests it may coincide with emplacement of Bed 12 and is, therefore, a subtle expression of more intense deformation along the margin proper. The St. George Unconformity correlates closely with emplacement of Bed 14, indicating that faulting and uplift inboard on the shelf accompanied collapse at the margin. These relationships illustrate the inboard-progressing, diachronous nature of deformation during this time, thereby supporting the interpretation that it is intimately related to continued convergence and encroachment of the subduction zone on the continent margin.

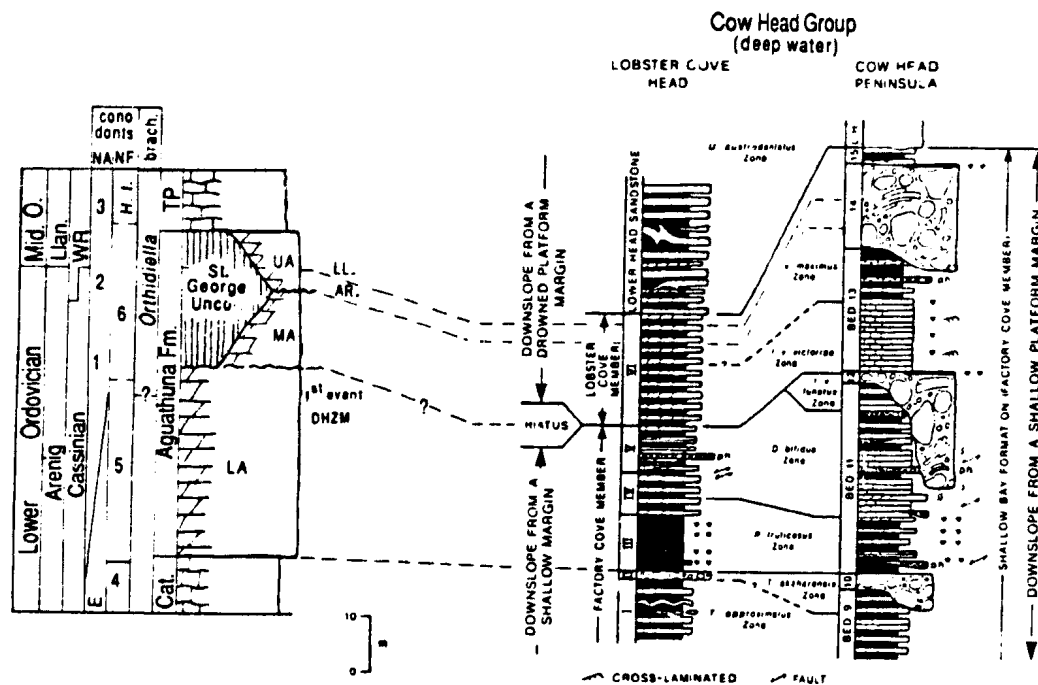


Figure 11.4 Stratigraphic sections showing correlations of lithologic units and synsedimentary deformation events between the Agathuna Formation and coeval deep water sediments of the Cow Head Group (the latter are from James *et al.*, 1987). Faunal zones are from Ross and James, 1987 and Williams *et al.*, 1987. WR, Whiterock; Llan., Llanvirn; Cat., Catoche Formation; LA, MA, UA, lower, middle and upper Agathuna; NF, Newfoundland; NA, North America; brach., brachiopod; H. t., *Histiodelle tableheadensis*.

CHAPTER 12

PHASE 2: DEPOSITION ON A TECTONICALLY UNSTABLE PLATFORM

The Table Point Formation (Chapter 4) records total inundation of the block-faulted and eroded platform and reestablishment of shallow marine environments during early Middle Ordovician (Whiterockian) time. Actual extent of these conditions further inboard on the continental shelf is difficult to determine because this period of time is represented by an erosional unconformity on the Mingan Islands, indicating either contemporaneous or somewhat later exposure and erosion (Desrochers, 1985).

Table Point limestones are compositionally and texturally much like other Paleozoic and modern platform carbonates. Moreover, there is a certain degree of correlation between the formation's three-phase depositional history (inundation, deepening, shoaling) with that recorded by same age sediments deposited on the passive, southwest margin of the North American continent, suggesting that sedimentation was partly controlled by eustasy (Chapter section 4.5, Figure 4.8). Table Point sequences, however, also bear structures that indicate concurrent tectonism, and are characterized by great lateral variation in total thickness and in the make-up and thickness of lithofacies assemblages which comprise them. Thus, these otherwise typical, shallow marine carbonates are interpreted to have been deposited on an unstable, differentially subsiding platform.

12.1 Synsedimentary Deformation Structures and Deposits

Evidence of synsedimentary, tectonic deformation is scattered but widespread both within and at the very top of the Table Point Formation. A list of deformation features and localities where they are found is in Table 12.1. They are described, illustrated, and discussed below.

Table 12.1 Deformation Features in the Table Point

Locality	Intraform.* Erosion Surfaces	Gravitational Slides	Pebbly Limestone Conglomerate	Fractures	Flaggy Conglomerate
Burnt Island	-----	-----	-----	1) echinoderm grainstone & 2) shale filled at the very top of the formation	locally at the very top of the formation
Pistolet Bay (west side)	-----	-----	present locally at the very top of the formation	shale filled at the very top of the formation	-----
Bakeapple Island	-----	-----	-----	shale-filled at the very top of the formation	-----
Hwy. 430 (roadcuts)	in BPU strata	-----	-----	shale filled at the very top of the formation	-----
Gargamelle Cove	-----	in the MSU limestones & at the very top of the formation	(component of gravitational slide masses)	carbonate mud filled directly below top gravitational slide	-----
River of Ponds Lake	-----	-----	very top of the formation	carbonate mud filled directly below top conglomerate	-----
Table Point	-----	several in the BPU & MSU	-----	-----	-----
DHZN (cores)	-----	discordant bedding in BPU strata	-----	-----	-----
Southwest Feeder	-----	-----	very top of the formation	-----	-----
Black Cove	in BPU strata	-----	-----	-----	-----
Agathuna Quarry	in BPU strata	-----	-----	-----	-----
Caribou Brook	-----	thin horizons of discordant bedding in the top 15 m	-----	-----	-----
Big Cove	-----	very top of the formation	-----	-----	-----

* = intraformational; BPU = Basal Peritidal Unit; MSU = Middle Subtidal Unit

12.1.1 Intraformational Unconformities

Description Basal Peritidal Unit (BPU) strata are cross-cut by an erosional surface at Aguathuna Quarry, Black Cove and in a Hwy. 430 roadcut near Hare Bay (Figures 11.1.a and 12.1). The surfaces display a maximum of 2-3 m erosional relief over distances of a few tens of metres and appear channelled. They are discontinuously overlain by pebbly conglomerate composed of Table Point-derived limestone lithoclasts, Aguathuna Formation-derived dolostone lithoclasts, skeletal fragments, and/or silica sand, granules and pebbles. Silica grains include simple quartz, chert and megaquartz, the latter two of which also form nodules and evaporite pseudomorphs in the Aguathuna.

Significance These disconformities are interpreted as subaerial erosion and dissolution surfaces. A subaerial origin is supported by lack of evidence of powerful marine currents in underlying and overlying sediments that could have caused significant erosion, as well the presence of karren on Aguathuna Formation dolostones in Aguathuna Quarry where the surface merges laterally with the St. George Unconformity (Figure 11.1.a). Channelling suggests they formed beneath flowing rather than standing water. Carbonate lithic fragments in overlying conglomerates indicate mechanical breakdown of underlying carbonates which may have been facilitated by fracturing of lithified limestones and dolostones caused by contemporaneous faulting or folding. Siliceous grains, in contrast, appear to be insoluble lags concentrated by dissolution of underlying carbonates. Their local abundance, and paucity everywhere of large carbonate clasts, suggest freshwater dissolution was more important than mechanical abrasion in generating the surfaces.

Unlike the St. George Unconformity, these erosional surfaces formed only locally on topographic highs. Fracturing and folding of underlying carbonates demonstrate that deformation preceded or accompanied exposure and erosion. The surfaces, therefore, are interpreted to have formed on

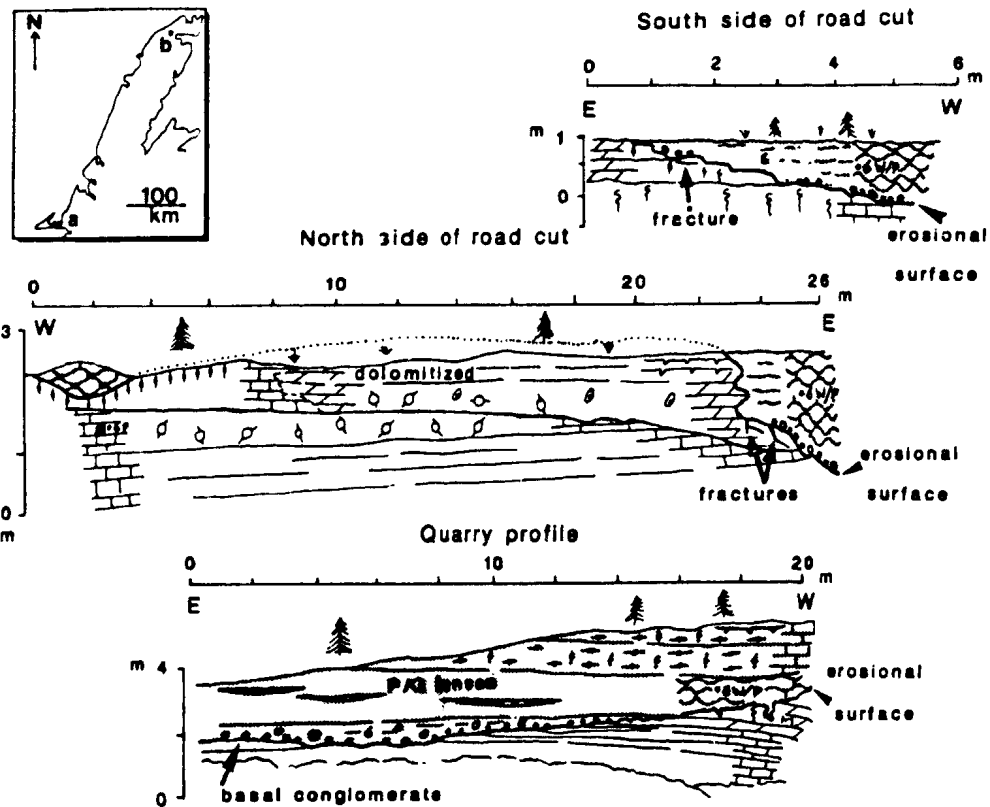


Figure 12.1 Intraformational erosion surface in the BPU; Hwy. 430 west-northwest of Hare Bay (b on inset map) (from Knight, 1986c). It lies ~15 m above the base of the Table Point (I. Knight, pers. comm. 1986) and cross-cuts folded and fractured BPU strata. Inset map also shows the location of Agathuna Quarry (a) where another prominent erosion surface is exposed (Figure 11.1.a).

platform blocks that for a period of time either did not subside or were suddenly uplifted. Basal Peritidal Unit sequences in which they occur are relatively thin and composed mostly of tidal flat deposits, indicating that underlying blocks were depositional highs that were inundated by marine waters late and/or experienced relatively slow subsidence - ie. areas that were more susceptible to renewed uplift during structural adjustments of the shelf. Formation of the surfaces, which expresses a change in shelf topography, may correlate with abrupt changes in the style of peritidal sedimentation in other areas (see Chapter section 12.2.2(ii), below).

12.1.2 Gravitational Slides

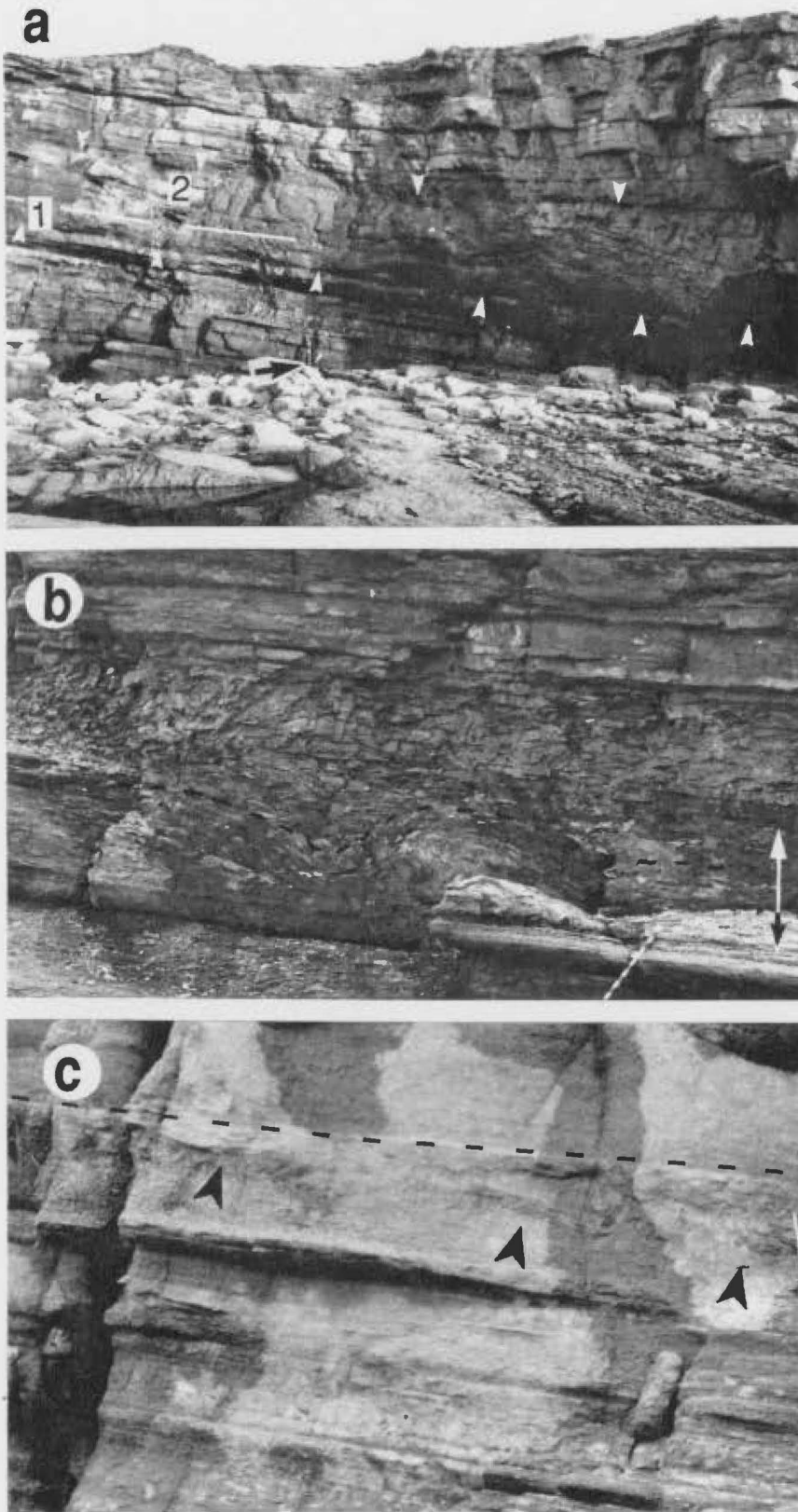
Description Horizons of folded, rotated and/or conglomeratic limestone are present in all subtidal lithofacies of the Table Point Formation locally (Table 12.1). They are underlain and overlain by undeformed strata and are interpreted to have formed by gravitational sliding.

Most slides occur within the platform sequence, enclosed by similar undeformed platform strata (Figure 12.2). They are generally less than 2-3 m thick and are bounded by a sharp, flat to gently inclined basal detachment and a flat or hummocky upper surface. Low relief depositional topography is obvious only above conglomerate domains of slide masses where clasts protrude above the top of the bed. Slides are commonly continuous along the length of the exposure (several tens of metres), but thin markedly or even pinch out laterally where the basal detachment cuts up-section (Figure 12.2.a,c). The deformed sediments are compositionally and texturally very similar or identical to underlying and overlying strata indicating that they are not highly allochthonous.

Style of deformation varies among the various lithologies affected and commonly changes laterally within an individual slide. For example, deformation in peloidal grainstone is manifest by folding (Figure

Figure 12.2 Gravitational slides in the Table Point Formation at Table Point. a) Amalgamated slides (1, 2) in burrowed wackestone; BPU. Detachment of slide 2 (dashed line) cuts down section and merges with the upper bounding surface of 1. Deformation changes (left to right) from gently folded to chaotically folded to conglomeratic (off photo) toward the interior of the slide. Metre stick (large arrow) for scale. b) Folded peloidal grainstone in a slide (arrow) in the BPU. Asymmetry indicates displacement to the left (north-northeast). Divisions on measuring stick are 10 cm. c) Cryptic slide in burrowed wackestone (basal detachment marked by arrows) above sponge bioherms in the MSU. Metre stick (right) for scale.

Figure 12.2



12.2.b) while in muddy, stylo-nodular limestones (Figure 12.2.a,c) it is manifest by symmetrical folding, chaotic folding and conglomerate domains. The latter are composed mostly of pebble-size clasts, but some domains also contain limestone blocks a few tens of centimetres to 3 m across. Gradational contacts between pebbly conglomerate and larger clasts indicate the conglomerate was generated by disintegration of incompletely lithified, nodular limestone during transport (Chapter section 4.3.4).

Although individual slides are proven to pinch out laterally in outcrop, several at Table Point can be correlated over fairly large distances with deformed horizons in adjacent areas. Slides in restricted subtidal limestones in the Basal Peritidal Unit at Table Point occur at about the same stratigraphic level as horizons of folded strata in the same lithofacies in cores from the Daniel's Harbour Zinc Mine area 13 km to the southeast. Two slides that occur above the horizon of sponge bioherms in Middle Subtidal Unit at Table Point have counterparts directly above the same sponge bioherm marker horizon at Gargamelle Cove 40 km to the north-northeast (Figures 12.2.c and 12.3). There is no way to demonstrate that slides in the widely separated areas are physically linked, but their probable contemporaneity demonstrates that the triggering mechanism operated over a large area.

Gravitational slides also occur locally at the top of the Table Point (Table 12.1). In contrast to those within the formation they are thicker and are directly overlain by deep-water sediments. One which caps the Table Point at Gargamelle Cove, and is inferred to be directly overlain by Goose Tickle Group clastics, is shown in Figure 12.4.a. It is 8-10 m thick and involves strata that are compositionally and texturally identical to underlying, in place, Middle Subtidal Unit limestone. The exposed base of the slide is exceptionally planar and is clearly defined only where directly overlain by limestone conglomerate. Underlying strata are flat-lying, but are cross-cut by high-angle,

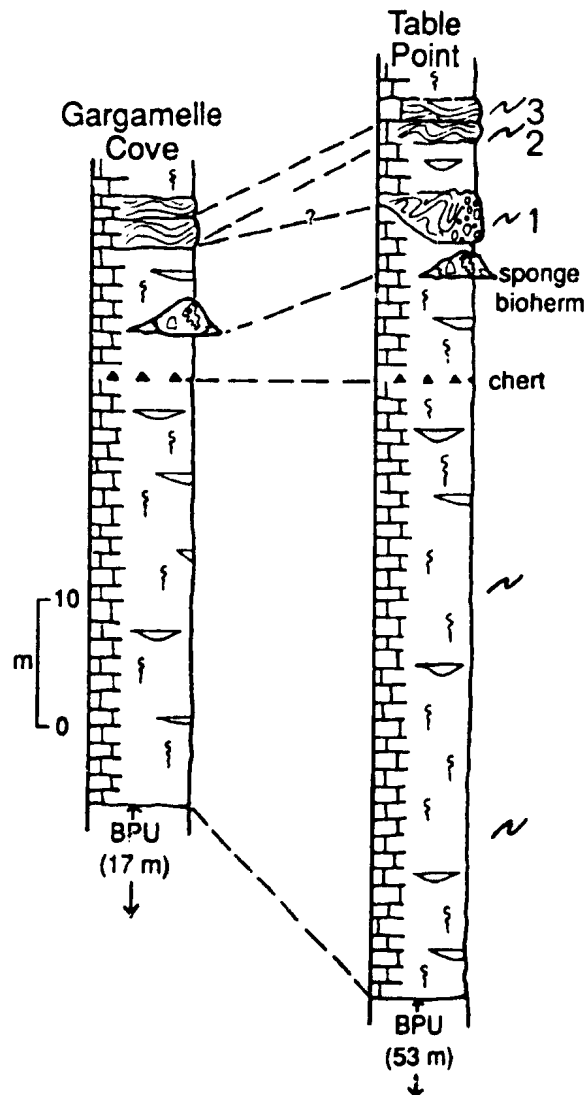
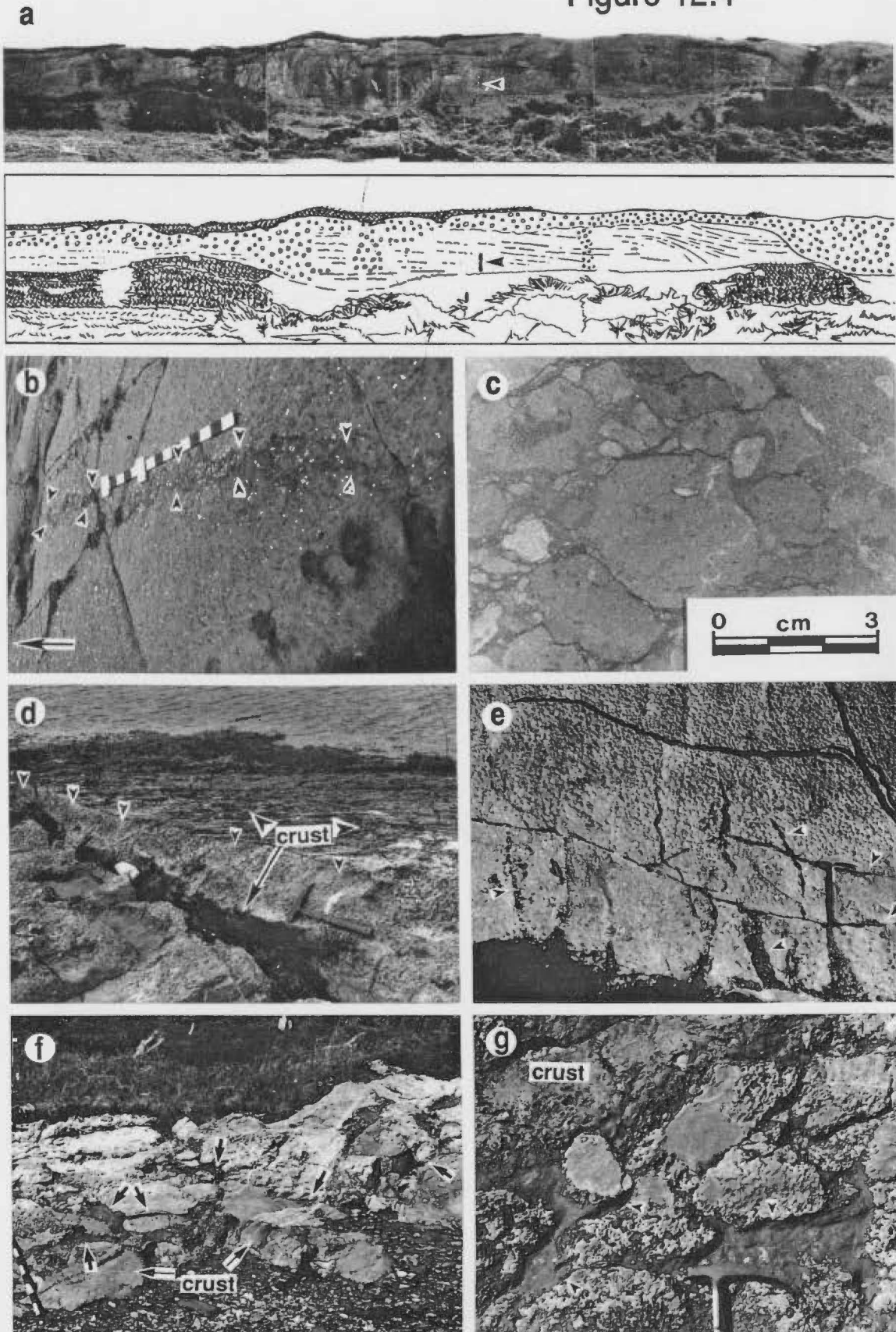


Figure 12.3 Measured sections in the Middle Subtidal Unit (MSU) at Gargamelle Cove and Table Point showing correlations between gravitational slide masses. Sections are hung on a prominent chert horizon interpreted as a time line (see Figure 4.4.e). Sponge bioherms in both sections are also inferred to be time correlative. Two thin slides at Gargamelle may correlate with the first thick slide above the bioherms at Table Point (1), but probably formed concurrently with the two, thin, superimposed deformed horizons further up section (2 and 3). Consistently greater thickness of MSU limestones between stratigraphic markers at Table Point, about 1.5 to 2 times greater than at Gargamelle, is interpreted to reflect greater subsidence in that area. Key to symbols is in Appendix A.

Figure 12.4 Synsedimentary deformation features at the top of the Table Point Formation. a) Photo mosaic (and line drawing) of the gravitational slide at the top of the Table Point exposed on the south shore of Gargamelle Cove. Contacts between relict, bedded limestone and conglomeratic limestone are gradational. Measuring stick (arrow) is 1.3 m high. b) Bedding plane view of a pebbly conglomerate-filled fracture (arrows) beneath the slide shown in a. (Large arrow marks the up direction for the photo). Divisions on measuring stick are 10 cm. c) Polished slab of pebbly limestone conglomerate from the base of the slide shown in a). d) Silica-dolomite crust-lined, black shale-filled fracture (arrows) at the top of the Table Point on Burnt Island peninsula. The crust is partly eroded from the platform surface and fracture wall. e) Upper bedding plane view of an echelon, shale-filled fractures (arrows) at the top of the Table Point on Bakeapple Island; surface dips moderately out of the page (see Figure 7.2.a). Hammer (lower right) for scale. f) Upper bedding plane view of the top of the platform on Burnt Island peninsula. Hummocky topography is generated by fractures that cross-cut (arrows) and a conglomeratic limestone that veneers Stromatolites mound limestone. The discontinuous distribution of the silica-dolomite crust atop the conglomerate is due to recent weathering. Divisions on measuring stick are 10 cm. g) Upper bedding plane view of flaggy limestone conglomerate at the top of the Table Point on Burnt Island peninsula. Interclast matrix is black shale (arrows). The discontinuous distribution of the silica-dolomite crust is due to recent weathering.

Figure 12.4



north/north-east-trending and east/southeast-trending fractures, some of which extend at least 3.5 m below the base of the slide (Figures 12.4.b and 12.5.a). The fractures are a few centimetres to 25 cm wide and up to at least 8 m long, and are filled with fine-grained, limestone pebble conglomerate, lime mud and/or blocky calcite.

Most of the slide is clast-supported, pebbly limestone conglomerate (Figure 12.4.c), but it also contains 0.5-0.8 m diameter, equidimensional, wackestone boulders and rafts over 3 m long. In the lower 4-6 m the conglomerate grades laterally and vertically into large, discontinuous areas of gently-dipping, stylo-nodular limestone that are interpreted as limbs of broad, disintegrating folds (Figure 12.4.a). Gradational contacts between the pebbly conglomerate, relict bedded areas, and large clasts indicate that the conglomerate was generated by disintegration of heterogeneously lithified, thin-bedded, nodular limestone during transport (Chapter section 4.3.4).

Gravitational sliding is also recognized at the top of Table Point sequences directly overlain by the Cape Cormorant Formation on the west side of Port au Port Peninsula. At Caribou Brook and in Big Cove proper disruption of Table Point limestones is evident by minor soft-sediment folding and discordant bedding at or near the top of the formation (Figures 6.1.a,c). On the coast between Cape Cormorant and Big Cove sea cliffs expose a large slide that involves at least the upper 10 m of the Table Point (Figure 6.3.a,b). Inaccessibility of the sea cliff precludes documenting relationships with inclosing strata and internal structure of the slide mass in detail. The basal contact with underlying limestones appears planar and the top of the slide seems to be erosionally truncated by the massive conglomerate at the base of the Cape Cormorant. Strata involved in the slide appear to be largely undeformed except at the far west, seaward end of the outcrop where they are folded, broken, and locally rotated.

Significance Gravitational sliding is a highly anomalous feature of

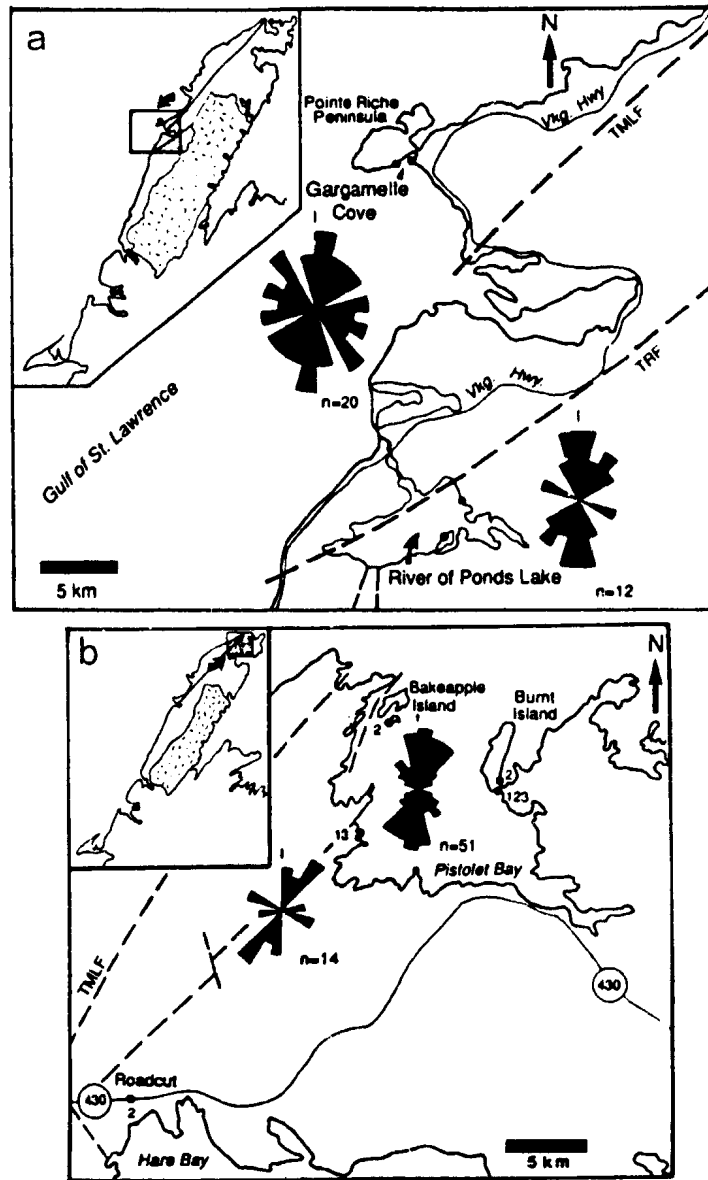


Figure 12.5 Location and orientation of synsedimentary fractures in the Table Point Formation. a) Fractures beneath the slide at the top of the Table Point at Gargamelle Cove and beneath the debris flow conglomerate at River of Ponds Lake. Data are plotted on equal area circular histograms; n = number of readings. Major Acadian faults are shown as heavy dashed lines. TMLF = Ten Mile Lake Fault; TRF = Torrent River Fault; Vkg. Hwy. = Viking Highway. b) Deformation features at the top of the Table Point in the Pistolet Bay area. 1 = grainstone filled fractures; 2 = black shale-filled fractures; 3 = limestone conglomerate veneer. Equal area circular histograms show the orientation of shale-filled fractures; n = number of readings. Major Acadian faults are shown as heavy dashed lines. TMLF = Ten Mile Lake Fault.

the shallow marine environments in which the Table Point Formation was deposited. The platform probably had very gentle depositional slopes, but the fact that most sediments are not deformed suggests that mass movement was not the norm. Two of the more plausible mechanisms which could have triggered sliding are seismic shocks or sudden, though not necessarily large, changes in depositional slope, both of which could have been related to displacements on nearby faults. Synsedimentary faulting is regionally expressed by differential subsidence of the platform, now manifested by great lateral and vertical variations in lithofacies distribution and thickness, aspects of the Table Point Formation which are addressed in Chapter section 12.2, below. Higher frequency of sliding around Table Point correlates with the great thickness of sediment that accumulated in that area, thereby supporting the interpretation that mass movement was triggered by displacements along nearby structures that controlled local subsidence. Correlation of slides over fairly large areas suggests that adjustments on local structures were the result of regional stresses generated outboard of the shelf where subduction and volcanism were ongoing.

There is little evidence that faulting usually produced submarine escarpments. This may be the case, however, for the first slide 6 m above the sponge bioherms at Table Point (Figures 12.2.c and 12.3) which contains clasts of pelmatozoan grainstone and sponges which suggest it came from the underlying bioherm horizon. It is possible that the bioherms were incorporated in a more proximal region of the slide where the basal detachment extended down further down section, but they may have been exhumed by vertical faulting.

Large slides at the top of the platform may have been triggered by similar mechanisms. Since they are directly overlain by deep-water sediments, however, powerful seismic shocks or sudden changes in slope are inferred to signal major structural displacements and rapid subsidence of the platform. Brittle fracturing of limestones beneath

the slide at Gargamelle is interpreted to have accompanied faulting or flexing of the platform which ultimately led to failure and downslope sliding of the overlying limestones. Conjugate fracture sets define either a northeast- or northwest-trending axis of least principal stress (Figure 12.5.a). The former orientation is nearly parallel to the strike of the adjacent Ten Mile Lake Fault and may indicate that fracturing was related to displacements along, or folding adjacent to, the Middle Ordovician ancestral fault.

Mass-movement related to faulting is a logical origin for the large slide at the top of the Table Point overlain by escarpment-derived Cape Cormorant Formation on the Port au Port Peninsula. Nevertheless, since the slide is directly overlain by a massive, debris flow megaconglomerate, sliding could have been triggered by sudden depositional loading during conglomerate emplacement.

12.1.3 Pebbly Limestone Conglomerate

Description Clast-supported, pebbly limestone conglomerate occurs at the top of the Table Point Formation in three sections (Table 12.1). It is interpreted to have been deposited by sediment gravity flow and is inferred to be directly overlain by deep water, fine-grained clastics of the Goose Tickle Group.

Beds range from at least 1.5 m to about 4 m thick. Outcrop on the northeast shore of River of Ponds Lake proves the base of the conglomerate there to be sharp and flat. Underlying limestones are flat lying but like beds beneath the slide at Gargamelle Cove they are cross-cut by narrow (1-3 cm), dolomitic mud-filled fractures (Figure 12.5.a). The fractures dominantly trend nearly north-south, but otherwise define irregular, polygonal domains about a metre across. Covered intervals succeed the conglomerates up section and nowhere are depositional contacts with overlying clastics exposed. The upper surface of the conglomerate exposed in Southwest Feeder is veneered by a 3-4 cm thick, black, siliceous and dolomitic crust similar to the hardground which

occurs at the top of the Table Point in the Pistolet Bay area (Chapter sections 4.4.2-4; Chapter section 12.1.4, below).

These conglomerates are composed of pebble-size, muddy, fossiliferous limestone clasts identical in composition and texture to immediately underlying strata, which appear to belong to the Middle Subtidal Unit of the Table Point. The conglomerate exposed on the River of Ponds Lake shoreline, however, also contains lithistid sponges, possibly alluding the debris to the Upper Subtidal Unit (sponge biostrome lithofacies) of the formation. That bed and the one in Southwest Feeder are massive and matrix-poor, containing only 10-15% lime mud matrix. They are texturally similar to conglomerate which makes up a large portion of the gravitational slide at the top of the Table Point Formation at Gargamelle Cove (Figure 12.4.c), but lack large clasts or relict bedded areas, and are instead interpreted to have been deposited by debris flow. In contrast, the conglomerate exposed on the island in River of Ponds Lake is weakly, normally-graded, and lime mud matrix decreases up through the bed and is replaced by sand- to granule-size limestone intraclasts or lithoclasts in the upper part of the bed. These features suggest deposition from a debris flow and overriding, high concentration turbidity current.

Significance Sediment gravity flows at the top of the platform sequence are also interpreted to have been triggered by seismicity or sudden changes in slope just prior to rapid subsidence of the platform into deep-water. Brittle fractured limestone beneath the conglomerate, at least locally, attests to flexing of the platform or faulting prior to, or during emplacement. Proximity to the northeast-trending Torrent River Fault suggests fracturing accompanied right lateral displacements along the ancestral fault (Figure 12.5.a). Textural similarities between the conglomerates and conglomeratic portions of slides (eg. at Gargamelle Cove) strongly suggest that the debris flows evolved from slides by incorporation of water into the disaggregating mass during

transport (Hampton, 1972). Proximity of River of Ponds Lake to Gargamelle Cove, plus similar trends in the fractures in underlying limestones, further suggest mass movement in both areas was caused by the same structural rearrangement of the platform.

12.1.4 Fractured Limestone and Flaggy Limestone Conglomerate

Description Echinoderm-algal limestone and Stromatolactis mound limestone at the very top of the Table Point Formation in the Pistolet Bay area are invariably cross-cut by one or more generations of sediment-filled fractures and/or are overlain by a discontinuous, flaggy, limestone conglomerate (Table 12.1; Figures 12.4.d-g and 12.5.b). Deformed limestones in turn are mantled locally by a phosphatic-siliceous-dolomitic crust interpreted as a submarine hardground (Chapter section 4.4.4), and abruptly overlain by Black Cove Formation shale. Relationships between the platform limestones, deformation structures, the mineralized hardground, and black shale are illustrated in Figure 12.6 and summarized below.

Early fractures - Earliest fractures are filled with tan, echinoderm grainstone (Figure 12.6). They occur only in Stromatolactis mound limestone on Burnt Island peninsula, are generally less than 10 cm wide and seem to be oriented at high-angles to bedding; their vertical extent is indeterminate. Geopetal sediment in Stromatolactis cavities indicate ~50 degrees rotation relative to bedding defined by the hardground-mantled platform surface.

This deformation is interpreted to have occurred in shallow water. Grainstone fracture-fillings indicate the depositional surface remained in shallow, normal marine water where crinoids and cystoids flourished and where sediments that accumulated on the seafloor were winnowed by moving water.

Later fractures - Fractures filled with black shale cross-cut both echinoderm-algal and Stromatolactis mound lithofacies limestone at the top of the Table Point at all outcrops in Pistolet Bay, and in a Hwy. 430

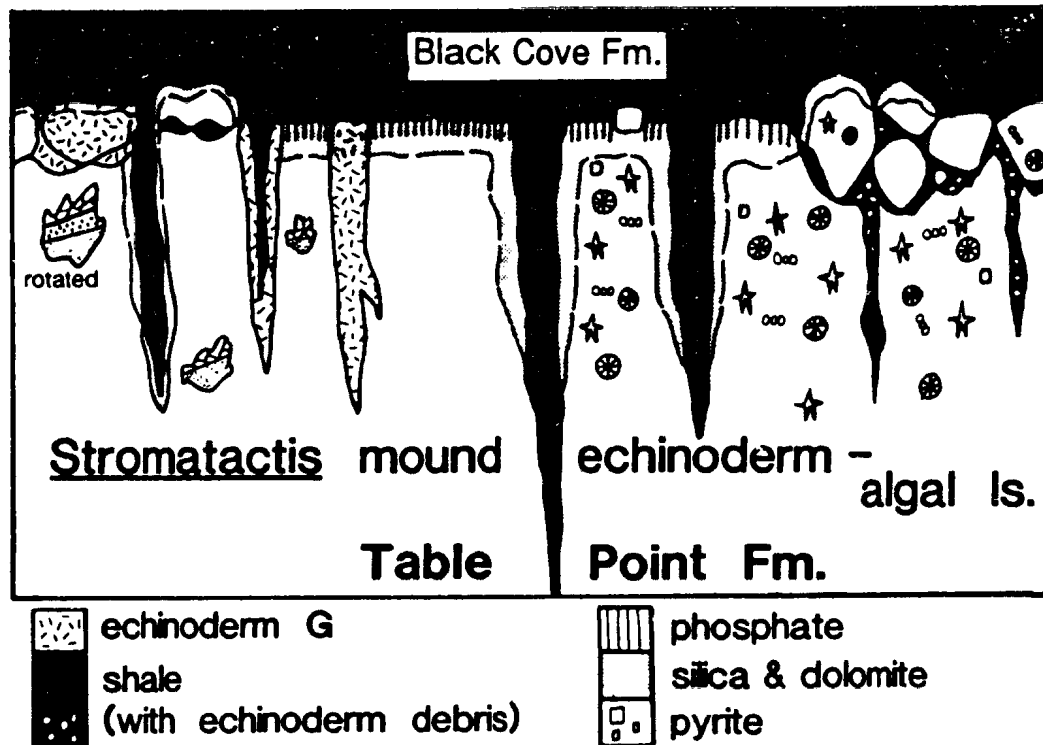


Figure 12.6 Schematic cross-section through the top of the Table Point in the Pistolet Bay area showing relationships between USU limestones, cross-cutting fractures, conglomerate veneer and their relationships to mineral phases of the hardground at the top of formation.

roadcut northwest of Hare Bay (Figures 12.4.d-f and 12.5.b). They range from less than 1 cm to 25 cm wide, are spaced 25-75 cm apart, and extend anywhere from 15 cm to at least 5 m below the top of the Table Point. Those at Bakeapple Island and in outcrop on the west coast of Pistolet Bay are strongly oriented north-northeast with a subordinate set trending east-southeast (Figure 12.5.b).

Cross-cutting relationships demonstrate that these fractures postdate echinoderm grainstone-filled fractures (Figure 12.6). Timing and environment of formation are more tightly constrained by their relationships to mineral phases of the hardground (Chapter section 4.4.4; Figure 12.6). The phosphatic layer, which occurs on both echinoderm-algal and mottled mound lithofacies limestone, is cross-cut by the shale-filled fractures, indicating that deformation occurred after the platform had subsided into relatively deep, dysaerobic or anoxic water. Silica and dolomite components of the hardground overprint the surficial phosphatic layer and replace carbonate sediment in the walls of the fractures (Figure 12.4.d), indicating an extended period of little or no sedimentation after deformation and prior to the onset of shale deposition.

Fracture-generated limestone conglomerate - Limestone conglomerate forms a discontinuous veneer at the top of the Table Point locally (Table 12.1; Figures 12.4.f,g, 12.5.b and 12.6). It is better developed atop massive, Stromatactis mound limestone than above echinoderm-algal limestone; maximum measurable thickness is about 80 cm.

On Burnt Island peninsula, where it is best exposed, the conglomerate is composed of angular to subround, flat pebbles and plate-shaped cobbles up to 40 cm long (Figure 12.4.f,g). Clast lithologies are a representative cross-section of limestones at or just below the top of the Table Point in the immediate area (ie. Stromatactis mound limestone, echinoderm grainstone, burrowed, peloidal, fossiliferous wacke-/packstone). Interclast porosity is variably occluded by echinoderm

grainstone, black shale, or black shale with abundant echinoderm debris. Shale-filled fractures associated with the conglomerate veneer do not cross-cut limestone clasts, but rather trend parallel to the margins of clasts, suggesting that they played a role in conglomerate formation (Figure 12.4.f).

Limestone cobble and boulder conglomerate composed of more equi-dimensional clasts occurs locally at the top of the Table Point exposed on the west Pistolet Bay coast (Figure 12.5.b). Clasts are compositionally and texturally allied to the echinoderm-algal lithofacies. Interclast porosity is filled with black shale with abundant trilobite and echinoderm fragments.

The absence of soft-sediment slump-folds and pebbly limestone conglomerate, which elsewhere are features of gravitational slides in the Table Point, suggests that this conglomerate was generated by in situ fragmentation of the platform and was not transported very far. Echinoderm grainstone matrix in the conglomerate locally indicates that it formed at least in part in shallow water, possibly at the same time that grainstone-filled fractures formed. Echinoderm grainstone clasts in the conglomerates further suggest that more than one episode of fracturing occurred in that setting. Flat, plate-shaped clasts that mantle the platform surface seem to have originated as broken limestone layers above bedding-parallel fractures, the formation of which could have been controlled by primary depositional or early diagenetic layering (Chapter section 4.3.4), or in the case of massive mound limestones, by the distribution of lithified crusts or incompletely filled Stromatolite cavities (Chapter section 4.4.3).

The intimate association of shale-filled fractures and conglomerate, plus the presence of shale matrix in the conglomerate locally, indicate that the conglomerate was also generated in part during later deformation of the platform in deep water. Limestone conglomerate at Burnt Island is mantled by the siliceous-dolomitic crust (Figure 12.4.f,g).

Although the crust overprints phosphatized sediment on adjacent Stromatactis mound and echinoderm-algal limestones, it is not clear whether clast surfaces are phosphatized, hence whether conglomerate formation preceded or post-dated phosphatization. One shale-filled fracture associated with the conglomerate contained small phosphatic pebbles suggesting that the conglomerate was probably generated in part after phosphatization and before silicification and dolomitization.

Significance These sediment-filled fractures and limestone conglomerates at the top of the Table Point record a protracted history of deformation that began in shallow water and continued as the platform subsided into deep water. Vertical fractures that cross-cut bedding and horizontal fractures that gave rise to flaggy conglomerate are dilational structures that are interpreted to have formed in response to tensile stress. As in the Gargamelle - River of Ponds area (Chapter sections 12.1.2 and 12.1.3) fracturing is interpreted to have occurred in response to regional faulting and/or broad flexing of the platform. The two possible origins cannot be differentiated by the available data. However, similarities between fracture trends in the Pistolet Bay area and those in the Gargamelle Cove - River of Ponds area, and their similar orientations with respect to northeast-trending, Acadian faults (Figure 12.5), suggest that fracturing was related to displacements along, or folding adjacent to, ancestral faults which ultimately controlled platform subsidence. In contrast, the absence of gravitational slides or sediment gravity flows from the top of the platform suggests that rapid subsidence in the Pistolet Bay area was not accompanied by a marked change in depositional slope.

12.2 Depositional Anomalies

There are several sedimentologic and stratigraphic aspects of the Table Point Formation that distinguish it from similar shallow marine carbonates deposited either on a stable, passive margin or on the

craton. They include: 1) great variation in depositional thickness of the formation, 2) rapid, nondirectional lateral changes and abrupt vertical changes in lithofacies and in the thickness of lithofacies assemblages that comprise the formation, and 3) anomalous peritidal depositional cycles.

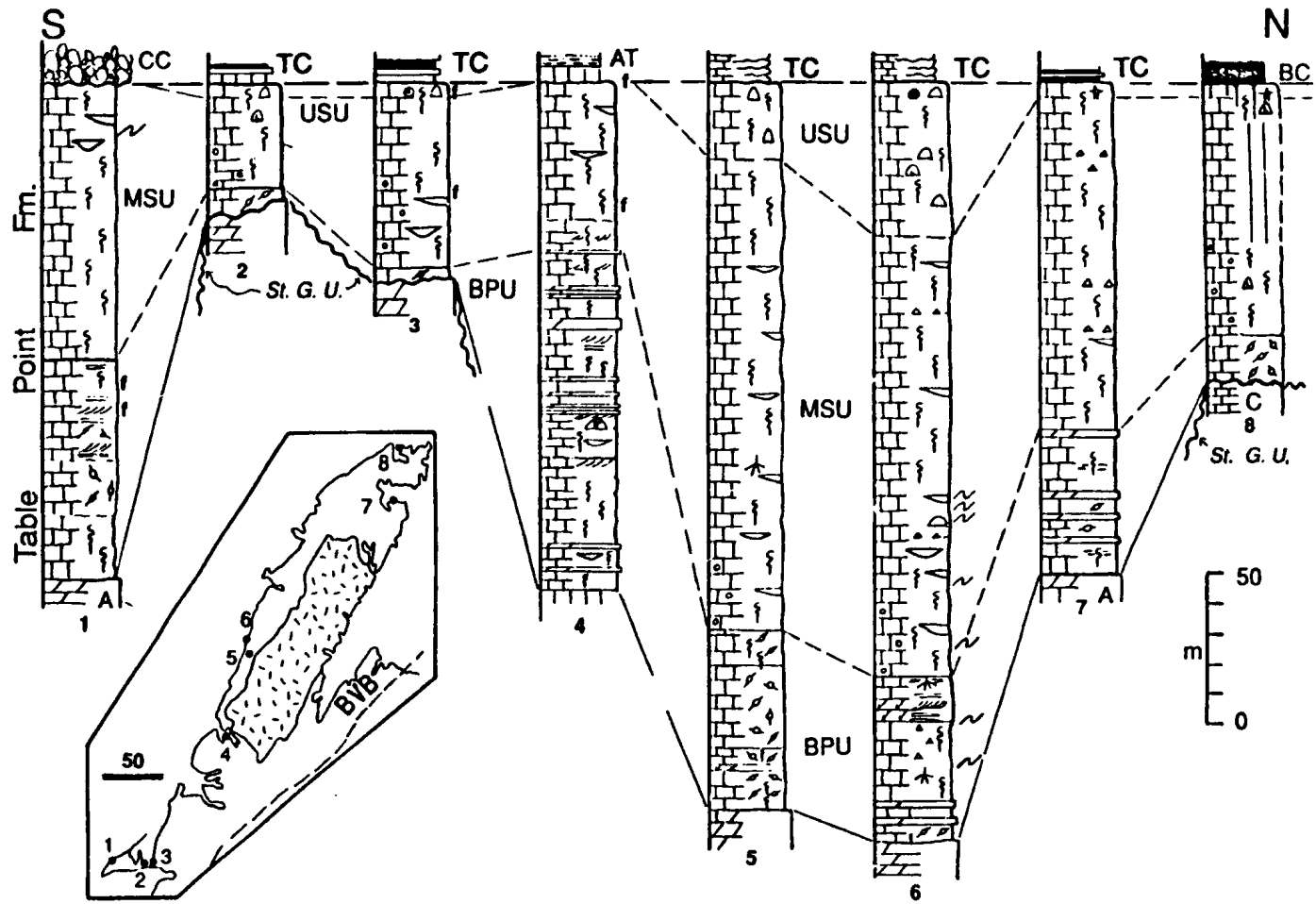
12.2.1 Variation in Formation Thickness

Description The most striking, first order anomaly of the Table Point Formation is great variation in depositional thickness (Figure 12.7). It ranges from as little as 60 m in Aguathuna Quarry to as much as 250 m at Table Point and does not vary systematically either along- or across-strike. Formation thickness roughly parallels thickness of the Basal Peritidal Unit and is also commonly greater where the burrowed, fossiliferous wackestone lithofacies dominates the Middle Subtidal Unit, and are thinner where the burrowed, peloidal packstone lithofacies is better developed.

Discussion Carbonates deposited on continental shelves commonly assume the shape of a seaward thickening wedge in which progressively thicker accumulations reflect the formation of buildups on, and increasing subsidence toward, the margin (Wilson, 1975). The thickness of sediment deposited in any given facies belt developed in a zone of relatively uniform subsidence, generally parallel to the shelf margin, is quite uniform.

Irregular along strike and across strike variations in the depositional thickness of the Table Point indicate that sediment accumulation was profoundly controlled by local rates of subsidence. Highly variable subsidence implies differential movement along synsedimentary faults and demonstrates that the fault block mosaic initiated during deposition of the Aguathuna Formation also characterized the platform during this time. Correlation between thick formation sequences, thick peritidal units, and comparatively deep, muddy subtidal sediments versus that between thin formation sequences, thin peritidal units, and shallow,

Figure 12.7 Cross-section of measured sections of the Table Point Formation. 1 = Caribou Brook. 2 = Aguathuna Quarry. 3 = Black Cove; section is locally faulted and may be thicker than shown. 4 = Shag Cliff; a large percentage of limestone in the section are replaced by sucrosic dolomite. Dolostone beds shown are very finely crystalline and are interpreted as syndepositional. 5 = DH-2512; drill core from the Daniel's Harbour Zinc Mine area, location shown in Figure 12.10. 6 = Table Point. 7 = Springs Inlet. 8 = Burnt Island; most of the Table Point section is faulted; thickness shown is representative of the formation in the immediate area. BPU = Basal Peritidal Unit; MSU = Middle Subtidal Unit (small circles in the limestone lithology symbol denotes the burrowed, peloidal packstone lithofacies); USU = Upper Subtidal Unit; (A) = Aguathuna Fm.; (C) = Catoche Fm.; (TC) = Table Cove Fm.; (CC) = Cape Cormorant Fm.; (AT) = American Tickle Fm.; (BC) = Black Cove Fm.; (BVB) = Baie Verte-Brompton line (BVB). Key to other symbols is in Appendix A.



peloidal subtidal sediments indicates that platform blocks characterized initially by high and low subsidence, respectively, commonly retained those signatures during this entire phase of platform sedimentation.

12.2.2 Variations in Lithofacies Assemblages

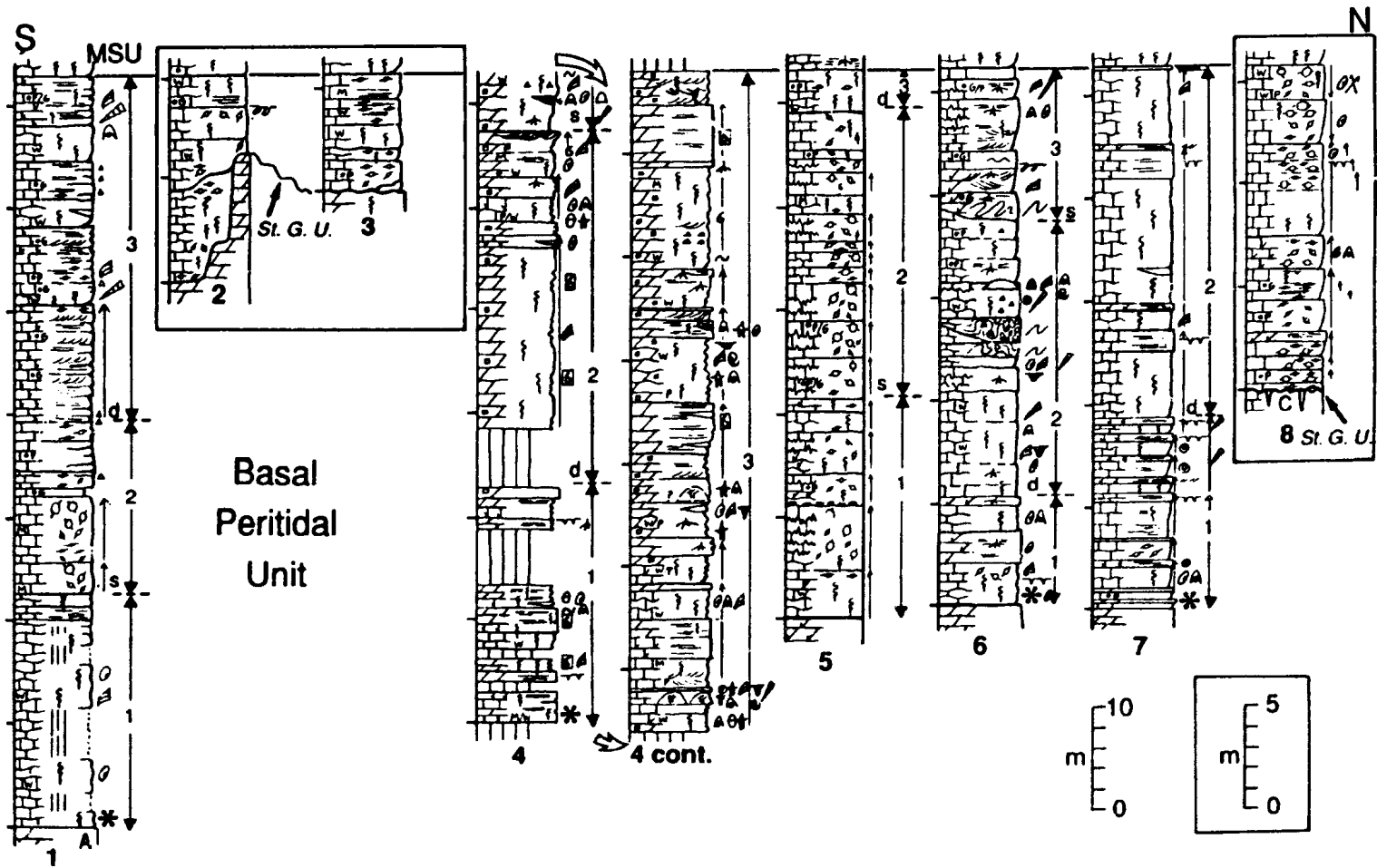
The second order, regional anomaly in Table Point Formation sequences is the considerable lateral variation in thickness of each of the three lithofacies assemblages (Basal Peritidal Unit (BPU), Middle Subtidal Unit (MSU), Upper Subtidal Unit (USU)), and in the vertical and lateral distribution of lithofacies which comprise them (Figure 12.7). The type of sediment deposited was fundamentally controlled by water depth while depositional thickness is thought to have been largely controlled by subsidence. The influence of differential subsidence and depositional topography on sedimentation is most pronounced in the BPU which records deposition in very shallow environments most sensitive to depth changes. It is manifest not only by regional variations in thickness, but also by marked variations in lithofacies, abrupt lateral and vertical changes in lithofacies (both locally and regionally), and by abnormal depositional sequences. Each of these aspects is described, illustrated and discussed below.

(i) Regional variations in thickness and lithofacies of the BPU

Description The BPU ranges from as little as 6 m at Black Cove to nearly 130 m at Shag Cliff in Bonne Bay (Figure 12.8). Thickness does not change systematically either along- or across-strike. Commonly, but with exception (eg. Port au Choix), sequences are thinner where they directly overlie the St. George Unconformity, especially where it is disposed low in the Aguathuna Formation or in the Catoche Formation, and are thicker where the unconformity occurs within the Aguathuna Formation or at least does not conspicuously mark the base of the Table Point Formation (Figure 12.8).

Similarly, the actual lithofacies that make-up BPU sequences vary markedly across the study area (Figure 12.8). Despite their

Figure 12.8 Cross-section of measured sections through the BPU. Locations are shown in Figure 12.7. Note that sections 2, 3, and 8 (boxed in) are drafted at a smaller scale (box in lower right). Asterisk (*) denotes sequences dominated by restricted, shallow subtidal lithofacies; other sequences are dominated by tidal flat sediments. Numbered sequences (1, 2, 3) delineated by large arrows to the right of the columns are characterized by distinctive suites of lithofacies or style of sedimentation. Letters above each sequence boundary denote whether the sequence records deepening (d) or shoaling (s) of the platform. Small, upward- and downward-pointing arrows to the right of the columns delineate small-scale shallowing- and deepening-upward sequences, respectively. Key to other symbols is in Appendix A.



differences, each sequence falls into one of two categories, those composed mostly of tidal flat deposits (ie. fenestral limestone, cryptalgal laminite) and those dominated by restricted, shallow subtidal sediments or burrowed, tidal flat deposits not readily distinguished from subtidal sediments. There are no detectable along- or across-strike trends in the distribution of these two types of sequences. However, there is commonly, but with exception (eg. Figure 12.8.5), positive correlation between thickness and proportion of restricted subtidal lithofacies.

Discussion Carbonate shoal complexes on passive margin shelves typically form either a strandline belt or a shelf edge complex (eg. Wilson, 1975; Grotzinger, 1986; Ross *et al.*, 1989). Sediments deposited in these belts typically thin in the direction of increasingly subtidal environments, either toward an inner shelf lagoon or toward the shelf edge. Moreover, if there are no marked along-strike changes in environmental conditions (eg. hydrodynamic energy, water depth, salinity, oxygenation, temperature, clastic influx, light penetration) the types of sediment deposited are very much the same along strike. Across-strike changes in the type of sediments deposited, in contrast, reflect changes in those environmental parameters away from the strand or shelf edge.

Neither thickness variations in the BPU nor the lateral distribution of the two types of BPU lithofacies assemblages clearly define either a strand or a linear, margin shoal complex. Although the precise location and configuration of the tectonized platform margin during this time are unknown, relative to the Baie Verte - Brompton Line which approximates its outline (Figure 12.7, inset map; Williams and St-Julien, 1982), the Table Point Formation outcrops occur in a 40-50 km wide belt at least 70 km landward of the margin. Potentially this distance would afford enough across-strike exposure to detect a directional change in peritidal sequence thickness and composition, though this is not the

case. Moreover, the outcrop belt, paralleling the ancient margin, includes a (present day) northeast-trending segment which during Middle Ordovician time faced low latitude trade winds and bore nearly directly the impact of wind driven waves, and a (present day) east-trending segment where prevailing, wind-driven waves were directed along the shelf (Scotese *et al.*, 1979; Dott and Batten, 1981). Therefore, detectable changes in peritidal lithofacies might be expected between BPU sequences both across-strike and between sequences at the tip of the Great Northern Peninsula and those in the Port au Port area, though this is not the case either.

One explanation for thickness and composition variations in BPU sequences is that they were deposited on and gradually filled in and buried an irregular topographic surface on a platform experiencing uniform subsidence. However, there is no compelling evidence that at the onset of deposition there was 120 m topographic relief on the platform, specifically on the St. George Unconformity, as is suggested by the maximum thickness difference among BPU sequences. Only 15 m erosional relief is measured on the unconformity at Aguathuna Quarry (Figure 11.1.a) and in the Daniel's Harbour Zinc Mine area it is visualized as a nearly flat, bevelled surface (Lane, 1990). This explanation is further discredited by the fact that some thick BPU sequences are mostly tidal flat deposits and some very thin sequences are mostly subtidal deposits, precisely opposite the predicted record of sedimentation had deposition been controlled solely by topography.

Heterogeneity among BPU sequences is instead interpreted to reflect irregular, but subtle depositional topography that was generated and perpetuated by differential subsidence of platform blocks, similar to circumstances envisaged for deposition of upper Aguathuna Formation dolostones above the St. George Unconformity. Initially only low areas on the platform were flooded and became sites of peritidal sedimentation while intervening areas remained subaerially exposed either because they

did not subside or were instead being uplifted. Deposition continued in subsiding low areas and began on the topographic highs only when those areas ceased to be uplifted and began to subside. Whether sedimentation occurred predominantly on tidal flats or mostly in restricted subtidal settings was determined by the interplay of local subsidence and sedimentation rates and eustatic sea level. This hypothesis is supported by the common correlation between thin BPU sequences and deeply truncated or completely eroded, underlying Aquathuna sequences. It further implies that thin BPU sequences correlate with the stratigraphically highest BPU sediments in thicker sequences and suggests that peritidal sedimentation across the entire platform ceased at the same time.

(ii) Abrupt lateral and vertical changes in BPU lithofacies

Description Basal Peritidal Unit sequences typically change significantly in character over short distances. This is clearly shown in Figure 12.8 in the contrasting BPU sequences at Caribou Brook and Aquathuna Quarry, and in DH-2512 and at Table Point. The thicker sequences also commonly record two abrupt changes in style of sedimentation up section.

Similar spatial relationships and temporal changes in sedimentation are recognized on a more local scale in sequences at the Daniel's Harbour Zinc Mine (Figure 12.9). In that area the BPU is ~55-60 m thick and is mostly fenestral limestone. In detail it consists of three subunits. The lower subunit is made up of small-scale, subtidal to intertidal or supratidal, shallowing-upward sequences. It is widespread, but thins out north of the mine and is incorporated in pipe breccias generated by dissolution collapse in two places adjacent to the mine. The middle subunit is either primarily fenestral, tidal flat limestone or mostly burrowed, subtidal wackestone. Only subtidal lithofacies are present north of the mine. The upper subunit is peloidal grainstone and/or burrowed, peloidal packstone deposited in environments transitional between exposed tidal flats and quiet, subtidal settings.

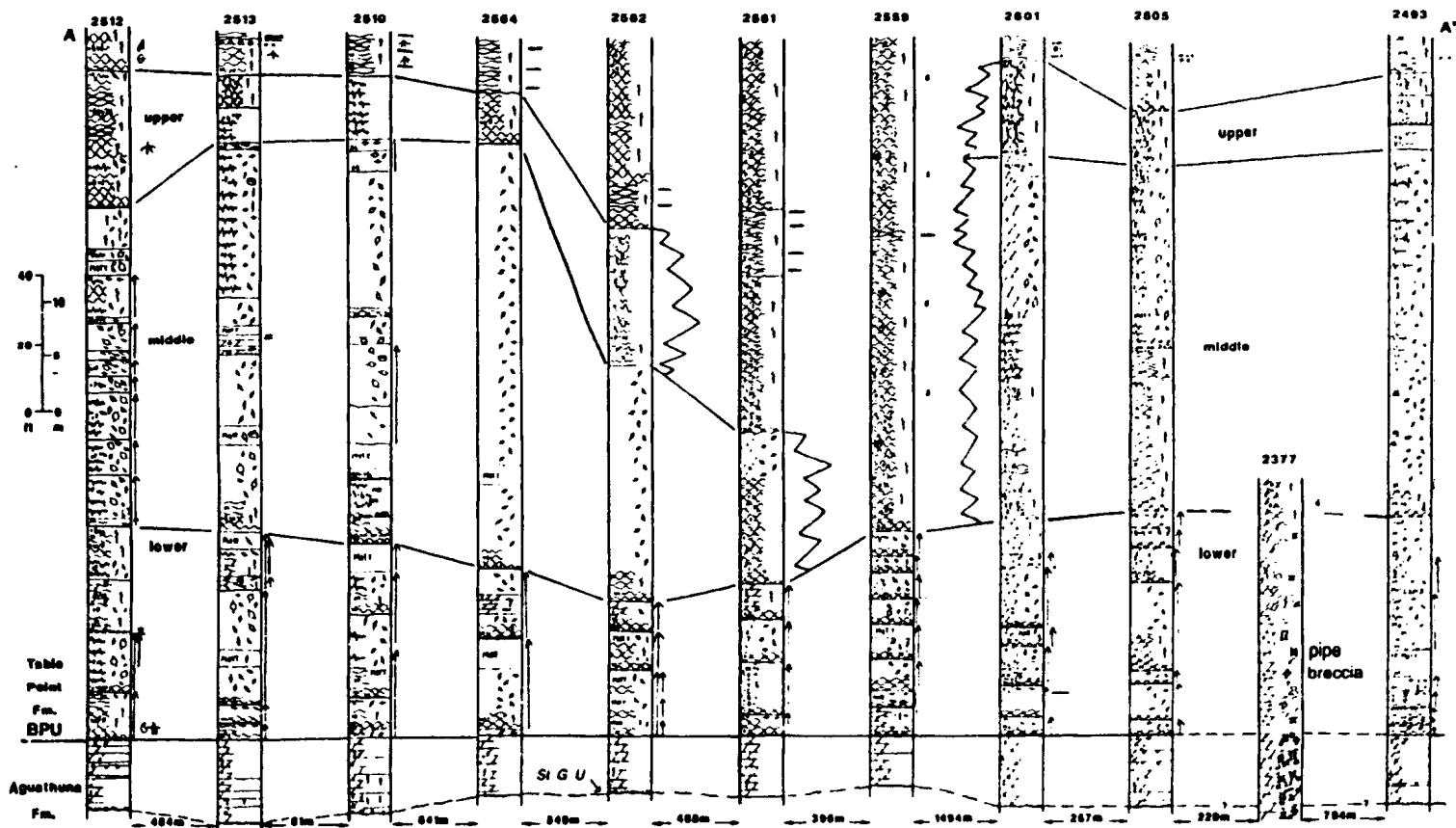


Figure 12.9 Cross-section of measured sections through the BPU in cores at the DHZM. Line of cross-section is in Figure 12.10.a. Vertical arrows to the right of the columns denote shallowing-upward sequences. DH-2559, 2551 and 2501 are partly or completely dolomitized; DH-2554, 2552, 2551, and 2377 are generated from logs described by G. C. O'Connell (Teck Corporation); variations in detail on the sections reflect the amount of detail provided on the original log. St. G. U., St. George Unconformity. Key to other symbols is in Appendix A.

It occurs only above middle subunit sequences composed of fenestral limestone.

The vertical and lateral distribution of the BPU subunits indicate two rather abrupt changes in water depth and style of sedimentation concomitant with structural rearrangement of the platform. Middle subunit lithofacies record sudden differentiation of the platform around the mine into areas of predominantly intertidal or subtidal deposition (Figure 12.10.b). This event correlates with the formation of pipe breccias near the zinc mine and was probably caused by displacements on preexisting faults which controlled development of the Trout Lake Breccia (TLB) during earliest deformation of the platform (Chapter 11) and influenced deposition of the Aguathuna Formation (Lane, 1990; Figure 12.10.a). It is also possible that formation of the central subtidal depression reflects dissolution collapse at some deeper stratigraphic level. As was the true for the TLB, however, dissolution would probably also have been controlled by adjacent structures. Moreover, horizons of slumped bedding in the subtidal limestones in some cores correlate approximately with gravitational slides in similar subtidal wackestone in the BPU at Table Point (Figure 12.8.6), suggesting that faulting was involved.

Subsequent deposition of upper subunit peloidal sand bodies only in areas that had previously been tidal flats indicates that topographic relief was maintained, while sudden flooding implies a rapid rise in sea level that may either have been eustatic or caused by an abrupt increase in the rate of regional subsidence (Figure 12.10.c). Evidence in support of the latter comes from approximately correlative peloidal grainstones in the BPU at Table Point which are folded and displaced in a slump or slide (Figure 12.8.6), and suggest faulting was involved.

Discussion A tripartite stratigraphy is recognized in most other relatively thick BPU sequences, but the changes in water depth inferred from the changes in lithofacies or styles of sedimentation are not

everywhere same (Figure 12.8). Therefore, although the changes are recorded regionally they cannot be attributed to eustasy. Instead they are interpreted to reflect sudden structural rearrangement of the platform and changes in the rate of local subsidence. Intraformational erosional surfaces in thin BPU sequences (Chapter section 12.1.1) may, in fact, correlate with one of these events. Since the rate changes were widespread it is reasonable to conclude that differential movement on local structures was ultimately controlled by regional stresses imposed by continued convergence along the continental margin.

(iii) Anomalous peritidal sequences

Description Peritidal lithofacies in many Table Point sections occur in discrete packages, most of which are readily interpreted as shallowing-upward sequences (Chapter section 4.2.3; Figures 12.8 and 12.9). They are highly variable in thickness (0.4-17 m) and cannot be correlated between adjacent areas. Moreover, they show no consistent directional change in thickness either along strike or up-section. Locally there are also vertical successions of lithofacies that are interpreted to record deepening-upward (Figure 12.8.8).

Discussion Shallow marine carbonates deposited on passive margins and in stable cratonic basins commonly consist of repeated shallowing-upward sequences (Wilson, 1967, 1975; James, 1984; Wilkinson, 1982) which, within a given facies belt, are compositionally similar, remarkably laterally continuous, and fairly uniform in thickness; variations are usually developed across strike (Wilson, 1967; Grotzinger, 1986). They may be generated under conditions of uniform subsidence and constant sea level by changes in sedimentation rate controlled by internal feedback mechanisms that control where in the system deposition occurs (autocyclic; eg. Ginsburg, 1971; Wilkinson, 1982), or in response to small scale changes in eustatic sea level caused by short period Milankovitch cycles (allocyclic; eg. Fischer, 1964; Hardie *et al.*, 1986).

BPU sediments in many places were deposited above a subaerial unconformity and, therefore, indicate a relative rise in sea level. Same age sediments deposited on the southwest, passive margin of the continent also record flooding during this time, suggesting that sea level rise was eustatic (Figure 4.8). Regionally, shallowing-upward sequences may have been formed in response to short term fluctuations associated with the sea level rise. Since these sediments accumulated entirely in shallow environments and lithofacies sequences demonstrate that sediment production kept pace and commonly exceeded sea level rise, it is postulated that the factor which determined the types, thickness, and, to some extent the sequences of sediment deposited, was rate of subsidence. Nonsystematic lateral variations in thickness of shallowing-upward sequences indicate that rates of subsidence varied across the shelf, while nonsystematic vertical changes in the thickness of shallowing-upward sequences indicate that local subsidence rate varied in time. Uncommon deepening-upward sequences further prove that locally subsidence rate did not merely overprint, but controlled the water depth and the type of sediment deposited.

12.3 Synthesis

The Table Point Formation records widespread inundation and reestablishment of typical marginal marine and then shallow subtidal carbonate environments over the entire, previously block-faulted platform. Anomalous sedimentologic and stratigraphic aspects of these sequences indicate that sedimentation was continuously influenced by regional and local tectonism.

Initial deposition in peritidal environments was profoundly influenced by low relief topography generated and perpetuated by differential subsidence of platform blocks and by subsidence itself. Flooding of the platform was a continuation of that which had begun earlier and is recorded by the upper Aguathuna Formation (Figure 11.3). There was

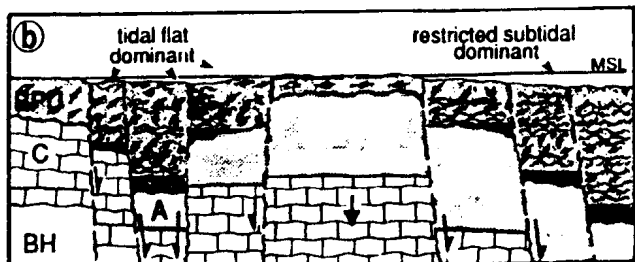
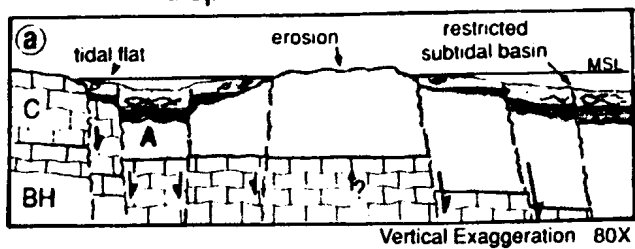
no single shoreline or regional paleoslope; flooding and peritidal sedimentation began on topographically low platform blocks while adjacent highs remained subaerially exposed (Figure 12.11.a). In contrast to when upper Aguathuna dolostones were deposited, environmental conditions were much less restricted, as indicated by the predominance of limestone, notably the large percentage of burrowed limestone which could be in part tidal flat deposits, paucity of syndepositional dolostone and apparent absence of evaporites. Less restrictive conditions imply that, despite irregular topography, circulation across the platform was much better than it had been during deposition of the Aguathuna Formation.

As flooding of the platform continued, thick sequences of peritidal sediments accumulated on blocks experiencing relatively rapid, continuous subsidence, whereas thin sequences were deposited on topographically high blocks where the onset of sedimentation was delayed and/or frequently interrupted by periods of subaerial exposure, some of which were accompanied by erosion and freshwater dissolution of previously deposited peritidal strata (Figure 12.11.b). The delicate balance between local subsidence, eustatic sea level and sedimentation rate determined where subtidal conditions predominated and where intertidal conditions were maintained. Episodes of tectonism that appear to have affected large areas, if not the entire platform, caused displacements along faults that further modified topography across the platform and caused rapid changes in the type of sediment deposited. Locally, it triggered gravitational sliding. On a shorter time scale, differential subsidence gave rise to both deepening upward and anomalous shallowing-upward sequences characterized by highly variable thickness and lateral discontinuity.

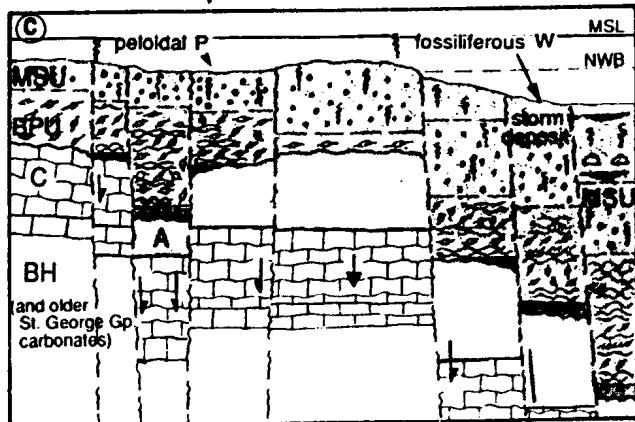
Peritidal sedimentation was everywhere followed by deepening of the platform and deposition in exclusively shallow subtidal environments, first on muddy, peloidal sand flats and then on a deeper, quieter muddy

Figure 12.11 Schematic vertical cross-section across the platform during deposition of the Table Point Formation. a) Initial inundation of the platform and deposition in peritidal environments. b) Deposition in peritidal environments near the end of BPU sedimentation. c) Sea level rise and deposition in exclusively shallow subtidal environments. d) Late stage shoaling. MSL = mean sea level. Arrows indicate relative subsidence.

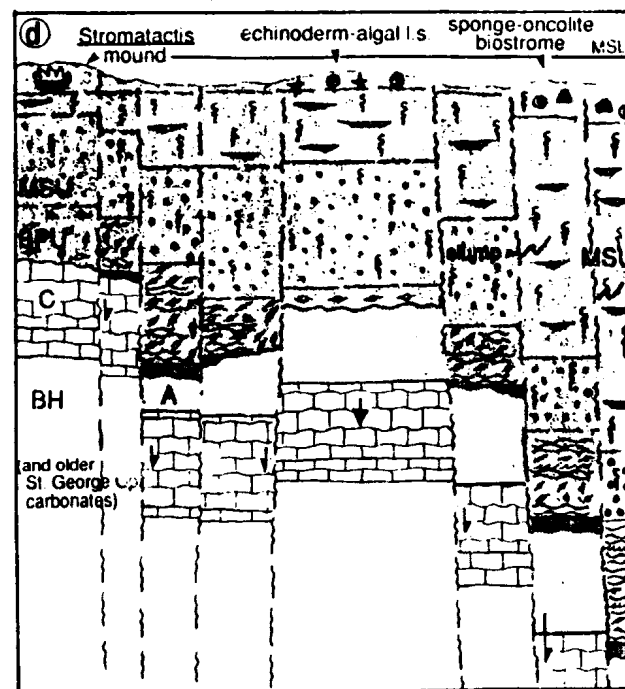
Deposition of the BPU



Deposition of the MSU



Deposition of the USU



sea floor (Figure 12.11.c). Continued differential subsidence of platform blocks created and perpetuated a low relief, submarine topography which determined how long sedimentation in comparatively shallow settings continued and, ultimately the total thickness of sediment deposited during this phase of sedimentation. Locally, displacements on faults that controlled subsidence triggered gravitational slides. Contemporaneous sliding in fairly widely separated areas suggests that displacements were caused by stresses transmitted over large areas of the platform.

Subtidal sedimentation was everywhere followed by shoaling of the platform and deposition in comparatively shallow subtidal, and locally intertidal environments (Figure 12.11.d). Low relief topography perpetuated by continued differential subsidence is expressed by the heterogeneous distribution of the three lithofacies deposited during this phase sedimentation, each of which must reflect a unique set of hydrodynamic conditions. Episodic faulting caused fracturing of early lithified Stromatactis mounds. More widespread deformation after shallow marine sedimentation ceased involved fracturing and mass transport of the uppermost platform strata in gravitational slides or sediment gravity flows locally, or surficial fracturing and formation of a discontinuous conglomerate veneer.

Northeast-trending faults are inferred to have most actively controlled differential subsidence and influenced sedimentation. In the Daniel's Harbour Zinc Mine - Table Point area a preexisting, northeast-trending fault zone is proven to have controlled the distribution of BPU lithofacies (Figure 12.10). More generally, in all areas where there is good stratigraphic control, abrupt lateral changes in lithofacies, thickness of lithofacies assemblages, and, more conspicuously, formation thickness, all commonly occur across northeast-trending Acadian structures. Displacements on the ancestors of these structures, though they apparently did not generate high-relief escarpments, are inferred

to have triggered gravitational sliding during deposition of the Table Point. In addition, the orientation of brittle fractures in limestones at or just below the top of the Table Point suggest that those structures were involved in regional deformation of the platform just prior to drowning.

12.4 Tectonic Significance

The Table Point Formation was deposited in shallow marine environments reestablished by flooding of a regional unconformity on the previously block-faulted and uplifted platform. By this time the actual margin of the shelf-wide platform had experienced catastrophic faulting, and tectonic collapse (James and Stevens, 1986; James *et al.*, 1987; James *et al.*, 1989). Carbonate sediment was no longer being generated and transported off-shelf, and deep water, continental slope and rise environments were being buried by siliciclastic flysch derived from a geologically complex terrane above the subduction zone composed of obducted oceanic elements and thrust slices of continental margin sediments scraped off the North American plate (Stevens, 1970). On the reestablished carbonate platform, destruction of the margin proper is signaled by improved circulation across the platform, inferred from the nature of basal, peritidal sediments of the Table Point Formation. Ongoing subduction and volcanism to the paleo-south is indicated by thin volcanic ash layers in the platform sequences.

Differential subsidence across the entire Table Point platform and episodic seismicity that triggered mass movement in the shallow marine carbonates are interpreted to be the local responses of the continental shelf to regional stresses imposed by continued convergence. These features distinguish Table Point carbonates from those deposited on the predeceasing, stable, passive margin and identify this platform as a component of the evolving foreland basin. Independent subsidence of platform blocks during this entire period of sedimentation indicates

that the structures that defined the block boundaries were linked to a common detachment fault, thereby further supporting the interpretation that the faults were reactivated, rift-related structures linked to basement.

The three phases of sedimentation (BPU, MSU, USU) recorded in Table Point Formation sequences indicate significant, temporal changes in relative sea level (Figure 12.12). BPU sediments deposited largely above the St. George Unconformity indicate a relative rise in sea level and define a phase during which sedimentation kept pace with, and commonly exceeded, the rate of sea level rise. Overlying MSU sediments indicate regional deepening of the platform, implying an increase in the rate of sea level rise that did not cause drowning, but did preclude accretion to sea level. The USU indicates regional shoaling and, therefore, a fall in relative sea level.

The two most critical factors that may have controlled sea level changes across the Table Point platform are eustasy and subsidence. The relative importance of each can be evaluated to a first approximation by comparing the relative sea level curve constructed from Table Point sequences with that constructed from Whiterockian strata deposited on the southwestern, passive margin of the North American continent (Figure 12.12.a,b). If the southwest U. S. A., passive margin experienced uniform subsidence and the sea level curve from that area is primarily eustatic, then the difference between it and the sea level curve from the Table Point must represent the component of tectonically-controlled, regional subsidence for the foreland basin platform.

The subsidence curve (Figure 12.12.c) shows that initial peritidal sedimentation corresponds to a period of abnormally slow crustal subsidence, possibly even continued differential uplift of the tectonized platform. This is consistent with the presence of subaerial unconformities within peritidal sequences locally, and accounts for the fact that many shallowing-upward sequences are anomalously thin. Tectonic uplift

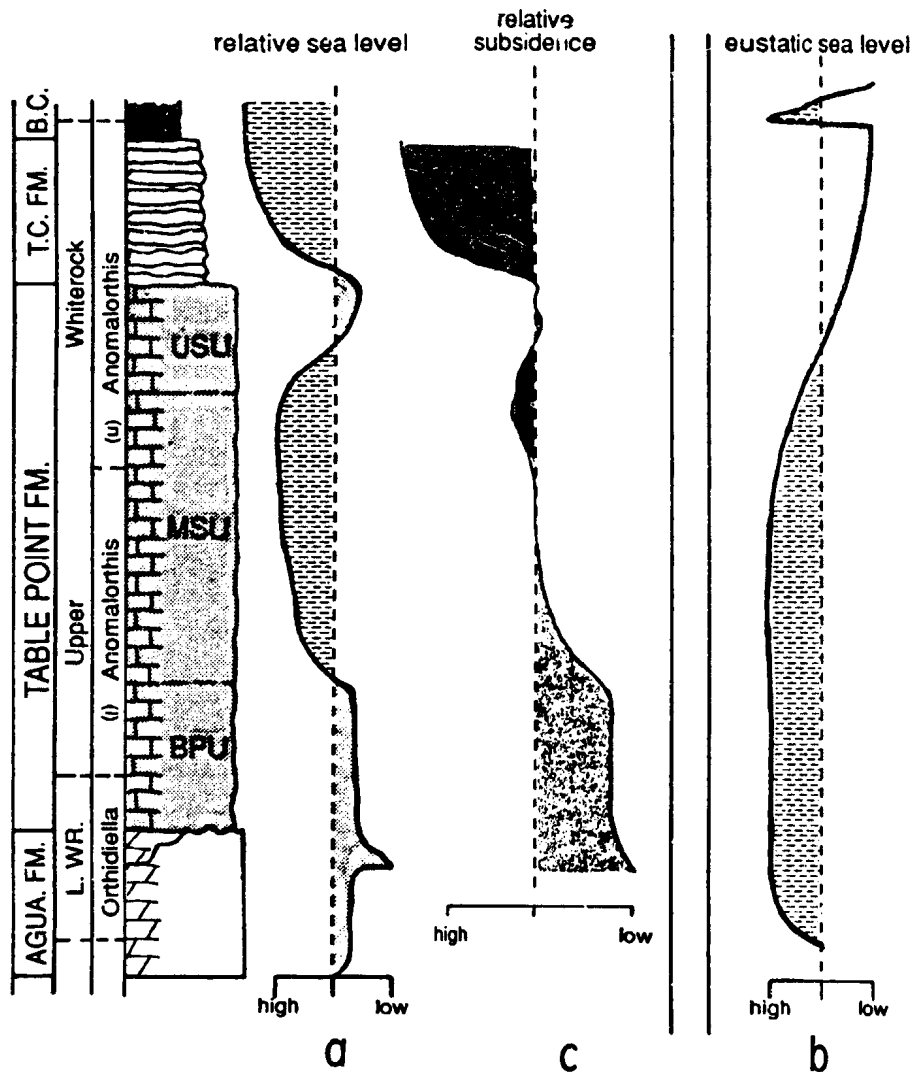


Figure 12.12 Relative sea level and subsidence curves for the Table Point Formation. a) Relative sea level curve constructed from carbonate lithofacies for Whiterockian age strata in western Newfoundland. Boundaries for the *Orthidiella* and the lower and upper *Anomalorthis* zones are approximate. b) Relative sea level curve for coeval strata deposited on the southwestern, passive margin of the North American continent (constructed from Ross *et al.*, 1989). c) Subsidence curve for the Table Point platform generated by addition of the two sea level curves. Negative intervals are phases during which regional subsidence was less than it was on the passive margin; positive intervals are phases when regional subsidence was greater than it was on the passive margin.

of the platform contemporaneous with eustatic sea level rise may, in fact, have minimized the duration and effects of exposure, erosion, and dissolution involved in prior formation of the St. George Unconformity.

Subsequent shallow subtidal sedimentation (MSU) must reflect a rather rapid increase in the rate of subsidence along the length of the foreland basin (Figure 12.12.c). Rapid subsidence negated, or at least countered, the slow down in the rate of eustatic sea level rise, or possibly even sea level fall at this point.

Late phase shoaling (USU) approximately coincides with a maximum, eustatic sea level low recorded on the passive margin (Figure 12.12.a, b). This suggests that tectonically-controlled subsidence slowed down considerably, permitting accretion of sediments to near sea level. However, since shoaling preceded tectonic deformation of the platform and was immediately followed by rapid deepening, it is possible that shoaling was a consequence of tectonic upwarping prior to platform destruction.

CHAPTER 13

PHASE 3: PLATFORM COLLAPSE

This phase of foreland basin development involved sudden deepening and drowning of the Table Point platform and deposition everywhere of deep-water sediments. Across western Newfoundland these events are recorded by three markedly different sedimentary sequences (Figure 13.1). In most places shallow water sedimentation was gradually superseded by deposition of muddy carbonates on a gently dipping slope and basin margin (Table Cove Formation). In several places, platform sedimentation ceased abruptly and was followed by deposition of black shale in an anoxic basin (Black Cove Formation). In one area, the far west side of Port au Port Peninsula, platform sedimentation was abruptly succeeded by deposition of lithoclastic conglomerate and calcarenite in a shale basin (Cape Cormorant Formation). The outcrop distribution of the three deep water units over the entire western Newfoundland platform is shown in Figure 13.2.

Three lines of evidence lead to the conclusion that drowning of the Table Point platform was caused by very rapid, tectonically-controlled subsidence. First, heterogeneity among the post-platform sediments, plus unequivocal evidence of tilting and, locally, faulting of the platform, indicate that deepening was not simply a consequence of eustatic sea level rise imposed on a gradually subsiding shelf. Second, under 'normal' circumstances carbonate production on platforms has the potential to outpace long-term sea level rise (Schlager, 1981); in the absence of some other factor that would inhibit carbonate production, such as deteriorating environmental conditions or influx of abundant clastics (eg. Whalen, 1988), drowning is most readily explained by exceptionally rapid sea level rise caused by subsidence (Schlager, 1981). Finally, deepening over the Table Point platform is precisely opposite to the effect predicted from the eustatic sea level curve

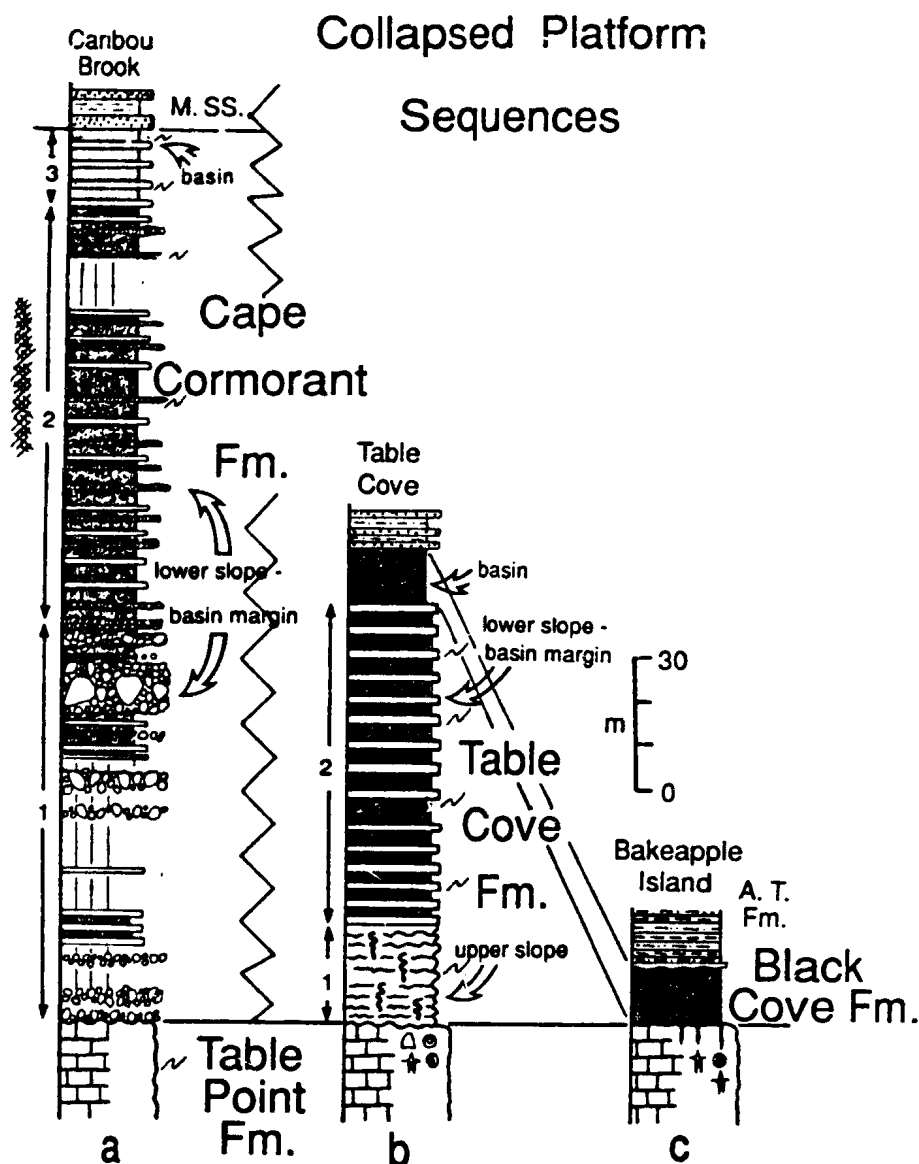


Figure 13.1 Type examples of collapsed platform sequences. a) Caribou Brook; platform disconformably overlain by escarpment- and platform - derived, deep-water carbonates of the Cape Cormorant Formation. 1 = megaconglomerate-ribbon limestone lithofacies; 2 = calcarenite-conglomerate lithofacies (hatched pattern marks the interval of black shale); 3 = green shale-calcarenite lithofacies. b) Table Cove; platform gradationally overlain by slope to basin margin carbonates of the Table Cove Formation. 1 = burrowed limestone lithofacies; 2 = ribbon limestone lithofacies. c) Bakeapple Island; platform abruptly overlain by black, basinal shale of the Black Cove Formation. Locations are shown in Figure 13.2. M.SS., Mainland Sandstone; AT, American Tickle Formation. Key to other symbols is in Appendix A.

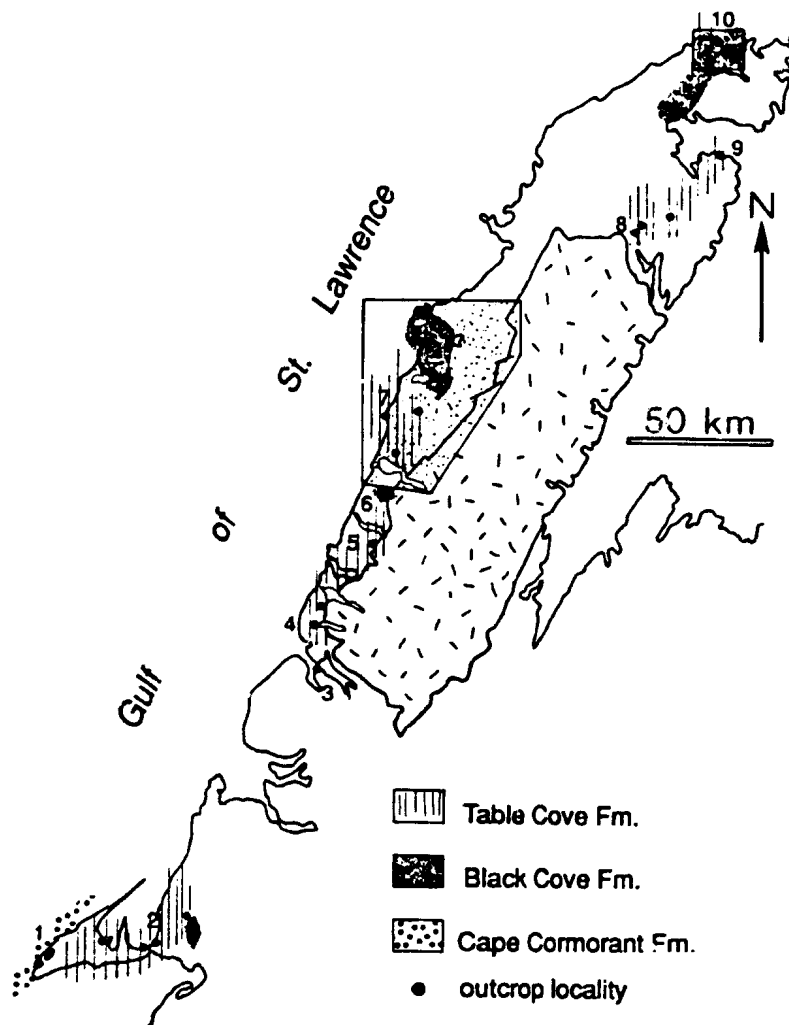


Figure 13.2 Aerial distribution of post-platform, deep-water formations. Numbered localities include: 1 = Caribou Brook; 2 = Black Cove; 3 = Shag Cliff; 4 = Bakers Brook; 5 = West Brook; 6 = Southwest Feeder; 7 = Table Point; 8 = Beaver Brook; 9 = Springs Inlet; 10 = Bakeapple Island. The depositional distribution of the Table Cove Formation between Shag Cliff and Southwest Feeder is not entirely certain. It is not present immediately above the platform at any localities, but it does outcrop in Bakers Brook and is structurally juxtaposed with the Table Point Formation in West Brook. Its absence from the Southwest Feeder section is thought to be depositional, but further south it is likely to be due to faulting. Stippled areas correspond to map areas in Figures 13.4 and 13.6.

generated from coeval strata deposited on the southwestern, passive margin of the North American continent (Figure 12.12).

The nature and distribution of the three post-platform, deep-water lithofacies shed light on the regional dynamics and configuration of the foreland basin during this stage of its development.

13.1 Deposition of the Table Cove Formation

The Table Cove Formation consists of thin-bedded, dark grey, muddy limestone and carbonate-rich shale deposited on a gently-dipping, carbonate slope and basin margin (Chapter 5). These strata gradationally overlie the platform, thereby signalling gradual subsidence accompanied by tilting of the platform in the areas they occur. Most sequences consist of either bioturbated, fossiliferous, upper slope limestones or burrowed, parted limestone deposited in a mid-slope setting, overlain by ribbon limestone deposited on the lower slope and basin margin (Figure 13.1.b). Those in which muddy hemipelagites dominate distal ribbon limestones were deposited on a gently-dipping ramp, while those consisting in large part of peloidal and spiculitic turbidites are inferred to have been deposited on a gently-dipping slope structurally separated from the adjacent relict platform (Figure 5.11). All sequences constitute a single, deepening-upward sediment package that records platform drowning, lateral migration of deep water environments and sediments over shallower ones, and eventually, basin formation.

The Table Cove Formation is similar in composition, texture, style of bedding, and distribution of physical and biogenic structures to other ancient, deep-water carbonate sequences (Cook and Enos, 1977 and papers therein; Cook and Taylor, 1977; Cook and Mullins, 1983 and references therein; McIlreath and James, 1984; James and Stevens, 1986). Its three dimensional distribution, however, distinguishes it from similar slope to basin deposits found either along a continental margin

proper or along intra-shelf or intra-cratonic platforms. It does not comprise a single, contiguous sediment package with a recognizable three dimensional geometry that can be linked to either a single adjacent platform or basin, or even to the strike of the ancient, northeast-trending continental margin. Instead, the formation is highly variable in thickness (10 m--130 m) and is not laterally continuous (Figures 5.1, 10.2 and 13.2). Furthermore, lateral changes in thickness and paleo-slope data indicate that there were several local slopes of different facing directions and that locally the facing direction reversed over time. Collectively these features indicate that there was no single, regional carbonate slope, and that the foundering platform was characterized by highly variable subsidence, as was true for the predeceasing Table Point platform.

The anomalous aspects of the Table Cove Formation itemized above are recognized regionally. They are most clearly illustrated in the Table Point area where the outcrop and subsurface data base is most extensive and provides a comparatively complete record of sedimentation during this phase of foreland basin development. Eight collapsed platform sequences from that area are shown in Figure 13.3; their locations are shown in Figure 13.4. Integration of sedimentologic, stratigraphic and structural data permits recognition of local dynamics and changes in foreland basin configuration.

Table Cove Formation slope deposited in this area range from 11.5 m to ~130 m thick and are inferred to be depositionally absent at Gargamelle Cove and River of Ponds Lake (Figure 13.3). (The significance of the latter sequences is addressed in Chapter section 13.2). Table Cove thickness and lithofacies make-up change markedly over short distances, with major changes occurring across northeast-trending, Acadian faults (Figures 13.3 and 13.4). Of these structures, the Torrent River and Ten Mile Lake faults are proven to have actively influenced sedimentation during earlier stages of foreland basin

Figure 13.3 Collapsed platform sequences in the Table Point area. Locations are in Figure 13.4; precise locations of DH-2512 and DH-2541 at the Daniel's Harbour Zinc Mine are in Figure 12.10. Sections are arranged generally from west to east across structural strike. Abbreviations TMI/TR, TC, PCP, etc. (top) correspond to major faults shown in Figure 13.4. Upper Subtidal Unit lithofacies are developed at the top of the underlying Table Point Formation (TP) everywhere except at Gargamelle Cove and River of Ponds Lake where the top of the platform is represented by a gravitational slide and debris flow conglomerate, respectively. Covered intervals above both sections are inferred to be underlain by fine-grained, Goose Tickle Group clastics. Arrows to the right of the Table Cove Formation (TC) sequences at Table Cove and Spudgels Cove show the general transport directions of gravitational slides in the slope deposits based on measurements of slump fold axes, imbricated bedding, and detachment surfaces (Figure 5.10 and Spudgel's Cove section in back pocket). BC = Black Cove Formation; AT = American Tickle Formation; M.SS. = Mainland Sandstone; congl. = conglomerate. Key to other symbols is in Appendix A.

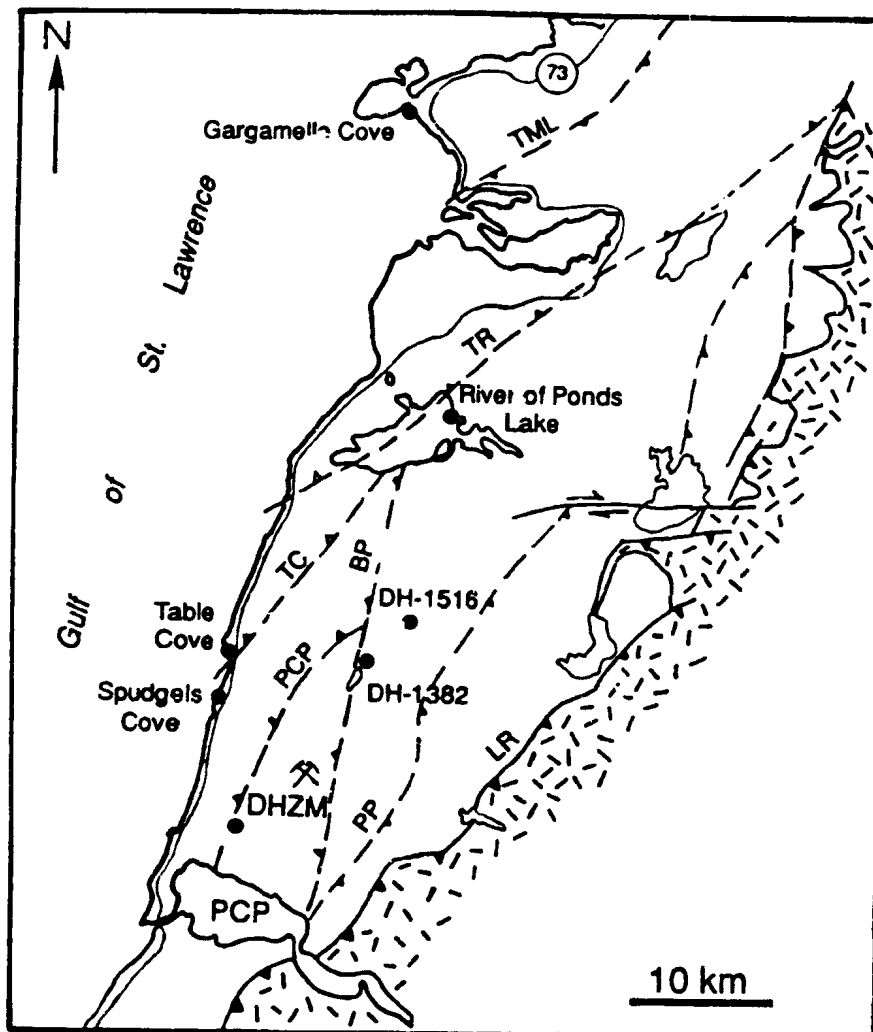


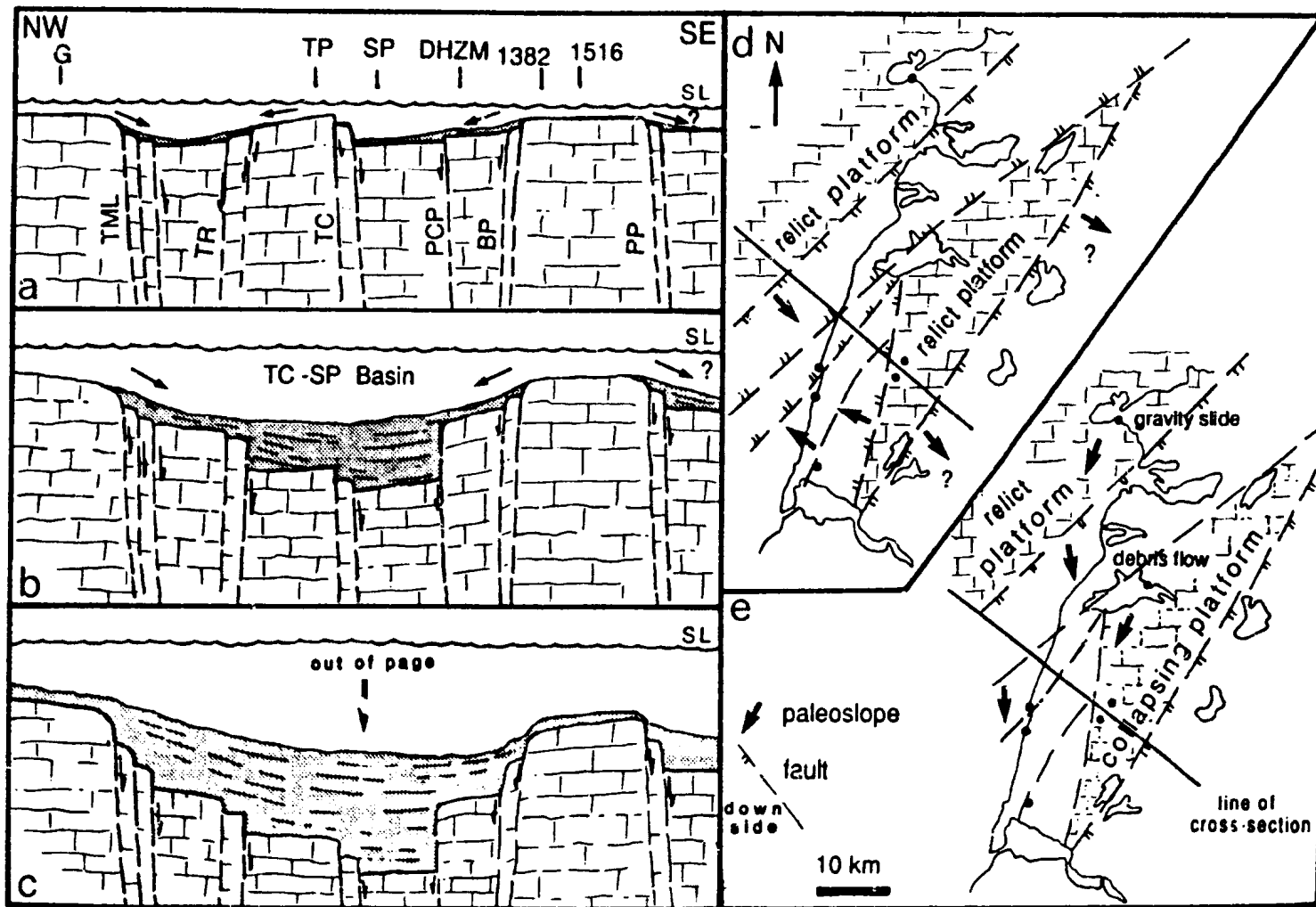
Figure 13.4 Map of the Table Point area showing the locations of measured sections in Figure 13.3. Faults shown are the major Acadian structures mapped by Cawood and Williams (1986), Grenier and Cawood (1988), and Grenier (1990). They are interpreted by Grenier (1990) as basement-linked faults of opposing facing directions that were generated during Late Precambrian rifting and reactivated with reverse sense displacement during Acadian orogenesis. TML = Ten Mile Lake Fault; TR = Torrent River Fault; IC = Table Cove Fault (informal name); PCP = Portland Creek Pond Thrust; BP = Bellburns Pond Thrust; PP = Parsons Pond Thrust; LR = Long Range Thrust.

development (Chapter sections 11.3, 12.1.1 and 12.1.2). Lateral changes in the collapsed platform sequences gives reason to believe that all of the structures actively controlled subsidence and influenced deposition of these deep water carbonates as well.

Among the Table Cove Formation sequences in the area there is a general westward-thickening trend (Figure 13.3) which suggests deposition on a single, differentially subsiding, easterly-dipping ramp. However, the strike of such a slope is not readily defined, nor does it appear to have been linear. Moreover, there is a reversal in the water depth gradient recorded by basal Table Cove lithofacies, specifically the presence of upper slope limestones at Table Cove and at the DHZM, and of deeper water, mid-slope, parted limestone between the those two areas at Spudgels Cove (Figure 13.3), which defies this simple reconstruction.

A more complex and changing configuration is indicated by paleoslope data from the Table Cove sequences at Table Cove and Spudgel's Cove (Figures 13.3 and 13.5). Data from the lowest strata in both localities indicate that deep-water sedimentation occurred initially on a northwest-facing slope flanked by a relict platform off to the southeast (Figure 13.3). The reversal in water depth indicated by basal Table Cove lithofacies between Table Cove and the DHZM (noted above), however, implies that this slope was not continuous and that deposition ensued on two, possibly three, separate, northwest-tilted blocks (Figure 13.5.a,d). Structures that defined the block boundaries are inferred to coincide with the northeast-trending Table Cove (new, informal name) and Portland Creek Pond faults. Paleoslope data from overlying ribbon limestones (Figure 13.3) indicate that as sedimentation and subsidence continued, basinal conditions were established in the Table Point-Spudgel's Cove area and slides were transported in from the southeast and the northwest, implying the presence of relict platforms and slopes of opposing facing directions on either side (Figure 13.5.b).

Figure 13.5 Schematic reconstruction of platform collapse in the Table Point area. Vertical cross-sections (a), b), and c)) show probable fault blocks defined by ancestors of major Acadian faults (abbreviations for them are the same as in Figure 13.4). Relative locations of the measured sections in Figure 13.3 along the line of cross-section (shown in c) and d)) are abbreviated in a) as: G, Gargamelle Cove; TP, Table Point; SP, Spudgels Cove; DHZM, DH-2512 and DH-2541; 1382, DH-1382; 1516, DH-1516. a) Initial faulting and subsidence created a subtle horst and graben terrane with relict, sediment producing platforms west of the Ten Mile Lake (TML) fault and east of the Bellburns Pond (BP) fault. A regional northwest-facing slope occurred between the two highs, but was rendered discontinuous along a fault block boundary (TC) east of Table Cove. Corresponding map view of foundering platform topography is shown in d). b) With continued subsidence, the crustal blocks between the Ten Mile Lake fault and the Portland Creek Pond Fault (PCP) joined to form a single, rapidly subsiding depression [TC-SP Basin]. Sediments derived from the eastern relict platform accumulated in a mid-slope environment on a northwest-facing slope in the Spudgels Cove area, while Table Cove, located in a more axial position, received sediments derived from both relict platforms, including gravitational slides from both adjacent slopes. Little sediment accumulated on either flanking relict platform. c) Later structural adjustments resulted in a regional south-southeast-facing slope away from the western relict platform. That high continued to supply sediment to deep-water environments and ribbon limestone accumulated everywhere between Table Cove and the DHZM. The eastern relict platform subsided rapidly and a thin, deep-water carbonate sequence was deposited on the south-dipping slope of that fault block (out of the page). Subsequent faulting or seismicity triggered mass movement of carbonates on the up-slope end of that block, resulting in deposition of exotic debris flow conglomerates on the local slope which marked the end of deep-water carbonate sedimentation in that area. Corresponding map view of the basin configuration is shown in e).



vert. exag. \approx 45X

Paleoslope data from the youngest ribbon limestones (Figure 13.3) indicate that the final phase of deep-water carbonate sedimentation accompanied regional tilting to the south-southeast, leaving a single, sediment-supplying relict platform off to the northwest until deep-water carbonate sedimentation ceased (Figure 13.5 c,e).

The comparatively thin Table Cove Formation sequences in DH-1516 and DH-1382 east of Table Cove (Figures 13.3 and 13.4) are located in the area that may have been the relict platform for the initial, northwest-dipping slope in the area (Figure 13.5.a,d). Their thinness alone, especially in contrast to the sequence at Table Cove, suggests that they were deposited on a different, independently subsiding crustal block. Its boundaries are inferred to coincide with the northeast-trending Bellburns Pond and Parsons Pond faults which appear to define a horst in the basement (Figure 13.4), and a topographic high in the foreland basin at this point in time (Figure 13.5.a,b,d). Initially it was a source for hemipelagic mud, sediment gravity flows and gravitational slides deposited in adjacent deep-water environments to the west and remained a relatively shallow area of little net sediment accumulation for at least as long as northwest-directed, gravitational sliding occurred in the Table Cove - Spudgel's Cove area (Figure 13.5.b). Subsequent subsidence and drowning occurred rapidly, possibly in response to down-faulting that eventually produced a regional, south-southeast dipping slope (Figure 13.5.c,e). Only upper slope carbonates were deposited on the northern end of the block (DH-1516, Figure 13.3), while upper slope sediments, followed by lower slope, ribbon limestone were deposited over its deeper, southwest end (DH-1382, Figure 13.3). Those ribbon limestones could have come either from upslope areas to the north or, possibly, from the relict platform to the west (Figure 13.5.c,e). Shallow water-derived, debris flow conglomerate that cap both of these sequences (Chapter sections 5.2.1(iv) and 5.4.1(iii)) probably came from an escarpment that exposed very shallowly buried platform carbonates.

They signal seismicity and/or a sudden change in depositional slope probably related to displacements on faults that led to rapid collapse of the platform block.

Lateral discontinuity of Table Cove sequences is recognized in all other regions of the study area where this critical interval of the foreland basin succession is well-exposed (Figures 10.2 and 13.2). Limited paleoslope data in other areas precludes determining slope directions with the same degree of certainty as in the Table Point area, but local depositional thinning (in the absence of evidence of slope reversal) suggests that other local slopes faced northward, southward and eastward. The highly irregular, three-dimensional distribution of the slope deposits is interpreted to reflect the checkerboard distribution of relict platforms which in turn indicates that regional foundering of the platform was accompanied by faulting that generated a low relief, horst and graben topography and permitted differential subsidence of crustal blocks during this phase of foreland basin evolution.

13.2 Deposition of the Black Cove Formation

The Black Cove Formation consists of black, laminated, graptolitic shale that was deposited in a deep, anoxic basin (Chapter 7). It abruptly overlies platform limestones locally (Figures 13.1.c and 13.2), but more commonly it gradationally overlies Table Cove Formation slope carbonates. In both cases, the shale signifies a period of starved sedimentation in areas deprived of platform-derived carbonate sediment prior to the influx of siliciclastic turbidites of the American Tickle Formation (Chapter 14).

The platform limestone-basinal shale contact marks a 'drowning unconformity' (Schlager and Camber, 1986; Schlager, 1989) generated by extremely rapid subsidence of the platform. It is accentuated locally in the Pistolet Bay area by a mineralized hardground at the top of the

platform (Figures 4.5.b, 12.4 and 12.6) that formed during a depositional hiatus prior to the onset of shale sedimentation. In that area, and in some others further south, the uppermost platform limestones are also fractured and/or have been disrupted and transported in a gravitational slide or debris flow, further attesting to tectonic deformation of the platform prior to, or during, subsidence (Chapter sections 12.1.2-4). The absence of deep-water carbonates from those sequences suggests that subsidence was so rapid as to preclude deposition of even a thin veneer of *in situ* generated carbonate, such as formed elsewhere in an upper slope setting. Minor dolomite in the basal Black Cove Formation shale, however, does point to the presence of contemporaneous carbonate sediment sources that were either very far away or had subsided to depths where very little sediment was produced and/or storm waves were no longer effective at entraining the sediment and transporting it off-platform.

These drowned platform sequences are not clustered in a specific zone or region, but instead are in isolated areas generally surrounded by sequences in which the platform is overlain by deep-water carbonates (Figure 13.2). Based on their relationships to the latter it appears that drowned sequences have two, somewhat different origins.

1) Drowned sequences at Gargamelle Cove and River of Ponds Lake (Figure 13.3) are interpreted to represent rapidly foundered, relict platforms. The depositional histories of Table Cove Formation sequences in adjacent areas (described above) indicate the drowned platform at River of Ponds Lake and the condensed Table Cove Formation slope sequences in DH-1516 and DH-1382 are located in the area that was a topographically high, sediment source area during initial subsidence of the platform (Figure 13.5.a,b,d). Rapid subsidence and starved sedimentation at River of Ponds Lake, therefore, is inferred to have occurred late, after the change to a regional, south-southeast-dipping slope and essentially coincident with deposition of the thin slope sequences in

DH-1516 and DH-1382 (Figure 13.5.c,e). A similar history is inferred for the drowned platform sequence at Gargamelle Cove, located structurally inboard of the thick carbonate slope sequences at Table Cove and Spudgel's Cove, which was also a sediment supplying, topographic high (Figure 13.5. b,c,e). Rapid subsidence and drowning of this block, however, is inferred to have occurred somewhat later, coincident with the end of deep-water carbonate sedimentation further south. In both of these area fracturing and mass movement of the uppermost platform limestones (Chapter sections 12.1.2-3) signal major changes in submarine topography, probably caused by displacements on faults that facilitated rapid collapse of these platform blocks.

2) Drowned platform sequences in the Pistolet Bay area, in contrast, are thought represent a sediment-starved basin formed over a rapidly foundered platform block at the downslope end of a newly formed, subsiding ramp. In that area black shale directly overlies a large area of the platform; Table Cove Formation slope deposits overlie the platform only locally on the northwest side of Pistolet Bay and on the south side of Hare Bay (Figures 13.2 and 13.6). Sequences shown in Figure 13.6 are presently separated by faults, most of them west-directed thrusts, that are interpreted to have formed during Acadian orogenesis. Those delineated on the accompanying maps are proven or inferred to have actively influenced sedimentation during earlier phases of foreland basin development (Chapter sections 11.3 and 12.1.4).

Two different models that account for drowning and deposition of deep-water shale directly atop the platform in this area are illustrated in Figure 13.7. A relict platform origin (Figure 13.7.a), identical to that envisaged for drowned sequences at River of Ponds and Gargamelle Cove, is supported by the previous sedimentation history of the underlying tectonized platform. Deep erosion on the St. George Unconformity, and deposition of both thin peritidal sequences at the base of the Table Point Formation and of relatively thin and grainy, complete platform

Figure 13.6 Cross-section of post-platform sequences in the Pistolet Bay area. 1 = Callieux Bay (Vaches Point); interstratified debris flow conglomerates are interpreted to have come from the upper slope or platform from which enclosing ribbon limestones derived (Chapter section 5.4.3), implying synsedimentary faulting before that platform was drowned. 2 = Bakeapple Island; 3 = west coast of Pistolet Bay; 4 = Burnt Island peninsula. Their locations are shown in the accompanying map. TP = Table Point Formation; TC = Table Cove Formation; BC = Black Cove Formation; AT = American Tickle Formation; DH = Daniel's Harbour Member. Key to other symbols is in Appendix A. The abbreviations *rls* and *sh* on the maps mark other outcrops where Table Cove Formation ribbon limestone and Black Cove Formation shale, respectively, overlie the platform. The ribbon limestone outcrop south of Cook's Harbour does not contain debris flow conglomerates. Faults delineated on the maps are only the major Acadian structures in the area (compare with Bostock et al., 1983; Knight, 1986a; Cawood, 1989); the amount of structural telescoping of the platform caused by these and other thrust faults in the area is unknown. The Ten Mile Lake Fault (TML) and the unnamed fault west of Burnt Island peninsula in Pistolet Bay are inferred to have been active during uplift of the platform and formation of the St. George Unconformity (Chapter section 11.3) and during deposition of Basal Peritidal Unit sediments of the Table Point Formation (compare BPU sequences at Bakeapple Island and Burnt Island peninsula, back pocket).

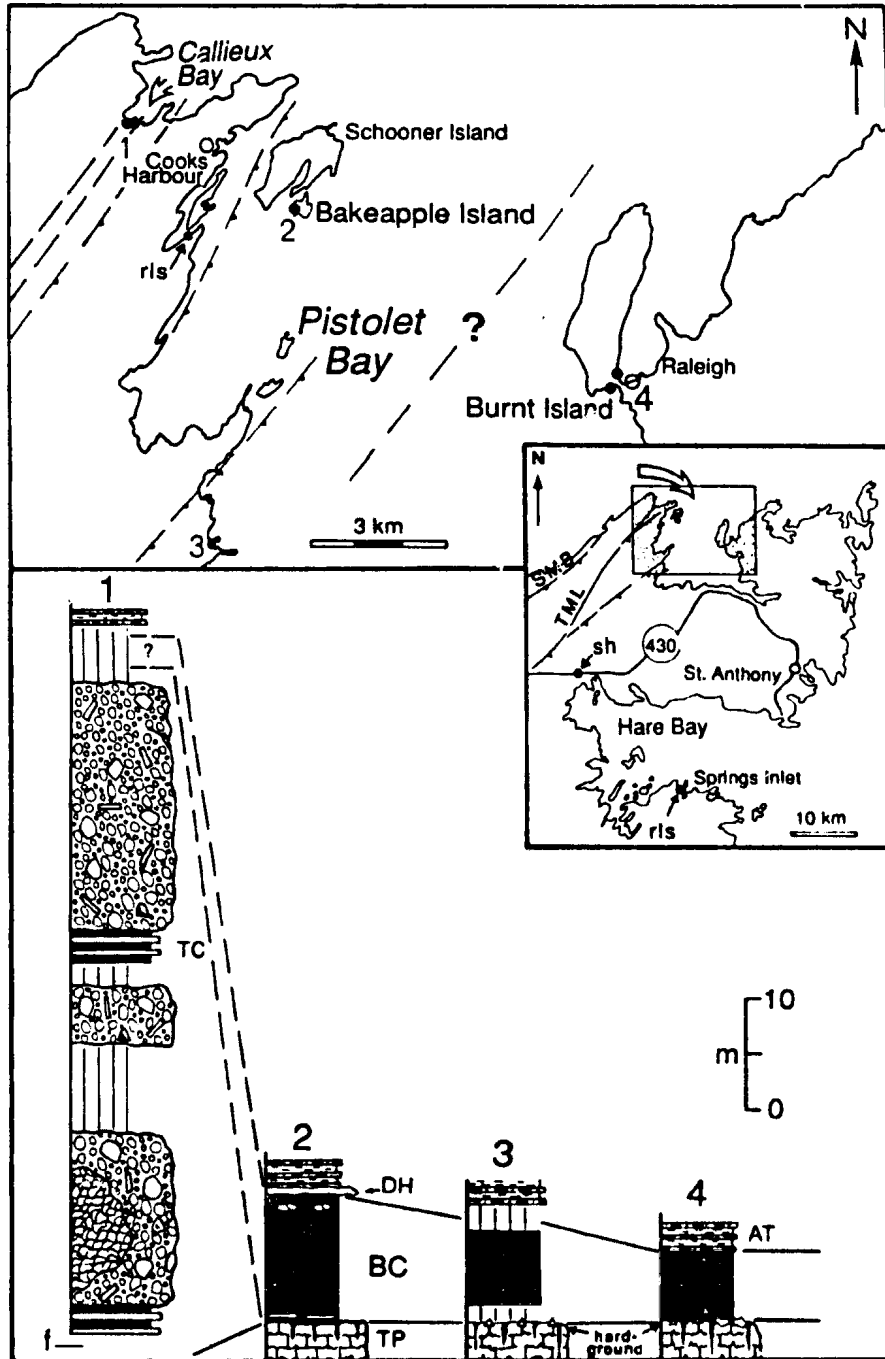
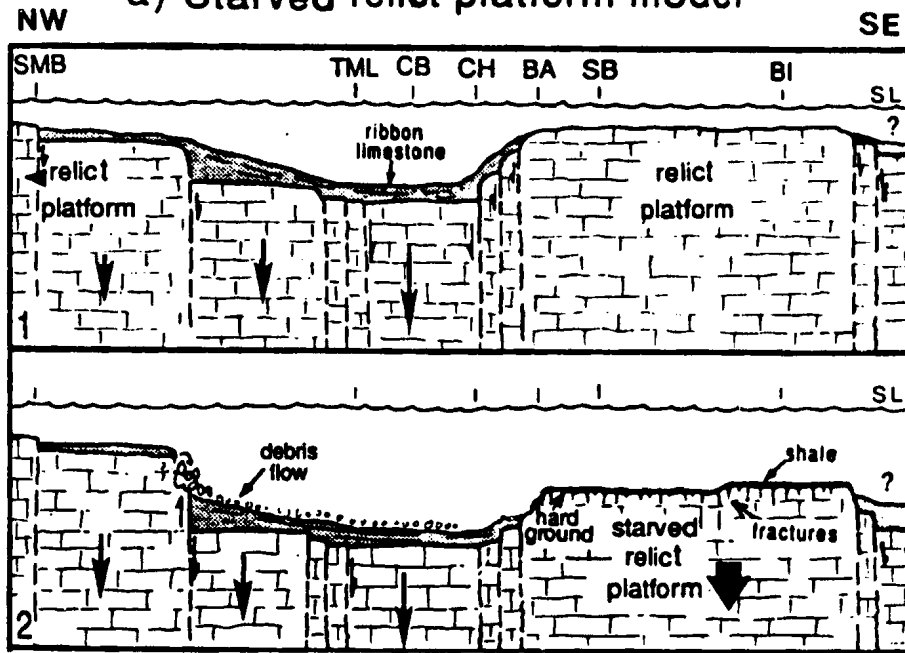
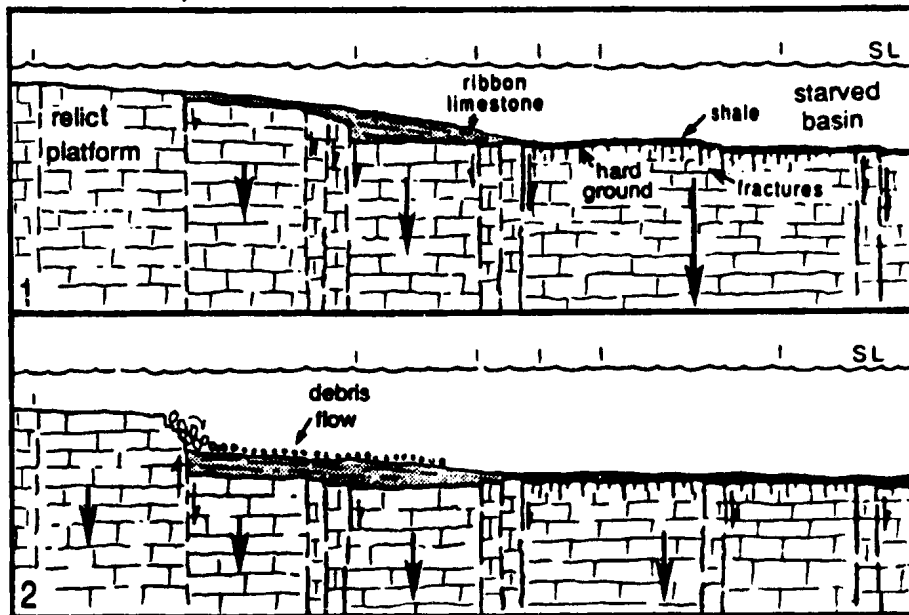


Figure 13.7 Models for platform collapse and generation of the drowning unconformity in the Pistolet Bay area. Line of cross-section extends roughly across structural strike from the St. Margaret Bay fault (SMB) to Burnt Island peninsula (BI); TML, Ten Mile Lake fault; CB, Callieux Bay; CH, Cooks Harbour; BA, Bakeapple Island; SB, west side of Pistolet Bay; locations are in Figure 13.6. a) Starved, relict platform model. 1 - Initial differential subsidence of the platform rendered the Pistolet Bay area a sediment producing, topographic high on the east flank of an incipient basin centered around Callieux Bay. 2 - Later displacements on faults resulted in fracturing, foundering, and hardground formation on the Pistolet Bay platform block and created an escarpment on the opposing platform from which debris flow conglomerates were generated. b) Starved basin model. 1 - Initial break-up and differential subsidence of the platform generated an easterly-dipping slope, the adjoining basin of which was formed by very rapid subsidence of the platform underlying Pistolet Bay. Fracturing and hardground formation accompanied subsidence. 2 - Later seismicity or faulting that affected the relict platform gave rise to debris flow conglomerates deposited on the lower slope-basin margin.

a) Starved relict platform model



b) Starved basin model



sequences (Figures 11.2, 12.7 and 12.8) indicate that the area had previously been a relatively slowly subsiding, submarine high. It could have retained that subsidence signature and persisted as an isolated relict platform during regional collapse. However, evidence in Aquathuna - Table Point sequences in other areas that the subsidence signature (rapid or slow) of individual platform blocks changed with time (eg. Port au Choix, Figure 11.2; DH-2512, Figures 12.7 and 12.8), proves that this was not necessarily the case. The alternative, starved basin origin for collapsed platform sequences in this area (Figure 13.7.b) is favoured for two reasons. First, there is no evidence of a west-facing slope immediately west of Bakeapple Island. The distribution of the deep-water carbonates, notably the presence of relatively thick sequences of Table Cove Formation ribbon limestones at Callieux Bay and south of Cooks Harbour, and of a few thin, discontinuous mudstone beds at the base of the Black Cove Formation at Bakeapple Island, suggest they were deposited on an easterly-facing slope supplied with sediment by a relict platform located off to the west. Second, debris flow conglomerates that are interpreted to have come from an escarpment in shallow water are interstratified with ribbon limestones only at Callieux Bay. Their distribution also suggests the presence of a relict platform located off to the west.

In summary, drowned platforms on which basinal shale was deposited resulted from both very rapid subsidence at the onset of platform collapse, and from later, abrupt subsidence of relict platforms that had acted as sediment sources for deep water environments. Starved conditions persisted in both settings until they came within reach of siliciclastic-bearing, turbidity currents, as dictated by distance from those encroaching systems and/or topography.

13.3 Deposition of the Cape Cormorant Formation

The Cape Cormorant Formation is composed of carbonate lithoclast,

debris flow conglomerates and calciturbidites, and lesser platform-derived, ribbon limestone, interstratified with shale that were deposited in deep-water, basin margin and basin settings (Chapter 6; Figure 13.1.a). These strata disconformably overlie the platform only on the far west side of the Port au Port Peninsula (Figures 13.2) and, like the previously described sequences, indicate extremely rapid subsidence of the platform. A low, angular unconformity between Table Point limestones and the basal Cape Cormorant conglomerate in Big Cove proper (Figure 6.1.c), and a large gravitational slide at the top of the platform exposed north of Big Cove (Figures 6.1.b and 6.3.b), suggest platform subsidence was accompanied by seismicity and an abrupt, albeit small change in depositional slope.

These deep-water sediments uniquely demonstrate that platform collapse was accompanied by catastrophic faulting and generation of high relief, submarine topography. The outstanding components of the sequences, namely polymictic, debris flow conglomerates and calciturbidites that came from an exhumed, Early Paleozoic platform succession, indicate that the basin was bounded along at least one margin by a fault scarp that exposed at least 500 m of buried platform carbonates. Coarseness and thickness trends in Cape Cormorant Formation sequences, in conjunction with paleoflow data, indicate that the main escarpment trended north-northeast and was located west of present day Cape Cormorant outcrops (Figure 6.19).

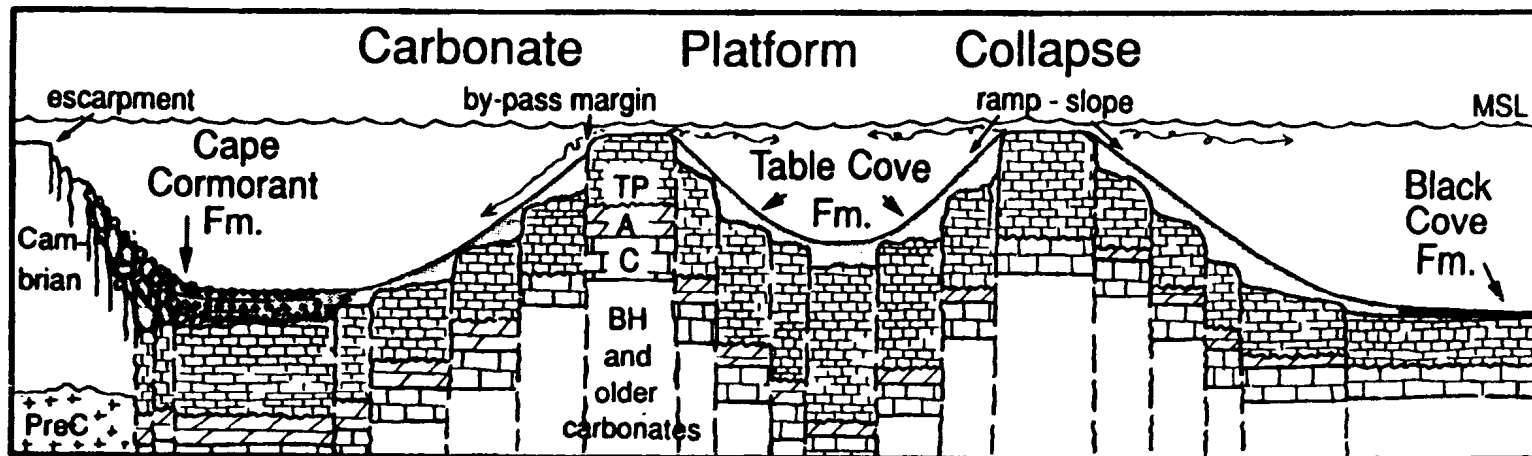
The vertical succession of lithofacies that make up the complete formation sequence at Caribou Brook (Figure 13.1.a) record: 1) rapid formation of, and prolonged deposition in, a fault-bounded basin, 2) gradual mass wasting of the bounding fault scarp and drowning of one or more adjacent relict platforms, and 3) basin filling, and possibly shoaling, accompanied by temporary reactivation of the faulted margin, and influx of siliciclastic turbidites. Despite the unique escarpment-derived components of the Cape Cormorant, the depositional history

parallels that of post-platform sequences in all other areas. Platform-derived ribbon limestone in the basal megaconglomerate-ribbon limestone lithofacies is equivalent to same-named strata in the upper Table Cove Formation. Black, laminated shale, a prominent component of the overlying calcarenite-conglomerate lithofacies, is equivalent to the Black Cove Formation. Greenish-grey, silty shale in the capping green shale-calcarenite lithofacies is equivalent to distal turbidite lithofacies at the base of the American Tickle Formation. These correlations indicate that the two types of collapse sequences were deposited contemporaneously.

13.4 Reconstruction and Discussion

Regional collapse of the Table Point platform was accompanied by block-faulting that involved reactivation of rift-related basement structures that reestablished a horst and graben topography across the foreland basin (Figure 13.8). Over most of the area, initial faulting generated a gentle, low relief submarine topography. Several localized carbonate slopes formed on tilted and differentially subsiding platform blocks, while very rapid subsidence of others created deep, starved, anoxic basins. Only locally at the onset of platform break-up and foundering was faulting of such magnitude as to generate a major, submarine escarpment that exhumed several hundred metres of old, buried platform carbonates. Later faulting that led to the ultimate demise of relic platforms in other areas, however, was accompanied by brittle fracturing and, either because of increased seismicity or sudden changes in slope, mass movement of the uppermost platform limestones.

Slopes of variable dips and the irregular, three-dimensional distribution of post-platform sequences indicate the foreland basin at this point in time was not a single, regional carbonate slope adjacent to an extensive, albeit dying, platform. Two aspects of the Table Cove Formation, however, suggest that the envisaged irregular topography was



vert. ex. \approx 50x

Figure 13.8 Schematic vertical cross-section across the western Newfoundland platform during the collapse stage (Phase 3) of foreland basin development. (No polarity across the platform is implied.) Differential subsidence of platform blocks that created relict, shallow-water platforms and gentle slopes and adjoining basins on which Table Cove Formation carbonates and Black Cove Formation shale were deposited was widespread. Catastrophic faulting that exhumed passive margin platform carbonates and created a deep-water basin into which resedimented carbonates and shale of the Cape Cormorant Formation occurred only locally. TP, Table Point Fm.; A, Aguathuna Fm.; C, Catoche Fm.

superimposed on a regional, eastward-dipping slope. First, the thickest formation sequences are restricted to the most inboard, western localities (eg. Table Point, Spudgel's Cove), while those in the east are consistently thin (eg. Beaver Brook, Black Cove). Although limited outcrop precludes establishing this across-strike trend everywhere, the thickness gradient does suggest that subsidence and drowning occurred more rapidly in outboard areas than in inboard areas, the net product being an oceanward-dipping slope. Second, conodont faunas reported from formation sequences at Little Springs Inlet (Hare Bay) and in the Port au Port area suggest they are slightly older than they are at Table Cove (Fåhraeus, 1970; Erdtmann, 1971; Stouge, 1984). Although the age difference between those sequences corresponds to only one conodont phylozone (Stouge, 1984), outboard to inboard diachronous collapse also implies a regional slope dipping off toward the subduction zone.

CHAPTER 14

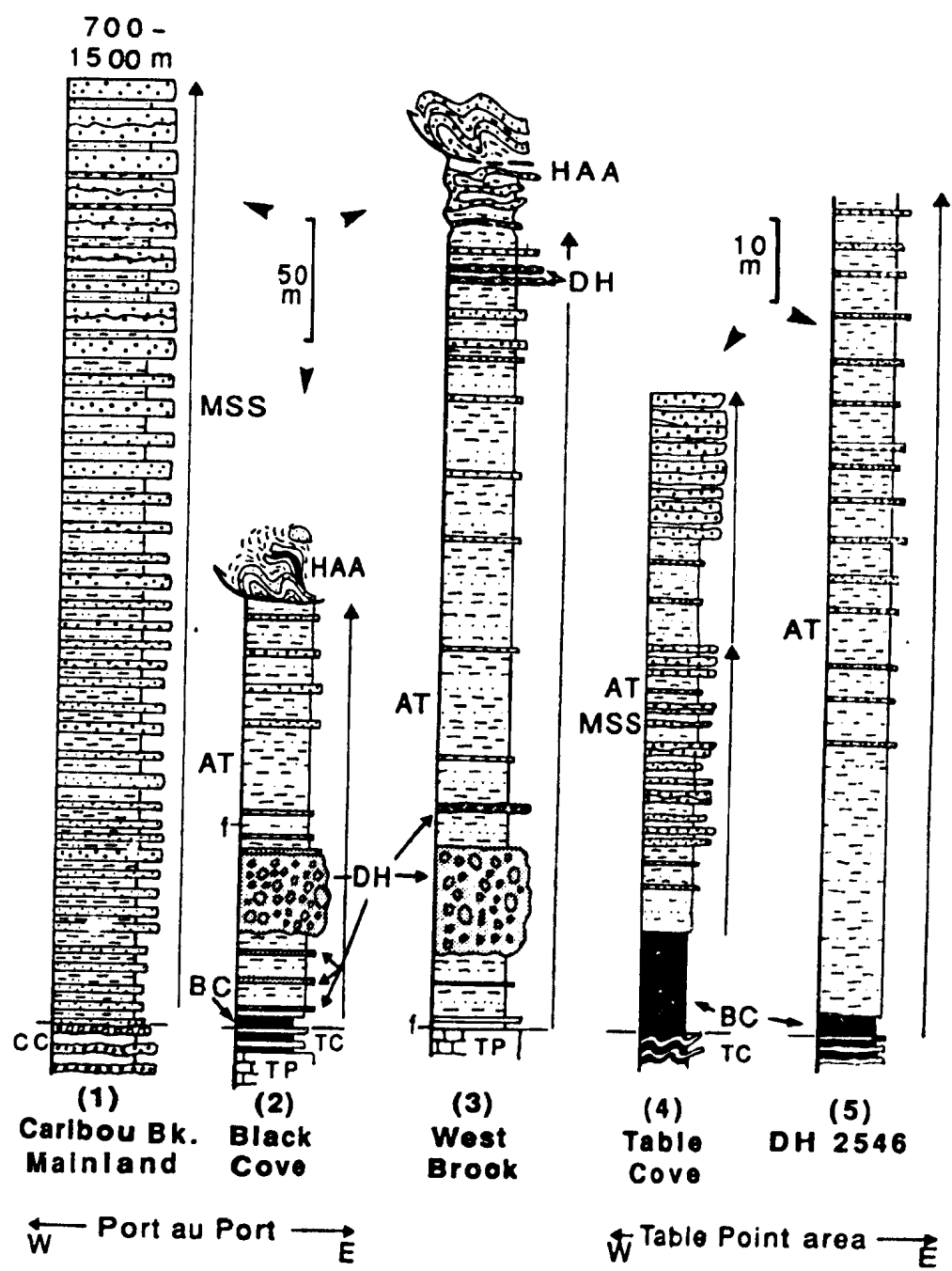
PHASE 4: DEPOSITION OF SILICICLASTIC SEDIMENTS

Platform collapse and deep-water carbonate sedimentation was everywhere followed by deposition of deep-water siliciclastic sediments of the Goose Tickle Group (Figure 14.1). In most places the demise of carbonate sedimentation was followed by a period of starved sedimentation during which black shale (Black Cove Formation; Chapter 7) was deposited. That phase of sedimentation was eclipsed by the influx of immature siliciclastic sediment (American Tickle Formation and Mainland Sandstone; Chapter 8) that was transported into and deposited in the foreland basin by turbidity currents. The turbidites buried the collapsed platform and continued to fill the foreland basin until allochthonous thrust slices of sedimentary and igneous rocks, tectonically assembled outboard of the continental shelf (Taconic Allochthons), were emplaced (Chapter 16).

14.1 Starved, Anoxic Basin Sedimentation

Starved sedimentation in deep, anoxic settings in the foreland basin is recorded by the relatively thin, but widespread Black Cove Formation composed of black, laminated, graptolitic shale (Figures 10.2 and 14.1). Most commonly it gradationally overlies ribbon limestones (Table Cove Formation) that were deposited in lower slope to basin margin environments. That stratigraphic relationship indicates that the shale accumulated in basins adjacent to carbonate slopes that lay beyond the reach of platform-derived hemipelagic suspensions and turbidity currents. Progressive decline and then elimination of platform-derived carbonate delivered to deep-water environments was caused by continued subsidence of relict platform and slope blocks which not only lowered them below depths at which biogenic carbonate was produced, but removed them from the zone of current and wave activity where surface sediments were

Figure 14.1 Cross-section of measured sections through the Goose Tickle Group. Locations are shown in Figure 14.3. BC, Black Cove Formation; AT, American Tickle Formation; MSS, Mainland Sandstone; DH, Daniel's Harbour Member; TC, Table Cove formation; TP, Table Point Formation. Arrows to the right of the columns indicate coarsening- and thickening-upward sequences. Section (1) is based on field observations of parts of the Mainland section by the writer and shows only general changes in sandstone-dominated lithofacies up-section. Sections (2-4) are from measured sections described by the writer. Section (5) is based on the original log for the core described by T. Lane, Teck Exploration.



entrained and transported out over adjacent slopes and basins. Starved conditions persisted until siliciclastic-bearing turbidity currents traveled into the basin. Regional variations in thickness of the shale above Table Cove Formation ribbon limestone (2-22 m; Figure 10.2) suggest that period of time varied considerably across the foreland basin.

Local deposition of black shale directly atop platform limestones (Chapter 13.2) also records very rapid subsidence of platform blocks, including both those that formed basins at the toes of carbonate slopes and those that had remained as sediment-supplying, relict platforms for some period of time (Figures 13.5 and 13.7). In contrast to those that formed basins, relict platform blocks were isolated, intrabasinal highs that initially escaped burial by coarser siliciclastics transported by turbidity currents traveling in topographic lows. Starved conditions persisted until subsidence of these high blocks and sediment accretion in adjacent low areas eliminated sea floor topography.

14.1.1 Origin and Significance of Anoxic Bottom Waters

Black Cove Formation shale uniquely records starved sedimentation, but anoxic conditions are not peculiar to the settings described above. Lower slope - basin margin ribbon limestones are interpreted to have been deposited under strongly dysaerobic or anoxic bottom waters, as are siliciclastic turbidites (Chapter sections 5.4.5 and 8.6).

There are two possible explanations for the presence of anoxic waters in what are inferred to have been the deepest environments of the foreland basin. One is that anoxia reflects subsidence of the tectonized platform to a depth at which it intercepted an oceanic, oxygen minimum zone (OMZ) (Figure 14.2.a). Along modern margins in open ocean settings OMZs are most well-developed in areas of coastal upwelling and high biologic productivity in surface waters, occurring as discontinuous lenses that intersect the shelf or slope at intermediate water depths ranging widely from as little as 50 m to 100 m or 500 m, and extending

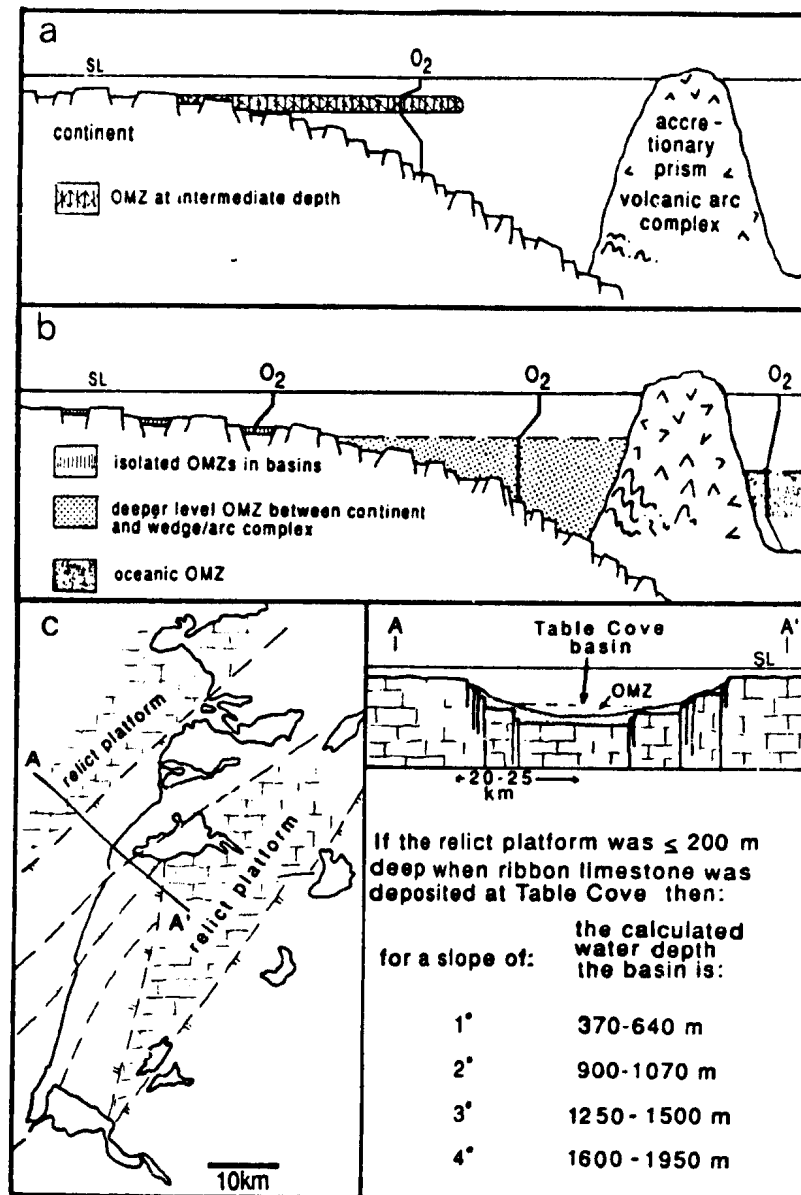


Figure 14.2 Models for the Oxygen Minimum Zone in the foreland basin. **a)** Tectonized platform subsides to the depth at which it intercepts the oceanic OMZ ($O_2 < 0.2$ ml/l). No specific depth range or lateral extent of the OMZ are implied. **b)** An OMZ forms in a thermohaline stratified water column in the foreland basin and/or in isolated basins of the block-faulted platform. **c)** Map and vertical cross-section across the foundered platform in the Table Point area (see also Figure 13.5) and depth ranges for the Table Cove basin in which ribbon limestones were deposited under strongly dysaerobic to anoxic conditions.

to depths of 1000-2000 m (Sverdrup *et al.*, 1942 in Heckel, 1977; Deuser, 1975; Burnett, 1977; Thiede and Van Andel, 1977; Vercoutere *et al.*, 1987). Whether similar conditions existed along the Middle Ordovician continental margin cannot be demonstrated. However, the presence of red shale in older continental slope and rise deposits of the Cow Head Group indicates that there was no permanent, oceanic OMZ that extended to the ocean bottom during Ordovician time (James and Stevens, 1986) and, therefore, persistence of anoxic conditions in the foreland basin implies that it did not subside below the depth of the oceanic OMZ.

The alternative explanation is that anoxia reflects stratification of the water column in the foreland basin resulting from restricted circulation imposed by adjacent land masses and submarine topography (Figure 14.2.b). Similar conditions presently characterize the Black Sea which is semi-enclosed by land and semi-isolated from oxygenated Mediterranean waters by a sill (Degens and Ross, 1974; Grasshoff, 1975; Demaison and Moore, 1980). The OMZ there comprises the entire bottom water mass, extending from ~150-250 m down to the bottom (~2000 m), and is maintained by a strong halocline that impedes exchange with the open ocean. Perhaps more analogous to the Middle Ordovician foreland basin are small, stratified basins that occur on otherwise open ocean shelves (Richards and Vaccarro, 1956; Thornton, 1984). The Cariaco Trench in the Caribbean Sea, for example, has a sill at ~200 m depth and an OMZ that extends from ~300 m to the bottom (1400 m) and is maintained by a strong thermocline that prevents vertical mixing in the water column.

This model for the origin of the OMZ in the foreland basin is favoured for several reasons. 1) The carbonate platform did subside to depths of at least 100-200 m (ie. carbonate production ceased), probably more, and so the water column could have become thermally stratified (eg. Heckel, 1977). 2) The foreland basin was semi-enclosed. Continental land to the west and the accretionary prism/island arc to the east would have defined a narrow sea (by ocean standards) in which vertical

mixing of the water column by wave activity would have been reduced by limited fetch of the basin (Byers, 1977). 3) Platform collapse generated submarine topography that would have impeded both lateral circulation and vertical mixing of basin waters. Development of anoxic bottom waters may have been exacerbated by exceptionally high biologic productivity in surface waters possibly stimulated by nutrients supplied by wind-blown volcanic material. Moreover, under warm and humid climatic conditions thermal stratification may have been coupled with salinity stratification that enhanced the density contrast of water masses and further limited vertical mixing.

Whether anoxia in the foreland basin is independent of an oceanic OMZ or not, water depth is not tightly constrained (see depth values above). Evidence that the foreland basin did not intercept oxygenated polar waters below an oceanic OMZ and that both deep-water carbonates and shale were deposited above the CCD (Chapter 7.6) implies depths of less than 4000 m, possibly less than 2000 m. This agrees with bathymetry of the foreland basin calculated for the Table Point area where relict platforms and a contemporaneous anoxic basin are identified and located with considerable confidence (Figure 14.4.c).

14.2 Siliciclastic Turbidite Sedimentation

The relatively short period of starved sedimentation was everywhere followed by deposition of siliciclastic turbidites, recorded by the American Tickle Formation and Mainland Sandstone of the Goose Tickle Group (Figures 10.2, 14.1 and 14.3). These strata are classic orogenic flysch, composed of compositionally and texturally immature sediments that came from a geologically complex source terrane and were deposited rapidly, but episodically, in a deep-water basin. Lithic fragments in the sandstones point to weathered and eroded sedimentary, volcanic, plutonic, and possibly metamorphic sources. Detrital chromite may link the sediment to ultramafic rocks which, together with the lithic

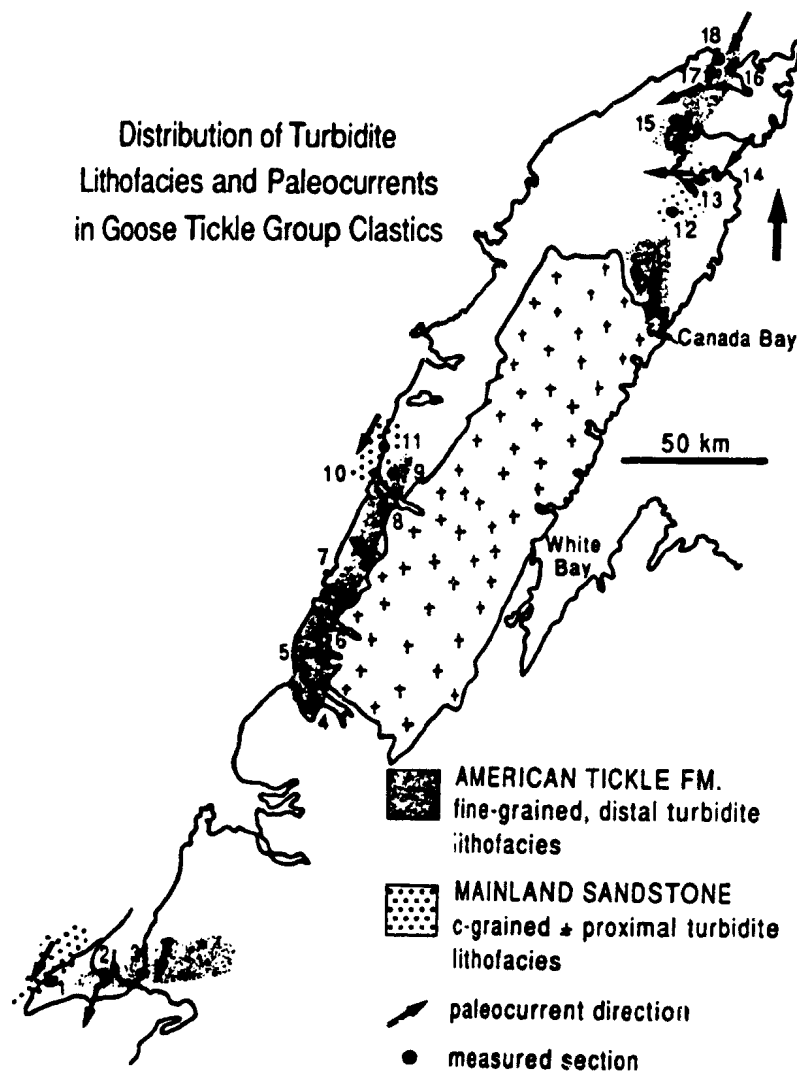


Figure 14.3 Map distribution of deep-water, siliciclastic turbidite lithofacies and paleocurrents. 1, Caribou Brook; 2) West Bay Center; 3) Black Cove; 4) Shag Cliff; 5) Baker's Brook; 6) Stag Brook; 7) West Brook; 8) Southwest Feeder; 9) Daniel's Harbour Zinc Mine; 10) Spudgel's Cove; 11) Table Cove; 12) Coles Pond; 13) American Tickle (not measured); 14) Springs Inlet; 15) Northern Arm; 16) Burnt Island; 17) west coast Pistolet Bay; 18) Bakeapple Island. Paleocurrents are from Williams and Smyth (1983), Williams (1985), Knight (1986c), Quinn (1988a) and this study. Lithofacies shown at Canada Bay is based on descriptions by Cummings (1983).

components, suggests the sediments came from the ophiolite-bearing, accretionary wedge (Humber Arm and Hare Bay allochthons) that was assembled in the subduction zone on the eastern margin of the foreland basin (Stevens, 1970).

These turbidites buried the collapsed platform and filled the foreland basin. Their current structures indicate regional transport to the south-southwest (Figure 14.3) and suggest the foreland basin was an elongate, northeast-trending, south-dipping trough that was filled with sediment deposited by currents traveling parallel to the basin axis. This regional morphology and pattern of sediment dispersal are common to other ancient flysch sequences deposited in other structurally confined foreland basins (Kuenen, 1957 and Haaf, 1959 cited in Reading, 1978; Morris, 1974; Nilsen, 1985; Ricci Lucchi, 1985).

Sedimentation continued until the accretionary prism was emplaced over this inboard region of the foreland basin. The thickness of sediment deposited is thought to have been a minimum of a few to several hundred metres. Structural truncation by the overlying allochthon in most places precludes determining the actual thickness, and accurate measurements of even those sequences are impossible to obtain in most places because exposures are incomplete and commonly folded and faulted. The approximate thickness of American Tickle Formation sequences in the Gros Morne area (Shag Cliff to West Brook) is 300-350 m (Figures 14.3 and 14.1.3). Predominance of deformed, siliciclastic turbidites in the mélange at the base of the overlying allochthon, however, suggests the pre-emplacment thickness was actually much greater. In contrast, the Mainland Sandstone on the west side of the Port au Port Peninsula, located beyond the Humber Arm Allochthon, has a directly measurable thickness of 700 m (Quinn, 1988a) and may be as much as 1500 m thick (Stevens, 1970).

14.3 Mechanism of Basin Filling

Turbidite lithofacies in many of the more complete formation sequences define a single, coarsening- and thickening-upward package which indicates that basin filling was accompanied by progradation of a turbidite-dominated depositional system in the basin (Figure 14.1). Shifting of proximal environments over distal ones is thought to reflect steady encroachment of the sediment source terrane and is the predictable product of continuous continentward migration of the accretionary prism in response to continued subduction. East to west progradation of the flysch away from the subduction zone is inferred from the presence of compositionally and texturally similar turbidites (Lower Head Sandstone) depositionally above Cow Head Group and other coeval continental slope and rise sequences that were incorporated as thrust slices in the accretionary prism (Humber Arm Allochthon) (Stevens, 1970; James and Stevens, 1986). An early Llanvirnian age of Lower Head sandstones and an early middle to late Llanvirnian age for Goose Tickle Group clastics demonstrate that the orogenic flysch is regionally diachronous across strike.

Two other salient aspects of the siliciclastic sequences shed more light on the configuration of the foreland basin and manner in which it was filled. First, there is no north to south, proximal to distal gradient defined by grain size, bed thickness, or sedimentary structures which parallels the regional paleocurrent data indicating that the sediment was supplied to the basin mostly or solely via its up-slope, northern end (eg. Ricci Lucchi and Valmori, 1980; Nilsen, 1985). Second, predominant lithofacies of the sequences define a west to east, proximal to distal environmental gradient across the inferred strike of the foreland basin (Figure 14.3), contradictory to the expected polarity of turbidite depositional environments away from a sediment source located east of the immediate basin.

The absence of a consistent north to south, proximal to distal

gradient in what is inferred to be an elongate trough suggests that sediment was supplied to the foreland basin at several points along its length. This is precisely what would be expected given a linear source terrane extending along the eastern margin of the basin and it has been documented in the older, equivalent Lower Head Sandstone (González-Bonorino, 1990) and in other ancient foreland basins and in modern trenches (Dzulynski *et al.*, 1959; Moore *et al.*, 1982a; Ricci Lucchi, 1985). Introduction of sediment at several points and deposition in separate systems is strongly suggested by reversals in texture along strike, such as is apparent in the turbidite sequences in the Gros Morne area between Southwest Feeder and Shag Cliff (Figure 14.3). More generally it is indicated by striking differences in the general appearance of the siliciclastic sequences in different areas of the foreland basin (Figure 8.3). Outcrop appearance reflects a combination of composition (eg. percentage of different types of lithic fragments, minerals, and matrix), texture, specifically, the range of grain sizes, and diagenesis (eg. abundance and types of cement), which are all inter-related and ultimately controlled by a local, available sediment supply.

Independent of the potentially numerous depositional systems along the length of the foreland basin, an across-strike, proximal to distal lithofacies pattern is defined by the nearly restricted distribution of proximal, sandstone-dominated turbidite lithofacies to the most western outcrop localities and predominance of thin-bedded and fine-grained lithofacies to the east (Figure 14.3). It is best illustrated in two small areas, namely around Table Point and on the Port au Port Peninsula, where contrasting proximal and distal lithofacies sequences are thought to have come from the same local source and are inferred to be essentially coeval (Figure 14.1). Thick-bedded, coarse-grained, channel-like sandstones with current structures indicating flow toward the south in the western-most outcrops in both areas (Figure 14.3) seem to define major depositional axes of the foreland basin. Their presence

inboard of distal turbidite lithofacies sequences and the complete lack of any western source area demand that sediment was locally transported westward, across the basin, by-passing areas close to the sediment source. Importantly, in both areas the depositional axis defined by proximal turbidites occurs precisely in areas that were previously rapidly subsiding basins - Table Cove and Spudgel's Cove, where anomalously thick sequences of Table Cove Formation slope and basin carbonates were deposited (Figure 13.3), and Caribou Brook, where a very thick succession of deep-water, lithoclastic carbonates and shale of the Cape Cormorant Formation were deposited (Figure 13.1.a). The correlation suggests that the location of depositional axes for the turbidites was determined by preexisting structural domains in the basin probably defined by relict submarine topography on the collapsed platform, and perhaps maintained by continued differential movement on bounding faults. Across-basin transport and by-passing of areas nearest the sediment source must also have been controlled by topography.

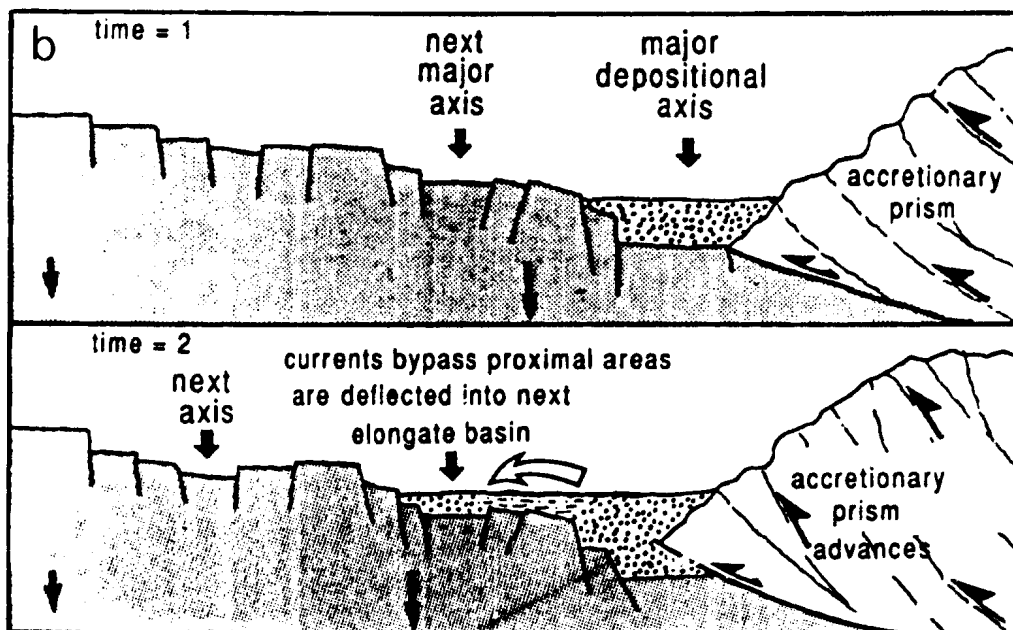
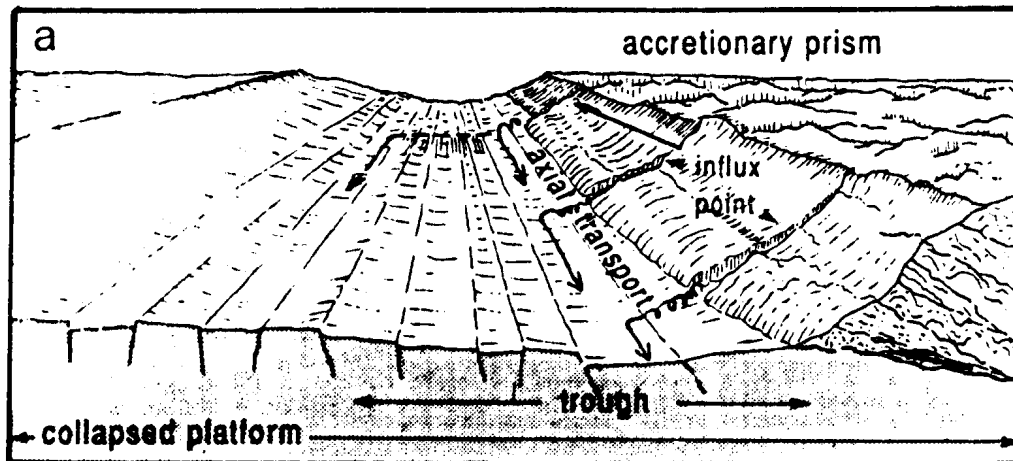
A model that accounts for the observed distribution of lithofacies in the autochthonous flysch is shown schematically in Figure 14.4. Turbidity currents flowing into the foreland basin from numerous points along its length were primarily funneled down the regional paleoslope in relict, elongate grabens of the block-faulted and collapsed platform, which became the major depositional axes of the turbidite systems (Figure 14.4.a). As the accretionary prism source advanced toward the continent, and the siliciclastics eroded from it prograded westward ahead of it, the depositional axes shifted to progressively more inboard structural depressions (Figure 14.4.b). Across-basin transport probably occurred along other depressions associated with major cross-faults, similar in origin and expression to transforms in oceanic crust (eg. Choukroume *et al.*, 1978), that were oriented at high angles to the predominant, northeast-trending structural grain.

Evidence in support of this model comes from American Tickle

Figure 14.4 Model for turbidite dispersal in the foreland basin.

a) Across-strike reconstruction of the foreland basin. Debris eroded from the accretionary prism is delivered to the foreland basin at several points along its length. Turbidity currents are deflected down the trough axis as dictated by the regional paleoslope. Across-basin transport occurs along other structural depressions associated with cross-faults oriented at high angles to the predominant structural grain. b) Vertical cross-sections across the foreland basin showing how subsidence-controlled, antecedent submarine topography controlled the location of depositional axes for the prograding orogenic flysch. Cross-faults that facilitated across-basin transport and westward shifting of the axes, which are not shown, are located up-slope (into the page) of the line of cross-section.

Mechanism of flysch dispersal



sequences in the Hare Bay - Pistolet Bay area which contradict many of the trends in sediment distribution and dispersal in other areas (Figure 14.5). First, defying the west to east, proximal-distal lithofacies gradient, basal siliciclastics of the formation at Springs Inlet, a comparatively eastern, outboard locality, are proximal turbidites. Their current structures indicate flow to the southwest, suggesting the sequence defines one major depositional axis in the foreland basin. Sandstone-dominated lithofacies at the base of the formation at Coles Pond, located along structural strike to the southeast, and predominance of fine-grained, distal turbidites further south and east around Canada Bay (Figure 14.5) suggest the sequence at Coles Pond records deposition in that same structural depression. Second, current structures in the turbidites at American Tickle indicate flow to the west (Figure 14.5). Depending on how consistent those data are (actual measurements are not published in Williams and Smyth, 1983), westward transport may indicate that that area is in the zone of a cross-fault that facilitated across-basin transport. Third, turbidite lithofacies at the base of American Tickle sequences around Pistolet Bay also define an east to west, proximal distal lithofacies trend (Figure 14.5) which may point to yet another major depositional axis of a separate turbidite system structurally inboard of the one inferred from the sequence at Springs Inlet. Finally, in that same area both Cumming (1983) and Quinn (1988a) describe coarsening-upward then fining-upward in the lower 100 m of the American Tickle Formation. This trend suggests progradation followed by abandonment of the depositional system, precisely the history expected with progressive shifting of major depositional axes of the basin toward the continent with time.

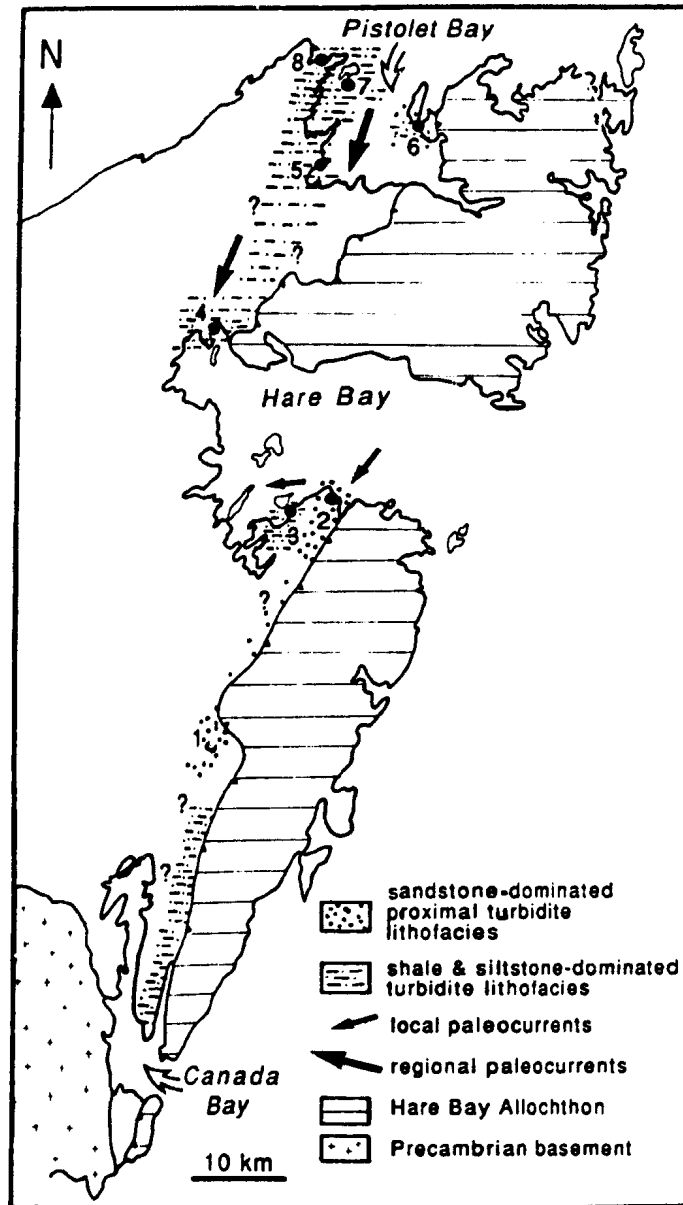


Figure 14.5 Map distribution of American Tickle Formation lithofacies and paleocurrents in the Hare Bay - Pistolet Bay area. 1, Coles Pond; 2, Springs Inlet; 3, American Tickle; 4, Northern Arm; 5, west side of Pistolet Bay; 6, Burnt Island peninsula; 7, Bakeapple Island; 8, Callieux Bay. Distributions of relatively proximal and distal lithofacies with respect to the regional northeast-trending structural grain suggest two major depositional axes for prograding flysch sequences. The most outboard appears to be located in a zone between Springs Inlet and Coles Pond; another more inboard axis is intercepted at Burnt Island. Paleocurrents are from Williams and Smyth (1983); Knight (1986c) and this study. Lithofacies data from Canada Bay is from Cummings (1983).

CHAPTER 15

PHASE 5: INTRABASINAL FAULTING

The final phase of foreland basin development prior to tectonic emplacement of allochthons, which overprinted siliciclastic turbidite sedimentation, was intrabasinal faulting. Faulting and uplift generated other submarine escarpments and exhumed the recently deposited, deep water and shallow water foreland basin succession and, to a limited extent, older passive margin carbonates. Material shed from the escarpments by mass wasting, was transported into the basin by debris flows and turbidity currents that deposited limestone lithoclast conglomerates and quartz-rich calcirudites and calcarenites of the Daniel's Harbour Member (Chapter 9; Figures 10.2 and 14.1). First generation debris flows and calciturbidites affected by subsequent faulting and uplift were incorporated and transported as clasts in second, possibly even third or fourth? generation flows. The distribution of the resedimented carbonate debris indicates that faulting occurred along nearly the entire length of the foreland basin (Figure 15.1), that it commenced shortly after siliciclastic turbidite sedimentation began in this region of the foreland basin, and that escarpments persisted as sources of debris for a significant period of time before transport and emplacement of allochthons (compare the Black Cove and West Brook sections in Figure 14.1).

15.1 Location of Escarpments

Lithoclasts which comprise Daniel's Harbour Member beds indicate they came from escarpments located in this general area of the foreland basin, that is, where the foreland basin developed on what had previously been a carbonate platform on a passive margin continental shelf; there are simply no lithoclasts exotic to the autochthonous succession present. The actual dimensions of the ancient platform, turned foreland

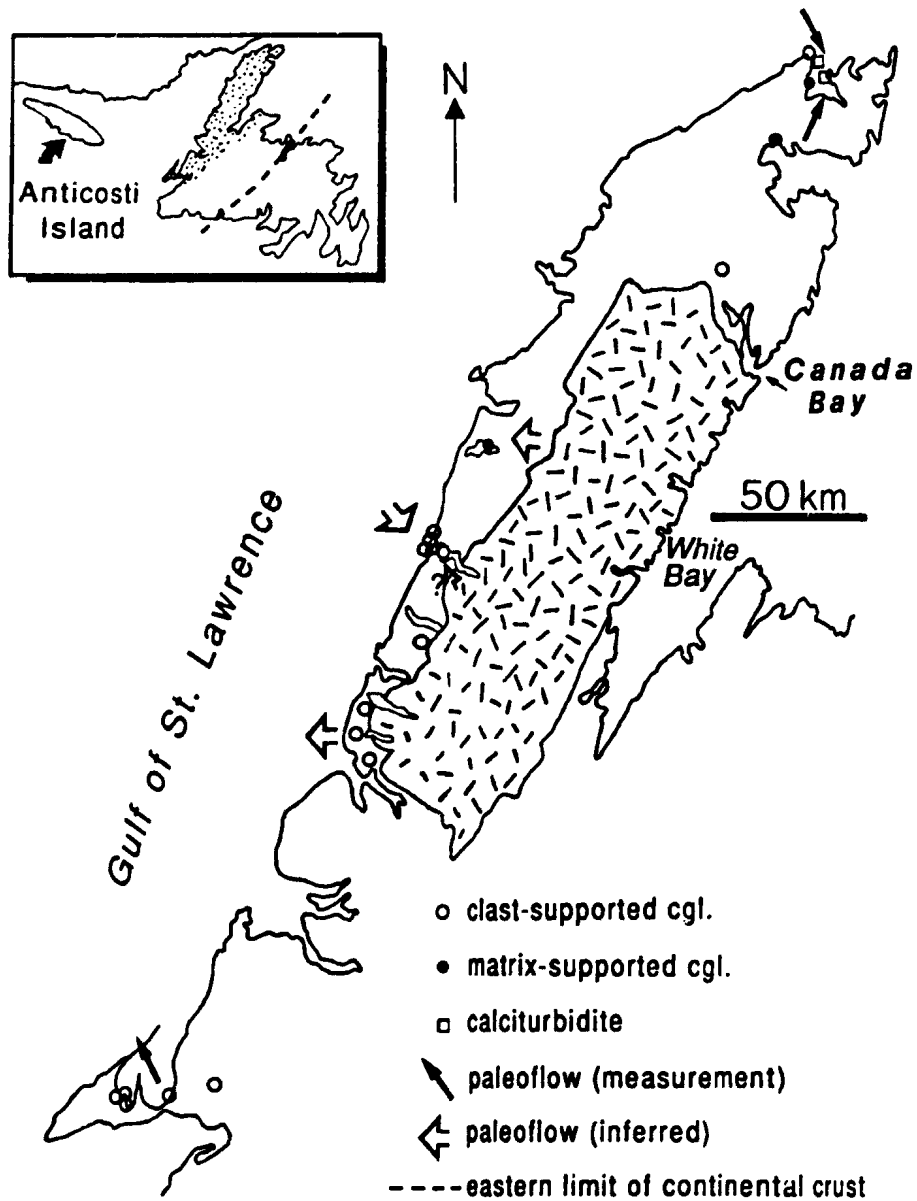


Figure 15.1 Regional distribution and transport directions for Daniel's Harbour Member beds.

basin, however, are not precisely known. The pre-foreland platform margin is thought to have been located at least as far east as White Bay where polydeformed, shelf carbonates occur (Lock, 1972; Williams, 1977; Figure 15.1). Deep crustal seismic lines, however, show that thickened continental crust extends about 125 km further east under central Newfoundland (Keen et al., 1986), so the margin of the platform could also have been much further east. Also, the ancient platform must have extended several tens of kilometres further west toward the continent; a Middle Ordovician foreland basin sequence is recognized in the subsurface as far inboard as Anticosti Island (Roliff, 1968; Figure 15.1, inset map). Consequently, the escarpments from which Daniel's Harbour Member beds were derived could have been located very near where the material was deposited, or could have been outside the actual outcrop area.

Two arguments support a hypothesis that fault scarp sources were generally very local. First, this area of the foreland basin is proven to have been dissected by numerous, basement-linked faults that influenced sedimentation during all previous phases of foreland basin development. It is reasonable to assume they could have been reactivated with catastrophic displacements at this point in time. Second, many of the debris flow conglomerates contain distinctive lithoclasts that tie them to intact stratigraphic sequences in the immediate area. For example, black chert clasts are conspicuous, although minor components of Daniel's Harbour Member conglomerates in the Gros Morne area where locally upper Table Point limestones contain numerous horizons of black, nodular chert. Similarly, large clasts of Stromatactis mound limestone and plates of peloidal, turbiditic ribbon limestone (sub-lithofacies B) are conspicuous components of the conglomerate in the Port au Port Peninsula area where those lithofacies are well-developed at the top of the Table Point Formation and in the Table Cove Formation, respectively. Also, large clasts of medium- and

coarse-grained sandstone are prominent components of the conglomerates in the Daniel's Harbour - Eastern Head area just north of which, at Spudgel's Cove and Table Cove, similar proximal turbidites comprise the Mainland Sandstone/American Tickle Formation. Finally, matrix-supported conglomerates in the Pistolet Bay - Hare Bay area are characterized by abundant shale matrix and clasts and scarcity of ribbon limestone clasts or plates, while in the immediate vicinity slope carbonates are not present in many autochthonous successions and platform limestones are directly overlain by black shale.

Major arguments against local derivation of Daniel's Harbour Member beds are these. First, no fault scarp sources are recognized in the area. Neither deeply-eroded autochthonous platform sequences mantled by siliciclastic turbidites, nor discordant, depositional contacts between platform carbonates and carbonate lithoclast talus or siliciclastic sediments that would identify a fault scarp are seen in outcrop. Admittedly, this may simply be a function of limited exposure or, in the latter case, obliteration by more recent faulting. Second, and perhaps more importantly, the foreland basin is visualized as a complex mosaic of discontinuously distributed lithostratigraphic units and lithofacies, and lithoclasts cited above as markers for correlation are simply not exclusive to the immediately adjacent autochthonous sequences; the sole exception seems to be peloidal, turbiditic ribbon limestone in the Port au Port area. Therefore, derivation from other, more distant sources is entirely possible. Debris flow conglomerates in the Daniel's Harbour area illustrate this point in reverse. They contain large clasts of Stromatactis mound limestone, but that lithofacies is not developed at the top of the Table Point Formation in outcrops in the immediate area.

Two arguments can be put forth in support of a hypothesis that most debris was shed from faults located outboard of the immediate area. First, most conglomerates are composed primarily of pebbly debris. Although this texture is thought to mostly reflect disintegration of

semi-lithified, stylo-bedded limestone clasts during transport, it also suggests that the material was far travelled and/or recycled, and that original sources may have been located at some distance away from where it was deposited. Second, nearly all Daniel's Harbour Member conglomerates bear a small percentage of dolostone clasts which are thought to have come from the Aguathuna Formation or the basal Table Point Formation, and of white fenestral limestone clasts which are thought to have come from the top of the Catoche Formation (Costa Bay Member). The mere presence of Catoche limestone clasts and paucity of dolostone clasts strongly suggests that the exhumed lithoclast source was a condensed foreland basin sequence, ie. one in which the Aguathuna Formation was very thin, or possibly absent, and below which fenestral limestones occur at the top of the Catoche. Both conditions are met east of the immediate area where the Costa Bay Member is recognized as a peritidal lithofacies restricted to the mid- to outer shelf (Knight and James, 1987), and where later tectonic uplift and extensive erosion and karstification is postulated to have occurred while deposition of Aguathuna sediments in very restricted peritidal settings occurred further west (Knight *et al.*, in press).

In small areas of the foreland basin, derivation of the resedimented carbonates can be assessed on the basis of specific compositional and textural data, and paleoflow indicators. A compilation of those interpretations are shown in Figure 15.1. The data and rationale are summarized below.

15.1.1 Port au Port Area

In this area Daniel's Harbour Member beds are present in virtually every outcrop of the American Tickle Formation between West Bay Centre Quarry and North Brook Anticline (Figure 15.2.a,b). The distribution of the debris flow conglomerates and calciturbidites in the measured sections does not define a single, obvious proximal- distal trend from which the general location of a source of the debris can be inferred

Figure 15.2 Daniel's Harbour Member beds in the Port au Port area. a) Simplified geologic map of the area showing the locations of sections in b) (modified from Williams, 1985). 1 = West Bay Centre Quarry; 2 = Piccadilly roadcut; 3 = Black Cove; 4 = Cold Brook Quarry. TMA, Table Mountain Anticline; PBA, Phillips Brook Anticline; NBA, North Brook Anticline; SL, Serpentine Lake. b) Measured sections through American Tickle Formation clastics with Daniel's Harbour Mbr. beds (shaded). TC, Table Cove Formation; BC, Black cove Formation; TP, Table Point Formation. Structural integrity of the Cold Brook section is not proven; the Table Point - Goose Tickle contact may be faulted (f). c) Paleocurrent data from Daniel's Harbour Mbr. calciturbidites at Black Cove. Megaripple orientation data come from the relatively coarse-grained lower parts of the calciturbidites. Ripple orientation, parting lination and graptolite orientation data come from the fine-grained tops of the beds.

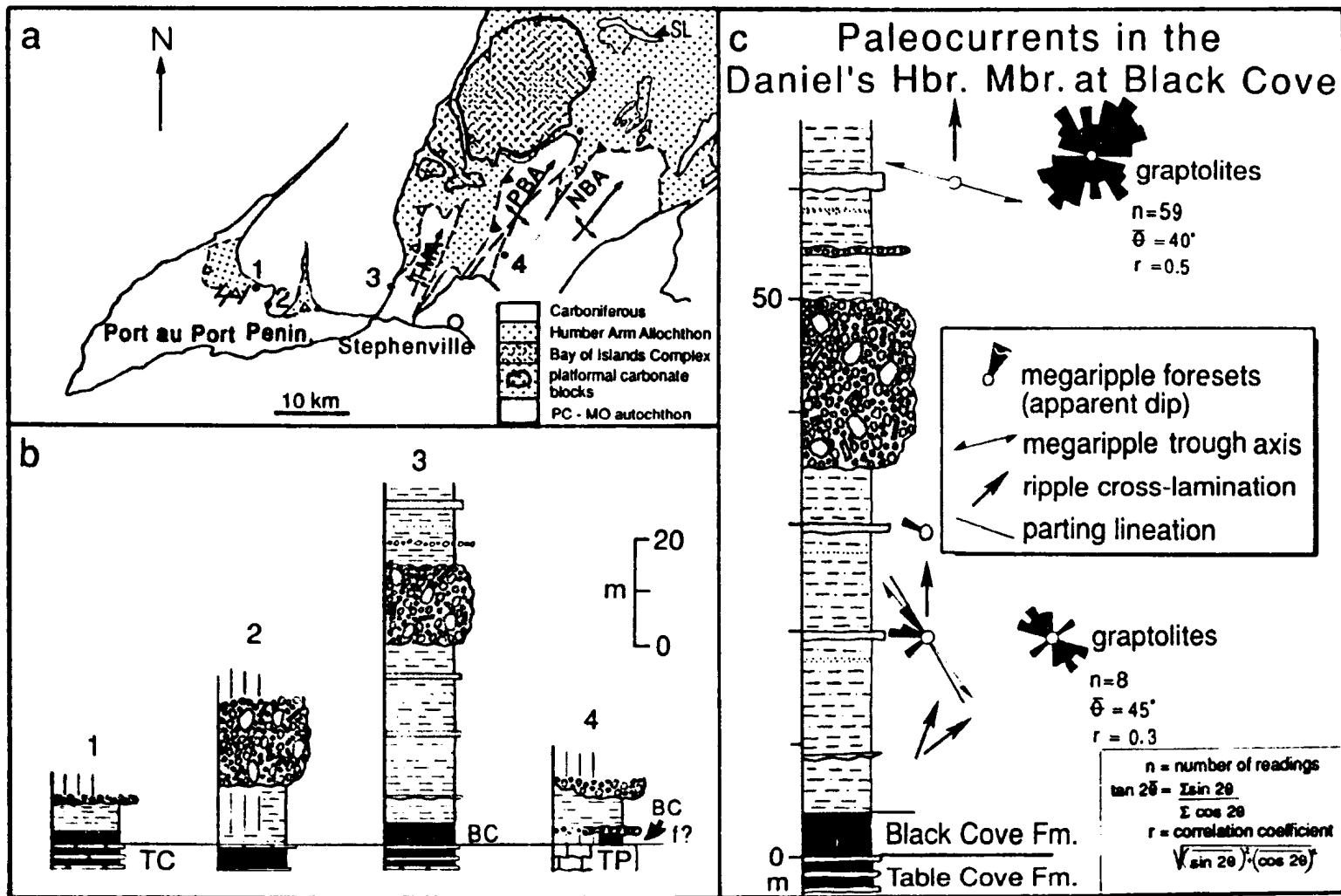


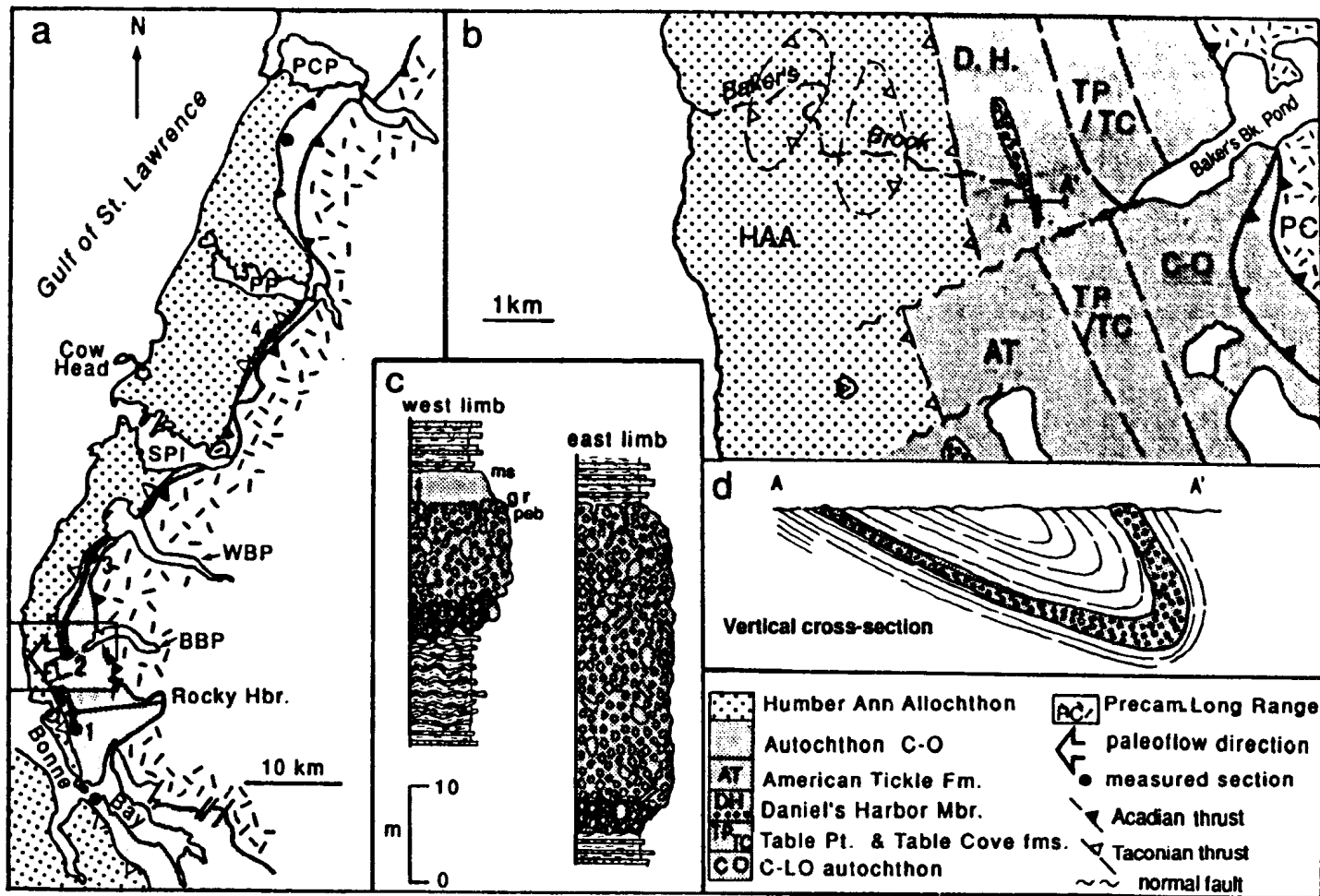
(Figure 15.2.b). Moreover, there are no structures in or at the base of the conglomerates that indicate transport direction(s) of the debris flows. Paleocurrent data from four calciturbidites at Black Cove indicate two directions of transport (Figure 15.2.c). Assuming that the beds came from the same escarpment, they are interpreted to indicate that the currents originated at a source located to the southeast and as they travelled northwest into the basin the tails of the currents were deflected or reflected back toward the east. Conglomerates in the section are inferred to have come from the same source.

Since the paleoflow data are from a single locality, their regional significance is suspect. However, the absence of Cape Cormorant Formation clasts in the conglomerates and the absence of Daniel's Harbour Member beds from the Mainland Sandstone on the west side of the peninsula, suggest an easterly provenance for all Daniel's Harbour Member beds, perhaps from faults located both outboard of and within the immediate outcrop area.

15.1.2 Gros Morne Area

In this area massive Daniel's Harbour Member conglomerates occur in virtually all American Tickle Formation sequences from just north of Bonne Bay to West Brook (Figure 15.3.a). The thickest beds may occur at the same stratigraphic level in the American Tickle Formation, but structural complexities preclude demonstrating this. There are no structures in the conglomerates from which transport direction can be determined. A reasonable assessment comes from lateral changes in the nature of the Daniel's Harbour Member in Baker's Brook (Figure 15.3.b). Based on bedding and cleavage orientation data from the conglomerates and enclosing American Tickle clastics, the two conglomerate outcrops in the brook (Figure 15.3.c) are interpreted to represent a single bed exposed on opposing limbs of a north-northwest-trending, east-facing, overturned syncline (Figure 15.3.d). The thinner debris flow conglomerate on the western limb and thick calciturbidite deposited atop

Figure 15.3 Daniel's Harbour Member beds in the Gros Morne area. a) Simplified geologic map of the area showing the locations of measured sections with Daniel's Harbour Member beds in the American Tickle Formation (from Williams et al., 1985b; Cawood and Williams, 1986; Williams and Cawood, 1989). 1 = Hwy. 430 roadcut; 2 = Bakers Brook; 3 = Stag Brook; 4 = West Brook. (Measured sections are in back pocket). BBP, Bakers Brook Pond; WBP, Western Brook Pond; SPI, St. Pauls Inlet; PP, Parsons Pond; PCP, Portland Creek Pond. Box outlines the area of the map in b). b) Geologic map of the area around Bakers Brook showing the outcrops of Daniel's Harbour Mbr. beds. c) Measured sections through Daniel's Harbour Mbr. outcrops in Bakers Brook. gr, granule; peb, pebble; ms, medium sand. d) Interpretative geologic cross-section along A-A' in c) illustrating westward-thinning of the debris flow conglomerate between the two outcrops in the brook.



it are interpreted as more distal deposits of the massive conglomerate exposed in the eastern limb. The directional change is interpreted to reflect transport to the west from a source located off to the east.

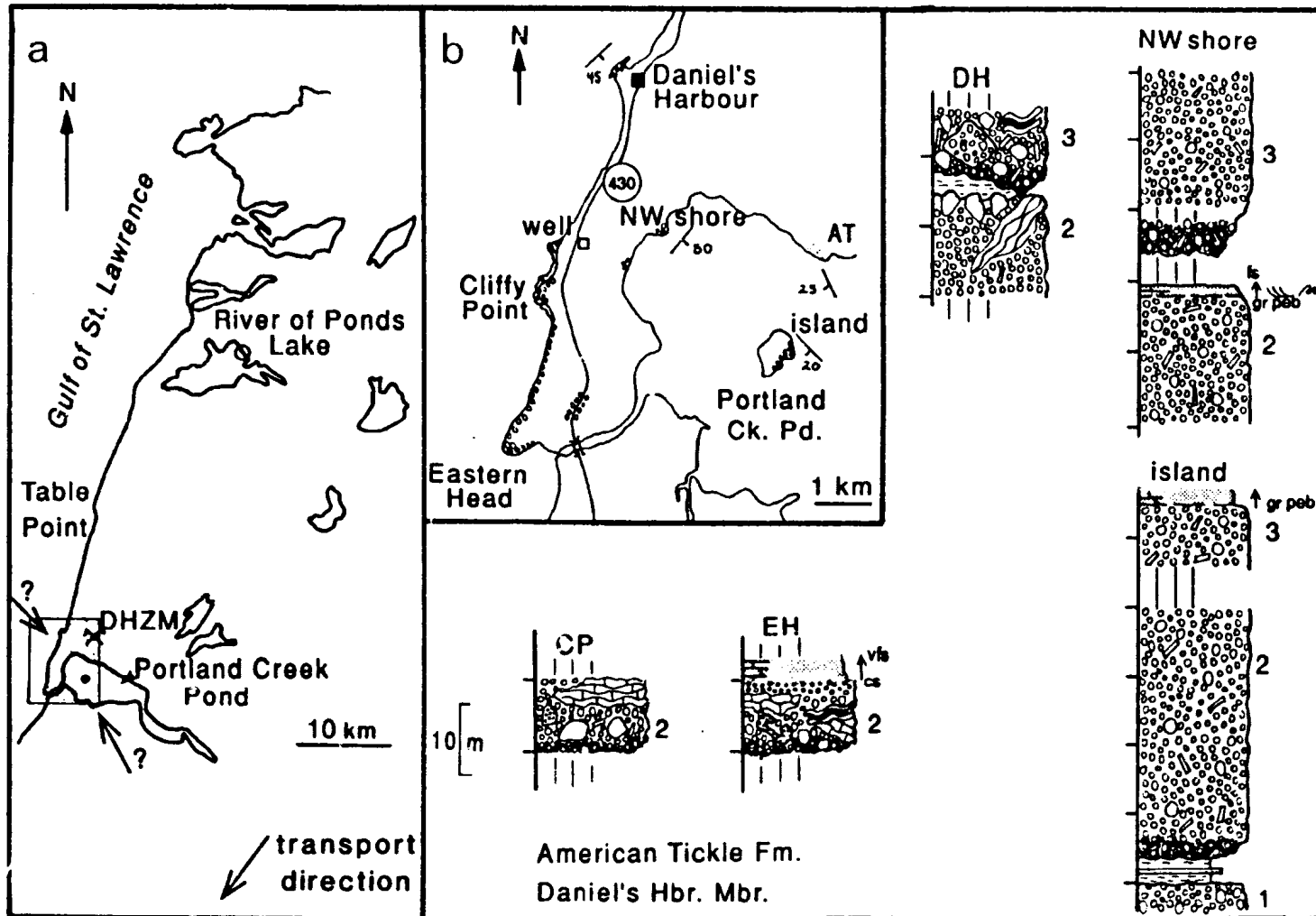
15.1.3 Table Point Area

At least two, possibly three or four, massive, clast-supported conglomerates, some with capping calciturbidites, punctuate the American Tickle Formation in the Daniel's Harbour and Portland Creek Pond area (Figure 15.4). Their precise stratigraphic position is unknown but, assuming they are components of the same autochthonous sedimentary sequence seen in drill cores from the Daniel's Harbour Zinc Mine, they must be more than 90 m above the base of the Goose Tickle Group (see for example DH-2546 in Figure 14.1).

Despite superb coastal exposure, the derivation and transport directions of Daniel's Harbour Member beds in this area cannot be uniquely determined. There are no sedimentary structures in either the debris flows or calciturbidites in any outcrops that indicate flow direction. Moreover, proximal to distal trends defined by changes in bed thickness, sediment texture, or the distribution of calciturbidites are equivocal. The latter is a consequence of both 1) the inability to place any of the Daniel's Harbour Member beds in a precise stratigraphic context, which introduces a high level of uncertainty in correlations made between outcrops, and 2) incomplete exposure, especially covered stratigraphic contacts with enclosing clastics which preclude determining actual bed thickness and proving the depositional presence or absence of overlying calciturbidites.

If correlations shown in Figure 15.4 are valid, then transport from the northwest toward the southeast is suggested by a west-northwest to east-southeast, proximal to distal trend defined by the presence of very large clasts in the conglomerates at Daniel's Harbour, as well as at Clifly Point and Eastern Head, and their apparent absence from the debris flows in Portland Creek Pond. This trend is paralleled by the

Figure 15.4 Daniel's Harbour Member beds in the Table Point area. a) Map showing the location of the enlarged map in b) (stippled area) and of the single Daniel's Harbour Mbr., conglomerate at River of Ponds Lake. b) Measured sections through Daniel's Harbour Mbr. clast-supported conglomerates and associated calciturbidites between Portland Creek Pond and Daniel's Harbour. CP, Clifly Point; EH, Eastern Head; DH, Daniel's Harbour; NW shore and island refer to locations in Portland Creek Pond. Numbers to the right of the columns denote possible correlations between the sections. Map shows the outcrop distribution of these beds (pebble pattern) and American Tickle Fm. clastics (AT) (stippled). "well" on the map northwest of Clifly Point marks the location of a water well drilled at the Daniel's Harbour Dairy that penetrated ~60 m of conglomerate underlain by at least 90 m of 'shale' (American Tickle clastics) and did not yet reach Table Cove Formation limestone (T. Lane, 1989, pers. comm.). The thickness of the conglomerate is similar to the composite thickness of the two beds at Daniel's Harbour, but the orientation of bedding in the subsurface at the Dairy is not known, so the significance of the thickness of the conglomerate is uncertain. *peb*, pebble; *gr*, granule; *cs*, coarse sand; *fs*, fine sand; *vfs*, very fine sand. Key to other symbols is in Appendix A.



apparent distribution of calciturbidite caps on debris flow conglomerates which are considered indicative of more distal reaches of sediment gravity flows. It is supported by the presence of large clasts of thick-bedded, coarse-grained, green sandstone, similar to turbidites that make-up the Mainland Sandstone/American Tickle Formation further north at Spudgel's Cove and Table Cove, and conceivably underlie the Gulf of St. Lawrence further west.

Nevertheless, derivation from the northwest and transport toward the southeast is undermined by the following. 1) Southeastward-fining of debris flow conglomerates may be an artifact of exposure rather than real; conglomerates in Portland Creek Pond are not nearly as extensively exposed as are those on the coast. 2) Proximal turbiditic sandstones in the enclosing flysch are not unique to that area; siliciclastic turbidites of other depositional systems were channelled down other, more outboard, structural depressions further east (Chapter section 14.3; Figure 14.5). 3) The presence of probably three massive debris flow conglomerates on the island in Portland Creek Pond suggest that area was more proximal to the debris source than those to the west. 4) If calciturbidites at Eastern Head proper and on the northwest shore of Portland Creek Pond are correlative, greater thickness at Eastern Head suggests that area was more proximal to the source of the flow. 5) The presence of sparse dolostone clasts and white fenestral limestone clasts in the debris flow conglomerates suggests derivation from the east.

Since all of the above arguments are also controvertible, it can only be concluded that either all resedimented carbonates came from the west-northwest or they originated from two escarpments, the second located in the immediate area off to the east-southeast.

Separated from this cluster of massive, clast-supported conglomerates is a thin, matrix-supported conglomerate exposed on River of Ponds Lake (Figure 15.4). That bed also lacks structures that indicate flow direction. However, distinctive clasts of dolomitic shale

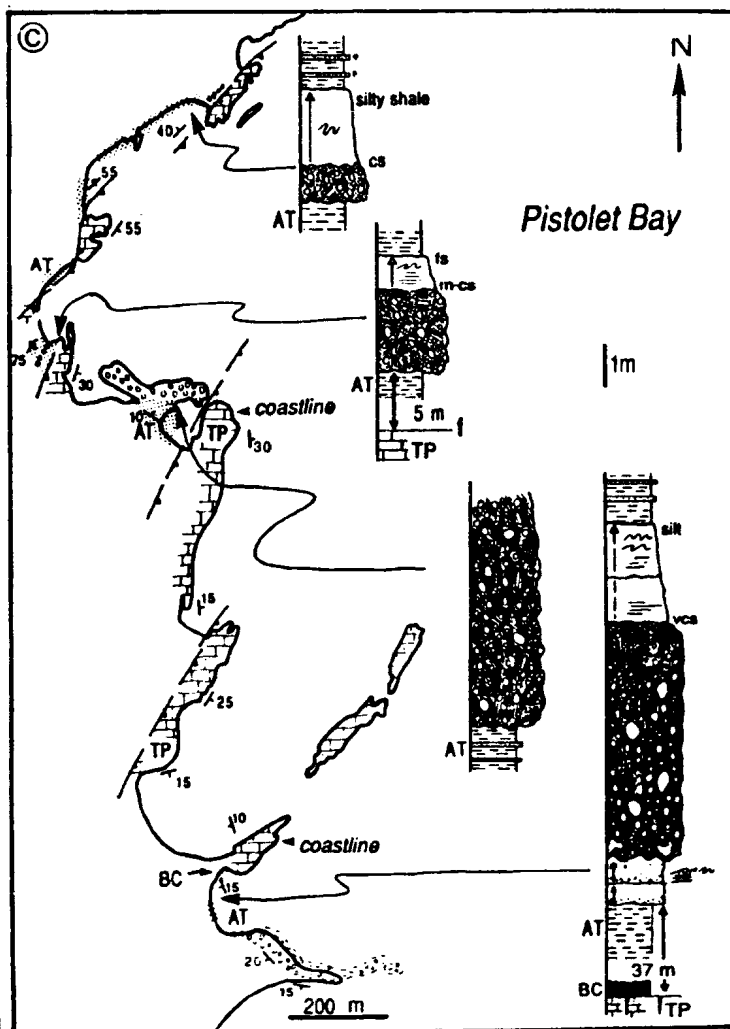
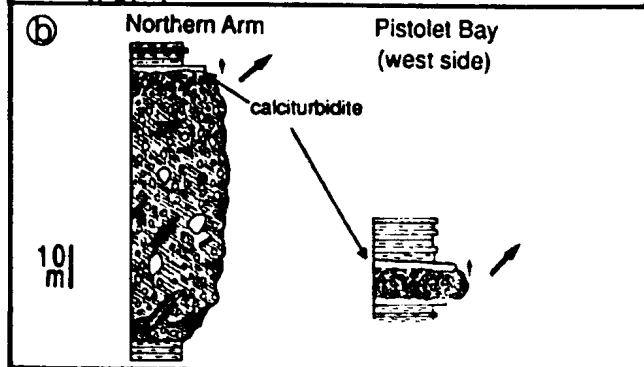
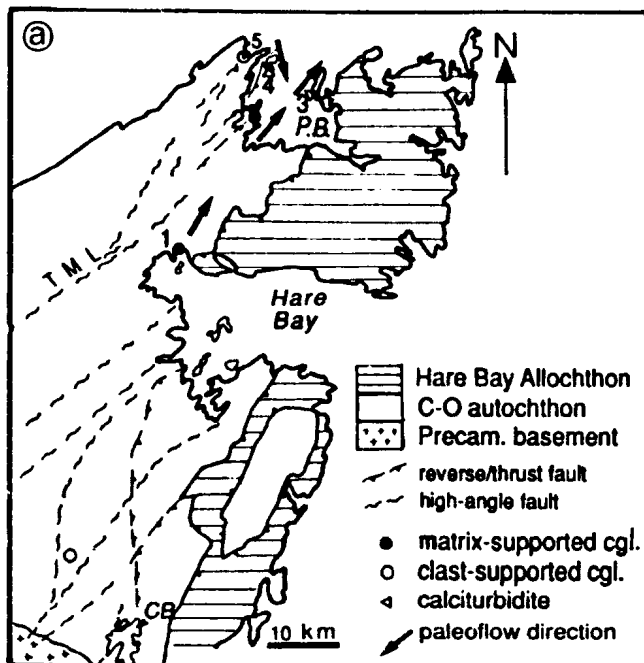
with mudstone nodules, comparable to lower Table Cove Formation lithofacies found only in the most eastern outcrops in the entire study area (eg. Beaver Brook and Baker's Brook Pond outlet), is thought to indicate that the flow came from an eastern source.

15.1.4 Hare Bay - Pistolet Bay Area

Both matrix-supported and clast-supported debris flow conglomerates and calciturbidites are interstratified with the flysch in the Hare Bay - Pistolet Bay area (Figure 15.5). Matrix-supported conglomerates at Northern Arm and in Pistolet Bay are compositionally and texturally similar enough to suggest they may be the same bed. Whether they are directly correlative or not, they do occur in the same major Acadian thrust slice, and so are inferred to be laterally equivalent, along with Daniel's Harbour Member calciturbidites on Burnt Island peninsula. Among these deposits, lateral changes in thickness of the conglomerates and current structures in the calciturbidites generally indicate transport to the northeast (Figure 15.5.a,c).

Although this local slope seems anomalous with respect to directions inferred from Daniel's Harbour beds in other area, it does mimic the local, structurally controlled topography existent during earlier passive margin sedimentation and is in turn mimicked by the present day structure of the area. First, paleocurrents in the Lower Cambrian Bradore Formation locally indicate transport to the north away from the Long Range Inlier (Knight and Saltman, 1980), suggesting that the Precambrian basement in that area was a structural high after rifting of the crust. Second, the entire Early Paleozoic sequence in the area dips gently northeast off the north end of the Long Range Inlier, a configuration attributed to uplift of the basement during Acadian orogenesis (Cawood and Williams, 1988; Grenier, 1990). Persistence of the local north-dipping slope implies reactivation of basement faults that overprinted and exaggerated the original structural configuration of the basement during both Taconian and Acadian orogenesis.

Figure 15.5 Daniel's Harbour Mbr. beds in the Hare Bay - Pistolet Bay (P.B.) area. a) Simplified geologic map showing the distribution of different types of Daniel's Harbour Member beds and transport directions for calciturbidites (after Bostock et al., 1983; Knight, 1986a, b; Cawood, 1989). 1 = Northern Arm, 2 = west side of Pistolet Bay; 3 = Burnt Island peninsula; 4 = Bakeapple Island; 5 = Callieux Bay. CB, Canada Bay; TML, Ten Mile Lake fault. Outlined, stippled area is enlarged in c). b) Measured sections at Northern Arm and on the west coast of Pistolet Bay transport; arrows show transport directions for overlying calciturbidites indicated by ripple cross-lamination. c) Lateral changes in a matrix-supported conglomerate and overlying calciturbidite exposed on the west coast of Pistolet Bay. TP, Table Point Fm.; BC, Black Cove Fm.; AT, American Tickle Fm. Key to other symbols is in Appendix A.



Matrix-poor, clast-supported conglomerate punctuates Goose Tickle clastics exposed along the west side of Callieux Bay (Vaches Point section, back pocket), and has been mapped over a small region south of Hare Bay (Figure 15.5.a), areas that are separated by too great a distance to suggest the conglomerates are a single bed. Those at Callieux Bay contain no structures that indicate flow direction, but are interpreted to have come from the west or northwest for a number of reasons. They occur in the same sequence in which Table Cove Formation ribbon limestones are punctuated by similar debris flow conglomerates interpreted to have come from the west (Chapter section 13.2; Figure 13.6). They contain rafts of both ribbon limestone and upper slope limestone, indicating derivation from a collapsed platform sequence in which deep-water carbonates were deposited, thereby excluding the area immediately to the east (Figure 13.6). Moreover, there are no comparable conglomerates in American Tickle Formation sequences further east. Finally, current structures in a Daniel's Harbour Member calciturbidite on Bakeapple Island indicate flow to the southeast (Figure 15.5.a) which, although not necessarily correlative with Callieux Bay conglomerates, demonstrate that some resedimented carbonates were transported into the basin from the northwest. The absence of both resedimented carbonate lithoclasts in the conglomerates and large Goose Tickle clastic clasts further suggests they are first generation debris flows.

Neither the thickness, nor derivation and transport direction of the clast-supported conglomerate south of Hare Bay are known. Its mapped distribution (Knight 1986a, b) suggests that it occurs at about the same stratigraphic level in the Goose Tickle as the thick, matrix-supported conglomerate at Northern Arm. It could have originated from any number of northeast-trending faults in the immediate area (Figure 14.5), several of which are proven to have influenced platformal carbonate sedimentation during early Ordovician time (Knight and Saltman, 1980). Furthermore, in light of evidence of a local northward-dipping

paleoslope it is reasonable to postulate that the conglomerate is a first generation debris flow that was subsequently remobilized by faulting and uplift in more distal regions of the basin and gave rise to the matrix-supported conglomerate deposited further north.

15.1.5 Summary

In summary, among Daniel's Harbour Member beds regionally there are many that are interpreted to have come from an easterly direction, but others that were transported away from escarpments located off to the northwest and to the south. Collectively the transport directions suggest that both local and outboard faults were involved. Importantly, they indicate transport mostly in directions other than down the regional paleoslope, which for the siliciclastic depositional systems was toward the south-southwest (Chapter 14), and demonstrate that faulting in the foreland basin recreated an irregular submarine topography with local slopes of variable facing directions.

15.2 Cause and Style of Intrabasinal Faulting

This episode of faulting marks the final phase of synsedimentary deformation in the foreland basin prior to emplacement of allochthonous thrust sheets. Tectonic emplacement of the allochthons on the ancient shelf, turned foreland basin, occurred in response to continued convergence and subduction of the North American continent. In this tectonic setting it is reasonable to postulate that faulting and uplift along nearly the entire length of the foreland basin occurred in response to regional compression. The shelfwide pattern of deformation attributed to Ordovician orogenesis supports this. In western outcrops, i.e. those in the study area, deformation is minor, recognized primarily by folding and shearing of Goose Tickle Group clastics immediately beneath the allochthons caused by their emplacement (Schillereff, 1980; Williams *et al.*, 1985b; Cawood *et al.*, 1988; Grenier, 1990). However, in more eastern, outboard regions, such as White Bay and Canada Bay, the entire

autochthonous succession is polydeformed and imbricately thrust (Williams, 1977; Williams and Smyth, 1983; Figure 15.1). West-directed thrust faults in the east indicate east-west compression, but since Ordovician overthrusts are not recognized further west, structures that exhumed the platform and overlying foreland basin succession in more inboard areas must have been high-angle faults with reverse sense displacements.

The depositional model constructed to explain the multi-generational nature of Daniel's Harbour Member debris flow conglomerates and calciturbidites calls upon propagation of faults and uplift toward the basin (Chapter section 9.7; Figure 9.8), which fits well with the east-west compressional regime depicted above. Given previous episodes of block-faulting, clearly the basins in which they were deposited were defined by submarine topography, in part relict from platform collapse and in part new in response to continued differential subsidence and uplift of crustal blocks. The fact that many of the resedimented carbonates came from easterly sources suggests that uplift was more common in outboard areas of the foreland basin, which is compatible with the regional pattern of increasing deformation toward the east. However, variations in flow directions indicate that faulting generated a more irregular topography characterized by escarpment-bounded slopes of different facing directions. This configuration demands that compressional stress was not solely transmitted by displacements on east-facing, reverse faults, but instead involved displacements on a complex system of high-angle faults, including those of both west and east polarity, and others trending at a high angle to the predominant structural trend. In this inboard region of the foreland basin that system of faults is thought to be the same network of basement-linked, normal faults and cross-faults that were generated during late Precambrian rifting of the continent and which were reactivated during previous phases of foreland basin development, initially influencing deformation and uplift of the

passive margin platform, later controlling sedimentation on the unstable, foreland basin platform, and finally dictating the manner in which the platform collapsed. The apparent absence of Daniel's Harbour Member beds from the Humber Arm area (Figure 15.1) indicates that that region was less susceptible to uplift. This is compatible with other sedimentologic evidence from passive margin platform carbonates (Levesque, 1977; Chow, 1986; Cowen and James, 1989) and coeval slope and rise strata (James and Stevens, 1986; Botsford, 1987; James *et al.*, 1987) that this was a fault-bounded, structurally low, reentrant in the continental margin.

CHAPTER 16

PHASE 6: EMPLACEMENT OF TACONIC ALLOCHTHONS

The final phase of foreland basin development and culmination of the Taconic Orogeny in western Newfoundland was emplacement of the Humber Arm and Hare Bay allochthons in the foreland basin (Figure 10.1). The allochthons are assemblages of imbricate thrust slices, the structurally lowest of which are Cambro-Ordovician age continental slope and rise strata and the upper slices of which are ophiolite and other igneous rocks of oceanic affinity (Stevens 1970; Church and Stevens, 1971; Williams and Stevens, 1974). Shaley *mélange*, a third major component, occurs both at the base of the allochthons and between thrust slices. The allochthons are interpreted as accretionary terranes, tectonically assembled from east to west, in a piggy-back fashion, above a southeast-dipping subduction zone between the North American continent and overriding oceanic plate (Church and Stevens, 1971; Malpas and Stevens, 1977). Although originally interpreted to have been transported and emplaced by gravitational sliding (Rodgers and Neale, 1963; Stevens, 1970; Church and Stevens, 1971; Williams and Stevens, 1974), current thought is that they were emplaced by thrusting (Cawood *et al.*, 1988; Waldron *et al.*, 1988).

16.1 Regional Extent

The allochthons form two isolated klippe atop the Cambro-Ordovician autochthonous sequence (Figure 16.1). It is not certain whether they define two separate accretionary wedges or if they are erosional remnants of a single allochthonous package. CAI (conodont alteration index) values for conodonts from platform carbonates, potentially a measure of burial depth and hence, true original allochthon extent, are equivocal. They seem to correspond more closely with proximity to the ophiolite rather than with the allochthons *per se*, and vary directly

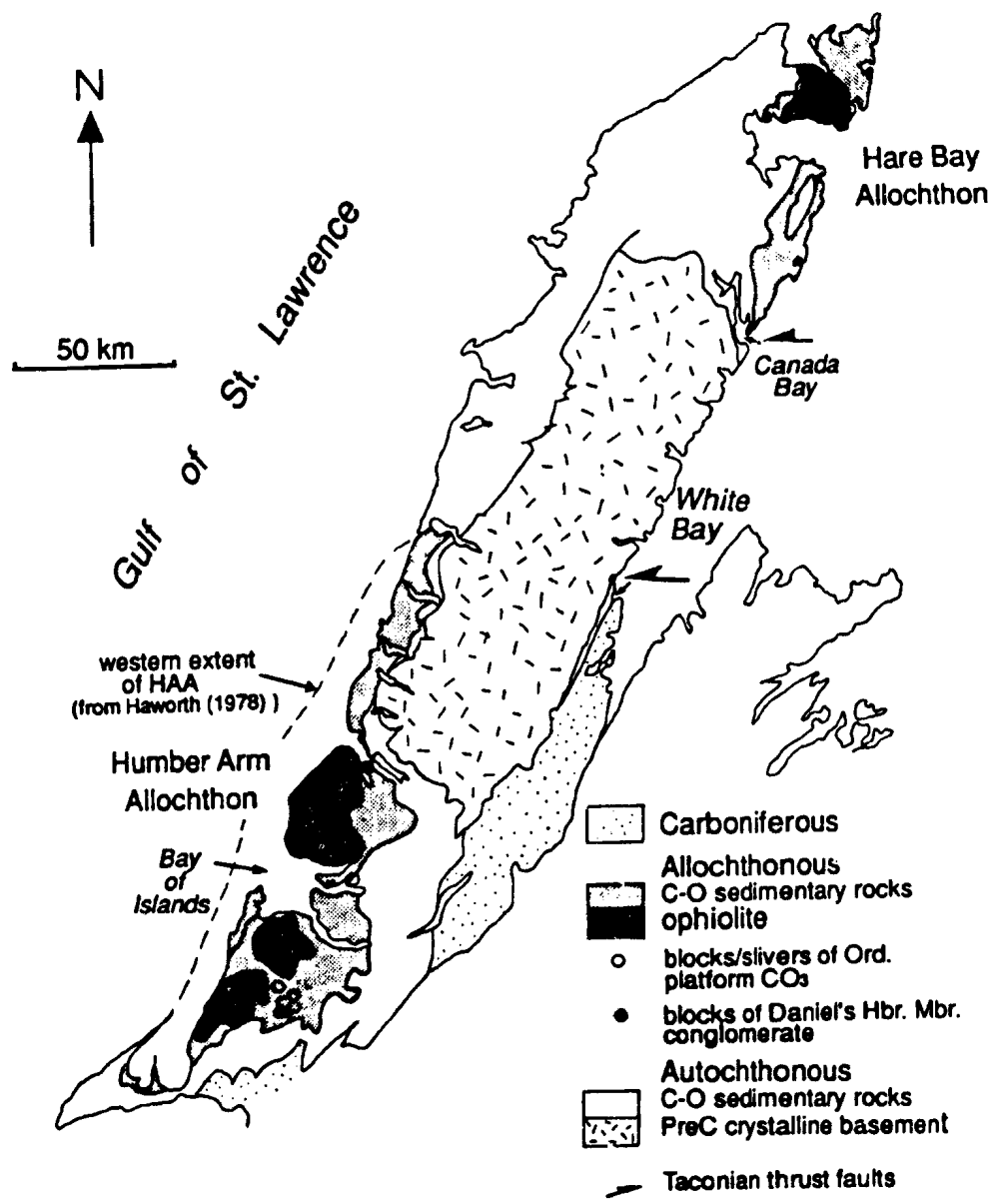


Figure 16.1 Map of western Newfoundland showing the distribution of Taconic allochthons and blocks or slivers of autochthonous carbonates in the Humber Arm Allochthon. SL, Serpentine Lake.

with degree of metamorphism associated with Acadian thrusting (Stouge, 1984, 1986; Cawood *et al.*, 1988), and so do not answer the question. Sedimentologic evidence from both the passive margin shelf/platform sequence and coeval slope and rise strata, however, which indicate that both the Humber Arm and Hare Bay regions were structurally low reentrants in the margin while the Long Range Inlier segment was a relative high (Levesque, 1977; Knight and Saltman, 1980; Williams and Smyth, 1983; Chow, 1986; James and Stevens, 1986; Botsford, 1987; James *et al.*, 1987; Cowen and James, 1989), also suggest that emplacement may have been controlled by basement structure and so present day outcrops may closely reflect the original distributions of the allochthons in the foreland basin. The Humber Arm Allochthon is proven on land to extend as far west as Lourdes on the Port au Port Peninsula and, on the basis of geophysical data, is interpreted to extend northeast along strike just offshore and under the Gulf of St. Lawrence as far north as the Bay of Islands and possibly as far north as Portland Creek Pond (Shearer, 1973; Haworth and Sanford, 1976; Haworth, 1978; Figure 16.1).

16.2 Nature of the Autochthon - Allochthon Contact

The allochthons are proven almost everywhere to overlie Goose Tickle Group clastics. Locally the contact is marked by a sharp thrust, but more commonly it is marked by a gradual transition from a folded and/or boudinaged American Tickle turbidite sequence to *mélange*. The basal *mélange* is a chaotic mixture of dark shale and scattered blocks of sedimentary and igneous rocks, most of which are correlative with those that make up the structurally higher and larger thrust slices (Schillereff and Williams, 1979; Williams and Godfrey, 1980; Williams and Smyth, 1983; Williams *et al.*, 1985b). Disintegrating blocks of turbiditic sandstone derived from the Goose Tickle Group, and possibly slightly older correlatives deposited in more outboard areas, are common components. Locally it also contains isolated blocks of Daniel's

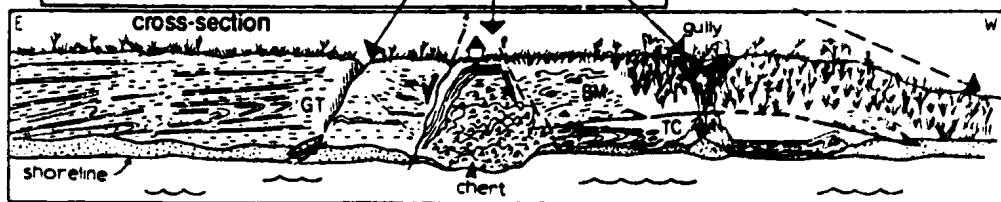
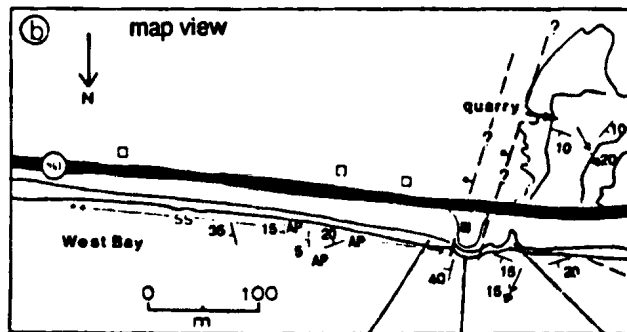
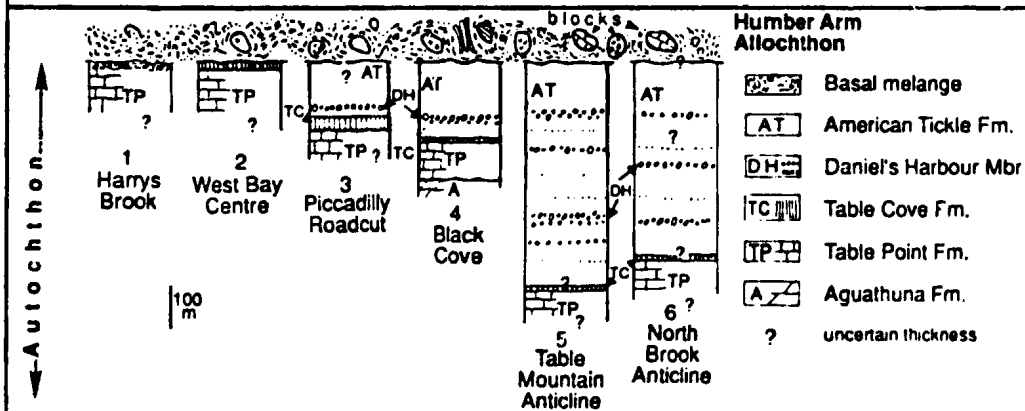
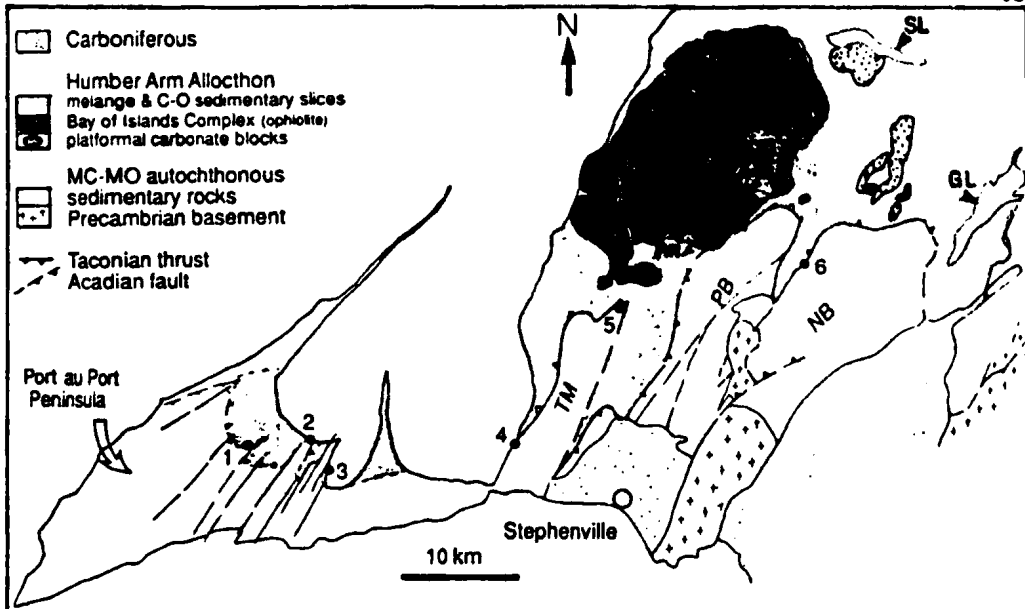
Harbour Member limestone conglomerate (Figure 16.1). The basal mélange and other mélanges that occur between higher structural slices are interpreted to have formed contemporaneously with allochthon assembly and emplacement by tectonic stripping of soft sediments beneath thrust slices and mass wasting during transport (Brückner, 1966; Stevens, 1965, 1970).

Poor exposure and/or post-emplacement folding and faulting of Goose Tickle strata in most sections preclude determining how far above the base of the Goose Tickle the autochthon-allochthon contact lies. Thickness measurements of even a few sections indicate a large amount of stratigraphic relief on that contact. It is recognized on a regional scale by contrasting American Tickle Formation sequences at Shag Cliff and West Brook, where the thickness is about 350 m, with that at Black Cove, where the American Tickle sequence beneath the allochthon is only about 170 m (Figure 14.1). It is also dramatically illustrated on a more local scale among sequences in the Port au Port area (Figure 16.2.a). From Table Mountain westward the basal mélange overlies progressively lower stratigraphic levels of the foreland basin sequence, partly incorporating Table Cove Formation ribbon limestones at West Bay Centre (Figure 16.2.b) and directly overlying the Table Point Formation in the vicinity of Harrys Brook.

16.3 Platform Carbonate Blocks in the Allochthons

Large blocks and slivers of platform carbonates occur locally in the Humber Arm Allochthon (Figure 16.1). The Serpentine Lake sliver (Figure 16.2.a) is among the largest (~3.5 km across) and consists of lower St. George Group through basal Table Point Formation dolostones and limestones (Williams and Godfrey, 1980; Godfrey, 1982). Several similar blocks, ranging from less than 1 km to about 5 km in length, occur in an area just a few kilometres south of Serpentine Lake and north of the Phillips Brook and North Brook anticlines (Schillereff, 1980; Williams

Figure 16.2 Contact relationships between the Humber Arm Allochthon and the autochthon in the Port au Port area. a) West to east cross-section of stratigraphic sections through the contact between Harrys Brook and Georges Lake (GL). 1) Harrys Brook (J. Waldron, 1990, pers. comm.), 2) West Bay Centre, 3) Piccadilly roadcut (the actual thickness of clastics above the Daniel's Harbour Member is not known), 4) Black Cove, 5) north Table Mountain (based on descriptions by Schillereff (1980), 6) North Brook Anticline (conjectural, based on unpublished field descriptions by P. A. Cawood, 1990, pers. comm.). b) Outcrop sketch of autochthon - allochthon contact relationships at West Bay Centre. Table Head carbonates here have been previously mapped as a block in the Humber Arm Allochthon (Schillereff and Williams, 1979; Williams, 1985). However, Table Cove, Black Cove and basal American Tickle strata in the quarry proper, where the autochthon - allochthon contact is not exposed, are interpreted by the writer to be in place, comprising the north end of a prominent ridge south of the quarry underlain by resistant Table Point Formation limestone and older carbonates. Deformation of these strata related to allochthon emplacement is expressed by a sedimentary dyke that cross cuts Black Cove Formation shale in the upper quarry floor. The dyke rock is mostly of coarse, nonferroan dolomite and intercrystalline blocky calcite cement, and contains scattered, angular grains of angular chert, quartz and feldspar, silica-replaced radiolarians, fragments of inarticulate brachiopods, and phosphatic and silty shale intraclasts. The latter are inferred to have been ripped from the wall rock and are aligned with their flat surfaces parallel to the dyke wall. The carbonate-rich composition and presence of radiolarians and brachiopods suggest the dyke formed by expulsion of fluids from the underlying ribbon limestones due to buildup of high fluid pressure caused by loading of the allochthon. Similar injection features are recognized at the actual base of the allochthon in other areas (Waldron et al., 1988).



and Godfrey, 1980; Williams and Cawood, 1989; Figure 16.2.a). Another carbonate sliver forms the Penguin Hills on the southeast side of Penguin Arm in the Bay of Islands (Lilly, 1963; Williams *et al.*, 1982; Figure 16.1). It is a little more than 1 km long and about 0.5 km wide and is broadly correlated with the St. George - Table Head platform sequence. All of these blocks are surrounded by *mélange* near the base of the allochthon.

The timing and mechanism of emplacement of the carbonate slivers and blocks has been controversial. Schillereff (1980) concluded that the sliver at Fox Island River (Phillips Brook anticline area) was a post-allochthon emplacement klippe, while Williams *et al.* (1982) and Godfrey (1982) interpreted the Penguin Hills klippe, and the Serpentine Lake and nearby slivers to be part of the assembled allochthon, an interpretation also offered for similar platform slices in the Taconic Allochthons in New York state (Zen, 1967; Rowley and Kidd, 1981), and strongly supported by their consistent occurrence in the basal *mélange* (Godfrey, 1982), a position which agrees with the general model for allochthon assembly, i.e. the structurally lowest components were accreted last and are the least far travelled. More recently Cawood *et al.* (1988) speculated that the isolated blocks may have been emplaced by gravitational sliding during Acadian uplift in the much same manner that ophiolite of the allochthons are thought to have reached their present day resting places (Cawood, 1989).

16.4 Model for Allochthon Emplacement in the Foreland Basin

Relief on the autochthon - allochthon contact suggests that the depth of detachment and incorporation of the underlying foreland basin sequence during allochthon emplacement varied across the basin. Evidence that the basal thrust cuts down section from east to west in the inferred direction of transport (Port au Port area) contradicts the behaviour of thrusts (Dahlstrom, 1970) and suggests that it did not

follow a simple staircase trajectory as it propagated across the basin (eg. Cawood *et al.*, 1988). Irregular stratigraphic relief on the contact may be an expression of out of sequence thrusting at the base of the allochthon during emplacement, as has been documented in the accretionary terrane of the Oman Mountains (Searle, 1985; Cooper, 1988) and has been called upon to explain the origin of platform carbonate slivers in the Taconic Allochthons in New York state (Rowley and Kidd, 1981). An alternative interpretation, shown schematically in Figure 16.3, is that stratigraphic relief on the contact is due to a combination of seafloor topography and sub-seafloor structural relief on the collapsed and buried platform preexisting from earlier episodes of block faulting (uplift and collapse) and later reverse faulting that gave rise to Daniel's Harbour Member conglomerates. Under such circumstances the basal thrust of the moving allochthons indiscriminately truncated different stratigraphic units occurring at different structural levels even as it propagated up-section; structurally high crustal blocks that were tectonically decapitated above the basal thrust gave rise to slivers of platform carbonates that were incorporated in the basal melange (see also Godfrey, 1982). This same mechanism has been invoked to explain stratigraphic relief on the base of the Valsugan Overthrust in the southern Alps (Bosellini and Doglioni, 1986). Such topographic and structural highs may have been scattered across the foreland basin, but those from which platform carbonates were stripped were likely located in outboard regions where the entire autochthonous succession was intensely deformed and imbricately thrust during Taconian orogenesis (Lock, 1972; Williams, 1977; Williams and Smyth, 1983; Figure 16.1) and therefore the platform was more consistently structurally elevated and more susceptible to detachment.

Emplacement of accretionary prism

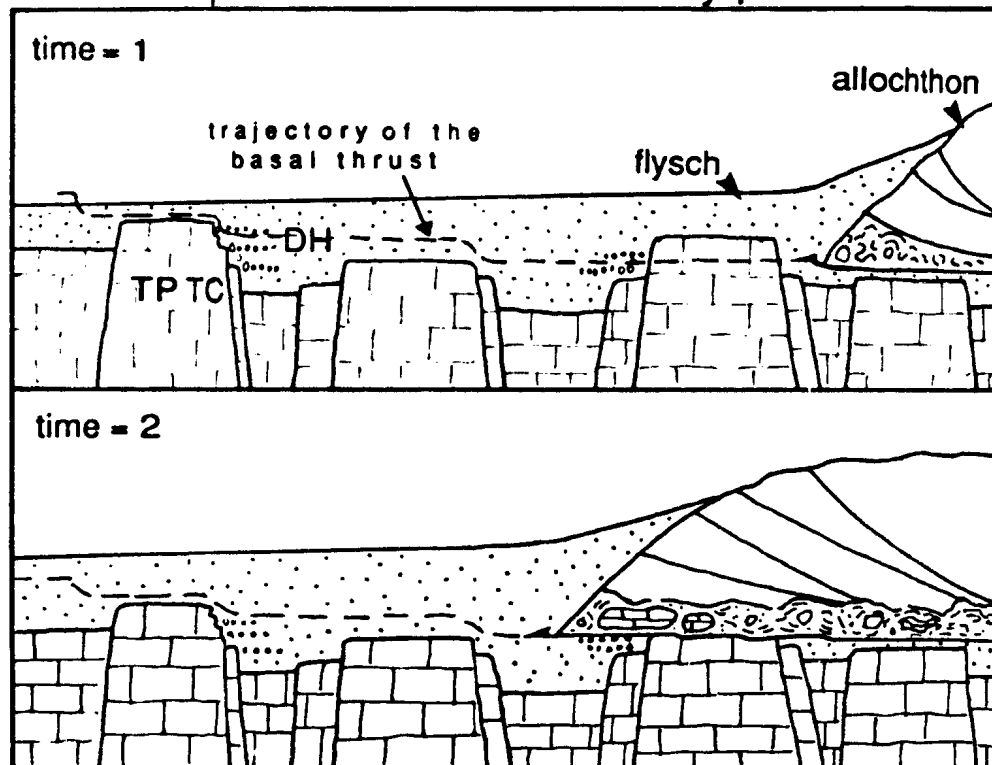


Figure 16.3 Tectono-sedimentary model for emplacement of Taconic allochthons in the foreland basin. Sub-seafloor structural relief on the collapsed, buried and uplifted foreland basin platform determines which stratigraphic units are displaced above the basal thrust of the advancing allochthon. Surficial, unlithified clastic sediments stripped off and incorporated in the allochthon were admixed with debris shed off the allochthonous thrust slices forming the mélangé at the base. Lithified platformal carbonates detached from structural highs in the basin survived as coherent blocks in the basal mélangé.

CHAPTER 17

MODEL FOR FORELAND BASIN DEVELOPMENT IN WESTERN NEWFOUNDLAND

The purpose of this chapter is to relate the six phases of sedimentation and tectonism discussed in Chapters 11-16 to morphologic features of, and tectonic processes operating at, a convergent plate margin.

17.1 Architecture and Mechanics of Convergent Margins

Morphologic features and tectonic regimes across a continent-ocean, convergent plate boundary, such as is envisaged for the North American continental margin in Newfoundland during middle Ordovician time (Malpas and Stevens, 1977), are illustrated in Figure 17.1. Major features of the overriding oceanic plate are the accretionary wedge and volcanic arc complex. The accretionary wedge develops under a compressional stress regime and is generated by stripping of surficial sediments off the down-going plate by thrusting (Seely *et al.*, 1974; Karig and Sharman, 1975) and structural incorporation of sediments deposited contemporaneously on the moving thrust slices (Shipley *et al.*, 1982). Accretionary wedges in modern oceans are discontinuously developed above subduction zones and vary in expression from low relief, submarine ridges to subaerially exposed archipelagos (eg. Moore *et al.*, 1982a, b; Shiki and Misawa, 1982; Karig *et al.*, 1987). Arc volcanism occurs 130-200 km behind the trench, commonly across an area 100-300 km wide (eg. Seely *et al.*, 1974; Westbrooke, 1982; Scholl *et al.*, 1983).

The outer rise, or peripheral upwarp (Figure 17.1), is a broad, gentle flexure that forms as an isostatic response to loading above the subduction zone (Walcott, 1970). Those documented in modern oceans occur 100-200 km from the trench, are 150 km to nearly 300 km wide, have amplitudes of a few hundred metres to 700 m, and are entirely submarine (Walcott, 1970; Caldwell and Turcotte, 1979). The outer trench slope, which is subjected to tensile stresses imposed by a combination of

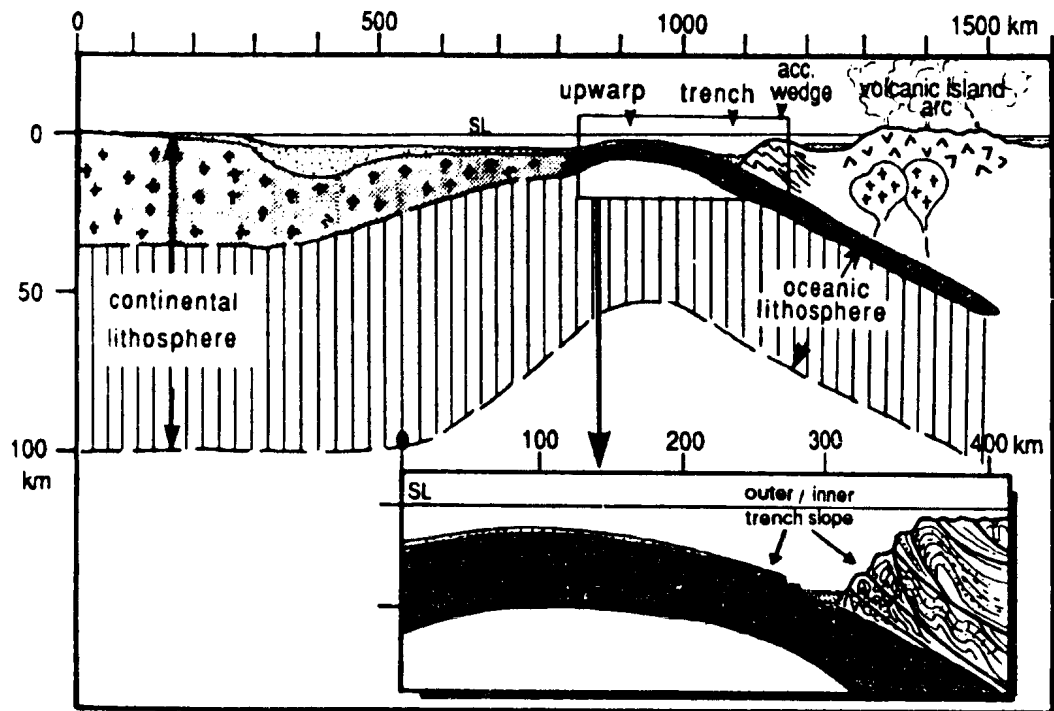


Figure 17.1 Schematic vertical cross-section through a continent-ocean subduction zone (modified from Press and Siever, 1982, Fig. 10-30 with data from references cited in text).

gravitational pull on the subducted plate and loading above the subduction zone, is deformed by offset on a series of normal faults (Hanks, 1979). Trenches in modern oceans are deep, ranging from 5000-10000 m where they are developed on oceanic crust (eg. Karig, 1970; Prince and Kulm, 1975; von Heune and Arthur, 1982), and from 1500-3500 m where they are developed on subducted continental crust (eg. Hamilton, 1977; Bowin et al., 1980). They are characteristically sites of rapid deposition from turbidity currents and other sediment gravity flows of debris commonly eroded from an adjacent accretionary prism - volcanic arc complex (Moore et al., 1982a). However, starved conditions occur in trenches where an accretionary terrain is not present, or is entirely submarine, or where sediment is trapped in forearc basins or faulted basins on the inner trench slope (Moore and Karig, 1976; Moore et al., 1982b). Sediment dispersal is typically along the axis of the trench, but structural barriers can block currents and trap sediment in local depressions (Prince and Kulm, 1975; Moore and Karig, 1976; Moore et al., 1982a).

The trench is under a compressional stress regime (Figure 17.1). Normal faults generated on the outer trench slope may be reactivated in the trench with reverse-sense displacement, and both the subducted plate and overlying trench-fill sediments may be involved in thrusting and consequently incorporated in the accretionary prism (Prince and Kulm, 1975; Kulm et al., 1982; Le Pichon et al., 1982).

As convergence between two plates occurs, the accretionary prism grows upward and outward, while the trench and sediments deposited in it migrate sympathetically ahead of the subduction zone across the subducted plate. Ideally, the history of convergence on any margin would consist of a series of depositional and tectonic phases that reflect migration through each of the morphotectonic settings described above.

17.2 Models for Lithosphere Flexure

Several physical models that show lithosphere response to loading have been constructed to simulate foreland basin development in response to overthrusting along a subduction zone. They differ fundamentally with respect to the designated rheological properties of the lithosphere, which has been variably regarded as a continuous elastic plate (eg. Jordan, 1981), a continuous uniform viscoelastic plate (eg. Walcott, 1970; Beaumont, 1978, 1981), and a continuous viscoelastic plate with a temperature-dependent viscosity (eg. Courtney and Beaumont, 1983; Quinlan and Beaumont, 1984), in each case overlying an inviscid or low viscosity sublayer. All models predict that 1) a load applied to a lithospheric plate causes down-bending of the plate beneath it and isostatic upwarping, or formation of a peripheral forebulge, and 2) movement of the load causes migration of the basin and forebulge in the same direction. The flexural response of an elastic plate differs from that of a viscoelastic plate in that the former does not relax to stress over time, so deformation caused by initial loading does not change, whereas relaxation of stress accommodated by flowage at lower levels in a viscoelastic plate causes the basin to deepen and become narrower while the forebulge becomes higher and migrates toward the basin.

Other variables factored into flexural models in order to more accurately portray the variability of convergent margin conditions include plate boundary conditions (infinite or semi-infinite), rate of loading, and episodic loading (Schedl and Wiltschko, 1984), as well as flexural rigidity of continental lithosphere as a function of its thermal properties, hence age, and size of the overthrust load (Stockmal *et al.*, 1986). Several predictions that stem from those models and their applications to the sedimentation and tectonic histories of foreland basins are summarized in Table 17.1.

Table 17.1 Predictions of Flexural Models

Model/ Critical Parameters	Predictions	Applications to Foreland Basins
<p>Schedl & Wiltschko (1984)</p> <ul style="list-style-type: none"> - plate boundary conditions - rate of loading - episodic loading & concurrent sedimentation 	<ol style="list-style-type: none"> 1) Deflections caused by loading on a semi-infinite elastic plate are greater than those on an infinite plate. 2) Rapid loading of a viscoelastic plate generates the same flexural response as loading on an elastic plate; time does not permit relaxation of stresses and deformation does not change with time. 3) Incremental loading of a viscoelastic plate followed by a period of relaxation during which the load (overthrust) is partially eroded and redeposited in the basin produces out of phase transgressions and regressions on the basinward and continentward side of the basin, respectively. Downward deflection in the basin is much greater than on uplift on the upwarp. 	<ol style="list-style-type: none"> 1) Changing plate boundary conditions in thrust terranes may be reflected in the sedimentary record; continent-continent, continent-island arc, continent-displaced terrane collisions are potentially distinguishable. 2) Foreland basins generated in response to rapid subduction will not record secondary, out of phase transgressions in the basin and regressions on the peripheral bulge. 3) Regressions caused by basinward migration of the peripheral bulge during lithosphere relaxation correspond to changes of only a few tens of metres and may be very subtly expressed in the sedimentary record.
<p>Steckmal <i>et al.</i> (1986)</p> <ul style="list-style-type: none"> - age of the continental margin - size (topographic expression) of the overthrust 	<ol style="list-style-type: none"> 1) Age of the margin influences flexural response only during initial stages of overthrusting; the flexural wavelength for an old margin (~120 m. y.) is greater than that for a young margin (~10 m. y). 2) Flexural rigidity of an old margin is greater than that of a young margin; overthrusting of an old margin creates a higher relief forebulge on an old margin than on a young margin. 3) As an overthrust overrides the continental slope a significant portion becomes subaerially exposed and subject to erosion. 4) As overthrusting occurs on progressively thicker lithosphere and the peripheral bulge migrates across ever thicker lithosphere beyond the hinge line, the rate of bulge migration decreases and the distance between it the overthrust decreases. When the forebulge arrives at or is beyond the hinge line, and that part of the shelf is at or very near sea level, uplift could render the entire area subaerially exposed until sediments fill the basin and prograde over the shelf. 5) A topographically high overthrust (~Himalayan type; frontal slope ~3°) creates a deeper basin/trench on continental lithosphere than a topographically low overthrust (Zagros Mts. type; frontal slope ~0.5°) (~16 km vs. ~3 km maximum). 6) As an overthrust approaches and arrives at the hinge line and an increasingly greater proportion is subaerially exposed, syn- and post-emplacment erosion accompanied by isostatic uplift causes progressive unroofing of the overthrust. 	<ol style="list-style-type: none"> 1) Given the same rate of convergence the amount of time between forebulge uplift of the continental shelf and its arrival at the trench for an old margin is greater than it is for a young margin. 2) Calculated uplift of ~400 m on a old margin that lies near sea level and an effective, flexurally-controlled isostatic amplification caused by erosion of ~2, could generate >800 m erosional relief. 3) Sediment starved conditions could persist in a trench adjacent to a submarine overthrust; sedimentation rate would increase progressively as subduction continues. 4) Unconformities generated by peripheral bulge uplift inboard of the hinge line potentially represent longer periods of time than those generated outboard of the hinge line. 5) Foreland basins forming adjacent to a topographically high overthrust terrane can accommodate a much greater thickness of overthrust-derived sediment than can a basin adjacent to a low terrane. 6) Upon final emplacement of the overthrust its structurally highest components are eroded; the youngest overthrust-derived sediments delivered to the foreland basin come from the structurally lowest, potentially metamorphosed elements of the overthrust.

17.3 Pre-convergence Configuration of the Continental Margin

Convergence and destruction of the early Paleozoic margin was preceded by a long, passive margin history that included continent rifting, which established the structural framework of the margin, and a long period of sedimentation, which determined the morphology of the margin immediately prior to convergence (James *et al.*, 1989). Both of these elements factored into later foreland basin development.

The passive margin history began with rifting of Grenville basement during late Precambrian and earliest Cambrian time and ended with uplift, erosion and formation of the St. George Unconformity during late early Ordovician time (James *et al.*, 1989; Figure 17.2). Figure 17.3 shows an interpretive reconstruction of the western Newfoundland margin prior to convergence. Given that seafloor spreading and opening of the Iapetus Ocean continued for at least 40-60 millions years (drift phase, Figure 17.2), and assuming a conservative rate of seafloor spreading to have been ~5 cm/yr (an average rate for modern spreading ridges, Press and Siever, 1982), the platform margin could have faced a major ocean 2000-2400 km wide. Cambro-Ordovician sediments deposited on the margin formed a continentward- and oceanward-tapering wedge, where the greatest thickness of sediment accumulated over extensionally thinned crust at the base of the continental slope. At the end of passive margin sedimentation the carbonate platform was at its widest (James *et al.*, 1989), but the precise location of its morphological margin is uncertain. It is placed east of White Bay in the Figure 17.3 because platform margin lithofacies do not occur in the autochthonous Cambro-Ordovician sequence west of White Bay, but coeval strata in White Bay (Coney Arm Group, Lock, 1972; Williams, 1977) include lithologies akin to both the platform (thick-bedded or massive carbonates) and the slope-rise (carbonate conglomerate), suggesting that that area, at least at some stage of platform evolution, did define or lie near the margin.

Figure 17.2 Early Paleozoic stratigraphy in western Newfoundland and its relationship to radiometrically dated igneous/tectonic events in western and central Newfoundland. Series ¹ from van Eysinga (1975); Series ² from Knight *et al.* (in press). Stratigraphy is from Stevens (1970), Williams and Stevens (1974), Williams (1975), Chow (1986), James and Stevens (1986), Knight and James (1987), Stenzel *et al.* (1990), and James and Cuffey (1989). Age data are from ¹ - Stukas and Reynolds (1974), ² - Williams *et al.* (1985a), ³ - Williams and Hiscott (1987), ⁴ - Dunning and Krough (1985), ⁵ - Dallmeyer (1977) recalculated with a new K decay constant by Dunning and Krough (1985), ⁶ - Dallmeyer and Williams (1975) recalculated with a new K decay constant by Dunning and Krough (1985), ⁷ - Archibald and Farrar (1976) recalculated with a new K decay constant by Dunning and Krough (1985), ⁸ - Williams *et al.* (1976), ⁹ - Kay and Eldridge (1968), ¹⁰ - Dunning *et al.*, (1987), Kay, (1975) and Arnott *et al.* (1985).

Platform

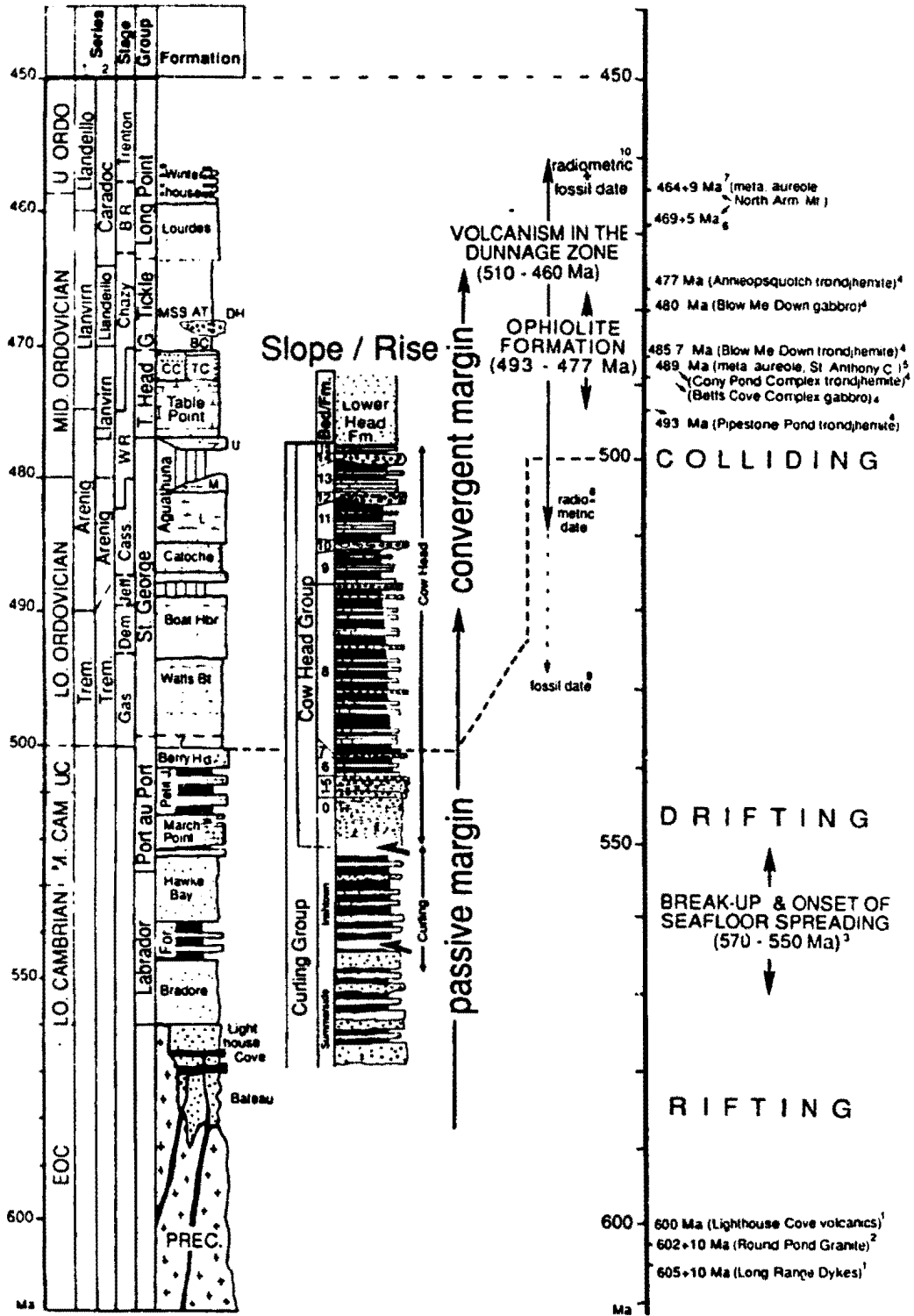
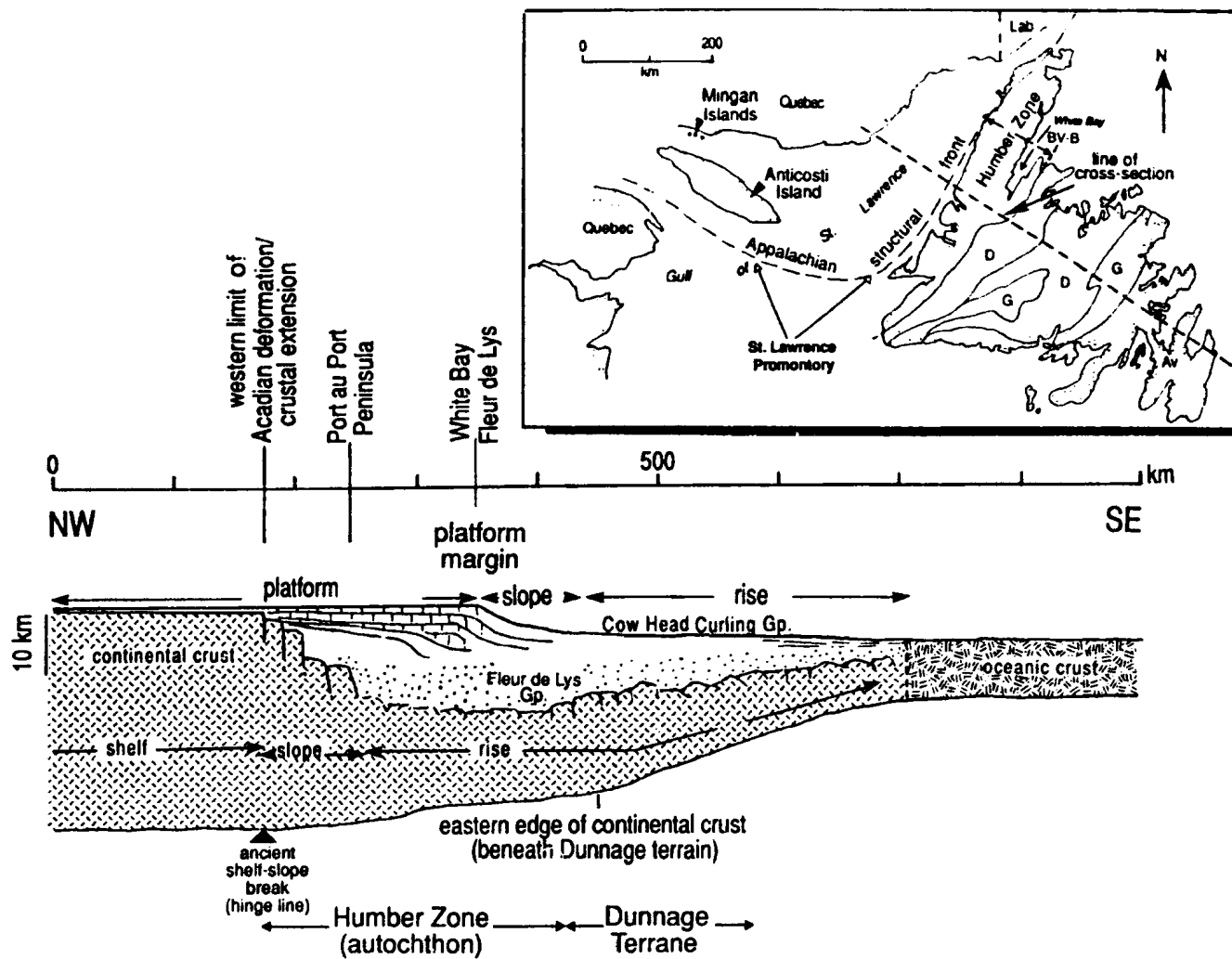


Figure 17.3 Interpretive reconstruction of the western Newfoundland margin at the end of passive margin development. Thickness, structure and lateral extent of Grenville basement are based on deep crustal seismic profiles (Keen *et al.*, 1986; Marillier *et al.*, 1989), and seismic and bathymetric profiles across modern passive margins (Heezen, 1974; Rabinowitz, 1974; Grow *et al.*, 1979; Hutchinson *et al.*, 1983). Autochthonous Cambro-Ordovician clastics and carbonates comprise the platform. A thick sequence of Late Precambrian-earliest Cambrian rift-related clastics overlies extensionally thinned crust at the base of the continental slope (Fleur de Lys Group; Williams and Stevens, 1974). Allochthonous Cambro-Ordovician clastics and carbonates form the continental slope and rise (Cow Head and Curling groups; Williams and Stevens, 1974; James and Stevens, 1986; Botsford, 1987). Slope and rise dimensions are based on modern day counterparts, which closely agree with restored widths generated by unstacking of imbricate thrust slices of slope and rise in the Humber Arm Allochthon (Williams, 1980). Inset map shows surficial tectono-stratigraphic zones across Newfoundland (from Williams (1979) and Williams *et al.* (1988); BV-B, Baie Verte-Brompton Line; D, Dunnage; G, Gander; Av, Avalon)) and the approximate line of cross-section for the margin profile.



17.4 Ocean Closing and Initial Subduction of the Continent

Closing of Iapetus Ocean began several million years before the effects of convergence were recorded on the platform. Subduction and island arc volcanism began as early as late Cambrian time, and then continued until late middle Ordovician time (Figure 17.2). Neither the location of the initial subduction zone with respect to the continental margin, nor its polarity are known.

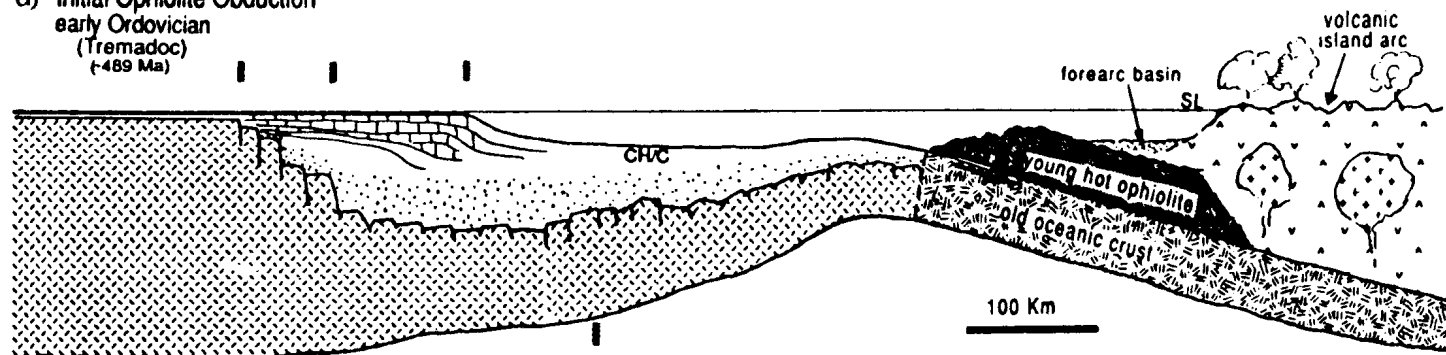
Actual subduction of the North American continent is interpreted to closely coincide with obduction of ophiolite onto the continental rise (Searle and Stevens, 1984; Dunning and Krough, 1985; Figure 17.4.a). Radiometric ages of several of the arc-related ophiolites indicate that they formed at least as early as early Ordovician (Tremadocian) time, well before the deformation of the platform occurred (Figure 17.2). Radiometric dates for metamorphic aureoles beneath ophiolites in the Hare Bay and Humber Arm allochthons indicate that obduction post-dated ophiolite formation by ~16 million years, and probably occurred diachronously from north to south along the subduction zone (Figure 17.2). Given that subduction continued for about 20 million years prior to ophiolite obduction, and assuming a conservative rate of convergence to have been ~2-5 cm/year (versus 4-11 cm/yr for modern subduction zones, Press and Siever, 1982), at least 400-1000 km of oceanic lithosphere was consumed. (See also Williams (1980)).

Ophiolite obduction initiated development of an accretionary prism above the subduction zone and evolution of a foreland basin on the outer edge of the continent (Figure 17.4.b). Substantial growth of the prism and arrival of relatively inboard areas of the continental rise at the subduction zone occurred by late early Ordovician time, recorded by deposition of turbiditic, siliciclastic sands derived from the wedge-arc complex (Lower Head Formation) directly on platform-derived, deep-water carbonates (Cow Head and Curling groups) (Figures 17.2 and 17.4.b). The period of time between earliest ophiolite obduction (489 Ma, radiometric

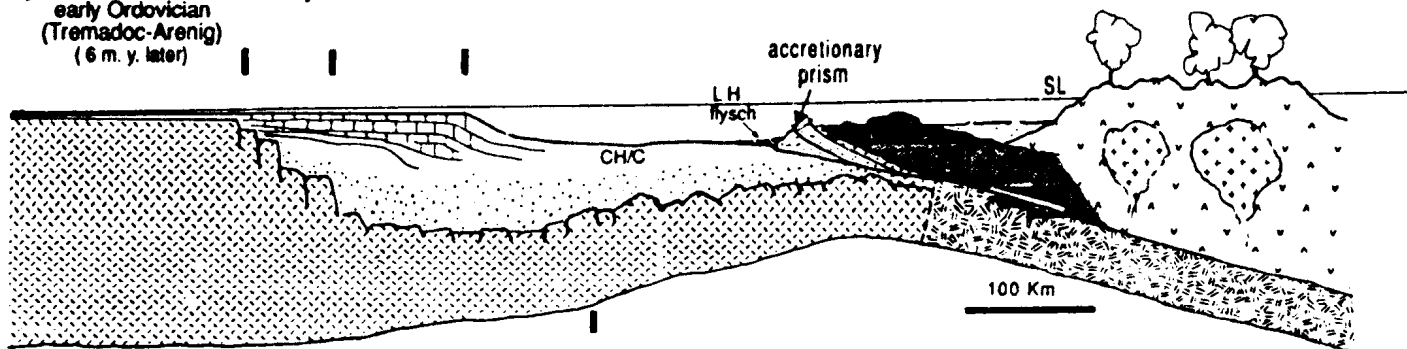
Figure 17.4 Interpretive cross-section across the margin during initial closing of Iapetus Ocean.

a) Newly-formed ophiolite generated within the island arc complex is obducted onto the outer edge of the continent above a southeast-dipping subduction zone. b) As subduction continues obducted oceanic elements and sedimentary rocks stripped off the downgoing continent are incorporated in an accretionary prism. Debris shed from the prism and adjacent arc complex are deposited in the trench. CH/C, Cow Head and Curling groups; LH, Lower Head Formation.

a) Initial Ophiolite Obduction
 early Ordovician
 (Tremadoc)
 (~489 Ma)



b) Formation of Accretionary Prism
 early Ordovician
 (Tremadoc-Arenig)
 (6 m. y. later)



date) and earliest deposition of flysch on the continental rise (-483 Ma, approximate date based on graptolites (Castlemainian Zone 2, Arenig Stage, J. Botsford and S. H. Williams, pers. comm., 1984, cited in James and Stevens, 1986; Figure 17.2) is only 6 million years, and implies relatively rapid formation of the accretionary prism.

17.5 Evolution of the Foreland Basin on the Platform

The Middle Ordovician foreland basin in western Newfoundland developed on old, cold and rigid, extensionally-thinned crust outboard of the original continental shelf-slope break, or hinge line of the margin (Figure 17.3). Initial deformation and each succeeding phase of deposition and tectonism record temporal changes in bathymetry and configuration in response to changes in style, direction and magnitude of stresses imposed by continued subduction of the North American continent. Sedimentation during each phase was influenced by synsedimentary faulting.

A model which takes into account the passive margin configuration and eustatic sea level, and relates each tectono-depositional phase of Middle Ordovician foreland basin development to morphotectonic regimes in the subduction zone is shown schematically via a series of time slice diagrams across the margin (Figure 17.5) and is summarized below.

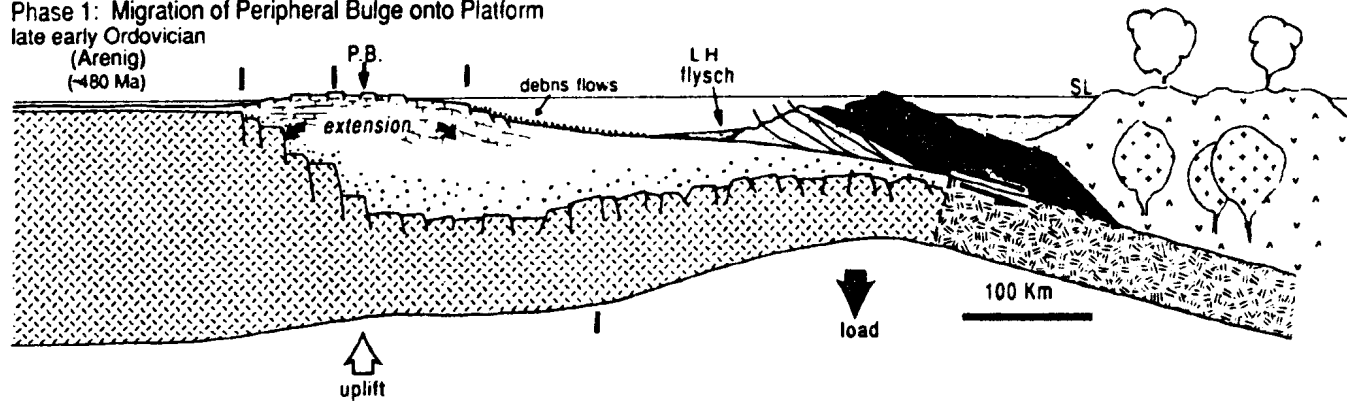
17.5.1 Phase 1: Faulting and Uplift

Earliest deformation which interrupted peritidal carbonate sedimentation (Aguathuna Formation) and culminated in formation of the regional St. George Unconformity during late early Ordovician time is interpreted to be the expression of migration of the peripheral forebulge onto the platform (Jacobi, 1981; Knight *et al.*, in press; Figure 17.5.a). Flexural uplift accompanied by extensional faulting transformed the flat, continuous platform into a mosaic of crustal blocks and generated a low relief, horst and graben topography. Differential uplift caused variation in duration of subaerial exposure

Figure 17.5 Tectonic model for foreland basin development on the platform in western Newfoundland. Tick marks on the cross-sections correspond to major boundaries delineated in Figure 17.3; shaded zone delineates the outcrop belt for this study. a) Phase 1: Deposition of Aguathuna Formation carbonates in very restricted, peritidal environments ceases as the entire platform is faulted and uplifted in response to migration of the peripheral bulge (P.B.) onto the platform. Subaerial exposure and karsting give rise to a regional unconformity (St. George Unconformity). The platform margin is concurrently destroyed by catastrophic faulting. b) Phase 2: Renewed deposition of carbonates in peritidal environments (Table Point Formation (TP)) occurs initially in response to eustatic sea level rise on the platform as uplift continues. Regional subsidence and deposition in subtidal environments occur as the peripheral bulge migrates onto the continent (shown). Differential subsidence facilitated by differential displacements on faults permit highly variable thicknesses of sediment to accumulate. Powerful seismic shocks or abrupt changes in slope trigger gravitational slides. The accretionary prism overrides the continental rise; surficial deep-water carbonates are incorporated at the base of the prism by thrusting, and siliciclastic sediments shed from the prism are deposited in the adjacent trench.

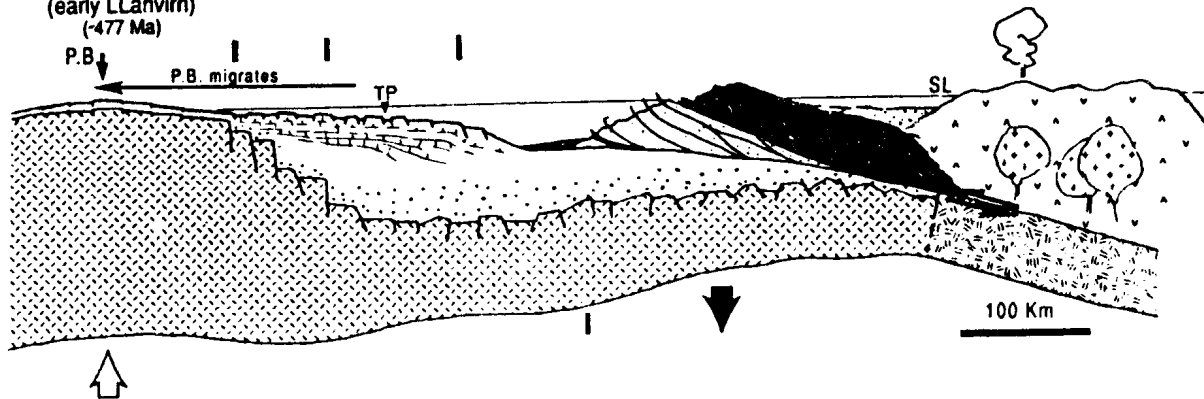
a)

Phase 1: Migration of Peripheral Bulge onto Platform
late early Ordovician
(Arenig)
(~480 Ma)



b)

Phase 2: Flooding and Renewed Shallow Water Carbonate Sedimentation
early middle Ordovician
(early Llanvirn)
(~477 Ma)



and in the depth of erosion across the platform. Approximately contemporaneous eustatic sea level rise (Figure 12.11) countered the effect of tectonic uplift, limiting the duration exposure and degree of erosion.

This episode of deformation approximately coincides with tectonic destruction of the platform margin proper, which is recorded in coeval deep-water, lower slope and rise deposits (James and Stevens, 1986; James *et al.*, 1987; Bed 14, Cow Head Group; Figure 17.2; Figure 17.5.a). After this point, carbonate sediment produced on the tectonized platform was no longer delivered to the adjacent lower slope and rise. Deposition of orogenic flysch (Lower Head Formation) above the youngest, deep-water carbonates (Figure 17.4) indicates that the outer continental rise at least 200 km seaward of the platform margin had arrived at the trench.

17.5.2 Phase 2: Sedimentation on an Unstable Platform

Renewed shallow marine carbonate sedimentation on an unstable platform (Table Point Formation) records marine flooding after uplift and demonstrates that the platform continued to be deformed by regionally imposed stress. Differential subsidence is interpreted to be an expression of normal faulting on preexisting structures and, hence, a tensile stress regime. Since platformal carbonate sequences record changes in bathymetry that do not agree with what would be expected by simple passage of the peripheral bulge (ie. progressive deepening), both tectonics and eustasy are inferred to have influenced deposition.

Periodic, vertical accretion to sea level, despite rising sea level (Figure 12.11) suggests that peritidal sedimentation occurred on the peripheral bulge when the platform was still experiencing tectonic uplift. Episodic displacement of the overthrust along the subduction zone, which triggered structural adjustments on the platform, in concert with small scale eustatic sea level changes, may account for abrupt changes in bathymetry and style of sedimentation recorded in these very shallow water sediments.

Subsequent platform deepening and wholly subtidal deposition coincide with continued eustatic sea level rise (Figure 12.11). However, since this occurred rather abruptly it is interpreted to partly reflect continentward-migration of the peripheral bulge (Figure 17.5.b). As concurrent sea level rise and tectonic subsidence did not result in platform drowning, it is inferred that the rate of sea level rise was small and that the amplitude of the forebulge was less than 100-200 m, depths at which carbonate sediment production would have declined significantly or ceased.

Late stage shoaling approximately coincides with eustatic sea level fall recorded on the western U. S. A. passive margin of the continent (Figure 12.11). The relatively subtle expression of this change in the foreland basin suggests that tectonic subsidence continued as sea level fell. An alternative explanation for regional shoaling is oceanward migration of the peripheral bulge back across the platform, a change in deformation caused by relaxation of the continental lithosphere during a period of time when subduction and overthrusting ceased (Table 17.1).

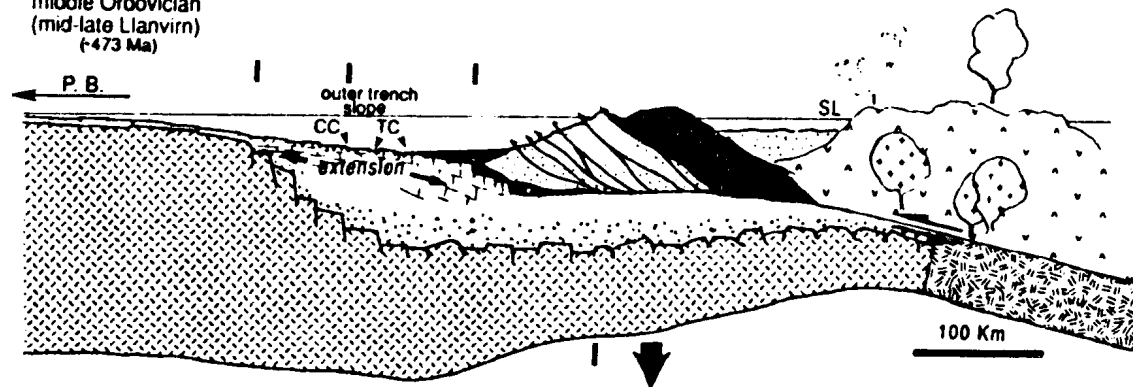
17.5.3 Phase 3: Platform Collapse

Synsedimentary faulting, differential subsidence, and ultimately regional drowning of the foreland basin platform is interpreted to record downward flexing and diachronous collapse of the platform as it moved toward, and formed the upper reaches of the outer slope of the trench (Figure 17.5.c). As this event approximately coincides with eustatic sea level fall (Figure 12.11), eustasy played no discernible role in sedimentation, and platform drowning is inferred to have been caused solely by very rapid, tectonically-controlled subsidence.

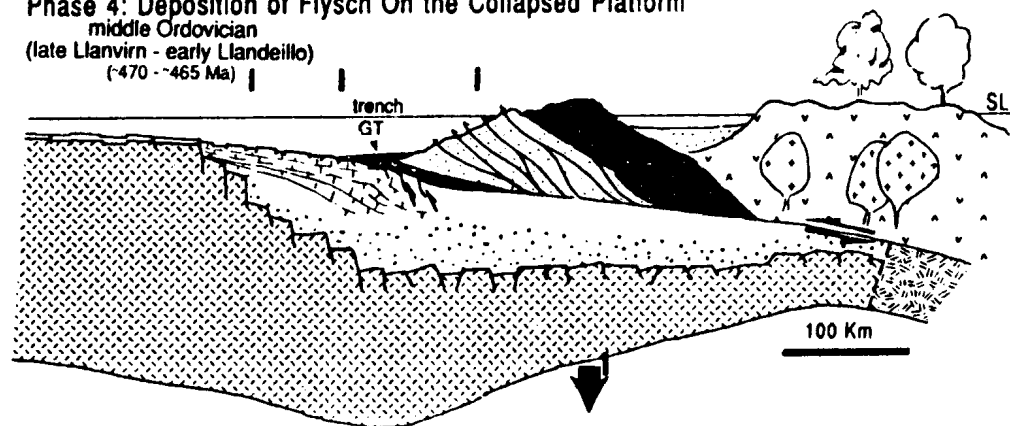
Synsedimentary faulting across the outer trench slope mostly generated a low relief, horst and graben topography in which horsts formed isolated, relict platforms that supplied sediment to flanking slopes and basins (Table Cove Formation). Rapidly foundered, sediment-starved blocks were blanketed by black shale (Black Cove Formation).

Figure 17.5 continued c) Phase 3: Collapse and drowning of the foreland basin platform occurs as it approaches the subduction zone and forms the outer trench slope. Tensile stresses reactivate preexisting faults with normal sense displacements regenerating a low relief, submarine horst and graben terrane. Horsts form relict platforms that remained in shallower water and supplied carbonate sediment to flanking slopes and adjacent basins (Table Cove Formation (TC)). Rapidly subsiding crustal blocks distant from relict platforms become starved basins and sites of black shale deposition (Black Cove Formation). Faulting locally generates a high relief, submarine encarpment which exposes old, passive margin carbonates that are redeposited in the adjacent basin by sediment gravity flows (Cape Cormorant Formation (CC)). The accretionary prism overrides the relict platform margin and the outermost platform is buried by prism-arc-derived siliciclastic turbidites. d) Phase 4: Carbonate sedimentation ceases and burial of the entire collapsed platform by siliciclastic sediment (Goose Tickle Group (GT)) occurs as it arrives at the trench. Debris shed from the prism-arc complex enter the trench at several points along its length. Sediment dispersal along and across the trench is controlled by submarine topography, both relict from the underlying collapsed platform and that regenerated by contemporaneous faulting (e), below).

c)
Phase 3: Foundering and Deep Water Sedimentation
 middle Ordovician
 (mid-late Llanvirn)
 (~473 Ma)



d)
Phase 4: Deposition of Flysch On the Collapsed Platform
 middle Ordovician
 (late Llanvirn - early Llandeilo)
 (~470 - ~465 Ma)



Catastrophic faulting that resulted in uplift and exposure of buried, passive margin carbonates that were subsequently eroded and redeposited in a rapidly formed basin (Cape Cormorant Formation) apparently occurred in only one area (far west Port au Port Peninsula). Regional reactivation of preexisting structures with normal sense displacement was caused by tensile stress imposed on the platform as it approached the trench.

The anomalously large amount of vertical displacement (≥ 500 m) on the Cape Cormorant fault, which relative to present-day geology is inferred to lie just west of the Port au Port Peninsula, indicates that either greater stress was concentrated in that area, or the geometry of the fault and/or its relations to adjacent faults made it weaker and more responsive to stress. Location of the fault at the St. Lawrence Promontory (Rankin, 1976; Thomas, 1977; Figure 17.3), may have rendered it the focus of stress during subduction. Moreover, apparent proximity of the fault to the western limit of extensionally-thinned continental crust (Figure 17.3) also suggests the structure may have been the high-angle, east-facing ramp of a major listric detachment generated during rifting (eg. Gibbs, 1984; Lister *et al.*, 1986). When subjected to tensile stress in the foreland basin this fault took up more strain (greater displacement) than any of the other more outboard, subordinate faults linked to it at depth.

Platform collapse cannot be correlated with any depositional or tectonic event recorded in continental margin sediments now comprising the Humber Arm and Hare Bay Allochthons; no strata younger than earliest middle Ordovician in age comprise the imbricate thrust slices (Figure 17.2). Rapid, regional subsidence of the foreland basin platform is, however, inferred to have occurred as the relict continental slope and carbonate platform margin entered the trench and were overthrust by the accretionary prism. Wholesale subsidence of the area of the platform exposed in western Newfoundland implies that the peripheral bulge had migrated further west onto the continent, probably beyond the hinge line

(Figure 17.5.c). That event is probably recorded by the post-Canadian - pre-middle Chazyan unconformity in the autochthonous sequence on the Mingan Islands located ~125 km inboard of the hinge (Nowlan, 1981; Desroches, 1985; Figure 17.3, inset map).

17.5.4 Phase 4: Deposition of Siliciclastic Sediments

The demise of deep-water carbonate sedimentation and rapid burial of the collapsed platform by siliciclastics (American Tickle Formation and Mainland Sandstone) derived from the accretionary prism-volcanic arc complex records arrival at the trench (Figure 17.4.d). Development of sediment-starved conditions prior to the influx of siliciclastic turbidites reflects a combination of great water depth (ie. an ever diminishing supply of shallow water-derived carbonate sediment), and submarine topography that dictated the direction and distance of turbidity current flow and siliciclastic sediment dispersal. Siliciclastic turbidites were dispersed down a regional, southwest-dipping paleoslope parallel to the trench axis. Preexisting structural domains controlled sediment dispersal down the axis and across the trench as subduction continued and turbidite systems prograded continentward.

By the time the collapsed platform was being buried by orogenic flysch, the leading edge of the accretionary prism must have overridden the relict platform margin (Figure 17.5.d). Because the prism would have been elevated topographically, more of it would have been exposed, and consequently eroded and redeposited in the trench.

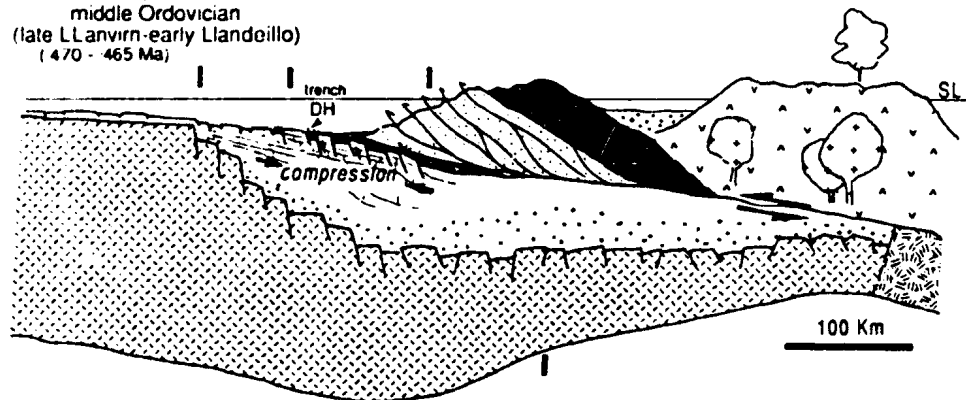
17.5.5 Phase 5: Intrabasinal Faulting

Faulting which generated submarine escarpments that exhumed and exposed to mass wasting and redeposition the entire foreland basin sequence and uppermost passive margin carbonates (Daniel's Harbour Member) also occurred in the trench (Figure 17.5.e). Uplift is interpreted to be an expression of reactivated preexisting faults with reverse-sense displacement in response to compression.

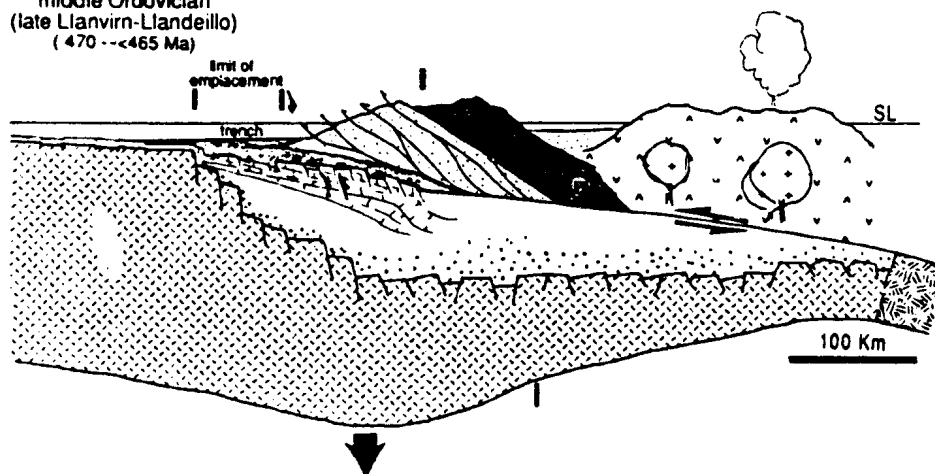
Imbricate thrusting occurred only in outboard localities of the

Figure 17.5 continued e) Phase 5: Compressional stress in the trench causes reactivation of preexisting faults that exhume the entire foreland basin sequence and the uppermost passive margin carbonates. Faulting regenerates an irregular submarine topography with slopes facing various directions. Mass wasting along the submarine escarpments gives rise to other carbonate sediment gravity flows that redeposit the material in local, intra-trench basins (Daniel's Harbour Member (DH)). f) Phase 6: Siliciclastic sedimentation ceases as the foreland basin is overthrust by the accretionary prism. Irregular sea floor topography and structural relief on the collapsed and buried platform permit the tops of structurally elevated blocks to be detached above the thrust and incorporated in mélangé at the base of the prism. Overthrusting stops a short distance outboard of the hinge line and siliciclastic sediments eroded from the prism fill the foreland basin.

e)
Phase 5: Uplift and Cannibalization of Foreland Basin Strata
 middle Ordovician
 (late Llanvirn-early Llandeillo)
 (470 - 465 Ma)



f)
Phase 6: Emplacement of the Accretionary Prism
 middle Ordovician
 (late Llanvirn-Llandeillo)
 (470 - c465 Ma)



platform (eg. White Bay, Canada Bay, Figures 17.3 and 17.5.e), but apparently no large thrust slices were incorporated in the accretionary prism. Reverse faulting in the interior of the platform may be an expression of minor thrusting on a low angle detachment at depth and sympathetic displacement on subordinate, higher-angle faults linked to it. Minor inboard faulting compared to outboard imbricate thrusting reflects decreasing intensity of stress away from the subduction zone. This deformation gradient may have been influenced by the relict platform margin that acted as a buttress to accretionary wedge displacement until subduction ceased.

17.5.6 Phase 6: Emplacement of the Accretionary Prism

Deep-water turbidite sedimentation ceased as the foreland basin was overthrust by the accretionary prism (Figure 17.4.f). As the prism moved continentward the basal thrust indiscriminately cross-cut underlying foreland basin strata. Surficial siliciclastics were incorporated and remoulded into mélangé at the base; some structurally elevated platform blocks were decapitated by the basal thrust and incorporated as coherent slivers in the basal mélangé. The leading edge of the accretionary prism was transported no further west than ~50 km outboard of the limit of rifted basement (near the base of the original continental slope), suggesting that its final resting place in the foreland basin was influenced either by structurally-controlled seafloor topography or the sub-seafloor structure of increasingly thick continental lithosphere. At this point an even greater proportion of the accretionary prism may have been subaerially exposed and an enormous amount of debris shed from it would have been supplied to the trench. The apparently great thickness of the Mainland Sandstone (1.5 km to as much as 5 km) deposited just west of the leading edge of the accretionary prism, and evidence that it changes in character from deep-water to shallow water up-section as it grades up into Llandeilo-age clastics at the base of the Long Point Group, suggest that the basin was filled to

near sea level.

17.6 Discussion

The pre-collision nature of the Newfoundland margin closely corresponds to the conditions specified by Stockmal et al. (1986) for their model of collision along an old continental margin. Comparison of the history of sedimentation and tectonics in the Taconian foreland basin with that predicted by the model provides further insight on dynamics along the Newfoundland margin.

1) The period of time between peripheral bulge uplift of the Newfoundland platform and burial by flysch (each phase realized as diachronous in nature) compares closely to the amount of time between those events in the model (15 m. yr. vs. 14 m. yr.; compare Phases 1-4 with their time steps II-IV, Stockmal et al. (1986), Figure 2). Moreover, the relative positions of the overthrust and peripheral bulge during uplift, collapse and burial of the interior platform proper for the model are comparable to those demonstrated or inferred for the Newfoundland foreland basin. This suggests that the rate of subduction along the Newfoundland margin averaged about 50 mm/year, the same as the value specified for the model. The actual rate more than likely varied, and probably decreased steadily as increasingly thicker continental lithosphere entered the subduction zone.

2) The amount of peripheral bulge uplift and erosion on the Newfoundland platform was much less than values predicted by the model (-60 m vs. 200-800 m; Table 17.1). This may indicate that the North American margin was much less rigid than the model assumes, or the effective load on the subduction zone was much less than the model employs, or migration of the peripheral bulge across the platform occurred too quickly for maximum uplift and erosion to have occurred. The other critical factor limiting the amount of erosion would have been concurrent eustatic sea level rise that dampened the effects of uplift.

3) The Taconian foreland basin was never exceptionally deep. It apparently did not subside to below either an oceanic Oxygen Minimum Zone or the CCD (ie. ≤ 4000 m, Chapter sections 7.6 and 14.1). Moreover, with the possible exception of the Mainland Sandstone on the far west side of Port au Port Peninsula, flysch sequences deposited atop the collapsed platform are not thick, a few hundred metres at most. Admittedly, almost all sequences except the Mainland Sandstone are structurally truncated by the overlying allochthon. Nevertheless, relatively shallow water depths and thin trench deposits correspond closely to the bathymetry and amount of sediment accumulation predicted by the model which specifies a topographically low, Zagros Mt.-like overthrust (Table 17.1), and suggests a similar low topography profile for the accretionary prism advancing over the Newfoundland basin.

4) Present day outcrop of the Humber Arm and Hare Bay allochthons (Figure 16.1) suggests the accretionary prism did not advance as far west as the hinge line of the ancient continental margin. This is supported by the apparent absence of the Humber Arm Allochthon above the Mainland Sandstone on the west side of Port au Port Peninsula, which instead appears to grade up into shallow marine, calcareous sandstone at the base of the Long Point Group (Figure 17.2). At present the Humber Arm Allochthon is ~200 km long, 50 km wide, and has a stratigraphic thickness of about 5 km (Williams and Cawood, 1989). The model predicts that when overthrusting beyond the hinge line occurs, the structurally lowest components of the prism become increasingly buried (Stockmal *et al.*, 1986, time steps V-VII in Figure 2). When movement ceases, erosion and concomitant isostatic uplift of the prism brings increasingly lower levels of the prism back up to the surface (time step VIII, in their Figure 2); stratigraphic unroofing and derivation of detritus from increasingly metamorphosed sources are recorded in sediments deposited in the foreland (Table 17.1). It is difficult to assess how the present day dimensions of the allochthons in the Taconian foreland basin compare

to their dimensions shortly after emplacement. There are remnants of a Llanvirnian-age, synemplacement sedimentary cover on the ophiolite capping the Humber Arm Allochthon (Casey and Kidd, 1981), but there is no evidence that the accretionary prism was deeply buried during emplacement, and as of yet no stratigraphic change in the metamorphic grade of detrital lithic fragments in the prism-derived flysch has been reported. In light of this negative evidence, it is postulated that the present-day Humber Arm and Hare Bay Allochthons closely approach in position and dimension (specifically with respect to their western boundaries) those of the accretionary prism when it reached its final emplacement position on the collapsed shelf. Low topographic expression probably limited the amount of erosion. When overthrusting ceased, removal from the zone of further erosion was probably caused by subsidence of the underlying continental lithosphere until isostatic equilibrium was reached.

17.7 Modern Analogue

A modern day plate margin that may serve as an analogue for Ordovician subduction of the North American continent is the collision zone between Australia and the Banda Arc along which convergence has occurred since the late Cenozoic (Hiscott, 1978; Rowley and Kidd, 1981; Shanmugam and Lash, 1982). Major elements of this geologically and geometrically complex region for which there appear to be counterparts in the Newfoundland orogen, and a bathymetric profile between Australia and Timor, are shown in Figures 17.6 and 17.7. The Australian shelf, which is underlain by a thick sequence of Mesozoic and Tertiary strata (Mollan *et al.*, 1970; Martison *et al.*, 1973), dips gently seaward away from the northwest coast of Australia and the southwest coast of New Guinea (Van Andel and Veevers, 1965). Water depth is mostly less than 100 m; low relief topography is defined by a system of shallow depressions and broad rises. The declivity of the shelf increases at depths of ~130 m, beyond which it slopes over 75-100 km to the bottom of

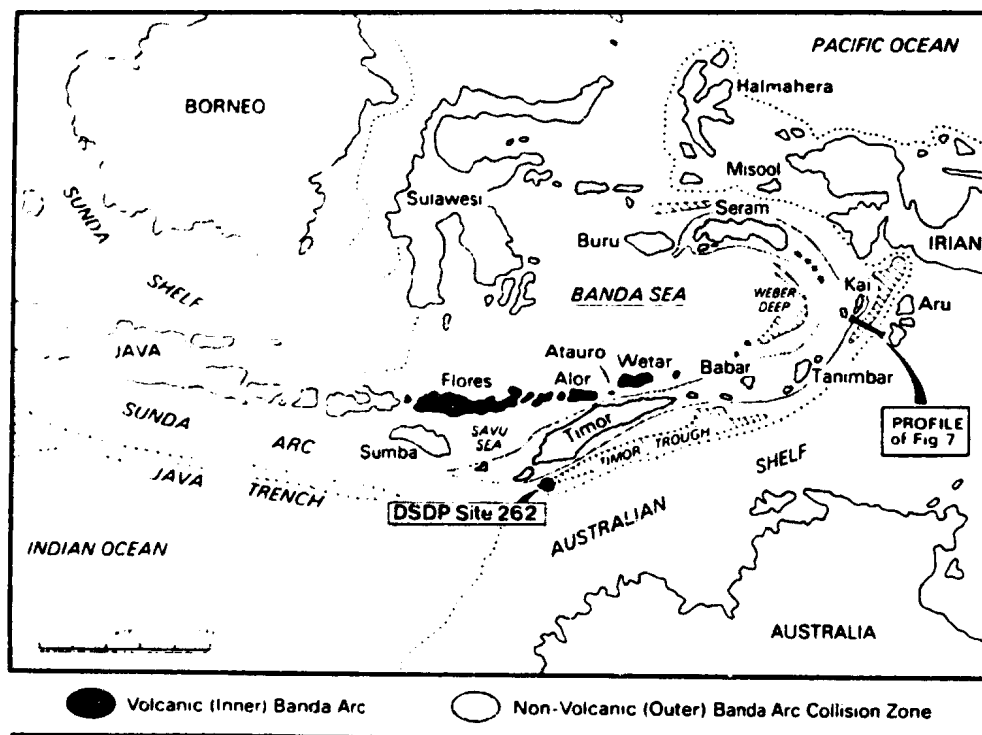


Figure 17.6 Location map of the Australia - Banda Arc collision zone (from Audley-Charles, 1986).

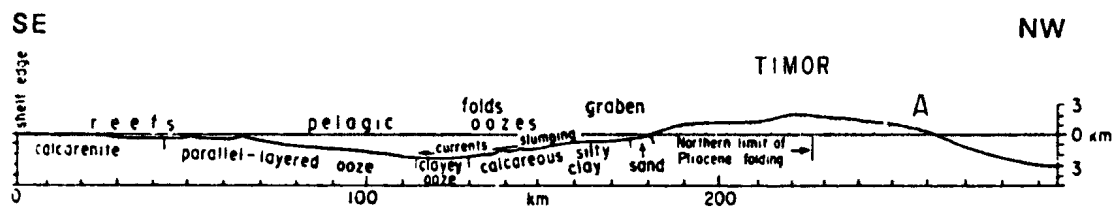


Figure 17.7 Bathymetric profile from the Australian shelf to Timor (from Veevers *et al.*, 1978).

the Timor-Seram Trough (Van Andel, 1965; Van Andel and Veevers, 1965). The Timor-Seram Trough is an arcuate system of structurally isolated, elongate depressions that range from <2--70 km wide and are 2000-3000 m deep (Van Andel and Veevers, 1967; Veevers *et al.*, 1978; Audley-Charles, 1986). The Outer Banda Arc is a discontinuous series of submarine ridges and islands (eg. Timor and Seram) composed of tectonically-imbricated rocks, mostly Mesozoic and Cenozoic strata of the Australian continental rise, plus some highly allochthonous sedimentary, igneous and metamorphic thrust slices of Asian or uncertain paleogeographic affinities (Audley-Charles, 1968; Audley-Charles *et al.*, 1979) and, locally, structurally isolated crustal blocks of the Australian continent (Jacobson *et al.*, 1978; Bowin *et al.*, 1980). The inner Banda Arc is a discontinuous series of volcanic submarine ridges and islands.

There is geophysical evidence that 30 km thick Australian continental crust extends seaward under the Timor-Seram Trough and the Outer Banda Arc (Jacobson *et al.*, 1978; Bowin *et al.*, 1980). There is also Sr⁸⁶/Sr⁸⁷ isotope data from Inner Arc volcanics which indicate contamination of the melts by continental crust and suggest that the Australian margin was being subducted during Miocene-Pliocene time (Whitford *et al.*, 1977). Two fundamentally different tectonic models have been proposed to account for these and other data and explain the present day expression of convergence in the area (Figure 17.C). Although additional geophysical data seems necessary to resolve significant discrepancies between the two models, comparison of this convergent zone with the subducted Newfoundland margin is justified for two reasons. 1) The overall morphologic expression of deformation of the Australian margin is quite similar to that envisaged for the evolving Middle Ordovician foreland basin. 2) Seismic and DSDP drill hole data indicate that shallow-water carbonates of the Australian shelf underlie the Timor Trough and extend at least 10 km further north under Timor (Veevers, 1971). Therefore, the deep-water continental rise

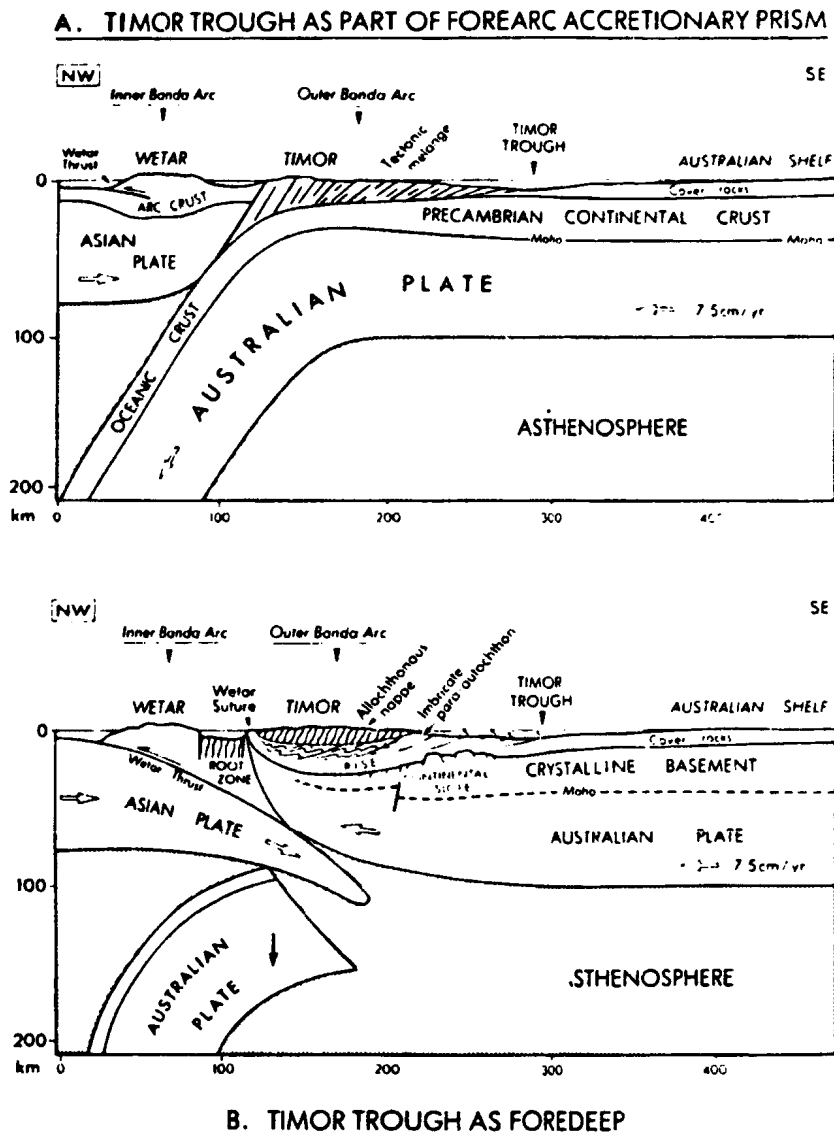


Figure 17.8 Tectonic models for the Australia - Banda Arc collision zone (from Audley-Charles, 1986). a) The Timor-Seram Trough is interpreted as the surface trace of a subduction zone dipping toward the Banda Sea; the Outer Arc is an accretionary prism constructed largely of sedimentary rocks scraped off the subducted Australian continental margin (eg. Hamilton, 1979; Bowin *et al.*, 1980; Karig *et al.*, 1987). This is identical to the model proposed for Taconian subduction along the Newfoundland margin. b) Jamming of the subduction zone by thick continental rise sediments results in a reversal in polarity of the Benioff zone and back-thrusting of the continental margin over the Inner Arc. The Outer Arc is a parautochthonous fold and thrust belt, and the Timor-Seram Trough is a flexural foredeep caused by loading of the imbricated rise sediments on the Australian continental margin (eg. Audley-Charles, 1981; 1986).

strata comprising Timor are allochthonous, and in precisely the same structural position as are Taconic allochthons with respect to autochthonous, Early Paleozoic platformal carbonates on the North American margin.

The pre-convergence history of the Australian margin is similar to that of the Early Paleozoic North American margin (Mollan *et al.*, 1970; Martison *et al.*, 1973; Bradshaw *et al.*, 1988; MacDaniel, 1988). Ocean closing, subduction of the Australian margin, and volcanism along the Inner Banda Arc began during the Miocene and continued until middle Pliocene time (~6-3 Ma; Audley-Charles, 1981). Arrival of proximal continental rise strata at the trench and overthrusting of allochthonous thrust slices onto the Australian margin occurred between early and middle Pliocene time (~5-3 Ma; Carter *et al.*, 1976; Audley-Charles *et al.*, 1979). Major folding, imbrication, and continentward displacement of continental rise strata occurred between latest Miocene and late Pliocene time (~6-1.8 Ma; Audley-Charles, 1968; Audley-Charles *et al.*, 1979). Collectively the timing of volcanism and major deformation events indicate that subduction essentially ceased ~3 million years ago, possibly due to jamming of the subduction zone by thick sedimentary deposits of the proximal continental rise (Audley-Charles, 1981). Since that time most deformation in response to continued convergence has been taken up by structural telescoping between and within the Inner and Outer Banda Arcs, manifest by shallow, diffuse seismicity and episodes of folding and faulting at Timor and Seram during the Pleistocene (Audley-Charles, 1968, 1981, 1986; Audley-Charles *et al.*, 1979; Bowin *et al.*, 1980). Veevers *et al.* (1978) calculate the rate of convergence to have decreased dramatically from ~5.8 cm/yr during the middle to late Pliocene to ~0.5 cm/yr from the Pleistocene to the present.

In its state of suspended animation the present day Australian margin resembles that envisaged for the Newfoundland margin during the Middle Ordovician. Dynamics across the margin in response to continued,

albeit decelerated, convergence are recorded in the uppermost Pliocene, Pleistocene and Recent carbonates. Salient aspects of the history that are common to the Newfoundland margin and demonstrate similar responses to convergence are summarized below.

1) Initial expression of convergence on the northwest Australia shelf was faulting, folding and uplift of the passive margin carbonate shelf during middle to late Miocene time, approximately coincident with allochthonous nappe emplacement and initial imbrication of continental rise strata in the Outer Banda Arc. The event is recorded by a regional subaerial unconformity that extends (in the subsurface) across the entire present day shelf, beneath the present day slope, the Timor Trough and edge of Timor proper, and is tentatively correlated with an exposure surface on the Australia mainland (Van Andel and Veevers, 1965; Mollan *et al.*, 1970; Veevers, 1971). Marked lateral variations in the amount of section missing indicate that the duration of exposure and/or amount of erosion varied across the area. As this deformation appears to be related to overthrusting at the margin (Veevers, 1971), it may be an expression of flexural uplift, and, therefore, is analogous to the Lower-Middle Ordovician St. George Unconformity.

2) Post-Miocene (unconformity) carbonate sedimentation on the present day shelf was controlled by syndimentary faulting and differential subsidence (Mollan *et al.*, 1970; Martison *et al.*, 1973; MacDaniel, 1988); total accumulations vary from 400-1000 m thick. Most active faults are linked to Paleozoic basement; some are reactivated rift-generated structures. Local and regional syndimentary tectonism during the Pleistocene is recorded by 1) discontinuous horizons of faulted, broken and chaotic bedding, 2) both local and more widespread subaerial unconformities, and 3) warping of the shelf into a system of large scale shallow depressions and broad rises (Van Andel and Veevers, 1965; Veevers, 1971).

The dynamics of this carbonate shelf and its post-uplift sedimentary

history parallel that recorded by the Table Point Formation deposited on a tectonically unstable platform. The fact that the Australian shelf has remained in very shallow water, that vertical accretion was accompanied by progradation (Veevers, 1971; MacDaniel, 1988), and that the sea floor was episodically exposed, suggest that sedimentation has continued on a broad peripheral upwarp which, like the subduction zone, has not migrated significantly since Pliocene time.

3) The foundered, outer portion of the passive margin shelf underlies the Australian slope (Veevers, 1971; Veevers *et al.*, 1978) which is presently the site of deposition of fine-grained, shelf-derived and pelagic carbonate muds (Van Andel and Veevers, 1967; Figure 17.7). A deepening-upward sequence above the Miocene unconformity seen in DSDP 262 core from the Timor Trough (Figure 17.6) indicates that 2300 m of subsidence (the depth of the present day trough axis) occurred in ~1.2 million years, during which ~100 m of carbonate mud was deposited. Although the slope profile along most of its length is fairly smooth, seismic profiles show a substructure of down-to-basin normal faults, mostly with <150 m displacements (Veevers, 1971; Jacobson *et al.*, 1978; Veevers *et al.*, 1978; Karig *et al.*, 1987). In general, differential subsidence related to faulting and its affect on sediment accumulation is most pronounced on the upper slope where sequences locally vary from 120-400 m thick (Veevers, 1971). Catastrophic faulting with exposed vertical escarpments up to 500 m high, and a comparatively steep gradient for the entire slope is recognized on the slope adjacent to Aru where curvature of the Banda Arc is greatest (Jacobson *et al.*, 1978; Figure 17.6).

The Australian slope is a suitable analogue for platform collapse on the outer trench slope recorded by both platform-derived, slope to basinal carbonates of the Table Cove Formation and the escarpment-derived, deep-water carbonates of the Cape Cormorant Formation. The thinness of most Table Cove sequences compared to that of slope

carbonates in DSDP 262 may be a reflection of more rapid foundering in response to continued rapid convergence (versus nearly stationary) along the Newfoundland margin. Localization of major faulting on the slopes of both the Australian and North American margins suggests that stresses related to convergence are amplified in curved regions and lead to gradients steeper than can be sustained without major fault displacements (eg. Jacobson *et al.*, 1978).

3) The Timor-Seram Trough, too distant from the Australian shelf to be supplied with abundant carbonate sediment, is presently the depositional site of radiolarian-rich clays derived primarily from the Outer Arc (Van Andel and Veevers, 1967; Veevers *et al.*, 1978; Figure 17.7). In the Timor Trough ~340 m of predominantly terrigenous mud have accumulated since the Pliocene. Seismic profiles show the sediments to be parallel layered and commonly disposed in a basinward-tapering wedge that onlaps the outer carbonate slope (Veevers *et al.*, 1978). Near the foot of the Outer Arc, however, they (and immediately underlying shelf to slope carbonates) are folded and uplifted by high-angle reverse faults that reflect compressive stresses in the trough, probably precursor to imbrication and incorporation in the Outer Arc (Veevers *et al.*, 1978; Karig *et al.*, 1987).

The origin, morphology, depth and, to a limited extent, the sedimentology of the basins comprising the Timor-Seram Trough render them suitable analogues for the foreland basin in which Goose Tickle Group clastics were deposited. Reverse faulting in response to compressive stress in the trough is precisely the mechanism by which Daniel's Harbour Member beds are interpreted to have been generated. The contrasting absence of Outer Arc-derived, turbiditic sands from the troughs may reflect trapping/ponding of coarse debris in structural basins on the rugged inner slope where they will not be delivered to the trough floor until upper slope basins are filled or tectonically disrupted.

In summary, there are striking similarities in bathymetry, styles of

sedimentation, and expressions of synsedimentary deformation related to convergence across the modern Australian margin and the ancient Newfoundland which are the product of arc-continent collision. Fundamental differences between sedimentation histories for both the platform/shelf and slope appear to be due to vastly different rates of convergence, specifically early cessation of subduction along the Australian margin.

CHAPTER 18
CONCLUSIONS

Middle Ordovician Table Head Group and Goose Tickle Group strata record foundering, burial and cannibalization of a foreland basin carbonate platform on the North American continental margin during initial stages of Taconian orogenesis. The succession reflects delicate interplay between sedimentation and tectonics during discrete stages of foreland basin development. Each stage corresponds to a specific morpho-tectonic regime across a continent - ocean subduction zone.

Passive margin sedimentation on the long-lived, late Precambrian - early Ordovician carbonate platform ended, and convergent margin sedimentation began with an episode of regional block-faulting and differential uplift. This event was caused by migration of a peripheral forebulge across the platform. It interrupted peritidal carbonate sedimentation (Aguathuna Formation, St. George Group), culminating in widespread formation of the erosional and karstified St. George Unconformity, and rendered the flat and coherent platform a complex mosaic of differentially subsiding blocks.

Shallow marine Table Point Formation carbonates deposited on the St. George Unconformity are the first record of sedimentation on this unstable platform along the western flank of the evolving foreland basin. Continuing deposition, synsedimentary faulting and differential subsidence resulted in platformal carbonates of greatly varying thickness, composition and facies. Such dynamics also gave rise to local intraformational unconformities in peritidal sequences, gravitational slides, abrupt lateral and vertical changes in lithofacies, and anomalous peritidal sequences. Nevertheless, tectonism was subtle enough that eustatic sea level changes still influenced sedimentation.

Deep-water carbonates and terrigenous clastics (Table Cove, Cape

Cormorant and Black Cove formations) deposited on Table Point limestone reflect tectonic drowning of the foreland basin platform. Diachronous collapse took place as the platform entered and formed the paleo-southeast-facing inner trench slope of the migrating subduction zone. Foundering was accompanied by synsedimentary extensional faulting and differential subsidence that generated a low-relief horst and graben topography across most of the area, and locally generated high relief submarine escarpments. Table Cove Formation strata accumulated under ever increasing water depth on newly-formed, gently-dipping carbonate slopes and basin margins, with carbonate sediment coming from adjacent, relict, shallow water platform blocks. Such slopes were discontinuous, faced various directions (and some changed over time), and subsided at different rates. Cape Cormorant Formation strata record catastrophic faulting in the Port au Port area and resedimentation of exhumed passive margin carbonates by sediment gravity flows in a structurally-isolated, deep-water basin on the inner trench slope. Localization of this major faulting was probably due to amplification of stress caused by convergence at the curvature of the St. Lawrence Promontory. Black Cove Formation shale covered abruptly subsiding platform blocks deprived of contemporaneous or resedimented carbonates. Such anoxic, sediment-starved conditions developed in deep-water basins adjacent to carbonate slopes. They were also generated on top of isolated, rapidly foundered, relict platforms.

The collapsed and fragmented platform was buried by terrigenous mud, silt, and immature sand (American Tickle Formation and Mainland Sandstone) as it entered the trench. This sediment came from the encroaching accretionary prism-volcanic arc complex and entered the trench at several points along its length. Most was transported and deposited by turbidity currents travelling down the south-southwest-dipping trench axis. Preexisting structural domains controlled location of major depositional axes of trench-parallel, progradational turbidite

systems, as well as sediment dispersal across the trench.

Reverse faulting and uplift of the foundered and buried platform in response to compression in the trench accompanied siliciclastic turbidite sedimentation and gave rise to resedimented carbonates of the Daniel's Harbour Member. Exhumed foreland basin carbonates and clastics shed from escarpments of various facing directions were transported by sediment gravity flows and redeposited in local intra-trench basins. Much of this debris was involved in more than one cycle of uplift, mass wasting, and gravity flow transport.

Sedimentation in the trench ceased as it was structurally overridden by the accretionary prism. Structurally elevated blocks were decapitated during prism emplacement and incorporated as coherent blocks and slivers in mélangé at the base of the accretionary prism.

REFERENCES

- Ahr, W. M., 1973, The carbonate ramp: an alternative to the shelf model: *Trans. Gulf Coast Assoc. Geol. Soc.*, v. 23, p. 221-225.
- Aigner, T., 1982, Calcareous tempestites: storm-dominated stratification in upper Muschelkalk limestone (Middle Trias, SW Germany), *in* Einsele, G., and Seilacher, A., eds., *Cyclic and Event Stratification*: New York, Springer-Verlag, p. 180-198.
- Aitken, J. D., 1966, Middle Cambrian to Middle Ordovician sedimentation, southern Rocky Mountains of Alberta: *Bull. Can. Petrol. Geol.*, v. 14, p. 405-441.
- Alberstadt, L. P., and Repetski, J. E., 1989, A lower Ordovician sponge-algal facies in the southern United States and its counterparts elsewhere in North America: *Palaios*, v. 4, p. 223-242.
- Alberstadt, L. P., and Walker, K. R., 1975, A receptaculitid-echinoderm pioneer community in a Middle Ordovician reef: *Lethaia*, v. 9, p. 262-272.
- Archibald, D. A., and Farrar, E., 1976, K-Ar ages of amphibolites from the Bay Islands ophiolite and the Little Port Complex, western Newfoundland, and their geological implications: *Can. Jour. Earth Sci.*, v. 13, p. 520-529.
- Arnott, R. J., McKerrow, W. S., and Cocks, L. R. M., 1985, The tectonics and depositional history of the Ordovician and Silurian rocks of Notre Dame Bay, Newfoundland: *Can. Jour. Earth Sci.*, v. 22, p. 607-618.
- Aspler, L. B., and Donaldson, J. A., 1986, Penecontemporaneous sandstone dykes; Nonacho Basin (early Proterozoic, Northwest Territories): horizontal injection in vertical, tabular fissures: *Can. Jour. Earth Sci.*, v. 23, p. 827-838.
- Audley-Charles, M. G., 1968, *The geology of Portuguese Timor*: Geol. Soc. London Mem. 4, 76 p.
- Audley-Charles, M. G., 1981, Geometrical problems and implications of large scale overthrusting in the Banda Arc - Australian, margin collision zone, *in* McClay, K. R., and Price, N. J., eds., *Thrust and Nappe Tectonics*: Geol. Soc. Lon. Spec. Publ. 9, p. 407-416.
- Audley-Charles, M. G., 1986, Timor-Tanimbar Trough: the foreland basin of the evolving Banda Orogen, *in* Allen, P. A., and Homewood, P., eds., *Foreland Basins*: Internat. Assoc. Sediment. Spec. Publ. 8., p. 91-102.
- Audley-Charles, M. G., Carter, D. J., Barber, A. J., Norwick, M. S., and Tjokrosoepetro, S., 1979, Reinterpretation of the geology of Seram: implications for the Banda Arc and northern Australia: *Jour. Geol. Soc. London*, v. 136, p. 547-568.
- Badiozamani, K., 1973, The Dorag dolomitization model - application to the Middle Ordovician of Wisconsin: *Jour. Sed. Petrology*, v. 43, p. 965-984.

- Baker, P. A., and Burns, S. J., 1985, Occurrence and formation of dolomite in organic-rich continental margin sediments: Am. Assoc. Petroleum Geologists Bull., v. 69, p. 1917-1930.
- Ball, M. M., 1967, Carbonate sand bodies of Florida and the Bahamas: Jour. Sed. Petrology, v. 37, p. 556-591.
- Ball, M. M., Shinn, E. A., and Stockman, K. W., 1967, The geologic effects of hurricane Donna in south Florida: Jour. Geol., v. 75, p. 583-597.
- Bally, A. W., 1982, Musings over sedimentary basin evolution: Phil. Trans. Royal. Soc., Ser. A, v. 305, p. 325-338.
- Barnes, C. R., 1984, Early Ordovician eustatic events in Canada, in Burton, D. L., ed., Aspects of the Ordovician System: Palaeont. Contrib., University of Oslo, No. 295, p. 51-64.
- Bathurst, R. G. C., 1975, Developments in Sedimentology 12: Carbonate sediments are their diagenesis: Amsterdam, Elsevier, 658 p.
- Bathurst, R. G. C., 1980, Stromatactis - origin related to submarine-cemented crusts in Palaeozoic mud mounds: Geology, v. 8, p. 131-134.
- Bathurst, R. G. C., 1987, Diagenetically enhanced bedding in argillaceous platform limestones: stratified cementation and selective compaction: Sedimentology, v. 34, p. 749-778.
- Baturin, G. N., 1982, Developments in Sedimentology 33: Phosphorites on the sea floor - origin, composition and distribution: Amsterdam, Elsevier, 343 p.
- Beaumont, C., 1978, The evolution of sedimentary basins on a viscoelastic lithosphere: theory and examples: Geophys. Jour. R. Astr. Soc., v. 55, p. 471-497.
- Beaumont, C., 1981, Foreland basins: Geophys. Jour. R. Astr. Soc., v. 65, p. 291-329.
- Belt, E. S., and Bussièrès, L., 1981, Upper Middle Ordovician submarine fans and associated facies, northeast of Quebec City: Can. Jour. Earth Sci., v. 18, p. 981-994.
- Benedict, G. L., III., and Walker, K. R., 1978, Paleobathymetric analysis in Paleozoic sequences and its geodynamic significance: Am. Jour. Sci., v. 278, p. 579-607.
- Berger, W. H., 1970, Planktonic foraminifera: selective solution and the lysocline: Mar. Geol., v. 8, p. 111-138.
- Berger, W. H., 1971, Sedimentation of planktonic foraminifera: Mar. Geology, v. 11, p. 325-358.
- Berger, W. H., 1974, Deep sea sedimentation, in Burk, C. A., and Drake, C. L., eds., The Geology of Continental Margins: New York, Springer-Verlag, p. 213-241.
- Bergström, S. M., 1979, First report of the enigmatic Ordovician microfossil Konyrium in North America: Jour. Paleontology, v. 53, p. 320-327.

- Bergström, S. M., Riva, J., and Kay, M., 1974, Significance of conodonts, graptolites, and shelly faunas from the Ordovician of western and north central Newfoundland: *Can. Jour. Earth Sci.*, v. 11, p. 1625-1660.
- Bernoulli, D., and Jenkyns, H. C., 1974, Alpine, Mediterranean, and central Atlantic Mesozoic facies in relation to the early evolution of the Tethys, in Dott, R. H., Jr., and Shaver, R. H., eds., *Modern and Ancient Geosynclinal Sedimentation*: SEPM Spec. Publ. 19, p. 129-160.
- Blatt, H., Middleton, G., and Murray, R., 1980, *Origin of sedimentary rocks*: Englewood Cliffs, NJ, Prentice-Hall Inc., 782 p.
- Boardman, R. S., Cheetham, A. H., and Rowell, A. J., eds., 1987, *Fossil invertebrates*: Palo Alto, CA, Blackwell, 713 p.
- Boardman, M. R. and Neumann, A. C., 1984, Sources of periplatform carbonates, northwest Providence Channel, Bahamas: *Jour. Sed. Petrology*, v. 54, p. 1110-1123.
- Boscence, D. W. J., Rowlands, R. J., and Quine, M. L., 1985, Sedimentology and budget of a Recent carbonate mound, Florida Keys: *Sedimentology*, v. 32, p. 317-343.
- Bosellini, A., and Doglioni, F., 1986, Inherited structures in the hanging wall of the Valsugana Overthrust (southern Alps, southern Italy): *Jour. Struct. Geol.*, v. 8, p. 581-583.
- Bostock, H. H., 1983, Precambrian rocks of the Strait of Belle Isle area: *Geol. Surv. Canada Mem.* 400, p. 1-73.
- Bostock, H. H., Cumming, L. M., Williams, H., and Smyth, W. R., 1983, *Geology of the Strait of Belle Isle Area, northwestern insular Newfoundland, southern Labrador, and adjacent Quebec*: *Geol. Surv. Canada Mem.* 400, 141 p.
- Botsford, J. B., 1987, *Depositional history of Middle Cambrian to Lower Ordovician deep water sediments, Bay of Islands, western Newfoundland* [unpubl. Ph. D. dissert.]: St. John's, Newfoundland, Memorial University of Newfoundland, 500 p.
- Bouma, A. H., 1962, *Sedimentology of some flysch deposits*: Amsterdam, Elsevier, 168 p.
- Bourgeois, J., and Smith, J. D., 1984, Paleohydraulic significance of hummocky cross-stratification (abstr.): *Sedimentology of shelf sands and sandstones*: Calgary, Can. Soc. Petroleum Geol. Research Symposium, Abstr., p. 27.
- Bourque, P.-A., and Gignac, H., 1983, Sponge-constructed *Stromatolites* mud mounds, Silurian of Gaspé, Québec: *Jour. Sed. Petrology*, v. 53, p. 521-532.
- Bourque, P.-A., Amyot, A., Desroches, A., Gignac, H., Gosselin, C., Lachambre, G., and Laliberté, J.-Y., 1986, Silurian and Lower Devonian reef and carbonate complexes of the Gaspé Basin, Québec - a summary: *Bull. Can. Petrol. Geol.*, v. 34, p. 452-489.
- Bourque, P.-A., Manet, B., et Roux, A., 1981, Algues siluriennes du synclinorium de la Baie des Chaleurs, Québec, Canada: *Revue de Micropaléontologie*, v. 24, p. 88-126.

- Boyce, W. D., Ash, J. S., and Knight, I., 1988, Biostratigraphic studies of Ordovician carbonate rocks in western Newfoundland, in Hyde, R. S., Walsh, D. G., and Blackwood, R. F., eds., Current Research, Newfoundland Dept. Mines Energy, Mineral Dev. Div., Report 88, p. 75-83.
- Bowen, Z. P., Rhoads, D. C., and McAlester, A. L., 1974, Marine benthic communities in the upper Devonian of New York: *Lethaia*, v. 7, p. 93-120.
- Bowin, C., Purdy, G. M., Johnston, C., Shor, G., Lawver, L., Hartono, H. M. S., and Jezek, P., 1980, Arc - continent collision in Banda Sea region: *Am. Assoc. Petroleum Geologists Bull.*, v. 64, p. 868-915.
- Bradley, D. C., and Kusky, T. M., 1986, Geologic evidence for rate of plate convergence during Taconic arc - continent collision: *Jour. Geol.*, v. 94, p. 667-681.
- Bradshaw, M. T., Yeates, A. N., Benyon, R. M., Brakel, A. T., Langford, R. P., Totterdell, J. M., and Yeung, M., 1988, Paleogeographic evolution of the North West Australia Shelf region, in Purcell, P. G., and Purcell, R. R., eds., *The Northwest Shelf, Australia*: Perth, *Petrol. Explor. Soc. Australia*, p. 29-54.
- Bridges, P. H., and Chapman, A. J., 1988, The anatomy of a deep water mud mound complex to the southwest of the Dinantian platform in Derbyshire, UK: *Sedimentology*, v. 35, p. 139-162.
- Broadhead, T. W., and Waters, J. A., 1980, Echinoderms: Notes for a Short Course: *University TN Studies in Geology* 3, 235 p.
- Broecker, W. S., 1974, *Chemical Oceanography*: New York, Harcourt Brace Jovanovich, 214 p.
- Bromley, R. G., 1967, Marine phosphorites as depth indicators: *Mar. Geol.*, v. 5, p. 503-509.
- Bromley, R. G., and Asgaard, U., 1972, A large radiating burrow-system in Jurassic micaceous sandstones in Jameson Land, east Greenland: *Rapp. Grønlands Geol. Unders.*, v. 49, p. 23-30.
- Bromley, R. G., and Eckdale, A. A., 1984, Chondrites: a trace fossil indicator of anoxia in sediments: *Science*, v. 222, p. 872-874.
- Bromley, R. G., and Mork, A., 1984, Phoebichnus ichnofacies in the condensed Lower Jurassic succession of Svalbard [unpubl. report]: *Continental Shelf Institute, Norway*, 13 p.
- Brooks, G. R., and Holmes, C. W., 1990, Recent carbonate slope sediments and sedimentary processes bordering a nonrimmed platform: southwest Florida continental margin, in Crevello, P. D., Wilson, J. L., Sarg, J. F., and Read, J. F., eds., *Controls on Carbonate Platform and Basin Development*: *SEPM Spec. Publ.* 44, p. 259-272.
- Brückner, W. D., 1966, Stratigraphy and structure of west central Newfoundland, in Poole, W. H., ed., *Guidebook, Geology of Parts of Atlantic Provinces*: *Ann. Mtg., Geol. Assoc. Canada, Mineral. Assoc. Canada*, p. 137-151.
- Burnett, W. C., 1977, Geochemistry and origin of phosphorite deposits from off Peru and Chile: *Geol. Soc. Am. Bull.*, v. 88, p. 813-823.

- Butler, G. P., 1969, Modern evaporite deposition and geochemistry of coexisting brines, the sabkha, Trucial Coast, Arabian Gulf: *Jour. Sed. Petrology*, v. 39, p. 70-89.
- Butler, R. W., 1982, The terminology of structures in thrust belts: *Jour. Struct. Geol.*, v. 4, p. 239-245.
- Byers, C. W., 1977, Biofacies patterns in euxinic basins: a general model, *in* Cook, H. E., and Enos, P., eds., *Deep-water Carbonate Environments: SEPM Spec. Publ.* 25, p. 5-18.
- Caldwell, J. G., and Turcotte, D. L., 1979, Dependence of the thickness of the elastic oceanic lithosphere on age: *Jour. Geophys. Res.*, v. 84, p. 7572-7576.
- Carter, D. J., Audley-Charles, M. G., and Barber, A. J., Stratigraphic analysis of island arc-continental margin collision in eastern Indonesia: *Jour. Geol. Soc. Lond.*, v. 132, p. 179-198.
- Casey, J. F., and Kidd, W. S. F., 1981, Parallochthonous group of sedimentary rocks unconformably overlying the Bay of Islands ophiolite complex, North Arm Mountain, Newfoundland: *Can. Jour. Earth Sci.*, v. 18, p. 1035-1050.
- Cawood, P. A., 1989, Acadian remobilization of a Taconian ophiolite, Hare Bay allochthon, northwestern Newfoundland: *Geology*, v. 17, p. 257-260.
- Cawood, P. A., Shaw, B. R., and Stevens, R. K., 1991, Comment on "Structure of the Appalachian deformation front in western Newfoundland: implications of multichannel seismic reflection data": *Geology*, v. 19, p. 1-4.
- Cawood, P. A., and Williams, H., 1986, Northern extremity of the Humber Arm Allochthon in the Portland Creek area, western Newfoundland, and relationships to nearby groups, *in* *Current Research, Part A. Geol. Surv. Canada Paper*, 86-1A, p. 675-682.
- Cawood, P. A., and Williams, H., 1988, Acadian basement thrusting, crustal delamination, and structural styles in and around the Humber Arm allochthon, western Newfoundland: *Geology*, v. 16, p. 370-373.
- Cawood, P. A., Williams, H., O'Brien, S. J., and O'Neill, P., 1988, Geologic cross-section of the Appalachian Orogeny: *Geol. Assoc. Canada, Mineral. Assoc. Canada, Can. Soc. Petroleum Geol. Field Trip Guidebook*, Trip 1B.
- Chamberlain, C. K., 1971a, Bathymetry and paleoecology of Ouachita geosyncline of southeastern Oklahoma as determined from trace fossils: *Am. Assoc. Petroleum Geologists Bull.*, v. 55, p. 34-50.
- Chamberlain, C. K., 1971b, Morphology and ethology of trace fossils from the Ouachita Mountains, southeastern Oklahoma: *Jour. Paleontology*, v. 45, p. 212-246.
- Chamberlain, C. K., 1977, Ordovician and Devonian trace fossils from Nevada: *Nevada Bur. Mines and Geology, Bull.*, v. 90, p. 1-24.
- Cherns, L., 1979, The environmental significance of *Lingula* in the Ludlow Series of the Welch Borderland and Wales: *Lethaia*, v. 12, p. 35-46.

- Choquette, P. W., and Steinen, R. D., 1980, Mississippian non-supratidal dolomite, Ste. Genevieve Limestone, Illinois Basin: evidence for mixed water dolomitization, in Zenger, D. H., Dunham, J. B., and Ethington, R. L., eds., Concepts and Models of Dolomitization: SEPM Spec. Publ. 28, p. 163-196.
- Choukroune, P., Francheteau, J., and Le Pichon, X., 1978, In situ structural observations along Transform Fault A in the FAMOUS area, Mid-Atlantic Ridge: Geol. Soc. Am. Bull., v. 89, p. 1013-1029.
- Chow, N., 1986, Sedimentology and diagenesis of Middle and Upper Cambrian platform carbonates and siliciclastics, Port-au-Port Peninsula, Newfoundland [unpubl. Ph. D. dissert.]: St. John's, Newfoundland, Memorial University of Newfoundland, 458 p.
- Chow, N., and James, N. P., 1986, Cambrian grand cycles: a northern Appalachian perspective: Geol. Soc. Am. Bull., v. 98, p. 418-429.
- Chow, N., and James, N. P., 1987, Facies-specific, calcitic and bimineralic ooids from Middle and Upper Cambrian platform carbonates, western Newfoundland, Canada: Jour. Sed. Petrology, v. 57, p. 907-921.
- Chowns, T. M., and Elkins, J. E., 1974, The origin of quartz geodes and cauliflower cherts through the silicification of anhydrite nodules: Jour. Sed. Petrology, v. 44, p. 885-903.
- Church, W. R., and Stevens, R. K., 1971, Early Paleozoic ophiolite complexes of the Newfoundland Appalachians as mantle - oceanic crust sequences: Jour. Geophys. Res., v. 76, p. 1460-1466.
- Cloud, P. E., 1948, Notes on Recent brachiopods: Am. Jour. Sci., v. 246, p. 241-250.
- Cohen, C. R., 1982, Model for a passive to active continental margin transition: implications for hydrocarbon exploration: Am. Assoc. Petroleum Geologists Bull., v. 66, p. 708-718.
- Coleman, J. M., and Prior, D. B., 1988, Mass wasting on continental margins: Ann. Rev. Earth and Plan. Sciences., v. 16., p. 101-110.
- Coniglio, M., 1985, Origin and diagenesis of fine-grained slope sediments: Cow Head Group (Cambro-Ordovician), western Newfoundland [unpubl. Ph. D. dissert.]: St. John's, Newfoundland, Memorial University of Newfoundland, 684 p.
- Coniglio, M., 1989, Neomorphism and cementation in ancient deep-water limestones, Cow Head Group (Cambro-Ordovician), western Newfoundland: Sedimentology, v. 65, p. 15-33.
- Coniglio, M., and James, N. P., 1988, Dolomitization of deep-water sediments, Cow Head Group (Cambro-Ordovician), western Newfoundland: Jour. Sed. Petrology, v. 58, p. 1032-1045.
- Cook, H. E., 1979, Ancient continental slope sequences and their value in understanding modern slope development, in Doyle, L. J., and Pilkey, O. H., Jr., eds., Geology of Continental Slopes: SEPM Spec. Publ. 27, p. 287-306.
- Cook, H. E., and Enos, P., eds., 1977, Deep-water carbonate environments: SEPM Spec. Publ. 25, 336 p.

- Cook, H. E., McDaniel, P. N., Mountjoy, E. W., and Pray, L. C., 1972, Allochthonous carbonate debris flows at Devonian bank ("reef") margins, Alberta, Canada: *Bull. Can. Petrol. Geol.*, v. 20, p. 439-497.
- Cook, H. E., and Mullins, H. T., 1983, Basin margin, in Scholle, P. A., Bebout, D. G., and Moore, C. H., eds., *Carbonate Depositional Environments*: Am. Assoc. Petroleum Geologists Mem. 33, p. 539-618.
- Cook, H. E., and Taylor, M. E., 1977, Comparison of continental slope and shelf environments in the Upper Cambrian and Lowest Ordovician of Nevada, in Cook, H. E., and Enos, P., eds., *Deep-water Carbonate Environments*: SEPM Spec. Publ. 25, p. 51-82.
- Cooper, D. J. W., 1988, Structure and sequence of thrusting in deep-water sediments during ophiolite emplacement in the south-central Oman Mountains: *Jour. Struct. Geol.*, v. 10, p. 473-485.
- Cooper, G. A., 1956, Chazy and related brachiopods: *Smiths. Misc. Coll.*, v. 127, 1245 p.
- Copeland, M. J., and Boltmon, T. E., 1985, Fossils of Ontario, Part 3: The eurypterids and phyllocarids: *Royal Ontario of Museum Life Sciences Misc. Publ.*, 48 p.
- Cossey, S. P. J., and Ehrlich, R., 1979, A conglomeratic, carbonate flow deposit, northern Tunisia; a link in the genesis of pebbly mudstones: *Jour. Sed. Petrology*, v. 49, p. 11-22.
- Courtney, R. C., and Beaumont, C., 1983, Thermally activated creep and flexure of the oceanic lithosphere: *Nature*, v. 305, p. 201-204.
- Cowen, C. A., and James, N. P., 1989, Stratigraphy and sedimentology of the Port au Port Group (Middle to Upper Cambrian), western Newfoundland: preliminary results, in Pereira, C. P. G., Walsh, D. G., and Blackwood, R. F., eds., *Current Research (1989)*, Newfoundland Dept. Mines, Geol. Surv. Newfoundland, Report 89-1, p. 55-61.
- Crevello, P. D., and Schlager, W., 1980, Carbonate debris sheets and turbidites, Exuma Sound, Bahamas: *Jour. Sed. Petrology*, v. 50, p. 1121-1147.
- Crimes, T. P., 1970, Trilobite tracks and other trace fossils from the Upper Cambrian of North Wales: *Jour. Geol.*, v. 7, p. 47-68.
- Crimes, T. P., 1973, From limestones to distal turbidites: a facies and trace fossil analysis in the Zumaya flysch (Paleocene-Eocene), North Spain: *Sedimentology*, v. 20, p. 105-131.
- Crimes, T. P., 1977, Trace fossils of an Eocene deep-sea sand fan, northern Spain, in Crimes, T. P., and Harper, J. C., eds., *Trace Fossils 2*: Seel House Press, Liverpool, p. 71-90.
- Crimes, T. P., and Harper, J. C., eds., 1970, *Trace fossils*: Seel House Press, Liverpool, 547 p.
- Cuffey, R. J., 1977, Bryozoan contributions to reefs and bioherms through geologic time: *Studies in Geology*, v. 4, p. 181-194.
- Cumming, L. M., 1983, Lower Paleozoic autochthonous strata of the Strait of Belle Isle area: *Geol. Surv. Canada Mem.* 400, p. 75-108.

- Curtis, C. D., 1977, Sedimentary geochemistry: environments and processes dominated by involvement of an aqueous phase: Phil. Trans. Royal Soc., Ser. A286, p. 352-372.
- Dahlstrom, C. D., 1970, Structural geology in the eastern margin of the Canadian Rocky Mountains: Bull. Can. Petrol. Geol., v. 18., p. 332-406.
- D'Alessandro, A., and Bromley, R. G., 1987, Meniscate trace fossils and the Muensteria-Taenidium problem: Paleontology, v. 30, p. 743-763.
- Dallmeyer, R. D., 1977, Diachronous ophiolite obduction in western Newfoundland: evidence from $^{40}\text{Ar}/^{39}\text{Ar}$ of the Hare Bay metamorphic aureole: Am. Jour. Sci., v. 277, p. 61-72.
- Dallmeyer, R. D., and Williams, H., 1975, $^{40}\text{Ar}/^{39}\text{Ar}$ ages for the Bay of Islands metamorphic aureole: their bearing on the timing of Ordovician ophiolite obduction: Can. Jour. Earth Sci., v. 12, p. 1685-1690.
- Davies, G. R., 1970, Algal laminated sediments; Gladstone Embayment, Shark Bay, Western Australia, in Logan, B. W., ed., Carbonate Sedimentation and Environments, Shark Bay, Western Australia: Am. Assoc. Petroleum Geologists Mem. 13, p. 169-205.
- Davies, I. C., and Walker, R. G., 1974, Transport and deposition of resedimented conglomerates: the Cap Enragé Formation, Cambro-Ordovician, Gaspé, Québec: Jour. Sed. Petrology, v. 44, p. 1200-1216.
- DeGrace, J. R., 1974, Limestone resources of Newfoundland and Labrador: Newfoundland Dept. Mines Energy, Min. Dev. Div. Rept. 74-2, 117 p.
- Degens, E. T., and Ross, D. A., eds., 1974, The Black Sea - geology, chemistry, and biology: Am. Assoc. Petroleum Geologists Mem. 20, 633 p.
- Delong, R. C., and Middleton, G. V., 1978, Ordovician carbonate megabreccias at Cape Cormorant, western Newfoundland: Submarine debris flows: Geol. Assoc. Canada, Mineral. Assoc. Canada, Geol. Soc. Am. Joint Ann. Mtg., Abstr. with Prgm., v. 3, p. 387.
- Demaison, G. J., and Moore, G. T., 1980, Anoxic environments and oil source bed genesis: Am. Assoc. Petroleum Geologists Mem. 64, p. 1179-1209.
- Demicco, R. V., 1985, Platform and off-platform carbonates of the Upper Cambrian of western Maryland, U. S. A.: Sedimentology, v. 32, p. 1-22.
- Desroches, A., 1985, The Lower and Middle Ordovician platform carbonates of the Mingan Islands, Quebec; stratigraphy, sedimentology, paleokarst, and limestone diagenesis [unpubl. Ph. D. dissert.]: St. John's, Newfoundland, Memorial University of Newfoundland, 454 p.
- Deuser, W. G., 1975, Reducing environments, in Riley, J. P., and Skirrow, G., eds., Chemical Oceanography, v. 3, 2nd ed.: London, Academic Press, p. 1-37.
- Dogllioni, C., and Bosellini, F., 1987, Eoalpine and mesoalpine tectonics in the southern Alps: Geol. Rundschau, v. 76, p. 735-752.

- Dott, R. H., Jr., 1963, Dynamics of subaqueous gravity depositional processes: *Am. Assoc. Petroleum Geologists Bull.*, v. 47, p. 104-128.
- Dott, R. H., Jr., 1964, Wacke, graywacke and matrix - what approach to immature sandstone classification: *Jour. Sed. Petrology*, v. 34, p. 625-632.
- Dott, R. H., Jr., and Batten, R. L., 1981, *Evolution of the Earth*: New York, McGraw-Hill, 573 p.
- Droxler, A. W., and Schlager, W., 1985, Glacial vs. interglacial sedimentation and turbidite frequency in the Bahamas: *Geology*, v. 13, p. 799-802.
- Dunning, G. R., Kean, B. F., Thurlow, J. G., and Swinden, H. S., 1987, Geochronology of the Buchans, Roberts Arm and Victoria Lake groups and Mansfield Cove Complex, Newfoundland: *Can. Jour. Earth Sci.*, v. 24, p. 1175-1184.
- Dunning, G. R., and Krough, T. E., 1985, Geochronology of ophiolites of the Newfoundland Appalachians: *Can. Jour. Earth Sci.*, v. 22, p. 1659-1670.
- Dzulynski, S., Ksiazkiewicz, M., and Kuenen, P. H., 1959, Turbidites in flysch of the Polish Carpathian Mountains: *Geol. Soc. Am. Bull.*, v. 70, p. 1089-1118.
- Eberli, G. P., 1987, Carbonate turbidite sequences deposited in rift-basins of the Jurassic Tethys Ocean. (eastern Alps, Switzerland): *Sedimentology*, v. 34, p. 363-388.
- Eberli, G. P., and Ginsburg, R. N., 1990, Cenozoic progradation of northwestern Great Bahama Bank, a record of lateral platform growth and sea-level fluctuations, in Crevello, P. D., Wilson, J. L., Sarg, J. F., and Read, J. F., eds., *Controls on Carbonate Platform and Basin Development*: SEPM Spec. Publ. 44, p. 339-351.
- Eckdale, A. A., and Berger, W. H., 1978, Deep-sea ichnofacies: modern organism traces on and in pelagic carbonates of the western equatorial Pacific: *Palaeogeogr., Palaeoclim., Palaeoecol.*, v. 23, p. 263-278.
- Eckdale, A. A., Bromley, R. G., and Pemberton, S. G., 1984, *Ichnology: trace fossils in sedimentology and stratigraphy*: SEPM Short Course No. 15, 317 p.
- Eder, W., 1982, Diagenetic redistribution of carbonate, a process in forming limestone-marl alternations (Devonian and Carboniferous, Rheinisches Schiefergebirge, W. Germany), in Einsele, G., and Seilacher, A., eds., *Cyclic and Event Stratification*: New York, Springer-Verlag, p. 98-112.
- Einsele, G., 1982, Limestone-marl cycles (periodites): diagnosis, significance, causes - a review, in Einsele, G., and Seilacher, A., eds., *Cyclic and Event Stratification*: New York, Springer-Verlag, p. 8-53.
- Embley, R. W., and Jacobi, R. D., 1977, Distribution and morphology of large submarine sediment slides and slumps on Atlantic continental margins: *Mar. Geotech.*, v. 2, p. 205-228.

- Enos, P., 1983, Shelf, in Scholle, P. A., Bebout, D. G., and Moore, C. H., eds., Carbonate Depositional Environments: Am. Assoc. Petroleum Geologists Mem. 33, p. 267-297.
- Enos, P., and Moore, C. H., 1983, Fore-reef slope environment, in Scholle, P. A., Bebout, D. G., and Moore, C. H., eds., Carbonate Depositional Environments: Am. Assoc. Petroleum Geologists Mem. 33, p. 507-537.
- Enos, P., and Perkins, R. D., 1979, Evolution of Florida Bay from island stratigraphy: Geol. Soc. Am. Bull., v. 90, p. 59-83.
- Erdtmann, B.-D., 1971, Ordovician graptolite zones of western Newfoundland in relation to paleogeography of the North Atlantic: Geol. Soc. Am. Bull., v. 82, p. 1509-1528.
- Eslinger, E., and Sellars, B., 1981, Evidence for the transformation of illite from smectite during burial metamorphism in the Belt Supergroup, Clark Fork, Idaho: Jour. Sed. Petrology, v. 81, p. 203-216.
- Ethington, R. L., and Clark, D. L., 1971, Lower Ordovician conodonts in North America, in Sweet, W. C., and Bergstrom, S. M., eds., Symposium on Conodont Biostratigraphy: Geol. Soc. Am. Mem. 127, p. 63-82.
- Ethington, R. L., and Clark, D. L., 1981, Lower and Middle Ordovician conodonts from the Ibex area, western Millard County, Utah: Brigham Young University Geology Studies, v. 28(2), p. 1-160.
- Fåhræus, L. E., 1970, Conodont-based correlations of Lower and Middle Ordovician strata in western Newfoundland. Geol. Soc. Am. Bull., v. 81, p. 2061-2076.
- Fåhræus, L. E., 1977, Correlation of the Canadian/Champlainian Series boundary and the Whiterock Stage of North America with western European conodont and graptolite zones: Bull. Can. Petrol. Geol., v. 25, p. 981-994.
- Farrel, S. G., 1984, A dislocation model applied to slump structures, Ainas Basin, South Central Pyrenees: Jour. Struct. Geol., v. 6, p. 727-736.
- Fenchel, T. M., and Riedl, R. J., 1970, The sulfide system: a new biotic community underneath the oxidized layer of marine sand bottoms: Mar. Biol., v. 7, p. 255-268.
- Finney, S. C., and Skevington, D., 1979, A mixed Atlantic-Pacific province Middle Ordovician graptolite fauna in western Newfoundland: Can. Jour. Earth Sci., v. 16, p. 1899-1902.
- Fischer, A. G., 1964, The Lofer cyclothems of the Alpine Triassic: Bull. Kansas State Geol. Surv., v. 169, p. 107-149.
- Fischer, A. G., and Garrison, R. E., 1967, Carbonate lithification on the sea floor: Jour. Geol., v. 75, p. 488-496.
- Flower, R. H., 1978, St. George and Table Head cephalopod zonation in western Newfoundland: Current Research, Part A, Geol. Surv. Canada, Paper 78-1A, p. 217-224.

- Föllmi, K. B., and Grimm, K. A., 1990, Doomed pioneers: gravity flow deposition and bioturbation in marine oxygen-deficient environments: *Geology*, v. 18, p. 1069-1072.
- Fortey, R. A., 1975, Early Ordovician trilobite communities: *Fossils and Strata*, v. 4, p. 339-360.
- Fortey, R. A., 1984, Global earlier Ordovician transgression and regressions and their biological implications, in Burton, D. L., ed., *Aspects of the Ordovician System: Palaeont. Contrib.*, University of Oslo, No. 295, p. 37-50.
- Franks, P. C., 1969, Nature, origin, and significance of cone-in-cone structures in the Kiowa Formation (Early Cretaceous), north-central Kansas: *Jour. Sed. Petrology*, v. 39, p. 1438-1454.
- Friedman, G. M., 1980, Dolomite as an evaporite mineral: evidence from the rock record and from sea-marginal ponds in the Red Sea, in Zenger, D. H., Dunham, J. B., and Ethington, R. L., eds., *Concepts and Models of Dolomitization: SEPM Spec. Publ.* 28, p. 69-80.
- Froitzheim, N., and Eberli, G. P., 1990, Extensional detachment faulting in the evolution of a Tethys passive continental margin, Eastern Alps, Switzerland: *Geol. Soc. Am. Bull.*, v. 102, p. 1297-1308.
- Fürsich, F. T., 1974, On *Diplocraterion* Torell, 1870 and the significance of morphological features in vertical, spreiten-bearing, U-shaped trace fossils: *Jour. Paleontology*, v. 48, p. 952-962.
- Fürsich, F. T., 1979, Genesis, environments, and ecology of Jurassic hardgrounds: *N. Jb. Geol. Paläont. Abh.*, v. 158, p. 1-63.
- Garrett, P., 1970, Phanerozoic stromatolites: noncompetitive ecologic restriction by grazing and burrowing animals: *Science*, v. 169, p. 171-173.
- Gautier, D. L., and Claypool, G. E., 1984, Interpretation of methanic diagenesis in ancient sediments by analogy with processes in modern diagenetic environments, in McDonald, D. A., and Surdam, R. C., eds., *Clastic Diagenesis: Am. Assoc. Petroleum Geologists Mem.* 33., p. 111-123.
- Gebelin, C. D., 1969, Distribution, morphology and accretion rate of recent subtidal algal stromatolites: *Jour. Sed. Petrology*, v. 39, p. 6-69.
- Ghibaudo, G., 1980, Deep-sea fan deposits in the Alacigno Formation (middle-upper Oligocene) of the Gordana Valley, northern Appenines, Italy: *Jour. Sed. Petrology*, v. 50, p. 723-742.
- Gibbs, A. D., 1984, Structural evolution of extension basin margins: *Jour. Geol. Soc. London*, v. 141, p. 609-620.
- Ginsburg, R. N., 1971, Landward movement of carbonate mud: new model for regressive cycles in carbonates (abstr.): *Am. Assoc. Petroleum Geologists Bull.*, v. 55, p. 340.
- Ginsburg, R. N., ed., 1975, *Tidal deposits*: New York, Springer-Verlag, 428 p.

- Ginsburg, R. N., Rezak, R., and Wray, J. L., 1971, Geology of calcareous algae (Notes for a short course): Sedimenta I, Comparative Sedimentology Laboratory, University of Miami, 61 p.
- Gnoli, M., and Serpagli, E., 1980, The problematic microorganism *Nuia* in the Lower Ordovician of Precordilleran Argentina and its paleogeographic significance: Jour. Paleontology, v. 54, p. 1245-1251.
- Godfrey, S. C., 1982, Rock groups, structural slices and deformation in the Humber Arm Allochthon at Serpentine Lake, western Newfoundland [unpubl. M. Sc. thesis]: St. John's, Newfoundland, Memorial University of Newfoundland, 182 p.
- Goldring, R., 1962, The trace fossils of the Baggy Beds (Upper Devonian) of North Devon, England: Paläontol. Z., v. 36, p. 232-357.
- González-Bonorino, G., 1990, Early development and flysch sedimentation in Ordovician Taconic foreland basin, west-central Newfoundland: Can. Jour. Earth Sci., v. 27, p. 1247-1257.
- Gorsline, D. S., Kolpack, R. L., Karl, H. A., Drake, D. E., Fleischer, P., Thornton, S. E., Schwalbach, J. R., and Savrda, C. E., 1984, Studies of fine-grained sediment transport processes and products in the California Continental Borderland, in Stow, D. A. V., and Piper, D. J. W., eds., Fine-grained Sediments: Deep-water Processes and Facies: Geol. Soc. London Spec. Publ. 15, p. 395-416.
- Grasshoff, K., 1975, The hydrochemistry of landlocked basins and fiords, in Riley, J. P., and Skirrow, J., eds., Chemical Oceanography, v. 2, 2nd ed.: New York, Academic Press, p. 456-597.
- Grenier, R., 1990, The Appalachian fold and thrust belt, Northwestern Newfoundland [unpubl. M. Sc. thesis]: St. John's, Newfoundland, Memorial University of Newfoundland, 214 p.
- Grenier, R., and Cawcod, P. A., 1988, Variations in structural style along the Long Range Front, western Newfoundland, in Current Research, Part B. Geol. Surv. Canada Paper 88-1B, p. 127-133.
- Grotzinger, J. P., 1986, Cyclicity and paleoenvironmental dynamics, Rocknest platform, northwest Canada: Geol. Soc. Am. Bull., v. 97, p. 1208-1231.
- Grow, J. A., Mattick, R. E., and Schlee, J. S., 1979, Multichannel seismic depth sections and interval velocities over outer continental shelf and upper slope between Cape Hatteras and Cape Cod, in Watkins, J. S., Montadert, L., and Dickerson, R. W., eds., Geological and Geophysical Investigations of Continental Margins: Am. Assoc. Petroleum Geologists Mem. 29, p. 56-83.
- Guilbault, J.-P., Hubert, C., et Mamet, B., 1976, *Nuia* et *Halysis*, deux algues Ordoviciennes énigmatiques des Basses-Terres du Saint-Laurent: Naturaliste Can., v. 103, p. 119-132.
- Haaf, E. Ten., 1959, Graded beds of the northern Apennines [unpubl. Ph. D. dissert.]: University of Groningen, The Netherlands, 102 p.
- Hallam, A., 1986, Origin of minor limestone-shale cycles; climatically induced or diagenetic: Geology, v. 14, p. 609-612.

- Hamilton, W., 1979, Tectonics of the Indonesian region: U.S. Geol. Surv. Prof. Paper 1078, 345 p.
- Hampton, M. A., 1970, Subaqueous debris flow and generation of turbidity currents [unpubl. Ph. D. dissert.]: Stanford, CA, Stanford University, 180 p.
- Hampton, M. A., 1972, The role of subaqueous debris flow in generating turbidity currents: Jour. Sed. Petrology, v. 42, p. 775-793.
- Hampton, M. A., 1975, Competence of fine-grained debris flows: Jour. Sed. Petrology, v. 45, p. 834-844.
- Hampton, M. A., 1979, Buoyancy in debris flows: Jour. Sed. Petrology, v. 49, p. 753-758.
- Hanks, T. C., 1979, Deviatoric stresses and earthquake occurrences at the outer rise: Jour. Geophys. Res., v. 84, p. 2343-2347.
- Häntzschel, W., 1975, Trace fossils and problematica, 2nd ed., in Teichert, C., ed., Treatise on Invertebrate Paleontology, Part W, Supp. 1, Geol. Soc. Am. and Univ. Kansas, Lawrence, p. 1-269.
- Häntzschel, W., 1970, Star-like trace fossils, in Crimes, T. P., and Harper, J. C., eds., Trace Fossils: Liverpool, Seel House Press, p. 201-214.
- Hardie, L. A., 1987, Dolomitization: a critical review of some current views: Jour. Sed. Petrology, v. 57, p. 166-183.
- Hardie, L. A., Bosellini, A., and Goldhammer, R. K., 1986, Repeated subaerial exposure of subtidal carbonate platforms, Triassic, northern Italy: evidence for high frequency sea level oscillations on a 10⁴ year scale: Paleooceanography, v. 1, p. 447-457.
- Hardie, L. A., and Shinn, E. A., 1986, Carbonate depositional environments modern and ancient, Part 3: Tidal flats: Colorado School of Mines Quarterly, v. 81, p. 1-74.
- Harms, J. C., Southard, J., Spearing, D. R., and Walker, R. G., 1975, Depositional environments as interpreted from primary sedimentary structures and stratification sequences: SEPM Short Course Lecture Notes 2, 161 p.
- Harris, A. G., and Sweet, W. C., 1989, Mechanical and chemical techniques for separating microfossils from rock, sediment, and residue matrix, in Feldmann, R. M., Chapman, R. E., and Hannibal, J. T., eds., Paleotechniques: Paleon. Soc. Spec. Publ. 4, p. 70-86.
- Harwood, G. M., and Towerz, P. A., 1988, Seismic sedimentologic interpretation of a carbonate slope, north margin of the Little Bahama Bank, in Austin, J. A., Schlager, W., et al., eds., Proc., ODP, Sci. Results, v. 101, College Station, TX (Ocean Drilling Program), p. 263-277.
- Haworth, R. T., 1978, Interpretation of geophysical data in the northern Gulf of St. Lawrence and its relevance to lower Paleozoic geology: Geol. Soc. Am. Bull., v. 89, p. 1091-1110.
- Haworth, R. T., and Sanford, B. V., 1976, Paleozoic geology of north-east Gulf of St. Lawrence: Geol. Surv. Canada Paper 76-1A, p. 1-5.

- Hays, J. D., Imbrie, J., and Shackleton, N. J., 1976, Variations of the earth's orbit: pacemaker of the ice ages: *Science*, v. 194, p. 1121-1132.
- Heckel, P. H., 1977, Origin of phosphatic black shale facies in Pennsylvanian cyclothems of Mid-continent North America: *Am. Assoc. Petroleum Geologists Bull.*, v. 61, p. 1045-1068.
- Heezen, B. C., 1974, Atlantic type continental margins, *in* Burk, C. A., and Drake, C. L., eds., *The Geology of Continental Margins*: New York, Springer-Verlag, p. 13-24.
- Hein, F. J., 1982, Depositional mechanisms of deep-sea coarse clastic sediment, Cap Enrage Formation, Quebec: *Can. Jour. Earth Sci.*, v. 19, p. 267-288.
- Heinberg, C., and Birkeland, T., 1984, Trace-fossil assemblages and basin evolution of the Vardekloft Formation (Middle Jurassic, central east Greenland): *Jour. Paleontology*, v. 58, p. 362-397.
- Helwig, J., 1970, Slump folds and early structures: *Jour. Geol.*, v. 78, p. 172-187.
- Hendry, M. D., 1987, Tectonic and eustatic control on late Cenozoic sedimentation within an active plate boundary zone, west coast, Jamaica: *Geol. Soc. Am. Bull.*, v. 99, p. 718-728.
- Hesse, R., 1986, Early diagenetic pore water/sediment interaction: modern offshore basins: *Geoscience Canada* 13, p. 165-196.
- Hiscott, R. N., 1977, Sedimentology and regional implications of deep-water sandstones of the Tourelle Formation, Ordovician, Quebec [unpubl. Ph. D. dissert.]: Hamilton, Ontario, McMaster Univ., 542 p.
- Hiscott, R. N., 1978, Provenance of Ordovician deep-water sandstones, Tourelle Formation, Quebec, and implications for initiation of the Taconic Orogeny: *Can. Jour. Earth Sci.*, v. 15., p. 1579-1597.
- Hiscott, R. N., 1980, Depositional framework of sandy mid-fan complexes of Tourelle Formation, Ordovician, Quebec: *Am. Assoc. Petroleum Geologists Bull.*, v. 64, p. 1052-1077.
- Hiscott, R. N., 1984, Ophiolitic source rocks for Taconic-age flysch: trace element evidence: *Geol. Soc. Am. Bull.*, v. 95, p. 1261-1267.
- Hiscott, R. N., and James, N. P., 1985, Carbonate debris flows, Cow Head Group, Western Newfoundland: *Jour. Sed. Petrology*, v. 55, p. 735-745.
- Hiscott, R. N., and Middleton, G. V., 1979, Depositional mechanics of thick-bedded sandstones at the base of a submarine slope, Tourelle Formation (Lower Ordovician), Quebec, Canada, *in* Doyle, L. J., and Pilkey, O. H., eds., *Geology of Continental Slopes*: SEPM Spec. Publ. 27, p. 307-326.
- Hiscott, R. N., and Middleton, G. V., 1980, Fabric of coarse, deep-water sandstones, Tourelle Formation, Quebec, Canada: *Jour. Sed. Petrology*, v. 50, p. 703-722.
- Hiscott, R. N., and Pickering, K. T., 1984, Reflected turbidity currents on an Ordovician basin floor, Canadian Appalachians: *Nature*, v. 311, p. 143-145.

- Hoffman, P. F., 1987, Early Proterozoic foredeeps, foredeep magmatism, and Superior-type iron-formations of the Canadian Shield, *in* Kröner, A., ed., Proterozoic Lithospheric Evolution: Am. Geophys. Union, Geol. Soc. Am., Geodynamic Series, v. 17, p. 85-98.
- Hoffman, P. F., and Bowring, S. A., 1984, Short-lived 1.9 Ga continental margin and its destruction, Wopmay Orogen: *Geology*, v. 12, p. 68-72.
- Houseknecht, D. W., 1986, Evolution from passive margin to foreland basin: the Atoka Formation of the Arkoma Basin, central U.S.A., *in* Allen, P. A., and Homewood, P., eds., Foreland Basins: Internat. Assoc. Sediment. Spec. Publ. 8, p. 327-345.
- Howard, J. D., 1975, The sedimentological significance of trace fossils, *in* Frey, R. W., ed., The Study of Trace Fossils: New York, Springer-Verlag, p. 131-146.
- Howard, J. D., 1978, Sedimentology and trace fossils, *in* Basan, P. B., ed., Trace Fossil Concepts: SEPM Short Course No. 5, p. 11-42.
- Hurst, J. M., and Surlyk, F., 1983, Initiation, evolution, and destruction of an early Paleozoic carbonate shelf, eastern North Greenland: *Jour. Geol.*, v. 91, p. 671-691.
- Hurst, J. M., and Surlyk, F., 1984, Tectonic control of Silurian carbonate-shelf margin morphology and facies, North Greenland: *Am. Assoc. Petroleum Geologists Bull.*, v. 68, p. 1-17.
- Hutchinson, D. R., Grow, J. A., Klitgord, K. D., and Swift, B. A. 1983, Deep structure and evolution of the Carolina Trough, *in* Watkins, J. S., and Drake, C. L., eds., Studies in Continental Margin Geology: *Am. Assoc. Petroleum Geologists Mem.* 34, p. 129-153.
- Illing, L. V., Wells, A. J., and Taylor, J. C. M., 1965, Penecontemporary dolomite in the Persian Gulf, *in* Pray, L. C., and Murray, R. C., ed., Dolomitization and Limestone Diagenesis: SEPM Spec. Publ. 13, p. 89-111.
- Irwin, H., Curtis, C., and Coleman, M., 1977, Isotopic evidence for source of diagenetic carbonates formed during burial of organic-rich sediments: *Nature*, v. 269, p. 209-213.
- Jacka, A. D., 1974, Replacement of fossils by length-slow chalcedony and associated dolomitization: *Jour. Sed. Petrology*, v. 44, p. 421-427.
- Jacobi, R. D., 1981, Peripheral bulge - a causal mechanism for the Lower/Middle Ordovician unconformity along the western margin of the northern Appalachians: *Earth Planet. Sci. Let.*, v. 56, p. 245-251.
- Jacobson, R. S., Shor, G. G., Jr., Kieckhefer, R. M., and Purdy, G. M., 1978, Seismic refraction and reflection studies in the Timor-Aru Trough system and Australian continental shelf, *in* Watkins, J. S., Montadert, L., and Dickerson, P. W., eds., Geological and Geophysical Investigations of Continental Margins: *Am. Assoc. Petroleum Geologists Mem.* 29, p. 209-222.
- James, N. P., 1984, Shallowing-upward sequences in carbonates, *in* Walker, R. G., ed., Facies Models, 2nd ed.: Geoscience Canada Reprint Series 1, p. 213-228.

- James, N. P., Barnes, C. R., Stevens, R. K., and Knight, I., 1989, Evolution of a lower Paleozoic continental-margin carbonate platform, northern Canadian Appalachians, in Crevello, P. D., Wilson, J. L., Sarg, J. F., and Read, J. F., eds., Controls on Carbonate Platform and Basin Development: SEPM Spec. Publ. 44, p. 123-146.
- James, N. P., Botsford, J. W., and Williams, S. H., 1987, Allochthonous slope sequence at Lobster Cove Head: evidence of a complex Middle Ordovician platform margin in western Newfoundland: Can. Jour. Earth Sci., v. 24, p. 1199-1211.
- James, N. P., and Cuffey, R. J., 1989, Middle Ordovician coral reefs, western Newfoundland, in Geldsetzer, H. H. J., James, N. P., and Tebbutt, G. E., eds., Reefs, Canada and Adjacent Areas: Can. Soc. Petroleum Geol. Mem. 13, p. 192-195.
- James, N. P., Klappa, C. F., Opalinski, P. R., Skevington, D., and Stevens, R. K., 1979, Carbonate sedimentation during fragmentation of a lower Paleozoic continental margin: Table Head Formation (Middle Ordovician), western Newfoundland - A preliminary report (abstr.): Geol. Assoc. Canada Ann. Mtg., Quebec, Prgm. with Abstr., v. 4, p. 59.
- James, N. P., and Stevens, R. K., 1986, Stratigraphy and correlation of the Cambro-Ordovician Cow Head Group, western Newfoundland: Geol. Surv. Canada Bull., 366 p.
- Johnson, A. M., 1965, A model for debris flow (unpubl. Ph. D. dissert.): University Park, PA, Penn. State University, 305 p.
- Johnson, A. M., 1970, Physical processes in geology: San Francisco, Freeman, Cooper, 577 p.
- Johnson, D. I., 1986, Early Ordovician (Arenig) conodonts from St. Pauls Inlet and Martin Point, Cow Head Group, western Newfoundland [unpubl. M. Sc. thesis]: St. John's, Newfoundland, Memorial University of Newfoundland, 231 p.
- Johnson, S. Y., 1986, Water-escape structures in coarse-grained, volcanoclastic, fluvial deposits of the Ellensburg Formation, south-central Washington: Jour. Sed. Petrology, v. 56, p. 905-910.
- Jones, B., Oldershaw, A. E., and Narbonne, G. M., 1979, Nature and origin of rubbly limestone in the Upper Silurian Red Bay Formation of Arctic Canada: Sed. Geol., v. 24, p. 227-252.
- Jordan, T. E., 1981, Thrust loads and foreland basin evolution, Cretaceous, western United States: Am. Assoc. Petroleum Geologists Bull., v. 65, p. 2506-2520.
- Karig, D. E., 1970, Ridges and basins of the Kermadec Island arc system: Jour. Geophys. Res., v. 75, p. 239-254.
- Karig, D. E., Barber, A. J., Charlton, T. R., Klemperer, S., and Hussong, D. M., 1987, Nature and distribution of deformation across the Banda Arc - Australian collision zone at Timor: Geol. Soc. Am. Bull., v. 98, p. 18-32.
- Karig, D. E., and Sharman, G. F., 1975, Subduction and accretion in trenches: Geol. Soc. Am. Bull., v. 86, p. 377-389.

- Kauffman, E. G., 1982, Ecology and depositional environments of chalk-marl and limestone-shale rhythms in the Cretaceous of North America (abstr.), in Einsele, G., and Seilacher, A., eds., *Cyclic and Event Stratification*: New York, Springer-Verlag, p. 97.
- Kay, M., 1975, Campbellton sequence; manganiferous beds adjoining the Dunnage Mélange, northeastern Newfoundland: *Geo. Soc. Am. Bull.*, v. 86, p. 105-108.
- Kay, M., and Eldridge, N., 1968, Cambrian trilobites in central Newfoundland volcanic belt: *Geol. Mag.*, v. 105, p. 372-377.
- Keen, C. E., Keen, M. J., Nichols, B., Reid, I., Stockmal, G. S., Colman-Sadd, S. P., O'Brien, S. J., Miller, H., Quinlan, G., Williams, H., and Wright, J., 1986, Deep seismic reflection profile across the northern Appalachians: *Geology*, v. 14, p. 141-145.
- Keith, B. D., and Friedman, G. M., 1977, A slope-fan-basin-plain model, Taconic sequence, New York and Vermont: *Jour. Sed. Petrology*, v. 47, p. 1220-1241.
- Kendall, A. C., 1984, Evaporites, in Walker, R. G., ed., *Facies Models*, 2nd ed.: *Geoscience Canada Reprint Series 1*, p. 259-296.
- Kendall, C. St. G. C., and d'E. Skipwith, P. A., 1968, Recent algal mats of a Persian Gulf lagoon: *Jour. Sed. Petrology*, v. 38, p. 1040-1058.
- Kendall, C. St. G. C., and Warren, J., 1987, A review of the origin and setting of tepees and their associated fabrics: *Sedimentology*, v. 34, p. 1007-1028.
- Kennedy, W. J., and Garrison, R. E., 1975, Morphology and genesis of nodular chalks and hardgrounds in the Upper Cretaceous of southern England: *Sedimentology*, v. 22, p. 311-386.
- Kern, J. P., 1978, Trails from the Vienna Woods: paleoenvironments and trace fossils of Cretaceous to Eocene flysch, Vienna, Austria: *Palaeogeog., Palaeoclim., Palaeoecol.*, v. 23, p. 231-262.
- Kinsman, D. J. J., 1969, Modes of formation, sedimentary associations and diagnostic features of shallow-water and supratidal evaporites: *Am. Assoc. Petroleum Geologists Bull.*, v. 53, p. 830-840.
- Klappa, C. F., and James, N. P., 1980, Small lithistid sponge bioherms, early Middle Ordovician Table Head Group, western Newfoundland: *Bull. Can. Petrol. Geol.*, v. 28, p. 425-451.
- Klappa, C. F., and James, N. P., 1989, Lithistid sponge bioherms, early Middle Ordovician, western Newfoundland, in Geldsetzer, H. H. J., James, N. P., and Tebbutt, G. E., eds., *Reefs, Canada and Adjacent Areas*: *Can. Soc. Petroleum Geol. Mem.* 13, p. 196-200.
- Klappa, C. F., Opalinski, P. R., and James, N. P., 1980, Middle Ordovician Table Head Group of western Newfoundland: a revised stratigraphy: *Can. Jour. Earth Sci.*, v. 17, p. 1007-1019.
- Klein, G. de V., 1974, Estimating water depths from analysis of barrier-island and deltaic sedimentary sequences: *Geology*, v. 2, p. 409-412.
- Kluth, C. F., and Coney, P. J., 1981, Plate tectonics of the ancestral Rocky Mountains: *Geology*, v. 9, p. 10-15.

- Knauth, L. P., 1979, A model for the origin of chert in limestone: *Geology*, v. 7, p. 274-277.
- Knight, I., 1983, Geology of the Carboniferous Bay St. George Subbasin, western Newfoundland, *in* Gibbons, R. V., ed., Newfoundland Dept. Mines and Energy, Mineral. Dev. Div., Mem. 1, 358 p.
- Knight, I., 1986a, Geology map of the Raleigh map sheet (2M/9), Newfoundland: Newfoundland Dept. Mines Energy, Mineral Dev. Div., Map 86-26, scale 1:50000.
- Knight, I., 1986b, Geology map of the Roddickton map sheet (12I/16), Newfoundland: Newfoundland Dept. Mines Energy, Mineral Dev. Div., Map 86-64, scale 1:50000.
- Knight, I., 1986c, Ordovician sedimentary strata of the Pistolet Bay and Hare Bay area, Great Northern Peninsula, Newfoundland, *in* Blackwood, R. F., Walsh, D. G., and Gibbons, R. V., eds., Current Research: Newfoundland Dept. Mines Energy, Mineral Dev. Div. Rept. 86-1, p. 147-160.
- Knight, I., and James, N. P., 1987, Stratigraphy of the St. George Group, (Lower Ordovician) western Newfoundland; the interaction between eustasy and tectonics: *Can. Jour. Earth Sci.*, v. 24, p. 1927-1952.
- Knight, I., James, N. P., and Lane, T. E., (in press), The Ordovician St. George Unconformity, northern Appalachians: the effects of convergent lithospheric plate dynamics at the St. Lawrence Promontory on the Sauk-Tippecanoe sequence boundary: *Geol. Soc. Am. Bull.*
- Knight, I., and Saltman, P., 1980, Platformal rocks and geology of the Roddickton map area, Great Northern Peninsula, *in* O'Driscoll, C. F., and Gibbons, R. V., eds., Current Research, Newfoundland Dept. Mines Energy, Mineral Dev. Div. Rept. 80-1, p. 10-28.
- Kranck, K., 1975, Sediment deposition from flocculated suspensions: *Sedimentology*, v. 22, p. 111-123.
- Krause, F. F., and Oldershaw, A. E., 1979, Submarine carbonate breccias - a depositional model for two-layer, sediment gravity flows from the Sekwi Formation (Lower Cambrian), Mackenzie Mountains, Northwest Territories, Canada: *Can. Jour. Earth Sci.*, v. 16, p. 189-199.
- Kreisa, R. D., 1981, Storm-generated sedimentary structures in subtidal marine facies with examples from the Middle and Upper Ordovician of southwestern Virginia: *Jour. Sed. Petrology*, v. 51, p. 823-848.
- Kreisa, R. D., and Bambach, R. K., 1982, The role of storm processes in generating shell beds in Paleozoic shelf environments, *in* Einsele, G., and Seilacher, A., eds., Cyclic and Event Stratification: New York, Springer-Verlag, p. 200-207.
- Książkiewicz, M., 1970, Observations on the ichnofauna of the Polish Carpathians, *in* Crimes, T. P., and Harper, J. C., eds., Trace Fossils: Liverpool, Seel House Press, p. 283-322.
- Kuenen, Ph. H., 1957, Longitudinal filling of oblong sedimentary basins: *Verhandel. koninkl. Ned. Geol. mijnbouw. Genoot.*, Geol. Ser., v. 18, p. 189-195.

- Kulm, L. D., Resig, J. M., Thornburg, T. M., and Schrader, H.-J., 1982, Cenozoic structure, stratigraphy and tectonics of the central Peru forearc, in Leggett, J. K., ed., Trench-Forearc Geology: Sedimentation and Tectonics on Modern and Ancient Active Plate Margins: Geol. Soc. London Spec. Publ. 10, p. 151-170.
- LaJoie, J., 1972, Slump fold axis orientation: an indication of paleoslope: Jour. Sed. Petrology, v. 42, p. 486-488.
- Land, L. S., and Moore, C. H., 1980, Lithification, micritization and syndepositional diagenesis of biolithites on the Jamaican island slope: Jour. Sed. Petrology, v. 40, p. 357-371.
- Lane, T. E., 1990, Dolomitization, brecciation and zinc mineralization and their paragenetic relationships in the upper St. George Group (Ordovician) at Daniel's Harbour, western Newfoundland [unpubl. Ph. D. dissert.]: St. John's, Newfoundland, Memorial University of Newfoundland, 565 p.
- Lash, G. G., 1988, Sedimentology and evolution of the Martinsburg Formation (Upper Ordovician) fine-grained turbidite depositional system, central Appalachians: Sedimentology, v. 35, p. 429-448.
- Laporte, L. F., 1967, Carbonate deposition near mean sea level and resultant facies mosaic: Manlius Formation (Lower Devonian) of New York: Am. Assoc. Petroleum Geologists Bull., v. 51, p. 73-101.
- Leckie, D. A., and Walker, R. G., 1982, Storm- and tide-dominated shoreline in Cretaceous Moosebar-Lower Gates interval: outcrop equivalents of Deep Basin gas trap, western Canada: Am. Assoc. Petroleum Geologists Bull., v. 66, p. 138-157.
- Le Pichon, X., Huchon, P., Angelier, J., Lybérís, N., and others, 1982, Subduction in the Hellenic Trench: probable role of a thick evaporite layer based on Seabeam and submersible studies, in Leggett, J. K., ed., Trench-Forearc Geology: Sedimentation and Tectonics on Modern and Ancient Active Plate Margins: Geol. Soc. London Spec. Publ. 10, p. 319-334.
- Levesque, R. J., 1977, Stratigraphy and sedimentology of Middle Cambrian to Lower Ordovician shallow water carbonate rocks, western Newfoundland [unpubl. M. Sc. thesis]: St. John's, Newfoundland, Memorial University of Newfoundland, 276 p.
- Lewis, K. B., 1970, Slumping on a continental slope inclined at 1-4 degrees: Sedimentology, v. 16, p. 97-110.
- Li, Y. H., Takahashi, T., and Broecker, W. S., 1969, Degree of saturation of CaCO₃ in the oceans: Jour. Geophys. Res., v. 74, p. 5507-5525.
- Lilly, H. D., 1963, Geology of the Hughs Brook - Goose Arm area, western Newfoundland: St. John's, Newfoundland, Dept. Geol., Memorial University of Newfoundland, Rept. 2, 123 p.
- Lister, G. S., Ethridge, M. A., and Symonds, P. A., 1986, Detachment faulting and the evolution of passive continental margins: Geology, v. 14, p. 246-250.

- Lock, B. E., 1972, Lower Paleozoic history of a critical area; eastern margin of the St. Lawrence platform in White Bay, Newfoundland, Canada: XXIV Intern. Geol. Cong., Montreal, Canada, Section 6, p. 310-324.
- Logan, B. W., Rezak, R., and Ginsburg, R. N., 1964, Classification and environmental significance of algal stromatolites: Jour. Geol., v. 72, p. 68-83.
- Logan, W. E., 1863, Geology of Canada: Geol. Surv. Canada, Progress to 1863.
- Lowe, D. R., 1975, Regional controls on silica sedimentation in the Ouachita System: Geol. Soc. Am. Bull., v. 86, p. 1123-1127.
- Lowe, D. R., 1982, Sediment gravity flows: II. Depositional models with special reference to the deposits of high density turbidity currents: Jour. Sed. Petrology, v. 52, p. 279-297.
- Lucas, G., and Reche-Frollo, M., 1964, "Traces en rosette" du flysch éocène de Jaca (Aragon). Essai d'interprétation: Bull. Soc. Géol. France, Sér. 76, p. 163-170.
- MacDaniel, R. P., 1988, The geological evolution and hydrocarbon potential of the western Timor Sea region, in Petroleum in Australia: The First Century: Austr. Petrol. Explor. Assoc. Publ., p. 270-284.
- Malpas, J., and Stevens, R. K., 1977, The origin and emplacement of the ophiolite suite with examples from western Newfoundland: Geotectonics, v. 11, p. 453-466.
- Mamet, B., et Roux, A., 1982, Sur le mode de croissance de Nuia, algue Incertae sedis: Geobios, v. 15, p. 959-965.
- Mamet, B. L., Roux, A., et Shalaby, H., 1984, Role des Algues calcaires dans la sédimentation ordovicienne de la plate-forme du Saint-Laurent: Geobios, Mém. Spéc. 8, p. 261-269.
- Marillier, F., Keen, C. E., Stockmal, G. S., Quinlan, G., Williams, H., Colman-Sadd, S. P., and O'Brien, S. J., 1989, Crustal structure and surface zonation of the Canadian Appalachians: implications of deep seismic reflection data: Can. Jour. Earth Sci., v. 26, p. 305-321.
- Marlowe, J. I., 1971, Dolomite, phosphorite, and carbonate diagenesis on a Caribbean seamount: Jour. Sed. Petrology, v. 41, p. 809-827.
- Martison, N. W., McDonald, D. R., and Kaye, P., 1973, Exploration of continental shelf off northwest Australia: Am. Assoc. Petroleum Geologists Bull., v. 57, p. 972-989.
- McCann, T., and Pickerill, R. K., 1988, Flysch trace fossils from the Cretaceous Kodiak Formation of Alaska: Jour. Paleontology, v. 62, p. 330-348.
- McIlreath, I. A., and James, N. P., 1984, Carbonate slopes, in Walker, R. G., ed., Facies Models, 2nd ed.: Geoscience Canada Reprint Series 1, p. 245-257.

- McKenzie, J. A., Hsu, K. J., and Schneider, J. F., 1980, Movement of subsurface waters under the sabkha, Abu Dhabi, U. A. E., and its relation to evaporite dolomite genesis, *in* Zenger, D. H., Dunham, J. B., and Ethington, R. L., eds., *Concepts and Models of Dolomitization*: SEPM Spec. Publ. 28, p. 11-30.
- Middleton, G. V., and Hampton, M. A., 1976, Subaqueous sediment transport and deposition by sediment gravity flows, *in* Stanley, D. J., and Swift, D. J. P., eds., *Marine Sediment Transport and Environmental Management*: New York, John Wiley and Sons, p. 197-218.
- Mitchum, R. M., Jr., Vail, P. R., and Thompson, S., III, 1977, Seismic stratigraphy and global changes of sea level, part 2: the depositional sequence as a basic unit of stratigraphic analysis, *in* Payton, C. E., ed., *Seismic Stratigraphy - Applications to Hydrocarbon Exploration*: Am. Assoc. Petroleum Geologists Mem. 26, p. 53-62.
- Mollan, R. G., Craig, R. W., and Lofting, M. J. W., 1970, Geologic framework of continental shelf off northwest Australia: *Am. Assoc. Petroleum Geologists Bull.*, v. 54, p. 583-600.
- Möller, N. K., and Kvingan, K., 1988, The genesis of nodular limestones in the Ordovician and Silurian of the Oslo Region (Norway): *Sedimentology*, v. 35, p. 405-420.
- Monty, C. L. V., Bernet-Rollande, M. C., and Maurin, A. F., 1982, Re-interpretation of the Frasnian classical "reefs" of the southern Ardennes, Belgium: *Ann. Soc. Géol. Belg.*, v. 105, p. 339-341.
- Moore, D. G., 1961, Submarine slumps: *Jour. Sed. Petrology*, v. 31, p. 343-357.
- Moore, G. F., Curray, J. R., and Emmel, F. J., 1982a, Sedimentation in the Sunda Trench and forearc region, *in* Leggett, J. K., ed., *Trench-Forearc Geology: Sedimentation and Tectonics on Modern and Ancient Active Plate Margins*: Geol. Soc. London Spec. Publ. 10, p. 245-285.
- Moore, G. F., Watkins, J. S., McMillen, K. J., Bachman, S. B., and others, 1982b, Facies belts of the Middle America Trench and forearc region, southern Mexico: results from Leg 66 DSDP, *in* Leggett, J. K., ed., *Trench-Forearc Geology: Sedimentation and Tectonics on Modern and Ancient Active Plate Margins*: Geol. Soc. London Spec. Publ. 10, p. 77-94.
- Moore, G. F., and Karig, D. E., 1976, Development of sedimentary basins on the lower trench slope: *Geology*, v. 6, p. 693-697.
- Moore, N. K., 1977, Distribution of benthic algal flora in Middle Ordovician carbonate environmental units of the southern Appalachians, *in* Ruppel, S. C., and Walker, K. R., eds., *The Ecostratigraphy of the Middle Ordovician of the Southern Appalachians (Kentucky, Tennessee, and Virginia)*, U. S. A.: A Field Excursion: *Studies in Geology No. 77-1*, University of Tennessee, p. 18-29.
- Morris, R. C., 1974, Sedimentary and tectonic history of the Ouachita Mountains, *in* Dickinson, W. R., ed., *Tectonics and Sedimentation*: SEPM Spec. Publ. 22, p. 120-142.
- Morris, R. W., and Kay, M., 1966, Ordovician graptolites from the Middle Table Head Formation of Black Cove, near Port-au-Port, Newfoundland: *Jour. Paleontology*, v. 40, p. 1223-1229.

- Müller, J., and Fabricius, F., 1974, Magnesian-calcite nodules in the Ionian deep sea: an actualistic model for the formation of some nodular limestones, in Hsü, K. J., and Jenkyns, H. C., eds., *Pelagic Sediments on Land and Under the Sea: Internat. Assoc. Sediment. Spec. Publ. 1*, p. 235-248.
- Mullins, H. T., and Cook, H. E., 1986, Carbonate apron models: alternatives to the submarine fan model for paleoenvironmental analysis and hydrocarbon exploration: *Sed. Geol.*, v. 48, p. 37-79.
- Mullins, H. T., Gardulski, A. F., and Hine, A. C., 1986, Catastrophic collapse of the west Florida carbonate platform margin: *Geology*, v. 167-170.
- Mullins, H. T., Heath, K. C., Van Buren, H. M., and Newton, C. R., 1984, Anatomy of a modern open-ocean carbonate slope: northern Little Bahama Bank: *Sedimentology*, v. 31, p. 141-168.
- Mullins, H. T., and Neumann, A. C., 1979, Deep-carbonate bank margin structure and sedimentation in the northern Bahamas in Doyle, L. J., and Pilkey, O. H., eds., *Geology of continental slopes: SEPM Spec. Publ. 27*, p. 165-192.
- Mullins, H. T., Neumann, A. C., Wilbur, R. J., and Boardman, M. R., 1980, Nodular carbonate sediment on Bahamian slopes: possible precursors to nodular limestones: *Jour. Sed. Petrology*, v. 50, p. 117-131.
- Musman, W. J., and Read, J. F., 1986, Sedimentology and development of a passive- to convergent-margin unconformity: Middle Ordovician Knox Unconformity, Virginia Appalachians: *Geol. Soc. Am. Bull.*, v. 97, p. 282-295.
- Mutti, E., and Ghuibauda, G., 1972, Un esempio di torbiditi di conoide sottomarina esterna: le Arenarie di San Salvatore (Formazione di Bobbio, Miocene) nell'Appennino de Piacenza: *Memorie dell'Accademia delle Scienze Fisiche, Matematiche e Naturali, Series 4(16)*, 40 p.
- Narbonne, G., 1984, Trace fossils in Upper Silurian tidal flat to basin slope carbonates of Arctic Canada: *Jour. Paleontology*, v. 58, p. 398-415.
- Naylor, M. A., 1980, The origin of inverse grading in muddy debris flow deposits - a review: *Jour. Sed. Petrology*, v. 50, p. 1111-1116.
- Neumann, A. C., and Land, L. S., 1975, Lime mud deposition and calcareous algae in the Bight of Abaco, Bahamas: a budget: *Jour. Sed. Petrology*, v. 45, p. 763-786.
- Nilsen, T. H., 1985, Chugach turbidite system, Alaska, in Bouma, A. H., Normark, W. R., and Barnes, N. E., eds., *Submarine Fans and Related Turbidite Systems: New York, Springer-Verlag*, p. 185-192.
- Normark, W. R., 1970, Growth patterns of deep sea fans: *Am. Assoc. Petroleum Geologists Bull.*, v. 54, p. 2170-2195.
- Normark, W. R., 1978, Fan-valleys, channels and depositional lobes on modern submarine fans: characters for the recognition of sandy turbidite environments: *Am. Assoc. Petroleum Geologists Bull.*, v. 61, p. 912-931.

- Nowlan, G. S., 1981, Stratigraphy and conodont faunas of the Lower and Middle Ordovician Romaine and Mingan Formations, Mingan Islands, Québec (abstr.): *Mar. Sed. and Atlan. Geol.*, v. 17, p. 67.
- O'Brien, N. R., 1970, The fabric of shale - an electron microscope study: *Sedimentology*, v. 15, p. 229-246.
- O'Brien, N. R., Nakazawa, K., and Tokuhashi, S., 1980, Use of clay fabric to distinguish turbiditic and hemipelagic siltstones and silts: *Sedimentology*, v. 27, p. 47-61.
- Paquette, J., Stearn, C. W., and Klappa, C. F., 1983, An enigmatic fossil of sponge affinities from Middle Ordovician rocks of western Newfoundland: *Can. Jour. Earth Sci.*, v. 20, p. 1501-1512.
- Pedley, H. M., and Bennett, S. M., 1985, Phosphorites, hardgrounds and syndepositional solution subsidence: a paleoenvironmental model from the Miocene of the Maltese Islands: *Sed. Geol.*, v. 45, p. 1-34.
- Pemberton, S. G., and Frey, R. W., 1982, Trace fossil nomenclature and the Planolites-Palaeophycus dilemma: *Jour. Paleontology*, v. 56, p. 843-881.
- Pemberton, S. G., and Frey, R. W., 1984, Ichnology of storm-influenced shallow marine sequence: Cardium Formation (Upper Cretaceous) at Seebe, Alberta: *Can. Soc. Petroleum Geol. Mem.* 9, p. 281-304.
- Perkins, R. D., and Enos, P., 1968, Hurricane Betsy in the Florida - Bahamas - geologic effects and comparison with Hurricane Donna: *Jour. Geol.*, v. 76, p. 710-717.
- Pickerill, R. K., 1980, Phanerozoic flysch trace fossil diversity - observations based on an Ordovician flysch ichnofauna from the Arcostook-Matapedia Carbonate Belt of northern New Brunswick: *Can. Jour. Earth Sci.*, v. 17, p. 1259-1270.
- Pickerill, R. K., 1981, Trace fossils in a Lower Paleozoic submarine canyon sequence - the Siegas Formation of northwestern New Brunswick, Canada: *Mar. Sed. and Atl. Geol.*, v. 17, p. 36-58.
- Pickerill, R. K., 1989, Compaginaticnus: a new ichnogenus from Ordovician flysch of eastern Canada: *Jour. Paleontology*, v. 63, p. 913-919.
- Pickerill, R. K., Fillion, D., and Harland, T. L., 1984a, Middle Ordovician trace fossils in carbonates of the Trenton Group between Montreal and Quebec City, St. Lawrence Lowland, Eastern Canada: *Jour. Paleontology*, v. 58, p. 416-439.
- Pickerill, R. K., Harland, T. L., and Fillion, D., 1984b, In situ lingulids from deep-water carbonates of the Middle Ordovician Table Head Group of Newfoundland and the Trenton Group of Quebec: *Can. Jour. Earth Sci.*, v. 21, p. 194-199.
- Pickerill, R. K., Fyffe, L. R., and Forbes, W. H., 1987, Late Ordovician - Early Silurian trace fossils from the Metapedia Group, Tobique River, western New Brunswick, Canada: *Mar. Sed. and Atl. Geol.*, v. 23, p. 77-88.

- Pickering, K. T., Stow, D. A. V., Watson, M. P., and Hiscott, R. N., 1986, Deep-water facies, processes and models: a review and classification scheme for modern and ancient sediments: *Earth Sci. Rev.*, v. 23, p. 75-114.
- Pierce, J. W., 1976, Suspended sediment transport at the shelf break and over the outer margin, in Stanley, D. J., and Swift, D. J. P., eds., *Marine Sediment Transport and Environmental Management*: Toronto, John Wiley, p. 437-460.
- Pierson, T. C., 1981, Dominant particle support mechanisms in debris flows at Mt. Thomas, New Zealand, and implications for flow mobility: *Sedimentology*, v. 28, p. 49-60.
- Pigram, C. J., Davies, P. J., Feary, D. A., and Symonds, P. A., 1989, Tectonic controls on carbonate platform evolution in southern Papua New Guinea: passive margin to foreland basin: *Geology*, v. 17, p. 199-202.
- Piper, D. J. W., 1978, Turbidite muds and silts on deep sea fans and abyssal plains, in Stanley, D. J., and Kelling, G., eds., *Submarine Canyon and Fan Sedimentation*: Strousburg, PA, Dowden Hutchinson and Ross, p. 163-176.
- Pitcher, M., 1964, Evolution of Chazyan (Ordovician) reefs of eastern United States and Canada: *Bull. Can. Petrol. Geol.*, v. 12, p. 632-691.
- Poole, F. G., 1974, Flysch deposits of Antler foreland basin, western United States, in Dickinson, W. R., ed., *Tectonics and Sedimentation*: SEPM Spec. Publ. 22, p. 58-82.
- Postma, G., 1983, Water-escape structures in the context of a depositional model of a mass flow dominated fan delta (Alrioja Formation, Pliocene, Almeria Basin, SE Spain): *Sedimentology*, v. 30, p. 91-103.
- Potter, P. E., Maynard, J. B., and Pryor, W. A., 1980, *Sedimentology of shale*: New York, Springer-Verlag, 306 p.
- Potter, P. E., Maynard, J. B., and Pryor, W. A., 1982, Appalachian gas bearing Devonian shales: statements and discussions: *Oil and Gas Journal*, v. 80, p. 290-318.
- Pratt, B. R., 1979, The St. George Group (Lower Ordovician), western Newfoundland: sedimentology, diagenesis and cryptalgal structure [unpubl. M. Sc. thesis]: St. John's, Newfoundland, Memorial University of Newfoundland, 254 p.
- Pratt, B. R., 1982, Stromatolitic framework of carbonate mud-mounds: *Jour. Sed. Petrology*, v. 52, p. 1203-1227.
- Pratt, B. R., and James, N. P., 1986, The St. George Group (Lower Ordovician) of western Newfoundland: a tidal flat island model for carbonate sedimentation in shallow epeiric seas: *Sedimentology*, v. 33, p. 313-343.
- Press, F., and Siever, R., 1982, *Earth*, 3rd ed.: San Francisco, CA, Freeman, 613 p.
- Prince, R. A., and Kulm, L. D., 1975, Crustal rupture and the initiation of imbricate thrusting in the Peru - Chile Trench: *Geol. Soc. Am. Bull.*, v. 88, p. 1639-1653.

- Pryor, W. A., and Van Wie, W. A., 1971, The "sawdust sand" - an Eocene sediment of floccule origin: *Jour. Sed. Petrology*, v. 411, p. 763-769.
- Purser, B. H., 1969, Synsedimentary marine lithification of Middle Jurassic limestones in the Paris Basin: *Sedimentology*, v. 12, p. 205-230.
- Quinlan, G. M., and Beaumont, C., 1984, Appalachian thrusting, lithospheric flexure, and the Paleozoic stratigraphy of the Eastern Interior of North America: *Can. Jour. Earth Sci.*, v. 21, p. 973-996.
- Quinn, L. A., 1988a, Distribution and significance of Ordovician flysch units in western Newfoundland, *in* Current Research, Part B. Geol. Surv. Canada Paper 88-1B, p. 119-126.
- Quinn, L. A., 1988b, Easterly derivation of Ordovician flysch in western Newfoundland (abstr.): *Geol. Assoc. Canada, Mineral. Assoc. Canada, Can. Soc. Petroleum Geol., Joint Ann. Mtg., Prog. with Abstr.*, 23-25 May 1988, St. John's, Newfoundland, v. 13, p. A101.
- Quinn, L. A., 1991, Foredeep sandstones of the Goose Tickle Group, western Newfoundland (abstr.): *Geol. Assoc. Canada, Miner. Assoc. Canada, Soc. Econ. Geol. Joint Ann. Mtg., Prog. with Abstr.*, 27-29 May, Toronto, Ontario, v. 16, p. A103.
- Quinn, L. A. and Williams, H., 1983, Humber Arm Allochthon at South Arm, Bonne Bay, western Newfoundland, *in* Current Research, Part A: Geol. Surv. Canada Paper 83-1A, p. 179-182.
- Rabinowitz, P. D., 1974, The boundary between oceanic and continental crust in the western North Atlantic, *in* Burk, C. A., and Drake, C. L., eds., *The Geology of Continental Margins*: New York, Springer-Verlag, p. 67-84.
- Rankin, D. W., 1976, Appalachian salients and recesses: Late Precambrian continental breakup and the opening of the Iapetus Ocean: *Jour. Geophys. Res.*, v. 81, p. 5605-5619.
- Raymond, P. E., 1925, Some trilobites of the Lower Middle Ordovician of eastern North America: *Mus. Compar. Zool. Bull.*, v. 67, p. 180.
- Read, J. F., 1980, Carbonate ramp to basin transitions and foreland basin evolution, Middle Ordovician, Virginia: *Am. Assoc. Petroleum Geologists Bull.*, v. 64, p. 1575-1612.
- Read, J. F., 1982, Geometry, facies, and development of Middle Ordovician carbonate buildups, Virginia Appalachians: *Am. Assoc. Petroleum Geologists Bull.*, v. 66, p. 189-209.
- Read, J. F., and Grover, G. A., 1977, Scalloped and planar erosion surfaces Middle Ordovician limestone, Virginia: analogues of Holocene exposed karst or tidal rock platform: *Jour. Sed. Petrology*, v. 47, p. 956-972.
- Reading, H. G., 1978, *Sedimentary environments and facies*: New York, Elsevier, 557 p.
- Reineck, H.-E., and Singh, I. B., 1980, *Depositional Sedimentary Environments*, 2nd ed.: New York, Springer-Verlag, 549 p.

- Reinhardt, J., 1977, Cambrian off-shelf sedimentation, central Appalachians, in Cook, H. E., and Enos, P., eds., Deep-water Carbonate Environments: SEPM Spec. Publ. 25, p. 83-112.
- Research on Cretaceous Cycles Group, 1986, Rhythmic bedding in Upper Cretaceous pelagic carbonate sequences: varying sedimentary response to climate forcing: *Geology*, v. 14, p. 153-156.
- Reudemann, R., 1934, Paleozoic plankton of North America: *Geol. Soc. Am. Mem.* 2, p. 1-144.
- Reudemann, R., 1947, Graptolites of North America: *Geol. Soc. Am. Mem.* 19, 625 p.
- Rhoads, D. C., and Morse, J. W., 1971, Evolutionary and ecologic significance of oxygen-deficient marine basins: *Lethaia*, v. 4, p. 413-428.
- Ricci Lucchi, F., 1985, Marnoso-Arenacea turbidite system, Italy, in Bouma, A. H., Normark, W. R., and Barnes, N. E., eds., *Submarine Fans and Related Turbidite Systems*: New York, Springer-Verlag, p. 207-216.
- Ricci Lucchi, F., and Valmori, E., 1980, Basin-wide turbidites in a Miocene, oversupplied deep-sea plain: a geometrical analysis: *Sedimentology*, v. 27, p. 241-270.
- Richards, F. A., 1957, Oxygen in the oceans, in Hedgepleth, J. W., ed., *Treatise on Marine Ecology and Paleoecology*: *Geol. Soc. Am. Mem.* 67, v. 1, p. 185-228.
- Richards, F. A., and Vaccaro, R. F., 1956, The Cariaco Trench, an anaerobic basin in the Caribbean Sea: *Deep-Sea Research*, v. 7, p. 163-172.
- Rickard, L. V., and Fisher, D. W., 1973, Middle Ordovician Normanskill Formation, eastern New York, age stratigraphic, and structural position: *Am. Jour. Sci.*, v. 273, p. 580-590.
- Ricken, W., 1985, Epicontinental marl-limestone alternation: event deposition and diagenetic bedding (Upper Jurassic, southwest Germany), in Bayer, U., and Seilacher, A., eds., *Sedimentary and Evolutionary Cycles*: Berlin, Springer-Verlag, p. 127-162.
- Riding, R., 1974, *Girvanella* and other algae as depth indicators: *Lethaia*, v. 8, p. 173-179.
- Robertson, A. H. F., 1987a, The transition from a passive margin to an Upper Cretaceous foreland basin related to ophiolite emplacement in the Oman Mountains: *Geo. Soc. Am. Bull.*, v. 633-653.
- Robertson, A. H. F., 1987b, Upper Cretaceous Muti Formation: transition of a Mesozoic carbonate platform to a foreland basin in the Oman Mountains: *Sedimentology*, v. 34, p. 1123-1142.
- Rodgers, J., 1965, Long Point and Clam Bank Formations, western Newfoundland: *Geol. Assoc. Canada, Proc.*, v. 16, p. 83-94.
- Rodgers, J., and Neale, E. R. W., 1963, Possible Taconic klippen in western Newfoundland: *Am. Jour. Sci.*, v. 261, p. 713-730.

- Roliff, W. A., 1968, Oil and gas exploration - Articositi Island, Québec: Geol. Ass. Canada, Proc., v. 19, p. 31-37.
- Ross, J. P., 1970, Distribution, paleoecology and correlation of Champlainian Ectoprocta (Bryozoa), New York state, part III: Jour. Paleontology, v. 44, p. 346-382.
- Ross, R. J., Jr., Adler, F. J., Amsden, T. W., *et al.*, 1982, The Ordovician system in the United States: Internat. Union Geol. Sci. Publ. 12, 73 p.
- Ross, R. J., Jr., and James, N. P., 1987, Brachiopod biostratigraphy of the Middle Ordovician Cow Head and Table Head Groups, western Newfoundland: Can. Jour. Earth Sci., v. 24, p. 70-95.
- Ross, R. J., James, N. P., Hintze, L. F., and Poole, F. G., 1989, Architecture and evolution of a Whiterockian (early Middle Ordovician) carbonate platform, Basin Ranges of western U. S. A., in Crevello, P. D., Wilson, J. L., Sarg, J. F., and Read, J. F., eds., Controls on Carbonate Platform and Basin Development: SEPM Spec. Publ. 44, p. 167-185.
- Ross, R. J., Valusek, J. E., and James, N. P., 1988, Nuia and its environmental significance: New Mex. Bur. Min. Res. Mem., v. 44, p. 115-121.
- Rowley, D. B., and Kidd, W. S. F., 1981, Stratigraphic relationships and detrital composition of medial Ordovician flysch of western New England; implications for the tectonic evolution of the Taconic Orogeny: Jour. Geol., v. 89, p. 199-218.
- Rubin, D. M., and Friedman, G. M., 1977, Intermittently emergent shelf carbonates: an example from the Cambro-Ordovician of eastern New York state: Sed. Geol., v. 19, p. 81-106.
- Rupke, N. A., 1975, Deposition of fine-grained sediments in the abyssal environment of the Alegro-Balaeric Basin, western Mediterranean Sea: Sedimentology, v. 22, p. 96-109.
- Ruppel, S. C., and Walker, K. R., eds., 1977, The ecostratigraphy of the Middle Ordovician of the southern Appalachians (Kentucky, Tennessee, and Virginia), U. S. A.: A field excursion: Studies in Geology No. 77-1, University of Tennessee, 171 p.
- Ruppel, S. C., and Walker, K. R., 1982, Sedimentology and distribution of carbonate buildups: Middle Ordovician, east Tennessee: Jour. Sed. Petrology, v. 52, p. 1055-1071.
- Savdra, C. E., Bottjer, D. J., and Gorsline, D. S., 1984, Development of a comprehensive oxygen-deficient marine biofacies model: evidence from Santa Monica, San Pedro, and Santa Barbara Basins, California continental borderland: Am. Assoc. Petroleum Geologists Bull., v. 68, p. 1179-1192.
- Schedl, A., and Wiltschko, D. V., 1984, Sedimentologic effects of a moving terrain: Jour. Geol., v. 92, p. 273-287.
- Schillereff, S., 1980, Relationships among rock groups within and beneath the Humber Arm Allochthon at Fox Island River, western Newfoundland [unpubl. M. Sc. thesis]: St. John's, Newfoundland, Memorial University of Newfoundland, 166 p.

- Schillereff, S., and Williams, H., 1979, Geology of the Stephenville map area, Newfoundland, *in* Current Research, Part A. Geol. Surv. Canada Paper 79-1A, p. 327-332.
- Schlager, W., 1981, The paradox of drowned reefs and carbonate platforms: Geol. Soc. Am. Bull., v. 92, p. 197-211.
- Schlager, W., 1989, Drowning unconformities on carbonate platforms, *in* Crevello, P. D., Wilson, J. L., Sarg, J. F., and Read, J. F., eds., Controls on Carbonate Platform and Basin Development: SEPM Spec. Publ. 44, p. 15-26.
- Schlager, W., and Camber, O., 1986, Submarine slope angles, drowning unconformities, and self-erosion of limestone escarpments: Geology, v. 14, p. 726-765.
- Schlanger, S. O., 1964, Petrology of the limestones of Guam: U. S. Geol. Surv. Prof. Pap. 403-D, 52 p.
- Scholl, D. W., Vallier, T. L., and Stevenson, A. J., 1983, Arc, forearc and trench sedimentation and tectonics: Amlia Corridor of the Aleutian Ridge, *in* Watkins, J. S., and Drake, C. L., eds., Studies in Continental Margin Geology: Am. Assoc. Petroleum Geologists Mem. 34, p. 413-439.
- Scholle, P. A., Arthur, M. A., and Eckdale, A. A., 1983, Pelagic environment, *in* Scholle, P. A., Bebout, D. G., Moore, C. H., eds., Carbonate Depositional Environments: Am. Assoc. Petroleum Geologists Mem. 33, p. 619-691.
- Schopf, T. J. M., 1980, Paleooceanography: Cambridge, MA, Harvard University Press, 341 p.
- Schuchert, C., and Dunbar, C. O., 1934, Stratigraphy of western Newfoundland: Geol. Soc. Am. Mem. 1, 123 p.
- Schwarzacher, W., and Fischer, A. G., 1982, Limestone-shale bedding and perturbations of the earth's orbit, *in* Einsele, G., and Seilacher, A., eds., Cyclic and Event stratification: New York, Springer-Verlag, p. 72-95.
- Scotese, C. R., Bambach, R. K., Barton, C., Van der Voo, R., and Ziegler, A. M., 1979, Paleozoic base maps: Jour. Geol., v. 87, p. 217-277.
- Searle, M. P., 1985, Sequence of thrusting and origin of culminations in the northern and central Oman Mountains: Jour. Struct. Geol., v. 7, p. 129-143.
- Searle, M. P., and Stevens, R. K., 1984, Obduction processes in ancient, modern and future ophiolites, *in* Gass, I. G., Lippard, S. J., and Shelton, A. W., eds., Ophiolites and Oceanic Lithosphere: Oxford, England, Alden Press, p. 303-320.
- Seely, D. R., Vail, P. R., and Walton, G. G., 1974, Trench slope model, *in* Burk, C. A., and Drake, C. L., eds., The Geology of Continental Margins: New York, Springer-Verlag, p. 249-260.
- Seilacher, A., 1962, Paleontological studies on turbidite sedimentation and erosion: Jour. Geol., v. 70, p. 227-234.

- Seilacher, A., 1967, Bathymetry of trace fossils: *Mar. Geol.*, v. 5, p. 413-428.
- Shanmugan, G., 1980, Rhythms in deep sea, fine-grained turbidite and debris flow sequences, Middle Ordovician, eastern Tennessee: *Sedimentology*, v. 27, p. 419-432.
- Shanmugan, G., and Lash, G. G., 1982, Analogous tectonics and evolution of the Ordovician foredeeps, southern and central Appalachians: *Geology*, v. 10, p. 522-566.
- Shanmugan, G., and Walker, K. R., 1983, Anatomy of the Middle Ordovician Sevier Shale Basin, eastern Tennessee: *Sed. Geol.*, v. 34, p. 315-337.
- Shearer, J. M., 1973, Bedrock and surficial geology of the northern Gulf of St. Lawrence as interpreted from continuous seismic reflection profiles: *Geol. Surv. Canada Paper 71-23*, p. 285-303.
- Sheehan, P. M., 1977, Ordovician and Silurian brachiopods from Ordovician shales and related deep water argillaceous rocks: *Lethaia*, v. 10, p. 267-286.
- Shiki, T., and Misawa, Y., 1982, Forearc geological structure of the Japanese Islands, in Leggett, J. K., ed., *Trench-Forearc Geology: Sedimentation and Tectonics on Modern and Ancient Active Plate Margins*: *Geol. Soc. London Spec. Publ. 10*, p. 5-26.
- Shinn, E. A., 1968, Burrows in Recent lime sediments of Florida and the Bahamas: *Jour. Paleontology*, v. 42, p. 879-894.
- Shinn, E. A., 1969, Submarine lithification of Holocene carbonate sediments in the Persian Gulf: *Sedimentology*, v. 12, p. 109-144.
- Shinn, E. A., 1983, Tidal flat, in Scholle, P. A., Bebout, D. G., and Moore, C. H., eds., *Carbonate Depositional Environments*: *Am. Assoc. Petroleum Geologists Mem. 33*, p. 171-210.
- Shinn, E. A., Ginsburg, R. N., and Lloyd, R. M., 1965, Recent supratidal dolomite from Andros Island, Bahamas, in Pray, L. C., and Murray, R. C., eds., *Dolomitization and Limestone Diagenesis*: *SEPM Spec. Publ. 13*, p. 112-123.
- Shinn, E. A., Lloyd, R. M., and Ginsburg, R. N., 1969, Anatomy of a modern carbonate tidal flat, Andros Island, Bahamas: *Jour. Sed. Petrology*, v. 39, p. 1202-1228.
- Shinn, E. A., and Robbin, D. M., 1983, Mechanical and chemical compaction in fine-grained shallow water limestones: *Jour. Sed. Petrology*, v. 53, p. 595-618.
- Shipley, T. H., Ladd, J. W., Buffler, R. T., and Watkins, J. S., 1982, Tectonic processes along the Middle America Trench inner slope, in Leggett, J. K., ed., *Trench-Forearc Geology: Sedimentation and Tectonics on Modern and Ancient Active Plate Margins*: *Geol. Soc. London Spec. Publ. 10*, p. 95-106.
- Sholkovitz, E., and Souter, A., 1985, Changes in the composition of the bottom water of the Santa Barbara Basin: effect of turbidity currents: *Deep-sea Research*, v. 22, p. 13-22.

- Soudry, D., and Lewy, Z., 1988, Microbially influenced formation of phosphate nodules and megafossil moulds (Negev, southern Israel): *Palaeogeog., Palaeoclim., Palaeoecol.*, v. 64, p. 15-34.
- Southgate, P. N., 1986, Depositional environment and mechanism of preservation of microfossils, upper Proterozoic Bitter Springs Formation, Australia: *Geology*, v. 14, p. 683-686.
- Srivastava, P., Stearn, C. W., and Mountjoy, E. W., 1972, A Devonian megabreccia at the margin of the Ancient Wall carbonate complex, Alberta: *Bull. Can. Petrol. Geol.*, v. 20, p. 412-438.
- Stait, K., 1988, Upper Canadian to Whiterockian (Ordovician) conodont biostratigraphy of the upper St. George Group, western Newfoundland [unpub. M. Sc. thesis]: St. John's, Newfoundland, Memorial University of Newfoundland, 494 p.
- Stait, K., and Barnes, C. R., 1988, Conodont biostratigraphy of the upper St. George Group (Canadian - Whiterock), western Newfoundland (abstr.): 5th Internat. Ordovician Symp., Memorial University of Newfoundland, St. John's, Newfoundland, Canada, p. 98.
- Stenzel, S. R., and James, N. P., in press, Shallow water *Stromatolites* mud mounds on a Middle Ordovician foreland basin platform, western Newfoundland, in Monty, C., Bridges, P., Boscence, P., and Pratt, B. R., eds., *Mud Mounds: Internat. Assoc. Sed. Spec. Publ.*
- Stenzel, S. R., Knight, I., and James, N., 1990, Carbonate platform to foreland basin: revised stratigraphy of the Table Head Group (Middle Ordovician), western Newfoundland: *Can. Jour. Earth Sci.*, v. 27, p. 14-26.
- Stevens, R. K., 1965, Geology of the Humber Arm, west Newfoundland [unpubl. M. Sc. thesis]: St. John's, Newfoundland, Memorial University of Newfoundland, 121 p.
- Stevens, R. K., 1970, Cambro-Ordovician flysch sedimentation and tectonics in west Newfoundland and their possible bearing on a proto-Atlantic Ocean: *Geol. Assoc. Canada Spec. Paper 7*, p. 165-177.
- Stockmal, G. S., Beaumont, C., and Boutilier, R., 1986, Geodynamic models of convergent model tectonics: transition from rifted margin to overthrust belt and consequences for foreland-basin development: *Am. Assoc. Petroleum Geologists Bull.*, v. 70, p. 181-190.
- Stockmal, G. S., and Waldron, J. W. F., 1990, Structure of the Appalachian deformation front, western Newfoundland: implications from multichannel seismic reflection data: *Geology*, v. 18, p. 765-768.
- Stouge, S., 1981, Conodonts of the Table Head Formation (Middle Ordovician), western Newfoundland [unpubl. Ph. D. dissert.]: St. John's, Newfoundland, Memorial University of Newfoundland, 413 p.
- Stouge, S., 1982, Preliminary conodont biostratigraphy of Lower to Middle Ordovician carbonates of the St. George Group, Great Northern Peninsula, Newfoundland: Newfoundland Dept. Mines Energy Rept. 82-3, 59 p.
- Stouge, S., 1984, Conodonts of the Middle Ordovician Table Head Formation, western Newfoundland: *Fossils and Strata*, v. 16, 145 p.

- Stouge, S., 1986, Conodont color variation in the Lower/Middle Ordovician strata of western Newfoundland, in Blackwood, R. F., Walsh, D. G., and Gibbons, R. V., eds., Current Research: Newfoundland Dept. Mines Energy, Mineral Dev. Div. Rept. 86-1, p. 177-178.
- Stouge, S., and Bagnoli, G., 1988, Early Ordovician conodonts from Cow Head Peninsula, western Newfoundland: *Palaeontographia Italica*, v. 75, p. 89-179.
- Stouge, S., and Boyce, W. D., 1983, Fossils of northwestern Newfoundland and southeastern Labrador: conodonts and trilobites: Newfoundland Dept. Mines Energy Rept. 83-3, 55 p.
- Stow, D. A. V., 1979, Distinguishing between fine-grained turbidites and contourites on the Nova Scotian deep water margin: *Sedimentology*, v. 26, p. 371-387.
- Stow, D. A. V., and Piper, D. J. W., eds., 1984, Fine-grained sediments: deep-water processes and facies: *Geol. Soc. London Spec. Publ.* 15, 659 p.
- Stow, D. A. V., and Shanmugam, G., 1980, Sequence of structures in fine-grained turbidites: comparison of Recent deep-sea and ancient flysch: *Sed. Geol.*, v. 25, p. 23-42.
- Stricker, G. D., and Carozzi, A. V., 1973, Carbonate microfacies of the Pogonip Group (Lower Ordovician) Arrow Canyon range, Clark County, Nevada, U. S. A.: *Soc. Nat. Petroles d'Aquitaine Centre Recherches Bull.*, v. 7, p. 499-541.
- Stukas, V., and Reynolds, D. H., 1974, $^{40}\text{Ar}/^{39}\text{Ar}$ dating of the Long Range dikes, Newfoundland: *Earth Planet. Sci. Let.*, v. 22, p. 256-266.
- Sverdrup, H. U., Johnson, M. W., and Flemming, R. H., 1942, The oceans, their physics, chemistry and general biology: New York, Prentice-Hall, 1087 p.
- Taylor, J. M. C., and Illing, L. V., 1969, Holocene intertidal calcium carbonate cementation, Qatar, Persian Gulf: *Sedimentology*, v. 12, p. 69-107.
- Thiede, J., and Van Andel, T. H., 1977, The paleoenvironment of anaerobic sediments in the Late Mesozoic South Atlantic Ocean: *Earth Planet. Sci. Let.*, v. 33, p. 301-309.
- Thomas, W. A., 1977, Evolution of Appalachian-Ouachita salients and recesses from reentrants and promontories in the continental margin: *Am. Jour. Sci.*, v. 277, p. 1233-1278.
- Thornton, S. E., 1984, Basin model for hemipelagic sedimentation in a tectonically active continental margin: Santa Barbara Basin, California, continental borderland, in Stow, D. A. V., and Piper, D. J. W., eds., *Fine-grained Sediments: Deep-water Processes and Facies: Geol. Soc. London Spec. Publ.* 15, p. 377-394.
- Toomey, D. F., 1967, Additional occurrences and extension of stratigraphic range of the problematic micro-organism *Nuia*: *Jour. Paleontology*, v. 41, p. 1457-1460.

- Toomey, D. F., and Ham, W. E., 1967, Pulchrilamina, a new mound-building organism from Lower Ordovician rocks of West Texas and southern Oklahoma: Jour. Paleontology, v. 41, p. 981-987.
- Toomey, D. F., and Klement, K. W., 1966, A problematic micro-organism from the El Paso Group (Lower Ordovician) of West Texas: Jour. Paleontology, v. 40, p. 1304-1311.
- Toomey, D. F., and Nitecki, M. H., 1979, Organic buildups of the Lower Ordovician (Canadian) of Texas and Oklahoma: Fieldiana Geology (New Series), no. 2, 181 p.
- Tucker, M. E., 1976, Quartz-replaced anhydrite nodules ('Bristol Diamonds') from the Triassic of Bristol District: Geol. Mag., v. 113, p. 569-574.
- Tuke, M. F., 1968, Autochthonous and allochthonous rocks in the Pistolet Bay area in northernmost Newfoundland: Can. Jour. Earth Sci., v. 5, p. 501-513.
- Vail, P. R., Mitchum, R. M., Jr., and Thompson, S., III, 1977, Seismic stratigraphy and global changes of sea level, part 4: global cycles of relative changes of sea level, in Payton, C. E., ed., Seismic Stratigraphy - Applications to Hydrocarbon Exploration: Am. Assoc. Petroleum Geologists Mem. 26, p. 83-97.
- Van Andel, T. H., and Veevers, J. J., 1965, Submarine morphology of the Sahul Shelf, northwestern Australia: Geol. Soc. Am. Bull., v. 76, p. 695-700.
- Van Andel, T. H., and Veevers, J. J., 1967, Morphology and sediments of the Timor Sea: Australia Bur. Min. Res., Geol. Geophys., Bull. No. 83, 173 p.
- Van Eysinga, F. W. B. (compiler), Geologic time table, 3rd ed.: Amsterdam, Elsevier.
- Van Wamel, W. A., 1974, Conodont biostratigraphy of the Upper Cambrian and Lower Ordovician of north-western Öland, south-eastern Sweden: Utrecht Micropaleont. Bull., v. 10, 126 p.
- Veevers, J. J., 1971, Shallow stratigraphy and structure of the Australian continental margin beneath the Timor Sea: Mar. Geol., v. 11, p. 209-249.
- Veevers, J. J., 1988, Morphotectonics of Australia's northwest margin - a review, in Purcell, P. G., and Purcell, R. R., eds., The North West Shelf, Australia: Perth, Petrol. Explor. Soc. Austral., p. 19-27.
- Veevers, J. J., Falvey, D. A., and Robins, S., 1978, Timor Trough and Australia: facies show topographic wave migrated 80 km during the past 3 m. y.: Tectonophysics, v. 45, p. 217-227.
- Vercoutere, T. L., Mullins, H. T., McDougall, K. M., and Thompson, J. B., 1987, Sedimentation across the central California oxygen minimum zone: an alternative coastal upwelling sequence: Jour. Sed. Petrology, v. 57, p. 709-722.
- von Heune, R., and Arthur, M. A., 1982, Sedimentation across the Japan Trench off north Honshu Island, in Leggett, J. K., ed., Trench-Forearc Geology: Sedimentation and Tectonics on Modern and Ancient Active Plate Margins: Geol. Soc. London Spec. Publ. 10, p. 27-48.

- Walcott, R. I., 1970, Flexural rigidity, thickness, and viscosity of the lithosphere: *Jour. Geophys. Res.*, v. 75, p. 3941-3954.
- Waldron, J. W. F., Turner, D., and Stevens, K. M., 1988, Stratal disruption and development of mélangé, western Newfoundland: effect of high fluid pressure in an accretionary terrain during ophiolite emplacement: *Jour. Struct. Geol.*, v. 10, p. 861-873.
- Walker, K. R., and Ferrigno, K. F., 1973, Major Middle Ordovician reef tract in east Tennessee: *Am. Jour. Sci.*, v. 273A, p. 294-325.
- Walker, K. R., and Keller, F. B., 1977, Tellico Formation, submarine fan, proximal to distal turbidite environments: *Studies in Geology* No. 77-1, University of Tennessee, p. 134-140.
- Walker, R. G., 1967, Turbidite sedimentary structures and their relationship to proximal and distal depositional environments: *Jour. Sed. Petrology*, v. 37, p. 25-43.
- Walker, R. G., 1975, Generalized facies models for resedimented conglomerates of turbidite association: *Geol. Soc. Am. Bull.*, v. 86, p. 737-748.
- Walker, R. G., 1978, Deep water sandstone facies and ancient submarine fans: models for exploration for stratigraphic traps: *Am. Assoc. Petroleum Geologists Bull.*, v. 62, p. 932-966.
- Walker, R. G., 1984, Turbidites and associated coarse clastic deposits, *in* Walker, R. G., ed., *Facies Models*, 2nd ed.: *Geoscience Canada Reprint Series 1*, p. 171-188.
- Walker, R. G., 1985, Geological evidence for storm transportation and deposition on ancient shelves, *in* Tillman, R. W., Swift, D. J. P., Walker, R. G., eds., *Shelf Sands and Sandstone Reservoirs: SEPM Short Course 13*, p. 243-302.
- Walker, R. G., and Mutti, E., 1973, Turbidite facies and facies associations, *in* Middleton, G. V., and Bouma, A. H., eds., *Turbidites and Deep Water Sedimentation: Anheim, CA, SEPM Pacific Section Short Course*, p. 119-157.
- Walker, R. G., Duke, W. L., and Leckie, D. A., 1983, Hummocky stratification: significance of its variable bedding sequences - discussion and reply: *Geol. Soc. Am. Bull.*, v. 94, p. 1245-1251.
- Wallace, M. W., 1987, The role of internal erosion and sedimentation in the formation of stromatolite mudstones and associated lithologies: *Jour. Sed. Petrology*, v. 57, p. 695-700.
- Wanless, H. R., 1979, Limestone response to pressure solution and dolomitization: *Jour. Sed. Petrology*, v. 49, p. 437-462.
- Wanless, H. R., Tedesco, L. P., and Tyrell, K. M., 1988, Production of subtidal tubular and surficial tempestites by Hurricane Kate, Caicos Platform, British West Indies: *Jour. Sed. Petrology*, v. 58, p. 739-750.
- Watkins, R., and Berry, W. B., 1977, Ecology of a Late Silurian fauna of graptolites and associated organisms: *Lethaia*, v. 10, p. 267-286.
- Watts, K. F., 1988, Triassic carbonate submarine fans along the Arabian platform margin, Sumaini Group, Oman: *Sedimentology*, v. 35, p. 43-71.

- Watts, K. F., and Blome, C. D., 1990, Evolution of the Arabian carbonate platform margin slope and its response to orogenic closing of a Cretaceous ocean basin, Oman, in Tucker, M. E., Wilson, J. L., Crevello, P. D., Sarg, J. R., and Read, J. F., eds., Carbonate Platforms: Facies, Sequences and Evolution: Intern. Assoc. Sediment. Spec. Publ. 9, p. 291-323.
- Weedon, G. P., 1986, Hemipelagic shelf sedimentation and climatic cycles: the basal Jurassic (Blue Lias) of S. Britain: Earth Planet. Sci. Let., v. 76, p. 321-335.
- Wendt, J., 1973, Cephalopod accumulations in the Middle Triassic Hallstatt-Limestone in Yugoslavia and Greece: N. Jb. Geol. Paläont. Monat., 1973, p. 624-640.
- Wendt, J., and Aigner, T., 1985, Facies patterns and depositional environments of Paleozoic cephalopod limestones: Sed. Geol., v. 44, p. 263-300.
- Westbrook, G. K., 1982, The Barbados Ridge Complex: tectonics of a mature forearc system, in Leggett, J. K., ed., Trench-Forearc Geology: Sedimentation and Tectonics on Modern and Ancient Active Plate Margins: Geol. Soc. London Spec. Publ. 10, p. 275-290.
- Whalen, M. T., 1988, Depositional history of an Upper Triassic drowned carbonate platform sequence: Wallowa terrane, Oregon and Idaho: Geol. Soc. Am. Bull., v. 100, p. 1097-1110.
- Whitford, D. J., Compston, W., Nicholls, I. A., and Abbott, M. J., 1977, Geochemistry of late Cenozoic lavas from eastern Indonesia; role of subducted sediments in petrogenesis: Geology, v. 5, p. 571-575.
- Whittington, H. B., 1965, Trilobites of the Ordovician Table Head Formation, western Newfoundland: Bull. Mus. Compar. Zool., Cambridge, MS, Harvard University, v. 132, p. 277-441.
- Whittington, H. B., and Kindle, C. H., 1963, Middle Ordovician Table Head Formation, western Newfoundland: Geol. Soc. Am. Bull., v. 74, p. 745-758.
- Wilkinson, B. H., 1982, Cyclic cratonic carbonates and Phanerozoic calcite seas: Jour. Geol. Education, v. 30, p. 189-203.
- Williams, H., 1975, Structural succession, nomenclature, and interpretation of transported rocks in western Newfoundland: Can. Jour. Earth Sci., v. 12, p. 1874-1894.
- Williams, H., 1977, The Coney Head Complex: another Taconic Allochthon in West Newfoundland: Am. Jour. Sci., v. 277, p. 1279-1295.
- Williams, H., 1978a, Geological development of the northern Appalachians: its bearings on the evolution of the British Isles, in Bowes, D. R., and Leake, B. E., eds., Crustal Evolution in Northeastern Britain and Adjacent Regions: Geol. Jour. Spec. Issue No. 10, Liverpool, Seel House Press, p. 1-22.
- Williams, H. (compiler), 1978, Tectonic-lithofacies map of the Appalachian Orogen: Memorial University of Newfoundland, Map No. 1.
- Williams, H., 1979, Appalachian Orogen in Canada: Can. Jour. Earth Sci., v. 16, p. 792-807.

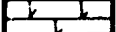
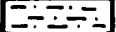
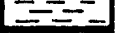
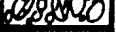
- Williams, H., 1980, Structural telescoping across the Appalachian Orogen and the minimum width of the Iapetus Ocean, *in* Strangway, D. W., ed., *The Continental Crust and Its Mineral Deposits: Geol. Assoc. Canada Spec. Paper 20*, p. 421-440.
- Williams, H., 1985, *Geology, Stephenville map area, Newfoundland: Geol. Surv. Canada, Map 1579A, 1:100000.*
- Williams, H., and Cawood, P. A., 1986, Relationships along the margin of the Humber Arm Allochthon between Georges Lake and Corner Brook, western Newfoundland, *in* *Current Research, Part A: Geol. Surv. Canada Paper 86-1A*, p. 759-756.
- Williams, H., and Cawood, P. A., 1989, *Geology, Humber Arm Allochthon, Newfoundland: Geol. Surv. Canada, Map 1678A, scale 1:250000.*
- Williams, H., Colman-Sadd, S. P., and Swinden, H. S., 1988, Tectonic-stratigraphic subdivision of central Newfoundland, *in* *Current Research, Part B: Geol. Surv. Canada Pap. 88-1B*, p. 91-98.
- Williams, H., Dallmeyer, R. D., and Wanless, R. K., 1976, Geochronology of the Twillingate Granite and Herring Neck Group, Notre Dame Bay, Newfoundland: *Can. Jour. Earth Sci.*, v. 13, p. 1591-1601.
- Williams, H., Gillespie, R. T., and Knapp, D. A., 1982, *Geology of Pasadena map area, Newfoundland, in Current Research, Part A. Geol. Surv. Canada Paper 82-1A*, p. 281-288.
- Williams, H., Gillespie, R. T., and van Breemen, O., 1985a, A late Precambrian rift-related igneous suite in western Newfoundland: *Can. Jour. Earth Sci.*, v. 22, p. 1727-1735.
- Williams, H., and Godfrey, S. C., 1980, *Geology of the Stephenville map-area, Newfoundland, in Current Research, Part A. Geol. Surv. Canada Paper 80-1A*, p. 217-221.
- Williams, H., and Hatcher, R. D., Jr., 1983, Appalachian suspect terranes, *in* Hatcher, R. D., Jr., Williams, H., and Zietz, I., eds., *Contributions to the Tectonics and Geophysics of Mountain Chains: Geol. Soc. Am. Mem. 158*, p. 33-53.
- Williams, H., and Hiscott, R. N., 1987, Definition of the Iapetus rift-drift transition in western Newfoundland: *Geology*, v. 15, p. 1044-1047.
- Williams, H., James, N. P., and Stevens, R. K., 1985b, Humber Arm Allochthon and nearby groups between Bonne Bay and Portland Creek, western Newfoundland, *in* *Current Research, Part A. Geol. Surv. Canada Paper 85-1A*, p. 399-406.
- Williams, H., and Smyth, W. R., 1983, *Geology of the Hare Bay Allochthon: Geol. Surv. Canada Mem. 400*, p. 109-141.
- Williams, H., and St-Julien, P., 1982, The Baie Verte-Brompton Line: early Paleozoic continent-ocean interface in the Canadian Appalachians, *in* St-Julien, P., and Béland, J., *Major Structural Zones and Faults in the Northern Appalachians: Geol. Assoc. Canada Spec. Paper 24*, p. 177-207.

- Williams, H., and Stevens, R. K., 1974, The ancient continental margin of eastern North America, *in* Burk, C. A., and Drake, C. L., eds., *The Geology of Continental Margins*: New York, Springer-Verlag, p. 781-796.
- Williams, S. H., Boyce, W. D., and James, N. P., 1987, Graptolites from the Lower-Middle Ordovician St. George and Table Head groups, western Newfoundland, and their correlations with trilobite, brachiopod, and conodont zones: *Can. Jour. Earth Sci.*, v. 24, p. 456-470.
- Williams, S. H., and Lockley, M. G., 1983, Ordovician inarticulate brachiopods from graptolitic shale at Dobb's Linn, Scotland; their morphologies and significance: *Jour. Paleontology*, v. 57, p. 391-400.
- Wilson, J. L., 1967, Carbonate-evaporite cycles in lower Duperow Formation of Williston Basin: *Bull. Can. Petrol. Geol.*, v. 15, p. 230-312.
- Wilson, J. L., 1969, Microfacies and sedimentary structures in 'deeper water' lime mudstones, *in* Friedman, G. M., ed., *Depositional Environments in Carbonate Rocks*: SEPM Spec. Publ. 14, p. 4-19.
- Wilson, J. L., 1975, *Carbonate facies in geologic history*: New York, Springer-Verlag, 471 p.
- Wilson, J. E., and Jordan, C., 1983, Middle shelf, *in* Scholle, P. A., Bebout, D. G., and Moore, C. H., eds., *Carbonate Depositional Environments*: Am. Assoc. Petroleum Geologists Mem. 33, p. 297-344.
- Woodcock, N. H., 1976, Structural styles in slump sheets: Ludlow Series, Powys, Wales: *Jour. Geol. Soc. London*, v. 132, p. 399-415.
- Woodcock, N. H., 1979, The use of slump structures as paleoslope orientation estimators: *Sedimentology*, v. 26, p. 83-99.
- Wray, J. L., 1977, *Calcareous algae. Developments in Paleontology and Stratigraphy*: Amsterdam, Elsevier, 185 p.
- Yurewicz, D. A., 1977, Sedimentology of Mississippian basin carbonates, New Mexico and west Texas - the Rancheria Formation, *in* Cook, H. E., and Enos, P., eds., *Deep-water Carbonate Environments*: SEPM Spec. Publ. 25, p. 203-220.
- Zankl, H., 1969, Structural and textural evidence of early lithification in fine-grained carbonate rocks: *Sedimentology*, v. 12, p. 241-256.
- Zen, E -an, 1967, Time and space relationships of the Taconic allochthon and autochthon: *Geol. Soc. Am. Spec. Paper* 97, 107 p.

APPENDIX A
KEY TO SYMBOLS

M	mudstone		radiolarian
W	wackestone		graptolite
P	packstone		phyllocard
G	grainstone		calcsphere
F	floatstone		<i>Pulchnilamina</i>
R	rudstone		<i>Halysis</i>
o	peloid		<i>Girvanella</i>
⊙	oncolite	Hed.	<i>Hedstroemia</i>
∞	intraclast		<i>Nuia</i>
∞	lithoclast		fenestra
	ostracode		<i>Stromatactis</i>
	(leperditiid)		stromatolite
	trilobite		mound
	arthropod antenna		
	brachiopod		horizontal burrow (<i>Planolites</i> and <i>Palaeophycus</i>)
	inarticulate brachiopod		bioturbation
	mollusc		peloid-filled burrow
	gastropod		pseudospar-filled burrow
	<i>Murchisoni</i>		burrows in shale
	<i>Maclurites</i>		dolomite/dolomitic burrow
	echinoderm		<i>Chondrites</i>
	cystoid		<i>Phoebichnus</i>
	bryozoan		ripples
	encrusting bryozoan		meganipples
	<i>Archaeoscyphia</i>		climbing ripples
	lithistid sponge		cross-lamination
	sponge holdfast		parallel lamination
	sponge spicule		normal grading
	<i>Lapidipanis</i>		clay flasers
	orthoconic cephalopod		mudstone lense
	coiled cephalopod		packstone lense
	unidentified skeletal fragment		
	mouldic fossil		

-  wrinkle marks
-  convolute lamination
-  fluid escape structure
-  flute
-  groove
-  loaded base
-  shale-filled fracture
-  desiccation crack
-  tepee structure
-  geopetal fabric
-  hardground
-  slump
-  chert nodule
-  nodular evaporite pseudomorph
-  concretion
-  calcite fracture
-  fault

-  limestone
-  dolostone
-  dolomitic limestone
-  sucrosic dolostone
-  sandstone
-  siltstone
-  shale (for Table Cove & Black Cove Fms.)
-  (for American Tickle Fm. & Mainland SS)
-  limestone (for Cape Cormorant Fm.)
-  conglomerate (for Daniel's Harbor Mbr.)

-  silica pebble conglomerate
-  bentonite
-  volcanic dyke

- Q quartz
- F feldspar
- PO₄ calcium phosphate
- Py pyrite
- g glauconite

TABLE POINT FM.

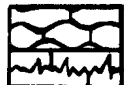
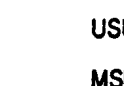
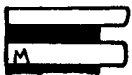
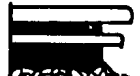
-  stylonodular bedding
-  microstylolitic bedding
- USU Upper Subtidal Unit
- MSU Middle Subtidal Unit
- BPU Basal Peritidal Unit

TABLE COVE FM.

-  interbedded M/W & calcareous shale
- 3B ribbon limestone lithofacies (type B)
- 3A ribbon limestone lithofacies (type A)
- 2 parted limestone lithofacies
- 1 burrowed limestone lithofacies

CAPE CORMORANT FM.

-  lithoclastic calcarenite/calcrudite & shale
-  polymictic conglomerate
- megacgl.-rls. megaconglomerate ribbon limestone lithofacies
- cgl.-calcarenite conglomerate-calcarenite lithofacies
- gn. shale-calc. green shale - calcarenite lithofacies

DANIEL'S HARBOR MBR.

-  clast-supported conglomerate
-  matrix-supported conglomerate
-  lithoclastic-quartz calcarenite

APPENDIX B

BRYOZOAN MOUNDS: TABLE POINT FORMATION

B.1 Description

Small, structureless mounds with abundant encrusting and minor nodule- and stick-like bryozoans occur at one, possibly two horizons in the Basal Peritidal Unit (BPU) of the Table Point Formation at Shag Cliff in Bonne Bay (Figure B.1; see also the measured section in back pocket). They are 0.5-1.4 m high and at least 1-1.5 m across, but limited exposure (vertical cross-sections over a few metres laterally in steeply-dipping beds) prevents determining their precise three dimensional morphology or lateral continuity. Bryozoan skeletons make up about 25-30% of the mounds, but they may not be arranged closely enough to form even an open framework. Those present include: 1) abundant, superimposed, mm-cm thick crustose colonies of Batostoma sp. indet., 2) common, cm-scale nodules of Nicholsonella? sp. indet., 3) rare fronds of Ceramoporella sp. indet., and 4) very rare, delicate branching (1-2 mm) Eridotrypa aff. mutabilis, and 5) a bifoliate? gen. and sp. indet. (identified by R. Cuffey, 1988, pers. comm.). Sediment between the bryozoans is fossil-poor wackestone. It is, however, both recrystallized and partially dolomitized, and it is difficult to determine to what extent textural and compositional features have been obliterated. Sediments flanking the mounds are relatively fossiliferous, muddy packstone with conspicuous mollusc fragments, small coiled cephalopods, and articulate brachiopods. They grade laterally away from the mound into muddier, burrowed fossiliferous packstone and wackestone. Low areas between two mounds seen in outcrop are partly filled with dolomitic mud.

The sedimentary sequence in which the bryozoan mounds occur is shown schematically in Figure B.1. They overlie flaggy-bedded, fossiliferous pack- /wackestone, and are overlain by a 25 cm thick, echinoderm-rich,

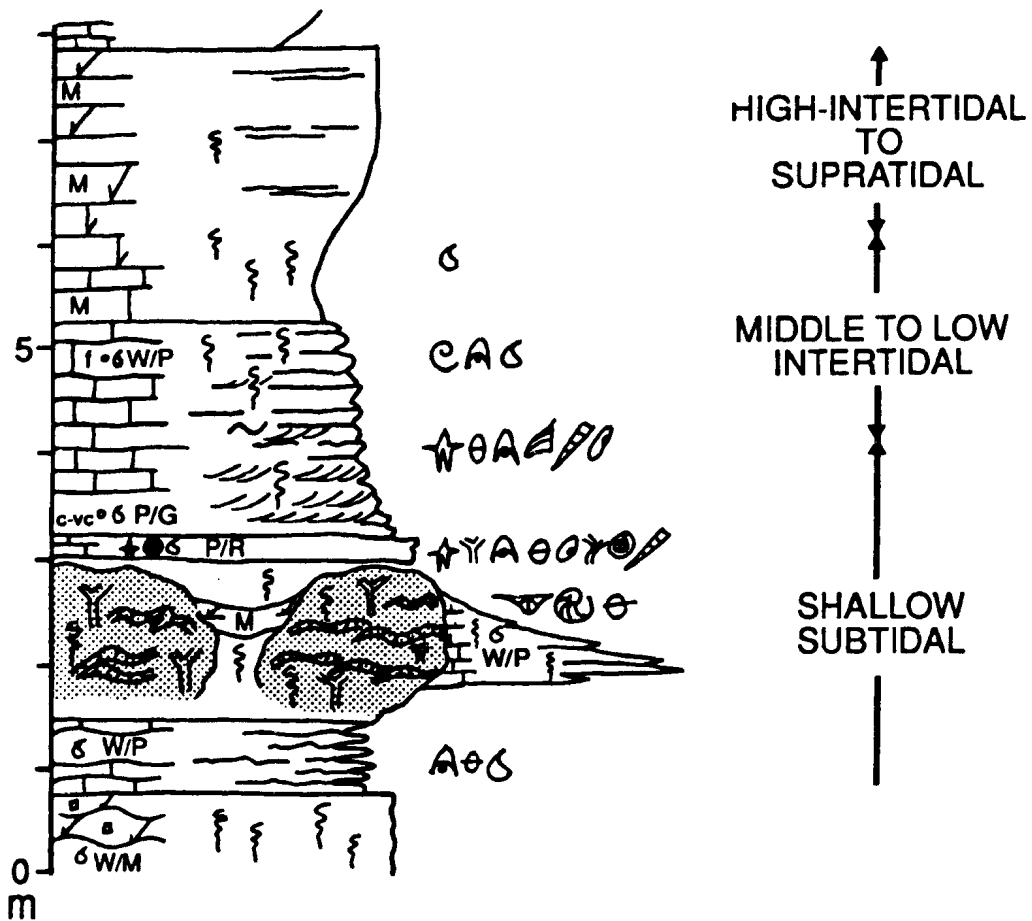


Figure B.1 Schematic measured section through bryozoan mounds and enclosing strata in the BPU at Shag Cliff in Bonne Bay. Key to symbols is in Appendix A.

intraclastic, oncolitic rudstone with large numbers of ostracodes and conspicuous small orthoconic cephalopods. Oncolites are 1-2 cm in diameter and are composed of Girvanella filaments around fragments of bryozoans, molluscs and trilobites. Most other skeletal fragments in the bed have micritized edges. The oncolitic sediments are in turn overlain by a 1.8 m thick, coarse- to very coarse-grained, vaguely ripple cross-stratified, echinoderm-rich, peloidal grainstone-packstone that becomes finer-grained and increasingly muddy and burrowed up section. These sediments are in turn overlain by partially burrowed, dolomitic cryptalgal laminite. The overall sequence is interpreted to record deposition in increasingly shallow and restricted environments.

These small bryozoan bioherms are the oldest reported from Middle Ordovician strata. Their appearance in the EPU of the Table Point places them in the uppermost lower Whiterock or basal upper Whiterock (Orthidiella - lower Anomalorthis zones, Figure 4.8). They appear to be the predecessors of more complex buildups in Chazy carbonates (uppermost Whiterock and younger, Figure 4.8; Ross *et al.*, 1982) which have been documented in several places in the southern Appalachians (Pitcher, 1964; Ross, 1970; Walker and Ferrigno, 1973; Alberstadt and Walker, 1975; Ruppel and Walker, 1977, 1982). Of the bryozoan genera present in the Table Point mounds, Batostoma, Nicholsonella, and Ceramoporella (Cheiloporella), along with several other genera not observed here, later became major components of both small mounds and large reefs during the Chazy.

B.2 Interpretation

These mounds are small organic buildups that formed in a quiet water to moderately agitated, relatively shallow subtidal environment. They were constructed mostly by irregularly stacked, sheet-like colonies of bryozoans and scattered stick-shaped forms that did not generate a rigid, wave-resistant structure, but which effectively trapped and

stabilized lime mud transported in the water column. The bryozoans appear to have colonized a comparatively grainy, but apparently stable substrate. Similar to their younger Chazyan counterparts they may have formed low relief patches of mud that protruded perhaps only 10-15 cm above the seafloor. Bryozoan diversity within the mounds remained low, but the surface of the mound was apparently colonized by other shelly invertebrates whose skeletons accumulated on the flanks.

Since there is no evidence of subaerial exposure the mounds are interpreted as wholly subtidal. Mound growth appears to have been controlled by the level of agitation of the water, which in the subtidal is inferred to increase with decreasing water depth. Considered in the context of the shallowing-upward sequence in which the mounds occur, the overlying coarse, oncolitic rudstone and cross-bedded grainstone indicate that growth stopped when current/wave agitation was strong enough to mobilize the sediment continuously. Sediments above these record sedimentation in progressively lower energy, more restricted environments determined by decreasing water depth along the shallow subtidal to supratidal topographic gradient. Girvanella oncolites in the sediments above the mounds may indicate depths of less than 10 m, possibly less than 3 m (Moore, 1977). Assuming no major change in sea level or tectonic pulse that changed the rate of subsidence, and minimal compaction, a comparable water depth of 7-8 m is reached by totalling the thickness of the shallowing-upward sequence from the base of a mound horizon up through the dolomitic, intertidal to supratidal cap (eg. Klein, 1974).

B.3 Discussion

Bryozoan mounds are unique to the Table Point Formation exposed in Bonne Bay. Similarly, the BPU of the formation is quite unlike BPU sequences in other areas: it is thicker than elsewhere (~120 m), it lacks fenestral limestone, and its diagnostic lithofacies indicating

restricted conditions and/or exposure is burrowed dolostone and dolomitic cryptalgal laminite (Lithofacies 1 and 3 in Table 4.1). Skeletal components in the subtidal lithofacies, notably a noticeable amount of echinoderm debris, and the apparent absence of algal-microbial mats in at least the lower zones of tidal flats suggest that marine waters approached more normal salinity and tidal flats were more agitated and less restricted than in other areas. Therefore it appears that bryozoan buildups developed because requisite environmental conditions, complexly defined by water depth, current and wave energy, salinity, and temperature, were unique to this area.

In light of other evidence that BPU sedimentation regionally was influenced by irregular topography generated by earlier block-faulting and uplift, and perpetuated by differential subsidence (discussed in Chapter section 12.2.2), more normal marine conditions in the Bonne Bay area implies that there were fewer or less effective barriers to circulation in adjacent outboard areas of the platform. This further suggests that Bonne Bay area was a relatively rapidly subsiding, structural low on the platform, a configuration supported by 1) the anomalously thick Aguathuna Formation sequence at Bonne Bay (Levesque, 1977; this study), 2) the potential absence of the St. George Unconformity either within the Aguathuna or at the Aguathuna - Table Point contact (Schuchert and Dunbar, 1934; Levesque, 1977; this study), and 3) the anomalously thick BPU sequence at the base of the Table Point.

Although their outcrop expression is poor, further study of these mounds is necessary to fully understand them and their evolutionary relationships to younger Chazyan buildups. Further research involving strategic sampling and petrographic examination would permit 1) identification of all bryozoan and other taxa present, 2) documentation of their distributions in the build-ups, and 3) critical evaluation of their roles in mound construction.

APPENDIX C

SYNSEDIMENTARY DEFORMATION: TABLE COVE FORMATION

C.1 Introduction

Table Cove Formation strata are commonly sheared, folded, faulted, and/or conglomeratic. Though not unique to, such deformation is pervasive only in relatively thick formation sequences. Based on criteria outlined by Helwig (1970) and Woodcock (1976) deformation is inferred to be synsedimentary rather than tectonic for the following reasons: 1) Deformed strata are commonly underlain and/or overlain by undeformed strata; overlying sediments are locally ponded in topography on top of deformed strata. 2) Folds within discrete deformed horizons locally (i) have different senses of asymmetry, (ii) are irregular or chaotic, and/or (iii) have curvilinear hinges. 3) Fold axes do not parallel either the axis of large-scale, tectonic folds or cleavage in the immediate area. 4) Folds lack or have only a weakly-developed axial planar cleavage which does not parallel tectonic cleavage. 5) Faults associated with folds do not have slickensides.

Many of the features listed above are complexly juxtaposed in discrete deformed horizons which are interpreted as gravitational slides. The term slide is used herein for all coherent packages of deformed strata displaced down-slope above a detachment surface that may have rotational (slump) and nonrotational (glide) deformation.

Thick Table Cove sequences with numerous slides are well-exposed at Table Cove and along the coast between Bellburns and Spudgel's Cove on the Great Northern Peninsula (Figure 1.2). Extensive along-strike outcrops (30 m-2 km) permit documentation of the types and distribution of deformation in slides in all three lithofacies. Several slides were mapped in detail and structures were plotted on low level aerial photographs. Orientations of fold axes and axis-parallel lineations (multiens), fold axial surfaces, inclined foliation in shear zones, faults

and imbricated beds were measured to determine transport directions (Woodcock, 1976, 1979; LaJoie, 1972; Figure 5.10 and Spudgel's Cove section in back pocket).

C.2 Types of Synsedimentary Deformation

Deformation features of slides in the Table Cove include: (i) faults, (ii) rotated and imbricated beds, (iii) pebbly and chaotic limestone conglomerate, (iv) sheared bedding, (v) folds, and (vi) quasi-conglomeratic limestone. Brief descriptions of these structures, their distributions and common relationships to each other in discrete slides, and interpretations are summarized in Table C.1. Outcrop examples are in Figure C.1.

The spectrum of structures and conglomerate fabrics indicates both brittle and ductile deformation of these sediments during sliding. Presence of both styles of deformation in all three Table Cove lithofacies implies that all sediments deposited along the slope to basin transect were at least partially lithified at the time of transport. Vertical and lateral variation in the type and degree of deformation within an individual slide demonstrates that stresses were heterogeneously distributed throughout the moving masses.

C.3 General Attributes of Slides in the Table Cove

Discrete slide masses in the Table Cove are defined by a basal detachment fault that parallels bedding and/or gently climbs up section; staircase trajectories identify these structures as soft-sediment analogues of hard rock thrusts (Butler, 1982). Where it parallels bedding, the basal detachment typically follows an argillaceous interbed, and is cryptic unless immediately underlying or overlying strata are deformed (Figures 5.5.a and C.1.g-1). Upper bounding surfaces have low relief depositional topography overlain and evened out by younger sediments (Figure C.1.a). In many cases in parted and ribbon limestones, the

Table C.1 Synsedimentary Deformation Structures, Table Cove Formation

Structure	Distribution in Slide Mass; Relationships to Other Structures	Formation Mechanism
<p>1) Fault</p> <p>Figures C.1.h-l, 5.3.a, 5.5.a, & 5.7.b</p>	<p>a) thrust; bedding parallel flats (commonly cryptic) & gently to moderately dipping ramps</p> <p>b) listric normal (0-15°) (uncommon)</p>	<p>brittle deformation: a) most propagated downslope in response to compression during transport &/or when sliding stopped; downslope-facing backthrusts generated when movement ceased</p> <p>b) - (i) propagated upslope in response to tensile stress during initial slope failure (ii) generated by tensile stress in culminations above ramps in slide masses</p>
<p>2) Rotated / Imbricated Beds</p> <p>Figure C.1.i,j</p>	<p>several decimetre to several metre thick, discontinuous packets of strata gently or moderately inclined relative to normal bedding</p> <p>(i) above basal detachment &/or splay thrusts (\pm comprising entire thickness of slide)</p> <p>(ii) between internal (thrust) detachments within a slide</p>	<p>brittle deformation: vertical & lateral displacement above, and stacking between thrusts</p> <p>(i) above splay thrusts linked to the basal detachment & terminating at the sediment-water interface during transport or when movement ceased</p> <p>(ii) between internal thrusts (duplex structure with a roof thrust) during transport</p>
<p>3) Folds</p> <p>Figures C.1.b-d, 5.5.a & 5.7.a</p>	<p>a) <u>multilayer</u> (most common)</p> <p>- complete spectrum of geometries & orientations: simple to chaotic, open to isoclinal, upright to recumbent</p> <p>- thinned limbs &/or extended or pinched off hinges common; (Amp.: <0.05-1 m; λ: 0.1-3 m)</p> <p>b) <u>single layer</u></p> <p>- open, symmetrical (\pm buckled hinges) to overturned, asymmetrical (commonly with faulted lower limbs (Amp.: <5 cm-20 cm; λ: 0.2-3 m)</p> <p>(i) discontinuous domains at slide base; grades laterally into sheared bedding</p> <p>(ii) discontinuous domains over entire slide thickness (mostly either multilayer open or chaotic); grades laterally into all types of conglomerate & undeformed bedding</p> <p>iii) discontinuous domains in slide mass</p>	<p>ductile deformation*</p> <p>(i) shearing in the subsurface during sliding</p> <p>(ii) buckling due to shear during displacement or compression when sliding stopped</p> <p>(iii) previous slope failure at the sediment-water interface or subsurface shear caused by differential movement between internal (thrust) detachments during transport</p> <p>* brittle failure for buckled fluid hinges & truncated limbs of drag folds below thrusts & lower limbs of some asymmetric, overturned folds</p>

Table C.1 continued

Structure	Distribution in Slide Mass; Relationships to Other Structures	Formation Mechanism
<p>4) Sheared Bedding</p> <p>Figures C.4.d,h & 5.5.a</p>	<p>(i) few cm or 10s of cm thick zone at slide base; grades laterally into chaotically folded bedding or pebbly or chaotic conglomerate; grades up into less deformed, folded &/or faulted bedding</p> <p>(ii) discontinuous domains within slide</p> <p>(iii) discontinuous domains below basal detachment of a slide</p>	<p>ductile deformation: differential movement between adjacent sediment layers during sliding (i) increasing velocity gradient away from slide base where frictional resistance is greatest</p> <p>(ii) differential movement between internal (thrust) detachments</p> <p>(iii) decreasing velocity gradient below basal detachment</p>
<p>5) Limestone Conglomerate</p> <p>a) Figure C.1.k</p>	<p>a) <u>pebbly</u>: massive, matrix-poor domains of pebble-size, equidimensional to elongate limestone clasts - weak, inclined foliation defined by relict primary bedding (local); low relief depositional topography on upper bounding surface on (iii)</p>	<p>brittle deformation: <u>in situ</u> disaggregation of well-lithified limestone beds in response to tight folding and intense shearing during transport</p>
<p>b) Figure C.1.l</p>	<p>b) <u>Chaotic</u>: massive mixtures of pebble-size limestone clasts and bedded limestone blocks 1-2 m across (clasts grade into pebbly debris); depositional topography on upper bounding surface; locally thinner than adjacent slide domains</p>	<p>brittle deformation: <u>in situ</u> disaggregation of well-lithified limestone beds either due to compressional faulting during transport or when movement ceased, or extensional pull-apart during initial slope failure</p>
<p>c) Figure C.1.e,f</p>	<p>c) <u>Quasi-conglomerate</u>: massive domains of round to irregular, vaguely-bounded, pebble-size limestone lumps; common gradational contacts between limestone lumps & argillaceous pseudospar matrix; cryptic folds defined by relict bedding locally; depositional topography on upper bounding surface</p>	<p>ductile deformation: folding & disarticulation of poorly-lithified sediments caused by shearing during sliding</p>

Figure C.1 Deformation structures in gravity slides; Table Cove Formation at Table Cove. a) Sediments ponded in topography on the upper bounding surface of a slide. b) Chaotically folded ribbon limestone. c) Recumbent folds at the base of a slide in ribbon limestone. Shale interbeds in adjacent undeformed sequences are 1-2 cm thick. d) Sheared beds (double arrow) gradationally overlain by folded (arrow) and disarticulated beds at the base of a slide in ribbon limestone. Shale interbeds in adjacent undeformed sequences are 1-2 cm thick. e) Quasi-conglomerate in ribbon limestone. Cryptic fold defined by relict bedding (arrow). Limestone and shale beds in adjacent undeformed sequences are 2-7 cm and 1-4 cm thick, respectively. f) Photomicrograph of quasi-conglomerate in e. Swirled, pseudosparitic matrix (not shale) is in sharp and gradational contact with round limestone lumps. st, stylolite. Bar scale is 2 mm long. g) Helicopter view of a segment of a large slide at the top of the parted limestone lithofacies exposed on the Bellburns coast. Black and white arrows point to two subsidiary faults (SP) linked to the basal detachment (BD) further to the right (north) off the photo. The basal detachment here parallels bedding. Folding in the hangingwall of the lowest fault indicates normal sense displacement. The upper fault is a splay thrust (ramp), the trajectory of which appears to have been controlled by the earlier-formed, extensional fault scarp. h) Basal detachment in ribbon limestone at Table Cove. Underlying beds are truncated; basal beds of the overlying slide are sheared (SE). i) Helicopter view of a large package of rotated and imbricated beds; upslope segment of the large slide shown in (a). Splay thrusts are cryptic; deformed beds in the footwall are pebbly conglomerate (black arrows). North-dipping bedding indicates transport to the south (left). j) Rotated and imbricated beds comprising the entire thickness of a slide in ribbon limestone; Table Cove. Splay thrusts (SP) are cryptic; arrow points to truncated drag fold in the footwall of one. Metre-stick for scale. k) Pebbly limestone conglomerate (arrows) at the base of a slide in parted limestone; Bellburns coast. Divisions on measuring stick are 10 cm. l) Helicopter view of chaotic limestone conglomerate domain comprising the entire thickness of a slide (~2 m) in ribbon limestone; Table Cove. Bedding dips ~30° south, into the page. Boulders in the foreground are loose beach sediment.

Figure C.1

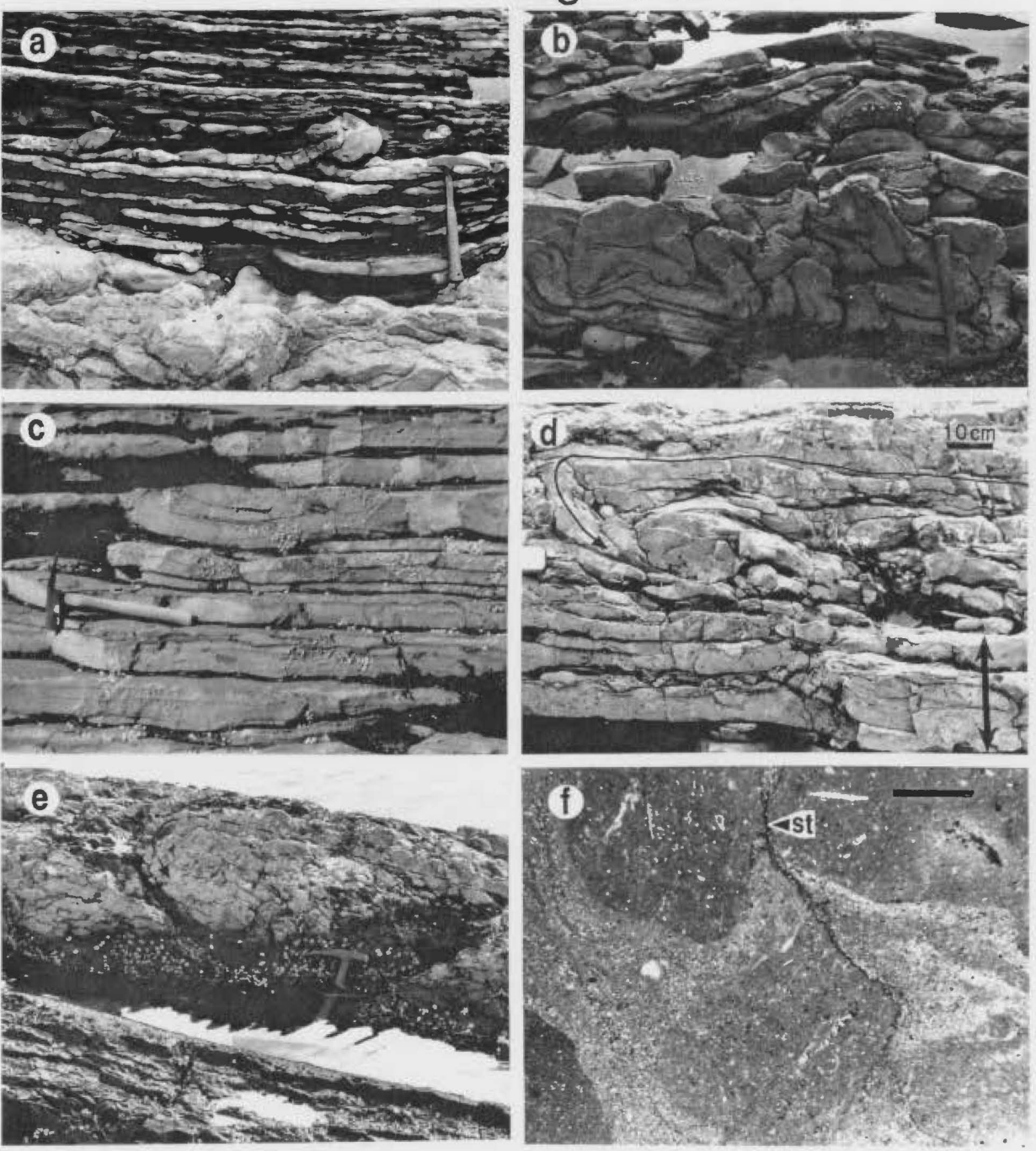
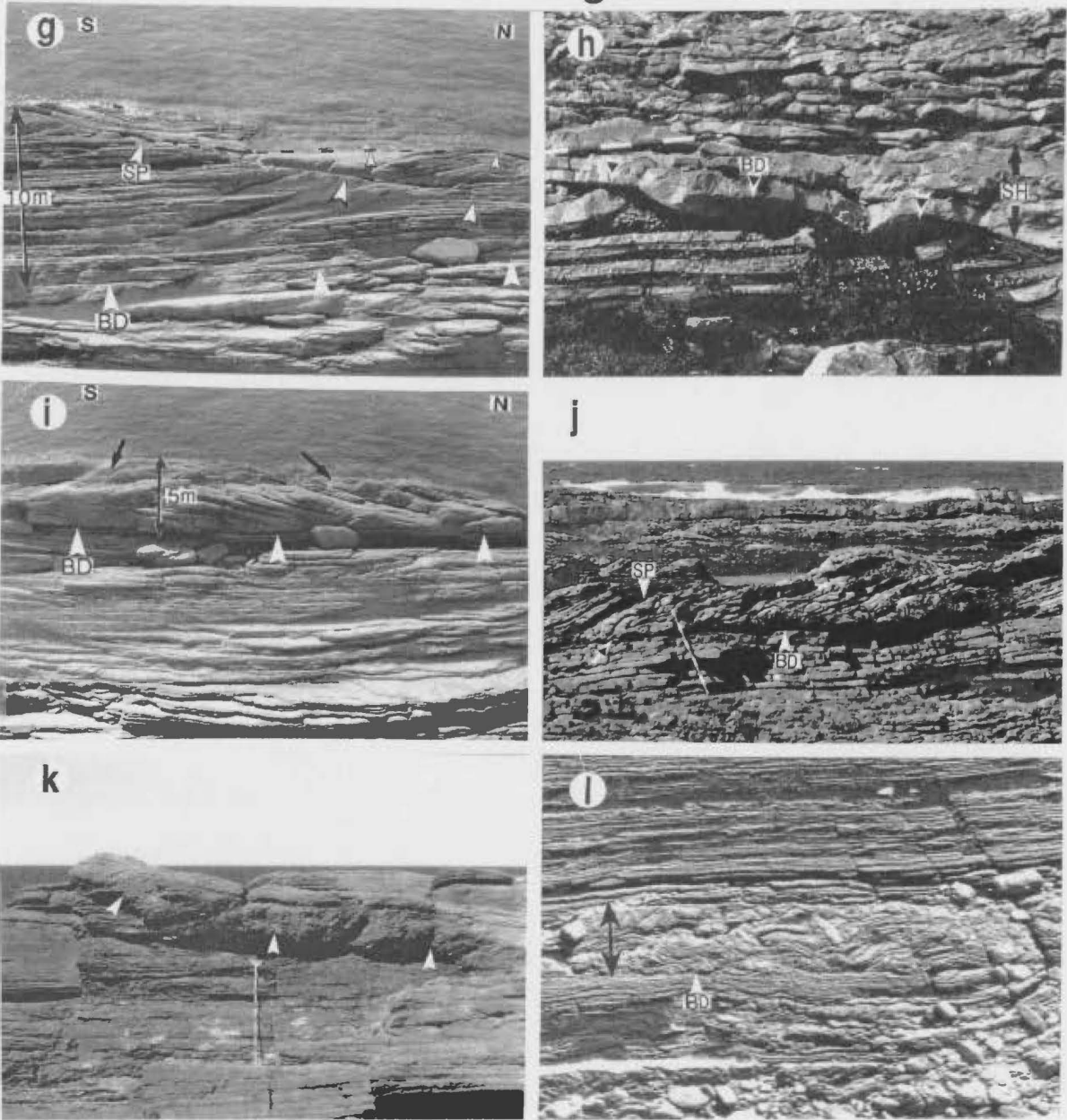


Figure C.1



upper bounding surface is the basal detachment of an overlying slide.

Slides range from less than 1 m to approximately 12 m thick. Most can be traced the length of the outcrop, ie. a few tens to a few thousand metres. They are much thinner than slides seen in seismic profiles across modern-day continental slopes and rises, which are several tens or hundreds of kilometres in lateral dimensions and involve several tens of metres of section (Lewis, 1970; Embly and Jacobi, 1977; Mullins et al., 1986; Coleman and Prior, 1988). Identification of such large structures in the Table Cove may be precluded by scale of the outcrop.

The amount of lateral displacement cannot be determined for most slides. Possible leading-edge overthrust segments of small slides in upper and middle slope limestone sequences indicate only a few metres or tens of metres of displacement. More distant transport is inferred for some slides in the lowest ribbon limestones at Table Cove where two opposing senses of displacement are recorded (Figure 5.10, back pocket). Strata comprising slides with structures indicating transport to the NW are more carbonate-rich, ie. composed of thicker and more continuous limestone beds, than are intercalated sequences with structures indicating displacement to the SE, which are more argillaceous and, locally, composed of nodular limestone. Based on carbonate content alone the latter are interpreted to have originated in a comparatively deep setting and are inferred to be relatively autochthonous, while the former are interpreted to have originated in a shallower position on a slope more proximal to a carbonate source, and are inferred to have been transported several hundred metres or a few kilometres into the basin.

C.4 Lithofacies Control on Deformation

In general, synsedimentary deformation in upper slope, burrowed limestones is minor and cryptic, while in deeper water parted and ribbon limestones it is more pervasive, complex, and well-defined by limestone: shale bedding. In the latter two lithofacies nearly every major bedding

plane break is either a basal detachment or upper bounding surface of a slide; in ribbon limestone, almost every limestone bed traced along strike is proven to be locally folded, faulted, rotated or sheared.

Careful study of slides at Table Cove and along the Bellburns coast prove that there are significant differences in thickness, in the distribution and proportion of ductile versus brittle deformation structures and/or fabrics, and in the style of brittle deformation among the three lithofacies, as well as up-section in the ribbon limestone lithofacies (Table C.2; Figures C.2-5).

Most factors that controlled these records of slope failure, such as magnitude of shear stresses that initiated failure, displacement velocity and velocity differentials within the slide, the distance of displacement and the mechanism by which movement ceased, and the slope angle, cannot be assessed. There is, however, close correlation between deformation style and lithofacies. Brittle failure structures predominate, and some are unique to, upper slope, middle slope, and the stratigraphically lowest ribbon limestone, while ductile deformation predominates and characterizes the highest ribbon limestones (Table C.2). Deformation style is interpreted to have been fundamentally controlled by the degree of lithification of incipient limestone beds, the up section change from predominantly brittle to ductile indicating decreasing lithification with increasing water depth. Precisely the same depth control on the degree of sea floor cementation has been documented along slopes of the Bahamas (Mullins *et al.*, 1980; Harwood and Towers, 1988).

Thickness of sediment packages involved in sliding is interpreted to have been controlled in part by both lithification state of incipient limestone beds and the relative abundance of intercalated, unlithified argillaceous sediment (Appendix D), which determined the shear strength of surficial sediment layers (Moore, 1961; Dott, 1963). Extensive, early lithification at very shallow depths below the sediment-water interface and paucity of shale in upper slope sediments rendered only

Table C.2 Gravitational Slides, Table Cove Formation

1) Burrowed Limestone Lithofacies

Thickness	Deformation Style ¹	Directional Changes	Interpretation
15-50 cm, rarely to 2 m (Figure C.2.a)	<u>BRITTLE</u> - knobby, imbricated bedding - pebbly conglomerate <u>ductile</u> - broad, open folds - ill-defined, small-scale chaotic folds	increases in thickness in the direction of transport	- surficial sediments well-lithified at the time of transport; thinness indicative of very shallow depths below the sediment-water interface at which sediments were sufficiently lithified to resist failure & down slope transport

2) Parted Limestone Lithofacies

1) 20-100 cm thick	<u>BRITTLE</u> - same as in the burrowed limestone lithofacies	degree of deformation increases in the direction of transport	- same as in the burrowed limestone lithofacies
2) 1-3 m thick (Figures 5.5.a, C.1.b, & C.2.b)	<u>DUCTILE</u> - folds (typically multilayer & asymmetric) - sheared bedding <u>BRITTLE</u> - pebbly conglomerate - thrust faults (common) - packets of rotated & imbricated bedding	degree of deformation increases in the direction of transport	- near surface sediments semi- to well-lithified at the time of transport; multi-layer folds are indicative of competency contrasts between limestone beds & shale partings; numerous internal detachments indicate argillaceous partings accommodated a great deal of stress by acting as glide planes during transport
3) 10-12 m thick (Figure C.1.g,i)	<u>BRITTLE</u> - pebbly conglomerate - numerous widely-spaced thrust faults - packets of rotated & imbricated bedding <u>ductile</u> - broad, open folds in strata between splay faults; minor drag folds	degree of deformation decreases in the direction of transport	- sediments fairly well-lithified at the time of transport; shear strength enhanced by the thickness of the sequence being displaced

3) Ribbon Limestone Lithofacies (26-35 m in the Table Cove section)

1.5-2 m thick (Figures C.2.j,l & C.3)	<u>DUCTILE</u> - folds (mostly chaotic) - sheared bedding <u>BRITTLE</u> * pebbly conglomerate * chaotic conglomerate - thrust faults & packets of rotated & imbricated bedding	thickness & degree of deformation decrease in the direction of transport	- surface sediments fairly well-lithified at the time of transport; limestone layers more susceptible to brittle failure during transport than in stratigraphically higher ribbon limestone
--	---	--	---

Table C.2 continued

3) Ribbon Limestone Lithofacies continued (35-62 m in the Table Cove section)

Thickness	Deformation Style	Directional Changes	Interpretation
2-4 m thick; decreases up- section (Figure C.3)	BRITTLE (especially in the lowest 10 m) - faults: complexly fault-bounded packets of rotated &/or imbricated beds ductile (increasingly in the upper 17 m) - folds (all styles; commonly recumbent &/or isoclinal) - sheared beds -quasi-conglomerate (incipient)	degree of deformation decreases in the direction of transport	(thick slides at base): surface sediments fairly well-lithified at the time of transport; strain accommodated by gliding along argillaceous interbeds rather than by folding; folding possibly also inhibited by greater overburden (thinner slides at top): surface sediments increasingly less well-lithified; less resistance to slope failure a function of lower shear strength (unlithified argillaceous layers & soft, incipient limestone beds)

3) Ribbon Limestone Lithofacies continued (62-72 m in the Table Cove section)

0.7-3 m thick (Figure C.4)	DUCTILE * quasi-conglomerate - sheared beds (commonly in the footwall & the hangingwall of the basal detachment) - folds (all types) brittle - uncommon/rare splay faults, internal detachments, & packets of rotated & imbricated bedding	quasi-conglomerate fades in the direction of transport	poorly-lithified incipient limestone beds & unlithified argillaceous layers impart little shear strength; surface sediments susceptible to failure even on low depositional slopes
-----------------------------------	---	--	--

3) Ribbon Limestone Lithofacies continued (72-93 m in the Table Cove section)

0.3-3 m thick (Figure C.4)	DUCTILE - folds - sheared beds (commonly in the footwall & the hangingwall of the basal detachment) - quasi-conglomerate (weakly developed) brittle (mostly in the top 3 m) - faults; complexly bound packets of folded & rotated bedding in the top 3-5 m	none	same as for the 62-93 m interval
-----------------------------------	---	------	----------------------------------

¹ predominant style is in CAPITAL letters; * signifies unique to the interval

Figure C.2 Slides in upper slope and middle slope limestones. a) Obscure deformation in the upper slope, burrowed limestone lithofacies; Table Cove. Basal detachment of the large slide is indistinct except where relict beds in the hangingwall of the ramp are rotated. Thin horizons of imbricated beds (IM, arrows) are more typical of this lithofacies. b) Complexly deformed strata in a slide in parted limestone; Bellburns coast. Measuring stick (10 cm divisions) rests on the anticlinal hinge of a large, multilayer fold; asymmetry indicates displacement to the left (south). Orientation of the fault (white arrows) splayed off the basal detachment (BD) indicates opposite displacement to the north.

Figure C.2

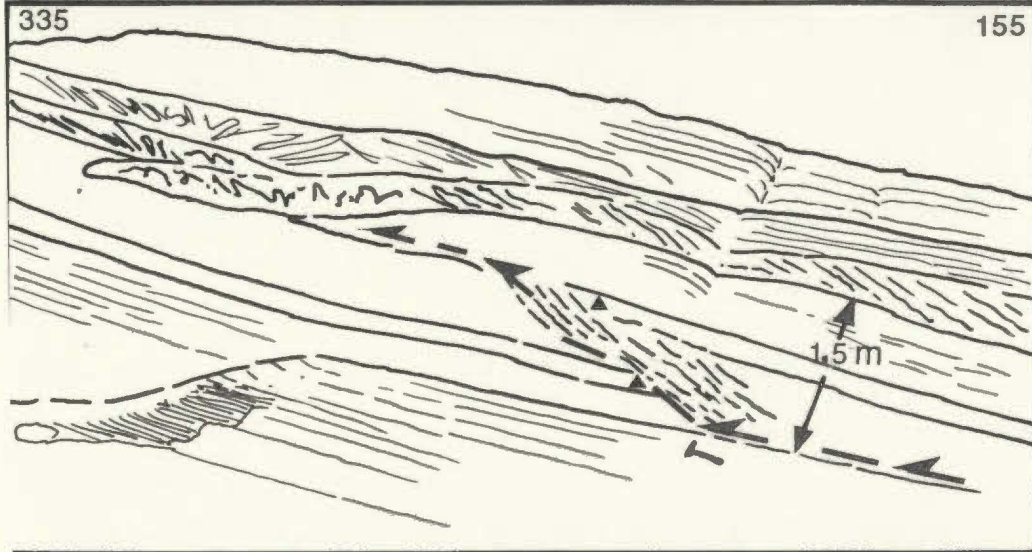


Figure C.3 Helicopter view of slides in the ribbon limestone lithofacies at Table Cove. Bedding dips -30° S (into the page). Overlap points among the three photos are marked by Xs. Metre values (right) correspond to height above the base of the formation. Every major bedding plane break corresponds to the basal detachment (BD) or upper bounding surface of a slide. There are more discrete slide masses than are delineated on the photos. Slides below 48.5 m are characterized by brittle deformation structures. Pebbly and chaotic limestone conglomerate (CH CGL) domains are unique to the lowest two slide masses in the field of view; complexly fault-bounded domains of rotated bedding comprise slides between 40.5 and 48.5 m. Sheared bedding and folds become increasingly common above 48.5 m. Quasi-conglomerates (Q) uniquely comprise discontinuous domains in slides above 58.5 m. ROT/IMB, rotated and/or imbricated bedding.

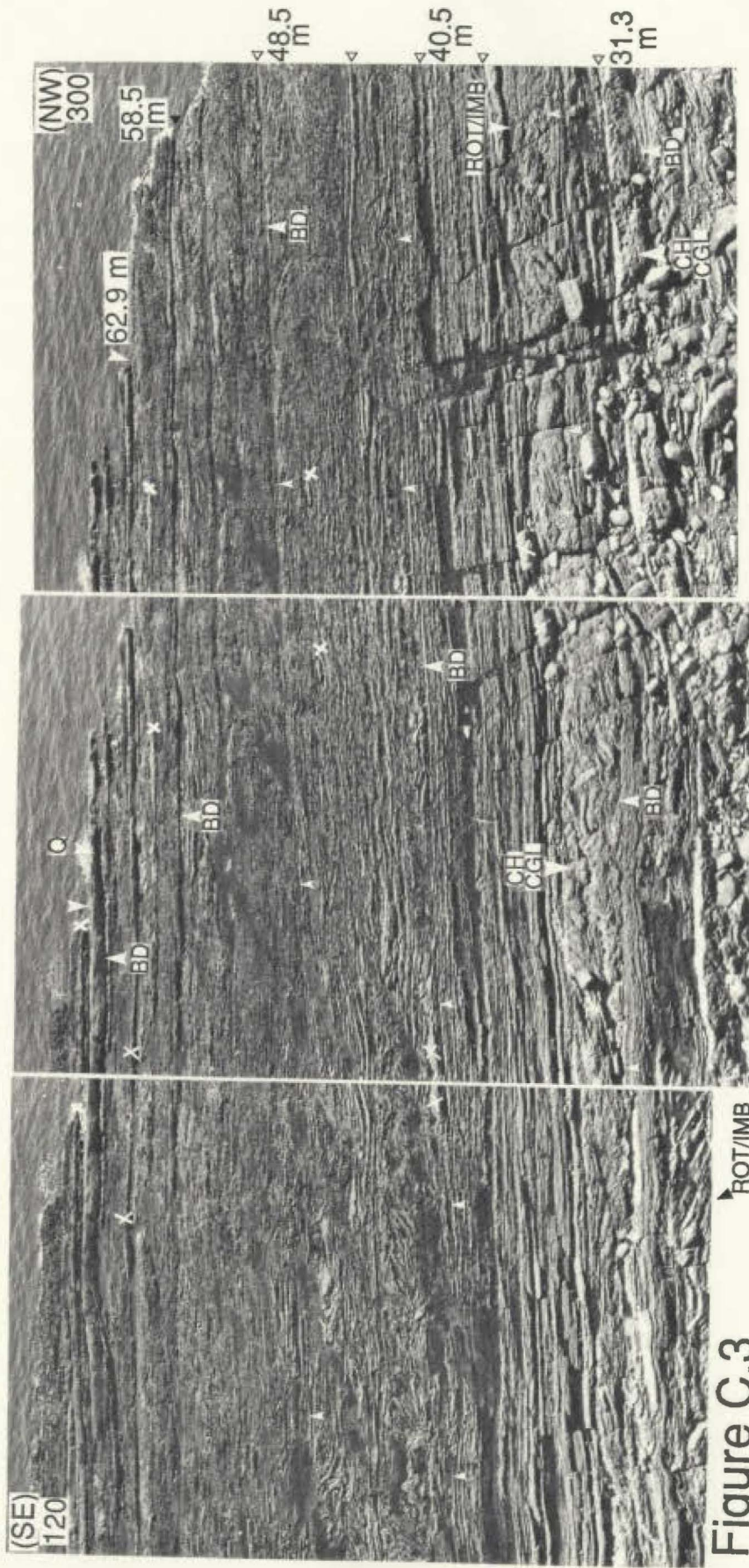
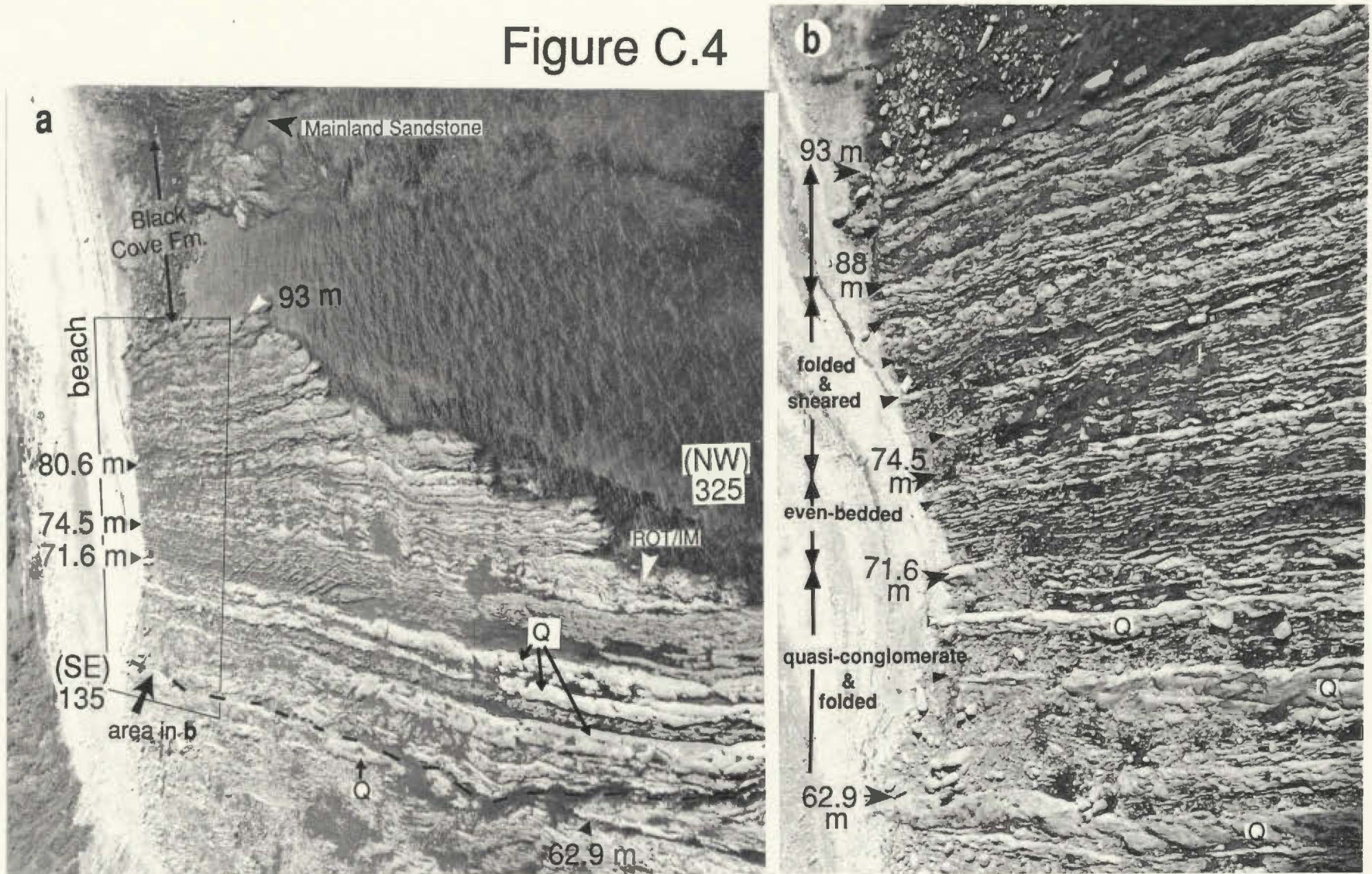


Figure C.3

Figure C.4 Helicopter views of thin slide masses in the upper 30 m of the ribbon limestone lithofacies at Table Cove. Bedding dips -25°S (into the page). Metre values correspond to height above the base of the Table Cove Formation. Abbreviations are the same as in Figure C.3. a) Every major bedding plane break corresponds to the basal detachment or upper bounding surface of a slide; there are even more discrete slides than are indicated by these breaks. Ductile deformation structures predominate in slides throughout the sequence. Quasi-conglomerates (Q) are unique to the 62.9-71.6 m interval; they fade to the southeast (in the direction of transport). The low angle detachment that truncates quasi-conglomerate at 62.9 m (dashed line) may be a ramp of a basal detachment that displaces all strata between 62.9-71.6 m. Further west (just off the photo) those strata are gently folded in what appears to be a hanging wall anticline. b) Close-up of area outlined in (a). Metre marked bedding plane breaks are either the base or top of a slide mass. Smaller arrows indicate basal detachments of other thin slides.

Figure C.4



the uppermost sediments susceptible to slope failure. Minimal early lithification of incipient limestones and abundant shale in the deepest ribbon limestones rendered those sediments susceptible to failure even on a very low angle depositional slope.

C.5 Discussion

The types and distribution of deformation structures documented in Table Cove Formation limestones at Table Cove and Bellburns-Spudgel's Cove are analogous to, if not more complicated than, deformation structures characteristic of hard rock, fold and thrust belts (eg. Butler, 1982). Decreasing thickness of slide masses in the direction of transport (Table C.2) in most cases is proven to be an expression of gradual climbing of the basal detachment up-section. Commonly observed decrease in the degree of deformation in the slide mass in the direction of transport is interpreted to reflect decreasing displacement above the basal detachment toward the leading edge of the slide (Farrel, 1984). Presence of true conglomerate domains in the slides, but absence of actual debris flow deposits, suggests that transport, disintegration and remoulding of sediments in the slides occurred so slowly that additional water necessary for the mass to flow was not incorporated into the slides during transport.

The morphology of basal detachments, predomination of contractional deformation structures, paucity of extensional structures, and the presence of backthrusts indicate the slide masses exposed at Table Cove and along the Bellburns coast are the leading edges, or toes, of the slides. This suggests that these exceptionally thick formation sequences are the product of synsedimentary, structural thickening, and that Table Cove sequences in adjacent areas that acted as sources for slide masses are likely structurally thinned.

APPENDIX D

ORIGIN OF BEDDING IN PARTED AND RIBBON LIMESTONE: TABLE COVE FORMATION

Rhythmically-interstratified limestone beds and argillaceous partings or interbeds are diagnostic of parted and ribbon limestone in the Table Cove Formation. Parted limestone is differentiated from ribbon limestone in these sequences by consistently thin (1-3 cm vs. 1-20 cm), burrowed limestone beds and comparatively thin (<1 cm versus 1-30 cm) argillaceous partings. This type of bedding in other ancient carbonate sequences has been interpreted as primary depositional layering (Schwarzacher and Fischer, 1982; Weedon, 1986), as an early diagenetic stratification (Hallam, 1986; Möller and Kvingan, 1988), and as bedding generated by pressure dissolution (Wanless, 1979). Field and petrographic aspects of parted and ribbon limestones in the Table Cove indicate that this bedding is largely defined by an early diagenetic stratification influenced by primary compositional layering and subsequently modified by pressure dissolution during burial (eg. Einsele, 1982; Ricken, 1985; Coniglio and James, 1990).

D.1 Primary Compositional Layering

Multiple hemipelagic and turbidite layers in discrete limestone beds in most ribbon limestones (Figures 5.7.d and 5.9.e) demonstrate that limestone beds do not record single depositional events. Similar layering was probably obliterated by burrowing in parted limestone and in the stratigraphically lowest ribbon limestone. Furthermore, argillaceous partings/interbeds have (or lack) sedimentary structures like those in enclosing and adjacent limestone beds, and contain similar benthic fossils. These features suggest that argillaceous layers are simply carbonate-depleted equivalents of limestone beds and that this layering records long period changes in composition of sediment delivered to the slope (Figure D.1.a).

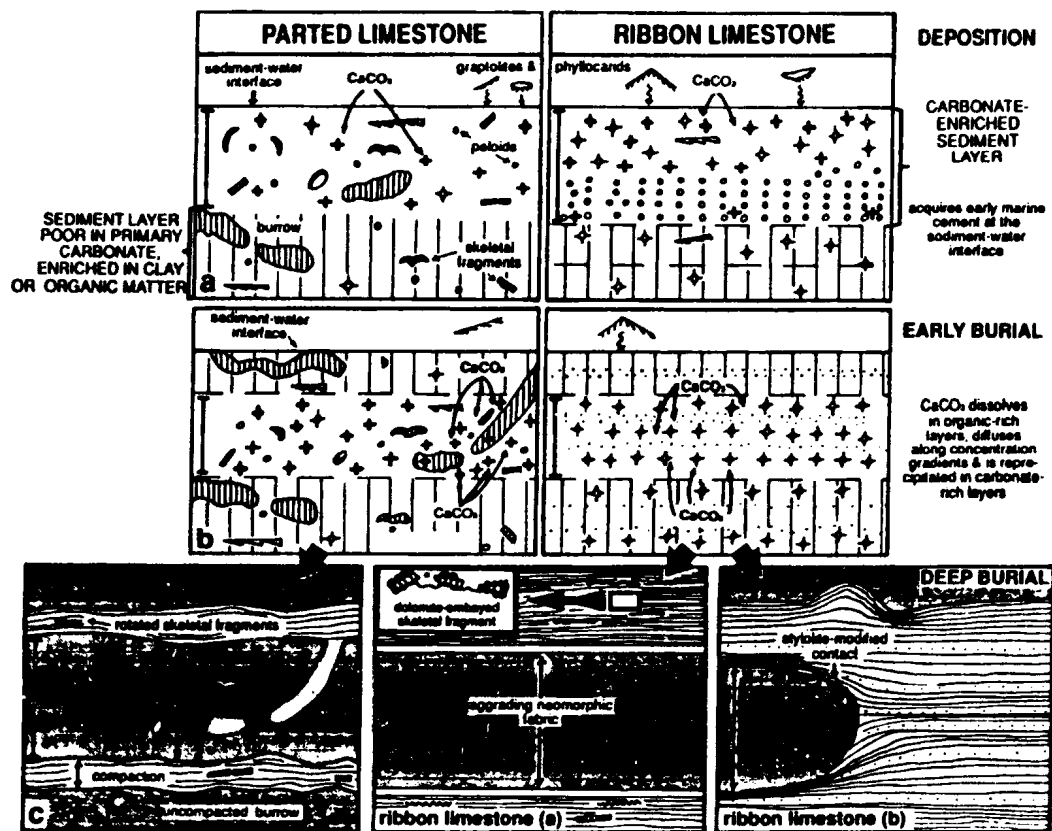


Figure D.1 Origin of bedding in parted and ribbon limestone. a) Sediment layers with different proportions of primary carbonate, clay, and/or organic matter are deposited on the slope. Carbonate-rich layers acquire CaCO_3 from seawater. b) Primary layering is accentuated by CaCO_3 redistribution in the shallow subsurface as sediments pass through diagenetic zones below the sediment-water interface. Carbonate-rich layers are lithified; carbonate-poor primary layers become more depleted of CaCO_3 . c) Mechanical compaction and pressure dissolution accentuate primary compositional layering and early diagenetic stratification. Poorly-lithified, carbonate-depleted layers are compacted and dissolved leaving insoluble residues.

Intuitively, the major compositional difference between the two primary sediment layers appears to have been the relative amounts of carbonate sediment and clay deposited. This interpretation is supported by argillaceous or silty pseudospar burrows in some limestone beds that indicate mixing of siliciclastics into limier sediment. Alternatively or in addition, there may have been periodic changes in abundance of organic matter and/or in proportions of aragonite, Mg-calcite and calcite delivered to the slope. In any case, this primary layering was retained, even in parted limestones, because of very little vertical mixing of the sediment by burrowers.

In Recent and Pleistocene deep water carbonates, repeated fluctuations in sediment composition and in the rates of carbonate production and dissolution correlate with cyclic climate changes (Hays *et al.*, 1976; Boardman and Neumann, 1984; Droxler and Schlager, 1985). Small-scale, limestone-shale rhythms in other ancient carbonate sequences have been attributed to similar, orbitally-forced, climate changes, or Milankovitch cycles (Eisele, 1982; Kauffman, 1982; Schwarzacher and Fischer, 1982; Research on Cretaceous Cycles Group, 1986). Therefore, limestone-shale rhythms in the Table Cove are also inferred to have been fundamentally controlled by climate cycles.

Table Cove sequences record sedimentation in progressively deeper slope environments and gradual elimination of shallow water carbonate sediment source areas by drowning (Chapter 5). If sedimentation was governed solely by periodic climate changes, and the sediments accumulated in an upslope- and downslope-thinning wedge or apron (Mullins and Cook, 1986), then the sedimentary sequence should show thickening then thinning of both limestone beds and argillaceous interbeds up section. Limestone beds at the top of Table Cove sequences are comparatively thin, but shale becomes the predominant lithology at the top of many of them. This implies an extraneous source of clay, most likely contributed by fine-grained suspensions generated by siliciclastic

turbidity currents operating in adjacent basinal areas, which may not have been climatically controlled.

D.2 Early Lithification

Synsedimentary deformation structures and fabrics in gravitational slides in parted and ribbon limestones indicate at least partial lithification of the sediments in the shallow subsurface (Appendix C; Figure D.2). Soft-sediment folds prove that the sediments were not totally lithified at the time of sliding. Synsedimentary faults and limestone conglomerate demonstrate that under certain conditions of stress imposed during transport sediments deformed in a brittle fashion.

Discrete clasts in pebbly conglomerate domains in slide masses are composed solely of limestone, indicating that only those sediment layers were lithified early. Open and/or undeformed burrows in many limestone beds (Figure 5.6.d.e) are also indicative of early lithification before significant burial (Shinn and Robbin, 1983). Shale partings and interbeds, in contrast, bend around and mimic topography on adjacent limestone beds, are composed of much thinner laminae than occur in adjacent limestones, and contain flattened, broken and/or rotated fossils (Figures 5.9.b.c). These features are evidence of mechanical compaction and indicate that the sediments were not lithified in the shallow subsurface. Furthermore, argillaceous layers commonly define basal detachments and internal detachments in gravitational slides (Appendix C), indicating that they were not lithified and so served as glide planes during downslope transport. The stratigraphic distribution ductile and brittle styles of deformation in gravitational slides further indicates that the degree of early lithification of precursor limestone layers decreased with increasing depth of the slope (Figure D.2; Appendix C).

Lithification may have involved precipitation of interparticle cement, but it is now manifested solely as neomorphic crystalline

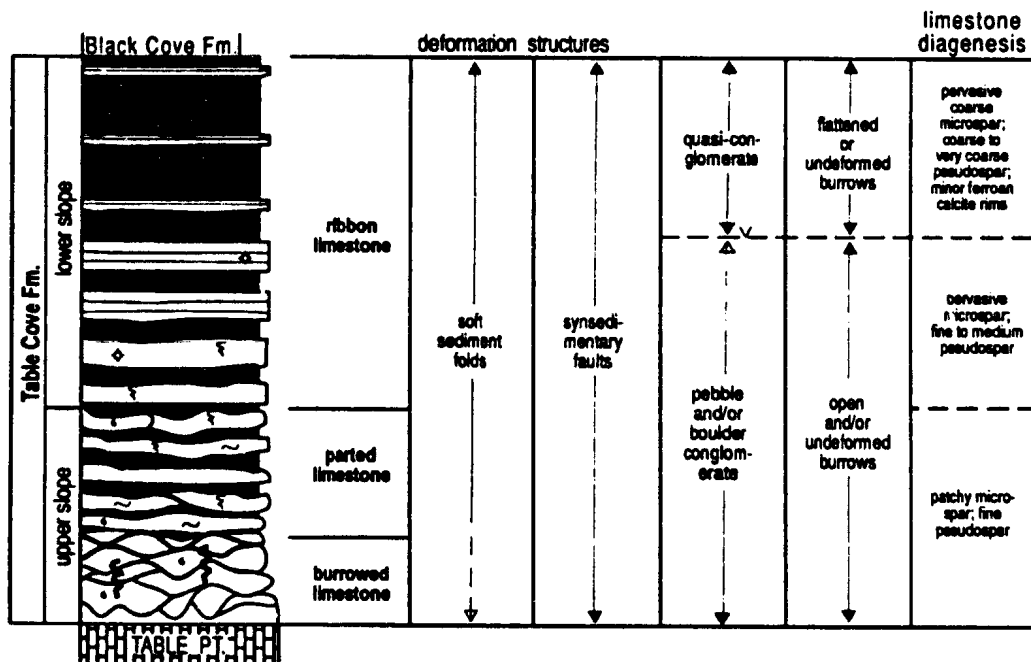


Figure D.2 Stratigraphic distribution of syndimentary deformation features and neomorphic crystal fabrics of parted and ribbon limestones in the Table Cove Formation.

fabrics. Neomorphism of micrite involves cannibalization of adjacent crystals and introduction of allochthonous carbonate; crystal size is considered an indirect measure of the distribution of carbonate nuclei in the sediment and the duration of the dissolution and precipitation processes (Bathurst, 1975). Therefore, comparatively fine microspar and pseudospar crystals in parted limestones (Figure 5.5.e) indicate numerous, closely-space nuclei and suggest that neomorphism, and hence lithification occurred rapidly. More pervasive and coarser microspar and pseudospar crystals in ribbon limestone beds (Figures 5.7.d,e and 5.9.d) suggest that primary carbonate grains that served as nuclei for precipitation were less abundant and that lithification occurred more slowly. In these sediments lithification may have been delayed because of a comparatively high concentration of clay (Zankl, 1969; Kennedy and Garrison, 1975). The stratigraphic distribution of the neomorphic fabrics, therefore, corroborates evidence from deformation features in slides that precursor limestone sediments deposited in shallower water high up on the slope were lithified more rapidly than those deposited in deeper water. A similar decrease in degree of sea floor cementation with increasing water depth occurs on the north slope of the Great Bahama Bank (Mullins *et al.*, 1980).

D.3 Diagenetic Stratification

Marginally-aggrading, neomorphic fabrics in limestone beds (Figure 5.7.e) are interpreted to reflect a decrease in the number of carbonate nuclei for calcite precipitation and record concretionary growth along upper and lower contacts of the beds (Coniglio, 1989; Möller and Kvingan, 1988). Such growth requires introduction of additional carbonate from adjacent sediments and indicates that selective, early lithification of precursor limestone beds was facilitated by precipitation of calcite from fluids originating in adjacent, precursor shale layers where CaCO_3 was concurrently being dissolved (Figure D.1.b).

Redistribution of calcium carbonate in the shallow subsurface, or 'diagenetic unmixing' (Hallam, 1986), is interpreted to occur as sediments pass through successive diagenetic zones which lie below and parallel the sediment-water interface (Eder, 1982; Möller and Kvingan, 1988; Coniglio, 1989; Figure D.3). Calcitic composition and uniformly dull luminescence signatures of neomorphic calcite crystals in the vast majority of limestone beds in both parted and ribbon limestones in the Table Cove indicate that precipitation occurred above the base of the sulphate reduction zone. However, very thin, bright luminescent, ferroan calcite rims on pseudospar crystals on the margins of some beds in ribbon limestones indicate that precipitation continued under more strongly reducing conditions, probably in the zone of fermentation. Normally the base of the sulphate reduction zone is controlled by diffusion of SO_4 down from the sediment-water interface and occurs at depths of less than 10 m below the sediment-water interface (Irwin *et al.*, 1977). In these sediments, however, it may have been partly controlled by progressive cementation of limestone layers and by the amount of organic matter in the sediments (Hesse, 1986), and so may have been only a few tens of centimetres or a few metres deep.

Variations in sediment composition which determined which sediment layers became lithified are speculative. Carbonate-rich sediment layers, because of their greater numbers of potential nuclei and perhaps greater porosity, may have acquired small quantities of cement precipitated directly from seawater which imposed a 'lithification signal' (Bathurst, 1987) that was preserved and perpetuated as the sediment passed through subsurface diagenetic zones. Sediment layers diluted by relatively high quantities of clay may not have acquired early cements either because clay particles reduced the numbers of calcite nuclei on which precipitation could occur or they mantled nuclei and prevented further precipitation (Zankl, 1969). Abundant organic matter in some sediment layers may have resulted in CO_2 build-up near the base of the

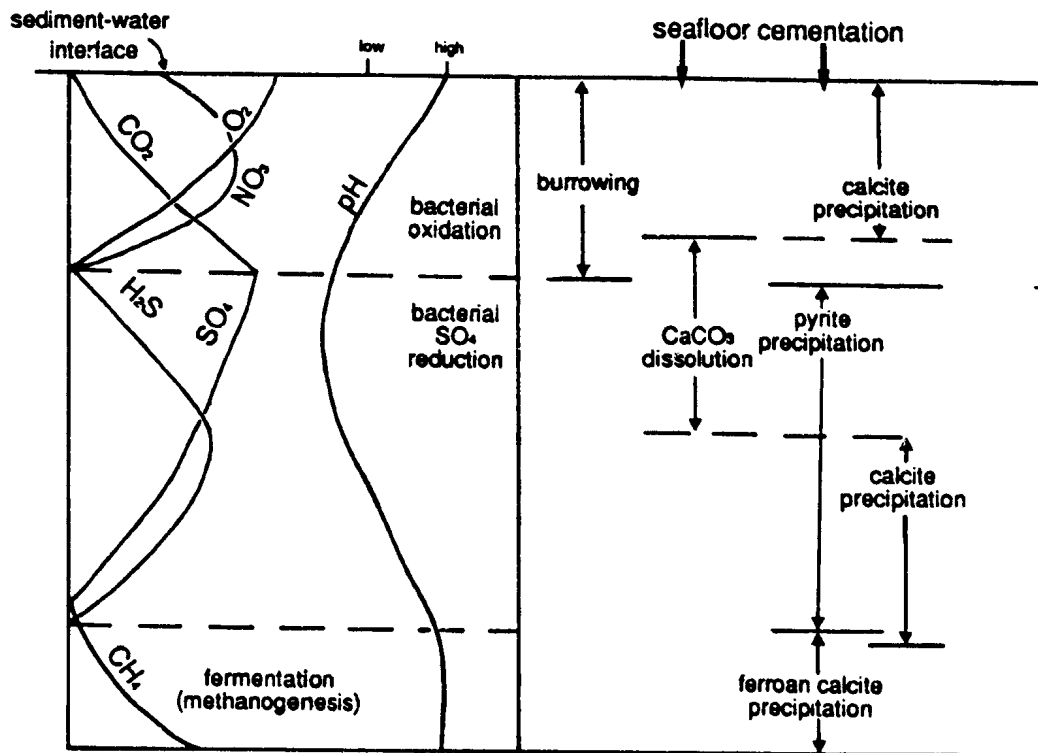


Figure D.3 Diagenetic zones, geochemical properties, and processes below the sediment-water interface (from Fenchel and Riedl (1970), Curtis (1977), Irwin *et al.* (1977) and Gautier and Claypool (1984)). Zones are defined by the manner in which organic matter is metabolized by bacteria. The thickness of the bacterial oxidation zone is determined by the depth and degree of burrowing. The base of the sulphate reduction zone is determined by diffusion of seawater SO₄ from the sediment-water interface.

bacterial oxidation zone, thereby generating acidic interstitial waters that either prevented calcite precipitation or caused dissolution.

More or less continuous limestone beds in parted limestones and in type A ribbon limestones (Figures 5.5.b and 5.7.a) indicate calcium carbonate dissolution and reprecipitation predominantly along vertical solute concentration gradients, whereas discontinuous limestone nodules in type B ribbon limestones (Figure 5.9.b) indicate vertical and lateral diffusion gradients. Although the weakly nodular fabric in parted limestones can be attributed to heterogeneity introduced by burrowing, paucity of burrows in ribbon limestones precludes a similar mechanism for the origin of stratabound limestone nodules in type B ribbon limestones. In addition, lack of evidence that tabular limestone beds are comprised of coalesced nodules (eg. vertical zones of pseudospar within limestone beds), suggests that nodular ribbon limestone sequences do not simply record incomplete carbonate redistribution. Neither a comparatively low abundance of primary carbonate sediment nor a relatively high abundance of detrital clay appear to have limited the extent of lithification. These sequences do, however, contain unusually large numbers of invertebrate fossils, and so it is postulated that high concentrations of organic matter imposed a strong, early diagenetic 'dissolution signature' that prevented more complete lithification.

D.4 Burial and Pressure Dissolution

Mechanical compaction and pressure dissolution are mostly confined to argillaceous layers that escaped early lithification (Figure D.1.c). Paucity of compaction features in limestone beds suggests that those layers were lithified before burial depths of 100 m (Shinn and Robbin, 1983). Compaction of argillaceous beds is demonstrated by flattened and/or broken skeletal fragments, and by rotated skeletal fragments and elongate silt grains parallel to bedding. Pressure dissolution is manifest by micro-stylolites that locally modify contacts between

limestone beds and argillaceous beds (Figure 5.9.c) and embayed contacts between calcite skeletal fragments and dolomite in argillaceous layers. Predominance of dolomite, quartz and feldspar silt, clays, and fine organic matter in argillaceous layers, and paucity of calcite grains, also indicates that they are insoluble residues of sediments subjected to intense pressure dissolution.

APPENDIX E

TRACE FOSSILS IN THE CAPE CORMORANT FORMATION

The following are descriptions and interpretations of trace fossils in the Cape Cormorant Formation. All occur on upper bedding planes of lithoclastic calcarenites; Planolites? also occurs on thick, mottled mudstone beds that are included as components of ribbon limestones (Table 6.1 (2)). The reader is referred to Figure 6.1.a for the Caribou Brook stratigraphic section referred to below.

E.1 ?Planolites

These are straight to slightly sinuous, sometimes branched, generally bedding-parallel burrows of variable dimension (Figure 6.12.a,i). They are a few centimetres to 40-50 cm long and 1-15 mm wide. Most are preserved in concave epirelief, or are flush with the top of the bed, and are filled with dark green carbonate silt or mud, reduced and/or dolomitized equivalents of enclosing sediment. On some beds they are preserved in convex epirelief.

?Planolites is by far the most common trace fossil in the Cape Cormorant Formation. It is interpreted as a feeding and/or locomotion burrow of a deposit-feeding organism, commonly an annelid (Häntzschel, 1975; Pemberton and Frey, 1982). The large variation in size of these burrows in the Cape Cormorant suggests they were generated by more than one type of worm. Planolites is eurybathic and euryhaline and is generally indicative of a low energy depositional regime that permitted fine, suspended sediment and organic matter to accumulate on the seafloor (Eckdale *et al.*, 1984).

Some burrows included here as Planolites may instead be Palaeophycus, a similar, but lined burrow interpreted to be the domicile and feeding burrow of a suspension-feeding organism, commonly a polychaete worm (Pemberton and Frey, 1982). Poor preservation of the

specimens precluded demonstrating that any were passively-filled, open structures in the sediment. Like Planolites, Palaeophycus is eurybathic and commonly found in fine-grained sediments, so differentiation between the two ichnogenera is not critical for environmental interpretation of these strata.

E.2 Syncoprulus (= Alcyonidiopsis)

This is a simple, slightly sinuous, subhorizontal burrow, the bottom of which is covered with elliptical, coarse sand-size, faecal pellets (Figure 6.12.b). It is uncertain whether the pellets fill the entire burrow, mantle only the floor of the burrow, or line the burrow walls. Exposed portions of the burrow are generally less than 10 cm long and 5-7 mm wide, generally. They are preserved in concave epirelief.

Syncoprulus occurs on several beds above 113 m in the Caribou Brook section. Specimens resemble Granularia (see Häntzschel, 1975, Figure 40) and Compaginathichnus (Pickerill, 1989), but are neither conspicuously branched, nor have meniscate internal structure. It is interpreted as a feeding burrow of a deposit-feeding organism (Chamberlain, 1977). Reported occurrences in other ancient siliciclastic and carbonate strata indicate it is eurybathic (eg. Chamberlain, 1977; Narbonne, 1984; Pickerill *et al.*, 1987).

E.3 Gordia marina?

This is a spaghetti-like mass of thin, smooth-walled, carbonate mud-filled, typically overlapping burrows (Figure 6.12.e). Burrows are 0.5-2 mm in diameter, are concentrated in areas 10-20 cm across, and are preserved in convex epirelief.

Gordia was recognized on only a few calcarenites in the upper 25 m of the Caribou Brook section. Pickerill (1981) interpreted it as a feeding burrow of a polychaete. The meandering-nature of the burrows is reminiscent of Helminthoida which is interpreted as a mining tunnel of a

soft-bodied, sediment ingesting invertebrate (Ksiaziewicz, 1970, Fig. 2j). Gordia is eurybathic, typically occurring in fine-grained sediments, but is particularly common to Paleozoic-age, deep water flysch (Pickerill, 1981; Narbonne, 1984; Pickerill et al., 1987; McCann and Pickerill, 1988, Figure 7).

E.4 Chondrites spp.

These are complex burrow systems consisting of a central, vertical shaft from which extends a whorl of branching, smooth-walled, gently-inclined tunnels (Figure 6.12.c,d). Three different sizes are present, possibly indicative of three different ichnospecies: i) tunnels 0.5-1 mm in diameter that form a branching network 1-1.5 cm across; ii) tunnels 3-4 mm in diameter that form a network 3-5 cm across; iii) tunnels 5-7 mm in diameter that define a fan-shaped, tunnel network 15-20 cm long and 12-15 cm wide. Most appear as clusters of small, dark green (reduced) carbonate silt or mud-filled circles and rays flush with or in concave epirelief on the bed.

Chondrites is conspicuous throughout most of the Caribou Brook section. It is interpreted as a feeding structure of a sessile, deposit-feeding organism (Häntzschel, 1975). It is eurybathic and has been documented in both siliciclastic and carbonate strata deposited in a wide range of environments, but is generally considered tolerant of low oxygen levels and therefore diagnostic of dysaerobic conditions at the sea floor (Bromley and Eckdale, 1984). Common recognition of Chondrites in the Cape Cormorant Formation by circular intersections of the upper, near vertical segments of the radiating tunnels indicates that the sediment-water interface was several millimetres (or possibly centimetres?) above the tops of the calcarenite beds.

E.5 Diplichnites

Diplichnites is a delicate surface trail consisting of two parallel

series of tracks (3.5 cm long and 1.5 cm wide), each track being 1-2 mm long, spaced 1-3 mm apart, and oriented nearly normal to the axis of the trail (for example, see Crimes, 1970, Plate 9).

Diplichnites was found in very fine-grained sediment at the top of one calcarenite at ~183 m in the Caribou Brook section. It is interpreted as the walking track of a trilobite across the sediment surface (Crimes, 1970). Reported occurrences in other ancient sequences (eg. several papers in Crimes and Harper, 1970; Pickerill, 1981; Eckdale et al., 1984; Pickerill et al., 1984a) indicate it is eurybathic; preservation of the track implies that the substrate was cohesive.

E.6 ?Diplocraterion

Burrows tentatively identified as Diplocraterion are straight, unlined and unbranched burrows filled with coarse-grained, lithoclastic sand (Figure 6.12.f). They are 7-10 mm wide and 20-55 mm long (average ~40 mm), are preserved in concave epirelief, and appear to be preferentially aligned in two directions (see Figure 6.8).

This burrow was found on the top of only one calcarenite in outcrops north of Caribou Brook equivalent to ~110 m in the Caribou Brook section (Figure 6.8.c). Although no vertical cross-sections through the structure were observed, the shape and fairly consistent length of the burrows and their apparently preferred orientation suggest it represents a cross-section through spreite of a U-shaped burrow such as Diplocraterion. Diplocraterion is interpreted as the dwelling burrow of a sessile, suspension-feeding polychaete (Goldring, 1962; Fürsich, 1974); the spreite are formed by vertical movement of the organism in the sediment. Documented occurrences of Diplocraterion in other ancient sequences indicate it is eurybathic (eg. Goldring, 1962; Ginsburg, 1975; Crimes, 1977; Eckdale et al., 1984), but is characteristically found in sandy sediments deposited in environments characterized by persistent currents and/or frequent sediment reworking. The orientation of these

burrows in the Cape Cormorant suggest they were constructed with anterior and posterior openings in up-current and down-current positions, respectively; bimodal orientations indicate two prevailing current directions.

Since the U-shape of these burrows could not be established, an alternative interpretation of these burrows is that they are segments of subhorizontal burrows such as Planolites or Palaeophycus, the apparent alignment of which may be merely coincidental.

E.7 Ichnogenus incertae type A

This is a very large, star-like trace fossil composed of a radiating whorl of straight to gently-sinuuous, rarely overlapping, bedding-parallel burrows (Figure 6.12.g). Each burrow is 1-1.5 cm wide and 35-50 cm long, and is preserved in concave epirelief. The entire radiating system is 80-100 cm in diameter. Poor preservation of the specimens precludes more detailed description.

This trace fossil occurs on the top three, possibly four calcarenites above 150 m in the Caribou Brook section. It is most similar in morphology and dimension (of both the burrows and entire burrow system) to Phoebichnus trichoides (Bromley and Asgaard, 1972) which has thus far only been documented in Mesozoic age, siliciclastic shelf sequences (Bromley and Asgaard, 1972; Bromley and Mork, 1984; Heinberg and Birkeland, 1984; Pemberton and Frey, 1984). Other diagnostic features of Phoebichnus, such as a central vertical shaft, annulated wall structure and meniscate infill, however, could not be determined for the Cape Cormorant specimens, so positive identification of the ichnogenus can not be made. Bromley and Asgaard (1972) interpret Phoebichnus as the complex feeding structure of a deposit feeder in a low-energy environment that was stationed in the central shaft and made excursions in the surrounding sediment.

This burrow system is also like other radiating traces described in

(ancient) flysch sequences in the Spain and Poland (Lucas and Rech-Frollo, 1965; Ksiazkiewicz, 1970), and has a strikingly similar Recent counterpart photographed on the deep sea floor (2000-5700 m) (see Häntzschel, 1970, Plate 1). Most of those ancient specimens, however, are smaller than the Cape Cormorant ones and commonly also have a central vertical shaft. They have been interpreted as trails of worms (Nowak, 1957) and as feeding structures of sessile bivalves (Lucas and Rech-Frollo, 1965). The origin of the more similar modern, deep-sea structure is yet uncertain, but is thought to have been produced by a large polychaete worm with many tentacles (Häntzschel, 1970).

E.8 Ichnogenus incertae type B

This burrow consists of clusters of small, sinuous, lined and possibly branched, bedding-parallel tubes (Figure 6.12.h). Each burrow is a few centimetres to ~10 cm long and are typically overlapped to form a braided stream-like pattern; inner and outer burrow diameters range from 2.5-3.3 mm and 4-4.7 mm in diameter, respectively. They are preserved in both convex and concave epirelief.

This burrow was observed on only a few calcarenites above 113 m in the Caribou Brook section. Its identity is not known. Clustering of the burrows is reminiscent of Chondrites and so it may also represent the feeding structure of a sessile, deposit feeding organism.

APPENDIX F
LITHOLOGIC DESCRIPTIONS AND CONODONT FAUNAS OF CARBONATE
LITHOCLASTS FROM THE CAPE CORMORANT FORMATION

Sixty-seven limestone and dolostone lithoclasts collected from Cape Cormorant Formation debris flow conglomerates at Caribou Brook and Big Cove were processed for conodonts using standard procedures (see summary in Harris and Sweet, 1989). Sample size depended largely on clast size, ranging from 0.2-3.5 kg; most were 1-2 kg. The list of samples processed, along with brief petrographic descriptions, and their ages as indicated by contained conodonts or inferred from composition [bracketed] are in Table F.1. [Bracketed] text in the Lithologic Description column is the original limestone composition and texture of epigenetic dolostone lithoclasts. Dolomite crystal sizes stated include: very fine/microcrystalline (0.01-<0.03 mm); fine crystalline (0.03-<0.1 mm); medium crystalline (0.1-0.2 mm); coarse crystalline (>0.2 mm). Abbreviations in the descriptions are: M, mudstone; W, wackestone; P, packstone; G, grainstone; F, floatstone; R, rudstone. Photographs of slabs and thin-section photomicrographs of several of these are in Figure 6.13.

Lists of conodonts recovered from the fossiliferous samples are in Table F.2; genera and species were identified by Felicity O'Brien (Department of Earth Sciences, Memorial University). Correlative Early Paleozoic platformal formations and members and deep-water, age equivalents in the Cow Head Group in column three were determined by comparison with Ordovician conodont faunas documented by Stouge (1981; 1982; 1984), Stouge and Boyce (1983), Stouge and Bagnoli (1988), Johnson, D. I. (1986), Ethington and Clark (1981), and Van Wamel (1974). Symbols preceding or following the names of selected species signify the following: ' - "A." iowensis is a Fauna B species; its presence may indicate it is longer ranging or possibly reworked; * = suggests Fauna

5, middle Catoche Fm., Laignet Point Mbr.; ** = suggests upper Catoche Fm.; *** = lower to upper Catoche (Stouge and Bagnoli, 1988); + = upper Boat Harbour Fm. below the "pebble bed" (see Stouge and Boyce, 1983, Figure 6); ++ = Bed 9 species; +++ = uppermost Bed 9 through most of Bed 11 in the Cow Head Group, earliest Arenig Paroistodus proteus zone. Early Ordovician conodont Faunas 1-5 are defined by Stouge (1982). Early Ordovician conodont Faunas A-E are defined by Ethington and Clark (1971). The letters A₁-A₅ refer to lithologic units defined by Stouge (1981, Fig. 3.2) in the Table Point Formation at Table Point. A₁ and A₂ correspond to the Basal Peritidal Unit of the Table Point; A₃ corresponds to the Middle Subtidal Unit and the sponge-oncolite biostrome of the Upper Subtidal Unit.

The reader is referred to Figure 6.15 for the stratigraphic column of the Cambro-Ordovician platformal sequence and to sections in James and Stevens (1986) for the coeval, deep-water Cow Head Group sequence.

**Table F.1 Lithoclasts Processed For Conodonts
(Cape Cormorant Formation)**

Sample Number and Mass	Lithologic Description	Age, Correlative Formation/Member
CB338 1.5 kg	Light brown, medium crystalline dolostone; nonferroan crystals with ferroan overgrowths 1) quartz, and 2) ferroan calcite intercrystalline cement. [oolitic-peloidal(?) G]	Barren [Cambrian]
CB33C 2.6 kg	Light green, fine-crystalline silty, peloidal dololaminite; ferroan crystals with minor chert intercrystalline cement.	Barren [?]
CB33D 0.4 kg	Green and tan, fine and medium-crystalline dolostone; nonferroan crystals with ferroan overgrowths, minor chert/chalcedony and abundant pyrite intercrystalline cement. [intraclastic, peloidal G with glauconite peloids, quartz silt, scattered ooids, and inarticulate brachiopod fragments]	Barren [Cambrian]
CB33E 0.9 kg	Grey, partly dolomitized, laminated M and quartz silty calcisiltite with minor glauconite and a glauconite and a few inarticulate brachiopod fragments.	Barren [Cambrian?]
CB33F 1.1 kg	Brown, medium to coarsely-crystalline dolostone; nonferroan crystals with megaquartz intercrystalline cement. [oolitic G]	Barren [Cambrian]
CB33G 1.7 kg	Light brown, intraclastic F with a peloidal G matrix with pelmatozoan and trilobite fragments; intraclasts of peloidal P and G \pm silty.	Latest Tremadoc Watts Bight Fm.
CB33H 0.7 kg	Grey, very fine, peloidal G with inarticulate brachiopod, echinoderm, and trilobite fragments and minor muscovite, biotite and glauconite; fine-laminated and partly replaced by ferroan dolomite.	Barren [Cambrian Cape Ann Mbr.? of Petit Jardin Fm.]
CB33I 3.5 kg	Mottled, fine-crystalline, sandy dolostone (off white, light brown, light grey-brown, green-grey, dark grey); nonferroan crystals with ferroan overgrowths. [fine, sandy ?peloidal G and laminated M with peloidal? G intraclasts and coarse-grained, quartz sand, fine, angular quartz silt, and minor glauconite, mica, and inarticulate brachiopods]	Barren [Cambrian]
CB33K 0.7 kg	Light tan, very fine peloidal G with trilobite, echinoderm, and mollusc fragments an <u>Nuia</u> .	Arenig Catoche Fm.
CB33L 1.3 kg	Medium brown, coarsely-crystalline dolostone; nonferroan crystals with ferroan overgrowths and 1) chert/chalcedony and 2) ferroan calcite intercrystalline cement. [syndimentarily fractured, laminated peloidal G (?) with M intraclasts and minor echinoderm fragments]	Barren [Cambrian?]
CB33M 0.8 kg	Very light brown, burrowed?, peloidal, intraclastic P with echinoderm, trilobite and sponge? fragments; pervasive neomorphism to microspar.	early to mid Arenig Catoche Fm.

Table F.1 continued

CB33W 0.3 kg	Intraclastic R with fine, peloidal, fossiliferous G matrix with fragments of inarticulate brachiopods, echinoderms and trilobites. Intraclasts of M, very fine peloidal G and peloidal, fossiliferous G. Patchily replaced by chalcedony and nonferroan dolomite. Similar to 0714-5.	Barren [?]
CB33O 0.9 kg	Light brown, fine-crystalline, sandy dolostone; nonferroan crystals with minor ferroan overgrowths and 1) chert and 2) ferroan calcite intercrystalline cement. [sandy, peloidal, intraclastic G with scattered ooids and minor glauconite]	Barren [Cambrian]
CB33P 1.0 kg	Mottled, light and medium brown, burrowed (dolomite) peloidal, fossil-bearing W/P with echinoderm, articulate brachiopod, ostracode, mollusc fragments, sponge spicules, <u>Girvanella</u> and <u>Nuia</u> ; similar to #396	Barren [Lower Ordovician, Catoche Fm.? or Boat Harbour Fm.]
CB 82 0.5 kg	Light brown and grey, fine intraclastic (very fine pyrite-defined) R/F with peloidal, fossiliferous W/P/G matrix bearing fragments of echinoderms, trilobites, and molluscs. Pervasively neomorphosed to microspar/pseudospar and partly replaced by nonferroan dolomite and silica.	Arenig lower to middle Catoche fm.
63 0.2 kg	Light brown, fine-crystalline sandy dolostone; nonferroan crystals with ferroan overgrowths and 1) megaquartz and 2) ferroan calcite intercrystalline cement. [peloidal, intraclastic, oolitic G with minor rounded quartz sand, echinoderm and trilobite fragments]	Barren [Cambrian]
66 0.1 kg	Brown and grey, very coarsely-crystalline, sandy dolostone; nonferroan crystals with ferroan overgrowths and 1) chert and 2) ferroan calcite intercrystalline cement. [quartzose, peloidal G with intraclasts, ooids, echinoderm fragments, and glauconite peloids]. Similar to 0714-7.	Barren [Cambrian]
77 1.0 kg	Brown and black clotted, peloidal, intraclastic, fossiliferous W with peloidal, intraclastic G patches with fragments of trilobites, gastropods, echinoderms, articulate brachiopods, sponge spicules, <u>Girvanella</u> , and <u>Halysis</u> (?) (all partially silicified and pyritized. (?thrombolite)	early Arenig Boat Harbour Fm.
112 0.4 kg	Mottled light grey and light brown, medium-crystalline dolostone; nonferroan crystals with ferroan overgrowths and 1) chert and 2) ferroan calcite intercrystalline cement. [oolitic, peloidal, intraclastic P/G]	Barren [Cambrian]
121 1.0 kg	Mottled medium brown and light brown, finely-crystalline dolostone; nonferroan crystals with nonferroan inter-crystalline cement. [oolitic G partly replaced by chert and chalcedony]	Barren [Cambrian]
143 0.5 kg	Mottled, medium brown-grey and dark brown-grey, silty, medium-crystal line dolostone; nonferroan crystals with chert intercrystalline cement. [uncertain original composition]	Barren [?]
149 0.2 kg	Pale army green, medium-crystalline dolostone; nonferroan crystals with ferroan rims, nonferroan overgrowths and chert intercrystalline cement. [uncertain original composition, G?]	Barren [?]

Table F.1 continued

158 1.4 kg	Light green, fine- to coarse-crystalline dolostone; nonferroan coarse crystals and ferroan fine crystals. [dololaminite breccia (vague) with minor quartz silt]	Barren [?]
173 ---	Brown, medium-crystalline dolostone; nonferroan crystals with 1) chert and 2) ferroan calcite intercrystalline cement. [oolitic (or peloidal) G]	Barren [Cambrian?]
192 0.7 kg	Mottled tan and pale army green, peloidal P with echinoderm, trilobite, gastropod, articulate brachiopod and <i>Girvanella</i> fragments; partly replaced by fine-crystalline, nonferroan dolomite.	Llanvirn Table Point Fm.
211 1.0 kg	Dark steel grey, slightly silty, fine- to medium-crystalline dolostone; nonferroan crystals with minor ferroan overgrowths and chert intercrystalline cement. [uncertain original composition, ?burrowed M/W]	Barren [?]
246 1.1 kg	Medium brown, medium-crystalline dolostone; nonferroan crystals with calcite cores. [finely laminated M(?)]	Barren [?]
261 1.1 kg	Light brown and blue grey (mottled), fossiliferous, burrowed W with fragments of sponge and spicules, articulate brachiopod and trilobite, echinoderm fragments, and <i>Girvanella</i> . Mostly replaced by fine-crystalline, nonferroan dolomite.	middle Arenig middle Catoche Fm.
263 1.7 kg	Light green and tan mottled, fine- to medium-crystalline dolostone; nonferroan crystals with with local ferroan calcite intercrystalline cement. [syndimentarily fractured M?]	Barren [?]
270 1.7 kg	Dark green-grey, intraclastic R with intraclastic, peloidal, fossil-bearing matrix; scattered ooids, fragments of echinoderms and trilobites and minor glauconite; intraclasts with ooids and quartz sand.	Barren [Cambrian]
297 0.3 kg	Mottled light brown and dark grey, burrowed, fossil-poor W with articulate brachiopod fragments. Mostly replaced by fine-crystalline, nonferroan dolomite.	early Arenig Catoche Fm.
302 1.1 kg	Dark grey brown, medium-crystalline dolostone; nonferroan crystals with minor chert intercrystalline cement. [peloidal-oolitic G with minor glauconite]	Barren [Cambrian]
395 1.0 kg	Speckled tan, white and brown grey, partly partly dolomitized, peloidal, intraclastic, fossiliferous P-G with echinoderm, trilobite, gastropod and articulate brachiopod fragments with pyritized rims. Thrombolite macrostructure.	early Arenig Boat Harbour Fm.
396 0.9 kg	Light grey and brown, burrow-mottled?, peloidal W with fragments of echinoderms, articulate brachiopods, molluscs, trilobites and <i>Girvanella</i> . Partly replaced by fine-crystalline, nonferroan dolomite.	early Arenig Boat Harbour Fm.
424 0.4 kg	Light brown, medium-crystalline dolostone; nonferroan crystals with ferroan calcite cores. [?fine peloidal G]	Barren [?]

Table F.1 continued

452 0.6 kg	Dark grey and black, peloidal, intraclastic, oolitic G with scattered round quartz sand and minor glauconite and echinoderm fragments.	Barren [Cambrian]
453 0.2 kg	Light brown, sandy, fine- to medium-crystalline dolostone; nonferroan crystals with ferroan crystals with ferroan overgrowths and chert intercrystalline cement. [quartzose, intraclastic, oolitic G]	Barren [Cambrian]
480 1.0 kg	Dark grey, fine, peloidal, intraclastic G with scattered ooids, quartz silt and echinoderm and trilobite fragments. Partly replaced by nonferroan dolomite.	Arenig lower to upper Catoche Fm.
515 0.2 kg	Dark grey-brown, medium- to coarsely crystalline dolostone; nonferroan crystals with nonferroan cement. [laminated, fine peloidal G(?)]	Barren [?]
536 0.2 kg	Light grey, fine- and medium-crystalline dolostone; nonferroan crystals with minor ferroan overgrowths and ferroan calcite intercrystalline cement. [syndimentarily cracked M with peloidal, intraclastic G-filled cracks with minor echinoderm fragments and ooids]	Barren [Cambrian?]
537 0.3 kg	Dark grey, fine- to medium-crystalline, silty dololaminite; nonferroan crystals with minor ferroan overgrowths and ferroan calcite intercrystalline cement. [M and quartz silty calcisiltite with minor glauconite, mica, and inarticulate brachiopod fragments]	Barren [Cambrian?, Cape Ann Mbr.?)
567 1.6 kg	Light grey, fine-crystalline dolostone; nonferroan crystals with minor ferroan overgrowths and calcite intercrystalline cement. [oolitic, intraclastic G with minor glauconite and quartz silt]	Barren [Cambrian]
583 0.5 kg	Medium brown, medium-crystalline dolostone; nonferroan crystals with ?dedolomitized ferroan calcite cores and minor chert intercrystalline cement. [laminated M or very fine peloidal G] Similar to C833L.	Barren [?]
0713-3 1.4 kg	Peloidal, intraclastic G/P with <u>Girvanella</u> , sponge spicules and orthoconic cephalopods. Partly replaced by nonferroan dolomite, pyrite and chalcidony.	Arenig? Catoche Fm.?
0714-5 2.2 kg	Peloidal, intraclastic P/G with abundant trilobite, echinoderm, and mollusc fragments and <u>Girvanella</u> . Partly replaced by medium-crystalline, nonferroan dolomite and chalcidony. Similar to 0830-7.	Arenig Catoche Fm.
0714-6 1.7 kg	Medium brown, fine-crystalline, sandy dolostone; nonferroan except for very finely-crystalline ferroan dolomite intraclasts. [Quartzose, peloidal, intraclastic P/G and peloidal, quartzose sandstone; bimodal quartz (very fine and very coarse; simple, chert, strained and coarse polycrystalline)] Similar to C833L.	Barren [Cambrian]

Table F.1 continued

0714-7 2.7 kg	Dark brown and green, very coarsely-crystalline dolostone; nonferroan crystals with very fine ferroan dolomite intraclasts. [Glaucopitic, echinoderm-rich, intraclastic G with a few ooids and inarticulate brachiopod fragments] Similar to #66.	Barren [Cambrian]
0718-5 2.0 kg	Light brown-grey, stylo-nodular, peloidal, fossiliferous, burrowed W/P with echinoderm, trilobite, mollusc and <u>Nuia</u> fragments.	early Arenig? Catoche Fm.?
0724-1 1.9 kg	Dark grey, intraclastic F with a silty, peloidal G matrix with minor echinoderm fragments and other unidentifiable fossils. Similar to #480.	Barren [Arenig?]
0724-4 2.1 kg	Off white, laminated M. Partly replaced by medium- to coarse-crystalline, nonferroan dolomite.	early Arenig Catoche Fm.
0724-6 0.9 kg	Mottled brown and grey, partly dolomitized, peloidal, intraclastic, fenestral G/P with trilobite, mollusc and ostracode fragments and <u>Girvanella</u> .	Barren [Ordovician, Table Point Fm.?
0724-7 2.1 kg	Tan with grey, swirly-mottled, microcrystalline pattern dolomite; nonferroan crystals. 'Pattern' defined by diffuse concentrations of very fine pyrite.	Barren [Cambrian, Berry Head Fm.?
0724-8A 2.0 kg	Light brown, partially dolomitized, peloidal, intraclastic, fossiliferous P/G with laminated internal sediment; trilobite, gastropod and echinoderm fragments commonly with pyritized rims. Thrombolite macrostructure.	early to middle Arenig Catoche Fm.
0724-8B 1.9 kg	Very light brown, peloidal, fossiliferous W/P/G with spiculitic sponges, echinoderm, mollusc, bite and ostracode fragments.	early Arenig lower Catoche Fm.
0727-2 2.3 kg	Light grey, spiculitic M with (tan) dolomitized burrows and scattered mollusc and trilobite fragments.	late Tremadoc/ early Arenig Boat Harbour Fm.
0727-3 1.9 kg	Light brown, dark brown and blue-grey mottled thrombolite; partly dolomitized, spiculitic, peloidal, fossiliferous W/P with sponges, echinoderms, trilobites, molluscs, and <u>Girvanella</u> and peloidal P mottles. Dolomite with calcite cores.	early to middle Arenig lower to middle Catoche Fm.
0727-8 2.3 kg	Mottled light brown and grey brown, fossil-poor M with fragments of trilobites, ostracodes, and articulate brachiopods and peloidal, intraclastic P/G laminae.	late Tremadoc Watts Bight Fm.
0727-10 2.4 kg	Light grey-brown, fine- to medium-crystalline dolostone; nonferroan crystals with calcite cores and minor calcite intercrystalline cement. [burrowed M with peloidal, intraclastic G laminae; fossil mouldic]	Barren [Arenig?]
0830-4 2.3 kg	Brown and tan mottled M. Partly replaced by medium- to coarse-crystalline, nonferroan dolomite.	Arenig - Llanvirn Table Point Fm. possibly Catoche Fm.
0830-7 2.0 kg	Mottled light brown, tan and blue-grey, peloidal, intraclastic P with fragments of gastropods, trilobites and echinoderms and sparse ooids.	early Arenig lower to middle Catoche Fm.

Table F.1 continued

0830-8 2.4 kg	Very dark grey, intraclastic R with glauconitic oolitic G matrix; intraclasts of very fine, silty peloidal G; ooid nuclei of trilobite, echinoderm and inarticulate brachiopod fragments; similar to #270. Partly replaced by coarsely-crystalline ferroan dolomite.	Sarren [Cambrian?]
0830-9 1.6 kg	White peloidal-intraclastic, fenestral P with small trilobite fragments.	Arenig - Llanvirn Table Point Fm. possibly Catoche Fm.
0831-2 2.0 kg	Mottled light brown and yellow-white, peloidal, intraclastic-fossiliferous W-P with fragments of echinoderms, trilobites, molluscs, <u>Nuia</u> , <u>Girvanella</u> and micritized spicules; partly dolomitized and partly silicified.	early Arenig Catoche Fm.
0831-4 2.5 kg	Light brown-grey, fine intraclastic R with a peloidal G matrix bearing few trilobite and echinoderm fragments.	latest Tremadoc Watts Bight Fm.
0831-6 2.3 kg	Mottled mound lithofacies limestone: light grey, burrowed, fossiliferous W with light brown peloidal, fossiliferous P mottles with trilobite, echinoderm, mollusc, ostracode, articulate brachiopod fragments and <u>Girvanella</u> . Small stromatolite cavities with internal sediment and cement.	Llanvirn Table Point Fm.
0831-7 2.3 kg	Grey-brown, stylo-nodular, interbedded very fine peloidal G and peloidal, spiculitic W/P with trilobite, <u>Nuia</u> , and <u>Girvanella</u> , molluscs, echinoderms and ostracodes.	Llanvirn? Table Point Fm.? possibly Catoche Fm.
CB-COC 1.5 kg	Mottled light brown and tan, partly dolomitized, peloidal, intraclastic P and fossil-poor W/M with small gastropods.	Arenig [Catoche Fm. or possibly Boat Harbour Fm.]

Table F.2 Conodont Faunal Lists
(Cape Cormorant Formation Lithoclasts)

Sample Number	Conodont Faunal List	Age, Correlative Platformal Formation or Member & Cow Neoc Group Units (e)
CB33G	<u>Loxodus bransoni</u> Furnish s.f. <u>Acanthodus uncinatus</u> Furnish s.f. <u>Eucharodus parallelus</u> (Branson and Mehl)++ "Acontiodus" cf. <u>A. iowensis</u> s.f. "Acontiodus" <u>staufferi</u> Furnish s.f. <u>Rossodus manitouensis</u> Repetski and Ethington <u>Scolopodus</u> sp. <u>Cordylodus intermedius</u> Furnish <u>Variabiliconus</u> sp.	late Tremadoc Fauna C Watts Bight Fm. ● Bed 8
CB33K	<u>Eucharodus parallelus</u> (Branson and Mehl)++ <u>Glyptoconus quadraplicatus</u> (Branson and Mehl)	Arenig Faunas 3/4;D Catoche Fm. ● Bed 9
CB33M	<u>Oneotodus simplex</u> Ethington and Brand <u>Glyptoconus quadraplicatus</u> (Branson and Mehl)	early - middle Arenig Faunas 3/4;D Catoche Fm. ● Bed 9
CB82	<u>Oneotodus costatus</u> "Scolopodus" <u>emarginatus</u> Barnes and Tuke <u>Drepanoistodus</u> sp. <u>Tropodus comptus</u> (Branson and Mehl) <u>Tropodus sweeti</u> (Serpagli) <u>Glyptoconus quadraplicatus</u> (Branson and Mehl) <u>Parapanderodus gracilis</u> (Ethington and Clark)+++	early - middle Arenig Faunas 3/4;D lower - middle Catoche Fm. ● Beds 9-11
#77	<u>Cornuodus longibasis</u> Lindström <u>Oneotodus</u> sp. <u>Drepanoistodus</u> sp. <u>Drepanodus gracilis</u> (Branson and Mehl) s.f. <u>Macerodus dianae</u> Fähræus and Nowlan+ <u>Juanognathus</u> sp. <u>Drepanodus? arcuatus?</u> Pander* "Acontiodus" <u>iowensis</u> Furnish <u>Oistodus</u> sp.	early Arenig Faunas 2;D Boat Harbour Fm.? ● Bed 8
#192	<u>Drepanoistodus</u> sp. <u>Parapanderodus arcuatus</u> Stouge	Llanvirn Table Point Fm.
#261	<u>Depikodus communis</u> (Ethington and Clark)*** <u>Parapaltodus</u> sp. <u>Fähræusodus marathonensis</u> (Bradshaw) <u>Tropodus sweeti</u> (Serpagli) <u>Oistodus multicorugatus</u> Harris <u>Juanognathus variabilis</u> Serpagli	middle Arenig Faunas 4/5 middle Catoche Fm. ● Beds 9-11
#297	<u>Glyptoconus quadraplicatus</u> (Branson and Mehl)	middle - upper Arenig Faunas 3/4;D upper Boat Harbour Fm./ Catoche Fm. ● Beds 8-9
#395	<u>Depikodus communis</u> Ethington and Clark*** <u>Drepanodus gracilis</u> (Branson and Mehl) s.f. <u>Eucharodus parallelus</u> (Branson and Mehl)++ <u>Glyptoconus quadraplicatus</u> (Branson and Mehl) <u>Acodus</u> sp. <u>Macerodus dianae</u> Fähræus and Nowlan+ <u>Ulrichodina</u> sp. <u>Tropodus sweeti</u> (Serpagli)	Arenig Faunas 2/4;D upper Boat Harbour Fm./ lower Catoche Fm. ● Beds 8 & 9

Table F.2 continued

#396	<u>Tropodus sweeti</u> (Serpagli)	early - middle Arenig Faunas 3/4 Boat Harbour or Catoche Fm. ● Beds 9 -11
#480	<u>Diaphrodus delicatus</u> (Branson and Mehl) <u>Tropodus comptus</u> (Branson and Mehl) <u>Acodus</u> sp. <u>Glyptoconus quadraplicatus</u> (Branson and Mehl) <u>Eucharodus parallelus</u> (Branson and Mehl)** <u>Oepikodus communis</u> (Ethington and Clark)***	Arenig Fauna 4;D Catoche Fm. ● Bed 9
0713-3	juvenile simple cones	Arenig?
0714-5	<u>Eucharodus parallelus</u> (Branson and Mehl)** <u>Glyptoconus quadraplicatus</u> (Branson and Mehl) <u>Oneotodus costatus</u> Ethington and Brand	early Arenig Faunas 3/4;D lower Catoche Fm. ● Bed 9
0718-5	<u>Tropodus comptus</u> (Branson and Mehl)	early Arenig? Fauna D ● Bed 9
0724-2	<u>Oepikodus communis</u> (Ethington and Clark)***	Arenig Faunas 4;D Catoche Fm. ● upper Bed 9
0724-4	<u>Drepanodus arcuatus</u> Pander* <u>Scolopodus? peselephantis</u> Lindström <u>Eucharodus parallelus</u> (Branson and Mehl)** <u>Parapanderodus elegans</u> Stouge <u>Drepanodus? gracilis</u> (Branson and Mehl) sensu Stouge 1984 <u>Oepikodus communis</u> (Ethington and Clark)***	early Arenig Faunas 4/5;D lower - middle Catoche Fm. ● Beds 9-11
0724-6	undiagnostic simple cones	-----?
0724-8A	<u>Tropodus sweeti</u> (Serpagli) <u>Prioniodus</u> sp. <u>Oepikodus communis</u> (Ethington and Clark)*** <u>Eucharodus parallelus</u> (Branson and Mehl)** <u>Drepanoistodus</u> sp. <u>Glyptoconus quadraplicatus</u> (Branson and Mehl) <u>Parapanderodus gracilis</u> Ethington and Clark***	early - middle Arenig Faunas 3/4;D lower middle Catoche Fm. ● Beds 9-11
0724-8B	<u>Juanognathus ?serpagli</u> Stouge <u>Tropodus sweeti</u> (Serpagli) "Accontiodus" <u>staufferi</u> Furnish s.f. "Scolopodus" <u>emarginatus</u> Barnes and Tuke <u>Trigonodus rectus</u> Stouge**	Arenig Fauna D Catoche Fm. ● Beds 9-11
0727-2	<u>Macerodus dianee</u> Fähræus and Nowlan†	late Tremadoc - earliest Arenig Fauna 2 Boat Harbour Fm. ● Bed 8
0727-3	<u>Eucharodus parallelus</u> (Branson and Mehl)** <u>Drepanodus gracilis</u> (Branson and Mehl) s.f. "Scolopodus" <u>emarginatus</u> Barnes and Tuke ?"Scandodus" <u>pseudoramus</u> <u>Oneotodus</u> sp. <u>Glyptoconus quadraplicatus</u> (Branson and Mehl)	early - middle Arenig Faunas 3/4;D lower - middle Catoche Fm. ● Beds 9-11

Table F.2 continued

0727-8	<u>Clavohamulus densus</u> Furnish <u>Macerodus diana</u> e Fähræus and Nowlan+ <u>Semiancontiodus</u> sp. <u>Loxodus bransoni</u> Furnish s.f.	late Tremadoc Faunas 2;C Watts Bight Fm. ● Bed 8
0830-4	<u>Trigonodus rectus</u> Stouge**	Arenig/Llanvirn units A.1 & A.2 of the Table Point Fm., possibly the Catoche Fm.?
0830-7	<u>Tropodus sweeti</u> (Serpagli) <u>Eucharodus parallelus</u> (Branson and Mehl)++ <u>Drepanodus gracilis</u> (Branson and Mehl) s.f. <u>Ulrichodina</u> sp. <u>Drepanodus arcuatus</u> Pander* <u>Glyptocoelus quadruplicatus</u> (Branson and Mehl) <u>Tropodus comptus</u> (Branson and Mehl) <u>Paraserratognathus abruptus</u> Repetski	early Arenig Faunas 3/4;D lower - middle Catoche Fm. ● Beds 9-11
0830-9	<u>Trigonodus rectus</u> Stouge**	Arenig/Llanvirn units A.1 & A.2 of the Table Point Fm., possibly the Catoche Fm.
0831-2	<u>Tropodus comptus</u> (Branson and Mehl) <u>Drepanoistodus</u> sp. <u>Oreotodus</u> sp. <u>Eucharodus parallelus</u> (Branson and Mehl)++ <u>Scolopodus? peselephantis</u> Lindström <u>Glyptocoelus quadruplicatus</u> (Branson and Mehl) <u>Oepikodus communis</u> (Ethington and Clark)*** <u>Tropodus sweeti</u> (Serpagli) "Scolopodus" <u>emarginatus</u> Barnes and Tuke <u>Drepanodus gracilis</u> (Branson and Mehl) s.f.	early Arenig Faunas 4/5;D/E middle Catoche Fm. ● Beds 9-11
0831-4	<u>Clavohamulus densus</u> Furnish "Acontiodus" <u>staufferi</u> Furnish s.f. <u>Loxodus bransoni</u> Furnish <u>Variabiliconus bassleri</u> (Furnish)++ <u>Rossodus</u> cf. <u>manitouensis</u> Repetski and Ethington	late Tremadoc Fauna C Watts Bight Fm. ● Bed 8, lower 9
0831-6	<u>Ansella jemtlandica</u> (Löfgren) <u>Histiodelle tableheadensis</u> Stouge <u>Drepanoistodus basiovalis</u> Sergeeva <u>Juanognathus serpaglii</u> Stouge <u>Protopanderodus</u> sp. <u>Paraistodus originalis</u> Sergeeva	Llanvirn unit A.2 of the Table Point Fm.
0831-7	<u>Tropodus comptus</u> (Branson and Mehl) <u>Oreotodus</u> sp. <u>Parapanderodus</u> sp. <u>Paraistodus originalis</u> Sergeeva <u>Juanognathus serpaglii?</u> Stouge	Llanvirn? Table Point Fm.?
CB-COC	<u>Oreotodus simplex</u> Ethington and Brand	early Arenig Fauna 0? Boat Hbr. Fm. or basal Catoche Fm. ● Bed 8?

Key to symbols: * = suggests Fauna 5, middle Catoche Fm., Laignet Point Mbr.; ** = suggests upper Catoche Fm.; *** = lower to upper Catoche in Stouge and Bagnoli (1989); + = upper Boat Harbour Fm. below the 'pebble bed'; ++ = Bed 9 species; +++ = uppermost Bed 9 through most of Bed 11, earliest Arenig, Paraistodus proteus zone

APPENDIX G
LITHOLOGIC DESCRIPTIONS AND CONODONT FAUNAS OF CARBONATE
LITHOCLASTS AND WHOLE ROCK SAMPLES FROM
THE DANIEL'S HARBOUR MEMBER

Twenty-one limestone, dolostone and siliciclastic lithoclasts and five whole rock samples from Daniel's Harbour Member conglomerates, plus one whole rock sample of Daniel's Harbour Member calcarenite were processed for conodonts using standard procedures (see summary in Harris and Sweet, 1989). Sample size depended on clast size, ranging from 0.7-2.4 kg; most were ~2 kg. The list of samples processed (sample number, collecting locality and size), along with brief lithologic descriptions, a list of conodonts recovered, and interpreted correlative formation are in Table G.1. Conodont genera and species were identified by Felicity O'Brien (Department of Earth Sciences, Memorial University). Correlative formations were determined by comparison with Ordovician conodont faunas documented by Stouge (1981; 1982; 1984), Stouge and Boyce (1983), Stouge and Bagnoli (1988), Johnson, D. I. (1986), Ethington and Clark (1981), and Van Wamel (1974). The letters A₁-A₃ and B₁-B₄ (under Correlative Formation) refer to lithologic units defined by Stouge (1981, Fig. 3.2) in the Table Point and Table Cove formations, respectively, at Table Point. A₁ and A₂ correspond to the Basal Peritidal Unit of the Table Point; A₃ corresponds to the Middle Subtidal Unit and the sponge-oncolite biostrome of the Upper Subtidal Unit; B₁ corresponds to the burrowed limestone lithofacies of the Table Cove; B₂ through B₄ correspond to the ribbon limestone lithofacies. Abbreviations for sample localities are as follows: BC, Black Cove; PIC, Piccadilly Roadcut; NARM, Northern Arm peninsula; PBAY, west Pistolet Bay; DH, Daniel's Harbour; CP, Clifty Point; EH, Eastern Head; WBC, West Bay Centre Quarry; PCP, Portland Creek Pond.

Table G.1 Lithologies and Conodont Faunas of Danie's Harbour
Member Clasts and Whole Rock Samples

Sample No. Locality 2 Mass		Correlative Formation
	Grey-brown, fossiliferous and/or peloidal limestone	
0726-13 (BC) 2.2 kg	Common out-sized boulder; grey-brown, burrowed, fossiliferous, peloidal, intraclastic wackestone with trilobites, ostracodes, echinoderms, bryozoans, <u>Nuis</u> , <u>Halysis</u> , <u>Girvanella</u> , and <u>Hetheredella</u> .	
	<u>Anella jemtlandica</u> (Löfgren) <u>Drepanodus arcuatus</u> Pander <u>Juanognathus serpaglii</u> Stouge <u>Loxodus? curvatus</u> Stouge <u>Parapaltodus simplicissimus</u> Stouge <u>Parapanderodus arcuatus</u> Stouge <u>Scalpellodus pointensis</u> Stouge <u>Semiacontiodus asymmetricus</u> Barnes and Poplawski	uppermost Table Point Fm., lower Table Cove Fm.* (mid A ₁ -B ₁)
	* <u>J. serpaglii</u> is not reported above B ₁ .	
0828-5 (BC) 2.2 kg	Common out-sized boulder; grey-brown, burrowed, fossil-poor wackestone with ostracodes, trilobites, echinoderms, bryozoans, gastropods, and sponge spicules, and <u>Girvanella</u> .	
	<u>Cordylodus? horridus</u> Barnes and Poplawski <u>Juanognathus</u> sp. <u>Loxodus? curvatus</u> Stouge <u>Parapanderodus arcuatus</u> Stouge <u>Periodon aculeatus</u> Hadding <u>Scolopodus oldstockensis</u> Stouge	lower Table Cove Fm.* (B ₁)
	* <u>S. oldstockensis</u> is reported only from B ₁ .	
0708-14 (PIC) 1.7 kg	Common, out-sized boulder; light brown, peloidal, very fossiliferous wackestone with ostracodes, trilobites, echinoderms, brachiopods, gastropods, sponge spicules, <u>Girvanella</u> , <u>Halysis</u> .	
	? <u>Erraticodon balticus</u> Dzik	Table Point Fm., lowermost Table Cove Fm. (A ₁ -lowest B ₁)
0811-11 (NARM) 1.7 kg	Boulder; grey-brown, burrowed, peloidal, intraclastic, fossiliferous wacke-/packstone (stylo-bedded) with ostracodes, trilobites, echinoderms, brachiopods, molluscs, sponge spicules, and <u>Halysis</u> .	
	<u>Anella jemtlandica</u> (Löfgren) <u>Drepanoistodus</u> cf. <u>venustus</u> Stauffer <u>Juanognathus serpaglii</u> Stouge <u>Parapaltodus simplicissimus</u> Stouge <u>Parapanderodus arcuatus</u> Stouge <u>Palaistodus originatus</u> Sergeeva <u>Protopanderodus</u> sp.	uppermost Table Point Fm., lower Table Cove Fm.* (A ₁ -B ₁)
	* <u>A. jemtlandica</u> is uncommon below A ₁ . <u>J. serpaglii</u> is not reported above B ₁ .	

Table G.1 continued

Sample No. Locality & Mass		Correlative Formation
Grey-brown fossiliferous and/or peloidal limestone (continued)		
0814-10 (PBAY) 1.7 kg	Boulder; dark grey trilobite rudstone with fine peloidal packstone matrix plus brachiopods, echinoderms and gastropods.	Lower Table Cove Fm.* (A ₃ -B ₄)
	<u>Acodus?</u> <u>mutatus</u> (?) <u>Ansella</u> <u>jemtlandica</u> (Löfgren) <u>Baltoniodus</u> sp. <u>Cordylodus?</u> <u>horridus</u> Barnes and Poplawski <u>Drepanodus</u> <u>arcuatus</u> Pander <u>Oistodus</u> <u>lanceolatus</u> Pander <u>Paltodus?</u> cf. <u>jemtlandicus</u> (Löfgren) <u>Parapaltodus</u> <u>flexuosus</u> Barnes and Poplawski <u>Parapaltodus</u> <u>simplicissimus</u> Stouge <u>Parpistodus</u> <u>originalis</u> Sergeeva <u>Periodon</u> <u>aculeatus</u> Madding <u>Polonodus?</u> sp. <u>Prioniodus</u> sp. <u>Protopanderodus</u> <u>varicosatus</u> Sweet and Bergström <u>"Scandodus"</u> <u>mysticus</u> Barnes and Poplawski <u>Walliserodus</u> <u>ethingtoni</u> Fähræus	
	*many of the species present are especially abundant in B ₁ ; several are not reported by Stouge (1984)	
Mottled <u>Stromatactis</u> limestone		
0725-5 (BC) 2.2 kg	Boulder (25X35 cm); fossil-poor wackestone with ostracodes, gastropods, spicules and <u>Girvanella</u> .	uppermost Table Point Fm.* (A ₃)
	<u>Ansella</u> <u>jemtlandica</u> (Löfgren) <u>Cordylodus?</u> <u>horridus</u> Barnes and Poplawski <u>Histioidella</u> <u>tableheadensis</u> Stouge <u>Parapanderodus</u> <u>arcuatus</u> Stouge <u>Periodon</u> <u>aculeatus</u> Madding <u>Polonodus?</u> <u>newfoundlandensis</u> Stouge <u>Scalpellodus</u> <u>biconvexus</u> (Bradshaw)	
	* <u>H. tableheadensis</u> does not occur above the very base of the Table Cove; <u>P.?</u> <u>newfoundlandensis</u> is restricted to A ₃ ; <u>S. biconvexus</u> is not reported above A ₃	
0829-3 (PIC) 2.3 kg	Boulder; peloidal, fossiliferous wackestone with peloidal wacke-/packstone mottles; echinoderms, ostracodes, trilobites, bryozoans, <u>Girvanella</u> and <u>Halysis</u> .	uppermost Table Point Fm.* (upper A ₃ -B ₄)
	<u>Ansella</u> <u>jemtlandica</u> (Löfgren) <u>Histioidella</u> <u>kristina</u> Stouge <u>Parapanderodus</u> <u>arcuatus</u> Stouge <u>Semiacontiodus</u> cf. <u>bulbosus</u> (Löfgren)	
	* <u>H. kristina</u> does not occur below the top of A ₃ ; <u>S.</u> cf. <u>bulbosus</u> recorded only in uppermost A ₃ and in B.	

Table G.1 continued

Sample No. Locality & Mass		Correlative Formation
Mottled <u>Stromatactis</u> limestone (continued)		
DH-55 (DH) 1.2 kg	Boulder; limestone with ostracodes, echinoderms, mollusc fragments, <u>Girvanella</u> , oncolites, and <u>Halysis</u> .	
	<u>Ansellia jemtlandica</u> (Löfgren)	uppermost Table Point Fm.*
	<u>Cordylodus? horridus</u> Barnes and Poplawski	(A ₃ -B ₁)
	<u>Cordylodus? sp.</u>	
	<u>Drepanodus sp.</u>	
	<u>Histiodelle tableheadensis</u> Stouge	
	<u>Juanognathus sp.</u>	
	<u>Parapaltodus simplicissimus</u> Stouge	
	<u>Parapanderodus arcuatus</u> Stouge	
	<u>Periodon sp.</u>	
	<u>Scalpellodus pointensis</u> Stouge	
	* <u>H. tableheadensis</u> does not occur above the very base of C ₁ ; Table Cove	
DH-58 (DH) 0.7 kg	Megaboulder (1.8X1.2X1.3 m); mottled <u>Stromatactis</u> lithofacies limestone as above plus brachiopods and sponge spicules.	
	<u>Ansellia jemtlandica</u> (Löfgren)	uppermost Table Point Fm.*
	<u>Cordylodus? horridus</u> Barnes and Poplawski	(A ₃ -B ₁)
	<u>Drepanoistodus cf. venustus</u> (Stauffer)	
	<u>Histiodelle kristina</u> Stouge	
	<u>Parapaltodus simplicissimus</u> Stouge	
	<u>Parapanderodus arcuatus</u> Stouge	
	<u>Periodon aculeatus</u> Hadding	
	<u>Protopanderodus asymmetricus</u> Barnes and Poplawski	
	<u>Protopanderodus cooperi</u> (Sweet and Bergström)	
	<u>Semiacontiodus asymmetricus</u> Barnes and Poplawski	
	* <u>H. kristina</u> does not occur below the top of A ₃ ; <u>P. simplicissimus</u> is uncommon below the very top of A ₃	
0917-2 (CP) 1.7 kg	Boulder; very fine peloidal, fossil-poor packstone with abundant spicules, sparse trilobites, ostracodes, and <u>Halysis</u> .	
	<u>Parapanderodus arcuatus</u> Stouge	Table Point Fm. (A ₃ -B ₄ ; species range)
Interbedded limestone and shale		
0920-3 (EH) 2.2 kg	Raft (>6X1.5 m); grey-brown, ribbon limestone; recrystallized, laminated mudstone/peloidal wackestone with sparse ostracodes and radiolarians.	
	<u>Cordylodus? horridus</u> Barnes and Poplawski	Table Cove Fm.
	<u>Drepanoistodus forceps</u> (Lindström)	(A ₃ -B ₄ ; species ranges)
	<u>Histiodelle kristina</u> Stouge	
	<u>Periodon aculeatus</u> Hadding	
	<u>Protopanderodus sp.</u>	

Table G.1 continued

Sample No. Locality & Mass		Correlative Formation
Interbedded limestone and shale (continued)		
0920-5 (EH) 2.4 kg	Reft (>5X1.5 m); grey-brown, burrowed parted limestone (mudstone) with sparse trilobites, ostracodes, brachiopods, mollusc fragments and radiolarians.	
	<u>Cordylodus?</u> <u>horridus</u> Barnes and Poplawski	Table Cove Fm.
	<u>Drepanoistodus</u> sp.	(A ₃ -B ₄ ; species ranges)
	<u>Juanognathus</u> sp.	
	<u>Parapanderodus arcuatus</u> Stouge	
0011-3 (NARM) 1.8 kg	Black argillaceous mudstone/calcareous shale; yellow-weathering; pyritic; well-developed cleavage.	
	Barren	
White fenestral limestone		
CP-45 (CP) 0.9 kg	Boulder; white, fenestral limestone; clotted, fine peloidal packstone with rare trilobites, gastropods, and <u>Girvanella</u> .	
	<u>Cornuodus longibasis</u> (Lindström)	Table Point Fm.
	<u>Loxodus?</u> sp.	(A ₂ -B ₄)
	<u>Parapanderodus</u> sp.	
DH-57 (DH) 0.7 kg	Boulder; white fenestral limestone with burrow mottles.	
	Barren	
0918-11 (CP) 2.1 kg	Boulder; white fenestral limestone; very fine peloidal grainstone with sparse ostracodes; blocky ferroan calcite cement.	
	Barren	
Dolostone		
BC55E (BC) 2.2 kg	Yellow-weathering, finely crystalline (0.02-0.05 mm) dolostone; nonferroan with minor ferroan overgrowths; structureless or with faint parallel lamination. (Sample composed of numerous pebble-size clasts in the conglomerate.)	
	Barren	

Table G.1 continued

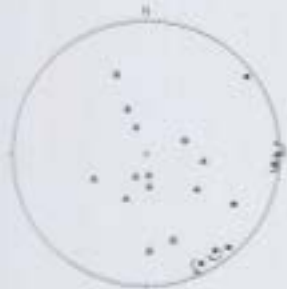
Sample No. Locality & Mass		Correlative Formation
	Limestone conglomerate (clast)	
DH-24 (DH) 1.5 kg	Mega-clast (10x1.5 m); small pebble, limestone conglomerate/	
	<u>Anella jemtlandica</u> (Löfgren) <u>Dischrognathus</u> sp. <u>Drepanodus? arcuatus</u> Pander <u>?Erraticodon balticus</u> Dzik <u>Parapaltodus simplicissimus</u> Stouge <u>Plectodina? sp. A</u> Stouge <u>Scalpellodus pointensis</u> Stouge <u>Semiacontiodus asymmetricus</u> Barnes and Poplawski <u>Semiacontiodus preasymmetricus</u> Stouge <u>Scalpellodus pointensis</u> Stouge	Table Point Fm., Table Cove Fm. (A,-B ₄)*
	* <u>Plectodina? sp. A</u> and <u>S. preasymmetricus</u> are reported only in the lower Table Point (A ₁ -A ₂).	
	Whole rock conglomerate	
WC-34B (WBC) 1.7 kg	Matrix-poor, pebble-grade conglomerate.	
	<u>Parapanderodus arcuatus</u> Stouge <u>Paroistodus originalis</u> Sergeeva <u>Protopanderodus rectus</u> (Lindström) <u>Ptiloncodus simplex</u> Harris	Table Point Fm., Table Cove Fm. (A,-B ₄) and St. George Gp.*?
	* <u>P. rectus</u> is a long-ranging species also reported in Arenigian strata (Van Wamel, 1974).	
0708-15 (PIC) 2.2 kg	Matrix-poor, pebble-grade conglomerate.	
	<u>Juanognathus serpaglii</u> Stouge <u>Paroistodus originalis</u> Sergeeva	Table Point Fm., Table Cove Fm. (A,-B ₄ ; species ranges)
CP-20 (CP) 1.5 kg	Matrix-poor, pebble-grade conglomerate.	
	<u>Anella jemtlandica</u> (Löfgren) <u>Cordylodus? horridus</u> Barnes and Poplawski <u>?Erraticodon balticus</u> Dzik <u>Histiodela kristina</u> Stouge <u>Parapaltodus simplicissimus</u> <u>Parapanderodus arcuatus</u> Stouge <u>Paroistodus originalis</u> Sergeeva <u>Tripodus laevis</u> Bradshaw	Table Point Fm., Table Cove Fm. (A,-B ₄) and St. George Group*
	* <u>I. laevis</u> is an Arenigian species reported from Beds 12-13 in the Green Point Fm. (Cow Head Group) (Johnson, 1986). Ethington and Clark (1981) recognize it as a middle Arenigian-lower Llanvirnian form, below the lower Whiterock.	

Table G.1 continued

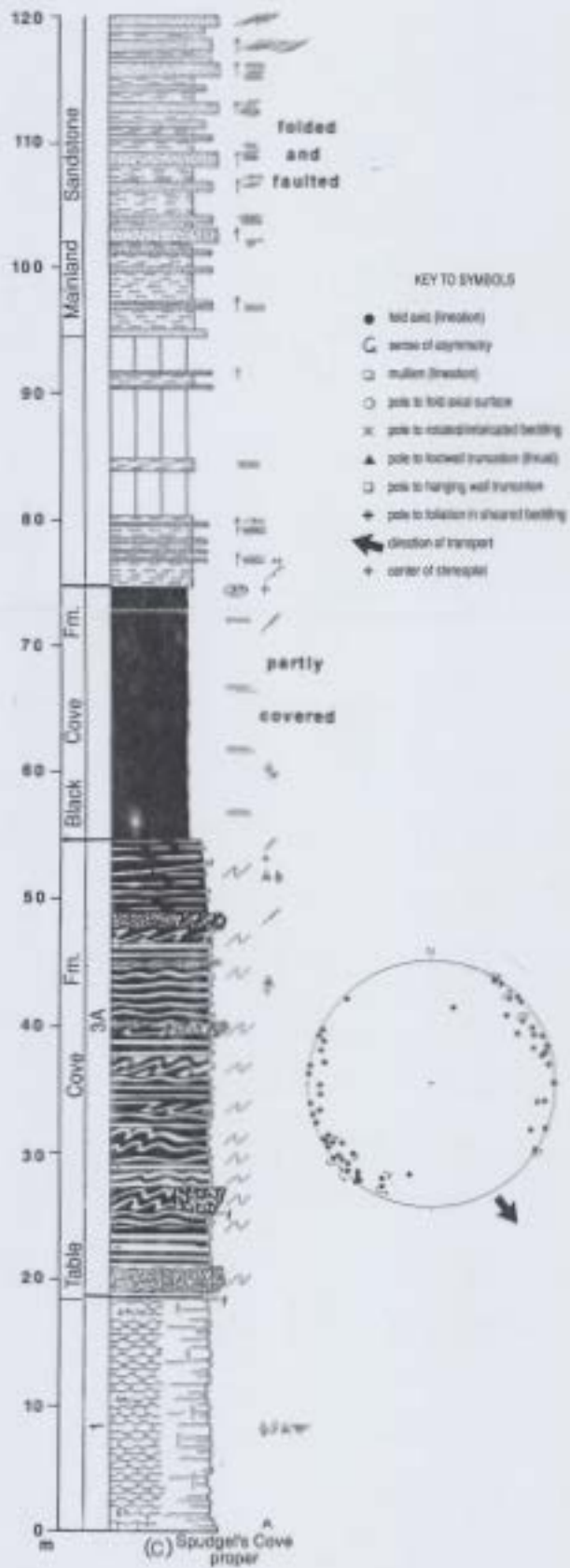
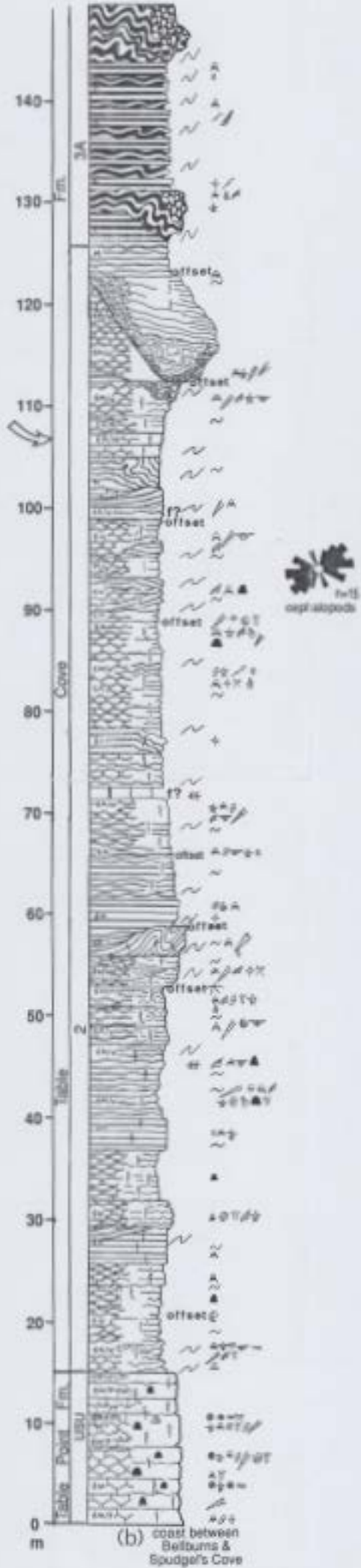
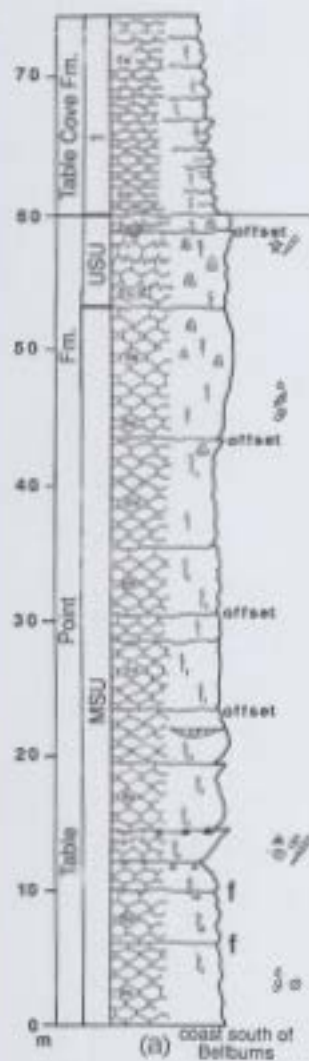
Sample No. Locality & Mass		Correlative Formation
Whole rock conglomerate (continued)		
0918-1 (CP) 2.1 kg	Matrix-poor, pebble-grade conglomerate.	
	<u>Parapanderodus arcuatus</u> Stouge	Table Point Fm., Table Cove Fm.
	<u>Pteronotodus crpytodens</u> (Mound)	(A ₂ -B ₄) and St. George Gp.*
* <u>P. crpytodens</u> is an Arenigian species reported from Bed 13 in the Green Point Fm. (Cow Head Gp.) (Johnson, 1986). Ethington and Clark (1981) recognize it as a lower Whiterockian, older than the lowest Table Point.		
PCP-13 (PCP)	Matrix-poor, pebble-grade conglomerate.	
	? <u>Erraticodon balticus</u> Dzik	Table Point Fm., Table Cove Fm.
	<u>Histiodelle tableheadensis</u> Stouge	(A ₁ -B ₄ ; species ranges)
	<u>Loxodus? curvatus</u> Stouge	
	<u>Parapaltodus simplicissimus</u> Stouge	
	<u>Parapanderodus arcuatus</u> Stouge	
	<u>Periodon aculeatus</u> Hadding	
	<u>Walliserodus ethingtoni</u> Fähræus	
Siliciclastic sediment		
CP 29 (CP) 2 kg	Greenish grey, very coarse-grained quartz lithic 'arenite' (QFL = 65-70%, <10-15%, >20%); matrix replaced by ferroan calcite and ferroan dolomite.	
	Barren	
0619-1 (PBAY)	Black, laminated calcareous shale/argillaceous mudstone; yellow-weathering; poorly-preserved graptolites.	
	Barren	
Daniel's Harbour Member Calcarenite (in situ)		
BC-46 (BC) 0.7 kg	Medium- to coarse-grained; <5-7% quartz, feldspar and lithic fragments (predominantly quartz. (Siliciclastic grains on average finer than carbonate grains.)	
	<u>Paroistodus</u> sp.	Table Point Fm., Table Cove Fm.
	<u>Parapanderodus arcuatus</u> Stouge	(A ₂ -B ₄)*
	<u>Scolopodus</u> cf. <u>oldstockensis</u> Stouge	
* <u>S.</u> cf. <u>oldstockensis</u> is reported only from B ₁ .		

APPENDIX H
LOCATIONS OF MEASURED SECTIONS

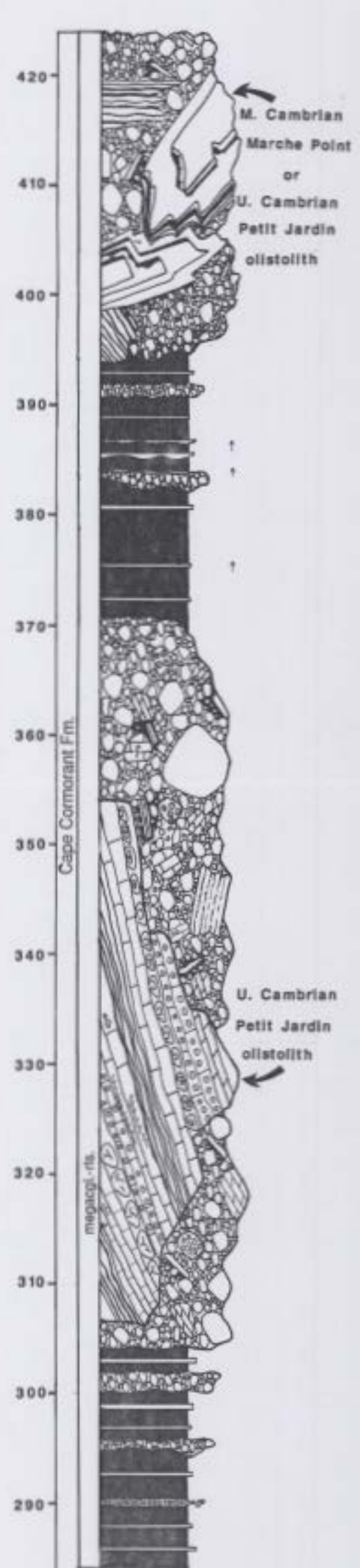
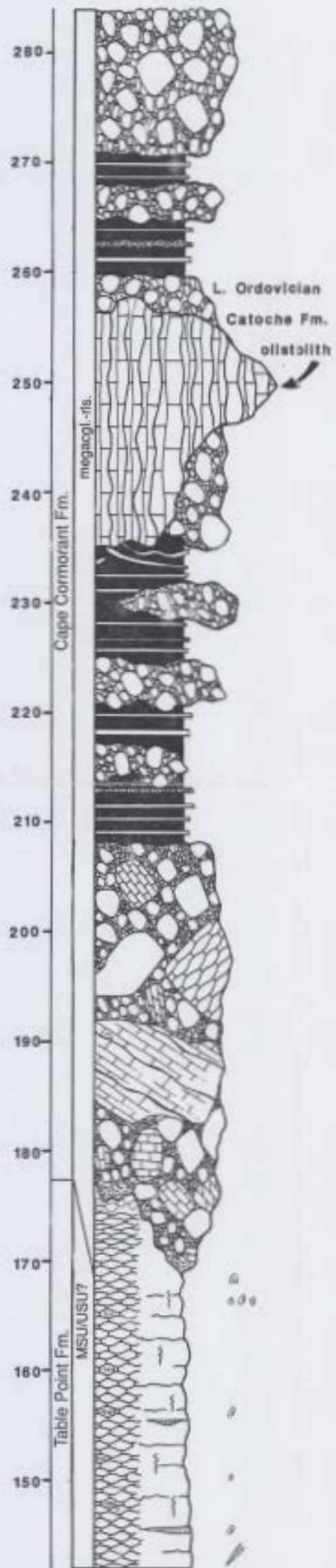
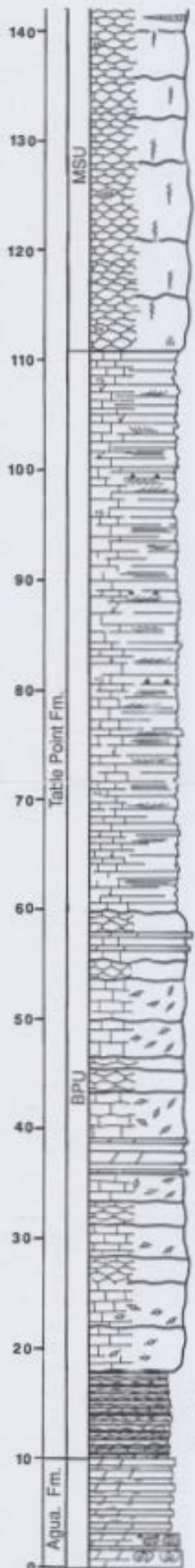
LOCATION	MAP NUMBER AND GRID REFERENCE
PORT AU PORT AREA	
Big Cove A	NTS 12B/11; UD 355777
Big Cove B	NTS 12B/11; UD 350750
Caribou Brook	NTS 12B/11; UD 377797
West Bay Center Quarry	NTS 12B/10; UD 583837
Piccadilly Park Roadcut	NTS 12B/10; UD 595830
Piccadilly Roadcut	NTS 12B/10; UD 590808
Agathuna Quarry	NTS 12B/10; UD 691718
Northwest Gravels	NTS 12B/10; UD 721797
Black Cove	NTS 12B/10; UD 745816
Cold Brook Quarry	NTS 12B/9W; UD 899882
GROS MORNE AREA	
Shag Cliff	NTS 12H/12; VE 378846
Bakers Brook	NTS 12H/12; VE 363994 to 349998
Stag Brook	NTS 12H/12; VE 377085
West Brook	NTS 12H/13; VF 595355
Southwest Feeder	NTS 12I/4; VF 581518
TABLE POINT AREA	
Portland Creek Pond (island)	NTS 12I/4; VF 608604
(shore)	NTS 12I/4; VF 585625
Eastern Head (south point)	NTS 12I/4; VF 562589
(north point)	NTS 12I/4; VF 566609
Cliffy Point	NTS 12I/4; VF 563615
Daniel's Harbour Zinc Mine	
DH-1516	NTS 12I/6 & 12I/5; VF 747811
DH-1382	NTS 12I/6 & 12I/5; VF 711786
US Borax (BO) #1	NTS 12I/6 & 12I/5; VF 732779
US Borax (BO) #2	NTS 12I/4; VF 617663
DH-2301	NTS 12I/6 & 12I/5; VF 615666
Spudgels Cove	NTS 12I/6 & 12I/5; VF 600706
Table Point/Table Cove	NTS 12I/5 & 12I/6; VF 616787/VF 620766
Gargamelle Cove (north side)	NTS 12I/11; VG 745166
(south side)	NTS 12I/11; VG 745163
River of Ponds Lake (shore)	NTS 12I/11; VF 777945
(island)	NTS 12I/6 & 12I/5; VF 764921
Daniel's Harbour	NTS 12I/4; UD 577653
HARE BAY - PISTOLET BAY AREA	
Beaver Brook	NTS 12I/16; WG 574437
Roddickton Quarry	NTS 12I/16; WG 575459
Springs Inlet (base)	NTS 2M/4; WG 806739
(top)	NTS 2M/4; WG 800748
Northern Arm	NTS 12P/8; WG 699917
Burnt Island (base)	NTS 2M/12; WH 870154
(top; SE corner)	NTS 2M/12; WH 869123
(top; SW corner)	NTS 2M/12; WH 868112
Pistolet Bay (west coast)	NTS 2M/12; WH 782084
Bakeapple Island (base)	NTS 2M/12; WH 802160
(top)	NTS 2M/12; WH 801158
Vaches Pt./Callieux Bay (base)	NTS 2M/12; WH 763179
(top)	NTS 2M/12; WH 769183



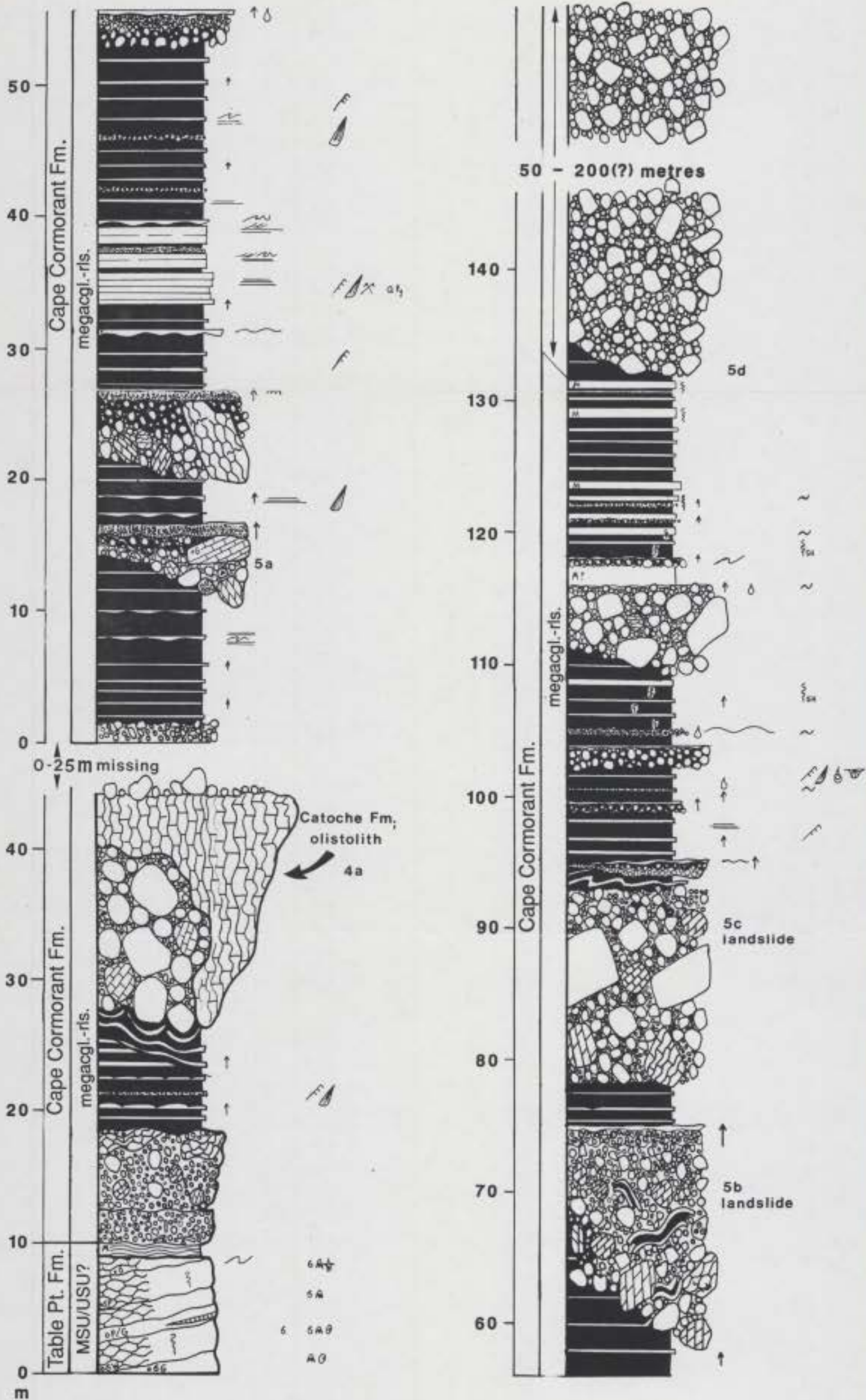
BELLBURNS / SPUDGEL'S COVE



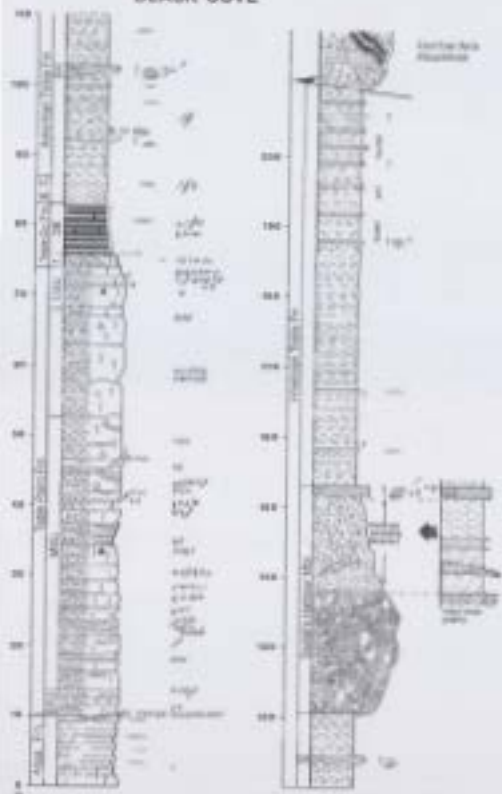
BIG COVE (A)



BIG COVE (B)



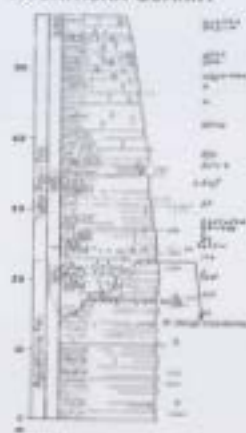
BLACK COVE



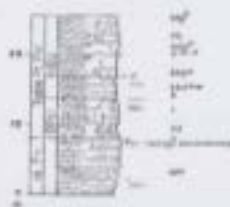
PICCADILLY ROADCUT



AGUATHUNA QUARRY



NW GRAVELS



WEST BAY CENTRE QUARRY

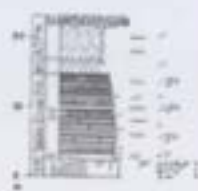
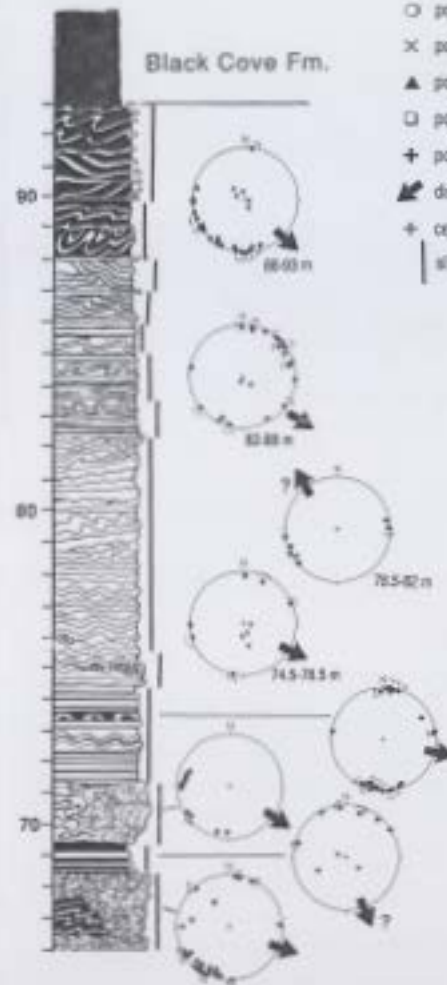
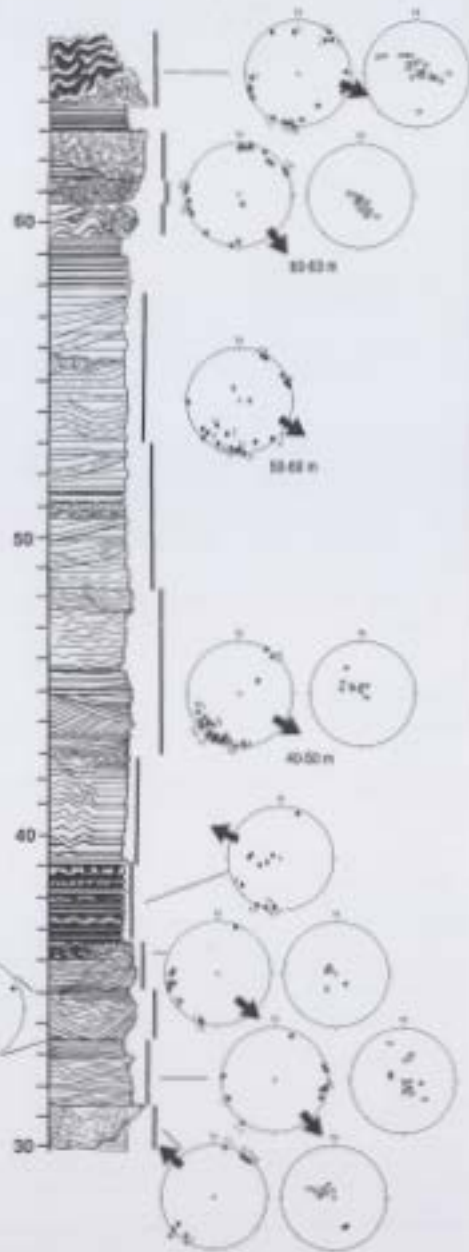


Figure 5.10

Table Cove Formation
at Table Cove:
paleoslope data



KEY TO SYMBOLS

- fold axis (lineation)
- C sense of asymmetry
- ▨ nullion (lineation)
- pole to fold axial surface
- × pole to rotated/intercalated bedding
- ▲ pole to footwall truncation (thrust)
- pole to hanging wall truncation
- + pole to foliation in sheared bedding
- ↖ direction of transport
- center of stereonet
- | side

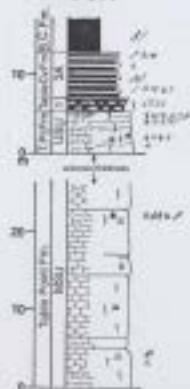
GARGAMELLE COVE



RIVER OF PONDS LAKE



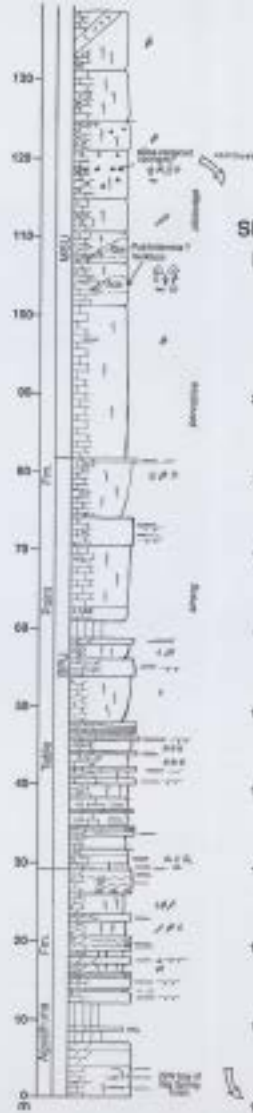
BEAVER BROOK



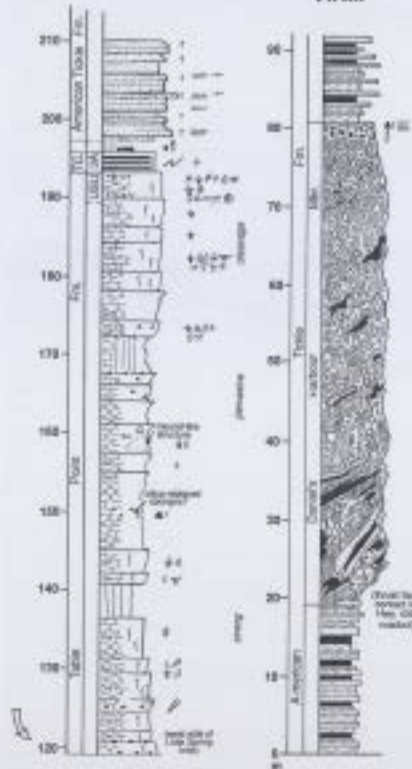
RODDICKTON QUARRY



SPRINGS INLET



NORTHERN ARM



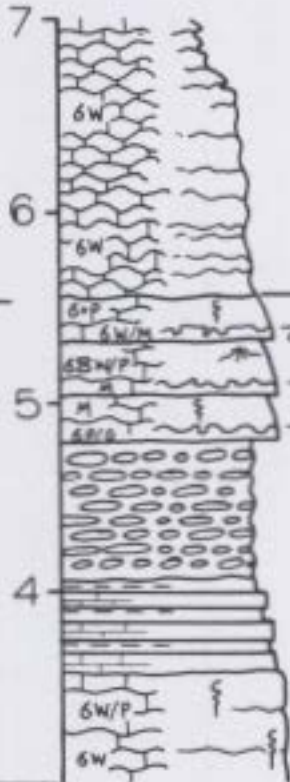
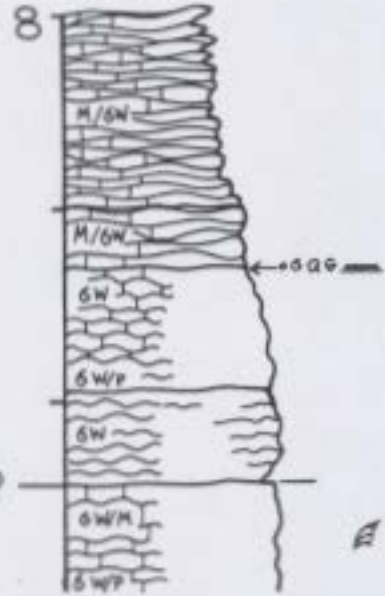
PROVINCIAL PARK ROADCUT SECTION

North side route 463

(east)

(west)

Table Cove Fm.

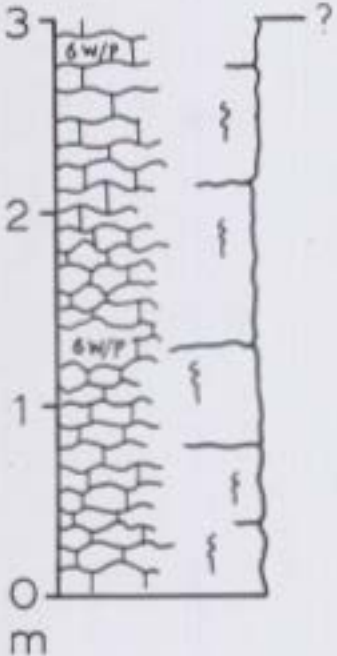


South side route 463

A6

A A
 B B

Table Point Fm.



SHAG CLIFF

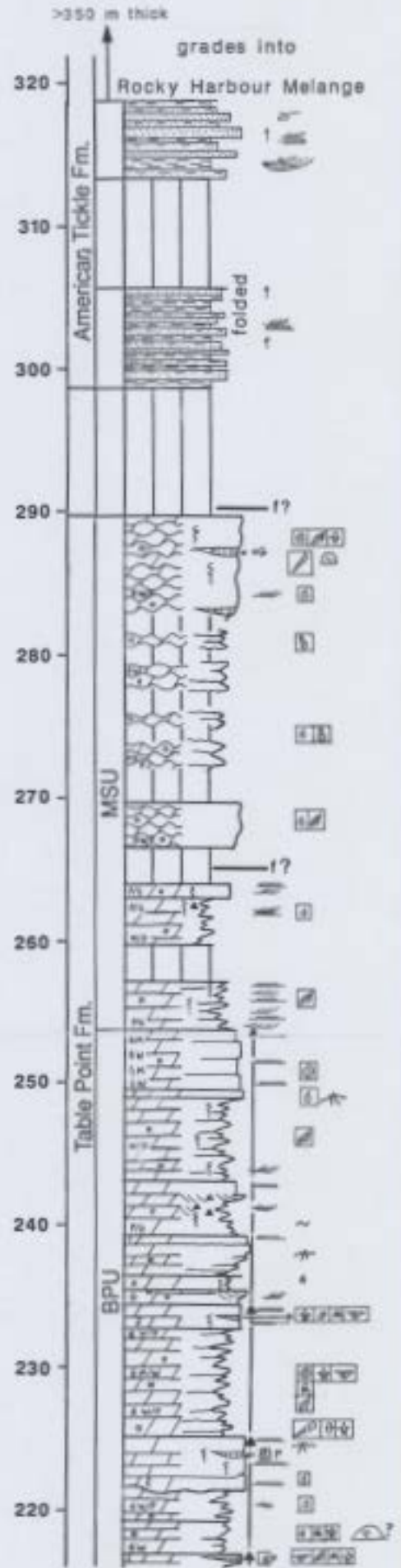
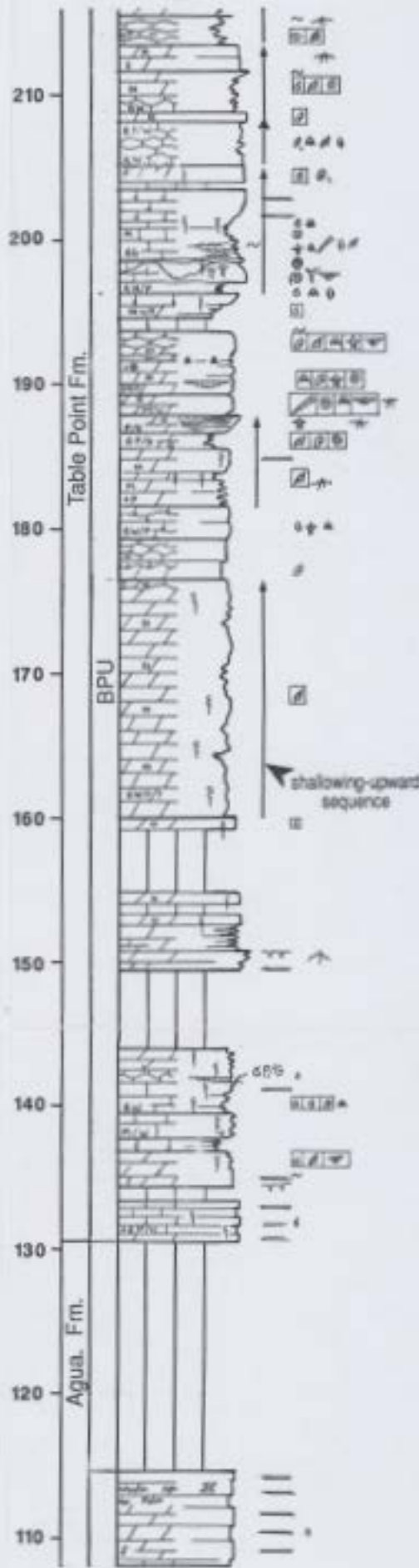
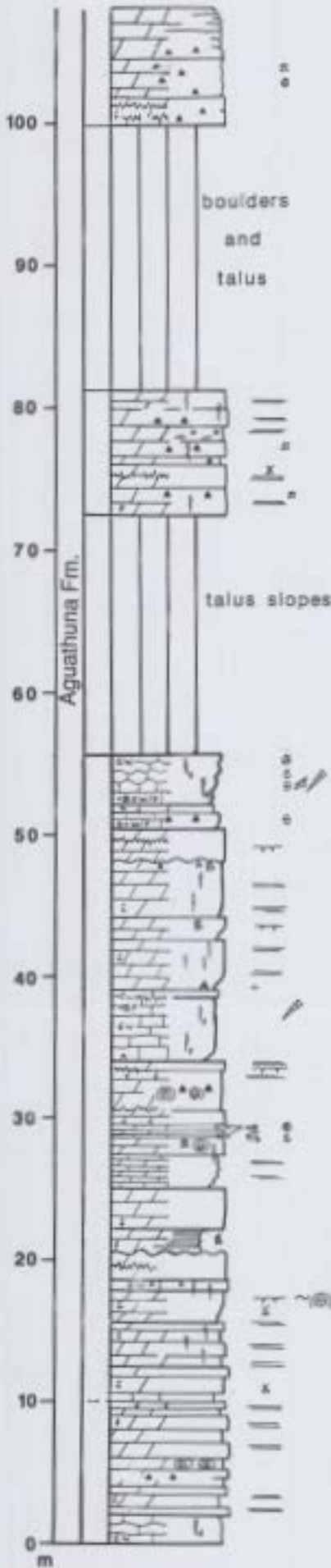


TABLE POINT

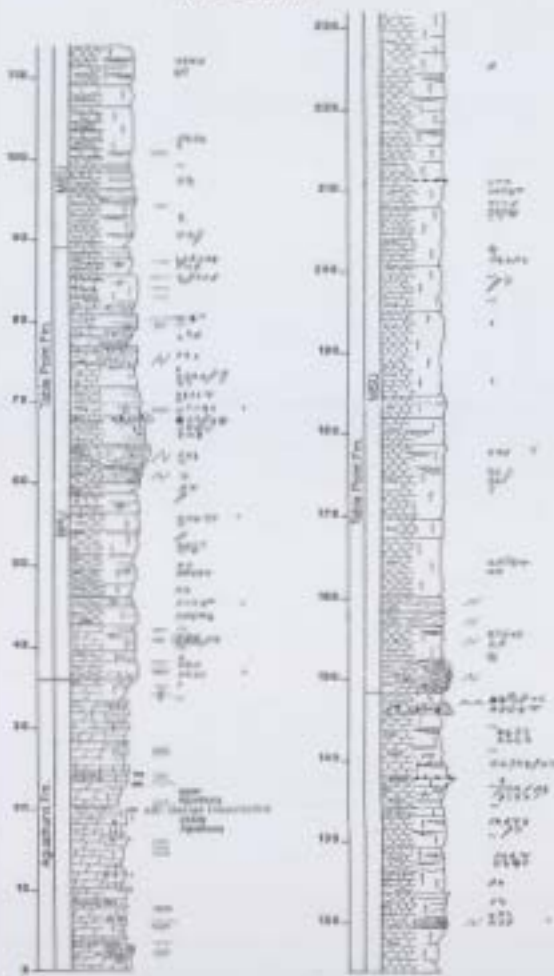


TABLE POINT (CONT.)

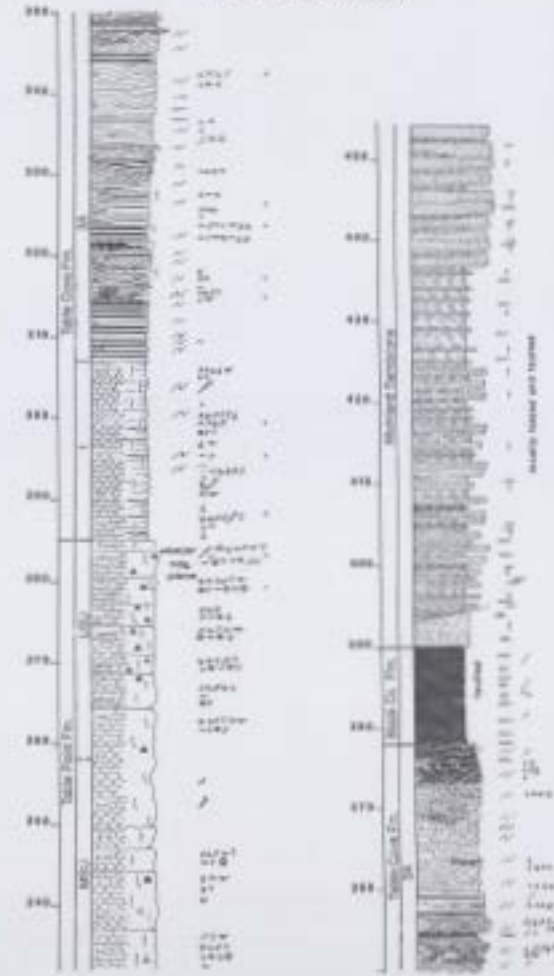
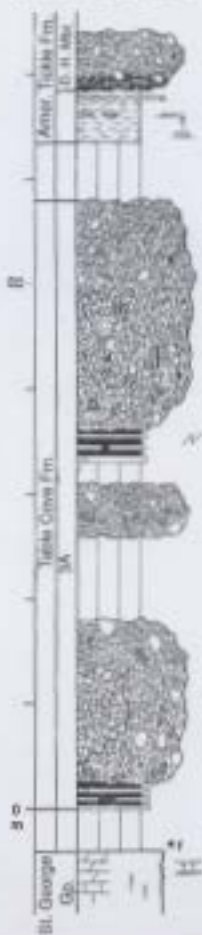


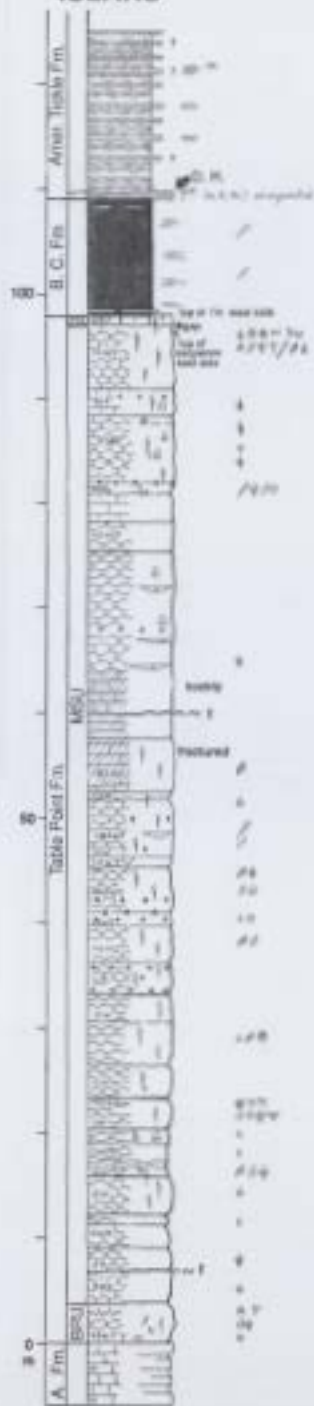
TABLE COVE - BELLBUNG



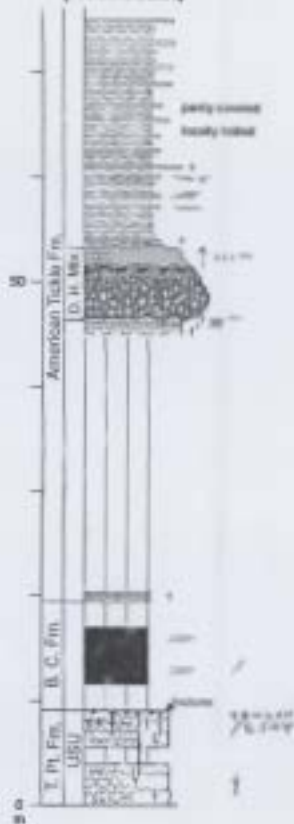
VACHES POINT



BAKEAPPLE ISLAND



PISTOLET BAY (west coast)



BURNT ISLAND

